

AD A 082404

LEVEL

9

1979 USAF

SUMMER FACULTY RESEARCH PROGRAM

DTIC
ELECTE
APR 1 1980
S D C

Research Report
Volume 3 of 3

Conducted by:
SOUTHEASTERN CENTER FOR
ELECTRICAL ENGINEERING EDUCATION
7300 LAKE ELLENOR DRIVE
ORLANDO, FLORIDA
DECEMBER, 1979

Approved for public release;
distribution unlimited.

80 9 26 049

PII Redacted

DDC FILE COPY

UNCLASSIFIED

SECURITY CLASSIFICATION OF THIS PAGE (When Data Entered)

REPORT DOCUMENTATION PAGE		READ INSTRUCTIONS BEFORE COMPLETING FORM
1. REPORT NUMBER AFOSR-TR- 80 - 02 49	2. GOVT ACCESSION NO.	3. RECIPIENT'S CATALOG NUMBER
4. TITLE (and Subtitle) 1979 USAF Summer Faculty Research Program Volume 3 of 3 A082403		5. TYPE OF REPORT & PERIOD COVERED Final
7. AUTHOR(s) Richard N. Miller		6. PERFORMING ORG. REPORT NUMBER
9. PERFORMING ORGANIZATION NAME AND ADDRESS Southeastern Center for Electrical Engineering Education 7300 Lake Ellenor Drive Orlando, Florida 32809		8. CONTRACT OR GRANT NUMBER(s) F49620-79-C-0038
11. CONTROLLING OFFICE NAME AND ADDRESS Air Force Office of Scientific Research/XOP Bldg. 410 Bolling Air Force Base, DC 20332		10. PROGRAM ELEMENT, PROJECT, TASK AREA & WORK UNIT NUMBERS 61102F 2305/D5
14. MONITORING AGENCY NAME & ADDRESS (if different from Controlling Office)		12. REPORT DATE December 1979
		13. NUMBER OF PAGES 719
		15. SECURITY CLASS. (of this report) UNCLASSIFIED
		15a. DECLASSIFICATION/DOWNGRADING SCHEDULE
16. DISTRIBUTION STATEMENT (of this Report) Approved for public release; distribution unlimited.		
17. DISTRIBUTION STATEMENT (of the abstract entered in Block 20, if different from Report)		
18. SUPPLEMENTARY NOTES		
19. KEY WORDS (Continue on reverse side if necessary and identify by block number) Summer Faculty Research Program		
20. ABSTRACT (Continue on reverse side if necessary and identify by block number) This Volume 3 of 3 volumes presents the final research reports of the 1979 Summer Faculty Research Program participants. The program designed to stimulate scientific and engineering interaction between university faculty members and technical personnel at the Air Force laboratories, centers, and divisions has four specific objectives: (1) To develop the basis for continuing research of interest to the Air Force at the faculty member's institution. (2) To further the research objectives of the Air Force.		

UNCLASSIFIED

SECURITY CLASSIFICATION OF THIS PAGE (When Data Entered)

- (3) To stimulate continuing relations among faculty members and their peers in the Air Force.
- (4) To enhance the research interests and capabilities of scientific and engineering educators.

UNCLASSIFIED

9

6

**USAF/SCEEE SUMMER FACULTY
RESEARCH PROGRAM (IND.)**

Volume III.

Conducted by

The Southeastern Center

for

Electrical Engineering Education

under 15

USAF Contract Number F49620-79-C-0038

PARTICIPANTS' RESEARCH REPORTS

Volume III of III

Submitted to

Air Force Office of Scientific Research

Bolling Air Force Base

Washington, D.C.

by

10

**Richard N. Miller / SFRP Director
Southeastern Center for
Electrical Engineering Education**

**AIR FORCE OFFICE OF SCIENTIFIC RESEARCH (AFSC)
NOTICE OF RELEASE TO THE
This document is released and is
approved for release under E.O. 12958-2 (b).
Distributed by
A. D. [unclear]
Technical Information Officer**

**Approved for public release;
distribution unlimited.**

**DTIC
SELECTED
APR 1 1980**

16 23-101

17 25

11 11 11

1-1-1-1-1-1

12 7

394

1979 USAF/SCEE SUMMER FACULTY RESEARCH PROGRAM

LIST OF PARTICIPANTS

NAME/ADDRESS

DEGREE, SPECIALTY, & LABORATORY
ASSIGNMENT

Dr. Yelagalawadi V. Acharya
Professor, Mechanical Engineering Dept.
West Virginia Tech
Montgomery, WV 25136
(304) 442-3289 [REDACTED]

Degree: D. Sc., Aeronautics, 1954
Specialty: Fluid Mechanics, Aero-
dynamics
Assigned: AFFDL (Wright-Patterson)
[REDACTED]

Dr. Adel A. Aly
Associate Professor
Dept. of Industrial Engineering
University of Oklahoma
202 W. Boyd, Suite 124
Norman, OK 73019
(405) 325-3721 [REDACTED]

Degree: PhD., Industrial Eng., 1975
Specialty: Applied OR, Math Prog.,
Facility design and location theory
and routing and distribution systems
Assigned: AFRADC (Griffiss)
[REDACTED]

Dr. Clarence A. Bell
Associate Professor
Dept. of Mechanical Engineering
Texas Tech University
Lubbock, TX 79409
(806) 742-3563 [REDACTED]

Degree: PhD., Mechanical Eng., 1971
Specialty: Vibrations, Dynamics,
Applied Mathematics
Assigned: AFWL (Kirtland)
[REDACTED]

Dr. Warren W. Bowden
Professor of Chemical Engineering
Rose-Hulman Institute of Technology
5500 Wabash Avenue
Terre Haute, IN 47803
(812) 877-1511 [REDACTED]

Degree: PhD., Chemical Eng., 1965
Specialty: Physical properties, Phase
equilibrium, Computer utilization
Assigned: AFAEDC (Arnold)
[REDACTED]

Mr. Barry D. Bullard
Instructor
Dept. of Engineering Technology
University of Central Florida
P.O. Box 25000
Orlando, FL 32816
(305) 275-2710/2268 [REDACTED]

Degree: MS, Electrical Eng., 1977
Specialty: Electronic Communications-
Antennas and Microwave
Assigned: SAMTEC (Patrick)
[REDACTED]

Dr. James A Cadzow
Professor, Dept. of Electrical Engineering
Virginia Polytechnic Institute
Blacksburg, VA 24061
(703) 961-5694 [REDACTED]

Degree: PhD., Electrical Eng., 1964
Specialty: Communications, Controls
& Digital Signal Processing
Assigned: AFRADC (Griffiss)
[REDACTED]

Dr. Malcolm D. Calhoun
Assistant Professor
Dept. of Electrical Engineering
Mississippi State University
Drawer EE
Mississippi State, MS 39762
(601) 325-3912/3073 [REDACTED]

Degree: PhD., Electrical Eng., 1976
Specialty: Electronics, Communications
Assigned: AFAL (Wright-Patterson)
[REDACTED]

1979 PARTICIPANTS
Page Two

NAME/ADDRESS

Dr. William R. Carper
Professor, Dept. of Chemistry
Wichita State University
Wichita, KS 67208
(316) 689-3120 [REDACTED]

Dr. Chi Hau Chen
Professor and Chairman
Electrical Engineering Dept.
Southeastern Massachusetts University
N. Dartmouth, MA 02747
(617) 999-8475 [REDACTED]

Dr. Donald C. Chiang
Professor
Division of Civil and Mechanical Engineering
Rose-Hulman Institute of Technology
5500 Wabash Avenue
Terre Haute, IN 47803
(812) 877-1511, EXT. 323 [REDACTED]

Dr. Aaron S. Collins
Assistant Professor
Electrical Engineering Dept.
Tennessee Technological University
Box 5004-TTU
Cookeville, TN 39501
(615) 528-3352 [REDACTED]

Dr. William A. Davis
Assistant Professor
Electrical Engineering Dept.
Virginia Polytechnic Institute
and State University
Blacksburg, VA 24061
(703) 961-6307 [REDACTED]

Dr. Alan S. Edelstein
Associate Professor, Dept. of Physics
University of Illinois at Chicago Circle
P.O. Box 4348
Chicago, IL 60680
(312) 996-5348/3400 [REDACTED]

Mr. Willard R. Fey
Associate Professor
Dept. of Industrial and Systems Engineering
Georgia Institute of Technology
Atlanta, GA 30332
(404) 894-2359 [REDACTED]

DEGREE, SPECIALTY, & LABORATORY
ASSIGNMENT

Degree: PhD., Physical Chemistry, 1963
Specialty: Kinetics, Molecular
Spectroscopy
Assigned: AFFJSRL (USAF Academy)
[REDACTED]

Degree: PhD., Electrical Eng., 1965
Specialty: Signal Processing, Pattern
Recognition and Communications
Assigned: AFGL (Hanscom)
[REDACTED]

Degree: PhD., Fluid Mechanics, 1965
Specialty: Fluid Mechanics, Thermo-
dynamics, Heat Transfer, Analog
Computer
Assigned: AFFDL (Wright-Patterson)
[REDACTED]

Degree: PhD., Electrical Eng., 1973
Specialty: Classical and Modern
Control Theory, Computers, Simulation,
Numerical Methods
Assigned: AFAL (Wright-Patterson)
[REDACTED]

Degree: PhD., Electrical Eng., 1974
Specialty: Electromagnetics
Assigned: AFWL (Kirtland)
[REDACTED]

Degree: PhD., Physics, 1963
Specialty: Solid State Physics,
Magnetism, Superconductivity
Assigned: AFML (Wright-Patterson)
[REDACTED]

Degree: MS, Electrical Eng., 1961
Specialty: System Dynamics
Assigned: AFESC (Tyndall)
[REDACTED]

1979 PARTICIPANTS

Page Three

NAME/ADDRESS

Dr. John T. Foley
Assistant Professor of Physics Dept.
Mississippi State University
Mississippi State, MS 39762
(601) 325-2806 [REDACTED]

Dr. Garabet J. Gabriel
Associate Professor
Dept. of Electrical Engineering
Notre Dame University
Notre Dame, IN 46556
(219) 283-7531 [REDACTED]

Dr. James A. Gessaman
Associate Professor of Biology Dept.
Utah State University
UMC 53
Logan, UT 84332
(801) 752-4100, EXT. 7876 [REDACTED]

Dr. Paul K. Grogger
Assistant Professor
Dept. of Geography and Environmental Studies
University of Colorado
Colorado Springs, CO 80907
(303) 598-3737, EXT. 273/217 [REDACTED]

Dr. William D. Gunther
Professor of Economics
University of Alabama
P.O. Box 650
University, AL 35486
(205) 348-7842 [REDACTED]

Dr. John Hadjiligiou
Associate Professor
Electrical Engineering Dept.
Florida Institute of Technology
P.O. Box 1150
Melbourne, FL 32901
(305) 723-3701, EXT. 217 [REDACTED]

Dr. Keith M. Hagenbuch
Assistant Professor of Physics
Behrend College of
Pennsylvania State University
Station Road
Erie, PA 16563
(814) 898-1511 [REDACTED]

DEGREE, SPECIALTY, & LABORATORY
ASSIGNMENT

Degree: PhD., Physics, 1977
Specialty: Optics
Assigned: APWL (Kirtland)
[REDACTED]

Degree: PhD., Electrical Eng., 1964
Specialty: Electromagnetics
Assigned: AFAPL (Wright-Patterson)
[REDACTED]

Degree: PhD., Zoology, 1968
Specialty: Thermoregulation, Ecological
Energetics
Assigned: USAFSAM (Brooks)
[REDACTED]

Degree: PhD., Geology
Specialty: Utilization of conservation
and solar energy, Investigation of
land use planning by remote sensing
Assigned: AFESC (Tyndall)
[REDACTED]

Degree: PhD., Economics, 1969
Specialty: Regional Economics
Assigned: AFESC (Tyndall)
[REDACTED]

Degree: PhD., Electrical Eng., 1970
Specialty: Digital Systems
Assigned: AFHRL/FTE (Williams)
[REDACTED]

Degree: PhD., Physics, 1967
Specialty: Electricity and Magnetism
Assigned: AFFDL (Wright-Patterson)
[REDACTED]

1979 PARTICIPANTS
Page Four

NAME/ADDRESS

DEGREE, SPECIALTY, & LABORATORY
ASSIGNMENT

Dr. Donald F. Hanson
Assistant Professor
Electrical Engineering Dept.
University of Mississippi
University, MS 38677
(601) 232-7231 [REDACTED]

Degree: PhD., Electrical Eng., 1976
Specialty: Numerical Solution of
Electromagnetics Problems
Assigned: AFWL (Kirtland)
[REDACTED]

Dr. Charles Hays
Associate Professor
Dept. of Manufacturing Technology
University of Houston
Houston, TX 77004
(713) 749-4652 [REDACTED]

Degree: PhD., Metallurgical Eng., 1973
Specialty: Metallurgy, Metallography,
Alloying, Materials requirements
Assigned: AFML (Wright-Patterson)
[REDACTED]

Dr. Michael J. Henschman
Associate Professor of Chemistry Dept.
Brandeis University
Waltham, MA 02154
(617) 647-2821 [REDACTED]

Degree: PhD., Chemistry, 1961
Specialty: Physical Chemistry,
Reaction Kinetics
Assigned: AFGL (Hanscom)
[REDACTED]

Dr. Manuel A. Huerta
Associate Professor of Physics Dept.
University of Miami
Coral Gables, FL 33124
(305) 284-2323 [REDACTED]

Degree: PhD., Physics, 1970
Specialty: Plasma Physics, MHD, Fluid
Mechanics, Electromagnetic Wave
Propagation and Doppler Radar, Acoustics
Tomography
Assigned: AFATL (Eglin)
[REDACTED]

Dr. Frank M. Ingels
Professor
Electrical Engineering Dept.
Mississippi State University
Drawer EE
Mississippi State, MS 39762
(601) 325-3912/6067 [REDACTED]

Degree: PhD., Electrical Eng., 1967
Specialty: Communications, Error
Correcting Codes, Signal Tracking
Electronics
Assigned: AFATL (Eglin)
[REDACTED]

Dr. Prasad K. Kadaba
Professor
Electrical Engineering Dept.
University of Kentucky
Lexington, KY 40506
(606) 258-2966/257-1856 [REDACTED]

Degree: PhD., Physics, 1950
Specialty: Microwave Absorption &
Dielectric Relaxation of various
materials, Microwave Measurements,
Magnetic Resonance, Application of
new techniques to evaluate toxic
effluents.
Assigned: AFML (Wright-Patterson)
[REDACTED]

Dr. Madhoo Kanai
Professor
Dept. of Physics
Clark University
Worcester, MA 01610
(617) 793-7366 [REDACTED]

Degree: PhD., Physics, 1969
Specialty: Transport Theory
Assigned: AFGL (Hanscom)
[REDACTED]

1979 PARTICIPANTS

Page Five

NAME/ADDRESS

Dr. William D. Kane, Jr.
Assistant Professor
Dept. of Management and Marketing
Western Carolina University
Cullowhee, NC 28723
(704) 227-7401, EXT. 26

Dr. Allen E. Kelly
Associate Professor of Civil Engineering
Oklahoma State University
Stillwater, OK 74074
(405) 624-5206

Dr. Robert V. Kenyon
Post Doctoral Fellow
Dept. of Optometry
University of California
Berkeley, CA 94705
(415) 642-7196

Dr. Keith Koenig
Assistant Professor
Dept. of Aerospace Engineering
Mississippi State University
Drawer A
Mississippi State, MS 39762
(601) 325-3623

Dr. John R. Lakey
Assistant Professor
Psychology Dept.
University of Evansville
Evansville, IN 47702
(812) 479-2531

Dr. Gordon K. Lee
Assistant Professor
Dept. of Electrical Engineering
Colorado State University
Ft. Collins, CO 80523
(303) 491-5767

Dr. Jack C. Lee
Associate Professor
Mathematics Dept.
Wright State University
Dayton, OH 45435
(513) 873-2433

DEGREE, SPECIALTY, & LABORATORY
ASSIGNMENT

Degree: PhD., Organizational Behavior,
1977
Specialty: Behavioral Science as it
applies to Management of Organizations
Assigned: AFHRL/ASR (Wright-Patterson)

Degree: PhD., Civil Eng., 1970
Specialty: Structural Eng. &
Mechanics
Assigned: AFATL (Eglin)

Degree: PhD., Physiological Optics, 197
Specialty: Visual Science, Eye
Movement Control Systems, Information
Processing for Motor Control
Assigned: AFHRL/FTE (Williams)

Degree: PhD., Aeronautics, 1978
Specialty: Bluff Body Separated Flows,
Laser Doppler Velocimetry
Assigned: AFFJSRL (USAF Academy)

Degree: PhD., Physiological Psychology,
1973
Specialty: Sensory Processors
Assigned: USAFSAM (Brooks)

Degree: PhD., Electrical Eng., 1978
Specialty: Multivariable Control
Systems
Assigned: AFATL (Eglin)

Degree: PhD., Statistics, 1972
Specialty: Multivariate Analysis and
Application of Statistics to different
Disciplines
Assigned: AFAMRL (Wright-Patterson)

1979 PARTICIPANTS

Page Six

NAME/ADDRESS

Dr. Robert D. Lyng
Assistant Professor
Dept. of Biological Sciences
Indiana University - Purdue University
2101 Coliseum Blvd. E.
Ft. Wayne, IN 46805
(219) 482-5798/5271 [REDACTED]

Dr. Arlyn J. Melcher
Professor of Administrative Sciences
Kent State University
Kent, OH 44242
(216) 672-2750 [REDACTED]

Dr. Bonita H. Melcher
Assistant Professor of Management
University of Akron
Akron, OH 44325
(216) 375-7037 [REDACTED]

Dr. Andrew U. Meyer
Professor of Electrical Engineering
New Jersey Institute of Technology
323 High Street
Newark, NY 07102
(201) 645-5468/5472 [REDACTED]

Dr. Jerrel R. Mitchell
Associate Professor of Electrical Engineering
Mississippi State University
P.O. Drawer EE
Mississippi State, MS 39762
(601) 325-3912/6064 [REDACTED]

Dr. William T. Morris
Professor
Dept. of Industrial and Systems Engineering
Ohio State University
1971 Neil Avenue
Columbus, OH 43210
(614) 422-2178 [REDACTED]

Dr. Stephen E. Mudrick
Assistant Professor
Dept. of Atmospheric Science
University of Missouri-Columbia
701 Hitt Street
Columbia, MO 65211
(314) 882-6591 [REDACTED]

DEGREE, SPECIALTY, & LABORATORY
ASSIGNMENT

Degree: PhD., Zoology, 1969
Specialty: Development Biology
Assigned: AFAMRL (Wright-Patterson)
[REDACTED]

Degree: PhD., Industrial Relations,
1964
Specialty: Organizational Analysis
Assigned: AFBRMC (Wright-Patterson)
[REDACTED]

Degree: DBA, Organization Theory &
Administration, 1975
Specialty: Organization Design
Assigned: AFBRMC (Wright-Patterson)
[REDACTED]

Degree: PhD., Electrical Eng., 1961
Specialty: Automatic Control Systems,
Application of System Analysis to
Biomedical Engineering
Assigned: AFAMRL (Wright-Patterson)
[REDACTED]

Degree: PhD., Electrical Eng., 1972
Specialty: Control Systems
Assigned: AFWL (Kirtland)
[REDACTED]

Degree: PhD., Industrial Eng., 1956
Specialty: Industrial Engineering,
Engineering Economics, Productivity
Improvement
Assigned: AFBRMC (Wright-Patterson)
[REDACTED]

Degree: PhD., Meteorology, 1973
Specialty: Dynamic Meteorology,
Numerical Modeling of Atmosphere
Assigned: AFGL (Hanscom)
[REDACTED]

1979 PARTICIPANTS

Page Seven

NAME/ADDRESS

DEGREE, SPECIALTY, & LABORATORY
ASSIGNMENT

Dr. William C. Mundy
Associate Professor of Physics
Pacific Union College
Angwin, CA 94508
(707) 965-7269 [REDACTED]

Degree: PhD., Physics, 1972
Specialty: Raman Spectroscopy &
Mie Scattering
Assigned: AFRPL (Edwards)
[REDACTED]

Dr. Maurice C. Neveu
Associate Professor
Dept. of Chemistry
State University of New York
Fredonia, NY 14063
(716) 673-3285 [REDACTED]

Degree: PhD., Physical-Organic
Chemistry, 1959
Specialty: Physical-Organic Chemistry,
Kinetics, Catalysis, Reaction Mechanisms,
Enzyme Chemistry
Assigned: AFATL (Eglin)
[REDACTED]

Dr. Charles E. Nuckolls
Associate Professor
Mechanical Engineering and Aerospace Science
University of Central Florida
P.O. Box 25000
Orlando, FL 32816
(305) 275-2242 [REDACTED]

Degree: PhD., Mechanical Eng., 1970
Specialty: Engineering Mechanics
Assigned: AFAEDC (Arnold)
[REDACTED]

Dr. Nicholas G. Odrey
Assistant Professor
Industrial Engineering Dept.
University of Rhode Island
103 Gilbreth Hall
Kingston, RI 02881
(401) 792-2455 [REDACTED]

Degree: PhD., Industrial Eng., 1978
Specialty: Manufacturing Engineering
Assigned: AFML (Wright-Patterson)
[REDACTED]

Dr. William J. Ohley
Assistant Professor
Dept. of Electrical Engineering
University of Rhode Island
Kingston, RI 02881
(401) 792-2505 [REDACTED]

Degree: PhD., Electrical Eng., 1976
Specialty: Biomedical Engineering
Assigned: AFHRL/ASR (Wright-Patterson)
[REDACTED]

Dr. John V. Oldfield
Professor
Dept. of Electrical and Computer Engineering
113 Link Hall
Syracuse, NY 13210
(315) 423-4443 [REDACTED]

Degree: PhD., Electrical Eng., 1958
Specialty: Computer-aided Electronic
Design, Graphical Display
Assigned: AFRADC (Griffiss)
[REDACTED]

Dr. John M. Owens
Associate Professor
Electrical Engineering Dept.
University of Texas
Arlington, TX 76019
(817) 273-2671 [REDACTED]

Degree: PhD., Electrical Eng., 1968
Specialty: Electrical Engineering
Assigned: AFRADC/ET (Hanscom)
[REDACTED]

1979 PARTICIPANTS
Page Eight

NAME/ADDRESS

Dr. Michael J. Pappas
Associate Professor of Mechanical Engineering
New Jersey Institute of Technology
323 High Street
Newark, NJ 07102
(201) 645-5367 [REDACTED]

Dr. Steven E. Poltrock
Assistant Professor
Dept. of Psychology
University of Denver
2030 S. York
Denver, CO 80210
(303) 753-2478 [REDACTED]

Dr. Douglas Preis
Assistant Professor of Electrical Engineering
Tufts University
Medford, MA 02115
(617) 628-5000, EXT. 287 [REDACTED]

Dr. Rangaiya A. Rao
Associate Professor
Dept. of Electrical Engineering
San Jose State University
S. 7th Street
San Jose, CA 95192
(408) 277-2459 [REDACTED]

Dr. Stephen M. Rappaport
Assistant Professor
Dept. of Biomedical and Environmental
Health Sciences
University of California
Berkeley, CA 94720

Dr. Jane A. Rysberg
Assistant Professor of Psychology
Ohio State University
1680 University Drive
Mansfield, OH 44906
(419) 755-4277 [REDACTED]

Dr. Michael C. Smith
Assistant Professor
Dept. of Insutrial Engineering
Oregon State University
Corvallis, OR 97331
(503) 754-2365 [REDACTED]

DEGREE, SPECIALTY, & LABORATORY
ASSIGNMENT

Degree: PhD., Mechanical Eng., 1970
Specialty: Structural Optmization
Assigned: AFFDL (Wright-Patterson)
[REDACTED]

Degree: PhD., Psychology, 1976
Specialty: Cognitive Psychology
Assigned: AFHRL/TTY (Lowry)
[REDACTED]

Degree: PhD., Electrical Eng., 1969
Specialty: Electromagnetics, Signal
Processing, Acoustics
Assigned: ESD (Hanscom)
[REDACTED]

Degree: PhD., Electrical Eng., 1966
Specialty: Semiconductor device
Physics and Technology, Solar
Cells, Semiconductor Crystal Growth,
III-V Compound Semiconductors,
Photodetectors, Microwave Devices,
Characterization of Semiconductors
Assigned: AFAL (Wright-Patterson)
[REDACTED]

Degree: PhD., Environmental Science
and Eng., 1974
Specialty: Industrial Hygiene
Assigned: USAFSAM (Brooks)
[REDACTED]

Degree: PhD., Educational Psychology,
1977
Specialty: Educational Psychology,
Cognitive Development
Assinged: AFHRL/PE (Brooks)
[REDACTED]

Degree: PhD., Industrial Eng., 1977
Specialty: Operations Analysis,
Analysis of Capital Investment, Health
Systems Design
Assigned: AFLC (Wright-Patterson)
[REDACTED]

1979 PARTICIPANTS

Page Nine

NAME/ADDRESS

Dr. Walther D. Stanaland
Assistant Professor
Dept. of Systems Science
University of Western Florida
Pensacola, FL 32504
(904) 476-9500, EXT. 495

Dr. Edwin F. Strother
Associate Professor
Dept. of Physics/Space Science
Florida Institute of Technology
Melbourne, FL 32901
(305) 723-3701, EXT. 326/240

Dr. Edgar C. Tacker
Professor
Dept. of Electrical Engineering
University of Houston
Houston, TX 77004
(713) 749-4416

Dr. Richard H. Tipping
Associate Professor
Physics Dept.
University of Nebraska
Omaha, NB 68182
(402) 554-2510

Dr. Pramod K. Varshney
Assistant Professor
Electrical and Computer Engineering
Syracuse University
Link Hall
Syracuse, NY 13210
(315) 423-4432

Dr. Ghasi R. Verma
Associate Professor
Dept. of Mathematics
University of Rhode Island
Kingston, RI 02881
(401) 792-2889

Dr. Ta-hsien Wei
Assistant Professor
Electrical Engineering Dept.
North Carolina A & T State University
Greensboro, NC 27411
(919) 379-7760

DEGREE, SPECIALTY, & LABORATORY ASSIGNMENT

Degree: PhD., Electrical Eng., 1979
Specialty: Electrical Properties of Dielectric Materials
Assigned: AFATL (Eglin)

Degree: PhD., Physics, 1971
Specialty: Experimental Physics
Assigned: AFGL (Hanscom)

Degree: PhD., Electrical Eng., 1964
Specialty: Systems (Decision Processes, Estimation, Control, and Modeling)
Assigned: AFFJSRL (USAF Academy)

Degree: PhD., Physics, 1969
Specialty: Molecular Spectroscopy
Assigned: AFGL (Hanscom)

Degree: PhD., Electrical Eng., 1976
Specialty: Communications and Computers
Assigned: AFRADC (Griffiss)

Degree: PhD., Mathematics, 1957
Specialty: Mathematics
Assigned: AFFDL (Wright-Patterson)

Degree: PhD., Physics, 1964
Specialty: Systems Engineering
Assigned: AFAPL (Wright-Patterson)

1979 PARTICIPANTS

Page Ten

NAME/ADDRESS

Dr. Herschel Weil
Professor
Electrical and Computer Engineering
University of Michigan
4517 East Engineering
Ann Arbor, MI 48109
(313) 764-4329

Dr. Bronel R. Whelchel
Associate Professor of Electronic
Data Processing
Tennessee State University
Nashville, TN 37203
(615) 320-3154

Dr. Charles R. Willis
Professor of Physics
Boston University
111 Cummington Street
Boston, MA 02215
(617) 353-2600

Dr. Dennis E. Wilson
Assistant Professor
Dept. of Engineering
University of South Carolina
Columbia, SC 29208
(803) 777-7118/4185

Dr. Gerald A. Woelfl
Assistant Professor
Dept. of Civil Engineering
Marquette University
1515 W. Wisconsin Avenue
Milwaukee, WI 53233
(414) 224-7384

Dr. John C. Wolfe
Assistant Professor
Dept. of Electrical Engineering
University of Houston
4800 Calhoun
Houston, TX 77004
(713) 749-2506

Dr. Richard G. Yalman
Professor of Chemistry
Antioch University
Yellow Springs Campus
Yellow Springs, OH 45387
(513) 767-7331

DEGREE, SPECIALTY, & LABORATORY
ASSIGNMENT

Degree: PhD., Applied Math, 1948
Specialty: Electromagnetic Theory
and Applications
Assigned: AFAPL (Wright-Patterson)

Degree: PhD., Education & Business
Administration
Specialty: Systems Analysis and
Design, Electronic Data Processing
Assigned: AFHRL/PE (Brooks)

Degree: PhD., Physics, 1957
Specialty: Theoretical Physics,
Quantum Optics, Statistical
Mechanics
Assigned: AFRADC/ET (Hanscom)

Degree: PhD., Mechanical Eng., 1976
Specialty: Viscous Flow, Analytical
and Approximate Methods
Assigned: AFAEDC (Arnold)

Degree: PhD., Civil Eng., 1971
Specialty: Highway and Construction
Materials
Assigned: AFESC (Tyndall)

Degree: PhD., Physics, 1974
Specialty: Electrical Engineering
Materials
Assigned: AFAL (Wright-Patterson)

Degree: PhD., Organic Chemistry, 1949
Specialty: Coordination Chemistry,
Organic Chemistry
Assigned: AFAL (Wright-Patterson)

PARTICIPANT LABORATORY ASSIGNMENT

1979 USAF/SCEEE SUMMER FACULTY RESEARCH PROGRAM

AFAEDC **AIR FORCE ARNOLD ENGINEERING DEVELOPMENT CENTER**
(Arnold Air Force Station)
1. Dr. Warren Bowden - Rose-Hulman Institute of Technology
2. Dr. Charles Nuckolls - University of Central Florida
3. Dr. Dennis Wilson - University of South Carolina

AFHRL/PE **AIR FORCE HUMAN RESOURCES LABORATORY**
(Brooks Air Force Base)
1. Dr. Jane Rysberg - Ohio State University
2. Dr. Bronel Whelchel - Tennessee State University

USAFSAM **UNITED STATES AIR FORCE SCHOOL OF AEROSPACE MEDICINE**
(Brooks Air Force Base)
1. Dr. James Gessaman - Utah State University
2. Dr. John Lakey - University of Evansville
3. Dr. Stephen Rappaport - University of California

AFRPL **AIR FORCE ROCKET PROPULSION LABORATORY**
(Edwards Air Force Base)
1. Dr. Bill Mundy - Pacific Union College

AFATL **AIR FORCE ARMAMENT DEVELOPMENT AND TEST CENTER**
(Eglin Air Force Base)
1. Dr. Manuel Huerta - University of Miami
2. Dr. Frank Ingels - Mississippi State University
3. Dr. Allen Kelly - Oklahoma State University
4. Dr. Gordon Lee - Colorado State University
5. Dr. Maurice Neveu - State University College of Fredonia/NY
6. Dr. Walter Stanaland - University of Western Florida

AFRADC **AIR FORCE ROME AIR DEVELOPMENT CENTER**
(Griffiss Air Force Base)
1. Dr. Adel Aly - University of Oklahoma
2. Dr. James Cadzow - Virginia Polytechnic Institute/State Univ.
3. Dr. John Oldfield - Syracuse University
4. Dr. Pramod Varshney - Syracuse University

AFGL **AIR FORCE GEOPHYSICS LABORATORY**
(Hanscom Air Force Base)
1. Dr. Chi Hau Chen - Southeastern Massachusetts University
2. Dr. Michael Henchman - Brandeis University
3. Dr. Madhoo Kanal - Clark University
4. Dr. Steven Mudrick - University of Missouri/Columbia
5. Dr. Edwin Strother - Florida Institute of Technology
6. Dr. Richard Tipping - University of Nebraska/Omaha

AFRADC/ET **AIR FORCE ROME AIR DEVELOPMENT CENTER**
(Hanscom Air Force Base)
1. Dr. John Owens - University of Texas
2. Dr. Charles Willis - Boston University

PARTICIPANT LABORATORY ASSIGNMENT (Continued)

ESD **ELECTRONICS SYSTEMS DIVISION**
(Hanscom Air Force Base)
1. Dr. Douglas Preis - Tufts University

AFWL **AIR FORCE WEAPONS LABORATORY**
(Kirtland Air Force Base)
1. Dr. Clarence Bell - Texas Tech University
2. Dr. William Davis - Virginia Polytechnic Institute/State Univ.
3. Dr. John Foley - Mississippi State University
4. Dr. Donald Hanson - University of Mississippi
5. Dr. Jerrel Mitchell - Mississippi State University

AFHRL/TTY **AIR FORCE HUMAN RESOURCES LABORATORY**
(Lowry Air Force Base)
1. Dr. Steven Poltrock - University of Denver

SAMTEC/TOEI **SPACE AND MISSILE TEST CENTER**
(Patrick Air Force Base)
1. Mr. Barry Bullard - University of Central Florida

AFESC **AIR FORCE ENGINEERING TECHNOLOGY OFFICE**
(Tyndall Air Force Base)
1. Mr. Willard Fey - Georgia Institute of Technology
2. Dr. Paul Grogger - University of Colorado/Colorado Springs
3. Dr. William Gunther - University of Alabama
4. Dr. Gerald Woelfl - Marquette University

AFFJSRL **AIR FORCE FRANK J. SEILER RESEARCH LABORATORY**
(United States Air Force Academy)
1. Dr. William Carper - Wichita State University
2. Dr. Keith Koenig - Mississippi State University
3. Dr. Edgar Tacker - University of Houston

AFHRL/FTE **AIR FORCE HUMAN RESOURCES LABORATORY**
(Williams Air Force Base)
1. Dr. John Hadjiioioliou - Florida Institute of Technology
2. Dr. Robert Kenyon - University of California

AFAL **AIR FORCE AVIONICS LABORATORY**
(Wright-Patterson Air Force Base)
1. Dr. Malcolm Calhoun - Mississippi State University
2. Dr. Aaron Collins - Tennessee State University
3. Dr. Rangaiya Rao - San Jose State University
4. Dr. John Wolfe - University of Houston
5. Dr. Richard Yalman - Antioch University

AFAMRL **AIR FORCE AEROSPACE MEDICAL RESEARCH LABORATORY**
(Wright-Patterson Air Force Base)
1. Dr. Jack Lee - Wright State University
2. Dr. Robert Lyng - Indiana Univ. - Purdue Univ./Ft. Wayne
3. Dr. Andrew Meyer - New Jersey Institute of Technology

PARTICIPANT LABORATORY ASSIGNMENT (Continued)

AFAPL AIR FORCE AEROPROPULSION LABORATORY
(Wright-Patterson Air Force Base)
1. Dr. Garabet Gabriel - Notre Dame University
2. Dr. Ta-hsien Wei - North Carolina A&T State University
3. Dr. Herschel Weil - University of Michigan

AFBRMC AIR FORCE BUSINESS RESEARCH MANAGEMENT CENTER
(Wright-Patterson Air Force Base)
1. Dr. Arlyn Melcher - Kent State University
2. Dr. Bonita Melcher - University of Akron
3. Dr. William Morris - Ohio State University

AFFDL AIR FORCE FLIGHT DYNAMICS LABORATORY
(Wright-Patterson Air Force Base)
1. Dr. Yelagalawadi Acharya - West Virginia Tech
2. Dr. Donald Chiang - Rose-Hulman Institute of Technology
3. Dr. Keith Hagenbuch - Pennsylvania State Univ./Behrend College
4. Dr. Michael Pappas - New Jersey Institute of Technology
5. Dr. Ghasi Verma - University of Rhode Island

AFHRL/ASR AIR FORCE HUMAN RESOURCES LABORATORY
(Wright-Patterson Air Force Base)
1. Dr. William Kane, Jr. - University of Western Carolina
2. Dr. William Ohley - University of Rhode Island

AFLC AIR FORCE LOGISTICS COMMAND
(Wright-Patterson Air Force Base)
1. Dr. Michael Smith - Oregon State University

AFML AIR FORCE MATERIALS LABORATORY
(Wright-Patterson Air Force Base)
1. Dr. Alan Edelstein - University of Illinois/Chicago Circle
2. Dr. Charles Hays - University of Houston
3. Dr. Prasad Kadaba - University of Kentucky
4. Dr. Nicholas Odrey - University of Rhode Island

RESEARCH REPORTS

1979 USAF-SCEEE SUMMER FACULTY RESEARCH PROGRAM

<u>VOLUME I</u> <u>Report No.</u>	<u>Title</u>	<u>Research Associates</u>
1	Thermodynamic and Aerodynamic Analysis of of High Speed Ejectors	Dr. Yelagalawadi Acharya
2	Optimum Design of Built-in-Test Diagnostic System	Dr. Adel A. Aly
3	Effects of Nuclear Blast Double Shock on Airborne Aircraft	Dr. Clarence A. Bell
4	Icing Testing with Models-Similitude Considerations	Dr. Warren W. Bowden
5	Shipboard Antenna Placement Optimization- (SAPO)	Mr. Barry D. Bullard
6	ARMA Spectral Estimation: An Efficient Closed Form Procedure	Dr. James A. Cadzow
7	A Study of Two Avionics Multiplex Simulation Models: SNS and MUXSIM	Dr. Malcolm D. Calhoun
8	Laser Candidate and Energetic Material Studies	Dr. William R. Carper
9	A Non-Linear Maximum Entropy Method for Spectral Estimation	Dr. Chi-Hau Chen
10	Computer Codes Applicable to the Determini- nation of Ejection Seat/Man Aerodynamic Parameters	Dr. Donald C. Chiang
11	Petri Net-Related Models for Avionics Systems	Dr. Aaron S. Collins
12	Bounding Signal Levels at Wire Terminations Behind Apertures	Dr. William A. Davis
13	Photoconductivity of Extrinsic Silicon	Dr. Alan S. Edelstein
14	System Analysis of the Environmental Tech- nical Information System (ETIS)	Mr. Willard Fey
15	The Uniqueness of Phase Retrieval From Intensity Measurements	Dr. John T. Foley
16	High Speed Electromagnetic Transients on Superconducting Coils	Dr. Garabet J. Gabriel

RESEARCH REPORTS (Continued)

<u>Report No.</u>	<u>Title</u>	<u>Research Associates</u>
17	Part I: Effects of Dehydration and Heat on Acceleration Response in Man Part II: Relationships Between Total Body Sweating Rate and Localized Sweating Rate	Dr. James A. Gessaman
18	The Utilization of Geothermal Resources at United States Air Force Bases	Dr. Paul K. Grogger
19	A Critical Evaluation of the USAF Methodology for Assessing the Socioeconomic Impact of Proposed Base Realignments	Dr. William D. Gunther
20	Analysis of the Advanced Simulator for Pilot Training (ASPT): Computer System Architecture	Dr. John Hadjiligiou
21	Optimized Holography of Microscopic Particles	Dr. Keith M. Hagenbuch

VOLUME II

22	Electromagnetic Diffraction by a Narrow Slit in an Impedance Sheet--E--Polarization	Dr. Donald F. Hanson
23	Part I: Technology Assessment on the Critical and Strategic Status of Tantalum Metal Part II: Technology Assessment Concerning the Current Status of Alloy and Coating Development Programs for Refractory Metal Systems Containing Cb, Mo, Ta, and W	Dr. Charles Hays
24	Gas Phase Reactions of Some Hydrated Ions	Dr. Michael J. Henschman
25	Detonation Physics of Nonideal Explosives with Analytical Results for Detonation Failure Diameter	Dr. Manuel A. Huerta
26	Cepstrum Analysis Techniques for Possible Applications to Seismic/Acoustic Ranging	Dr. Franklin M. Ingels
27	A NMR Study of Absorbed Water in the Anodized Oxide Layer and Paper Spacer of Electrolytic Capacitors	Dr. Prasad K. Kadaba
28	On Remote Sensing of the Atmospheric Temperature: An Analysis of the Discrepancy Between the Measured and Calculated Values of the Radiance	Dr. Madhoo Kanai
29	A Heuristic Model of Air Force Maintenance Performance	Dr. William Kane, Jr.

RESEARCH REPORTS (Continued)

<u>Report No.</u>	<u>Title</u>	<u>Research Associates</u>
30	An Evaluation of a Method for Assessing Aircraft Structural Damage from Multiple Fragment Impact	Dr. Allen E. Kelly
31	Groundwork for Oculomotor Research in Simulators	Dr. Robert V. Kenyon
32	Redesign of a Laser Doppler Velocimeter System for Unsteady, Separated Flow Studies	Dr. Keith Koenig
33	Electromyographic Correlates of Flight-Crew Performance	Dr. John R. Lakey
34	Investigation of Time-to-Go Algorithms for Air-to-Air Missiles	Dr. Gordon K. F. Lee
35	Some Statistical Analysis Issues for System Simulation Research	Dr. Jack C. Lee
36	Effects of Hydrazine on Pregnant ICR Mice	Dr. Robert D. Lyng
37	Organizational Analysis of an Acquisition Organization	Dr. Arlyn J. Melcher
38	Organizational Analysis of An Acquisition Organization	Dr. Bonita S. Melcher
39	Dynamics of Two-Dimensional Eye-Head Tracking	Dr. Andrew U. Meyer
40	Optimization of the Feed Forward Technique for Beam Control in the APT	Dr. Jerrel R. Mitchell
41	Predicting the Impacts of USAF Personnel Cuts	Dr. William T. Morris
42	Attempts to Simulate "Realistic" Atmospheric Motion with a Simple Numerical Model	Dr. Stephen Mudrick

VOLUME III

43	Plume Properties Measurement Research in a Solid Rocket Motor Exhaust	Dr. Bill Mundy
44	A Search for New Fuel Components in Non-Ideal Explosives Mixtures	Dr. Maurice C. Neveu
45	Vibration Diagnostics for Turbofan Engines	Dr. Charles E. Nuckolls
46	Goal Programming: Functional Decomposition and Consideration Within an Integrated Computer-Aided Manufacturing Decision Support System (IDSS)	Dr. Nicholas G. Odrey

RESEARCH REPORTS (Continued)

<u>Report No.</u>	<u>Title</u>	<u>Research Associates</u>
47	A Computer Model of Saccadic Suppression	Dr. William J. Ohley
48	Special-Purpose Processors for the Image-Processing Requirements of Automatic Feature Extraction Systems	Dr. John V. Oldfield
49	Magnetostatic Wave Decay and Filter Devices	Dr. John M. Owens
50	Improved Methods for Large Scale Structural Synthesis	Dr. Michael Pappas
51	Educational Implications of Cognitive Research on Imagery	Dr. Steven E. Poltrock
52	Adaptive Signal Processing for Array Antennas	Dr. Douglas Preis
53	Deep Levels in $Al_xGa_{1-x}As$	Dr. Rangaiya A. Rao
54	Development of Air-Sampling and Analytical Method for Diisocyanates	Dr. Stephen M. Rappaport
55	Civilian Appraisal System	Dr. Jane A. Rysberg
56	A Study of Opportunistic Maintenance Policies for the F100PW100 Aircraft Engine	Dr. Michael C. Smith
57	Error Analysis for a Radio-Frequency Systems Simulation Facility	Dr. Walter D. Stanaland
58	A High Altitude Tethered Aerostat System Study	Dr. Edwin F. Strother
59	Pattern Recognition/Image Processing in Optical Tracking	Dr. Edgar C. Tacker
60	Atmospheric Absorption of Radiation by H_2O and CO_2	Dr. Richard H. Tipping
61	Study and Evaluation of SIIDS and ADPT Systems	Dr. Pramod K. Varshney
62	Stability Analysis of the Lower Branch Solutions of the Falkner-Skan Equations	Dr. Ghasi R. Verma
63	Inductance Matrix of a Permanent Magnet Alternator	Dr. Ta-hsien Wei
64	Analysis for Coherent Anti-Stokes Raman Spectroscopy (CARS)	Dr. Herschel Weil

RESEARCH REPORTS (Continued)

<u>Report No.</u>	<u>Title</u>	<u>Research Associates</u>
65	An Investigation of One and Three Parameter Item Response Models with Implications for Computerized Adaptive Testing	Dr. Bronel R. Whelchel
66	Modulated Spontaneous Raman Effect for Laser All-Optical Frequency Standards	Dr. Charles R. Willis
67	Unsteady Laminar Boundary Layers Due to Transverse Cylinder & Free Stream Oscillations	Dr. Dennis E. Wilson
68	Response of Airfield Pavement to Large Magnitude Dynamic Loads	Dr. Gerald A. Woelfl
69	Analysis of the Role of High Brightness Electron Guns in Lithography	Dr. John C. Wolfe
70	Impurities in Communications Grade GaAs	Dr. Richard G. Yalman

UNITED STATES AIR FORCE

SUMMER FACULTY RESEARCH PROGRAM

PARTICIPANTS' RESEARCH REPORTS

1979 USAF - SCEE SUMMER FACULTY RESEARCH PROGRAM

Sponsored by the

AIR FORCE OFFICE OF SCIENTIFIC RESEARCH

Conducted by the

SOUTHEASTERN CENTER FOR ELECTRICAL ENGINEERING EDUCATION

FINAL REPORT

PLUME PROPERTIES MEASUREMENT RESEARCH IN A SOLID ROCKET MOTOR EXHAUST

Prepared by:	Bill Mundy
Academic Rank:	Associate Professor
Department and University:	Department of Physics and Computer Science Pacific Union College
Research Location:	Air Force Rocket Propulsion Laboratory, Propulsion Analysis Division, Plume Analysis Group
USAF Research Colleague:	Dr. T. D. McCay
Date:	September 12, 1979
Contract No:	F49620-79-C-0038

PLUME PROPERTIES MEASUREMENT RESEARCH
IN A SOLID ROCKET MOTOR EXHAUST

by

Bill Mundy

ABSTRACT

The objective of this experiment is to characterize the gaseous and particulate properties of solid rocket motor exhaust plumes. The effort involves in situ plume measurements using an IR emission/absorption system, a UV emission system, and a Mie scattering system (which utilizes laser scattering and transmission instrumentation)¹. The IR measurements contain information about the average gas temperature of the plume, the UV system investigates the UV signatures of the plume and the Mie data is related to the size of the particulates in the plume.

This report contains a description of the diagnostic system and its refinement.

ACKNOWLEDGMENTS

It was a privilege to participate in the 1979 USAF - SCEE Summer Faculty Research Program. Special thanks go to Dr. T. D. McCay who notified the author of the research opportunity and with whom the author worked. Dr. Dave Mann provided valuable encouragement. The support and interest of the test group at the Solid Propellant/Component Test Area (1-32) was appreciated. The technical support of Al Marcos, Joe Merril and Ernie Steinbrenner were expecially notable.

I. INTRODUCTION:

Improvement in solid rocket motor propellants and characterization of their plume signatures require information about combustion species and temperatures to guide propellant formulation efforts. Efforts to develop low visibility plumes need information about the size, number density and index of refraction of plume particulates in order to evaluate candidates for low visibility propellants.

The switch to low visibility propellants results in a plume which is optically thin, no longer dominated by thick particulate gray body emission. Hence it is possible to use light scattering and molecular absorption and emission techniques to help determine combustion efficiency and to define those species that are responsible for plume signatures.

AFRPL is developing a program to obtain and analyze plume data in conjunction with propellant evaluation test firings using the Ballistic Test and Evaluation System (BATES) motor. This program is designed to determine:

- 1) size and number density of smoke particulates,
- 2) species concentrations and temperatures at the motor exit plane,
- 3) signatures in the ultraviolet (UV) and infrared (IR) spectral regions.

Analysis of transmission and Mie scattering data of laser light is used to determine the number density and size distribution of particulates in the exhaust of a solid rocket motor². Infrared emission/absorption measurements are used to obtain information about species concentrations and temperatures in the plume³ and a UV spectrometer is used to measure the UV radiance of the plume.

II. OBJECTIVES OF THE RESEARCH EFFORT:

The activities planned for the summer were to:

- 1) refine and optimize the BATES laser scattering and transmission instrumentation and measurements (including calibrations),
- 2) Obtain preliminary transmission and Mie scattering data for typical solid propellants,

- 3) finalize Mie scattering deconvolution code,
- 4) analyze and assess Mie scattering data and technique,
- 5) report on the state of the art and developed capabilities at RPL for particulate size measurements for reduced visibility solid propellant plumes.

The goals achieved during the summer were primarily related to the first item above but did include the IR and UV systems as well as the Mie system.

III. REFINEMENTS:

The Mie scattering and transmission measurement system consists of an argon laser, a laser power meter for transmission measurements, and six scattered light detectors placed at various angles in a plane normal to the plume axis (See Fig. 1). The scattering detector assemblies incorporate photodetectors in front of which are 0.1 nm interference filters centered at 514.5 nm to separate the scattered laser light from plume emitted radiation. A system of electrically actuated polarizers and shutters in front of the detector allows data to be obtained for various polarizations of scattered light.

Refinements of this part of the system included a) verifying that no thermal focusing of the laser beam occurred in the rocket plume by taking a photograph of a rectangular grid of lines as seen through the plume (the grid lines were not optically distorted), b) inserting field stops in front of the detectors to define the plume region from which scattering data is obtained and c) developing a point light source technique for aligning the detector optics.

For accurate analysis of the Mie data it is essential to have an accurate system calibration. Prior to the efforts of this summer, several calibration techniques had been tried which were unsuitable primarily because they did not replicate the geometrical relation between the laser beam and the detectors. So several alternate calibration schemes were tested including Rayleigh scattering in air and Rayleigh scattering in water. Although both of these methods had the potential of yielding calibration data from the same region from which Mie data were obtained using the same laser beam and optics, the signals were too weak to be detected by the optical system.

A third approach was to use an argon discharge tube lined up so that its axis was coincident with the laser path from which Mie data was obtained. Again the signal was buried in the noise. Finally an 18 inch fluorescent tube was masked so that only a 2 mm strip parallel to its axis was exposed. The light intensity was adequate and a suitable signal, which appeared to be unpolarized, was obtained after the 60 Hz line signal was suppressed.

Spurious spikes that occurred in the signals from the scattering detectors were investigated. Comparison with signals that occurred when a Tesla coil was operated in the neighborhood of the detectors indicated that the spikes were due to RF pulses that occurred in the rocket plume.

Except that a unique cam mechanism is employed for rapid spectral scans, both the IR and UV systems utilize conventional spectroscopic techniques.

The IR system consists of a 1273 K black body, chopper and lens on one side of the rocket plume and a second lens, chopper and 0.22 m focal length spectrometer with an InSb detector on the other side (See Fig. 2). The detector signal is fed to two lock-in amplifiers at the two chopper frequencies to give signals proportional to plume absorption and emission. The IR system is calibrated by using N₂ purged path between the black body and the spectrometer. This calibration is repeated with the black body at the plume centerline location.

Ultraviolet data is obtained using a 0.22 m focal length spectrometer with a photomultiplier tube. The spectrometer is focused on the centerline of the rocket plume about 5 cm down stream of the exit plane. Calibration of the system is performed using a quartz-halogen standard lamp placed at the focus point.

Refinements of the IR and UV systems consisted primarily of aligning optics, stabilizing electronic components and verifying calibration procedures.

IV. MEASUREMENTS:

Figure 3 shows the laser transmission power meter output, together with motor chamber pressure and the 15° scattering detector output which was obtained during a typical rocket motor firing.

The two interruptions of the laser beam which permit plume radiance measurements are apparent at 0.82 sec and 2.1 sec. The sequence for inserting the polarization filters and shutter is: vertical polarizer, no polarizer, horizontal polarizer and shutter.

After corrections for detector calibration, ambient light level, detector dark current and plume radiance, the angular intensity data (See Fig. 4) can be used to determine the particle size distribution using the inversion of angular scattering technique developed by Curry^{2,4,5}. Results from the inversion program were not yet available at the time of this report.

Figs. 5 and 6 show typical IR and UV data. While reduction and analysis of this data is straight forward it was not a part of the summer activity reported here.

V. RECOMMENDATIONS:

The calibration procedure for the IR system needs to be refined to eliminate the spurious signals due to reflections from the calibration system and it would be desirable to increase the frequencies of both choppers by a factor of three to insure that chopping periods are shorter than any signal scan times.

The Mie scattering system is close to the edge of the applied state-of-the-art and is still in the research and development stage. Initial measurements already indicate that the system is capable of obtaining suitable signals. The basic concept and design of the system appears to be valid, but to obtain data of suitable quality from a well defined region in the rocket plume, refinements are needed. The scattering detectors need to be redesigned to provide for flexible but stable alignment and focus. Field stops need to be included in the design to provide a well defined field of view. (A two lens system may be necessary to achieve a sharply defined field.) It would seem to be sensible to redesign one detector to be thoroughly tested (including stress, thermal and shock exposures) in the lab followed by further tests at the rocket stand before rebuilding the entire detector system.

Because of the sophistication of the experiment, a high-level technological support is needed.

In particular, this experiment needs the assignment of a large fraction of the time of a qualified electronic test and design engineer and a spectroscopist, or light scattering scientist. Skilled electro-optical technicians and experienced datum operators also need to be available. All of these positions would be benefited by a continuity in assignment.

Because of the complexity of the instrumentation, a reliable system is essential. This requires careful design work and testing of all components is important. To verify the feasibility of this measurement technique quite a complete system is necessary. Because this is yet a development and not a test effort there continues to be a need to be flexible in short term (monthly) deadlines. Due to the nature, complexity and priority of the experiments, it is probably not suitable for summer research efforts until such time that general feasibility is established. At that point, certain aspects of the experiment and many aspects of the data interpretation would be amenable to a summer research program.

REFERENCES

1. D. M. Mann, T. D. McCay, E. Steinbrenner and W. A. Danne, "Initial In Situ Property Measurements in a SRM Exhaust" 11th JANNAF Exhaust Plume Technology Meeting (April 1978)
2. J. W. L. Lewis, B. P. Curry and D. P. Weaver, "Determination of the Size Distribution Function for Particles In a Hypersonic Flow Field", AEDC - TR - 77 - 101 (July 1978)
3. L. E. Brewer and C. C. Linbaugh, "Infrared Band Model Technique for Combustion Diagnostics", Applied Optics 11, 1200 (1972)
4. J. V. Dave, "Determination of Size Distribution of Spherical Polydispersions using Scattered Radiation Data", Applied Optics 10, 2035 (1971).
5. L. C. Chow and C. L. Tieu, "Inversion Technique for Determining the Droplet Size Distribution in Clouds: Numerical Examination", Applied Optics 15, 378 (1976)

LASER SCATTERING SYSTEM SCHEMATIC

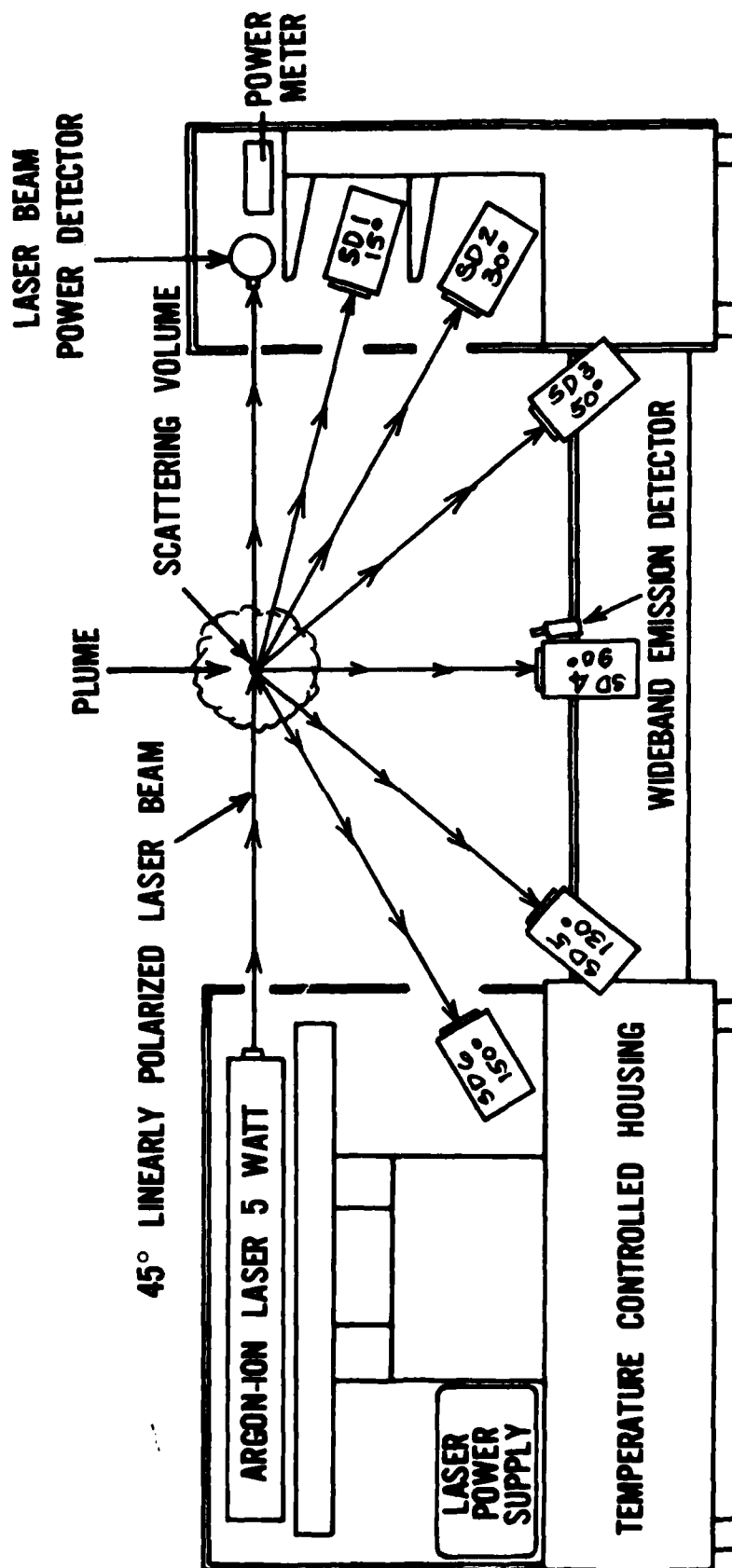


FIGURE 1

INFRARED MULTIWAVELENGTH EMISSION-ABSORPTION SYSTEM

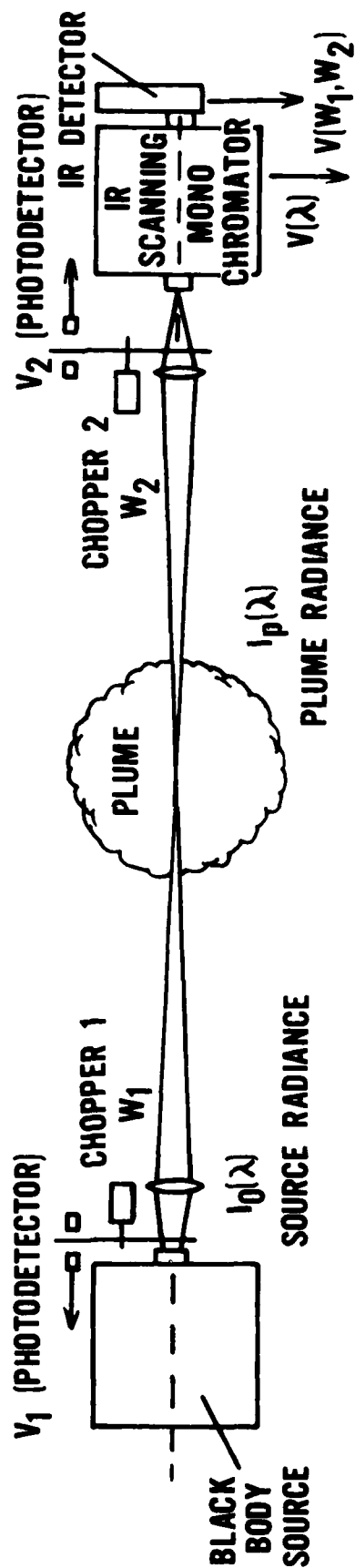


FIGURE 2

REDUCED SMOKE PROPELLANT LASER SCATTERING SIGNAL

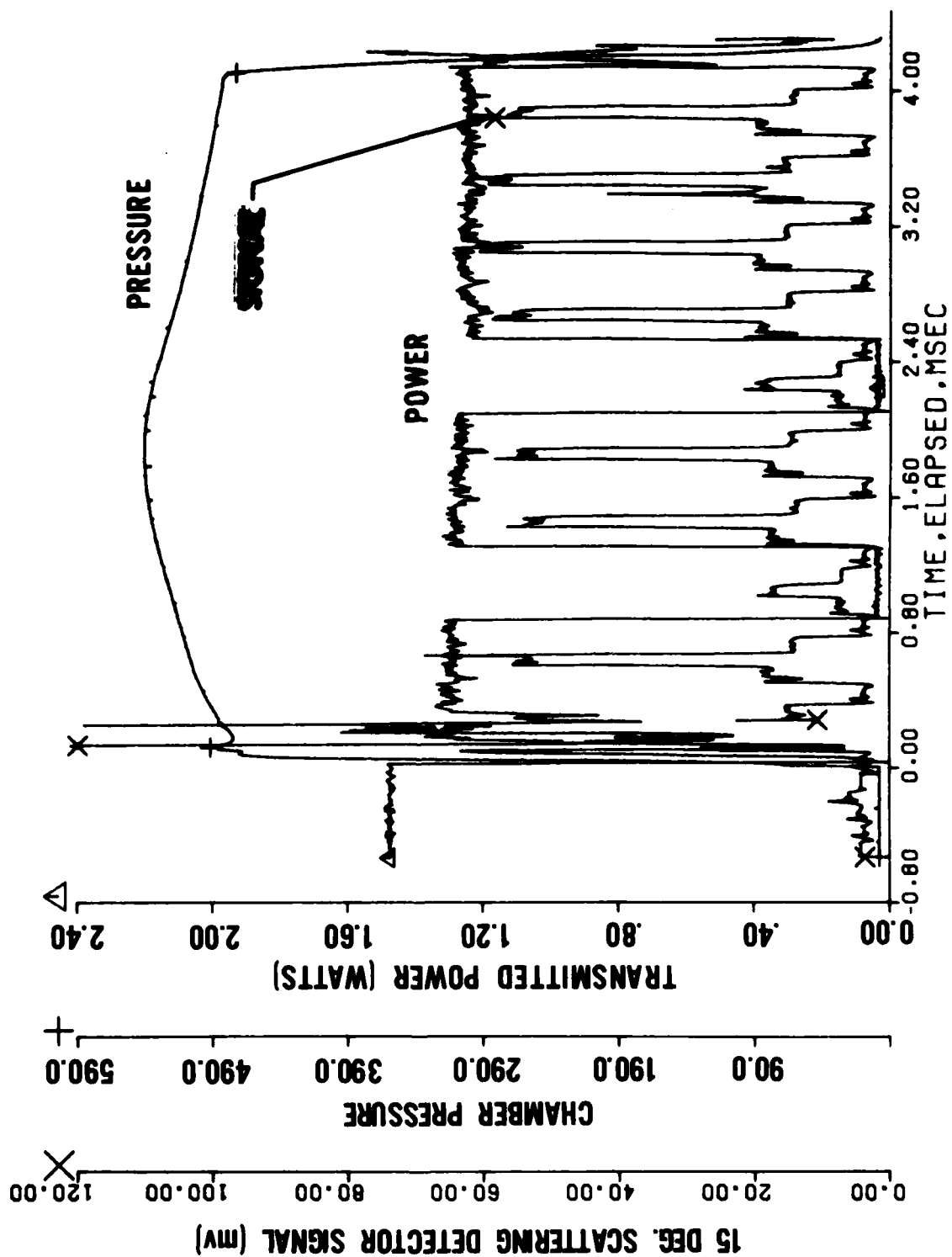


FIGURE 3

RELATIVE SCATTERING SIGNAL AS A FUNCTION OF POLAR ANGLE

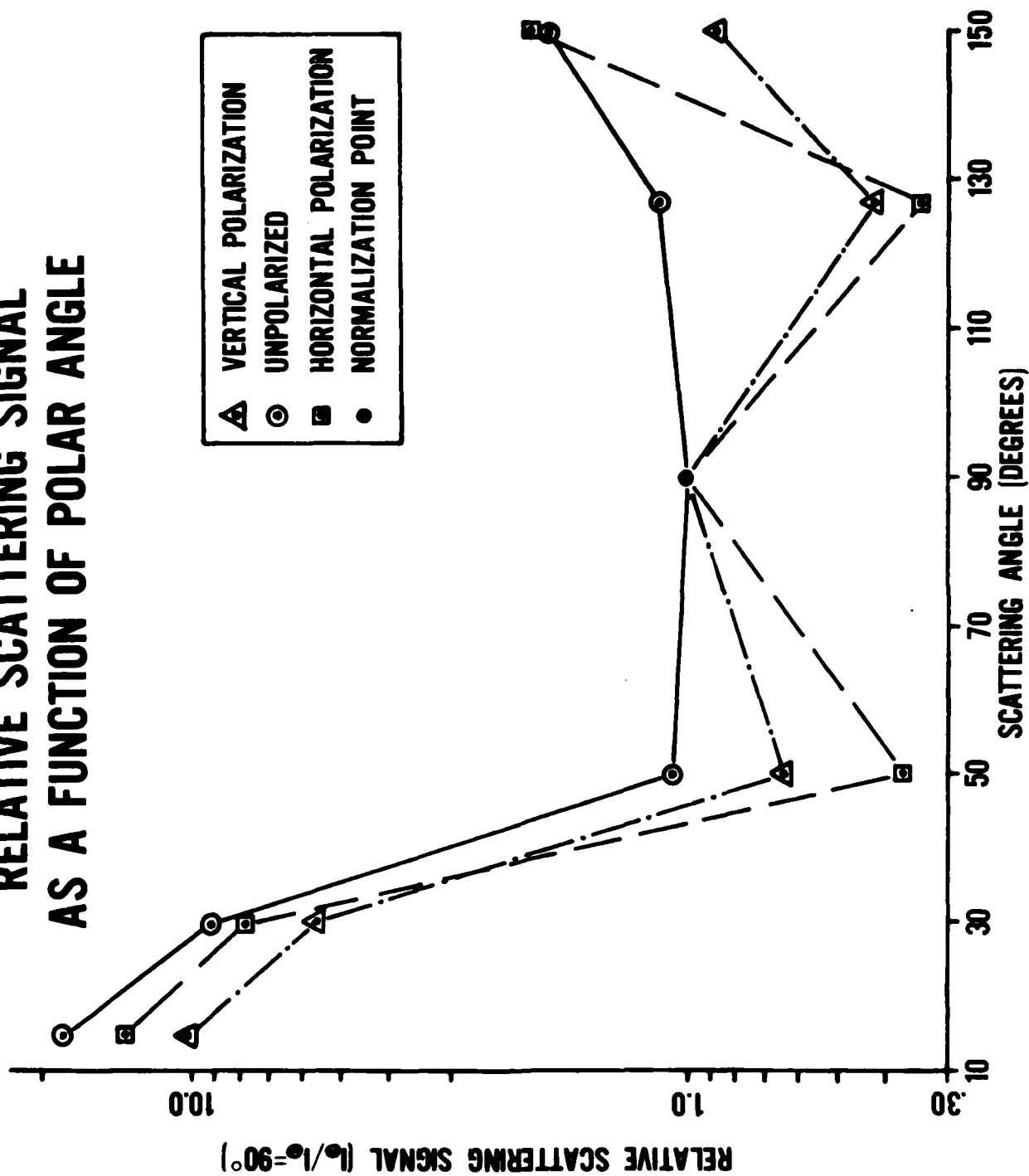


FIGURE 4

TOTAL IR RADIANCE CHANNEL SIGNAL FOR REDUCED SMOKE MOTOR

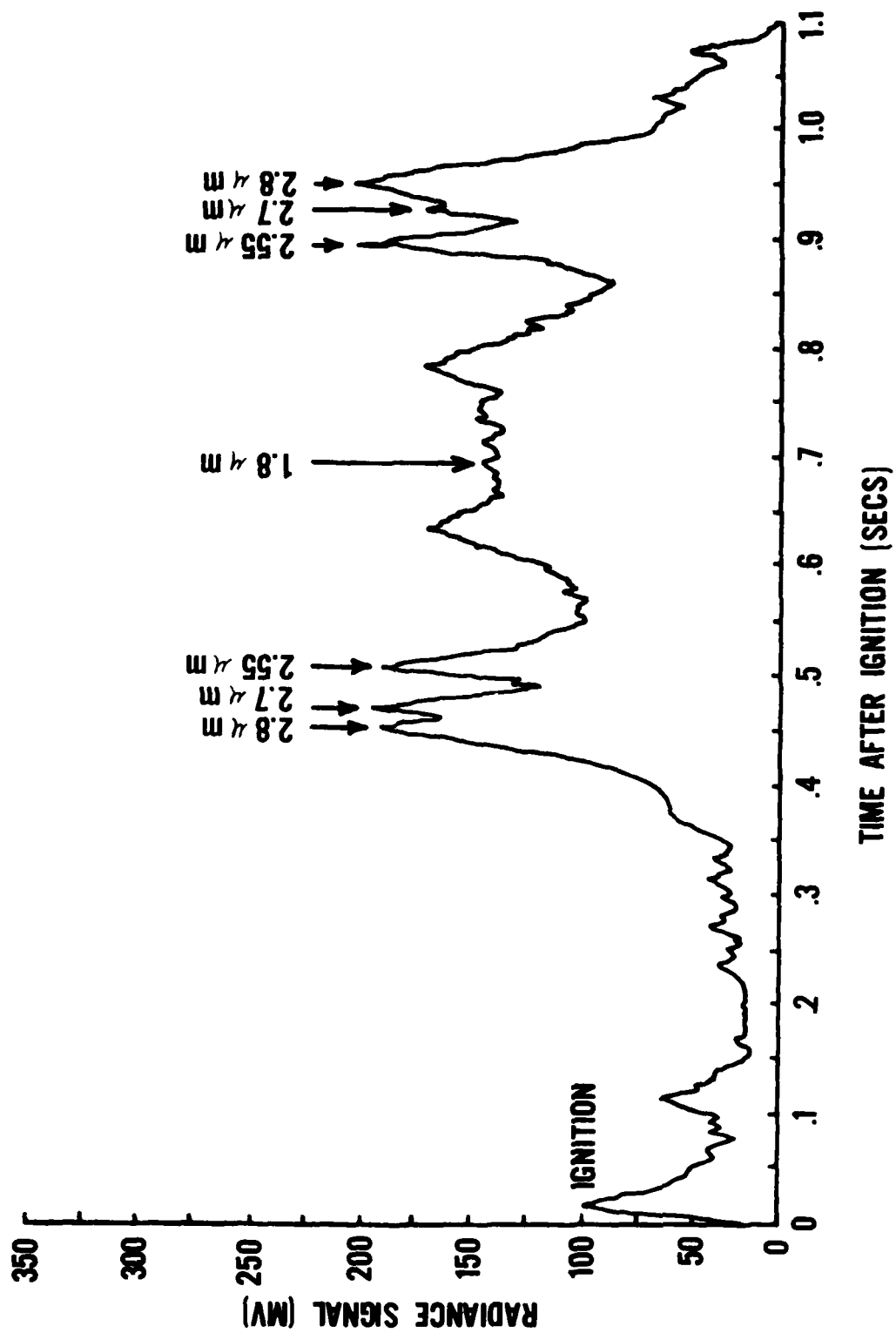


FIGURE 5

PLUME ULTRAVIOLET RADIATION

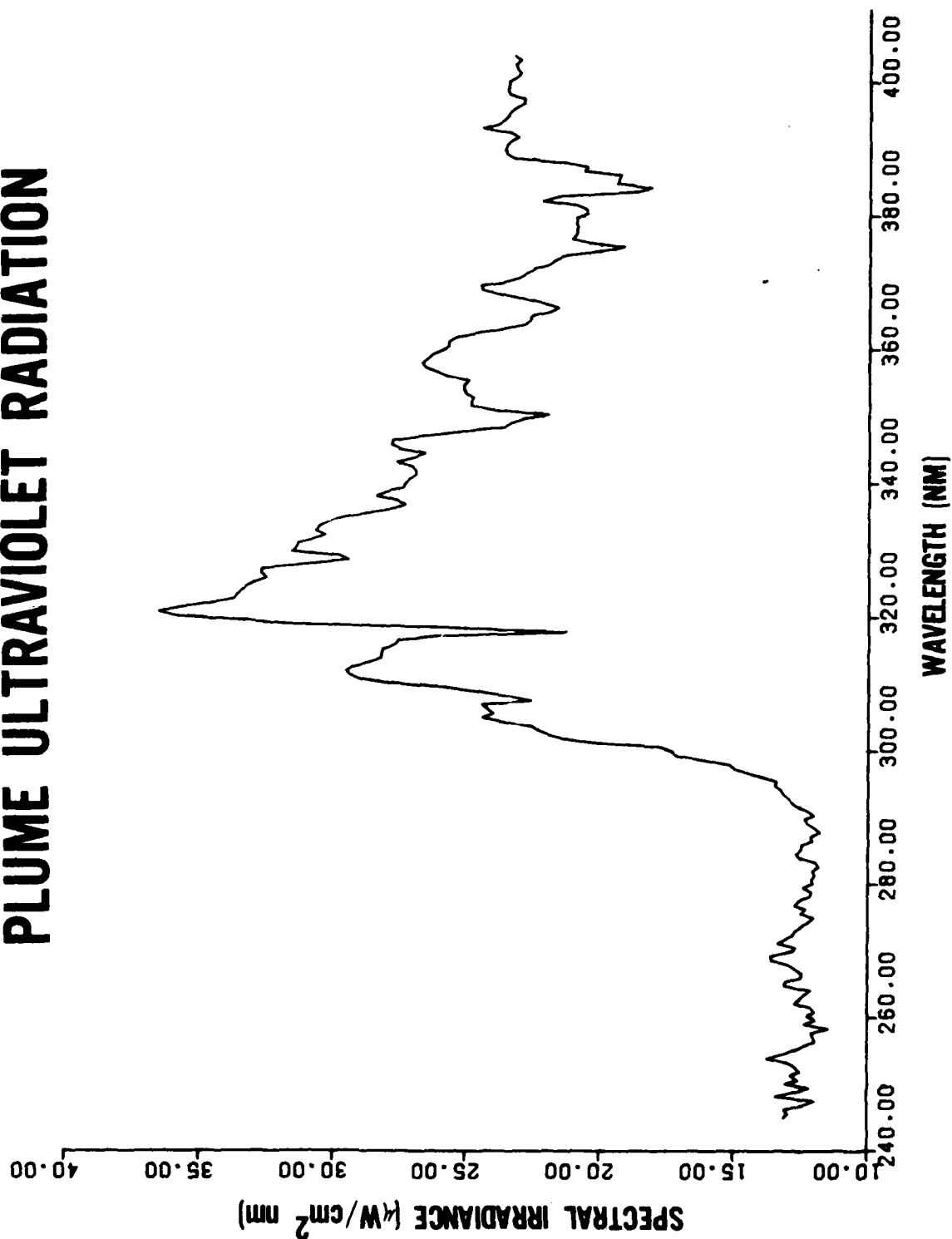


FIGURE 6

A SEARCH FOR NEW FUEL COMPONENTS
IN NON-IDEAL EXPLOSIVES MIXTURES

by

M.C. Neveu

ABSTRACT

A number of compounds were synthesized and tested for explosive properties as well as for the formation of eutectic mixtures with ammonium nitrate. In the class of nitro-azo compounds studied, one of these, C.I. 12075, was found to have good explosive characteristics when mixed with ammonium nitrate. The tetrammonium nitrate of anthraquinone and its nitro derivative were synthesized. These did not show the explosive properties that might have been expected on the basis of their structures. The tetranitro derivatives of two isomeric biphenols were synthesized. Their ammonium and potassium salts showed excellent explosive characteristics. No formation of eutectic mixtures with ammonium nitrate was observed for any of the compounds studied.

1979 USAF - SCEEE SUMMER FACULTY RESEARCH PROGRAM

SPONSORED BY

AIR FORCE OFFICE OF SCIENTIFIC RESEARCH

CONDUCTED BY THE

SOUTHEASTERN CENTER FOR ELECTRICAL ENGINEERING EDUCATION

A SEARCH FOR NEW FUEL COMPONENTS

IN NONIDEAL EXPLOSIVES MIXTURES

PREPARED BY:	Maurice C. Neveu
ACADEMIC RANK:	Associate Professor
DEPARTMENT AND UNIVERSITY :	Chemistry Department State University College, Fredonia, NY
RESEARCH LOCATION:	High Explosives Research and Development Facility, Air Force Armament Laboratory Eglin AFB, FL
USAF RESEARCH COLLEAGUE :	Irving Akst
DATE:	23 August 1979
CONTRACT NO:	F49620-79-C-0038

ACKNOWLEDGEMENTS

The author would like to thank the Air Force Systems Command, the Air Force Office of Scientific Research, and the Southeastern Center for Electrical Engineering Education for the opportunity to participate in a very exciting and stimulating research effort at the High Explosives Research and Development Facility of Eglin Air Force Base. Special recognition is also due to Dr. Richard N. Miller, Director of the Summer Faculty Research Program for a well-organized program and a great deal of help in the logistics involved in leaving one's home for the summer.

He would also like to express his appreciation for the efforts of Dr. Martin Zimmer, Research Director at the Eglin Armament Laboratory, for helping in obtaining the best match between the author's abilities and the research effort. He would also like to extend his thanks to the personnel at the High Explosives Research and Development Facility. Particular mention should be made of Majors Paul Jendrek and James Holt for maintaining a very well-equipped laboratory facility and for their efficient administration of it; of Mr. Irving Akst and Dr. Michael Coburn for very helpful discussions on explosives; of Mr. Nicholas Loverro, and Lieutenants Stephanie Richards, Douglas Loverro, and Douglas Hufnagle for much technical assistance in the laboratory; and of Mrs. Sara Thigpen for secretarial help. Finally, he would like to thank Mr. Thomas Floyd and Dr. William Howard for putting up with the running of messy compounds in the Differential Scanning Calorimeter and to all the members of the facility for providing a congenial atmosphere.

I. INTRODUCTION:

In view of the United States' high productive capacity for the manufacture of ammonium nitrate as well as its low cost and ease of production, its use as a component in explosive mixtures seems extremely attractive. Mixtures of ammonium nitrate and other chemical compounds have been found to have good explosive characteristics but have not produced the theoretically predicted effect based upon available thermodynamic data. Thus, these explosive mixtures are often referred to as non-ideal explosives.

Optimization of the explosive characteristics of non-ideal explosive mixtures can be obtained with effectively small particle size and high intimacy of the components of these mixtures. Thus, mixtures whose components form eutectic mixtures, mixed crystals, or solid solutions can be expected to possess short distances between particles of the different components which would result in a faster reaction.

II. OBJECTIVES:

It was decided to test the explosive characteristics and eutectic properties of aromatic nitro compounds having azo groups. These azo groups are known to facilitate the detonation of an explosive and are known as trigger linkages. Another series of compounds which seemed promising is based on 1,4,5,8-tetramino anthraquinone (Figure 1) and its derivatives. The rationale behind the interest in this latter compound as a component in non-ideal explosives is its resemblance, structurally, to ethylene diamine (Figure 2) whose dinitrate salt mixed with ammonium nitrate is an excellent non-ideal explosive and forms a eutectic melting at 103.8 C.^o

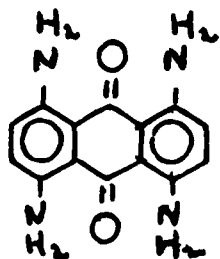


FIGURE 1

1,4,5,8-TETRAMINOANTHRAQUINONE

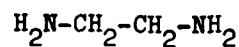


FIGURE 2

ETHYLENE DIAMINE

It was also decided to extend this study to nitrated derivatives of both, o,o'-biphenol (Figure 3) and p,p'-biphenol (Figure 4). The reason for the interest in these nitrated phenolic compounds is their very close structural resemblance to picric acid (Figure 5), a well-known explosive.

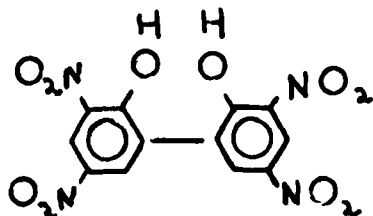


FIGURE 3

3,3',5,5'-TETRANITRO-o,o'-BIPHENOL

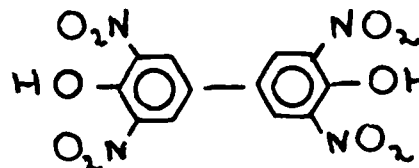


FIGURE 4

3,3',5,5'-TETRANITRO-p,p'-BIPHENOL

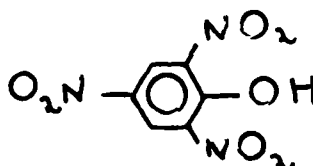


FIGURE 5

PICRIC
ACID

A great portion of the data desired can be obtained by Differential Scanning Calorimetry whereby enthalpic changes such as melting, crystallographic phase transitions, or chemical changes, explosive or otherwise, can be detected and measured from the endo- and exothermal bands and peaks that appear on the thermograms. Additional or corroborating evidence can be obtained by use of a polarizing microscope equipped with a hot stage assembly whereby phase transitions can be observed visually. Explosive properties can be assessed by making use of the drop-hammer sensitivity test. It might be mentioned at this point that the interest in azo compounds and the anthraquinone derivatives stems from their availability as dyes thus giving them an abundant and relatively inexpensive source of supply.

III. AROMATIC NITRO COMPOUNDS WITH AZO GROUPS:

A promising compound in this class was a commercially available dye from American Cyanamid Company having the commercial name Permanent Red GG or Permaton Orange XL. Consultation of the reference work Colour Index showed it to have the following identification number: 12075 and the structure shown in Figure 6.²

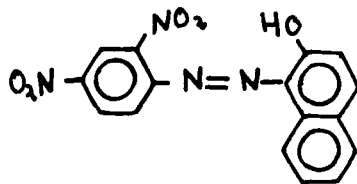


FIGURE 6 - C.I. 12075

The presence of nitro groups in this compound is expected to lead to explosive characteristics and the presence of the trigger linkage, the azo group $-N=N-$ is expected to sensitize the explosive reaction.

Drop-hammer tests on C.I. 12075 neat were negative.

A mixture with ammonium nitrate (50% by weight) showed good explosive properties as well as good stability characteristics.

A Differential Scanning Calorimeter (DSC) thermogram showed a strong exothermic peak at 330°C for neat C.I. 12075. The DSC scan of the mixture with ammonium nitrate did not show eutectic formation.

The mixture showed a strong exothermic peak at 275°C indicating a destabilization, perhaps caused by the presence of molten ammonium nitrate (melting point 169.6°C). The neat C.I. 12075 had shown a sharp endothermic peak just preceding its exothermic decomposition peak indicating a melting followed by explosive decomposition.

C.I. 12075 was subjected to the following nitration conditions: a) dissolving in concentrated sulfuric acid and then adding concentrated nitric acid to the resulting solution, stirring at room temperature overnight followed by quenching in water b) stirring overnight with 98% nitric acid followed by quenching in water. In both cases a brownish solid was obtained whose DSC scan shows no endo or exothermic peaks up to a temperature of 430°C. A mixture with ammonium nitrate showed no eutectic formation or exothermic peak in the DSC scan. An endothermic peak at 280°C was observed corresponding to the lowering of the melting point of the neat compound.

Another dye manufactured by American Cyanamid Company as Diarylide Orange, PermanentOrange G, or Diarylide Yellow having Colour Index identification number C.I. 21110. This compound has two -N=N- azo trigger linkages but no nitro groups. A DSC scan showed an exotherm at 327°C but no endotherm corresponding to a melting point. A mixture with ammonium nitrate showed no eutectic formation. The exotherm in this case occurred at 247°C, again conceivably a decomposition reaction taking place in the molten ammonium nitrate at a temperature appreciably lower than in the case of the neat compound. Nitrations were carried out in the methods a) and b) described for C.I. 12075 to yield a brown solid. The nitration product's DSC scan showed neither endo- or exothermic peaks up to a temperature of 320°C. A mixture with ammonium nitrate did not result in eutectic formation as shown by DSC scan. An endotherm was observed at 275°C, again perhaps indicating a depression of the melting point of the neat compound caused by ammonium nitrate impurity.

An alternative method of nitration similar to one used by Moir³ was developed during the course of these investigations. In this method, the compound to be nitrated is dissolved in concentrated sulfuric acid maintained at 100°C. The resulting solution is stirred for several hours at that temperature. An excess of concentrated nitric acid is then added to the solution at a temperature of 70°C and stirring is continued until solid product precipitates out. The solid is then filtered using sintered glass funnels. The nitration of Fat Red 2B manufactured by American Hoechst Corporation (C.I. 26105) was carried out in this fashion. The structure of this compound is given in Figure 7.

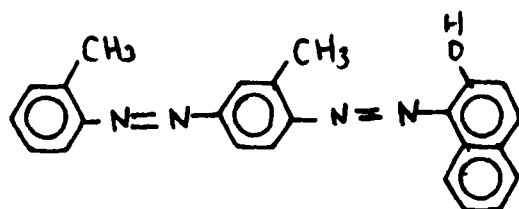


FIGURE 7 - C.I. 26105

The nitration would be expected to place one or several nitro groups on the naphthalene ring which initially has an -OH group capable of directing and activating nitration on the ring system to which it is attached. Thus, with one or several nitro groups and two azo trigger linkages, the nitration product might be expected to have explosive properties. The nitrated compound was obtained in good yield, 2.1 grams from a starting amount of C.I. 26105 of 3.8 grams. Its DSC scan showed no endothermic peaks. There was no sharp exotherms but only a gradual shift towards the exothermic side of the chart-paper was observed. A mixture with ammonium nitrate showed no eutectic formation, an endothermic peak corresponding to melting of ammonium nitrate appearing at 170°C. This was followed immediately by a fairly broad exotherm again indicating a reaction in the molten ammonium nitrate. Drop-hammer tests on the nitrated C.I. 26105, however, did not reveal any explosive properties for this compound.

Nitrated C.I. 26105 was converted to its ammonium and its potassium salt by neutralization of the phenolic -OH group. The ammonium salt was formed by dissolving the compound in an excess of warm concentrated ammonia, cooling the resulting solution, and filtering the resulting precipitate. The potassium salt was obtained by

dissolving the nitrated C.I. 26105 in warm methanol and exactly neutralizing it with a stock aqueous KOH solution of known concentration. The ammonium salt showed no DSC scan peaks up to 450°C. Mixing the ammonium salt with ammonium nitrate showed no eutectic formation. An exothermic peak occurring at 220°C was observed, again indicating a reaction in molten ammonium nitrate. The potassium salt showed a very strong and sharp DSC scan exotherm at 350°C. A eutectic did not form when the potassium salt was mixed with ammonium nitrate. Neither salt showed explosive properties with the drop-hammer test.

IV. ANTHRAQUINONES

As outlined in section II. OBJECTIVES, an attractive possibility as a component in a non-ideal explosives mixture is 1,4,5,8-tetramino anthraquinone (Figure 1) or one of its derivatives. This compound is available as a dye manufactured by General Aniline and Film Corporation known as Celliton Blue BB Extra Concentrated for Printing and has a Colour Index identification number 64500. The tetranitrate salt of C.I. 64500 by dissolving it in a hundred-fold excess of 1.6 M nitric acid and stirring at 25°C for three hours. About three-fourths of the resulting solution was allowed to evaporate. Acetonitrile was then added to the reduced solution until crystals appeared. These were filtered with a sintered glass funnel and dried in a vacuum oven to give a black-blue solid. Drop-hammer tests on this solid showed low sensitivity in explosive properties. No explosions were obtained with the 2.5 kg hammer up to a drop-height of 200 cm. Similar

results were obtained with a mixture of ammonium nitrate and the tetranitrate salt of C.I. 64500. Change to a 5 kg hammer resulted in an explosion at a drop-height of 200 cm for both the neat tetranitrate and for the mixture.

DSC scans were taken of C.I. 64500 and its derivatives and the mixtures with ammonium nitrate. C.I. 64500 itself showed no peaks, endothermic or exothermic, up to a temperature of 420°C. The tetranitrate has a very sharp exothermic peak centered at 155°C. This peak disappears when the scan is run up to 170°C, the calorimeter cooled down to 140°C, and then heated back up through 155°C, thus indicating that the peak is due to the decomposition of the material under study. A mixture of the tetranitrate and ammonium nitrate shows the persistence of the ammonium nitrate melting endotherm followed immediately by an exothermic peak centered around 172°C. Again here, eutectic formation does not seem to take place. The shift of the exotherm from 155°C to 172°C may be due to the poorer thermal conductivity of the ammonium nitrate. A mixture of ammonium nitrate and C.I. 64500 gave a DSC scan in which the ammonium nitrate melting endotherm was missing. No corresponding endotherm below this temperature of 169°C to indicate eutectic formation was observed. An exothermic peak centered at 220°C was observed. It is likely that a reaction occurs between the ammonium nitrate and the C.I. 64500 in which the ammonium nitrate is converted to ammonia and the C.I. 64500 is converted to a nitrate salt, not necessarily the tetranitrate, and that the nitrate salt decomposes at 220°C.

C.I. 64500 was subjected to various nitration conditions in order to convert it into a nitro derivative of the tetranitrate salt. Again methods a) and b) described for C.I. 12075 were used but product could not be isolated. The adaptation of the Moir method described for the nitration of C.I. 21110 produced a good yield of a brown fluffy crystals after the reaction mixture was quenched in water, taken up in methanol and then ether, and finally allowed to stand in the deep-freeze compartment of a refrigerator overnight. This compound showed a DSC scan endothermic peak at 280°C. A mixture with ammonium nitrate diminished this peak and gave rise to a new endothermic peak centered at 310°C, the ammonium nitrate peak, again, having been removed. Again, this seems to suggest: salt formation of free amino groups which apparently had not undergone neutralization during the nitration reaction or that it had reverted back to the free amino group during isolation. A more detailed study of the structures of these compounds, particularly by Nuclear Magnetic Resonance Spectroscopy seems to be needed. Drop-hammer test on this compound proved to be negative.

V. NITROBIPHENOLS

As outlined in II. OBJECTIVES the nitration of o,o'-biphenol and p,p'-biphenol to yield the anticipated nitrobiphenols (Figures 3 and 4) seemed like an interesting avenue to follow in the search of a fuel component in non-ideal explosives.

The nitration conditions suggested by Moir³ described in section III gave excellent yields of the nitro derivatives. p,p'-Biphenol under these conditions yielded about 50 percent of the theoretical amount of yellow crystals melting at 221°C. This melting point is in exact agreement with that reported by Moir³ for the compound shown in Figure 4 which will be given the abbreviation p,p'-TNBP. Drop-hammer tests on this compound were negative. The p,p'-TNBP was converted into the diammonium salt adding it to an excess of concentrated ammonia. A red solid was obtained. It was observed that the diammonium salt conversion could be carried out merely in the presence of ammonia fumes as shown by the yellow crystals' turning to a red color when a beaker of concentrated ammonium hydroxide was kept in the vicinity of the crystals. The diammonium salt gave positive drop-hammer tests with a 2.5 kg hammer at 150 cm. This data suggests a practical application in which a non-explosive is converted to an explosive by a very ready and facile uptake ammonia. It might also be mentioned in passing that the diammonium salt is listed in the Colour Index as an Acid Dye known as Palatine Orange with identification number C.I. 10311.

The p,p'-TNBP gives a DSC scan with three endotherms occurring at 162°C, 189°C, and 222°C. The first two of these correspond to phase transitions and the third to melting. This was confirmed by hot-stage microscopy. The diammonium salt showed a DSC scan exothermic peak occurring at 267°C. Mixing

with ammonium nitrate did not result in the lowering of the melting point of ammonium nitrate as observed by DSC scans, thus indicating absence of eutectic formation for both p,p'-TNBP and its diammonium salt. These results were also confirmed by hot-stage microscopy. The dipotassium salt of p,p'-TNBP was made by neutralization with a stock aqueous KOH solution of known concentration and also by exchange between excess potassium nitrate and the diammonium salt. In both cases, a reddish solid was obtained whose DSC scan displayed a strong, sharp exotherm at 350°C. A mixture with ammonium nitrate showed a sharp exotherm at 210°C and the persistence of the ammonium nitrate melting point endotherm, indicating reaction in the ammonium nitrate melt.

In an analogous manner, nitration of o,o'-biphenol was carried out to yield a yellow solid, presumably having the structure shown in Figure 3 which will be given the abbreviation o,o'-TNBP. Again, in a similar fashion as for p,p'-TNBP, the diammonium and the dipotassium salts were formed. The ammonium salt showed a DSC scan endotherm centered at 259°C and the potassium salt showed a very strong and sharp exotherm at 350°C. In both cases no eutectic formation was observed in mixtures with ammonium nitrate.

Preliminary drop-hammer tests showed excellent explosive properties for the potassium salts of o,o'-TNBP and of p,p'-TNBP. The ammonium salt of o,o'-TNBP also had some explosive properties and that of p,p'-TNBP also had excellent properties as noted previously.

VI. RECOMMENDATIONS

As mentioned in the previous section, the ammonium and potassium salts of the isomeric tetranitrobiphenols showed excellent explosive properties. The tetranitrobiphenols themselves were found to be non-explosive but reacted extremely readily with gaseous ammonia to form the explosive ammonium salts. The process was accompanied with a color change from yellow to red. A possible application of this set of facts may involve in situ explosive mixtures, that is, explosive mixtures formed at the site of use from non-explosive materials. An example of this is a mixture of ethylene diamine and ammonium nitrate, both non-explosives which, upon heating, converts into ethylene diamine dinitrate and ammonia. If an excess of ammonium nitrate is used, an explosive mixture of ethylene diamine dinitrate and unreacted ammonium nitrate results. However, the ammonia gas liberated interferes with the explosive properties of this mixture. If non-explosive tetranitrobiphenol were to be added to this system, it could scavenge the ammonia as it is liberated and convert to its explosive ammonium salt. Thus, the removal of the interfering ammonia and the formation of the explosive compound in the same operation would be expected to lead to enhanced explosive properties for this system. In addition, the color change occurring at the same time might be helpful in indicating whether all of the tetranitrobiphenol had been converted to the ammonium salt.

Possible follow-on research might include the following projects. Expansion in the area of the search for explosives forming eutectics with ammonium nitrate. This could involve the study of a collection of about forty dyes at hand which have either nitro and azo functions or a polyamino anthraquinone structure. Conversion of these into a variety of salts could be carried out and DSC scans carried out to detect any eutectic formation. Further nitration of some of these dyes by the methods developed in this work might also be carried out and eutectic formation of the various salts of the nitrated products investigated.

An interesting extension of the investigation of the explosive properties of nitrated biphenol salts would be an attempt to make a hexanitrobiphenol, 2,2',4,4',6,6'-hexanitro-m,m'-biphenol (Figure 8) by the nitration of m,m'-biphenol (Figure 9). m,m'-Biphenol, however, is not commercially available as were o,o'- and p,p'-biphenol and must be made by a five-step synthesis starting with o-anisidine (Figure 10).⁴

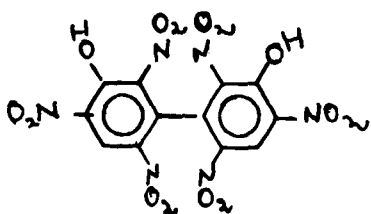


FIGURE 8

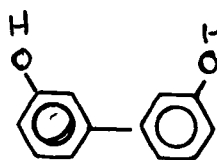


FIGURE 9

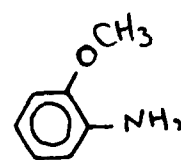


FIGURE 10

The hexanitrobiphenol has a structure very similar to that of picric acid (Figure 5, section II). There are two

picric acid molecules joined together by the bond between the two benzene rings. Its ammonium salt would be expected to have as good or better explosive properties as ammonium picrate, a known explosive. The hexanitrobiphenol might further be investigated relative the the in situ explosives and eutectic formation with ammonium nitrate.

Another important avenue to pursue is the verification of the various nitrated derivatives as to structure. It is an urgent matter to determine whether the derivatives do indeed have the structures imputed to them. A very important tool in this respect is the Nuclear Magnetic Resonance Spectrometer(NMR). This instrument which was not available at Eglin AFB but is available at my academic institution at State University College, Fredonia, N.Y. could be used for this elucidation of structure. Another measurement that might establish the extent of nitration would be elemental analysis to give percent carbon and hydrogen. Such analyses might be conducted at State University of N.Y. at Buffalo.

Finally, it might be advantageous to carry out a theoretical study which would give the desired parameters of size and structure for success in eutectic formation with ammonium nitrate. Such a study might start out by looking at the various parameters possessed by ethylene diamine dinitrate and extrapolating from there. The question of the nature of eutectic formation and the reasons underlying its existence should also be delved into.

REFERENCES

1. I. Akst and J. Hershkowitz, "Explosive Performance Modification by Cosolidification of Ammonium Nitrate with Fuels," Technical Report 4987, Picatinny Arsenal, Dover, N.J., October, 1976
2. Colour Index, third edition, published by the Society of Dyers and Colourists, Yorkshire, England, 1975
3. J. Moir, "New Derivatives of Diphenol," Journal of the Chemical Society, Vol. 91, pp. 1305-1311, 1907
4. L. Mascarelli and B. Visintin, Gazz. chim. ital., Vol. 62, pp.358-368, 1932

1979 USAF - SCEEE SUMMER FACULTY RESEARCH PROGRAM

Sponsored by the

AIR FORCE OFFICE OF SCIENTIFIC RESEARCH

Conducted by the

SOUTHEASTERN CENTER FOR ELECTRICAL ENGINEERING EDUCATION

FINAL REPORT

VIBRATION DIAGNOSTICS FOR TURBOFAN ENGINES

Prepared by:	Charles E. Nuckolls, Ph.D., P.E.
Academic Rank:	Associate Professor
Department and University:	Mechanical Engineering and Aerospace Sciences, University of Central Florida
Research Location:	Arnold Engineering Development Center, Arnold AFS, TN 37389; Engine Test Facility, Tech- nology Applications Branch, Propulsion Section
USAF Research Colleague:	Grant T. Patterson, Ph.D.
Date:	August 31, 1979
Contract No.:	F49620-79-C-0038

VIBRATION DIAGNOSTICS FOR
TURBOFAN ENGINES

by

C. E. Nuckolls

ABSTRACT

The feasibility of gas turbine engine condition assessment by analysis of the signal from a case mounted accelerometer is discussed. Case responses due to other excitations, such as multiple pure tones due to blade passage, overwhelm and obscure that due to the distressed component, such as a rotor bearing. Techniques for extraction of a periodic signal from noise are discussed. Recommendations are made with regard to a experimental program to verify feasibility of the technique and other possible schemes for condition monitoring.

ACKNOWLEDGEMENT

The author would like to thank the Air Force Systems Command, Air Force Office of Scientific Research and the Southeastern Center for Electrical Engineering Education for providing the opportunity to study and perform research in the area of gas turbine engine condition monitoring. Special acknowledgement is due Dr. Richard Miller, Director of the Summer Faculty Research Program, for a well coordinated program.

Finally, he would like to thank Dr. Grant T. Patterson and Mr. Dave Lansford of the Arnold Engineering Development Center for their assistance and guidance throughout the program.

I. INTRODUCTION:

The use of vibration measurements as a diagnostic tool has been well established in several engineering disciplines. The nonobtrusive techniques are generally referred to as Mechanical Signature Analysis. When successfully applied, information may be obtained about subsystems which is otherwise inaccessible. Furthermore, this information can be obtained during normal operation. If properly interpreted, this information can provide early warning of an incipient failure. Such a diagnostic system would obviously be of assistance to AEDC/ETF in its mission of test and evaluation of turbine engines for the USAF. The object of this research effort has been to investigate the feasibility of developing an on-line automated vibration monitoring and out-of-tolerance warning system.

A vast amount of literature exists in the area of Mechanical Signature Analysis. An excellent review has been written by Volin [1]. Most of these record experiences and successes in the petrochemical industry based on simple surveillance of the overall vibration level or the frequency spectrum. An excellent four-part series by Mitchell [2] discusses the design of such systems.

For more complex systems such as the turbofan engine, the concept of a Symptom Fault Matrix [3] is needed. This is shown schematically in Figure 1. A system utilizing this scheme has recently been installed at Oklahoma City--Air Logistics Center [4]. It was designed primarily to assist with trim balancing of rebuilt engines and detects such faults as rotor unbalance or misalignment and seal rub.

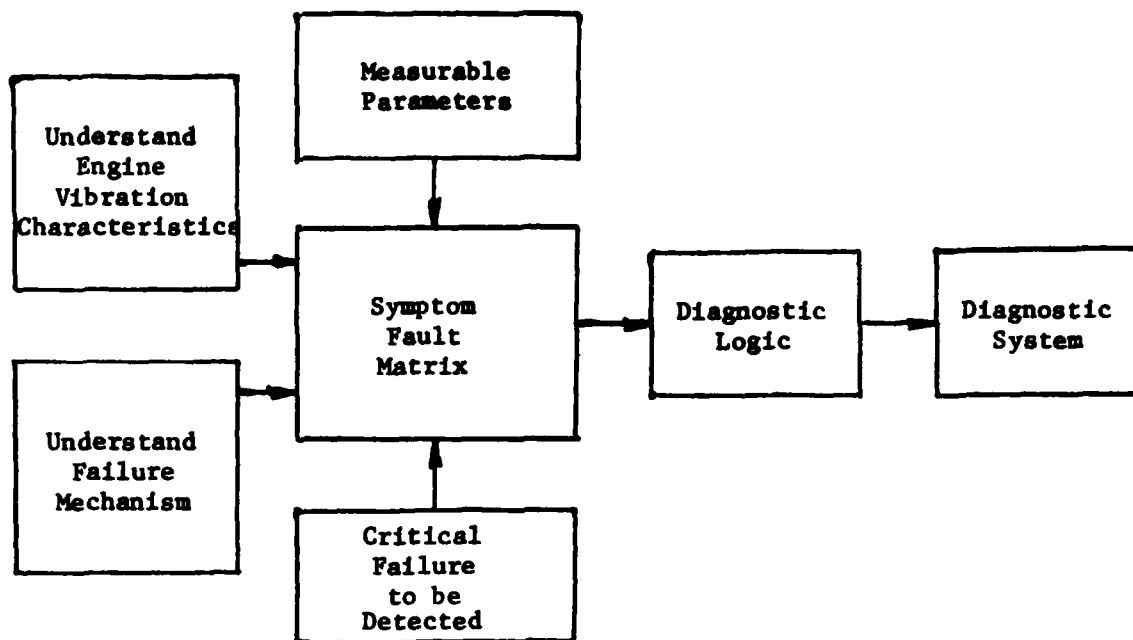


FIGURE 1 - SYMPTOM FAULT MATRIX

This study is directed toward development of a more comprehensive system, capable of detecting other faults, including bearing, gear or blade failure. When dealing with a system as complex as the turbofan engine, it is essential that one have a complete understanding of the engine vibration characteristics and of the failure mechanism before attempting to establish the discriminators in the Symptom Fault Matrix.

The situation seems to be comparable to that of the helicopter, at least in complexity. A great amount of work has been done on the helicopter diagnostics system problem. Houser and Drosjack [5] summarized the work done prior to 1973 in a most comprehensive report for the USAAMRDL. Each of the potential diagnostic discriminants shown in Figure 2 were discussed and evaluated. Much of that information is relevant to the task undertaken here in that a great deal of experience with various diagnostic schemes is available. Houser concluded that a workable diagnostic system for helicopter use was several years away.

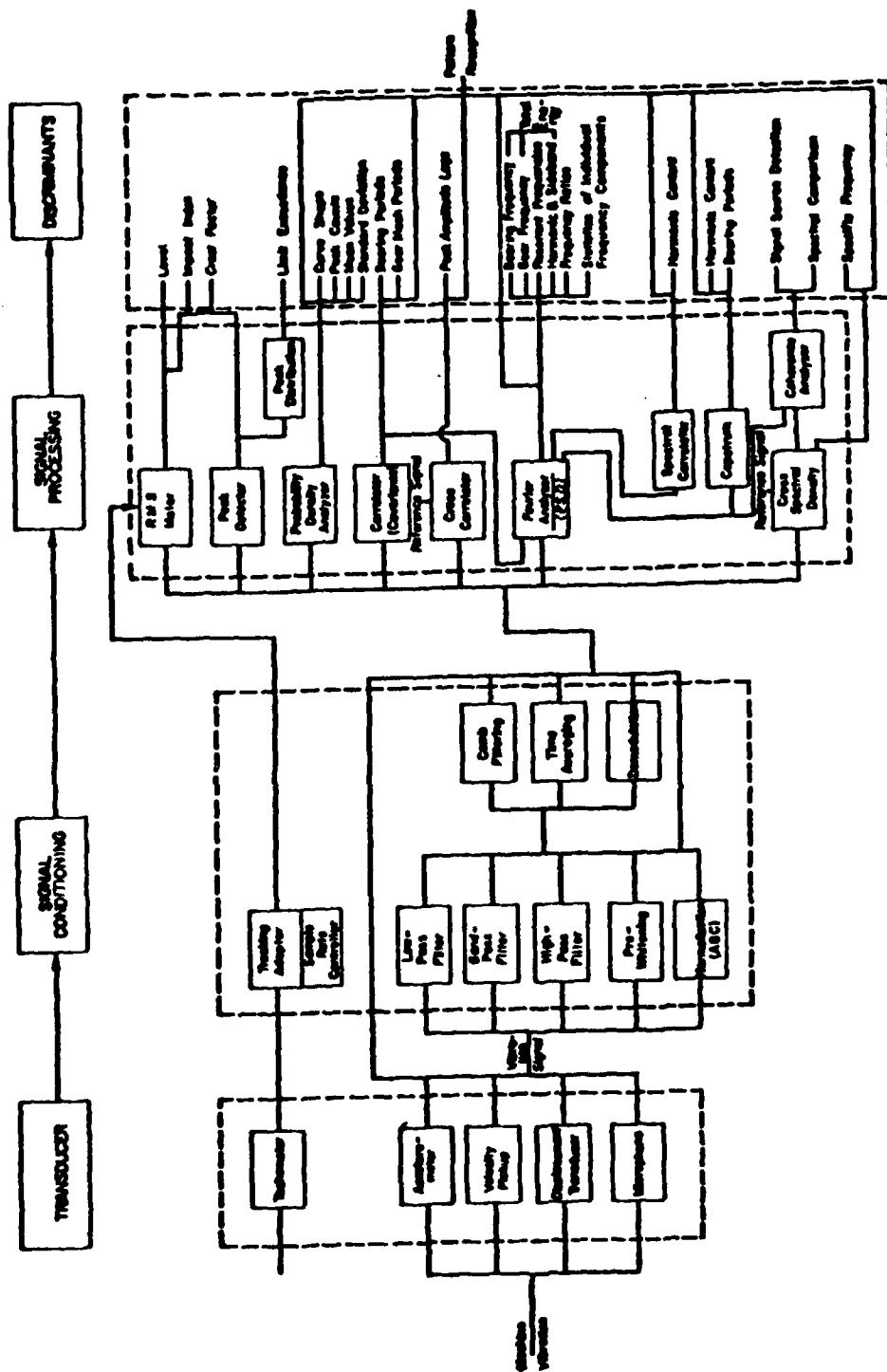


Figure 2. Potential Diagnostic Systems.

In 1978, Murphy from Bell Helicopter [6] concluded that a cost effective diagnostic system for helicopter propulsion systems is currently feasible, using engine "coast down" to indicate tip rub or defective bearings, engine overall rms vibration level to indicate foreign object damage or rotor unbalance, bearing temperature to indicate failure in tail rotor drive shaft bearings, and spectrometric oil analysis together with oil pressure and temperature measurements for the transmission and gearbox. Vibration signal analysis techniques for the transmission still require development.

II. OBJECTIVES:

The objectives of this project were:

- (1) Recommend the proper instrumentation to measure the vibration environment as determined to exist for a typical aircraft gas turbine engine operating at a high power setting.
- (2) Determine the amount of instrumentation (number of transducers) required and their placement on the test engine to affect measurement of critical component vibrations with minimum cost and complexity in mounting and placement.
- (3) Determine proper analysis techniques. Analyze engine component vibration characteristics. Specify any improvement required to present ETF or AEDC procedures or equipment to aid analysis.
- (4) Investigate the feasibility of developing an on-line automated vibration monitoring and out-of-tolerance warning system.

III. MEASURABLE PARAMETERS:

It may be assumed that the only data available are dynamic parameters measured on the engine case. Some engines are equipped with bill-of-material motion (velocity) transducers, but this cannot be assumed. Further, only external attachment of transducers is permitted. Only piezoelectric accelerometers are considered to be suitable because of their much advanced state of development, light weight, ease of mounting, wide dynamic range, extended frequency response, and emphasis of high frequency components within the signal.

Transducer location is as important as the transducer itself. In general, the transducer should be as close as possible to the part or

parts being monitored. Consider the signal generated by a bearing defect, for example.

Defect induced vibration is usually attributed to an impulse generated by the passing of a rolling element over the localized defect. At constant rotational speed, these impacts generate a periodic sequence of wavelets as depicted in Figure 3.



FIGURE 3 - TYPICAL BEARING SIGNATURE

Each wavelet is represented as the free damped response of some structural mode excited by the impacts of the rolling element passing over the defect, of the form

$$x(t) = \sum_j A e^{-\alpha(t-jT)} \sin[\omega_c(t-jT)] U(t-jT) \quad (1)$$

wherein

T = period of repetition

U = unit step function

A = amplitude parameter

α = damping parameter

ω_c = characteristic frequency of structural resonance

This is modified by the path of propagation from the vibration source (bearing) to the transducer so that the actual signal might be of the form

$$y(t) = \sum_i \left\{ \sum_j A_i e^{-\alpha_i(t-jT_i)} \sin[\omega_{ci}(t-jT_i)] U(t-jT_i) \right\} X_{hi}(t) \quad (2)$$

wherein

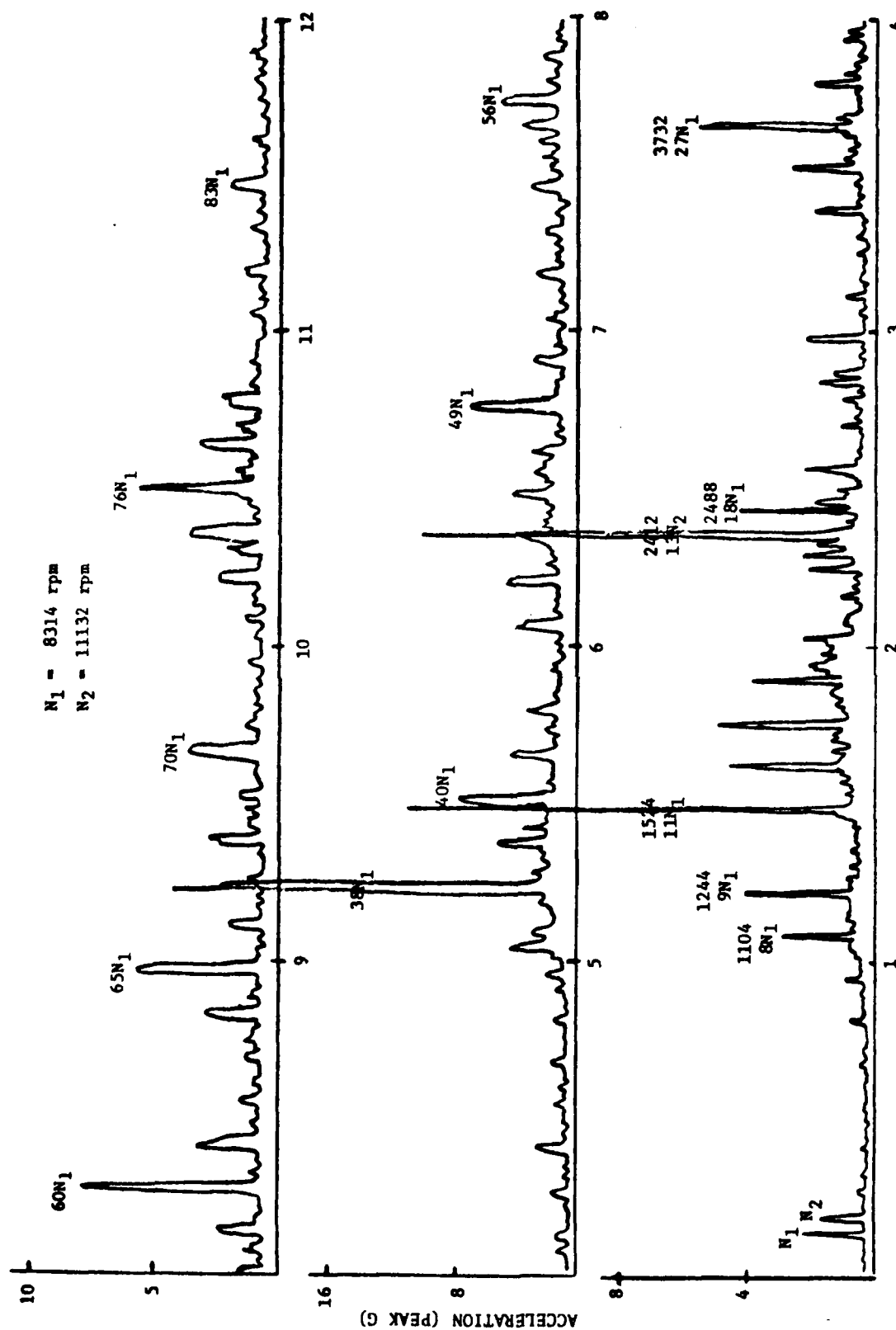
$h(t)$ = impulse response of the propagation path

X = convolution operator

The summation on i is included because there are many sources of vibration in addition to the bearings, or perhaps several propagation paths. The h_i are very complex frequency sensitive functions in general and are virtually impossible to predict analytically. If needed, they should be determined experimentally. They are introduced here only to emphasize the importance of transducer location and to point out that the signal will be complex and most likely will contain periodic components or noise which overwhelms the signal of interest. As a rule of thumb, there is a loss in signal level of 6 to 14 dB across any interface between the source and transducers. Other than that, the signal due to a bearing should propagate throughout the structure.

It may be that the amplitude of the signal as described by equation (1) is not strongly dependent upon speed of operation, but at the point of transducer attachment (equation (2)) it is. Therefore, any discriminators which are ultimately selected can only be used at given speeds for both rotors. Since the speed ratio between rotors depends upon the inlet conditions, this also requires that the inlet conditions are identical.

Vibration spectra are presented in Figures 4 and 5 for two operating conditions. The accelerometer was mounted on the front flange of the engine, sensing in the radial direction. Note in Figure 4 the presence of virtually every harmonic of the speed of the fan or low pressure rotor (N_1). Since there are 38 blades and 60 blades in the first and second stage fans respectively, it is not surprising that there exist peaks in the spectrum at $38N_1$ and $60N_1$ and their harmonics. The presence of the other multiple pure tones (MPT) are discussed extensively in the literature [7, 8, 9]. They are due to interaction between shock waves generated at supersonic tip speed. It is not the purpose of this study to investigate this phenomena, but its existence as a complicating feature must be considered. Even though N_1 was small enough that blade tip speed was



FREQUENCY (KHZ)
 FIGURE 4 - FREQUENCY SPECTRUM OF INLET CASE ACCELERATION
 ENGINE CONDITION: PLA 50° 12/9/5°

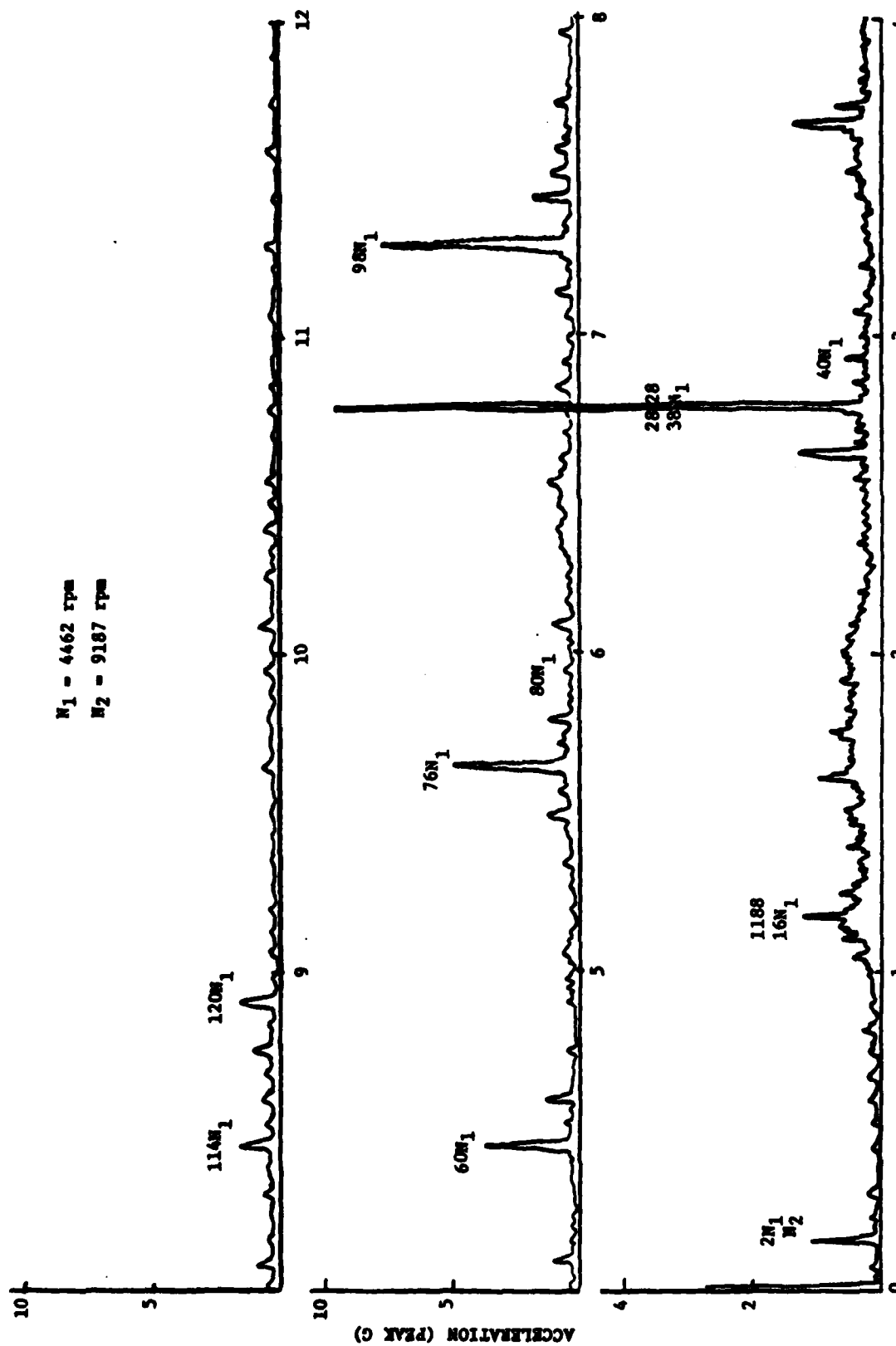


FIGURE 5 - FREQUENCY SPECTRUM OF INLET CASE ACCELERATION
 ENGINE CONDITION: IDLE 12/12/20°

subsonic for the case of Figure 5, the harmonics of N_1 are still present.

It would be ideal if only one transducer were required to diagnose various failure modes. But in view of the behavior described in equation (2), and illustrated in Figures 4 and 5, this is highly doubtful. The number required will depend upon the number and level of faults desired to be detected.

IV. CRITICAL FAILURES OR FAULTS:

The most prevalent failure modes and their relative importance are not known to this author. It is assumed that a symptom fault matrix with ability to identify the following conditions should ultimately be developed.

Unbalance

- High speed rotor

- Low speed rotor

Bearing failure

- Spalling/pitting/fretting

- Brinelling

- Corrosion

Gear failure

- Wear

- Pitting/spalling/scoring

- Fracture

Blade failure

- Foreign object damage

- Fatigue

- Stress rupture

Blade tip rub

V. PHYSICAL PHENOMENA

Bearing Failure

Vibration based methods for the detection of localized or surface defects such as spalls, corrosion spots and brinelling are considered here; other techniques based on temperature measurements or the checking of lubrication contamination are not.

The repetition rates for roller/ball bearings are given by the following equations (see Appendix A for their derivation) for defects on the outer race, inner race and roller, respectively.

$$f_o = \frac{n}{2} f_n \left(1 - \frac{d}{D} \cos \beta \right) \quad (3)$$

$$f_i = \frac{n}{2} f_n \left(1 + \frac{d}{D} \cos \beta \right) \quad (4)$$

$$f_b = \frac{D}{d \cos \beta} f_n \left(1 - \left(\frac{d}{D} \right)^2 \cos^2 \beta \right) \quad (5)$$

wherein

n = number of rollers/balls

d = ball diameter

D = pitch diameter

f_r = relative rotational speed between inner and outer race

β = contact angle

For the main engine bearings of the F100 engine these repetition rates are tabulated in Table 1.

Bearing No.	1	2	3	4	5
D	4.728	5.5118	7.4804	7.75	4.055
d	0.5512	0.750	0.90625	0.62992	0.4331
n	20	18	20	32	22
β	0	24°	23°	0	0
f_r	$N_1/60$	$N_1/60$	$N_2/60$	$N_2/60$	$N_1/60$
f_o/f_r	8.834	7.881	14.803	14.699	9.825
f_1/f_r	11.166	10.118	17.197	17.30	12.175
f_b/f_r	8.461	7.920	13.291	12.22	9.256

TABLE 1 - F100 MAIN ENGINE BEARING ORDERS

It is hypothesized that a periodic sequence of wavelets will be generated with these repetition rates, as discussed in the section on Measurable Parameters.

Early work in this area by Babkin and Anderson [10] was based on changes in the frequency spectrum as damage progressed. It was reported that the presence of localized defects would be manifested in the spectrum at those frequencies given by equations (3), (4), and (5). As pointed out by Braun and Datner [11] and Badgley [12], there are complications which require sophisticated signal conditioning circuitry. These are that there may be multiple defects, the defect signal will be altered by the propagation path between the defect and the accelerometer, many other signatures from other parts of the machinery exist (and are of much greater amplitude than those due to bearing defects). Even if the signal were as shown in Figure 3, it should be thought of as vibration at the characteristic frequency of the wavelet which is amplitude modulated at the defect repetition rate—only the characteristic frequency, not the modulating frequency, appears in the frequency spectrum. Simple spectral analysis is unsuitable as a diagnostic technique without further processing. A processing technique is desired such that the conclusion would be unaffected by the presence of other periodic signals or random signals and which would be unaffected by sensor location.

One well-known technique for extracting a periodic signal from a noisy waveform is Time Domain Averaging [13]. Assuming that this can be accomplished, Braun and Datner [11] suggest that the RMS value of the averaged signal be computed whereas Badgley [12] recommends demodulation--generation of an enveloping waveform--followed by spectral analysis.

Another approach proposed by Dyer and Stewart [14] should be mentioned. They report that the vibration signal generated by a healthy bearing is a stationary random process whose probability density function is Normal/Gaussian. With incipient damage, changes occur in the tails of the distribution. By monitoring the fourth moment (Kurtosis), the defect can be detected at an earlier stage than by monitoring the RMS value or peak value or crest factor. Use of this technique requires that the waveform not be contaminated by other signatures which means that the sensor must be located on the bearing housing. Since this sensor location requirement cannot be met, this technique was not seriously considered.

When using the concept of time domain averaging, two questions immediately arise. The first deals with how many sections of waveform must be averaged and the second with a proper repetition rate. At first glance, it seems that the repetition rate should be exactly one of those given by equations (3), (4), (5). But the contact angle varies slightly with thrust load and slippage might occur between the balls and races; consequently, the repetition rate is not known with precision a priori and the averaging process must be repeated several times with repetition rates in the vicinity of the nominal values. So the question reduces to one of closeness of spacing of the search frequencies.

A reasonable spacing for use with the above frequency search is recommended by Braun and Datner [11] as:

$$\Delta f = \frac{1}{CN} \frac{f_i}{f_c/f_i} \quad (6)$$

wherein

N = number of averages used

C = factor between 2 and 20

f_1 = repetition rate

f_c = characteristic frequency of wavelet

With regard to the number of averages which must be used, Braun [13] recommends

$$N > \frac{\alpha}{\pi^2 F} \quad (7)$$

wherein

α = desired attenuation of fundamental component of periodic signal to be rejected

$F = f/f_1 - K$

f = fundamental frequency of periodic signal to be rejected

$K = 0, 1, 2, 3, \dots$ such that $F \geq 1.0$

Serious difficulties with use of this technique are foreseen. First, the required attenuation (α) is not known but could easily be as great as 100. The frequency difference F is not known either; but for example, if $F = 0.01$ and $\alpha = 100$, then $N > 1000$. Further, if $f_1 = 3000$ Hz, $f_c = 30,000$ Hz (and $N = 1000$), then $f = 0.15$ Hz. Nevertheless, it is recommended that this technique be tried—that is, an iterative frequency search by use of time averaging with frequencies (averaging repetition rates) spaced according to (6), centered around nominal frequencies given by (3), (4), and (5), plotting the overall RMS value of the averaged waveform vs frequency.

Gear Failure

The primary frequency associated with geared systems is the gear mesh frequency--the product of the number of teeth and the rotational speed. This is because there are small deviations from the true involute profile as a result of tooth deflection--resulting in tooth engagement shocks or dynamic loads. The vibratory portion of this mesh dynamic force may be viewed as a periodic phenomena whose frequency spectrum consists of lines at the gear mesh frequency and its harmonics.

Any periodic meshing error leads to a cyclic load pattern with a maximum and a minimum mesh force occurring once per revolution. Such amplitude modulation can be represented in the frequency domain by sidebands as shown in Figure 6.

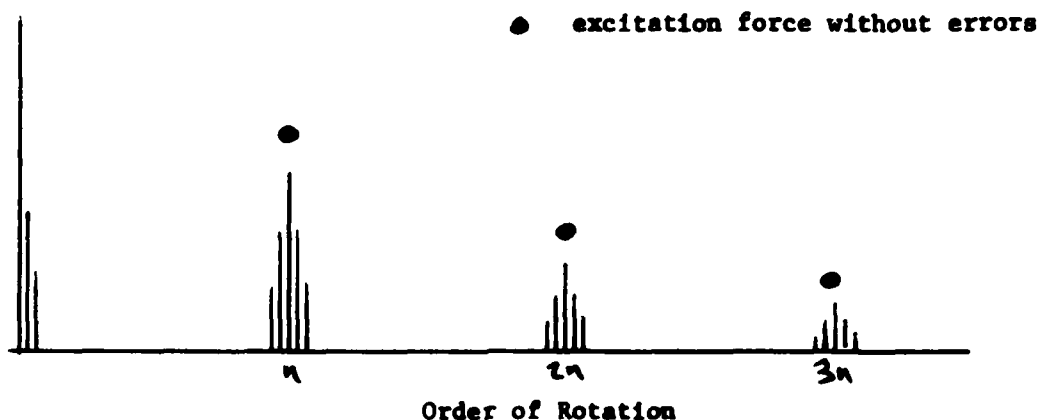


FIGURE 6

Note that the sidebands are symmetrical about the harmonics of the tooth mesh frequency. Also note that the amplitudes at the harmonics of the mesh frequency are smaller than for the case of no errors [15]. Periodic meshing errors might be due to

- (1) eccentric gears
- (2) tooth spacing errors
- (3) shaft vibration--which usually takes place at the same frequency as the rotational speed--having the same effect as eccentricity.

On the other hand, for gear pairs with arbitrary tooth spacing errors or defects, the fundamental period of the periodic mesh force must be the number of tooth intervals required to reestablish contact for a given tooth pair--which may take several revolutions. This introduces spectral lines of very low order; and if the tooth spacing errors are random, the symmetry of the sidebands is destroyed [15].

Signals due to gear meshing errors must be transmitted through the shafting and bearings into the structure before detection by the accelerometer. Consequently, all comments with regard to time averaging apply--with the exception that the repetition rate is known precisely.

Gear meshing orders for all meshing pairs in the F100 series 1 engine are given in Table II. These are all referred to the high pressure rotor ($N_2/60$).

GEAR PAIR	ORDER
I and II	73
III and IV	55.7
A and B	9.2
C and D	39.6
E and F	55.6
F and G	55.6
H and J	19.7
K and L	29.6
M and N	18.2
P and R	63.1
S and T	38.3
U and V	14.9
X and Y	14.9

TABLE II - GEAR MESH ORDERS, F100 ENGINE

Rotor Unbalance

The most commonly encountered forces which cause vibration of a gas turbine engine rotor are those produced by mass unbalance which may be distributed along and about the rotor axis. Rotation of the unbalanced masses at the speed of the rotor cause effective forces acting radially outward from the rotors axis--proportional to the mass of the unbalance and the square of the rotor speed. They may be oriented at any angle, circumferentially. As a result, the rotor whirls about the bearing axis. This is a synchronous motion--in the direction of rotation and at the speed of rotation. If the distribution of the unbalanced forces were similar to one of the mode shapes, extremely large amplitudes would result at the corresponding critical speeds.

The third critical speed is frequently within the operating speed range and the first two must be traversed in startup and shutdown, but the rotor responds to lesser extent to the unbalanced forces at any speed of operation. An excellent description of this phenomena and a complete rotor dynamic evaluation of eight turbine engines in the Air Force inventory is presented in a report by MTI, January, 1978 [16]. The F100 was not included in that study but apparently will be in a follow-on project. A diagnostic system similar to the one presently in use at OC-ALC, as mentioned earlier [4], might be incorporated at AEDC to detect unbalance.

Antifriction bearings commonly used in aircraft turbine engines have low damping characteristics. Consequently, squeeze film dampers are usually incorporated in series with the bearings. They are quite effective in controlling shaft whirl, whether synchronous or nonsynchronous, and the resulting orbital motion of the damper journal is circular [17]. For this reason the very subtle subject of whirl due to causes other than unbalance will not be discussed.

Turbine Blade Tip Contact

Only one paper was discovered which dealt with tip rub. It had to do with modeling of blade tip contact from a wear point of view [18]. It would seem that the phenomena would involve stick-slip motion or chatter and that some of the extensive literature that exists in the machine tool area might be relevant, but this was not pursued. It is also possible that the tip contact might not be uniform and could lead to a nonsynchronous whirl of the rotor as discussed by Den Hartog [19]. Such whirl occurs in a direction opposite that of rotation, at the critical frequency rather than at the speed of operation--usually about 40 to 50 percent of rotation speed. This is in contrast to whirl due to aerodynamic effects (which is synchronous) such as that due to circumferential variation of blade tip clearance [20].

The diagnostic system at OC-ALC reports the symptom of seal rub to be broad band vibration in the frequency range 1 KHZ to 10 KHZ [4].

It has been reported [21] that blade irregularities can be observed either directly in the time domain, using digital averaging techniques or in the frequency domain by comparing the shape of the spectrum with that of a mechanically perfect rotor. The example given, however, is for the case of a blade which is completely missing rather than just being bent or damaged.

As discussed earlier [7], it has been reported that multiple pure combination tones are generated as a direct result of small amplitude variations in the blade-attached shocks, due to normal manufacturing tolerances. These shocks propagate at different speeds creating shock interval variations forward of the fan, and the power spectrum depends critically upon variations of the intervals between shocks. Since fan irregularities due to manufacturing tolerances are not duplicated from fan-to-fan, the MPT noise spectra will vary from fan-to-fan.

This suggests that minor blade damage might be detected if a custom baseline is used rather than a generic one. The spectral shape of the MPT will be modified by structural resonance if an accelerometer is used--therefore, comparisons must be made based upon exactly the same rotor speed as that from which the custom baseline was generated. Use of a pressure transducer might circumvent this problem, however, especially if averaging in the frequency domain is performed on ratio spectra (order expressed relative to N_1).

Combined Effects

It has been reported that failure in a bearing increases the energy content of gear sidebands [5]. No quantitative explanation for this phenomenon is available and it is not clear how advanced the bearing degradation actually was. The possibility of interaction between failure modes exists and can complicate the use of a particular failure discriminant. Extensive experience with known defects present will be required before these combined effects can be evaluated.

VI. RECOMMENDATIONS

The nature of the signal which might be expected from various defects within an engine have been discussed. In principle, these can be detected by use of case mounted transducers, with appropriate

signal conditioning and choice of discriminators. An extensive experimental program will be required to verify this, however, a program which should include implantation of known defective components. With this general conclusion in mind, recommendations are made with respect to implementation of specific techniques which are presently available and to future developmental effort.

Failure Mode Analysis

The order of importance of various failure modes should be determined. No known information is available which describes the frequency of occurrence or severity of failure modes of interest to AEDC/ETF. This information is needed because the sensitivity of diagnostic technique varies between failure modes.

Data File

It is virtually impossible to make a decision as to the effectiveness of application of a given technique without actual testing. Some have recommended that a file of tape recorded data be developed. More failure implant data is definitely needed, but until the type and location of transducer have been standardized, the accumulation of a data file would be of little benefit.

Instrumentation

The data reduction capabilities available through use of the SD360 Digital Signal Processor and PDP11 appear to be adequate at the present time.

The BBN accelerometer model 506, presently in use at AEDC/ETF, appears to be ideal for this application. This endorsement, however, is based only upon perusal of the specification sheet and not on successful use of the accelerometer. The main advantage of the BBN-506 is that a charge amplifier is not required. It is very lightweight (mass of 2gm) and its mounted resonant frequency is 55 KHZ, but neither is an overwhelming factor. For the F100 engine the highest gear mesh frequency is 73 N₂ which is approximately 15 KHZ, and blade pass frequency could be as high as 20 KHZ, but most gear, bearing and blade pass frequencies are much lower. Most piezoelectric accelerometers

have resonant frequencies in the range 35 to 50 KHZ which should be acceptable. Sensitivity of 10 mv/g is typical.

Acoustic sensitivity is not mentioned in the BBN specification sheet but is worthy of investigation, particularly since the acoustic environment depends upon the test cell being used. This can be checked by suspending an accelerometer in the test cell very close to the case mounted one and evaluating either the cross correlation function or the coherence function between the two.

Accelerometer failure has been experienced in each test of this summer research program; no data in which we have genuine confidence was taken. It is recommended that if accelerometer failure again occurs a change be made to Endevco accelerometers, even though charge amplifiers are required and cost per channel might be greater.

Structural Dynamics

Any dynamic signal originating in a machine will be affected by structural characteristics before reaching a transducer. Knowledge of these characteristics might be helpful in selecting transducer placement and mounting. Determination of such structural characteristics would involve analytical procedures such as finite element or other lumped parameter techniques and experimental procedures such as shaker or pulse excitation to validate the analytical model. With a model available, one could optimize transducer placement and determine signal path transfer functions. It is felt, however, that development of an analytical model is not justified, that transducer location can be selected by trial and error. Recommended locations are flanges near the struts which support the bearing housings.

Mounting of the accelerometer is of equal importance. There is no point in having a large accelerometer natural frequency if high frequencies cannot be transmitted through the mount. Still thinking in terms of case mounting, it would be best if the accelerometer could be bonded directly to an exterior flange. This not being possible, a small solid accelerometer block which is bolted to the flange should be used. Aluminum is recommended since the modulus to weight ratio is about the same as that for steel and rigidity, not strength,

have resonant frequencies in the range 35 to 50 KHZ which should be acceptable. Sensitivity of 10 mv/g is typical.

Acoustic sensitivity is not mentioned in the BBN specification sheet but is worthy of investigation, particularly since the acoustic environment depends upon the test cell being used. This can be checked by suspending an accelerometer in the test cell very close to the case mounted one and evaluating either the cross correlation function or the coherence function between the two.

Accelerometer failure has been experienced in each test of this summer research program; no data in which we have genuine confidence was taken. It is recommended that if accelerometer failure again occurs a change be made to Endevco accelerometers, even though charge amplifiers are required and cost per channel might be greater.

Structural Dynamics

Any dynamic signal originating in a machine will be affected by structural characteristics before reaching a transducer. Knowledge of these characteristics might be helpful in selecting transducer placement and mounting. Determination of such structural characteristics would involve analytical procedures such as finite element or other lumped parameter techniques and experimental procedures such as shaker or pulse excitation to validate the analytical model. With a model available, one could optimize transducer placement and determine signal path transfer functions. It is felt, however, that development of an analytical model is not justified, that transducer location can be selected by trial and error. Recommended locations are flanges near the struts which support the bearing housings.

Mounting of the accelerometer is of equal importance. There is no point in having a large accelerometer natural frequency if high frequencies cannot be transmitted through the mount. Still thinking in terms of case mounting, it would be best if the accelerometer could be bonded directly to an exterior flange. This not being possible, a small solid accelerometer block which is bolted to the flange should be used. Aluminum is recommended since the modulus to weight ratio is about the same as that for steel and rigidity, not strength,

is the important factor. Calculation of the mount natural frequency is difficult because effective lengths are not known and the boundary conditions are less than ideal--block dimensions should simply be kept as small as possible.

Operating Conditions

Operating conditions are bound to have a significant influence on the monitored vibration. Sensitivity of the various discriminators to operating conditions must be determined. Use of a data file might be helpful in this regard, if it existed.

Implant Program

This author remains skeptical about the possibility of detecting a main engine bearing defect through case acceleration monitoring. Nevertheless, the scheme discussed in the Bearing section of this report should be tried. Such data manipulation, however, would be useless unless a defect was present. It is recommended that a cooperative project with either OC-ALC or SA-ALC be undertaken. A defective bearing should be implanted and test data gathered under whatever operating conditions are available at the Air Logistics Center. The presence of a known defect justifies experimentation with accelerometer location and orientation in an attempt to isolate the signal. Use of both radial and longitudinal accelerometer orientations, mounted on various flanges at which the structure between the bearing and transducer is as stiff as possible should be investigated. Without a more complete set of engine drawings than what has been made available, a more specific recommendation for accelerometer location cannot be made.

Multiple Pure Tone/Blade Damage

Statements have been made in the literature that the spectral shape of the MPT is critically dependent upon the uniformity of blade spacing. If these statements are correct, this suggests that the MPT spectrum might be of use in detection of minor blade damage. Experimental data should be collected to substantiate this. In particular, it should be determined whether or not the MPT spectrum

is repeatable for a given engine under identical operating conditions. If it is repeatable, then its sensitivity to changes in operating conditions should be investigated and defects must be implanted to determine their effect on the MPT spectra. If their effect is significant, then variation in MPT spectra between engines should be investigated to determine whether a generic baseline may be established or custom baselines are required.

Development of Specific Techniques

The following ideas are not in keeping with the original intent of this study, i.e. use of non-obstrusive diagnostic techniques, but appear to merit further development.

Resonant Technique/Dipstick

In the event of failure of the recommended scheme to detect a bearing defect, use of a "dipstick" to provide a direct mechanical path between the bearing and the external transducer should be considered. This would require engine modification but may not be so extensive that it could not be accommodated, particularly at the design stage. A primary advantage of such a scheme is that it would be insensitive to other sources of excitation. It might then be possible to take advantage of discriminators based on probability density functions, such as Kurtosis, rather than just the spectrum. Further, it has been observed that speed variations have not caused large changes in distressed bearing signal magnitudes (refer to equation (1)). Once the information carrying resonance has been determined, it might be used over the entire operating speed range. Some preliminary calculations are included in Appendix B.

Perturbation

Torsional oscillations are rarely discussed in terms of diagnostics. This is probably because angular acceleration is difficult to measure and the defects of interest provide little torsional excitation. Nevertheless, it would seem that defects such as fatigue cracks in a turbine disk or perhaps even in a blade would change the torsional frequency response and impulse response.

It is well known that when a linear system is subjected to white noise excitation, the cross correlation function between the input and response is the same as the impulse response. The difficulty with this idea is providing a continuous torsional perturbation as input. A recent article by Cottingham [22] discusses the successful use of pseudo-random binary noise (PRBN) as a small continuous perturbation in fuel flow to measure various engine dynamic response parameters. These parameters have involved control systems and the corresponding frequency response was limited to very low frequencies (≤ 10 HZ). It is recommended that an analytical model of the engine be developed to display its torsional response and determine the range of excitation frequencies required for use of this technique. Also, the use of a PRBN perturbation in fuel flow should be investigated to determine whether its spectrum can be extended to cover the required range. Other means of inducing a continuous random torsional disturbance should be sought.

Cross-Correlation with Stored Version of Signal

Other well known techniques exist for the extraction of a periodic signal buried in extraneous noise, namely auto correlation. This technique was not suggested because other periodic components are present besides the one of interest. However, if the signal of interest is known, then cross-correlation is an even more powerful tool. The total waveform consisting of the desired signal plus noise is cross-correlated with a stored version of the signal. An implant program would be required to determine a proper version of the signal to be stored. Perhaps all fan, compressor and turbine blades can be removed and the rotor driven externally with a defective bearing in place. Without the blade, the MPT (and the case resonance they excite) will not be present and a reasonable stored version of the signal can be recorded. Likely a family of such signals will be required but the number of different signals to be stored should not be prohibitive. It is recommended that feasibility of this scheme be investigated.

REFERENCES

1. Volin, Rudolph H., "A Review of Mechanical Signature Analysis", Proceedings--Institute of Environmental Sciences, 1978, pp. 357-362.
2. Mitchell, J. S., "Monitoring Machinery Health--I, II, III, IV", Power, March, May, July, August, 1977.
3. McTasney, R., A. R. Rio and W. A. Troha, "Turbine Engine Automated Trim Balancing and Vibration Diagnostics", ASME 78-GT-129, April, 1978.
4. Faneule, F., "Turbine Engine Automated Trim Balancing and Vibration Diagnostics, Volume II", Final Report, PRAM Project No. 34276-02, MTI 79-TR14, February, 1979.
5. Houser, D. R. and M. J. Drosjack, "Vibration Signal Analysis Techniques", USAAMROL-TR-73-101, December, 1973, AD 776397.
6. Murphy, J. A., "Diagnostic System Requirements for Helicopter Propulsion Systems", Journal of Aircraft, Volume 15, No. 6, June, 1978, pp. 333-338.
7. Pickett, G. F., "Prediction of the Spectral Content of Combination Tone Noise", Journal of Aircraft, Volume 9, September, 1972, pp. 658-663.
8. Vaidva, P. G. and K. S. Wang, "Nonlinear Resonance as the Cause of Multiple Pure Tones", Journal of Aircraft, Volume 15, August, 1978, pp. 526-533.
9. Feiler, C. E. and E. W. Conrad, "Fan Noise from Turbofan Engines", Journal of Aircraft, Volume 13, February, 1976, pp. 128-134.
10. Babkin, A. S. and J. J. Anderson, "Mechanical Signature Analysis of Ball Bearings by Real Time Spectrum Analysis", Journal of Environmental Sciences, January/February, 1973, pp. 9-17.
11. Braun, S. and B. Datner, "Analysis of Roller/Ball Bearing Vibrations", Transactions of the ASME, Journal of Mechanical Design, Volume 101, January, 1979, pp. 118-125.
12. Garg, R. H., et. al., Machinery Vibration Seminar Course Notes, General Technology Incorporated, June, 1978.

13. Braun, S., "The Extraction of Periodic Waveforms by Time Domain Averaging", *Acustica*, Volume 32, No. 2, 1975, pp. 69-77.
14. Dyer, D., and R. M. Stewart, "Detection of Rolling Element Bearing Damage by Statistical Vibration Analysis", *Transactions of the ASME, Journal of Mechanical Design*, Volume 100, April, 1978, pp. 229-235.
15. Remmers, E. P., "Gear Mesh Excitation Spectra for Arbitrary Tooth Spacing Errors, Load and Design Contact Ratio", *Transactions of the ASME, Journal of Mechanical Design*, Volume 100, October, 1978, pp. 715-722.
16. Turbine Engine Rotor Dynamic Evaluation, Volume 1, AFAPL-TR-76-81, January, 1978.
17. Cunningham, R. E., "Steady-state Unbalance Response of a Three-Disk Flexible Rotor on Flexible, Damped Supports", *Transactions of the ASME, Journal of Mechanical Design*, Volume 100, July, 1978, pp. 563-573.
18. Burton, R. A., S. R. Kilapadti and S. R. Heckmann, "Modeling of Turbine Blade Tip Contact", *Transactions of the ASME, Journal of Engineering for Power*, October, 1976, pp. 435-440.
19. Den Hartog, J. P., Mechanical Vibration, 4th Edition, McGraw-Hill, 1956
20. Alford, J. S., "Protecting Turbomachinery from Self Excited Rotor Whirl", *Transactions of the ASME, Journal of Engineering for Power*, October, 1965, pp. 333-344.
21. Barschdorff, D., "Theory of Periodic Turbomachine Noise and Determination of Blade Damage from Noise Spectrum Measurements", AGARD-CP-165 on Diagnostics and Engine Condition Monitoring, April, 1974.
22. Cottingham, R. V. and C. B. Pease, "Dynamic Response Testing of Gas Turbines", *Transactions of the ASME, Journal of Engineering for Power*, Volume 101, January, 1979, pp. 95-100.
23. Darlow, M. S., et. al., "Application of High Frequency Resonance Techniques for Bearing Diagnostics in Helicopter Gearboxes", Prepared for USAAMRDL, October, 1974, AD/A-004 014.

Appendix A
Bearing Pass Frequencies

Each of the references [7, 8, 9, 11] present formulae for the repetition rate of impacts resulting from a defect in the inner race, outer race or roller. Comparison of these formulae reveal the presence of several confusing discrepancies due to typographical errors. For that reason, their derivation is presented here.

Assuming no slipping at the point of contact of the ball with the races, a ball or roller bearing can be analyzed kinematically like an epicyclic gear train. Figure A-1 defines the symbology used in the following analysis. The angular velocities are first expressed relative to the ball carrier

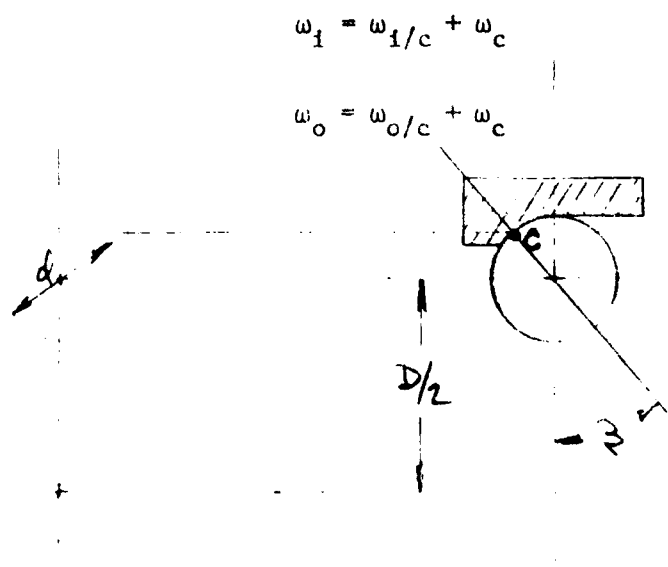


FIGURE A-1

wherein

- D = pitch diameter
- d = ball diameter
- β = contact angle

C = point of contact

ω_o = angular velocity of outer race

ω_i = angular velocity of inner race

ω_c = angular velocity of ball carrier

Transposing ω_c and dividing the first equation by the second equation leads to

$$\frac{\omega_i - \omega_c}{\omega_o - \omega_c} = \frac{\omega_{i/c}}{\omega_{o/c}} = \left(\frac{\omega_i}{\omega_o} \right)_c$$

The reason for performing this manipulation was so that the right-hand side, RHS, can now be evaluated as if it were a simple gear train. The effective ball diameter is now $d \cos \beta$.

$$\left(\frac{\omega_i}{\omega_o} \right)_c = - \frac{D + d \cos \beta}{D - d \cos \beta}$$

The negative sign means that the inner and outer races rotate in opposite sense relative to the carrier.

Now define $\omega_r = \omega_{i/o} = \omega_i - \omega_o$ to be the angle velocity of the inner race relative to the outer race.

$$\frac{(\omega_r + \omega_o) - (\omega_{c/o} + \omega_o)}{\omega_o - (\omega_{c/o} + \omega_o)} = \text{RHS}$$

In terms of ω_r and $\omega_{c/o}$ the angular velocity of the outer race ω_o does not appear and it is helpful for purposes of visualization to let the outer ring be fixed. Thus,

$$\frac{\omega_r - \omega_{c/o}}{-\omega_{c/o}} = - \frac{D + d \cos \beta}{D - d \cos \beta}$$

Solving for the angular velocity of the ball set (carrier) relative to the outer race

$$\omega_{c/o} = \frac{\omega_r}{2} \left(1 - \frac{d}{D} \cos \beta \right)$$

A localized defect in the outer race would be impacted by each of the N balls in every revolution of the ball set relative to the outer race. Frequency associated with an OUTER RACE DEFECT would be

$$f_o = \frac{N}{2} f_r (1 - \frac{d}{D} \cos \beta) \quad (A-1)$$

wherein

$$f_r = \frac{RPM_1 - RPM_o}{60}$$

Frequencies associated with a defect in the inner race can be expressed in a similar way except that the angular velocity of the carrier relative to the inner race is needed.

$$\begin{aligned} \omega_c &= \omega_{c/i} + \omega_{i/o} + \omega_o \\ \omega_{c/o} &= \omega_c - \omega_o = \omega_{c/i} + \omega_r \\ \omega_{c/i} &= \omega_{c/o} - \omega_r \\ \omega_{c/i} &= \frac{\omega_r}{2} (1 - \frac{d}{D} \cos \beta) - \omega_r \\ \omega_{c/i} &= -\frac{\omega_r}{2} (1 + \frac{d}{D} \cos \beta) \end{aligned}$$

Disregard the negative sign. Each of the N balls impacts a defect in the inner race once per relative revolution, therefore

$$f_i = \frac{N}{2} f_r (1 + \frac{d}{D} \cos \beta) \quad (A-2)$$

For frequencies associated with a ball defect, compute the angular velocity of the ball relative to the ball carrier. For each such revolution the defect will have contacted both inner and outer races. For this we need the arcs of contact described during unit time. Refer to Figure A-2.

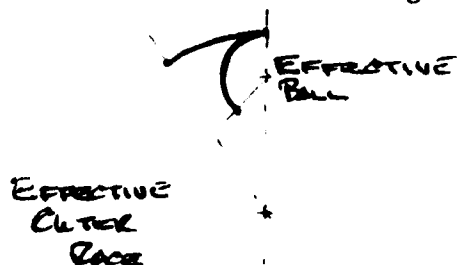


FIGURE A-2

Since the arc lengths are equal,

$$(D + d \cos \beta) \omega_{c/o} = (d \cos \beta) \omega_{b/c}$$

Solving for the angular velocity of the ball relative to the carrier.

$$\omega_{b/c} = \frac{\omega_r}{2} \frac{D}{d \cos \beta} (1 - (\frac{d}{D})^2 \cos^2 \beta)$$

Therefore frequencies associated with a ball defect are

$$f_b = \frac{D}{d \cos \beta} f_r (1 - (\frac{d}{D})^2 \cos^2 \beta) \quad (A-3)$$

It should be noted that the $\cos \beta$ factor in the denominator of equation (A-3) is not present in any of the cited articles. Contact angles are nominally in the neighborhood of 20° so this error leads to more confusion than anything else. It should be pointed out that contact angle depends upon the bearing geometry but that only its initial value is known, its actual value being dependent upon assembly methods and thrust loads as well. The same formulas hold for roller bearings with $\beta = 0$.

Appendix B

Resonant Structure/Dipstick

Vibration at the bearing as depicted in Figure 3 and equation (1) consists of the ringing of some structural mode - perhaps the outer race of the bearing itself. A study of the natural modes and frequencies of various bearings used in helicopters has been made by MTI [23]. The calculated resonant frequencies ranged from 1 KHZ to 30 KHZ. Good correlation was achieved between theoretical and experimental values of natural frequency. They were unable to predict, however, which mode would be excited by the distressed bearing. It is not yet well understood why some resonances are excited and others are not. Experimentally, the stronger resonances appeared to have frequencies in the range 12 KHZ - 24 KHZ. The characteristic frequency ω_c of equation (1) can therefore be expected to be of this range.

Feasibility of design of a "dipstick" to provide a direct mechanical path from the bearing to an external transducer is investigated here. It would be ideal for the dipstick/bearing/bearing housing to have a characteristic frequency in the same range as before because it has been observed that speed variations have not caused large changes in defect signal magnitudes and once the information carrying resonance has been determined, it could be used over the entire operating speed range. Since the dipstick length must be 16" to 18" this may or may not be possible. A combined theoretical and experimental study would be required to verify the feasibility.

It is felt that a resonant structure which can be excited by the defect signal should be used because it would be least sensitive to an unwanted signal. It might be necessary to tune the resonant frequency of the dipstick system to the bearing pass frequency and admit that it can be used only at discrete rotor speed.

If the dipstick could be modeled as a uniform rod which is fixed at one end (the bearing) and free at the other (the transducer), then its natural frequency for longitudinal vibration will be [19]

$$\omega = \frac{N\pi}{2L} \sqrt{\frac{E}{\rho}} \quad N = 1, 3, 5, \dots \quad (B-1)$$

wherein ω = circular natural frequency
 E = modulus of elasticity
 L = dipstick length
 ρ = mass density

Assuming that the material is steel this reduces to $fL = 50.66 (10^3)$. If $L = 18"$, then $f = 2814$ HZ. The greatest bearing pass frequency for the F100 engine is $17.3 N_2/60$. Thus, if $N_2 = 9761$ rpm, the bearing pass frequency will coincide with the resonant frequency of the dipstick. The minimum bearing pass frequency for bearings on the high speed rotor is $12.22 N_2/60$, which would require that $N_2 = 13839$ rpm. These speeds can be reduced by attaching a concentrated mass at the free end of the dipstick, still remaining within the operating range.

For the low speed rotor, the maximum and minimum bearing pass frequencies are $12.175 N_1/60$ and $7.881 N_1/60$ respectively and a concentrated mass at the free end of the dipstick would definitely be required to reduce the first natural frequency to the operating range. Assuming that N_1 maximum is 9000 rpm, then the dipstick frequency should be

$$f = (7.881)(9000)/60 = 1182 \text{ HZ}$$

The rotor speed required at the other bearing pass frequency would be $N_1 = 5825$ rpm, which is well within the operating range.

The characteristic equation in this case is

$$\beta \tan \beta = \frac{M_{\text{rod}}}{M_{\text{concentrated}}}$$

wherein
$$\beta = \frac{\omega L}{\sqrt{E/\rho}}$$

For a frequency of 1182 HZ, dipstick length of 18" and weight of 0.25 pounds a concentrated weight of 0.488 pounds is required.

Just on the basis of providing a mechanical path for the distressed bearing signal, use of a dipstick appears to be feasible, but requires further theoretical and experimental study and investigation of compatibility with spatial neighbors.

1979 USAF - SCEEE SUMMER FACULTY RESEARCH PROGRAM

Sponsored by the

AIR FORCE OFFICE OF SCIENTIFIC RESEARCH

Conducted by the

SOUTHEASTERN CENTER FOR ELECTRICAL ENGINEERING EDUCATION

FINAL REPORT

GOAL PROGRAMMING: FUNCTIONAL DECOMPOSITION AND
CONSIDERATION WITHIN AN INTEGRATED COMPUTER-AIDED
MANUFACTURING DECISION SUPPORT SYSTEM (IDSS)

Prepared by:	Nicholas G. Odrey
Academic Rank:	Assistant Professor
Department and University:	Department of Industrial Engineering University of Rhode Island
Research Location:	A.F. Materials Laboratory (LT) Wright-Patterson AFB, Ohio
USAF Research Colleague:	Mr. Richard J. Mayer
Date:	August 10, 1979
Contract No:	F49620-79-C-0038

GOAL PROGRAMMING: FUNCTIONAL DECOMPOSITION AND
CONSIDERATION WITHIN AN INTEGRATED COMPUTER-AIDED
MANUFACTURING DECISION SUPPORT SYSTEM (IDSS)

by

Nicholas G. Odrey

ABSTRACT

Intrinsic to the Integrated Computer-Aided Manufacturing (ICAM) Air Force program is the incorporation of various analytical techniques to the architectures derived for manufacturing from developed methodologies. This report presents the methodology of the mathematical programming technique termed goal programming and illustrates a tutorial example of the technique using accepted ICAM Definition (IDEF) methodology. Consideration is given to the implementation of the goal programming technique to the ICAM Decision Support System (IDSS). A general functional model decomposition is also presented for the goal programming technique.

ACKNOWLEDGMENTS

The author would like to thank the Air Force Systems Command, Air Force Office of Scientific Research, and the Southeastern Conference of Electrical Engineering Education for providing him the opportunity to spend an extremely interesting and professionally expanding summer at the Air Force Materials Laboratory, Wright-Patterson Air Force Base.

The author would particularly like to thank Mr. Richard J. Mayer, Mr. Gerald Shumaker, and Mr. Dennis E. Wisnosky of the Computer Integrated Manufacturing Branch for introducing him to the ICAM program and providing an extremely good and professionally interactive working atmosphere. Thanks are also due to the other members of the ICAM program office for numerous informative discussions.

I. INTRODUCTION:

The problems addressed in this project report pertain to the Air Force program on Integrated Computer - Aided Manufacturing (ICAM). The ICAM program incorporates elements of design, information systems, manufacturing technology, logistics management, and human factors into an integrated computer based system. Specifically, ten major thrust areas exist for the ICAM program. These thrust areas range from the architecture or model of manufacturing, to the data base-data automation systems, to systems for planning and group technology, to the simulation, modeling, operation research aspects, and to the shop-floor systems and support activities (30). Various benefits are expected to be derived from the ICAM program. Pay - offs will not only be in the "hard" technical areas of manufacturing technology but also in aspects such as organizational management. Significant beneficial contributions are expected for the nation, its defense and security, higher education institutions, and in overall national productivity gains with a strengthening of the nation's international competitive position.

Intrinsic to the ICAM program is the definition and implementation of various analytical techniques to the architectures derived for manufacturing from developed methodologies. Such methodologies are based on ICAM Definition (IDEF) Methodologies which are currently in the developed, redesign or developmental stages (1, 26). The analytical techniques are a part of the ICAM Decision Support System (IDSS) (2,3,4), an ongoing project with needs to incorporate additional techniques, further expand (decompose) existing analytical techniques following IDEF methodologies, build composite models (with a goal to reach a level of commonality between models), and integrate the techniques with shop-floor (manufacturing) operations. The primary problem addressed in this project report is to introduce the methodology of the mathematical programming technique termed goal programming and to illustrate a working model of the technique using accepted IDEF functional methodology.

In traditional mathematical programming, the assumptions are such that a function is clearly an objective relationship or a constraint relationship. In reality, it is very difficult to make such a dichotomous distinction. Typically, in reality, a decision maker attempts to achieve a set of goals to the fullest possible extent while subjected to conflicting goals, limited resources, substandard or incomplete information, and constrained personal ability to analyze the complex environment. This report on goal programming presents the fundamental mathematical structure of goal programming, and an IDEF Version 0 (IDEF₀) model of the goal programming methodology.

The mathematical technique of goal programming is a procedure that allows simultaneous solution to a system of complex multiple objectives, whether the problem deals with a single goal or with multiple subgoals. Priorities are placed on higher-order goals and lower-ordered goals with lower ordered goal considered only after the higher-order goals are satisfied or have reached their desired limit.

The concept of goal programming was first introduced in 1961 in an investigation of unsolvable linear programming problem. As stated then by Charnes and Cooper (13).

Closely related to the analysis of contradictions in unsolvable problems is the issue which will be called "goal attainment". Management sometimes sets such goals even when they are unattainable within the limits of available resources, for a variety of reasons. For example, such goals may be established to provide incentives or to judge accomplishments, or they may be used as a safeguard to ensure that long-run considerations are not obliterated by immediately attainable objectives, etc. Any constraint incorporated in the functional will be called a "goal". Whether goals are attainable or not, an objective may then be stated in which optimization gives a result which comes "as closely as possible" to the indicated goals.

In goal programming, one approach is to refer to objectives as being the result of three classes: (1) decision-maker desires (or aspirations), (2) limited resources, and (3) "legal" restrictions i.e. any other explicit or implicit restrictions placed on the choice of the decision variables. The third class of "legal" restrictions typically would include restrictions such as a physical requirement that certain variable(s) be nonnegative, or a contractual requirement(s) that specifies that certain variables equal or exceed a certain minimum value.

Various authors have contributed to the development of goal programming and studies have shown the mathematical feasibility of stochastic goal programming (14). A brief sampling of references in the field are given at the end of this report. To identify just a few applications, goal programming has been considered in capital budgeting (17), manpower planning (10), multiple-response simulation (8), aggregate planning of production and workforce (15), Input-Output modeling (9), and curve and response surface fitting (21). The reader is referred to two excellent reviews of goal programming by Ignizio (19) in 1978 and by Charnes and Cooper in 1977 (12). Lee's text (23) presents cases of goal programming applications, with the production planning study being of particular interest from the ICAM viewpoint.

II. OBJECTIVES OF THE RESEARCH EFFORT

The objectives of this project were:

- (1) To develop a functional model via the Structured Analytical Design Technique (SADT) for the methodology of goal programming within the ICAM program.
- (2) To investigate procedures for implementation of the goal programming methodology to the manufacturing engineering area.
- (3) To aid in the review of industrial efforts in functional modeling pertaining to Group Technology Classification and Coding (GTCC) systems.

- (4) To aid in the development of a description dynamics model and a performance dynamics (simulation) model.
- (5) To initialize a literature review on Lionieff input-output modeling techniques and to initiate investigation to its feasibility as a hierarchical structure manufacturing econometric technique within ICAM.
- (6) To initiate development of a composite statistical decomposition with emphasis on experimental design techniques to drive simulation models of the ICAM Decision Support System (IDSS).

Due to space limitations and for consistency, the first two objectives are the subject of this report. The latter two objectives are still in initial research and developmental stages and have been recommended by the ICAM program office for continuing investigation.

III BASIC CONCEPTS OF GOAL PROGRAMMING

Goal programming has been viewed as an "extension" of linear programming (LP) and as a general framework from which traditional single-objective models such as LP appear as special cases. Since goal programming notation has not been standardized, the notation and format presented in this report will follow the work of Ignizio (18). The following tutorial example is used to illustrate the "common" linear programming formulation which then serves as a basis to introduce the basic concepts of goal programming:

Example Problem: A company manufacturing two types of products. The profit of product 1 is \$5/unit and of product 2 is \$4/unit. The maximum weekly demand is estimated to be 3000 parts of product 1 and 2000 parts of product 2. Both products have material requirements which can be satisfied "in - house" at a maximum rate of 4000 parts/week, irrespective of the specific product.

A linear programming formulation would typically state a single objective: maximization of profit. Decision variables (x_1, x_2) could be specified as; x_1 = number of units produced of product 1 per week; x_2 = number of units produced of product 2 per week where, for simplicity, x_1 and x_2 are assumed to be continuous variables. A linear programming model would then be:

$$\begin{aligned}
 &\text{maximize } z = 5x_1 + 4x_2 && (\text{profit/week}) \\
 &\text{such that: } x_1 + x_2 \leq 4000 && (\text{mat'l req's}) \\
 & && x_1 \leq 3000 \quad (\text{Product 1 demand}) \\
 & && x_2 \leq 2000 \quad (\text{Product 2 demand}) \\
 & && x_1, x_2 \geq 0
 \end{aligned} \tag{1}$$

As an introduction to goal programming formulation, the problem can be considered from a different point of view. Instead of stating a single objective to maximize profit, suppose that the company has two goals: (1) Obtain a profit of \$10,000/week, (2) To minimize the purchase of materials from outside the company. An alternative linear programming model for this example could be formulated to find x_1 and x_2 (defined as previous) to

$$\begin{aligned}
 &\text{minimize } z = n_1 + p_2 \\
 &\text{such that: } 5x_1 + 4x_2 + n_1 - p_1 = 10000 \\
 & && x_1 + x_2 + n_2 - p_2 = 4000 \\
 & && x_1 \leq 3000 \\
 & && x_2 \leq 2000 \\
 & && x_i, n_i, p_i \geq 0 \quad (i=1,2)
 \end{aligned} \tag{2}$$

Note that in this formulation the first two constraints represent the company's two goals. By minimizing n_1 , we are effectively attempting to minimize the amount by which we fail to achieve the profit goal. Similarly, by minimizing p_2 , we are attempting

to minimize the amount of materials purchased from outside the company. The above model was chosen to demonstrate an error that would occur in subsequent formulation of a goal programming approach if the same objective function is retained. This point will be more fully elaborated upon later in this section of the report.

To develop the example from a goal programming viewpoint, the goal programming functional relationships for product demand must also be specified and formulated, prioritized objectives considered, and an achievement function formulated. These concepts are more fully developed and presented in the following paragraphs.

Typically, with goal programming formulation, the functional relationships are of the form

$$f_i(\bar{x}) + n_i - p_i = b_i \quad (i=1,2,\dots,m) \quad (3)$$

where the goals or objectives, G_i , are expressed as a function of the decision variables, i.e., $G_i = f_i(\bar{x})$ for $i = 1, \dots, m$ goals. Thus, for our example, $\bar{x} = (x_1, x_2)$ and the goal G_1 = profit per week (the first objective function) is expressed as follows:

$$G_1 = 5x_1 + 4x_2 \quad (4)$$

In goal programming, it is important to note that every objective function must have an associated value on the right-hand side, i.e. the b_i 's ($i=1,\dots,m$). The associated b_i value for the goal G_i reflects the value that $f_i(\bar{x})$ must satisfy, exceed, or be less than ($f_i(\bar{x}_i) = b_i$). To reflect the underachievement or overachievement of an objective function, negative (n_i) and positive (p_i) deviation variables are introduced. For any choice of decision variables (x_1, x_2), the value of n_i reflects the negative deviation from b_i , whereas the value of p_i reflects the positive deviation. Thus, the first objective function (equation 4) for our example is fully expressed as

$$5x_1 + 4x_2 + n_1 - p_1 = 10000 \quad (5)$$

where $b_1 = 10,000$. Similarly, to obtain the functional relationship format of equation 3, the second objective function is expressed as

$$x_1 + x_2 + n_2 - p_2 = 4000 \quad (6)$$

Following this format, the last two demand constraints for products 1 and 2 of the example problem are expressed respectively as

$$x_1 + n_3 - p_3 = 3000 \quad (7)$$

$$x_2 + n_4 - p_4 = 2000 \quad (8)$$

In many cases, objectives must be satisfied. Such objectives are termed absolute objectives. In such cases, either p_1 or n_1 must equal zero. Consider, for example, the second objective function for material requirements given by equation (6). If the decision were to set $(x_1, x_2) = (2500, 2000)$, then we would produce 4500 units of products 1 and 2 per week and the positive deviation would be $p_2 = 500$: If only "in - house" material can be used (no supplier materials available to make the products), such that it was not feasible to produce more than 4000 products per week, then the above solution would not be implementable. Thus, the only feasible solution must have $p_2 = 0$, and in this case the objective is an absolute objective.

An additional concept is the determination of a "target value" for a given b_1 . As an example, consider the profit per week goal, G_1 , represented by equation (4). The question that can arise is what value of b_1 should be placed on the right-hand-side of the equation. Naturally, from a strict mathematical sense, unlimited profits would be desirable, but from a realistic decision-making viewpoint, the value should reflect an upper bound (or target value) for the objective under consideration. Thus, if in the opinion of the decision-maker, it would be impossible to expect a weekly profit greater than \$10,000 for the example problem considered, then this value would serve as the right-hand-side value, b_1 such that

$$G_1 = 5x_1 + 4x_2 = 10000$$

or, in goal programming format, and as previously expressed by equation (5),

$$5x_1 + 4x_2 + n_1 - p_1 = 10000$$

Values of (x_1, x_2) would then be selected so as to minimize the value of n_1 , the underachievement for this goal.

Fundamental to the goal programming approach is the concept of prioritized levels for the objective functions. The distinction is made between prioritized absolute objectives which must be assigned priority level one, and the remaining nonabsolute objectives sets which are grouped and assigned respective priority levels. Of importance to note is that within any given priority level the objective must be commensurable, i.e. have a common unit of measure. Additionally, a key assumption within goal programming is that preemptive priorities, P , can be established for each objective or groups of objectives by the decisions maker(s) and the analyst(s). The highest priority is denoted as P_1 , the next as P_2 ($P_1 P_2$) regardless of any multiplier associated with P_2 .

The preemptive priority concept has served as a point of contention of investigators of the goal programming approach (which need not include the concept of preemptive priorities). It seems that other approaches are both encumbered by more restrictive assumptions and are less efficient. One such other approach is an effort to find the "nondominated solution set" (i.e. most efficient set, etc.). As noted by Ignizio (18),

.... While the author (Ignizio) does not personally believe that such methods (nondominated solution set) are as practical or efficient as the goal programming approach...it is still of interest to consider... this related field of multiple objective decision analysis (it should be noted that multiple objective methods that do not employ preemptive priorities are not, in the strict sense of the term, goal programming)..

As previously noted, the preemptive priority concept assumes that objectives may be arranged in prioritized ordered sets with

priority assignments such that $P_k \gg P_{k+1}$. It should be noted that preemptive priorities do not represent numbers, are never replaced by numbers, and the attainment of objectives at any specific priority level is immeasurable preferred (\gg) to the attainment of an objective set at any lower priority level. The assumption of preemptive priorities, although it may not always be a valid assumption, has been found to be applicable to a significantly large number of real world cases. Methodology does exist for objective rankings, weighing factor assignments to objectives within priority levels, etc., but are beyond the scope of this report.

Important to the practical implementation of the goal Programming methodology is the determination, structuring and prioritization of input goals. Current ICAM contractual efforts (3) on decision - alternatives and their relation to the ICAM architecture of manufacturing have noted (to identify just two) activity X Goal matrices and Goals X Performance Measures matrices as a means of determining how accurate goals are met, etc. Such implementation considerations are beyond the scope of this report. One possible suggested framework is that of the Interpretive Structural Modeling (ISM) (25) technique. Such a technique has considered a hierarchical structure for decision analysis (28). Requirements, some accomplishments, and the basic mathematics of the technique have been given in the text by Sage(27).

The final step in the goal programming modeling formulation is the attainment of the achievement function. In general, the achievement function (or vector) has the following form (18):

$$\text{minimise } \bar{a} = \{P_1[g_1(\bar{n}, \bar{p})], \dots, P_K[g_K(\bar{n}, \bar{p})]\} \quad (9)$$

where $g_j(\dots)$ is a linear functional of the deviation variables, P_j is the priority associated with g_j , and $j=1,2,\dots,K \leq M$, i.e.

the total number of objectives equals M and are greater than or equal to the number of preemptive priorities. Thus, the achievement vector, \bar{a} , has a dimension equal to the number of preemptive priority levels among the objectives and is an ordered vector since the subscripts, j , of g_j associate the respective priority levels.

Alternately, the preceding general form for the achievement function can also be expressed as

$$\text{minimize } \bar{a} = \{g_1(\bar{n}, \bar{p}), \dots, g_K(\bar{n}, \bar{p})\} \quad (10)$$

or

$$\text{minimize } \bar{a} = (a_1, a_2, \dots, a_K) \quad (11)$$

where $a_j = g_j(\bar{n}, \bar{p})$, $j = 1, 2, \dots, K$. Such expressions are sometimes preferred so that there is no misunderstanding associated with the interpretation of the priorities, P_j , associated with the goals, g_j .

To formulate the achievement function, three possibilities are available to minimize a linear function of the deviation variables. It is desired to select the decision variables, \bar{x} , such that $f_1(\bar{x})$:

- (1) is equal or greater than the value of b_1 , or
- (2) equal or less than the value of b_1 , or
- (3) exactly equal to the value of b_1 .

For a typical goal programming objectives function i.e., $f(\bar{x}) + n_1 - p_1 = b_1$ the procedure to obtain the first possibility listed of $f_1(\bar{x}) \geq b_1$ is to minimize the deviation variable, n_1 . For the second case of $f_1(\bar{x}) \leq b_1$, we wish to minimize p_1 , and for the third possibility of $f_1(\bar{x}) = b_1$, the linear function of the deviation variables, $n_1 + p_1$, is minimized. Thus, for any type of goal or constraint, we wish to minimize the nonachievement of the goal constraint by minimizing specific deviation variables or their linear combination.

To properly formulate an achievement function for the example problem given, consider as absolute the objectives (Priority one by

definition) of never exceeding demand. To satisfy such absolute objectives, p_3 and p_4 , the positive deviation variables associated with the objectives are minimized. The second priority is taken to maximize profit (i.e. minimize n_1), and the third priority is taken as minimizing material purchases outside the company (i.e. minimize p_2). The example goal programming model with the achievement function for such a priority structure is expressed as follows:

$$\begin{aligned} \text{minimize } \bar{a} &= \{(p_3 + p_4), (n_1), (p_2)\} \\ \text{such that: } &5x_1 + 4x_2 + n_1 - p_1 = 10000 \\ &x_1 + x_2 + n_2 - p_2 = 4000 \\ &x_1 + n_3 - p_3 = 3000 \\ &x_2 + n_4 - p_4 = 2000 \\ &\bar{x}, \bar{p}, \bar{n} \geq 0 \end{aligned} \quad (12)$$

It should be noted that the formulation of the goal programming model, particularly the prioritization and achievement function formulation, is intrinsically dependent on the analyst's knowledge and understanding of the problem. Such attributes are prerequisite to the proper structuring of the model.

For the original introduction to goal programming formulation as stated by the model given by equation(s) (2), it was pointed out that an error existed in the achievement function formulation. Consider again the original two objectives of the example problem.

- (1) Obtain a profit of \$10,000 week, i.e.,

$$5x_1 + 4x_2 + n_1 - p_1 = 10000$$

- (2) To minimize the purchase of materials from outside the company, i.e.,

$$x_1 + x_2 + n_2 - p_2 = 4000$$

If we interpret the first objective as not rigid, i.e. we aspire

to obtain a level of profit of \$10,000 per week, rather than maximizing profit, we can then minimize n_1 , the negative deviation from goal 1. In essence, the amount by which we underachieve the profit goal is then minimized. Similarly, for the second goal, minimization of p_2 is an attempt to minimize the amount of purchased materials from outside the company. Thus, the model would have (if we considered the goals separately):

$$\text{and} \quad \begin{aligned} \text{minimize } z &= n_1 \\ \text{minimize } z &= p_2 \end{aligned}$$

For the example as given by equation (2), deviation variables were taken from both goals and the linear sum, $n_1 + p_2$, minimized. As previously noted the deviation variables associated with different goals must be commensurable, i.e. it must be possible to find weighting factors such that a meaningful summation is possible. The example given is a case of noncommensurable deviation variables and as such is not implementable.

In summary, a linear goal programming model has the following general formulation:

$$\text{Find } \bar{x} = (x_1, x_2, \dots, x_j)$$

so as to

$$\text{minimize } \bar{a} = \{[g_1(\bar{n}, \bar{p})], \dots, [g_k(\bar{n}, \bar{p})]\}$$

such that

$$\sum_{j=1}^J C_{ij} x_j + n_i - p_i = b_i \quad \text{for all } i$$

$$\bar{x}, \bar{n}, \bar{p} \geq 0$$

where C_{ij} is the coefficient of decision variable x_j in the i th objective

The analyst currently has available models and solution techniques for not only linear goal programs (LGP), but also for nonlinear goal programs (NLGP), linear integer goal programs (LIGP), and linear, zero one, goal programs. As noted by Iginizio (19), and particularly for linear goal programming problems,..."all the tools required for sensitivity analysis are available as well as a concept...of duality...."Algorithms and computerized codes do exist and are available for the various types of goal programming formulations.

IV GOAL PROGRAMMING FUNCTIONAL MODEL DECOMPOSITION

A decomposition for the goal programming methodology following the IDEF functional decomposition technique has been given in Appendix A. The viewpoint taken is that goal programming can serve as a general framework from which traditional single-objective models such as linear programming, non-linear programming, etc. appear as special cases. The decomposition given in Appendix A includes a nodal diagram and the functional activity boxes with data flows (arrows) indicated as controls, inputs, outputs, and mechanisms. Given below are the specific nodes of the decomposition and their respective activity definitions. As an illustration of the goal programming functional decomposition methodology, the previous example problem is embedded within the following nodal breakdown. Statements or equations of the example as they pertain to a specific node are given within brackets immediately following the node identification and description. For convenience, the example problem is repeated as follows:

Example Problem: A company manufactures two types of products. The profit of product 1 is \$ 5/unit and of product 2 is \$4/unit. The maximum weekly demand is estimated to be 3000 parts of product 1 and 2000 parts of product 2. Both products have material requirements which can be satisfied "in - house" at maximum rate of 4000 parts/week, irrespective of the specific product.

The goal programming decomposition is as follows:

AO: Do Goal Programming

A1: Formulated Program Objectives

A11: Determine Decision Variables

[x_1 : number of units produced of product 1 per week]

[x_2 : number of units produced of product 2 per week]

A12: Formulate Program Objective Function(s)

A121: List Project Objectives

(a) [Obtain a profit of \$10,000/week]

(b) [Minimize the purchase of materials
from outside the company]

(c) [To never exceed demand]

A122 : List Project Restrictions

A1221: List Resource Restrictions

[4000 parts/wk "in - house"
material availability]

A1222: List Variable Restrictions

(a) [$0 \leq x_1$ (parts/week)]

(b) [$0 \leq x_2$ (parts/week)]

A1223: List Legal Restrictions

[n/a (not applicable)]

Note: A1222 and A1223 are sometimes combined as one node entitled Legal restrictions. With the decomposition as given it is intended to separate the decision variables that satisfy a physical requirement of nonnegativity from contractual "Legal" restrictions.

Note: The purpose of node A123 and subsequent subnode is to attempt to minimize the total number of objectives and to mathematically formulate the left - hand - side of the objective functions. A minimizable solution may exist if one objective dominates another, or objectives considered of minor or negligible importance are eliminated to reduce the number of objectives.

A123: Quantify Minimal Subsystem Objectives

A1231: Identify Subsystems

- a) [Profit: (Obtain a profit of \$10,000/wk)]
- b) [Mat'l requirements: (minimize the purchase of mat'ls from outside the company)]
- c) [Demand: (To never exceed demand)]

A1232: Formulate Subsystem(s) Objective(s) Function(s)

- a) [$G_1 = 5x_1 + 4x_2$ (profit/week)]
- b) [$G_2 = x_1 + x_2$ (Mat'l requirements)]
- c) [$G_3 = x_2$ (Product 1)]
- d) [$G_4 = x_2$ (Product 2)]

A1233: Minimize Objectives within Subsystems

[same as A1232 example with G_3 and G_4 within Demand Subsystem]

A2: Determine Goal Programming

A21: Assign Priority Level(s) to Objective Function(s)

A211: List Minimal Subsystem Objective

[The output list obtained from A1233 is used]

A2111: State Absolute Objectives

[To never exceed demand]

A2112: State Lower - Level Objectives

- a) [Obtain a profit of \$10,000/wk]
- b) [Minimize the purchase of material from outside the company]

A212: Assign Priorities to Subsystem(s) Objective(s)

A2121: Assign absolute priorities

[P_1 : To never exceed demand]

A2122: Group nonabsolute objectives

- a) [Group 1: Obtain a profit of \$10,000/week]
- b) [Group 2: Minimize the purchase of materials from outside the company]

A2123: Assign nonabsolute priorities

- a) [P_2 : Obtain a profit of \$10,000/week]
- b) [P_3 : Minimize the purchase of materials from outside the company]

continuous, identify as linear goal programming model]
i.e.

$$\begin{aligned} \text{minimize } \bar{a} &= \{(p_3 + p_4), (n_1), (p_2)\} \\ \text{such that: } 5x_1 + 4x_2 + n_1 - p_1 &= 10000 \\ x_1 + x_2 + n_2 - p_2 &= 4000 \\ x_1 + n_3 - p_3 &= 3000 \\ x_2 + n_4 - p_4 &= 2000 \\ \bar{x}, \bar{n}, \bar{p} &\geq 0 \end{aligned}$$

A32: Solve Specific Model

[Use existing computer package to obtain solution
and do sensitivity analysis]

V CONCLUSIONS

This brief report has attempted to demonstrate via a tutorial example feasibility of the multiple objective function decision analysis technique known as goal programming within the ICAM Decision Support System (IDSS). Some basic conclusions are as follows:

1. The capability does currently exist to handle multiple objective decision analysis.
2. The concept of prioritized objectives would seem to be a valuable aid in implementation of goal programming to manufacturing scene.
3. The goal programming methodology has been shown applicable to many real - world problems.
4. The goal programming formulation is amenable to the Structured Analysis Design Technique (SADT) methodology.
5. Indications are that the goal programming approach would be of benefit to a Decision Support System.

VI RECOMMENDATIONS

Recommendations for future research and development efforts for integration of goal programming to the integrated computer - aided

manufacturing scene are as follows:

1. To develop an information model (IDEF₁) for the programming methodology.
2. To develop tutorial models including basic graphical solution techniques as instructional aids in presenting the goal programming methodology.
3. To further the literature review and build up examples (case studies) of increasing complexity; reiterate on the Functional and Informational models for further definition and decomposition.
4. To investigate the applicability of Interpretive Structuring Methodology (ISM) or similar techniques as a means of possible implementation of prioritized objectives input.
5. To further develop and refine computer packages of goal programming and tailor them for ICAM.
6. To incorporate the goal programming methodology at various hierarchical levels for industrial decision - makers.
7. To investigate within the IDEF₀ methodology feasibility of goal programming as a global mathematical programming model.
8. To investigate the applicability of goal programming to the engineering design function and to the engineering design/manufacturing engineering interface.

Recommendations pertaining to other investigations initialized but not developed sufficiently enough to be a part of this report are as follows:

1. To investigate the feasibility of Lontieff Input-Output modeling techniques as a basis for overall ICAM hierarchical manufacturing econometric modeling.
2. To develop a composite statistical model with the viewpoint of "driving" simulation models of the manufacturing scene.

REFERENCES

1. _____, "Integrated Computer - Aided Manufacturing (ICAM): Task I - Final Report", AFML - TR - 78 - 148 under contract no. F33615-77-C-501, WPAFB, OH, Nov. (1978)
2. _____, "Integrated Computer Aided Manufacturers Decision Support Systems" Interim report (13 Jan. 1978 through 12 April, 1979) under AFML contract no. F33615-78-C-5114, Volumes I and II, WPAFB, OH, April, (1979)
3. _____, "ICAM Decision Support Systems" Interim report (13 April 1979 through 13 July 1979) under AFML contract no. F33-615-78-C-5114, WPAFB, OH, (1979)
4. _____, "ICAM Decision Support System: Task 3 Final Technical Report (DRAFT)", under AFML contract no. F33615-78-C-5231, WPAFB, OH, Feb. 26, (1979)
5. _____, "Architect's Manual: ICAM Definition Method "IDEF" (Version 0)", SofTech, Inc., Sept., (1978)
6. Ackoff, R.L., Sasieni, M.W., "Fundamentals of Operations Research", John Wiley & Sons, (1968)
7. Beale, E.M.L., "The Significance of Recent Developments in Mathematical Programming" in P.L. Hammer and G. Zoutendijk, "Mathematical Programming in Theory and Practice", New Holland Publishing Co., (1974)
8. Biles, W.E., Swain, J.J. "Optimization of Multiple-response Simulation Models" Proc. of 7th Annual Pittsburgh Conference on Modeling and Simulation, pp 991-996, vol. 8, pt. 2, (1977)
9. Blair, P.D., "Multiobjective Programming and Regional Energy Planning" Proc. of 9th Annual Pittsburgh Conference on Modeling and Simulation, pp. 25-31, vol. 9, pt. 1, (1978)
10. Charnes, A., Nilhaus, R.J. "A Goal Programming Model for Manpower Planning" Management Science Research Report 115, Carnegie - Mellon Univ., Pittsburgh, (1968)
11. Charnes, A., Cooper, W.W., "Goal Programming and Multiple

- Objective Optimizations" Center for Cybernetic Studies Report
CCS - 250, The University of Texas, Austin, (1975)
12. Charnes, A., Cooper, W.W., "Goal Programming and Multiple Objective Optimizations", European Journal of Operational Research, 1, pp 39-54, (1977)
 13. Charnes, A., Cooper, W.W. "Management Models and Industrial Applications of Linear Programming", John Wiley & Sons, Inc., (1961)
 14. Contini, B. "A Stochastic Approach to Goal Programming" Operations Research, pp. 576-586, May-June, (1968)
 15. Goodman, D.A., "A Goal Programming Approach to Aggregate Planning of Production and Workforce", Management Science, vol. 20, No. 12, pp. 1569-1570, Aug., (1974)
 16. Haseman, W.D., Kellner, M.I., "Decision Support Systems: Their Nature and Structure", Proc. of 7th Annual Pittsburgh Conference on Modeling and Simulation, pp. 853-858, vol. 8, pt. 2, (1977)
 17. Hawkins, C.A., Adams, R.A., "A Goal Programming Model for Capital Budgeting", Fin. Mgmt., pp 52-57, 3, (1974)
 18. Ignizio, J.P., "Goal Programming and Extensions" Lexington Books, D.C. Heath and Co., (1976)
 19. Ignizio, J.P. "A Review of Goal Programming: A Tool for Multiobjective Analysis" J. Opl. Res. Soc., pp. 1109-1119, vol. 29, 11, (1978)
 20. Ignizio, J.P., "The Modeling of Systems Having Multiple Measures of Effectiveness" "Proc. of 7th Annual Pittsburgh Conference on Modeling and Simulation", pp 1091-1093, vol. 7, pt. 2, (1977)
 22. Ijiri, Y., "Management Goals and Accounting for Control", Rand - McNally: Chicago, (1965)
 23. Lee, S.M., "Goal Programming for Decision Analysis", Auerbach Publishers, Inc., (1972)
 24. Lee, S.M., Moore, L.J., "Optimizing Transportation Problems with Multiple Objectives", AIIE Trans., vol. 5, no. 4, Dec., (1973)
 25. Malone D.W., "Interpretive Structural Modeling: An Overview and Status Report" Proc. of 6th Annual Pittsburgh Conference on

- Modeling and Simulation, pp. 767-772, vol. 6, pt. 2, (1975)
27. Ross, D.T., "Integrated Computer - Aided Manufacturing (ICAM): Task II - Final Report (Volume II: Technical Foundations for Characterizations)" AFML - TR - 77 - 218, vol. II, under AFML contract no. F33615-77-C-5012, WPAFB, OH, December, (1977)
27. Sage, A.P., "Methodology for Large Scale Systems", McGraw - Hill Book Co., (1977)
28. Sage, A.P., Rajala, D.W., "On Structural Relationships in Decision Analysis" Proc. of 7th Annual Pittsburgh Conference on Modeling and Simulation, pp. 1199 - 1204, vol. 7, pt. 2, (1976)
30. Wisnosky, D.E., "ICAM Program Prospectus" AFML, ICAM Program Office, WPAFB, OH, 1 June (1978)

APPENDIX A

Included within this appendix are the nodal diagram and the corresponding functional decomposition diagrams for the goal programming methodology. The lay-out and syntax of the figures are given following the methodology of the ICAM program.

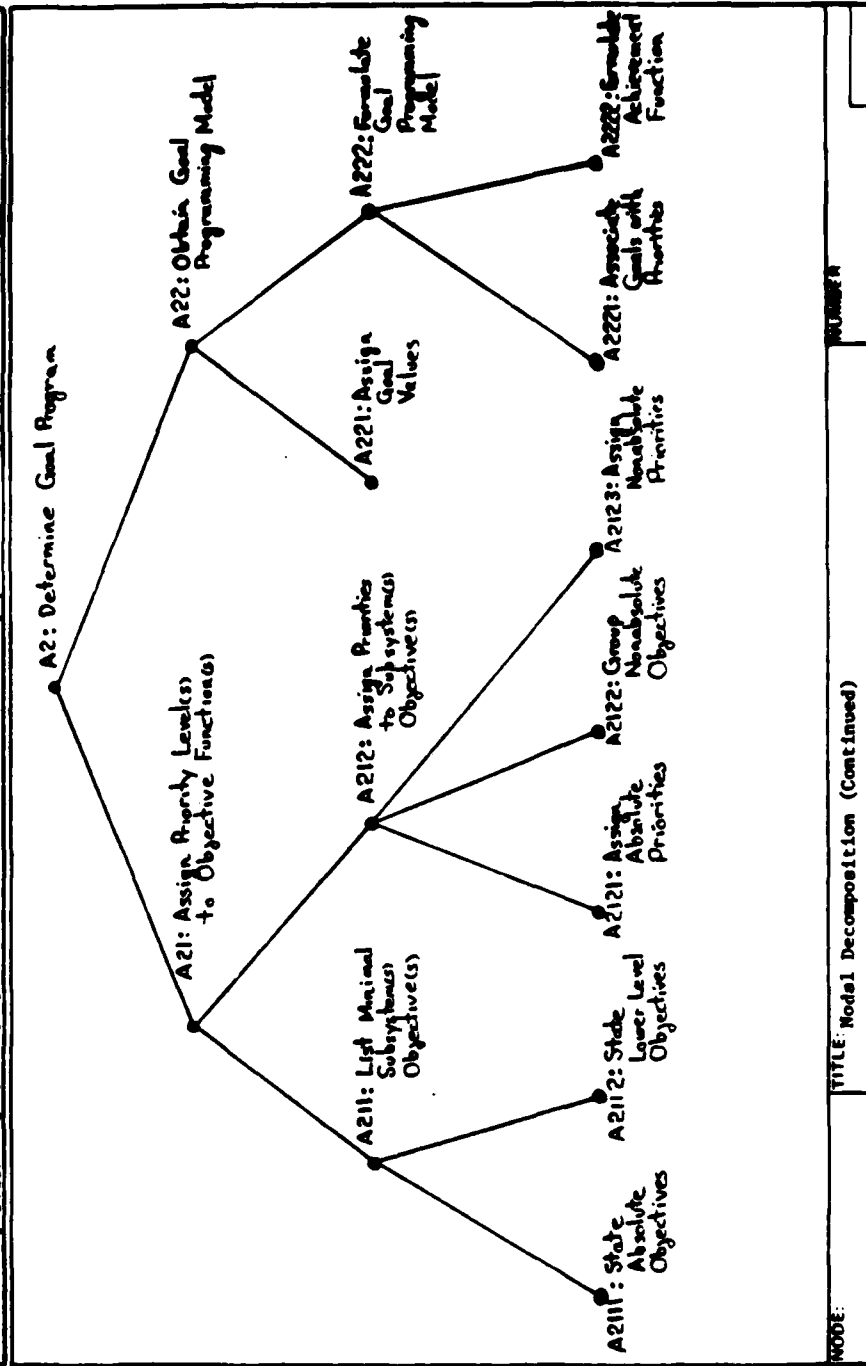
ST 252

USED AT:	AUTHOR: Odrey, N.G. PROJECT: IDSS TASK1/2	DATE: 8/10/79 REV.	WORKING DRAFT RECOMMENDED PUBLICATION	READER	DATE	CONTEXT:
NOTES: 1 2 3 4 5 6 7 8 9 10						


```

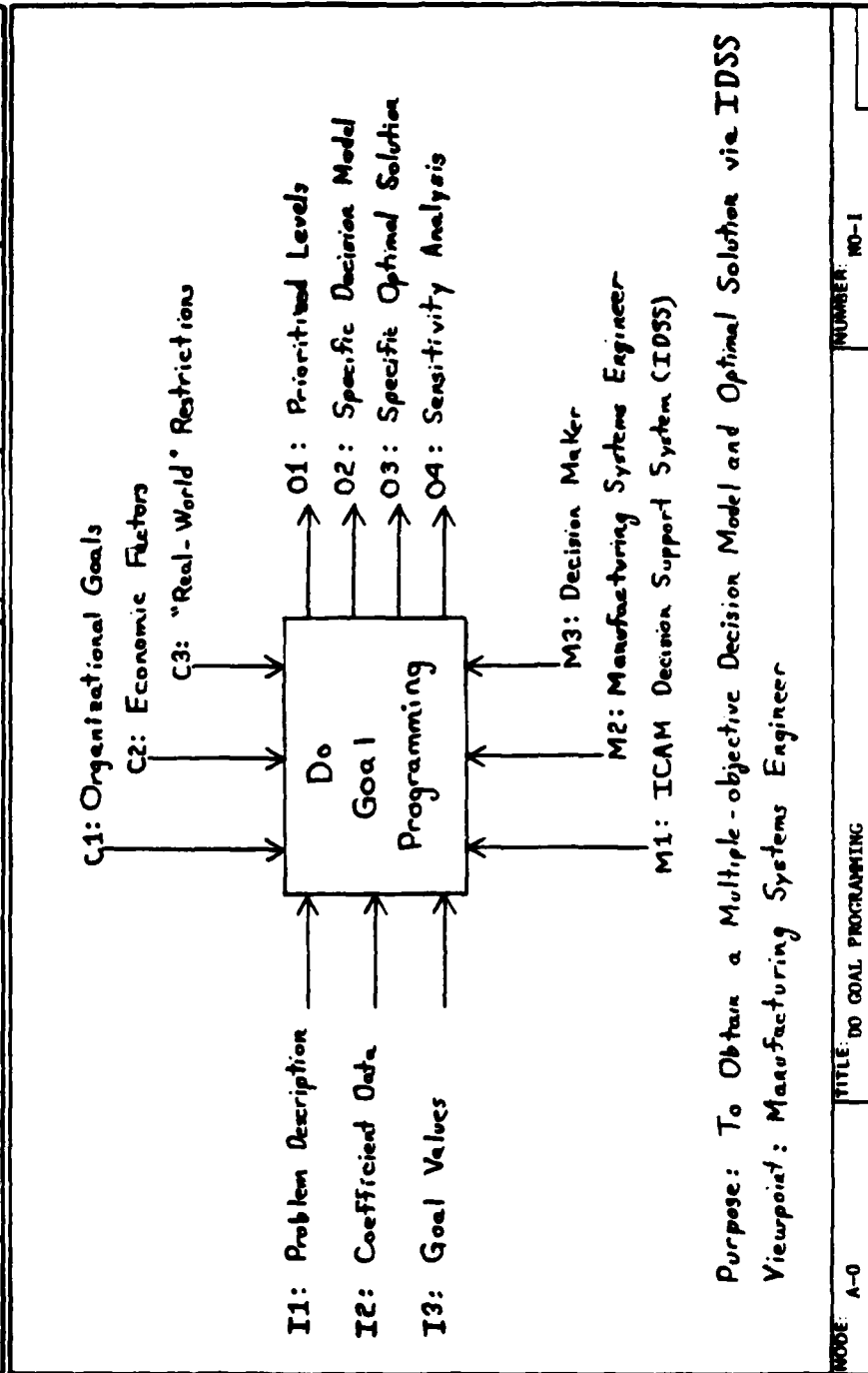
graph TD
    AO[AO: Do Goal Programming] --> A1[A1: Formulate Program Objectives]
    AO --> A2[A2: Determine Goal Program (see next page)]
    AO --> A3[A3: Solve Decision Model]
    A1 --> A11[A11: Determine Decision Variables]
    A1 --> A12[A12: Formulate Program Function(s)]
    A1 --> A13[A13: Solve Specific Model]
    A12 --> A121[A121: List Project Objective(s)]
    A12 --> A122[A122: List Project Restrictions]
    A12 --> A123[A123: Quantify Minimal Subsystem(s) Objective(s)]
    A121 --> A1211[A1211: List Resource Restrictions]
    A121 --> A1212[A1212: List Variable Restrictions]
    A121 --> A1213[A1213: List Logical Requirements]
    A122 --> A1221[A1221: List Resource Restrictions]
    A122 --> A1222[A1222: List Variable Restrictions]
    A122 --> A1223[A1223: List Logical Requirements]
    A123 --> A1231[A1231: Identify Subsystems]
    A123 --> A1232[A1232: Formulate Subsystem(s) Objective(s)]
    A123 --> A1233[A1233: Minimize Objective within Subsystem(s)]
  
```

MODE:	TITLE: Nodal Decomposition: Do Goal Programming	NUMBER:
-------	---	---------



ST 252

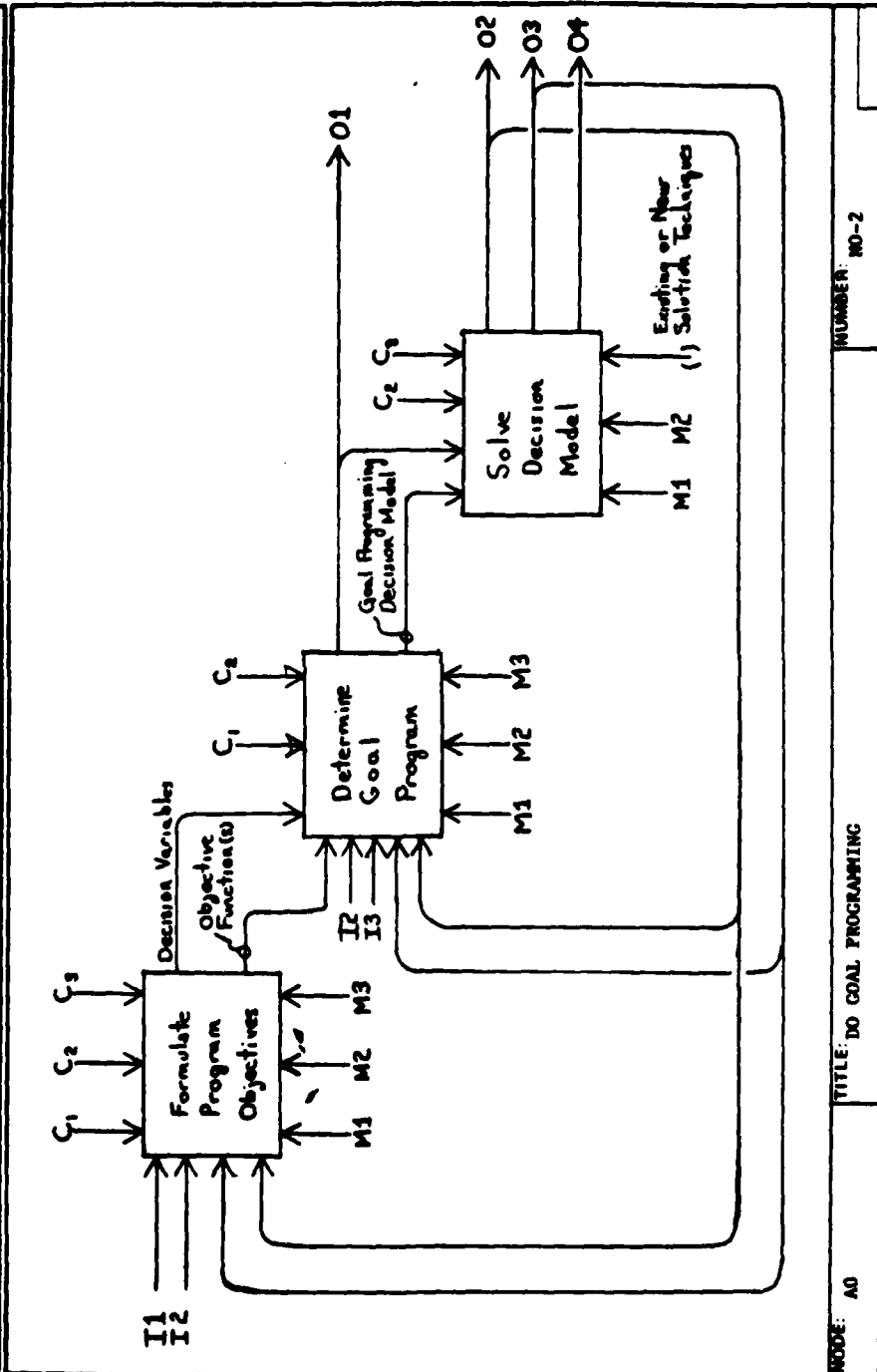
USED AT:	AUTHOR: Odrey, R.G.	DATE: 8/10/79	WORKING	READER	DATE	CONTEXT:
PROJECT: IDSS TASK 1/2	REV:		DRAFT			TOP
NOTES: 1 2 3 4 5 6 7 8 9 10			RECOMMENDED			
			PUBLICATION			



MODE: A-0	TITLE: DO GOAL PROGRAMMING	NUMBER: NO-1
-----------	----------------------------	--------------

ST 252

USED AT:	AUTHOR: Odroy, M.C.	DATE: 8/10/79	WORKING	READER	DATE	CONTEXT:
	PROJECT: IDSS TASK1/2	REV:	DRAFT			ZZZ
	NOTES: 1 2 3 4 5 6 7 8 9 10		RECOMMENDED			A-0
			PUBLICATION			



MODE: A0 TITLE: IDSS GOAL PROGRAMMING

NUMBER: NO-2

ST 252

USED AT:	AUTHOR: Odrey, N.C. PROJECT: IDSS TASK1/2	DATE: 8/10/79 REV:	WORKING DRAFT RECOMMENDED PUBLICATION	READER	DATE	CONTEXT: VZ <input type="checkbox"/> A0 <input type="checkbox"/>
NOTES: 1 2 3 4 5 6 7 8 9 10						

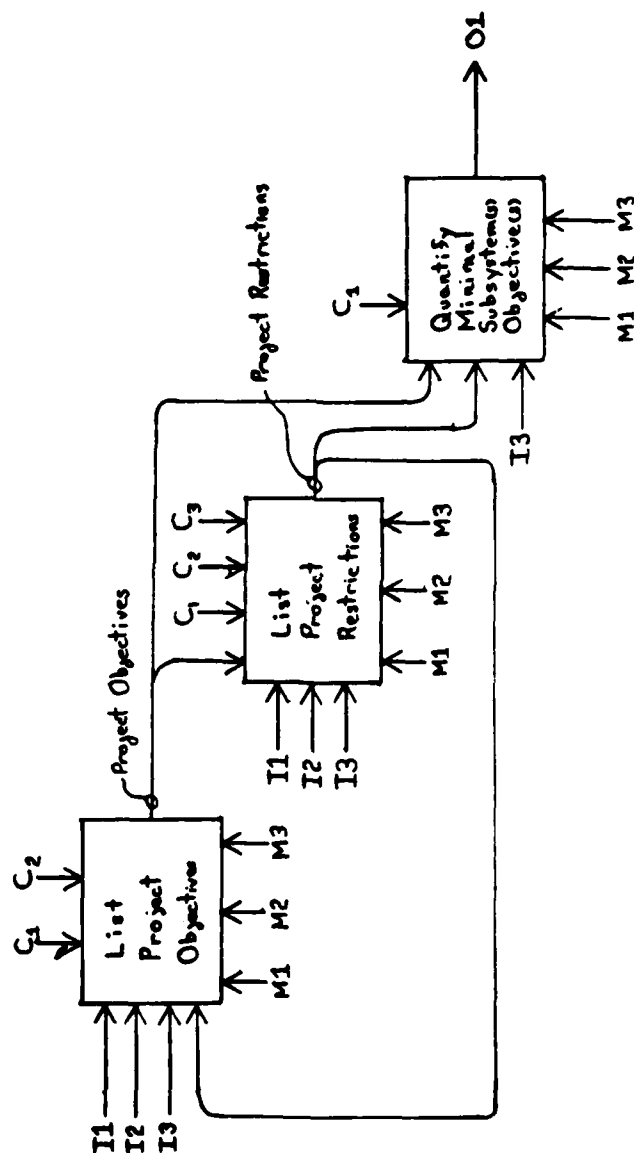

```

graph LR
    subgraph DV [Determine Decision Variables]
        I1_1[I1] --> DV
        I3[I3] --> DV
        I4[I4] --> DV
        C1[C1] --> DV
        C2[C2] --> DV
        C3[C3] --> DV
        DV --> I1_2[I1]
        DV --> I2[I2]
        DV --> M1[M1]
        DV --> M2[M2]
        DV --> M3[M3]
    end
    subgraph FPF [Formulate Program Objective Functions]
        I1_2 --> FPF
        I2 --> FPF
        C1 --> FPF
        C2[C2] --> FPF
        C3[C3] --> FPF
        M1 --> FPF
        M2[M2] --> FPF
        M3[M3] --> FPF
        FPF --> O1[O1]
        FPF --> O2[O2]
    end
    I1_2 --- DV2[Decision Variables]
    I2 --- DV2
    M1 --- DV2
    M2 --- DV2
    M3 --- DV2
    DV2 --> FPF
  
```


MODE: A1	TITLE: FORMULATE PROGRAM OBJECTIVES	NUMBER: NO-3
----------	-------------------------------------	--------------

ST 252

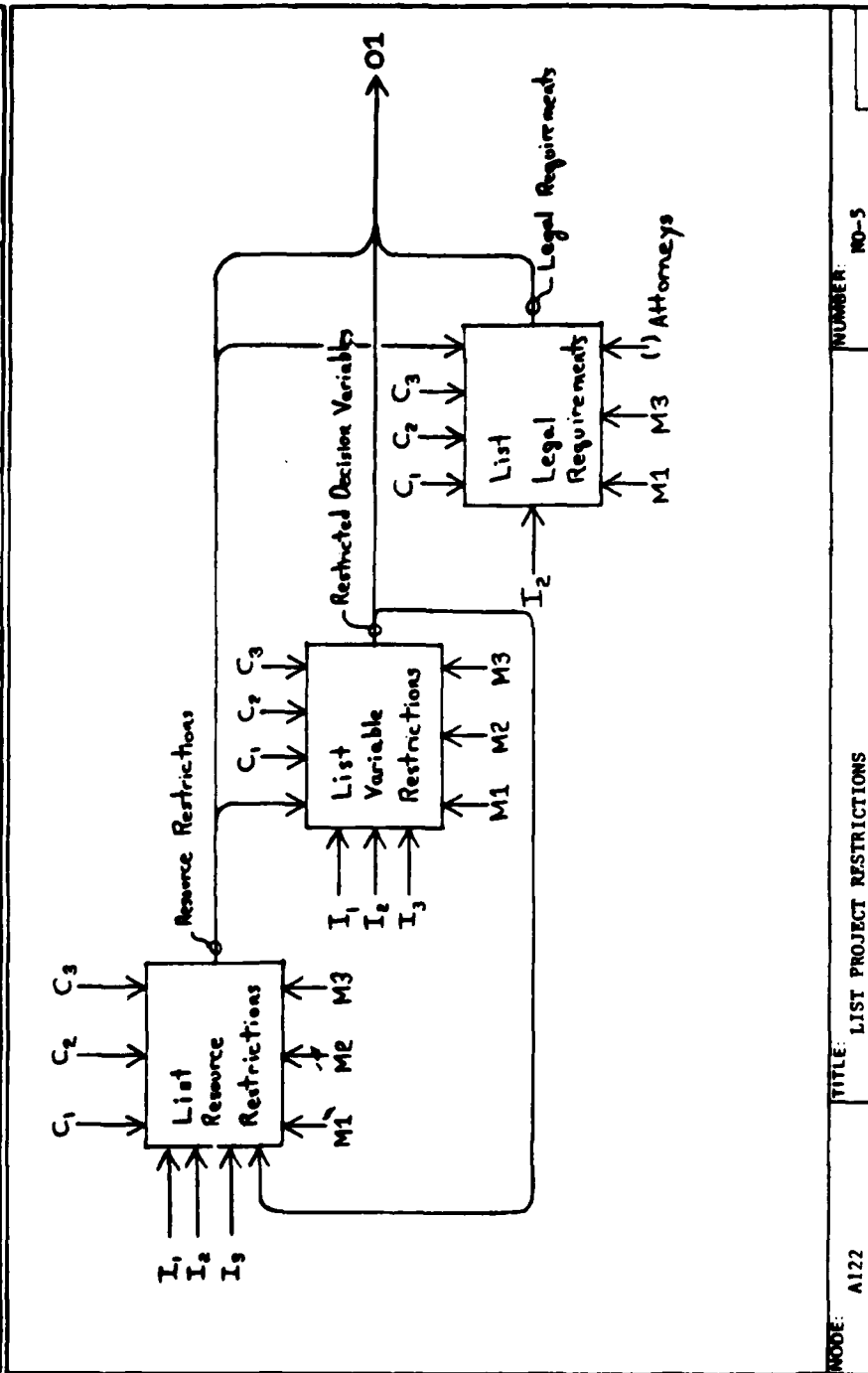
USED AT:	AUTHOR: Odroy, N.G.	DATE: 8/10/79	WORKING	READER	DATE	CONTEXT:
	PROJECT: IDSS TASK1/2	REV:	DRAFT			<input type="checkbox"/>
	NOTES: 1 2 3 4 5 6 7 8 9 10		RECOMMENDED			<input checked="" type="checkbox"/>
			PUBLICATION			A1



MODE: A12	TITLE: FORMULATE PROGRAM OBJECTIVE FUNCTION(S)	NUMBER: NO-4
-----------	--	--------------

87232

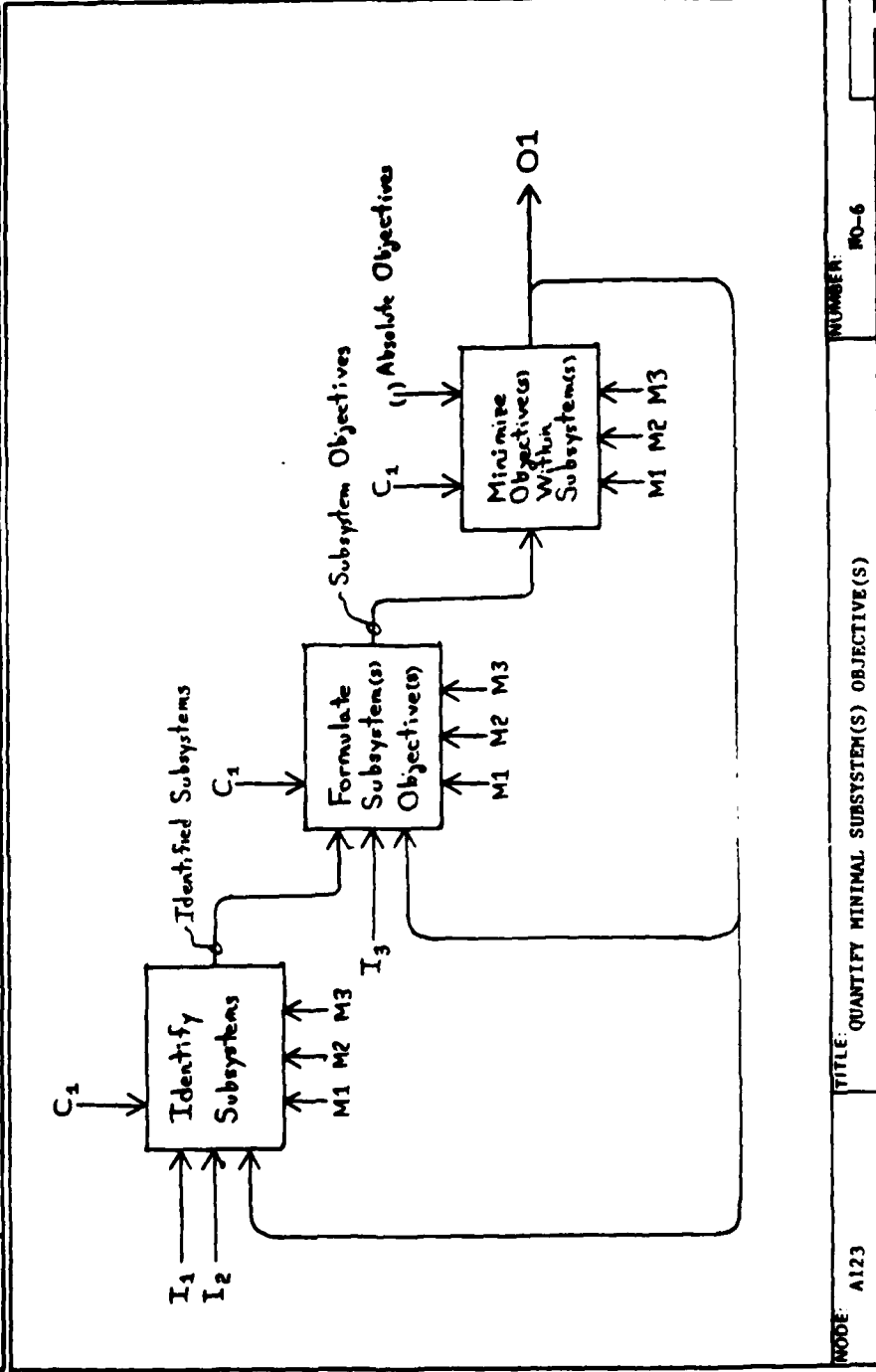
USED AT:	AUTHOR: Odrey, M.C.	DATE: 8/10/79	READER:	DATE:	CONTEXT:
	PROJECT: IDSS TASK1/2	REV:	WORKING		<input type="checkbox"/>
	NOTES: 1 2 3 4 5 6 7 8 9 10		DRAFT		<input type="checkbox"/>
			RECOMMENDED		<input checked="" type="checkbox"/>
			PUBLICATION		<input type="checkbox"/>
				A12	



MODE: A122	TITLE: LIST PROJECT RESTRICTIONS	NUMBER: NO-5
------------	----------------------------------	--------------

ST 132

USED AT:	AUTHOR: Odrey, W.G. PROJECT: IDSS TASK 1/2	DATE: 8/10/79 REV:	WORKING <input checked="" type="checkbox"/>	READER	DATE	CONTEXT: <input type="checkbox"/> <input type="checkbox"/> <input checked="" type="checkbox"/>
	NOTES: 1 2 3 4 5 6 7 8 9 10		DRAFT <input type="checkbox"/>	RECOMMENDED <input type="checkbox"/>		A12
			PUBLICATION <input type="checkbox"/>			



MODE: A123	TITLE: QUANTIFY MINIMAL SUBSYSTEM(S) OBJECTIVE(S)	NUMBER: MO-6
------------	---	--------------

ST 252		AUTHOR: O'Grady, N.G.		DATE: 8/10/79		WORKING		READER		DATE		CONTEXT:	
USED AT:		PROJECT: IDSS TASK1/2		REV:		DRAFT		RECOMMENDED				A0	
NOTES:		1		2		3		4		5		6	
		7		8		9		10					

Assign Priority
Level(s) to
Objective
Function(s)

↑ I1
↑ I2
↑ I4
↑ I5

↑ C2
↑ C3

↑ M1
↑ M2
↑ M3

Prioritized Objectives

↑ C1
↑ C2
↑ C3

Obtain
Goal
Programming
Model

↑ I2
↑ I3
↑ I4
↑ I5

↑ M1
↑ M2

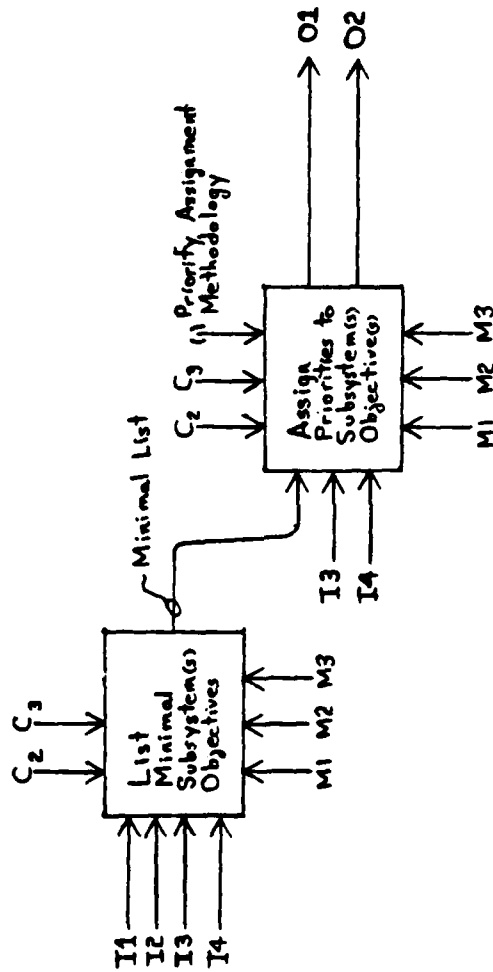
↑ O1

↑ O2

MODE: A2	TITLE: DETERMINE GOAL PROGRAM	NUMBER: NO-7
----------	-------------------------------	--------------

ST 232

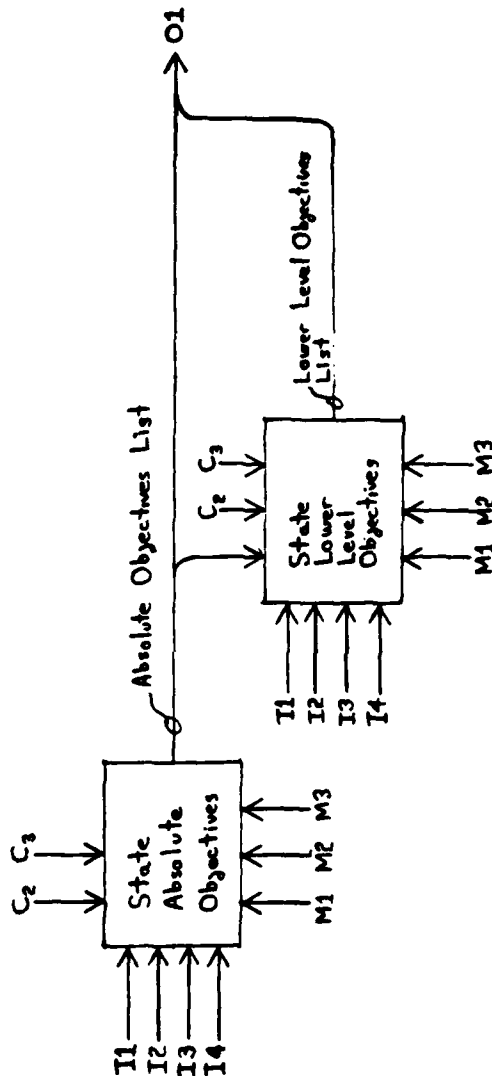
USED AT:	AUTHOR: Odrey, N.G.	DATE: 8/10/79	WORKING	READER	DATE	CONTEXT:
	PROJECT: IDSS TASK1/2	REV:	DRAFT			<input checked="" type="checkbox"/>
	NOTES: 1 2 3 4 5 6 7 8 9 10		RECOMMENDED			<input type="checkbox"/>
			PUBLICATION			A2



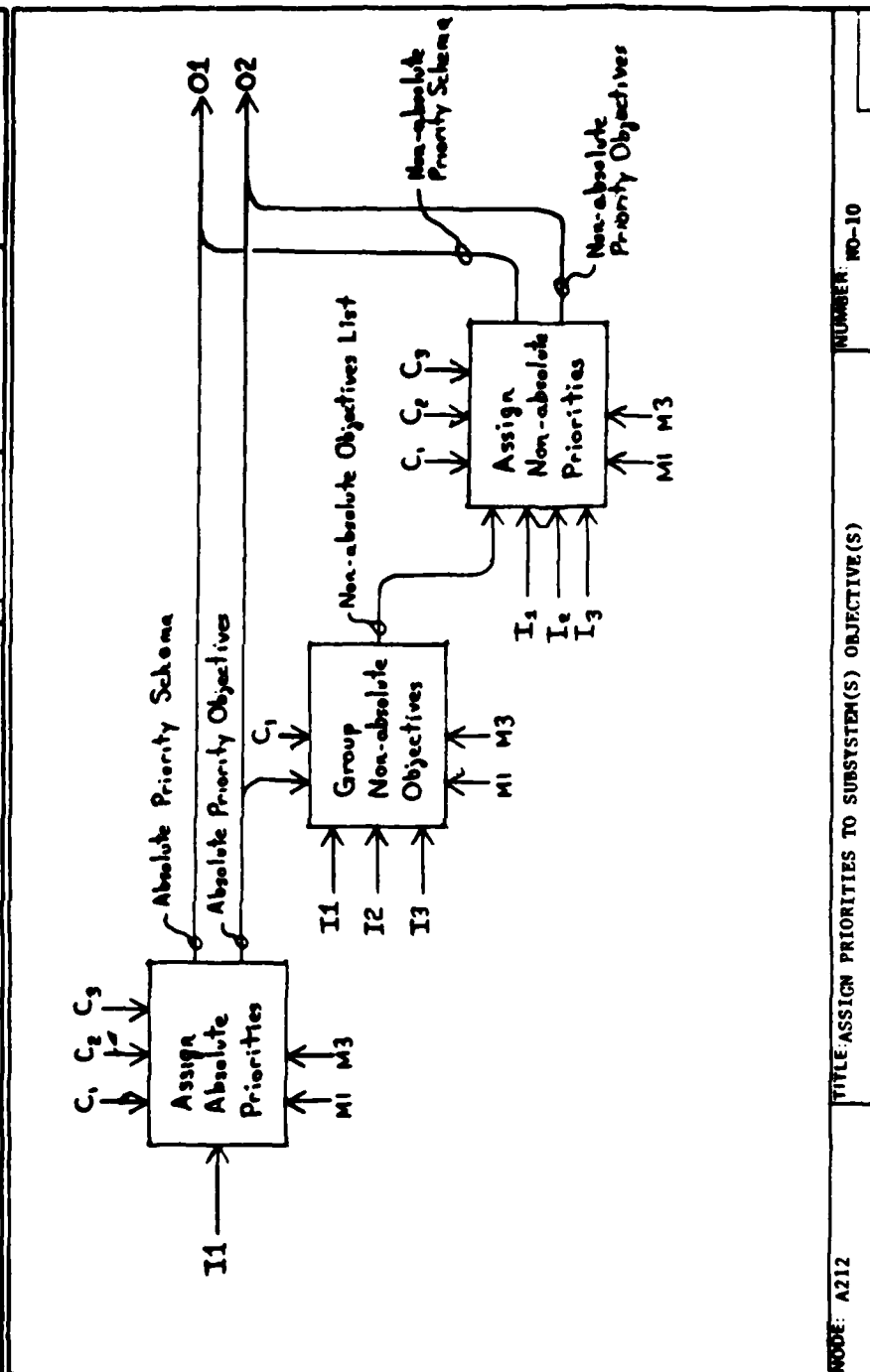
MODE A21	TITLE: ASSIGN PRIORITY LEVEL(S) TO OBJECTIVE FUNCTION(S)	NUMBER: NO-8
----------	--	--------------

ST252

USED AT:	AUTHOR: Odrey, M.C. PROJECT: IDSS TASK1/2	DATE: 8/10/79 REV:	WORKING <input checked="" type="checkbox"/> DRAFT <input type="checkbox"/> RECOMMENDED <input type="checkbox"/> PUBLICATION	READER	DATE	CONTEXT: <input checked="" type="checkbox"/> A21 <input type="checkbox"/>
NOTES: 1 2 3 4 5 6 7 8 9 10						

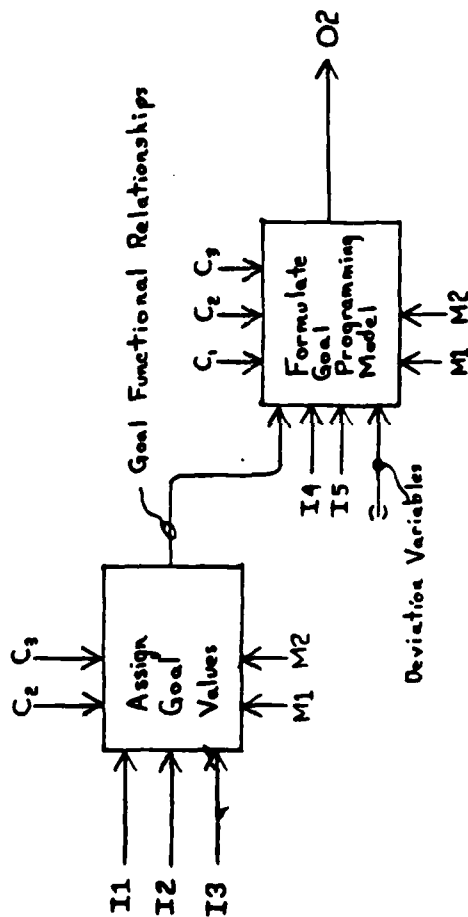


MODE: A211	TITLE: LIST MINIMAL SUBSYSTEM(S) OBJECTIVE(S)	NUMBER: NO-9
------------	---	--------------



ST 752

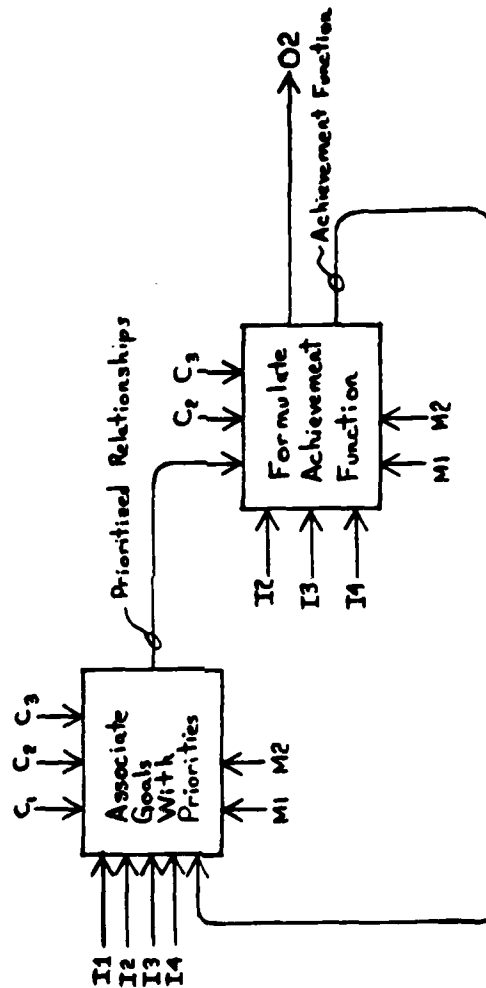
USED AT:	AUTHOR: Odrey, N.G. PROJECT: IDSS TASK1/2	DATE: 8/10/79	WORKING	READER	DATE	CONTENT:
	NOTES: 1 2 3 4 5 6 7 8 9 10	REV.	DRAFT	RECOMMENDED		<input type="checkbox"/> A2
			PUBLICATION			



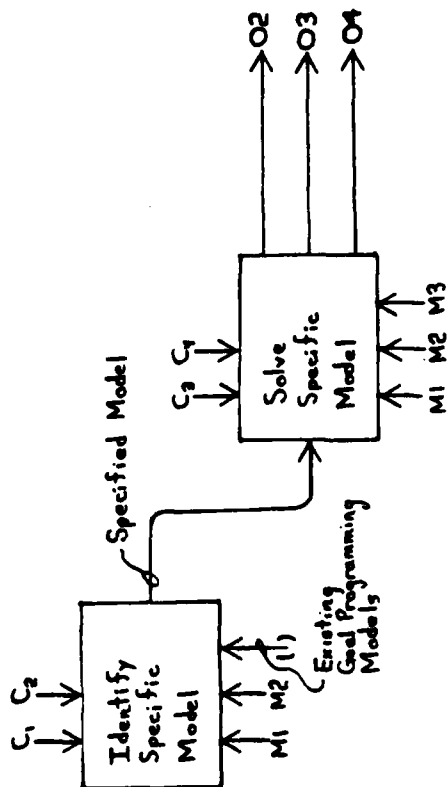
MODE: A22	TITLE: OBTAIN GOAL PROGRAMMING MODEL	NUMBER: NO-11
-----------	--------------------------------------	---------------

ST 252

USED AT:	AUTHOR: Ogrey, R.G.	DATE: 8/10/79	READER:	DATE:	CONTEXT:
PROJECT: IDSS TASK1/2		REV:			
NOTES: 1 2 3 4 5 6 7 8 9 10			WORKING		
			DRAFT		
			RECOMMENDED		
			PUBLICATION		
					A22



MODE: A222	TITLE: FORMULATE GOAL PROGRAMMING MODEL	NUMBER: WD-12
------------	---	---------------



1979 USAF - SCEEE SUMMER FACULTY RESEARCH PROGRAM

Sponsored by the

AIR FORCE OFFICE OF SCIENTIFIC RESEARCH

Conducted by the

SOUTHEASTERN CENTER FOR ELECTRICAL ENGINEERING EDUCATION

FINAL REPORT

A COMPUTER MODEL OF SACCADIC SUPPRESSION

Prepared by:	William J. Ohley
Academic Rank:	Assistant Professor
Department and University:	Department of Electrical Engineering University of Rhode Island
Research Location:	Human Resources Laboratory, Simulation Techniques Wright-Patterson AFB, OH
USAF Research Colleague:	Kenneth R. Boff
Date:	August 13, 1979
Contract No.:	F49620-79-C-0038

A COMPUTER MODEL OF SACCADIC SUPPRESSION

by

William J. Ohley

ABSTRACT

Suppression of vision during the course of voluntary saccadic eye movements has been well documented. However, the mechanisms which result in these observations are not clear. Moreover, the amount and types of visual suppression reported differ widely. It is not presently possible to accurately predict the efficacy of suppression for an individual in a given situation. However, the exploitation of suppression has been suggested for visual display systems. Thus, based on currently available data, this report provides a preliminary model for quantitative prediction of saccadic suppression. The model relies on the use of the line spread function, modulation transfer function, and temporal transfer function in conjunction with convolution mathematics and a postulated psychophysical detection process. Results are shown which facilitate explanation of typical suppression experiments. This is done by considering the visual system to be at least two-dimensional in time and space. The effects of visual stimulation during saccades are then seen to be a combination of the interaction between the time-space properties of the stimulus, those of the visual system, and a psychophysical detector. Since the model is composed entirely of software, it should be possible to examine a larger and more complex number of visual situations than would be experimentally feasible. In this way, baseline engineering design requirements can be specified. Furthermore if initial development of hardware proves difficult, the model, with suitable refinements, could provide an effective means for exploring alternative solutions. Suggestions for further research are also given.

ACKNOWLEDGMENTS

The support of the Air Force Office of Scientific Research, the Air Force Systems Command and the Southeastern Center for Electrical Engineering Education is gratefully acknowledged.

The author wishes to express his gratitude to the staff of the Human Resources Laboratory at Wright-Patterson AFB for a most stimulating and productive summer. In particular, Dr. Ken Boff for his provocative discussions; Dr. Don Gum for helping identify a problem area, Capt. Mike Ingalls for help in seeing the problem's scope; Dr. Gordon Eckstrand's advice on constraining the investigation was timely, as was Dr. Bill Askren's signature on my invoices. Mike Nicol, Lt. Jeff Rubin, TSgt Ed Sanderlin, and Bill (Schelker made the HRL *STARS* computer readily available and useful for this project (despite my attempts to crash the system). Colleen Burns and Carolyn Runyon put up with typing this manuscript and material for several briefings. Those outside HRL also provided valuable input: Ed Martin, Jim Basinger, and Art Ginsburg. It was especially enjoyable to run a "few" miles with Dr. Bill Kane, my colleague in the summer program.

Finally thanks to Allegheny Airlines for always arriving 5 hours late in Rhode Island, and to Michele for putting up with this cross country commuter existence for 10 weeks.

I. INTRODUCTION

Eye movements play an enormous part in how we perceive the visual world. When described by velocity and duration, there are several types of eye motion. As one particular type, saccades can be classified by their high velocity ($100^{\circ} - 400^{\circ}/\text{sec}$) and macro movement ($1^{\circ} - 80^{\circ}$). While frequently voluntary, they can also occur involuntarily (i.e. during high velocity tracking of a moving object).

Voluntary saccades occur when one switches gaze from some portion of the visual field to another, for example, returning to the beginning of a line while reading. During that time, the reader is usually not aware of the page blurring past in the opposite direction. Thus the retinal image is said to be suppressed. Late during the last century, experiments on suppression in visual perception during saccadic movements were reported. Since that time, there has evolved a large body of literature dealing directly with the phenomenon of saccadic suppression.

In a typical experiment designed to measure suppression, the subject is presented with a visual stimulus (i.e. a test flash) that is triggered to occur either immediately before, during or after a saccade. The visibility of the flash when compared to fixation thresholds is usually reported as reduced. The reduction in visibility begins before eye movement and continues until after the eye comes to rest again. However, when visibility is graphed versus the time of stimulus occurrence, it is found to be a minimum only during a portion of the saccadic movement.

The problem addressed by this investigation is motivated by Air Force requirements in advanced visual display systems for flight simulation. Recently it has been suggested that saccadic suppression can be exploited by allowing reduction in display resolution during times of suppression. In order to implement a system which relies on saccadic suppression for its success, it is desirable that the characteristics of this type of human visual processing be predictable. A computer based mathematical model of saccadic suppression will make it possible to examine a larger and more complex number of visual situations than would be experimentally feasible. Furthermore, in the event of system hardware problems this analysis could provide an effective means for methodically exploring alternative design solutions.

II. OBJECTIVES

The objectives of this project were:

1. To review the research literature applicable to modeling the process of saccadic suppression.
2. To develop a mathematical description of the process that could predict for example, how much suppression may occur in a given situation.
3. To implement the model and evaluate its preliminary results.
4. To make recommendations concerning the use of saccadic suppression in visual display systems.

III. BACKGROUND

Matin (18) has extensively reviewed both the historic and modern work on saccadic suppression. Carpenter's text (65) deals with more recent investigations as well as the general area of eye movements. In terms of the development of the model discussed in this report, the pertinent literature may be divided into four areas. 1. Saccadic suppression. 2. Spatial and temporal properties. 3. Eye movements 4. Visual processing.

1. Saccadic Suppression.

While the reference list contains several papers (19 - 22) prior to Matin's review, this report will deal primarily with subsequent work. Brooks et al (15) demonstrated, for stroboscopic test flashes, on various backgrounds, that similar time courses of suppression could be produced by "normal" saccadic eye movement and by "saccading" the visual image across the retina during eye fixation. Thus it was indicated that a large amount of suppressive effects may be due to retinal stimulation alone. Mitrani et al (16) also suggested that a significant amount of visual deterioration results from the movement of contours over the retinal field. Matin (14) considered the response of the visual system when eye muscles are paralyzed. He suggested a hybrid theory in which both actual eye movement and retinal stimulation can cause suppression. In related work, Shebilske (13) supported an "in flow" over an "out flow" theory of visual direction constancy during saccades. That is, the visual system relies on feedback from actual eye movement and position to interpret retinal stimulation.

While most suppression work has centered on stationary test flash visibility, Stark et al (12) experimentally showed suppression of image displacement. Furthermore, under static eye stimulus conditions, Sakitt (11) suggested that visual information may be available to the brain even though the observer indicates that the stimulus was not seen.

Bridgeman (10) criticized Brooks et al (15) by arguing in favor of an "extra retinal signal" arising during saccades to cause threshold elevations. Brooks et al (9) argued against this theory - maintaining that the primary source of suppression was due to the pattern of retinal stimulation.

Volkman et al (8) demonstrated elevation in contrast sensitivity during saccades. They conclude that both optical and neural effects combined to produce suppression. However, a larger amount of suppression appeared due to retinal stimulation than any extra-retinal signal.

The most recent work in saccadic suppression is represented in abstract form (1 - 7). Bridgeman et al has demonstrated saccadic suppression psychophysically in the cat (1), Brooks et al investigated perception of image motion during saccades (2), Impelman et al (3) and White et al (4) showed masking effects. Cohn et al (5) suggest that suppression may be due entirely to "uncertainty in the frame of reference." In addition Volkman et al (6) separate the effects of contrast sensitivity and retinal smear, while Wurtz et al (7) were concerned with retinal smear suppression.

Based on the literature, the following general conclusions can

be drawn: Suppression occurs for a variety of visual discrimination tasks i.e., contrast sensitivity, threshold, and perceived direction. Suppression can be obtained by "saccading" an image across a fixated eye. While stronger suppression occurs when the stimulus is more complex than simple flashes, it also occurs to a lesser extent during saccades over a low detail visual field. Although not tested experimentally, it has been suggested that the apparent large amount of suppression in the real world is due primarily to the complexity of the visual image.

Given the intended application, there appears to be a lack of data on saccadic suppression in several areas: (1) suppression in the presence of a coexisting stimulus or task, as might occur in a simulator cockpit; (2) quantitative results of suppression in a multi-colored environment. In any event, there have been no attempts to quantitatively predict the results of a suppression experiment either for simple test flashes or for more complex situations.

2. Spatial and Temporal Properties.

Because the saccadic suppression literature indicates the importance of retinal stimulation in obtaining elevated thresholds, literature pertaining to the visual system's spatial and temporal properties was investigated. The static spatial properties of the visual system have generally been described by several investigators in either of two ways: (1) By using some test of visibility

such as threshold sensitivity, the response to a series of spatial frequency sine waveforms has been obtained. This yields a transfer characteristic of the system in the frequency domain: the Modulation Transfer Function (MTF) (Legge 29, 40, Furchner et al (3) Graham (31), Carlson et al (32), Spitzberg et al (43), Kelley et al (44).) The results obtained depend on the stimulus intensity and wavelength as well as such factors as retinal location. (2) The inverse Fourier transform of the MTF (assuming a linear system) yields the Line Spread Function (LSF) (also called the Receptive Field Sensitivity Function). This function has recently been measured psychophysically by obtaining the visual response to two thin spatial lines, one 70% the intensity of the other. The visibility of the brighter line is found to be a function of how close the two lines are in space. By appropriate analysis, the LSF can be deduced. (Wilson et al (33), Wilson (25), Gelber et al (26), Limb et al (34), Hines (39).

It has also recently been shown that the spectral and spatial properties of the system can be modified by the temporal properties of the stimulus. Wilson, (25). In addition to a series of spatial Fourier filters, there is evidence that both temporal "transient" and "sustained" channels exist as well. (Mezrich (24), Arend (38), Spitzberg et al (43), Wilson (25).) It could be said that the visual system filters in both space and time - and that these processes appear to interact. Spitzberg et al (43) demonstrate relationships between sustained-transient and high-low spatial frequency responses.

The temporal properties have been studied extensively in the past (using test flashes etc) to obtain the "temporal modulation transfer function" (71). Recently King-Smith et al (33) have employed a stabilization apparatus to investigate visual time response.

However, there does not appear to be an experiment in which both the time response and line spread functions are simultaneously derived. The closest work in this area is Wilson (35) and Arend (38).

3. Eye Movements

There have been a number of investigations concerning the interaction of visual perception and saccadic eye movements. Prablanc et al (63) reported on the dependency of corrective saccades on retinal reafferent signals. Corrective saccades are small and immediately follow large saccades so that a target can be brought into the central fovea. They found that target stimulation must be available to the retina at certain times during the large primary saccade in order for the correction saccade to be accurate. Furthermore, latency in corrective saccadic response may be modified by appropriate timing of the stimulus. Coren et al (62) studied perception of the size of a circle inscribed by a circularly moving target. They showed that for high target velocity, the initiation of saccades to keep up with the object also resulted in more accurate perception of the circle size. In the smooth tracking phase, the circle appears to shrink as the angular velocity of the object increases.

Lisberger et al (61) investigated the number of corrective saccades as a function of total saccadic length. It was found that the longer primary saccade exhibited more corrective saccades than the shorter ones. However, results were also a function of target conditions and subjects. Hallett (60) demonstrated that "important visual stimulation can occur during saccades," This was observed in an experimental situation which altered the target position during an initial saccade. Hallett et al (59) presented additional evidence that saccades are "goal directed towards the physical location of the target . . . this is possible only if retinal image position and eye position information are correlated." Becker (57) suggests that visual information is not necessary for corrective saccades to occur. However he contends this disagreement with Prablanc et al (63) is most likely due to experimental conditions. Dimitrov et al (58) examined saccadic eye movement in terms of a stereoscopic image (Bela Julesz' Figure). They conclude that despite the unusual experimental conditions, the dependence of the maximum velocity and duration of the saccades on amplitude was not altered. Viviani et al (54) showed that for voluntary and optokinetic oblique saccades, a curved rather than straight path is followed. Furthermore there was a systematic dominance of the horizontal over the vertical component.

Komoda et al (53) investigated the accuracy of two dimensional saccades in the absence of retinal stimulation. They concluded, because of the relatively high accuracy, that the saccades are programmed on the basis of memory. Hansen et al (52) reiterated this finding by examining the accuracy of eye position information for motor control. They concluded that large errors in controlling eye position in the dark are due to poor spatial memory.

In further experiments, Prablanc et al (50) suggest that if extra-retinal signals do play a part in saccadic positional error, then they are not very sensitive, and in "normal" situations visual feedback is the dominating factor. Henson (47, 49) altered the visual feedback to the oculomotor system during large saccades to eliminate the need

for a "correction" saccade. The saccadic system was found to learn after a few minutes to undershoot the target as before. This result demonstrates the "corrective" saccadic mechanism to be a deliberate one.

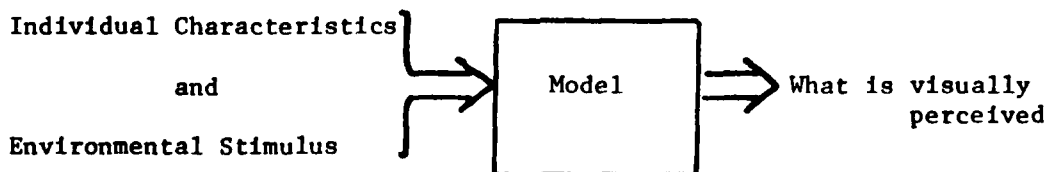
Despite the substantial number of investigations that have examined the relationship of saccadic eye movements and vision it is not entirely clear how the systems interact. There is apparently a combination of both retinal and extra retinal signals that effect resulting eye motion. The exact effects seem to be functions of both the situation and the individual.

4. Visual Processing

This section of the literature review is not well developed. The papers included here only scratch the surface of what may prove to be valuable information in modeling saccadic suppression. Several papers on meta contrast may have impact on perception during saccades (66, 70) since a meta contrast masking effect can be observed - apparent suppression occurring before eye movement. However, it may also be possible to explain this on the basis on time delays. For those familiar with system theory, a non-causal (meta contrast) system can be made causal with a sufficient time shift. Other types of masking have been investigated recently by Mateeff et al (69), Grunau (68), and King-Smith (68). It can also be noted here that Cornsweet (71) provides a wealth of information on visual perception in terms of linear and non-linear systems.

IV. MODEL DEVELOPMENT AND PRELIMINARY RESULTS

The model developed in this investigation is an attempt to combine information from the several areas of vision literature reviewed in section III. It is assumed to have the following form:



The input to the model are an individual's visual characteristics and the environmental stimulus. The output desired is a prediction of what was visually perceived.

First the individual's characteristics are considered, and the following general assumptions are made:

1. Visual acuity is "normal".
2. Range of illumination level and contrast is small.
3. Visual characteristics don't change during the saccadic time interval.
4. Model is restricted to black and white illumination.
5. Most suppression is due to retinal stimulation, extra retinal factors are secondary.

These assumptions allow the consideration of a lumped linear time invariant system. It is recognized that the eye and brain are probably non-linear, time varying, and non-causal as well. However, a linear analysis initially can provide some insight into a complex problem. Furthermore, it is quite likely that much of the stochastic, non-linear, or time varying,

effects are a result of psychophysical processes. Thus it is useful to divide the model into two parts: 1. Sensor, and 2. Psycho-physical detector.

To characterize the sensor portion of the model, data from the literature on line spread functions (LSF), modulation transfer functions (MTF) and temporal transfer functions (TTF) is utilized. The LSF or MTF describe the spatial properties of the system while the temporal properties are derived from the TTF. To make predictive use of this data, the concepts of impulse response and convolution integrals must be considered. Using the well known convolution integral, for a linear time invariant system in the time domain:

$$g(t) = \int_{-\infty}^{\infty} h(\tau) f(t-\tau) d\tau \quad (1)$$

where $g(t)$ is the output, $f(t)$ the input and $h(t)$ the impulse response, or system function. If only one spatial direction, i.e. the horizontal, is considered in conjunction with time, the system function is in general, a function of time and space:

$$g(x,t) = \int_{-\infty}^{\infty} \int_{-\infty}^{\infty} h(x,\tau) f(x-\tau, t-\tau) dx d\tau \quad (2)$$

Thus if one knows the time-space properties of the system, $h(x,t)$, the resulting time space function, $g(x,t)$, can be derived from any input function $f(x,t)$. Let $f(x,t)$ represent the intensity of illumination at some horizontal position x on the retina at some time t . Then $g(x,t)$ can be the representation of that illumination pattern arriving at the visual cortex as modified by $h(x,t)$.

Next it is assumed that:

$$h(x,t) = h_1(x) h_2(t) \quad (3)$$

This implies that $h(x,t)$ is separable - or symmetric to both the time and space axis. Then functional forms for $h_1(x)$ and $h_2(t)$ can be obtained from LSF, MTF and TTF data. Since the LSF is simply the Fourier transform of the MTF (assuming linearity), LSF data from Wilson (25) was used to describe $h_1(x)$:

$$h_1(x) = \exp\left(-\frac{x^2}{\sigma_e^2}\right) - \frac{K\sigma_e}{\sigma_i} \exp\left(-\frac{x^2}{\sigma_i^2}\right) \quad (4)$$

Where $\sigma_e = .064$, $\sigma_i = .193$, $K = .90$ and x is eccentricity in degrees. Recent investigations have shown that the LSF is a function not only of horizontal position x , but of where on the retina it is measured. The above numbers are for 0° eccentricity (at the fovea). While the form of LSF remains double gaussian, the constants σ_e , σ_i , K change significantly as one moves several degrees on the retina. Furthermore, it is also shown by Wilson and others (25, 38) that the temporal pattern of the stimulus affects its spatial perception.

These effects were not included in the model at this time. The retina is considered to be horizontally homogeneous and described by equation (4). However, several different values for σ_e , σ_i and K were examined to estimate how important they are to the system. The form of $h_2(t)$ was then estimated. Here from the data in (71) and (33):

$$h_2(t) = \exp(-t/\tau) \quad (5)$$

$$\tau = 2.0 \text{ msec}$$

Again several values of τ were also examined.

By combining (3) and (4):

$$h(x,t) = \left[\exp\left(-\frac{x^2}{\sigma_x^2}\right) - \frac{k\sigma_x}{\sigma_t} \exp\left(-\frac{x^2}{\sigma_t^2}\right) \right] \cdot \exp(t/\tau) \quad (6)$$

$h(x,t)$ is shown graphed in figure (1).

In order to predict $g(x,t)$, it remains now to describe $f(x,t)$, the space-time course of retinal stimulation during a saccadic eye movement. If it is assumed that stimulus is a spot of light that is turned on and then off as it is swept across the retina at constant velocity, in the space time plane $f(x,t)$ would look like Figure (2). Here it runs essentially diagonal across the plane-for each new instant, a new spatial location is stimulated. If, on the other hand, the movement in the x direction is stopped while the light remains on, then at that point the pulses would run parallel to the t axis. This is shown occurring in Figure (2) starting at $t = 25$ msec.

In naturally occurring saccades, a straight line relationship does not exist between the horizontal angle and time. Yarbus (64) gives it as a cosine relation:

$$x = \frac{x_0}{2} \left(1 - \cos \frac{\pi}{T} t \right) \quad (7)$$

Where t is time in seconds, x is the rotation angle in degrees, T is total saccade duration time, and x_0 is the final angle at the end of the saccade. For a light spot of intensity I_0 turned on at $t=0$ and off at $t=t_1$, Equation (7) yields:

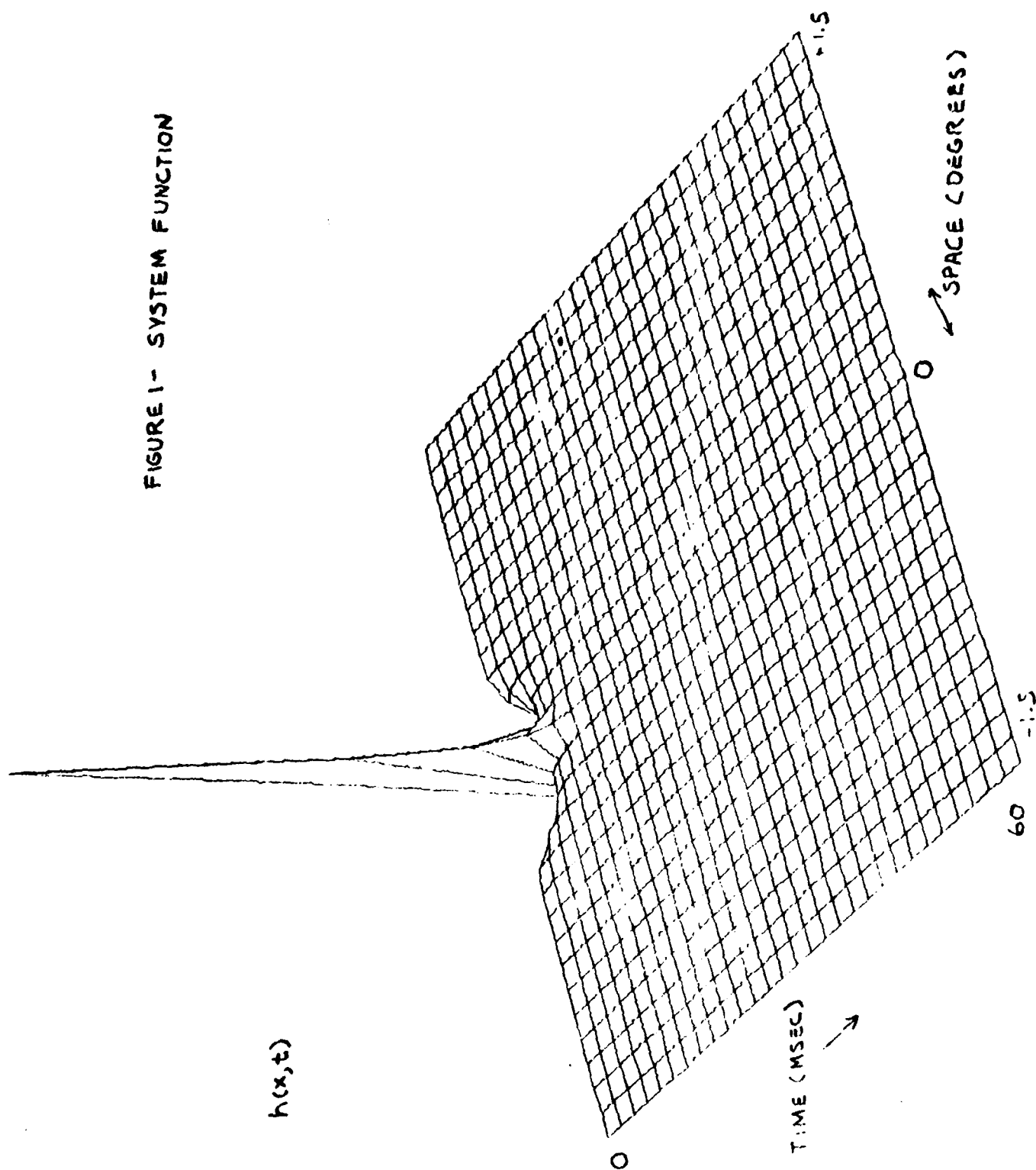
$$f(x,t) = \begin{cases} I_0, & 0 < t < t_1 \text{ AND } x_0 < x < \frac{x_0}{2} \left(1 - \cos \frac{\pi}{T} t \right) \\ 0, & \text{OTHERWISE} \end{cases} \quad (8)$$

Using equation (6) and (8), the resulting $g(x,t)$ can be predicted for a given experimental condition. It is useful to examine a particular saccadic suppression experiment (Matin(21)). The subject was required to make voluntary left to right 40° horizontal saccades between two fixation points. At the 1° position, detected by oculometer, a slit of light located beneath the right fixation point was then turned on. The slit was left on for varying times during the course of the saccade. The subject then compared the apparent length of the slit - (it was often seen as a blur in the visual field) to a comparison line displayed 500 msec after the saccade ended. (Figure 3a). The results for various illumination levels are shown in Figure 3b. The ordinate is perceived slit length and the abscissa is duration of slit illumination. Essentially, the blur was only perceived when the slit was turned off during the saccade. When left on past end of eye movement ($t > 30$ msec), the length of the blur decreased until only the slit itself was perceived. The blur was said to be suppressed.

To simulate this experiment, results were obtained from the model for two basic conditions: 1. Slit turned off before the end of the saccade and 2. Slit left on past the end of the saccade.

Applying the model consisted of solving equation (2). In order to obtain solutions to the convolution integral several methods were considered - one could use an FFT (Fast Fourier Transform) and work the solution in the frequency domain. However, this algorithm was not available in the HRL Stars system. Thus, a direct discrete solution

FIGURE 1- SYSTEM FUNCTION



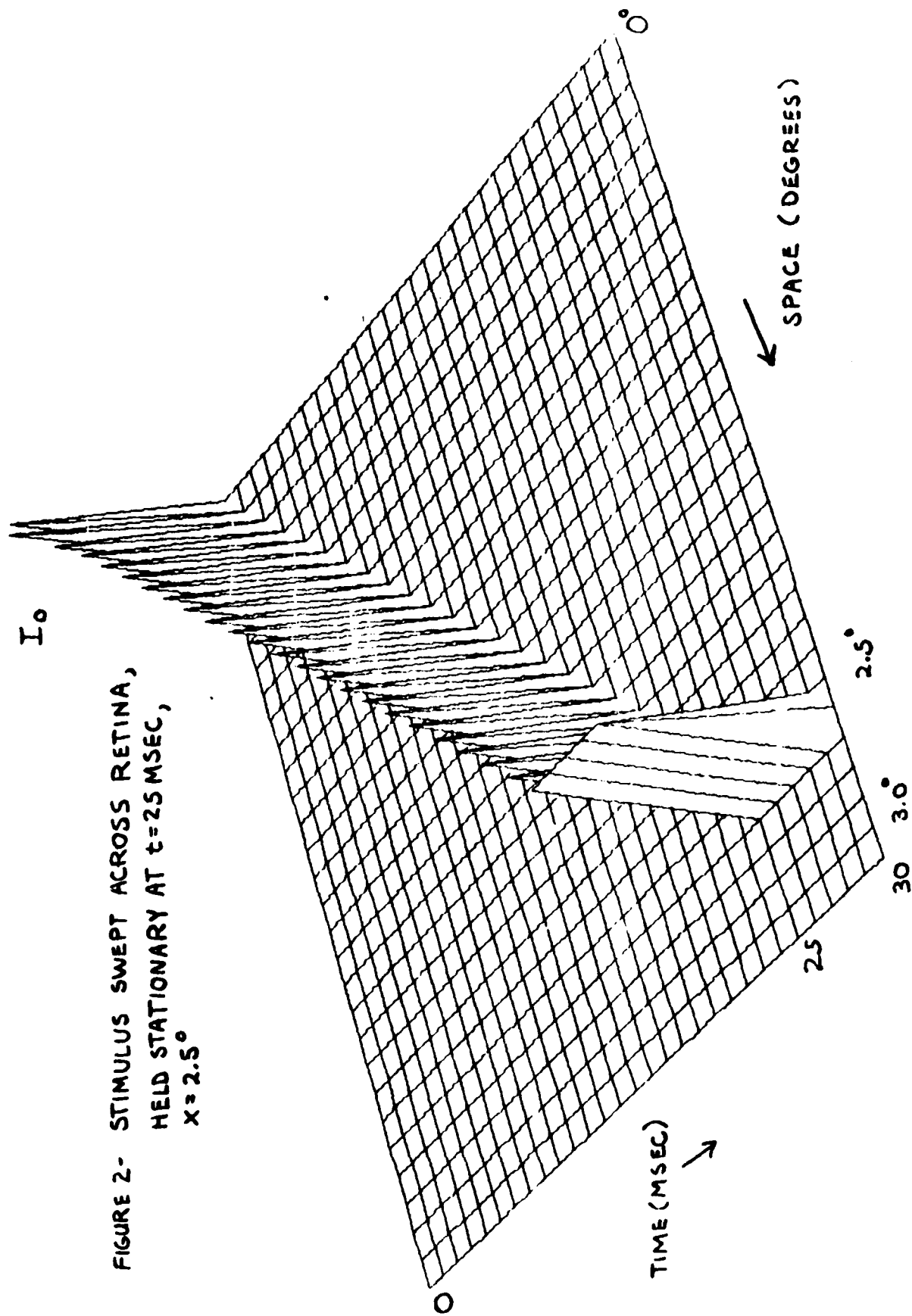
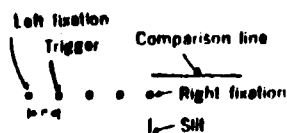


FIGURE 2- STIMULUS SWEEP ACROSS RETINA,
HELD STATIONARY AT $t=25$ MSEC,
 $x=2.5^\circ$

A.



B.

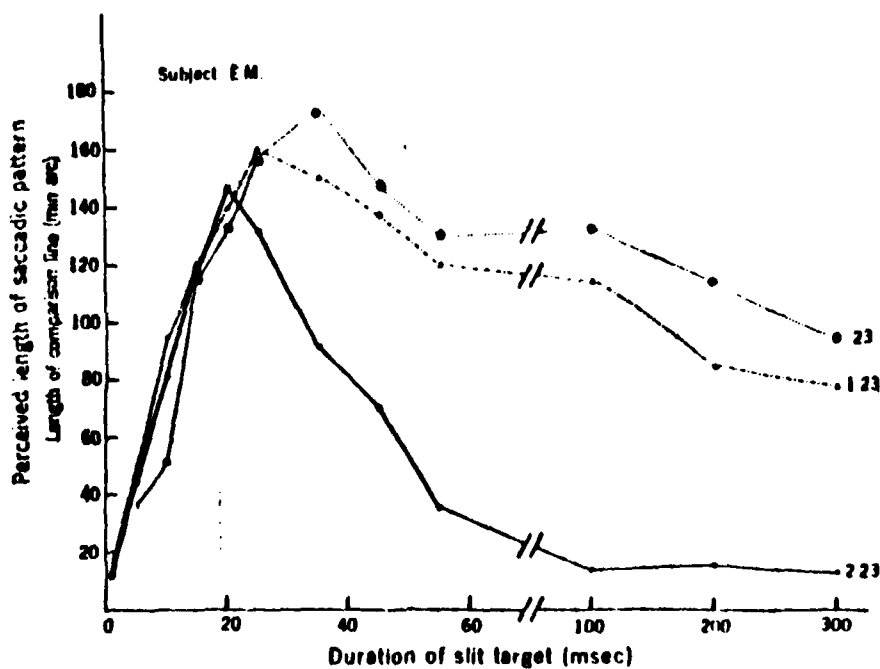


FIGURE 3 - MATIN'S EXPERIMENT

to the two-dimensional convolution was then implemented. Because of memory and system execution time limitations, a 30 X 30 array was chosen to represent the space-time plane ($t=0-30$ msec; $x = 0-3.0$ degrees). Each 3 dimensional plot is the result of 15 minutes execution and plotting time; the computer program is in Appendix 1.

Figure 4 shows the input $f(x,t)$ with the saccade ending at $t=15$ msec but with the slit illuminated during the post saccadic period ($t=15-25$ msec). Not shown but used as an input wave form was an $f(x,t)$ that was identical to figure 4 with the exception that $f(x,t) = 0$ at $t=15$ msec - simulating the slit turning off before the saccade end. The resulting $g(x,t)$ for both stimulus conditions are shown in figures 5 and 6. The output of the model at this point consists only of the $g(x,t)$ function. To complete the model, a psychophysical detection process must be postulated to predict what was seen. This portion of the model was not computer implemented during this phase of the work. However, a number of possibilities for the detector are suggested by comparing $g(x,t)$ to experimental results. These are presented in the following discussion section.

IV. DISCUSSION

The two response functions, $g(x,t)$, in figures 5 and 6 are substantially different. This is to be expected since two different input functions were used. If a simple detector is postulated in which a shape is seen only if its overall intensity is sufficiently different from the background, (contrast detection); then it is possible to draw some conclusions.

In figure 6, all of the peaks produced by the stimulus are essentially the same amplitude until the saccade end-- here the final peak is somewhat higher. But since the stimulus had been turned off at this point, all that is seen in $g(x,t)$ is an exponential decay in both time and space. A contrast detector should perceive each peak equally well, hence a spatial blur is seen. (The peaks really should be more continuous, however the time and space numerical integration increments were made large to conserve computation time.) It is easy to explain the large peak at the saccade end by recalling the cosine function relating space to time (Equation 7). This relation implies that the eye slows down towards the saccade end. As the eye slows down, for the same stimulus intensity, there is more temporal and less spatial integration taking place. Thus a brighter but spatially smaller light source is perceived. If $f(x,t) = 0$ at some time sooner than in figure 5, (before the eye slows down) the peaks in $g(x,t)$ would be even more similar in size. This interpretation compares favorably to observations noted by Martin in his slit experiment; long blurs were seen when the slit was extinguished before the end of the saccade, but the blur became shorter and the slit at the end of the blur became increasingly more pronounced as the light duration increased past the saccade end.

In Figure 6, the slit is left on after horizontal motion ceases. The eye continues to respond temporally at a single spatial position. Thus $g(x,t)$ develops a substantial peak in its response. The same type of detector as previously postulated would then dictate perception of only this peak - since it is much

FIGURE 4 - INPUT STIMULUS
SIMULATING SACCADIC;
SACCADIC END AT $t=15\text{MS}$,
 $x=1.4^\circ$; STIMULUS ON
UNTIL $t=25\text{MS}$

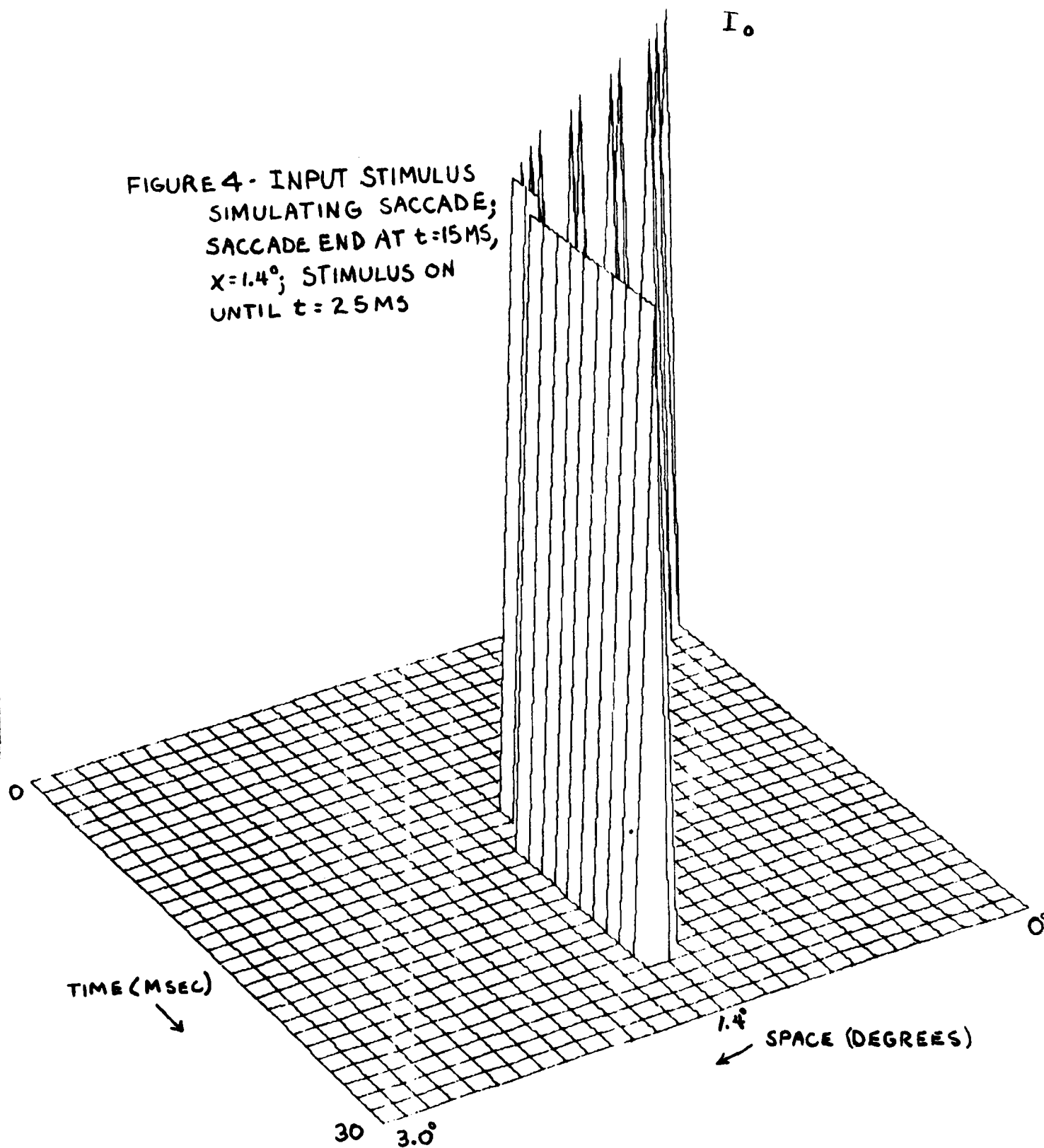


FIGURE 5- RESPONSE OF MODEL TO SACCADIC STIMULUS,
STIMULUS TURNED OFF AT SACCADE END - $t = 15\text{MS}$, $x = 14^\circ$

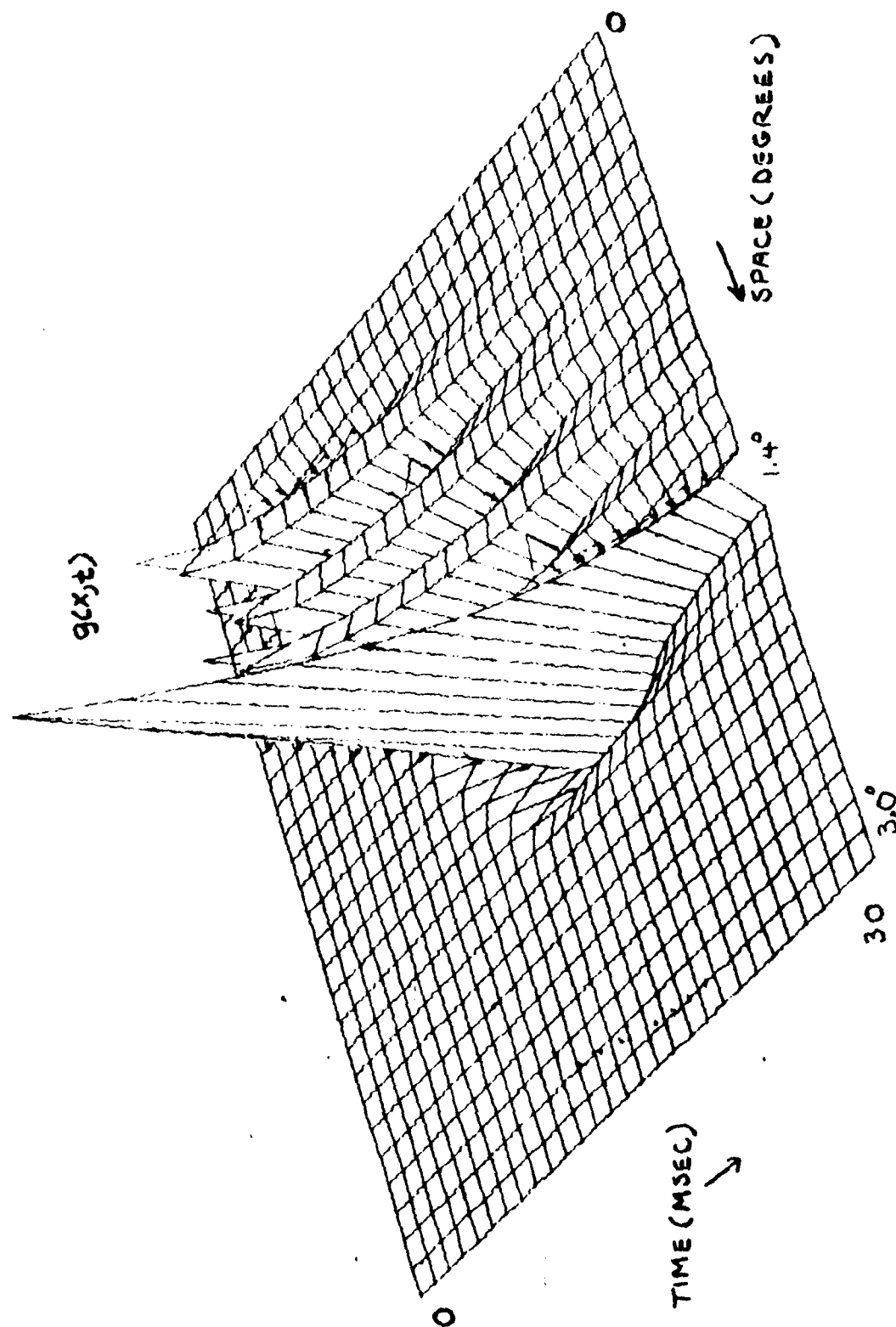
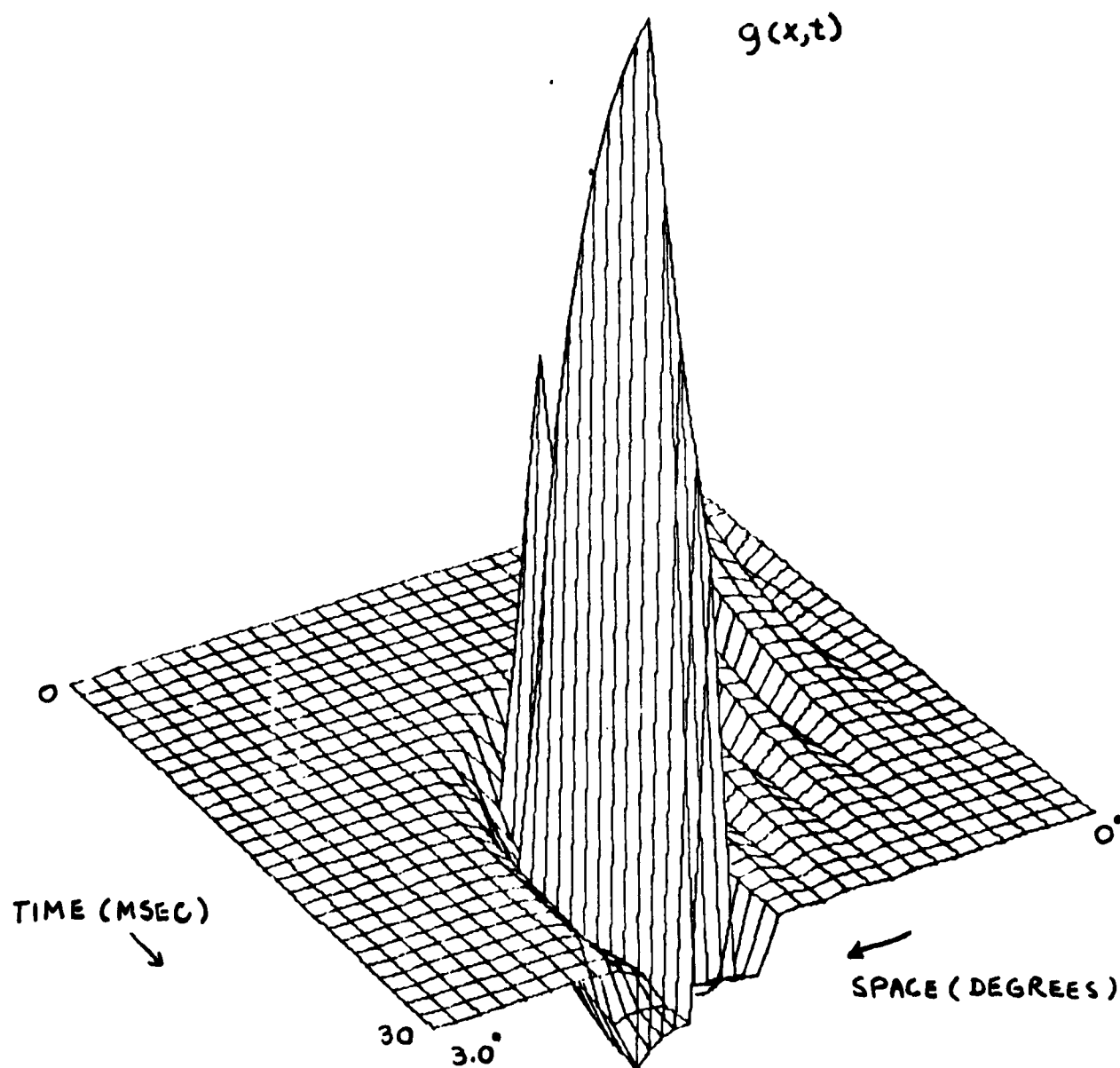


FIGURE 6- RESPONSE OF MODEL TO SACCADIC STIMULUS,
STIMULUS ON PAST SACCADIC END ($t=15\text{MS}$, $x=1.4^\circ$)
UNTIL $t=25\text{MS}$.



larger than any other disturbance in $g(x,t)$. This corresponds to the perception of only a slit - no blur, and a high degree of suppression. Simply stated, suppression is postulated to occur primarily because the temporal integration for a point on the retina is much greater when the eye is slow or fixating than while in a saccade. The resulting blurred image will be masked (or ignored) if there is, due to the system response, a more intense signal reaching the visual cortex at the saccade end. The question remaining is: How close in time or space must two signals be in order for suppression to occur?

This process can be represented mathematically as a detector. A type of detection has been postulated for the time domain by other investigators - it is essentially a finite time integrator: (36, 37)

$$\int_{t-\tau}^t \{g(t)\}^2 dt \geq K \Rightarrow \text{DETECTION} \quad (9)$$

$\tau \approx 200 \text{ msec}$

It is likely that spatial detectors of similar form are at work as well. The scope of this work has left formal investigation of the detector part of the model to a follow up study. However, it is expected that the detection process will be grounded in stochastic mathematics.

VI. CONCLUSIONS

The model presented in this investigation attempts to integrate spatial and temporal properties of the visual system, eye movements, and psychophysical processes. By doing this, it appears possible to understand some of the mechanisms that result in saccadic suppression.

The results of this report, while laying some ground work for a model also provide a few general conclusions.

1. Saccadic suppression is rarely 100%. It is both a function of stimulus pattern and psychophysical interpretation.
2. Based on the line spread function, temporal modulation transfer function and a suitable detection scheme, it should be possible to predict suppression magnitude for a number of situations.
3. The model could suggest the conditions for maximizing and minimizing suppression.

V. RECOMMENDATIONS

Recommendations from this work can be classified into three areas: 1. Implications of current literature and model results. 2. Suggestions for specific experiments. 3. Proposal to improve the effectiveness of the model.

1. Implications of Literature and Model

- a. Suppression is a relative phenomenon measured by percentage. It is not likely to achieve 100% suppression 100% of the

time. A more fundamental question to ask is: What will be tolerable in a visual display system? i.e., 50% suppression 75% of the time. Seeing is a question of perception. A stimulus may be presented that enhances the chances of suppression - but there is no guarantee that the subject will or will not perceive the stimulus.

- b. It should be possible to predict average suppression in a large number of situations.
- c. The model indicates that a combination of the visual system's spatial and temporal properties, and retinal stimulation are important determinants for predicting suppression during saccades.

2. Suggestions for Experiments

- a. Individuals should be tested for line spread function (LSF) and temporal transfer function (TTF) and then tested for saccadic suppression. The expected pay off would be a data set that directly relates some fundamental visual properties to suppression. It would also enable validation of the model's structure. Furthermore, information about the psychophysical detection process could be extracted.
- b. Most all saccadic suppression literature is derived from experiments that test vision without any coexisting task. Because of possible exploitation of suppression in a multi-sensory environment (i.e. a cockpit simulator), interactive effects should be studied. It is not possible at present to predict whether there would be more, less or the same suppression effects.
- c. Color and its effect on saccadic suppression is yet another area that has received little attention. At least a "base line" experiment is suggested.

3. Proposal to Improve Model

- a. The model presented in this report is quite crude and has resulted in only general statements about vision during saccadic movements. Steps to be taken to improve the model will be detailed in a "mini-grant" application. Only an outline is given here.
 - 1. Mathematical representation of detectors will be derived for the time-space domain
 - 2. Model out put will be generated to enable comparison with psychophysical experiments
 - 3. Convolution Algebra will be more precise
 - 4. Time course of eye accelerative effects will be included
 - 5. Retinal inhomogeneous spatial effects will be added

APPENDIX 1 - Computer Program for Two Dimensional Convolution

```

DIMENSION IAU(1024),PT(7),Z(30,30),WORK(120)
DIMENSION HX(300,30),F(300,30),G(300,30)
DATA 11/18INC1/
DO 10I=1,30
  XI=I-1
DO 10J=1,30
  XJ=J-1
  HX(I,J)=(EXP(-(1.1*XI/1064)**2)-.9*(.064/.193)*EXP(-
1  (1.1*XI/.193)**2))*PI*(EXP(-.001*XJ/.01)-.004*EXP(-.001*XJ/2.5))
C    DO TIME CONV
10  CONTINUE
DO 65I=1,30
DO 65J=1,30
  G(I,J)=F(I,J)*0.
65  CONTINUE
DO 64J=1,30
  I=15*(1-COS(13.14/30)*J))
  F(I,J)=10.
64  CONTINUE
DO 70I=1,30
DO 70N=1,I
DO 70J=1,30
DO 70K=1,J
  IF ((I-N).LE.0) GO TO 69
  IF ((J-K).LE.0) GO TO 69
  G(I,J)=G(I,J)+F(I,J)*HX((I-N),(J-K))*0.4
69  CONTINUE
70  CONTINUE
DO 75I=1,30
DO 75J=1,30
  Z(I,J)=G(I,J)
75  CONTINUE
DO 45I=1,30
45  WRITE(108,3) (Z(I,J),J=1,18)
3  FORMAT(5X,18F9.3)
  XMIN=YMIN=0
  ZMIN=0.
  XMAX=YMAX=ZMAX=1
  ZMAX=0
C    FIND MAX AND MIN
DO 55I=1,30
DO 55J=1,30
  IF (Z(I,J).GT.ZMAX) ZMAX=Z(I,J)
  IF (Z(I,J).LT.ZMIN) ZMIN=Z(I,J)
55  CONTINUE

```

THIS PAGE IS BEST QUALITY PRACTICABLE
FROM COPY FURNISHED TO DDC

```

      OUTPUT ZMAX,ZMIN
      H=Q=10
      NX=NY=30
      N=30
      TH=GAM=60
      IVIS=1
      PT(1)=11
      CALL THREE(XMIN,YMIN,ZMIN,XMAX,YMAX,ZMAX,PT(1),
1 Q,H,NX,NY,N,WORK,Z)
      CALL VIEW(TH,GAM,Q,IVIS)
      CALL PLOT(20,,0,,1)
      CALL CLRPLT
      END

```

THIS PAGE IS BEST QUALITY PRACTICABLE
FROM COPY FURNISHED TO DDC

REFERENCES

Saccadic Suppression

Abstracts

1. Bridgeman, B., Nelken, N., Heit, G., "Saccadic Suppression Determined Pysophysically in the Cat: Proc. ARVO 1979 p. 101
2. Brooks, B., Yates, J., Coleman, R., "How well can we see Image Motion Due to Saccadic Eye Movements: Proc. ARVO 1978 p. 138
3. Impelman, D., Brooks, B., "Backward and Forward Visual Masking During Saccades.: Proc. ARVO 1978, p. 138
4. White, C., Holtzman, J., "Visual Masking During Saccadic Eye Movements: Proc. ARVO 1977 p. 106
5. Cohn, T., Stark, L., Greenhouse, D. "Saccadic Suppression Maybe Due Entirely to Uncertainty in the Frame of Reference, "Proc. ARVO, 1977, p. 106
6. Volkman, F., Moore, R., Riggs, L., "Separable Effects on Contrast Sensitivity of Saccades and of Image Smear on the Retina" Proc. ARVO, 1977, p. 106
7. Wurtz, R., Campbell, F., "Why we Do Not See a Smear During Saccadic Eye Movements.: Proc. ARVO, 1977, p. 106

Papers

8. Volkman, F., Figgs, L., White, K., Moore, R., "Contrast Sensitivity During Saccadic Eye Movements, : Vis Res. Vol 18 pp 1193-1199 1978
9. Brooks, B., Fuchs, A., "Reply to Dr. Bridgemans' Letter," Vis. Res. Vol 17 pp 325-326, 197
10. Bridgeman, B., "Feplly to Brooks and Fuchs: Exogenous and Endogenous Contributions to Saccadic Suppression: Vis Res Vol 17 pp 323-324 1977
11. Sakitt, B., "Information Received from Unseen Lights", Vis. Res. Vol. 16 pp 782-784, 1976
12. Stark, L., Kong, R., Schwartz, S., Hendry, D., Bridgeman, B., "Saccadic Suppression of Image Displacement," Vis. Res. Vol 16 pp 1185-1187, 1976
13. Shebilske, W., "Extra Retinal Information in Corrective Saccades and Inflow vs. Outflow Theories of Visual Direction Constancy," Vis. Res. Vol 16 pp 621-628, 1976
14. Matin, I., "A possible hybrid mechanism for modification of visual direction associated with Eye Movements - The Paralyzed Eye Experiment Reconsidered " Perception, Vol 5 pp 233-239 1976

15. Brooks, B., Fuchs, A., "Influence of Stimulus Parameters on Visual Sensitivity During Saccadic Eye Movement.", Vis. Res. Vol 15 pp 1389-1398
16. Mitrani, L., Radil-Weiss, T., Yakimoff, N., Mateeff, S., Bozkov, V., "Determination of Vision Due to Contour Shift Over the Retina During Eye Movements," Vis. Res., Vol 15 pp 877-878, 1975
17. Mohler, G., Cechner, R., "Saccadic Suppression in the Monkey," Vis. Res. Vol 15 pp 1157-1160, 1975
18. Matin, E., "Saccadic Suppression: A Review and An Analysis," Psychol., Bull., Vol 81 pp 899-917 1974
19. Matin, L., Matin, E., "Visual Perception of Direction and Voluntary Saccadic Eye Movements." Biblio. Ophthal Vol. 82, pp 358-368, 1976
20. Matin, L., "Eye Movements and Perceived Visual Direction," Handbook of Sensory Physiology Vol VII, Visual Psychophysics pp 332-380, 1972
21. Matin, E., Clymer, A., Matin, L., "MetaContrast and Saccadic Suppression," Science, Vol 178, pp 179-182
22. Mackay, D., "Elevation of Visual Threshold by Displacement of Retinal Image," Nature, Vol 225, pp 90-92, 1970

Spatial and Temporal Properties

Papers

23. Wilson, H., Phillips, G., Bentschlen, I., Hülz, R., "Spatial Probability Summation and Disinhibition in Psychophysically Measures Line Spread functions," Vis. Res. Vol 19 pp 593-598 1979
24. Mezrich, J. "Modification of Spatial Frequency Processing Rates with Multiple Frequency Stimuli," Vis. Res. Vol 18 pp 1505-1507 1979
25. Wilson, H., "Quantitative Characterization of two types of Line Spread Function Near the Fovea," Vis. Res. Vol 18 pp 971-981, 1978
26. Glezer V.D., Gauzelman, V., Tsherbach, T., Dudkin, K., "Comments on Organization and Spatial-Frequency Characteristics of Receptive Fields in the Visual Cortex," Vis. Res. Vol 18, pp 887-889, 1978
27. Switkes, E., Mayer, M., Sloan, J., "Spatial Frequency Analysis of the Visual Environment: Anisotropy and the Carpentered Environment Hypothesis," Vis. Res. Vol 18 pp 1393-1399 1978
28. Caelli, T., Preston, G., Howell, E., "Implications of Spatial Summation Models for Processes of Contour Perception: A Geometric Respective," Vis. Res. Vol 18 pp 723-734 1978
29. Legge, G., "Sapce Domain Properties of a Spatial Frequency Channel in Human Vision," Vis. Res. Vol 18 pp 959-969 1978
30. Furchner, C., Thomas, J., Campbell, F., "Detection and Discrimination of Simple and Complex Patterns at Low Spatial Frequencies," Vis. Res. Vol 17, pp. 827-836

THIS PAGE IS BEST QUALITY PRACTICABLE
FROM COPY FURNISHED TO DDC

31. Graham, "Visual Detection of Aperiodic Spatial Stimuli by Probability Summation Among Narrowband Channels," Vis. Res. Vol 17 pp 637-652 1977
32. Carlson, C., Cohen, R., Gorog, I., "Visual Processing of Simple Two-Dimensional Sine-Wave Luminance Gratings," Vis. Res. Vol. 17 pp 351-358 1977
33. King-Smith, P., Riggs, L., Moore, R., Butler, T. "Temporal Properties of the Human Visual Nervous System," Vis. Res. Vol 17, pp 1101-1106 1977
34. Limb, J., Rubinstein, C., "A Model of Threshold Vision Incorporating Inhomogeneity of the Visual Field," Vis. Res. Vol 17, pp 371-384, 1977
35. Weisstein, N., Harris, C., Berbaum, K., Tangrey, J., Williams, A., "Contrast Reduction by Small Localized Stimuli: Extensive Spatial Spread of Above-Threshold Orientation-Selective Masking," Vis. Res. Vol 17, pp. 341-350, 1977
36. Rashbass, C., "Unification of two contrasting models of the visual increment threshold," Vis. Res. Vol 16, pp 1281-1283, 1976
37. Broekhuijsen, M., Rashbass, C., Veringa, F., "The threshold of Visual Transients," Vis. Res. Vol 16 pp 1285-1289, 1976
38. Arend, L. "Temporal Determinants of the Spatial Contrast Threshold MTF" Vis. Res., Vol 16 pp 1035-1042 1976
39. Hines, M., "Line Spread Function Variation Near the Fovea," Vis. Res. Vol 16 pp 567-572, 1976
40. Legge, G., "Adaptation to a Spatial Impulse: Implications for Fourier Transform Models of Visual Processing," Vis Res Vol 16 pp 1467-1418 1976
41. McCarter, A, Roehrs, T., "A Spatial Frequency Analogue to Mach Bands," Vis. Res. Vol 16, pp 1317-1321
42. Kelly, C., "Pattern Detection and the Two-Dimensional Fourier Transform: Flickering Checkerboards and Chromatic Mechanisms," Vis Res Vol 16, pp 277-287 1976
43. Spitzberg, R., Richards, W., "Broad Band Spatial Filters in the Human Visual System., " Vis. Res. Vol 15 pp 837-841 1975
44. Kelly, D., Magnuski, H., "Pattern Detection and the Two-Dimensional Fourier Transform: Circular Targets," Vis. Res. Vol 15 pp 911-915, 1975

Eye Movements

Papers

45. Mitrani, L., Dimitrov, G., Yakimoff, N. Mateef, S., "Oculomotor and Perceptual Localization During Smooth Eye Movements," Vis Res. Vol 19 pp 609-612 1979

46. Haegerstrom-Portnoy, G., Brown, B., "Contrast Effects on Smooth-Pursuit Eye Movement Velocity," Vis. Res. Vol 19, pp 169-174 1979
47. Henson, D. B., "Investigation into Corrective Saccadic Eye Movements for Refixation Amplitudes of 10 Degrees and Below," Vis. Res. Vol 19 pp 57-61, 1979
48. Mitrani, L., Dimitrov, G., "Pursuit Eye Movements of a Disappearing Moving Target," Vis. Res. Vol 18, pp 537-539 1978
49. Henson, D., "Corrective Saccades: Effects of Altering Visual Feedback," Vis. Res. Vol 18 pp 63-67 1978
50. Prablanc, C., Masse, D., Echallier, J., "Error-Correcting Mechanisms in Large Saccades," Vis. Res. Vol 18 pp 557-560, 1978
51. Holtzman, J., Sedgwick, H., Festinger, L., "Interaction of Perceptually Monitored and Unmonitored efferent Commands for Smooth Pursuit Eye Movements," Vis. Res. Vol 18 pp 1545-1555 1978
52. Hansen, R., Skavenski, A., "Accuracy of Eye Position Information for Motor Control," Vis Res. Vol 17 pp 919-926 1977
53. Komeda, M., Festinger, L., Sherry, J., "The Accuracy of Two-Dimensional Saccades in the Absense of Continuing Retinal Stimulation," Vis Res Vol 17, pp 1231-1232 1977
54. Viviani, P., Berthoz, A., Tracey, D., "The Curvature of Oblique Saccades," Vis. Res. Vol 17, pp. 661-664
55. Kowler, E., Steinman, R., "The Roles of Small Saccades in Counting," Vis. Res. Vol 17 pp 141-146, 1977
56. Ono, H., Nakamizo, S., "Saccadic Eye Movements During Changes in Fixation to Stimuli at Different Distances" Vis. Res. Vol 17 pp 233-238 1977
57. Becker, W., "Do Correction Saccades Depend Exclusively on Retinal Feedback? A Note on the Possible Role of Non-Retinal Feedback," Vis. Res. Vol 16, pp 425-427, 1976
58. Dimitrov, G., Yakimoff, N., S., Mitrani, L., "Saccadic Eye Movements on Bela Julesz' Figure," Vis. Res. Vol 16, pp 411-414 1976
59. Hallett, P., Lightstone, A., "Saccadic Eye Movements to Flashed Targets." Vis. Res. Vol 16, pp 107-114, 1976
60. Hallett, P., Lightstone, A., "Saccadic Eye Movements Towards Stimuli Triggered by Prior Saccades." Vol 16, pp 99-106, 1976
61. Lisberger, S., Fuchs, A., King, W., Evimer, J., "Effect of Mean Reaction Time of Saccadic Responses to Two-Step Stimuli with Horizontal and Verticle Components," Vis Res Vol 15, pp 1021-1025 1975

62. Coren, S., Bradley, D., Hoenig, P., Girgus, J., "The Effect of Smooth Tracking and Saccadic Eye Movements on the Perception of Size: The Shrinking Circle Illusion," Vis. Res. Vol 15, pp 49-55, 1975
63. Prablanc, C. Jeannerod, M., "Corrective Saccades: Dependence on Retinal Reafferent Signals," Vis. Res. Vol 15 pp 465-469, 1975

Books

64. Yarbus, A. "Eye Movements and Vision," Plenum Press 1967
65. Carpenter, R., "Movements of the Eyes." Pion, London, 1977

Visual Processing

Papers

66. Stoper, A., Mansfield, J., "Meta-Contrast and Paracontrast Suppression of a Contourless Area," Vis. Res Vol 18 pp 1669-1674, 1978
67. King-Smith, P., Riggs, L., "Visual Sensitivity to Controlled Motion of a Line or Edge," Vis. Res. Vol 18, pp 1509-1520, 1978
68. Grunau, M., "Interaction between Sustained and Transient Channels: Form Inhibits Motion in the Human Visual System," Vis. Res. Vol 18, pp 197-201, 1978
69. Mateeff, S., Yakimoff, N., Mitizain, I., "Some Characteristics of the Visual Masking by Moving Contours," Vis. Res. Vol 16., pp 489,492, 1976
70. Bridgeman, B., "Correlates of Metacontrast in Single Cells of the Cat Visual System," Vis Res Vol 15, pp 91-99, 1975

Books

71. Cornsweet, N. "Visual Perception" Academic Press, 1970
72. Uttal, W. "The Psychobiology of Sensory Coding" Harper and Row, 1973

THIS FILE IS BEST QUALITY FRAGMENT
FROM COPY FURNISHED TO DDC

1979 USAF - SCEEE SUMMER FACULTY RESEARCH PROGRAM

Sponsored by the

AIR FORCE OFFICE OF SCIENTIFIC RESEARCH

Conducted by the

SOUTHEASTERN CENTER FOR ELECTRICAL ENGINEERING EDUCATION

FINAL REPORT

A COMPUTER MODEL OF SACCADIC SUPPRESSION

Prepared by:	William J. Ohley
Academic Rank:	Assistant Professor
Department and University:	Department of Electrical Engineering University of Rhode Island
Research Location:	Human Resources Laboratory, Simulation Techniques Wright-Patterson AFB, OH
USAF Research Colleague:	Kenneth R. Boff
Date:	August 13, 1979
Contract No.:	F49620-79-C-0038

A COMPUTER MODEL OF SACCADIC SUPPRESSION

by

William J. Ohley

ABSTRACT

Suppression of vision during the course of voluntary saccadic eye movements has been well documented. However, the mechanisms which result in these observations are not clear. Moreover, the amount and types of visual suppression reported differ widely. It is not presently possible to accurately predict the efficacy of suppression for an individual in a given situation. However, the exploitation of suppression has been suggested for visual display systems. Thus, based on currently available data, this report provides a preliminary model for quantitative prediction of saccadic suppression. The model relies on the use of the line spread function, modulation transfer function, and temporal transfer function in conjunction with convolution mathematics and a postulated psychophysical detection process. Results are shown which facilitate explanation of typical suppression experiments. This is done by considering the visual system to be at least two-dimensional in time and space. The effects of visual stimulation during saccades are then seen to be a combination of the interaction between the time-space properties of the stimulus, those of the visual system, and a psychophysical detector. Since the model is composed entirely of software, it should be possible to examine a larger and more complex number of visual situations than would be experimentally feasible. In this way, baseline engineering design requirements can be specified. Furthermore if initial development of hardware proves difficult, the model, with suitable refinements, could provide an effective means for exploring alternative solutions. Suggestions for further research are also given.

ACKNOWLEDGMENTS

The support of the Air Force Office of Scientific Research, the Air Force Systems Command and the Southeastern Center for Electrical Engineering Education is gratefully acknowledged.

The author wishes to express his gratitude to the staff of the Human Resources Laboratory at Wright-Patterson AFB for a most stimulating and productive summer. In particular, Dr. Ken Roff for his provocative discussions; Dr. Don Gum for helping identify a problem area, Capt. Mike Ingalls for help in seeing the problem's scope; Dr. Gordon Eckstrand's advice on constraining the investigation was timely, as was Dr. Bill Askren's signature on my invoices. Mike Nicol, Lt. Jeff Rubin, TSgt Ed Sanderlin, and Bill Schelker made the HRL *STARS* computer readily available and useful for this project (despite my attempts to crash the system). Colleen Burns and Carolyn Runyon put up with typing this manuscript and material for several briefings. Those outside HRL also provided valuable input: Ed Martin, Jim Basinger, and Art Ginsburg. It was especially enjoyable to run a "few" miles with Dr. Bill Kane, my colleague in the summer program.

Finally thanks to Allegheny Airlines for always arriving 5 hours late in Rhode Island, and to Michele for putting up with this cross country commuter existence for 10 weeks.

I. INTRODUCTION

Eye movements play an enormous part in how we perceive the visual world. When described by velocity and duration, there are several types of eye motion. As one particular type, saccades can be classified by their high velocity ($100^{\circ} - 400^{\circ}/\text{sec}$) and macro movement ($1^{\circ} - 80^{\circ}$). While frequently voluntary, they can also occur involuntarily (i.e. during high velocity tracking of a moving object).

Voluntary saccades occur when one switches gaze from some portion of the visual field to another, for example, returning to the beginning of a line while reading. During that time, the reader is usually not aware of the page blurring past in the opposite direction. Thus the retinal image is said to be suppressed. Late during the last century, experiments on suppression in visual perception during saccadic movements were reported. Since that time, there has evolved a large body of literature dealing directly with the phenomenon of saccadic suppression.

In a typical experiment designed to measure suppression, the subject is presented with a visual stimulus (i.e. a test flash) that is triggered to occur either immediately before, during or after a saccade. The visibility of the flash when compared to fixation thresholds is usually reported as reduced. The reduction in visibility begins before eye movement and continues until after the eye comes to rest again. However, when visibility is graphed versus the time of stimulus occurrence, it is found to be a minimum only during a portion of the saccadic movement.

The problem addressed by this investigation is motivated by Air Force requirements in advanced visual display systems for flight simulation. Recently it has been suggested that saccadic suppression can be exploited by allowing reduction in display resolution during times of suppression. In order to implement a system which relies on saccadic suppression for its success, it is desirable that the characteristics of this type of human visual processing be predictable. A computer based mathematical model of saccadic suppression will make it possible to examine a larger and more complex number of visual situations than would be experimentally feasible. Furthermore, in the event of system hardware problems this analysis could provide an effective means for methodically exploring alternative design solutions.

II. OBJECTIVES

The objectives of this project were:

1. To review the research literature applicable to modeling the process of saccadic suppression.
2. To develop a mathematical description of the process that could predict for example, how much suppression may occur in a given situation.
3. To implement the model and evaluate its preliminary results.
4. To make recommendations concerning the use of saccadic suppression in visual display systems.

III. BACKGROUND

Matin (18) has extensively reviewed both the historic and modern work on saccadic suppression. Carpenter's text (65) deals with more recent investigations as well as the general area of eye movements. In terms of the development of the model discussed in this report, the pertinent literature may be divided into four areas. 1. Saccadic suppression. 2. Spatial and temporal properties. 3. Eye movements. 4. Visual processing.

1. Saccadic Suppression.

While the reference list contains several papers (19 - 22) prior to Matin's review, this report will deal primarily with subsequent work. Brooks et al (15) demonstrated, for stroboscopic test flashes, on various backgrounds, that similar time courses of suppression could be produced by "normal" saccadic eye movement and by "saccading" the visual image across the retina during eye fixation. Thus it was indicated that a large amount of suppressive effects may be due to retinal stimulation alone. Mitrani et al (16) also suggested that a significant amount of visual deterioration results from the movement of contours over the retinal field. Matin (14) considered the response of the visual system when eye muscles are paralyzed. He suggested a hybrid theory in which both actual eye movement and retinal stimulation can cause suppression. In related work, Shebilske (13) supported an "in flow" over an "out flow" theory of visual direction constancy during saccades. That is, the visual system relies on feedback from actual eye movement and position to interpret retinal stimulation.

While most suppression work has centered on stationary test flash visibility, Stark et al (12) experimentally showed suppression of image displacement. Furthermore, under static eye stimulus conditions, Sakitt (11) suggested that visual information may be available to the brain even though the observer indicates that the stimulus was not seen.

Bridgeman (10) criticized Brooks et al (15) by arguing in favor of an "extra retinal signal" arising during saccades to cause threshold elevations. Brooks et al (9) argued against this theory - maintaining that the primary source of suppression was due to the pattern of retinal stimulation.

Volkman et al (8) demonstrated elevation in contrast sensitivity during saccades. They conclude that both optical and neural effects combined to produce suppression. However, a larger amount of suppression appeared due to retinal stimulation than any extra-retinal signal.

The most recent work in saccadic suppression is represented in abstract form (1 - 7). Bridgeman et al has demonstrated saccadic suppression psychophysically in the cat (1), Brooks et al investigated perception of image motion during saccades (2), Impelman et al (3) and White et al (4) showed masking effects. Cohn et al (5) suggest that suppression may be due entirely to "uncertainty in the frame of reference." In addition Volkman et al (6) separate the effects of contrast sensitivity and retinal smear, while Wurtz et al (7) were concerned with retinal smear suppression.

Based on the literature, the following general conclusions can

be drawn: Suppression occurs for a variety of visual discrimination tasks i.e., contrast sensitivity, threshold, and perceived direction. Suppression can be obtained by "saccading" an image across a fixated eye. While stronger suppression occurs when the stimulus is more complex than simple flashes, it also occurs to a lesser extent during saccades over a low detail visual field. Although not tested experimentally, it has been suggested that the apparent large amount of suppression in the real world is due primarily to the complexity of the visual image.

Given the intended application, there appears to be a lack of data on saccadic suppression in several areas: (1) suppression in the presence of a coexisting stimulus or task, as might occur in a simulator cockpit; (2) quantitative results of suppression in a multi-colored environment. In any event, there have been no attempts to quantitatively predict the results of a suppression experiment either for simple test flashes or for more complex situations.

2. Spatial and Temporal Properties.

Because the saccadic suppression literature indicates the importance of retinal stimulation in obtaining elevated thresholds, literature pertaining to the visual system's spatial and temporal properties was investigated. The static spatial properties of the visual system have generally been described by several investigators in either or two ways: (1) By using some test of visibility

such as threshold sensitivity, the response to a series of spatial frequency sine waveforms has been obtained. This yields a transfer characteristic of the system in the frequency domain: the Modulation Transfer Function (MTF) (Legge (29), 4, Arhner et al (3) Graham (31), Carlson et al (32), Spitzberg (43), Kelley et al (44).) The results obtained depend on the stimulus intensity and wavelength as well as such factors as retinal location. (2) The inverse Fourier transform of the MTF (assuming a linear system) yields the Line Spread Function (LSF) (also called the Receptive Field Sensitivity Function). This function has recently been measured psychophysically by obtaining the visual response to two thin spatial lines, one 70% the intensity of the other. The visibility of the brighter line is found to be a function of how close the two lines are in space. By appropriate analysis, the LSF can be deduced. (Wilson et al (33), Wilson (25), Gelman et al (26), Limb et al (34), Hines (39).

It has also recently been shown that the spectral and spatial properties of the system can be modeled by the temporal properties of the stimulus. Wilson, (25). In addition to a series of spatial Fourier filters, there is evidence that both temporal "transient" and "sustained" channels exist as well (Mezrich (24), Arend (38), Spitzberg et al (43), Wilson (25).) It could be said that the visual system filters in both space and time - and that these processes appear to interact. Spitzberg et al demonstrate relationships between sustained-transient and high spatial frequency responses.

The temporal properties have been studied extensively in the past (using test flashes etc) to obtain a "temporal modulation transfer function" (71). Recently Smith et al (33) have employed a stabilization apparatus to investigate visual time response.

However, there does not appear to be an experiment in which both the time response and line spread functions are simultaneously derived. The closest work in this area is Wilson (35) and Arend (38).

3. Eye Movements

There have been a number of investigations concerning the interaction of visual perception and saccadic eye movements. Prablanc et al (63) reported on the dependency of corrective saccades on retinal reafferent signals. Corrective saccades are small and immediately follow large saccades so that a target can be brought into the central fovea. They found that target stimulation must be available to the retina at certain times during the large primary saccade in order for the correction saccade to be accurate. Furthermore, latency in corrective saccadic response may be modified by appropriate timing of the stimulus. Coren et al (62) studied perception of the size of a circle inscribed by a circularly moving target. They showed that for high target velocity, the initiation of saccades to keep up with the object also resulted in more accurate perception of the circle size. In the smooth tracking phase, the circle appears to shrink as the angular velocity of the object increases.

Lisberger et al (61) investigated the number of corrective saccades as a function of total saccadic length. It was found that the longer primary saccade exhibited more corrective saccades than the shorter ones. However, results were also a function of target conditions and subjects. Hallett (60) demonstrated that "important visual stimulation can occur during saccades," This was observed in an experimental situation which altered the target position during an initial saccade. Hallett et al (59) presented additional evidence that saccades are "goal directed towards the physical location of the target . . . this is possible only if retinal image position and eye position information are correlated." Becker (57) suggests that visual information is not necessary for corrective saccades to occur. However he contends this disagreement with Prablanc et al (63) is most likely due to experimental conditions. Dimitrov et al (58) examined saccadic eye movement in terms of a stereoscopic image (Bela Julesz' Figure). They conclude that despite the unusual experimental conditions, the dependence of the maximum velocity and duration of the saccades on amplitude was not altered. Viviani et al (54) showed that for voluntary and optokinetic oblique saccades, a curved rather than straight path is followed. Furthermore there was a systematic dominance of the horizontal over the vertical component.

Komoda et al (53) investigated the accuracy of two dimensional saccades in the absence of retinal stimulation. They concluded, because of the relatively high accuracy, that the saccades are programmed on the basis of memory. Hansen et al (52) reiterated this finding by examining the accuracy of eye position information for motor control. They concluded that large errors in controlling eye position in the dark are due to poor spatial memory.

In further experiments, Prablanc et al (50) suggest that if extra-retinal signals do play a part in saccadic positional error, then they are not very sensitive, and in "normal" situations visual feedback is the dominating factor. Henson (47, 49) altered the visual feedback to the oculomotor system during large saccades to eliminate the need

for a "correction" saccade. The saccadic system was found to learn after a few minutes to undershoot the target as before. This result demonstrates the "corrective" saccadic mechanism to be a deliberate one.

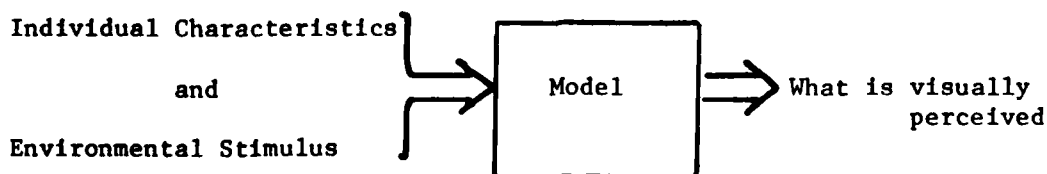
Despite the substantial number of investigations that have examined the relationship of saccadic eye movements and vision it is not entirely clear how the systems interact. There is apparently a combination of both retinal and extra retinal signals that effect resulting eye motion. The exact effects seem to be functions of both the situation and the individual.

4. Visual Processing

This section of the literature review is not well developed. The papers included here only scratch the surface of what may prove to be valuable information in modeling saccadic suppression. Several papers on meta contrast may have impact on perception during saccades (66, 70) since a meta contrast masking effect can be observed - apparent suppression occurring before eye movement. However, it may also be possible to explain this on the basis on time delays. For those familiar with system theory, a non-causal (meta contrast) system can be made causal with a sufficient time shift. Other types of masking have been investigated recently by Mateeff et al (69), Grunau (68), and King-Smith (68). It can also be noted here that Cornsweet (71) provides a wealth of information on visual perception in terms of linear and non-linear systems.

IV. MODEL DEVELOPMENT AND PRELIMINARY RESULTS

The model developed in this investigation is an attempt to combine information from the several areas of vision literature reviewed in section III. It is assumed to have the following form:



The input to the model are an individual's visual characteristics and the environmental stimulus. The output desired is a prediction of what was visually perceived.

First the individual's characteristics are considered, and the following general assumptions are made:

1. Visual acuity is "normal".
2. Range of illumination level and contrast is small.
3. Visual characteristics don't change during the saccadic time interval.
4. Model is restricted to black and white illumination.
5. Most suppression is due to retinal stimulation, extra retinal factors are secondary.

These assumptions allow the consideration of a lumped linear time invariant system. It is recognized that the eye and brain are probably non-linear, time varying, and non-causal as well. However, a linear analysis initially can provide some insight into a complex problem. Furthermore, it is quite likely that much of the stochastic, non-linear, or time varying,

effects are a result of psychophysical processes. Thus it is useful to divide the model into two parts: 1. Sensor, and 2. Psychophysical detector.

To characterize the sensor portion of the model, data from the literature on line spread functions (LSF), modulation transfer functions (MTF) and temporal transfer functions (TTF) is utilized. The LSF or MTF describe the spatial properties of the system while the temporal properties are derived from the TTF. To make predictive use of this data, the concepts of impulse response and convolution integrals must be considered. Using the well known convolution integral, for a linear time invariant system in the time domain:

$$g(t) = \int_{-\infty}^{\infty} h(\tau) f(t-\tau) d\tau \quad (1)$$

where $g(t)$ is the output, $f(t)$ the input and $h(t)$ the impulse response, or system function. If only one spatial direction, i.e. the horizontal, is considered in conjunction with time, the system function is in general, a function of time and space:

$$g(x,t) = \int_{-\infty}^{\infty} \int_{-\infty}^{\infty} h(x,\tau) f(x-\xi, t-\tau) d\xi d\tau \quad (2)$$

Thus if one knows the time-space properties of the system, $h(x,t)$, the resulting time space function, $g(x,t)$, can be derived from any input function $f(x,t)$. Let $f(x,t)$ represent the intensity of illumination at some horizontal position x on the retina at some time t . Then $g(x,t)$ can be the representation of that illumination pattern arriving at the visual cortex as modified by $h(x,t)$.

Next it is assumed that:

$$h(x,t) = h_1(x) h_2(t) \quad (3)$$

This implies that $h(x,t)$ is separable - or symmetric to both the time and space axis. Then functional forms for $h_1(x)$ and $h_2(t)$ can be obtained from LSF, MTF and TTF data. Since the LSF is simply the Fourier transform of the MTF (assuming linearity), LSF data from Wilson (25) was used to describe $h_1(x)$:

$$h_1(x) = \exp\left(-\frac{x^2}{\sigma_e^2}\right) - \frac{K\sigma_e}{\sigma_i} \exp\left(-\frac{x^2}{\sigma_i^2}\right) \quad (4)$$

Where $\sigma_e = .064$, $\sigma_i = .193$, $K = .90$ and x is eccentricity in degrees. Recent investigations have shown that the LSF is a function not only of horizontal position x , but of where on the retina it is measured. The above numbers are for 0° eccentricity (at the fovea). While the form of LSF remains double gaussian, the constants σ_e , σ_i , K change significantly as one moves several degrees on the retina. Furthermore, it is also shown by Wilson and others (25, 38) that the temporal pattern of the stimulus affects its spatial perception.

These effects were not included in the model at this time. The retina is considered to be horizontally homogeneous and described by equation (4). However, several different values for σ_e , σ_i and K were examined to estimate how important they are to the system. The form of $h_2(t)$ was then estimated. Here from the data in (71) and (33):

$$h_2(t) = \exp(-t/\tau) \quad (5)$$

$$\tau = 2.0 \text{ msec}$$

Again several values of τ were also examined.
By combining (3) and (4):

$$h(x,t) = \left[\exp\left(-\frac{x^2}{\sigma_x^2}\right) - \frac{k\sigma_x}{\sigma_t} \exp\left(-\frac{x^2}{\sigma_t^2}\right) \right] \cdot \exp(t/\tau) \quad (6)$$

$h(x,t)$ is shown graphed in figure (1).

In order to predict $g(x,t)$, it remains now to describe $f(x,t)$, the space-time course of retinal stimulation during a saccadic eye movement. If it is assumed that stimulus is a spot of light that is turned on and then off as it is swept across the retina at constant velocity, in the space time plane $f(x,t)$ would look like Figure (2). Here it runs essentially diagonal across the plane-for each new instant, a new spatial location is stimulated. If, on the other hand, the movement in the x direction is stopped while the light remains on, then at that point the pulses would run parallel to the t axis. This is shown occurring in Figure (2) starting at $t = 25$ msec.

In naturally occurring saccades, a straight line relationship does not exist between the horizontal angle and time. Yarbus (64) gives it as a cosine relation:

$$x = \frac{x_0}{2} \left(1 - \cos \frac{\pi}{T} t \right) \quad (7)$$

Where t is time in seconds, x is the rotation angle in degrees, T is total saccade duration time, and x_0 is the final angle at the end of the saccade. For a light spot of intensity I_0 turned on at $t=0$ and off at $t=t_1$, Equation (7) yields:

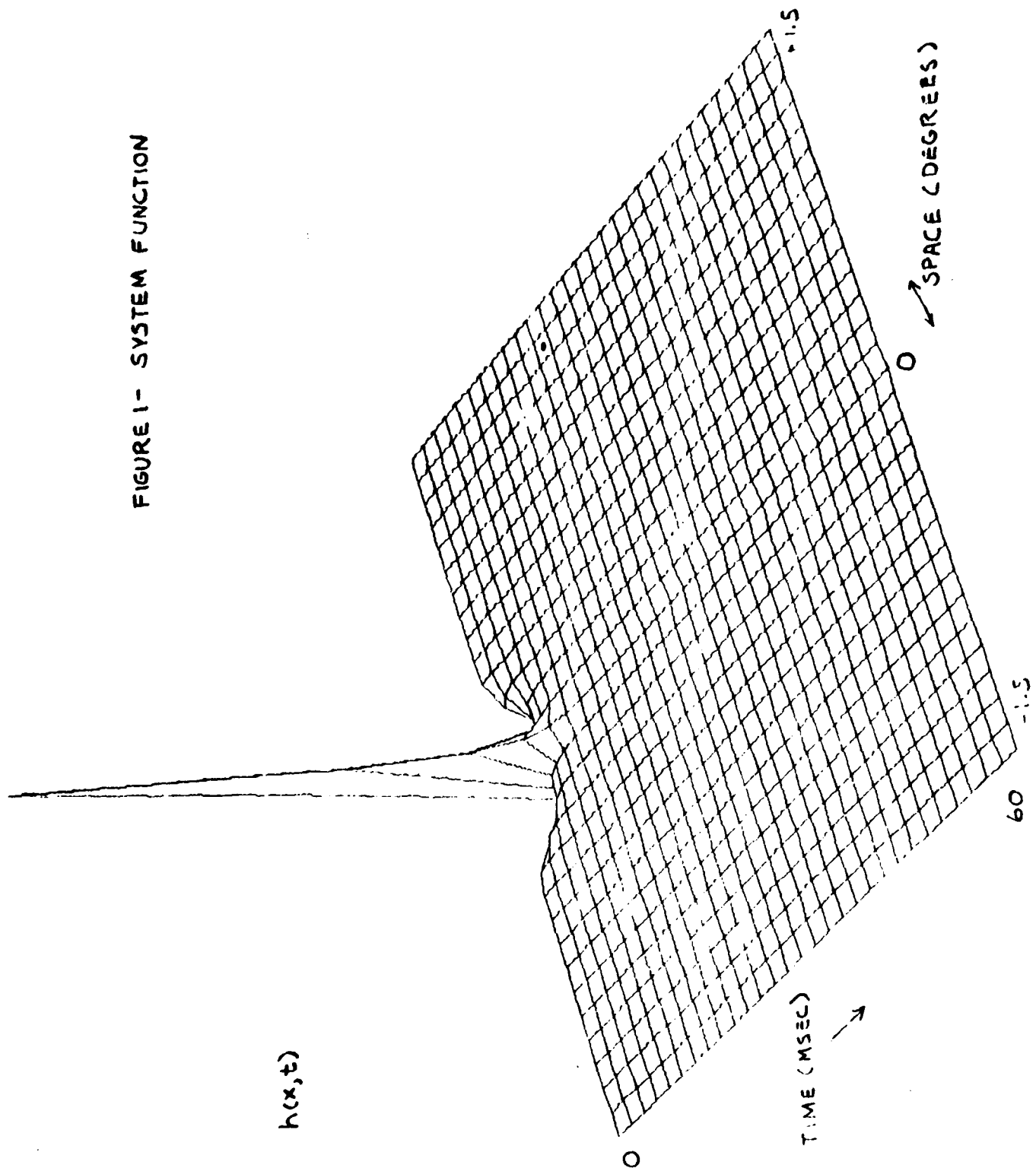
$$f(x,t) = \begin{cases} I_0, & 0 < t < t_1, \text{ AND } x_0 < x < \frac{x_0}{2} \left(1 - \cos \frac{\pi}{T} t \right) \\ 0, & \text{OTHERWISE} \end{cases} \quad (8)$$

Using equation (6) and (8), the resulting $g(x, t)$ can be predicted for a given experimental condition. It is useful to examine a particular saccadic suppression experiment (Matin(21)). The subject was required to make voluntary left to right 40° horizontal saccades between two fixation points. At the 1° position, detected by oculometer, a slit of light located beneath the right fixation point was then turned on. The slit was left on for varying times during the course of the saccade. The subject then compared the apparent length of the slit - (it was often seen as a blur in the visual field) to a comparison line displayed 500 msec after the saccade ended. (Figure 3a). The results for various illumination levels are shown in Figure 3b. The ordinate is perceived slit length and the abscissa is duration of slit illumination. Essentially, the blur was only perceived when the slit was turned off during the saccade. When left on past end of eye movement ($t > 30$ msec), the length of the blur decreased until only the slit itself was perceived. The blur was said to be suppressed.

To simulate this experiment, results were obtained from the model for two basic conditions: 1. Slit turned off before the end of the saccade and 2. Slit left on past the end of the saccade.

Applying the model consisted of solving equation (2). In order to obtain solutions to the convolution integral several methods were considered - one could use an FFT (Fast Fourier Transform) and work the solution in the frequency domain. However, this algorithm was not available in the HRL Stars system. Thus, a direct discrete solution

FIGURE 1- SYSTEM FUNCTION



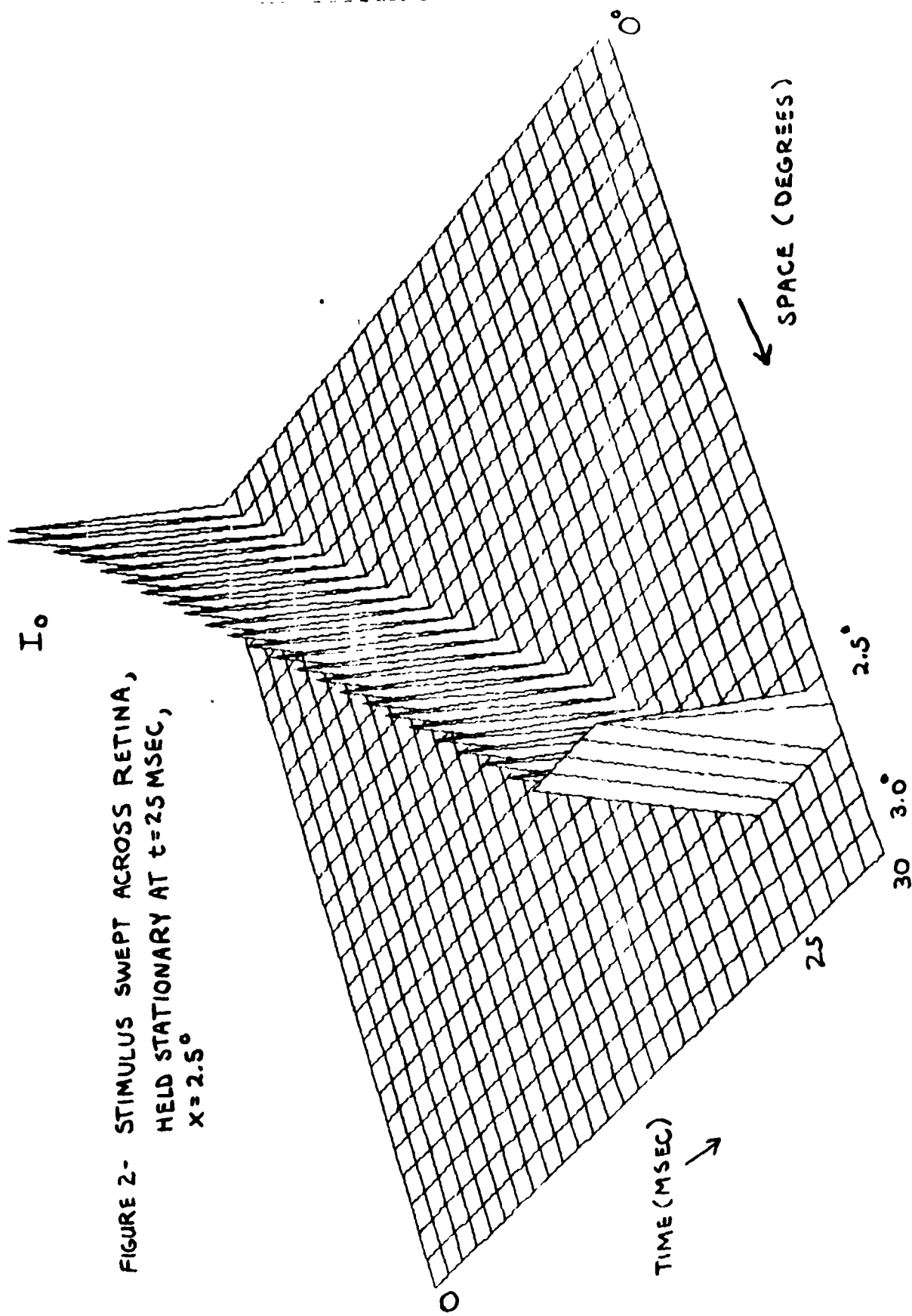
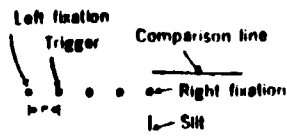


FIGURE 2- STIMULUS SWEEP ACROSS RETINA,
HELD STATIONARY AT $t=25$ MSEC,
 $x=2.5^\circ$

A.



B.

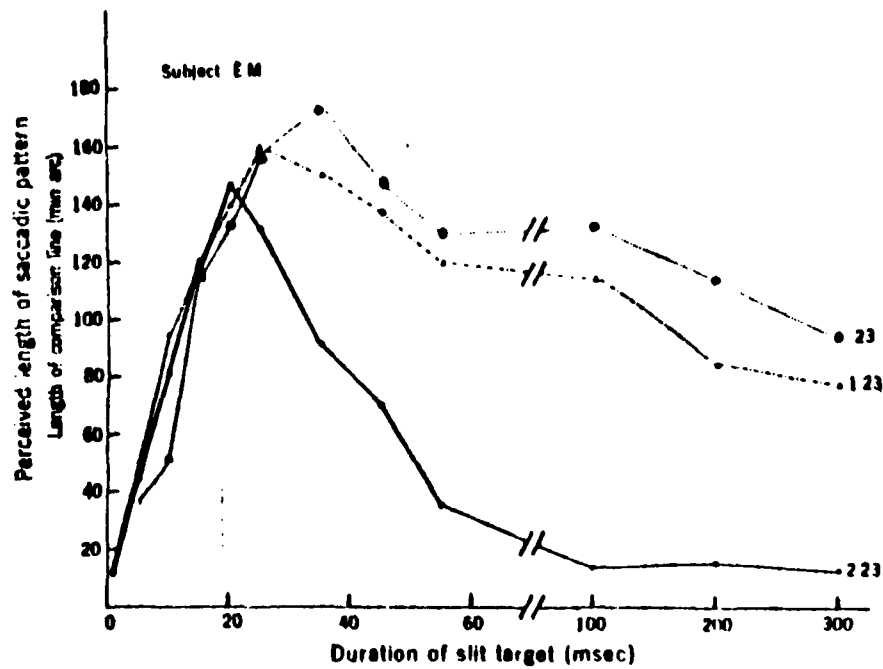


FIGURE 3 - MATIN'S EXPERIMENT

to the two-dimensional convolution was then implemented. Because of memory and system execution time limitations, a 30 X 30 array was chosen to represent the space-time plane ($t=0-30$ msec; $x = 0-3.0$ degrees). Each 3 dimensional plot is the result of 15 minutes execution and plotting time; the computer program is in Appendix 1.

Figure 4 shows the input $f(x,t)$ with the saccade ending at $t=15$ msec but with the slit illuminated during the post saccadic period ($t=15-25$ msec). Not shown but used as an input wave form was an $f(x,t)$ that was identical to figure 4 with the exception that $f(x,t) = 0$ at $t=15$ msec - simulating the slit turning off before the saccade end. The resulting $g(x,t)$ for both stimulus conditions are shown in figures 5 and 6. The output of the model at this point consists only of the $g(x,t)$ function. To complete the model, a psychophysical detection process must be postulated to predict what was seen. This portion of the model was not computer implemented during this phase of the work. However, a number of possibilities for the detector are suggested by comparing $g(x,t)$ to experimental results. These are presented in the following discussion section.

IV. DISCUSSION

The two response functions, $g(x,t)$, in figures 5 and 6 are substantially different. This is to be expected since two different input functions were used. If a simple detector is postulated in which a shape is seen only if its overall intensity is sufficiently different from the background, (contrast detection); then it is possible to draw some conclusions.

In figure 6, all of the peaks produced by the stimulus are essentially the same amplitude until the saccade end-- here the final peak is somewhat higher. But since the stimulus had been turned off at this point, all that is seen in $g(x,t)$ is an exponential decay in both time and space. A contrast detector should perceive each peak equally well, hence a spatial blur is seen. (The peaks really should be more continuous, however the time and space numerical integration increments were made large to conserve computation time.) It is easy to explain the large peak at the saccade end by recalling the cosine function relating space to time (Equation 7). This relation implies that the eye slows down towards the saccade end. As the eye slows down, for the same stimulus intensity, there is more temporal and less spatial integration taking place. Thus a brighter but spatially smaller light source is perceived. If $f(x,t) = 0$ at some time sooner than in figure 5, (before the eye slows down) the peaks in $g(x,t)$ would be even more similar in size. This interpretation compares favorably to observations noted by Martin in his slit experiment; long blurs were seen when the slit was extinguished before the end of the saccade, but the blur became shorter and the slit at the end of the blur became increasingly more pronounced as the light duration increased past the saccade end.

In Figure 6, the slit is left on after horizontal motion ceases. The eye continues to respond temporally at a single spatial position. Thus $g(x,t)$ develops a substantial peak in its response. The same type of detector as previously postulated would then dictate perception of only this peak - since it is much

FIGURE 4 - INPUT STIMULUS
SIMULATING SACCADIC;
SACCADIC END AT $t=15\text{MS}$,
 $x=1.4^\circ$; STIMULUS ON
UNTIL $t=25\text{MS}$

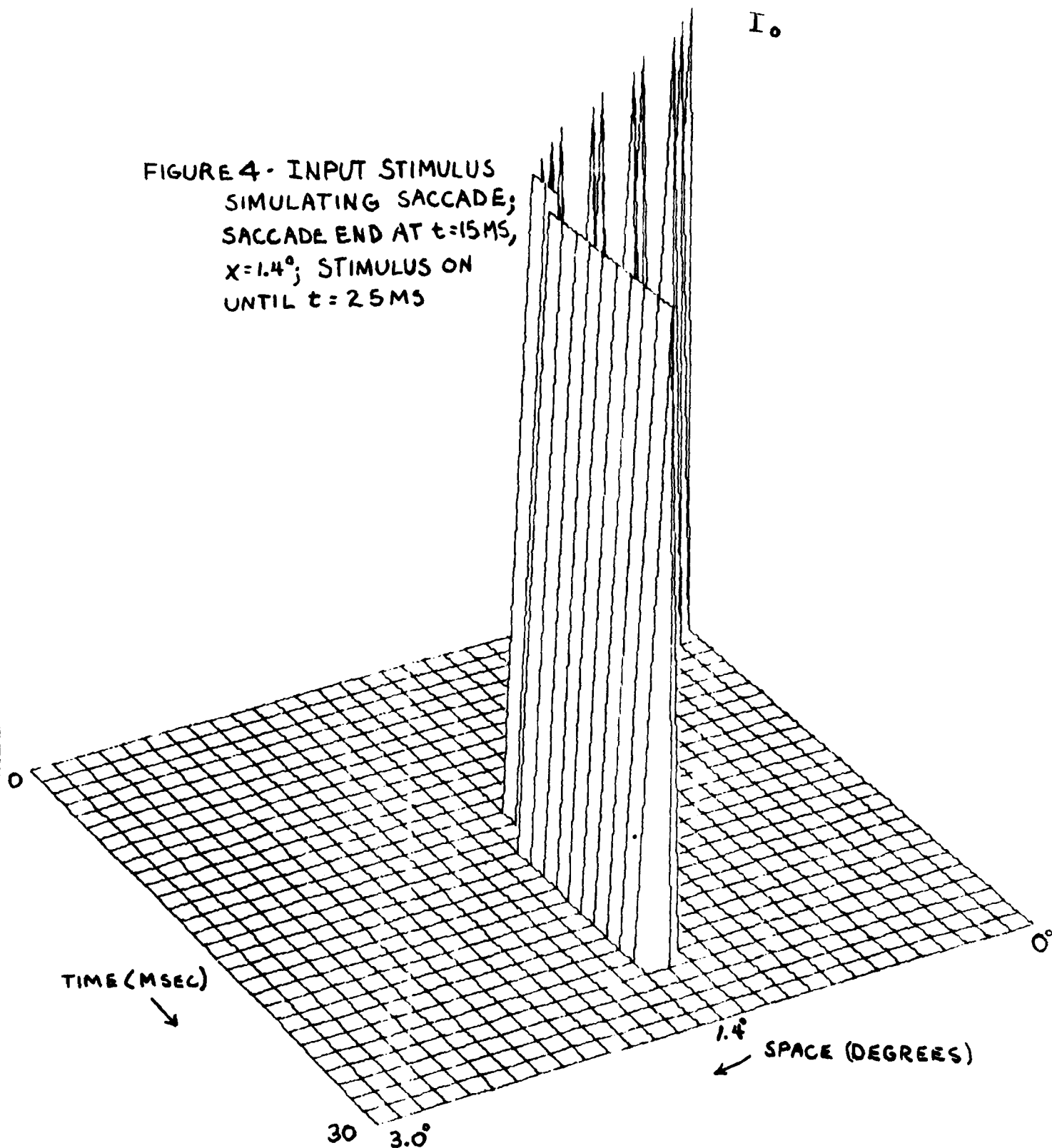


FIGURE 5 - RESPONSE OF MODEL TO SACCADIC STIMULUS,
STIMULUS TURNED OFF AT SACCADIC END - $t = 15\text{MS}$, $x = 14^\circ$

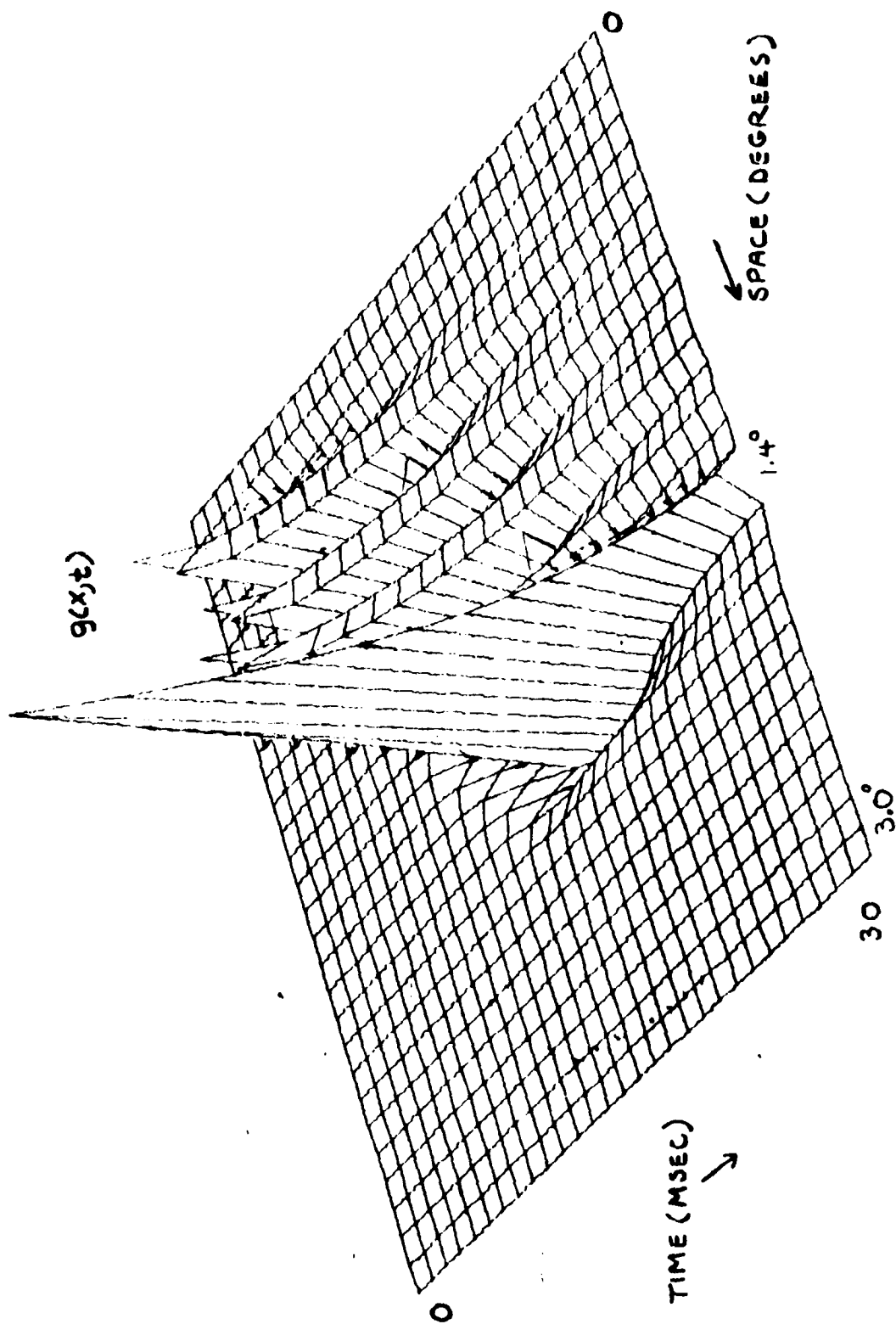
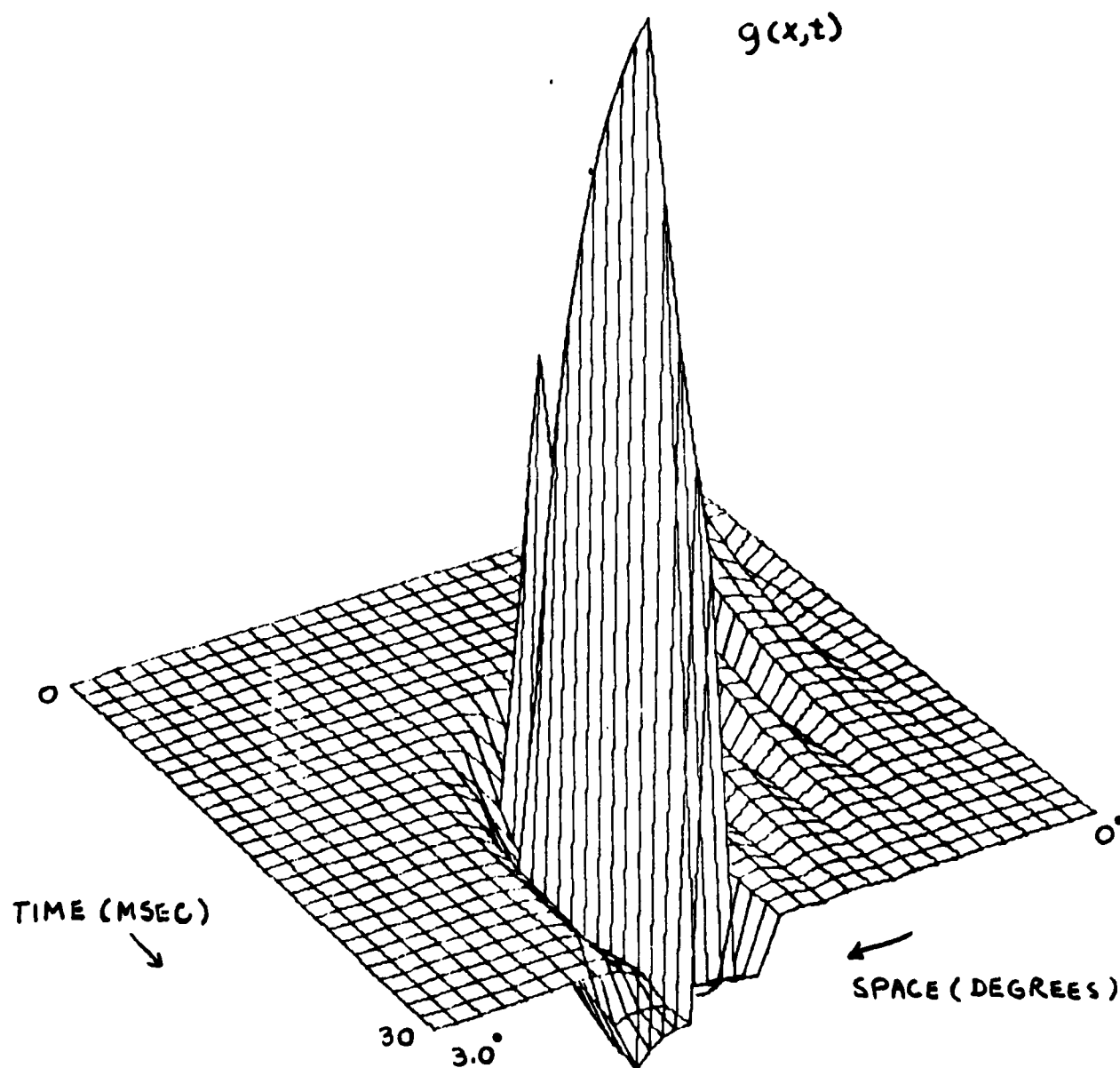


FIGURE 6- RESPONSE OF MODEL TO SACCADIC STIMULUS,
STIMULUS ON PAST SACCADIC END ($t=15\text{MS}$, $x=1.4^\circ$)
UNTIL $t=25\text{MS}$.



larger than any other disturbance in $g(x,t)$. This corresponds to the perception of only a slit - no blur, and a high degree of suppression. Simply stated, suppression is postulated to occur primarily because the temporal integration for a point on the retina is much greater when the eye is slow or fixating than while in a saccade. The resulting blurred image will be masked (or ignored) if there is, due to the system response, a more intense signal reaching the visual cortex at the saccade end. The question remaining is: How close in time or space must two signals be in order for suppression to occur?

This process can be represented mathematically as a detector. A type of detection has been postulated for the time domain by other investigators - it is essentially a finite time integrator: (36, 37)

$$\int_{t-\tau}^t \{g(t)\}^2 dt \geq K \Rightarrow \text{DETECTION} \quad (9)$$

$\tau \approx 200 \text{ msec}$

It is likely that spatial detectors of similar form are at work as well. The scope of this work has left formal investigation of the detector part of the model to a follow up study. However, it is expected that the detection process will be grounded in stochastic mathematics.

VI. CONCLUSIONS

The model presented in this investigation attempts to integrate spatial and temporal properties of the visual system, eye movements, and psychophysical processes. By doing this, it appears possible to understand some of the mechanisms that result in saccadic suppression.

The results of this report, while laying some ground work for a model also provide a few general conclusions.

1. Saccadic suppression is rarely 100%. It is both a function of stimulus pattern and psychophysical interpretation.
2. Based on the line spread function, temporal modulation transfer function and a suitable detection scheme, it should be possible to predict suppression magnitude for a number of situations.
3. The model could suggest the conditions for maximizing and minimizing suppression.

V. RECOMMENDATIONS

Recommendations from this work can be classified into three areas: 1. Implications of current literature and model results. 2. Suggestions for specific experiments. 3. Proposal to improve the effectiveness of the model.

1. Implications of Literature and Model

- a. Suppression is a relative phenomenon measured by percentage. It is not likely to achieve 100% suppression 100% of the

time. A more fundamental question to ask is: What will be tolerable in a visual display system? i.e., 50% suppression 75% of the time. Seeing is a question of perception. A stimulus may be presented that enhances the chances of suppression - but there is no guarantee that the subject will or will not perceive the stimulus.

- b. It should be possible to predict average suppression in a large number of situations.
- c. The model indicates that a combination of the visual system's spatial and temporal properties, and retinal stimulation are important determinants for predicting suppression during saccades.

2. Suggestions for Experiments

- a. Individuals should be tested for line spread function (LSF) and temporal transfer function (TTF) and then tested for saccadic suppression. The expected pay off would be a data set that directly relates some fundamental visual properties to suppression. It would also enable validation of the model's structure. Furthermore, information about the psychophysical detection process could be extracted.
- b. Most all saccadic suppression literature is derived from experiments that test vision without any coexisting task. Because of possible exploitation of suppression in a multi-sensory environment (i.e. a cockpit simulator), interactive effects should be studied. It is not possible at present to predict whether there would be more, less or the same suppression effects.
- c. Color and its effect on saccadic suppression is yet another area that has received little attention. At least a "base line" experiment is suggested.

3. Proposal to Improve Model

- a. The model presented in this report is quite crude and has resulted in only general statements about vision during saccadic movements. Steps to be taken to improve the model will be detailed in a "mini-grant" application. Only an outline is given here.
 - 1. Mathematical representation of detectors will be derived for the time-space domain
 - 2. Model out put will be generated to enable comparison with psychophysical experiments
 - 3. Convolution Algebra will be more precise
 - 4. Time course of eye accelerative effects will be included
 - 5. Retinal inhomogeneous spatial effects will be added

APPENDIX 1 - Computer Program for Two Dimensional Convolution

```

DIMENSION IAP(1024),PT(7),Z(30,30),WORK(120)
DIMENSION HX(300,30),F(300,30),G(300,30)
DATA 11/18INC1/
DO 10 I=1,30
  XI=I-1
DO 10 J=1,30
  XJ=J-1
  HX(I,J)=(EXP(-(1+XI/1064)**2))*.9*(.064/.193)*EXP(-
1  (1+XI/.193)**2))*(EXP(-.001*XJ/.01))-.004*EXP(-.001*XJ/2.5))
C    DO TIME CONV
10  CONTINUE
DO 65 I=1,30
DO 65 J=1,30
  G(I,J)=F(I,J)+0.
65  CONTINUE
DO 64 J=1,30
  I=15*(1-COS(13.14/30)*J))
  F(I,J)=10.
64  CONTINUE
DO 70 I=1,30
DO 70 N=1,I
DO 70 J=1,30
DO 70 K=1,J
  IF ((I-N).LE.0) GO TO 69
  IF ((J-K).LE.0) GO TO 69
  G(I,J)=G(I,J)+F(I,J)*HX((I-N),(J-K))*.04
69  CONTINUE
70  CONTINUE
DO 75 I=1,30
DO 75 J=1,30
  Z(I,J)=G(I,J)
75  CONTINUE
DO 45 I=1,30
45  WRITE(108,5) (Z(I,J),J=1,18)
5    FORMAT(5X,18F9.3)
  XMIN=YM1N=0
  ZMIN=0
  XMAX=YMAX=ZMAX=1
  ZMAX=0
C    FIND MAX AND MIN
DO 55 I=1,30
DO 55 J=1,30
  IF (Z(I,J).GT.ZMAX) ZMAX=Z(I,J)
  IF (Z(I,J).LT.ZMIN) ZMIN=Z(I,J)
55  CONTINUE

```

THIS PAGE IS BEST QUALITY PRACTICABLE
FROM COPY FURNISHED TO DDC

```

      OUTPUT ZMAX,ZMIN
      H=Q=10
      NX=NY=30
      N=30
      TH=GAM=60
      IVIS=1
      PT(1)=11
      CALL THREEED(XMIN,YMIN,ZMIN,XMAX,YMAX,ZMAX,PT(1),
1 Q,H,NX,NY,N,WORK,Z)
      CALL VIEWITH,GAM,Q,IVIS)
      CALL PLOT(20,,0,,1)
      CALL CLRPLT
      END

```

THIS PAGE IS BEST QUALITY PRACTICABLE
FROM COPY OF ORIGINAL TO 100

REFERENCES

Saccadic Suppression

Abstracts

1. Bridgeman, B., Nelken, N., Heit, G., "Saccadic Suppression Determined Psychophysically in the Cat: Proc. ARVO 1979 p. 101
2. Brooks, B., Yates, J., Coleman, R., "How well can we see Image Motion Due to Saccadic Eye Movements: Proc. ARVO 1978 p. 138
3. Impelman, D., Brooks, B., "Backward and Forward Visual Masking During Saccades.: Proc. ARVO 1978, p. 138
4. White, C., Holtzman, J., "Visual Masking During Saccadic Eye Movements: Proc. ARVO 1977 p. 106
5. Cohn, T., Stark, L., Greenhouse, D. "Saccadic Suppression Maybe Due Entirely to Uncertainty in the Frame of Reference, "Proc. ARVO, 1977, p. 106
6. Volkman, F., Moore, R., Riggs, L., "Separable Effects on Contrast Sensitivity of Saccades and of Image Smear on the Retina" Proc. ARVO, 1977, p. 106
7. Wurtz, R., Campbell, F., "Why we Do Not See a Smear During Saccadic Eye Movements.: Proc. ARVO, 1977, p. 106

Papers

8. Volkman, F., Figgs, L., White, K., Moore, R., "Contrast Sensitivity During Saccadic Eye Movements, : Vis Res. Vol 18 pp 1193-1199 1978
9. Brooks, B., Fuchs, A., "Reply to Dr. Bridgemans' Letter," Vis. Res. Vol 17 pp 325-326, 197
10. Bridgeman, B., "Reply to Brooks and Fuchs: Exogenous and Endogenous Contributions to Saccadic Suppression: Vis Res Vol 17 pp 323-324 1977
11. Sakitt, B., "Information Received from Unseen Lights", Vis. Res. Vol. 16 pp 782-784, 1976
12. Stark, L., Kong, R., Schwartz, S., Hendry, D., Bridgeman, B., "Saccadic Suppression of Image Displacement," Vis. Res. Vol 16 pp 1185-1187, 1976
13. Shebilske, W., "Extra Retinal Information in Corrective Saccades and Inflow vs. Outflow Theories of Visual Direction Constancy," Vis. Res. Vol 16 pp 621-628, 1976
14. Matin, L., "A possible hybrid mechanism for modification of visual direction associated with Eye Movements - The Paralyzed Eye Experiment Reconsidered " Perception, Vol 5 pp 233-239 1976

THIS PAGE IS BEST QUALITY PRACTICABLE
FROM COPY FUNCTION TO DEC

15. Brooks, B., Fuchs, A., "Influence of Stimulus Parameters on Visual Sensitivity During Saccadic Eye Movement.", Vis. Res. Vol 15 pp 1389-1398
16. Mittrani, L., Radil-Weiss, T., Yakimoff, N., Mateeff, S., Bozkov, V., "Determination of Vision Due to Contour Shift Over the Retina During Eye Movements," Vis. Res., Vol 15 pp 877-878, 1975
17. Mohler, G., Cechner, R., "Saccadic Suppression in the Monkey," Vis. Res. Vol 15 pp 1157-1160, 1975
18. Matin, E., "Saccadic Suppression: A Review and An Analysis," Psychol., Bull., Vol 81 pp 899-917 1974
19. Matin, L., Matin, E., "Visual Perception of Direction and Voluntary Saccadic Eye Movements." Biblio. Ophthal Vol. 82, pp 358-368, 1976
20. Matin, L., "Eye Movements and Perceived Visual Direction," Handbook of Sensory Physiology Vol VII, Visual Psychophysics pp 332-380, 1972
21. Matin, E., Clymer, A., Matin, L., "MetaContrast and Saccadic Suppression, Science, Vol 178, pp 179-182
22. Mackay, D., "Elevation of Visual Threshold by Displacement of Retinal Image," Nature, Vol 225, pp 90-92, 1970

Spatial and Temporal Properties

Papers

23. Wilson, H., Phillips, G., Bentschlen, I., Hiltz, R., "Spatial Probability Summation and Disinhibition in Psychophysically Measures Line Spread functions," Vis. Res. Vol 19 pp 593-598 1979
24. Mezrich, J. "Modification of Spatial Frequency Processing Rates with Multiple Frequency Stimuli," Vis. Res. Vol 18 pp 1505-1507 1979
25. Wilson, H., "Quantitative Characterization of two types of Line Spread Function Near the Fovea," Vis. Res. Vol 18 pp 971-981, 1978
26. Glezer V.D., Gauzelman, V., Tsherbach, T., Dudkin, K., "Comments on Organization and Spatial-Frequency Characteristics of Receptive Fields in the Visual Cortex," Vis. Res. Vol 18, pp 887-889, 1978
27. Switkes, E., Mayer, M., Sloan, J., "Spatial Frequency Analysis of the Visual Environment: Anisotropy and the Carpentered Environment Hypothesis," Vis. Res. Vol 18 pp 1393-1399 1978
28. Caelli, T., Preston, G., Howell, E., "Implications of Spatial Summation Models for Processes of Contour Perception: A Geometric Respective," Vis. Res. Vol 18 pp 723-734 1978
29. Legge, G., "Sapce Domain Properties of a Spatial Frequency Channel in Human Vision," Vis. Res. Vol 18 pp 959-969 1978
30. Furchner, C., Thomas, J., Campbell, F., "Detection and Discrimination of Simple and Complex Patterns at Low Spatial Frequencies," Vis. Res. Vol 17, pp. 827-836

THIS PAGE IS BEST QUALITY PRACTICABLE
FROM COPY FURNISHED TO DDC

31. Graham, "Visual Detection of Aperiodic Spatial Stimuli by Probability Summation Among Narrowband Channels," Vis. Res. Vol 17 pp 637-652 1977
32. Carlson, C., Cohen, R., Gorog, I., "Visual Processing of Simple Two-Dimensional Sine-Wave Luminance Gratings," Vis. Res. Vol. 17 pp 351-358 1977
33. King-Smith, P., Riggs, L., Moore, R., Butler, T. "Temporal Properties of the Human Visual Nervous System," Vis. Res. Vol 17, pp 1101-1106 1977
34. Link, J., Rubinstein, C., "A Model of Threshold Vision Incorporating Inhomogeneity of the Visual Field," Vis. Res. Vol 17, pp 371-384, 1977
35. Weisstein, N., Harris, C., Berbaum, K., Tangney, J., Williams, A., "Contrast Reduction by Small Localized Stimuli: Extensive Spatial Spread of Above-Threshold Orientation-Selective Masking," Vis. Res. Vol 17, pp. 341-350, 1977
36. Rashbass, C., "Unification of two contrasting models of the visual increment threshold," Vis. Res. Vol 16, pp 1281-1283, 1976
37. Broekhuijsen, M., Rashbass, C., Veringa, F., "The threshold of Visual Transients," Vis. Res. Vol 16 pp 1285-1289, 1976
38. Arend, L. "Temporal Determinants of the Spatial Contrast Threshold MTF" Vis. Res., Vol 16 pp 1035-1042 1976
39. Hines, M., "Line Spread Function Variation Near the Fovea," Vis. Res. Vol 16 pp 567-572, 1976
40. Legge, G., "Adaptation to a Spatial Impulse: Implications for Fourier Transform Models of Visual Processing," Vis Res Vol 16 pp 1467-1418 1976
41. McCarter, A; Roehrs, T., "A Spatial Frequency Analogue to Mach Bands," Vis. Res. Vol 16, pp 1317-1321
42. Kelly, C., "Pattern Detection and the Two-Dimensional Fourier Transform: Flickering Checkerboards and Chromatic Mechanisms," Vis Res Vol 16, pp 277-287 1976
43. Spitzberg, R., Richards, W., "Broad Band Spatial Filters in the Human Visual System., " Vis. Res. Vol 15 pp 837-841 1975
44. Kelly, D., Magnuski, H., "Pattern Detection and the Two-Dimensional Fourier Transform: Circular Targets," Vis. Res. Vol 15 pp 911-915, 1975

45. Mather, G., "Oculomotor and Movement," Vis Res. Vol 19

46. Haegerstrom-Portnoy, G., Brown, B., "Contrast Effects on Smooth-Pursuit Eye Movement Velocity," *Vis. Res.* Vol 19, pp 169-174 1979
47. Henson, D. B., "Investigation into Corrective Saccadic Eye Movements for Refixation Amplitudes of 10 Degrees and Below," *Vis. Res.* Vol 19 pp 57-61, 1979
48. Mitrani, L., Dimitrov, G., "Pursuit Eye Movements of a Disappearing Moving Target," *Vis. Res.* Vol 18, pp 537-539 1978
49. Henson, D., "Corrective Saccades: Effects of Altering Visual Feedback," *Vis. Res.* Vol 18 pp 63-67 1978
50. Prablanc, C., Masse, D., Echallier, J., "Error-Correcting Mechanisms in Large Saccades," *Vis. Res.* Vol 18 pp 557-560, 1978
51. Holtzman, J., Sedgwick, H., Festinger, L., "Interaction of Perceptually Monitored and Unmonitored efferent Commands for Smooth Pursuit Eye Movements," *Vis. Res.* Vol 18 pp 1545-1555 1978
52. Hansen, R., Skavenski, A., "Accuracy of Eye Position Information for Motor Control," *Vis Res.* Vol 17 pp 919-926 1977
53. Komeda, M., Festinger, L., Sherry, J., "The Accuracy of Two-Dimensional Saccades in the Absence of Continuing Retinal Stimulation," *Vis Res* Vol 17, pp 1231-1232 1977
54. Viviani, P., Berthoz, A., Tracey, D., "The Curvature of Oblique Saccades," *Vis. Res.* Vol 17, pp. 661-664
55. Kowler, E., Steinman, R., "The Roles of Small Saccades in Counting," *Vis. Res.* Vol 17 pp 141-146, 1977
56. Ono, H., Nakamizo, S., "Saccadic Eye Movements During Changes in Fixation to Stimuli at Different Distances" *Vis. Res.* Vol 17 pp 233-238 1977
57. Becker, W., "Do Correction Saccades Depend Exclusively on Retinal Feedback? A Note on the Possible Role of Non-Retinal Feedback," *Vis. Res.* Vol 16, pp 425-427, 1976
58. Dimitrov, G., Yakimoff, N., S., Mitrani, L., "Saccadic Eye Movements on Bela Julesz' Figure," *Vis. Res.* Vol 16, pp 411-414 1976
59. Hallett, P., Lightstone, A., "Saccadic Eye Movements to Flashed Targets." *Vis. Res.* Vol 16, pp 107-114, 1976
60. Hallett, P., Lightstone, A., "Saccadic Eye Movements Towards Stimuli Triggered by Prior Saccades." Vol 16, pp 99-106, 1976
61. Lisberger, S., Fuchs, A., King, W., Evner, L., "Effect of Mean Reaction Time of Saccadic Responses to Two-Step Stimuli with Horizontal and Vertical Components," *Vis Res* Vol 15, pp 1021-1025 1975

62. Coren, S., Bradley, D., Hoenig, P., Girgus, J., "The Effect of Smooth Tracking and Saccadic Eye Movements on the Perception of Size: The Shrinking Circles Illusion," *Vis. Res.* Vol 15, pp 49-55, 1975
63. Prablanc, C., Jeannerod, M., "Corrective Saccades: Dependence on Retinal Reafferent Signals," *Vis. Res.* Vol 15 pp 465-469, 1975

Books

64. Yarbus, A. "Eye Movements and Vision," Plenum Press, 1967
65. Carpenter, R., "Movements of the Eyes," Pion, London, 1977

Visual Processing

Papers

66. Stoper, A., Mansfield, J., "Meta-Contrast and Paracontrast Suppression of a Contourless Area," *Vis. Res.* Vol 18 pp 1669-1674, 1978
67. King-Smith, P., Riggs, L., "Visual Sensitivity to Controlled Motion of a Line or Edge," *Vis. Res.* Vol 18, pp 1509-1520, 1978
68. Grunau, M., "Interaction between Sustained and Transient Channels: Form Inhibits Motion in the Human Visual System," *Vis. Res.* Vol 18, pp 197-201, 1978
69. Mateeff, S., Yakimoff, N., Mitizain, I., "Some Characteristics of the Visual Masking by Moving Contours," *Vis. Res.* Vol 16., pp 489,492, 1976
70. Bridgeman, B., "Correlates of Metacontrast in Single Cells of the Cat Visual System," *Vis Res* Vol 15, pp 91-99, 1975

Books

71. Cornsweet, N. "Visual Perception" Academic Press, 1970
72. Uttal, W. "The Psychobiology of Sensory Coding" Harper and Row, 1973

1979 USAF - SCEEE SUMMER FACULTY RESEARCH PROGRAM

Sponsored by the

AIR FORCE OFFICE OF SCIENTIFIC RESEARCH

Conducted by the

SOUTHEASTERN CENTER FOR ELECTRICAL ENGINEERING EDUCATION

FINAL REPORT:

SPECIAL-PURPOSE PROCESSORS

FOR THE IMAGE-PROCESSING REQUIREMENTS

OF AUTOMATIC FEATURE EXTRACTION SYSTEMS

Prepared by:	John V. Oldfield Ph.D.
Academic Rank:	Professor
Department and University:	Department of Electrical and Computer Engineering Syracuse University
Research Location:	
(Air Force Base)	Griffiss AFB
(Laboratory)	RADC
(Division)	Intelligence & Reconnaissance
(Branch)	IRRE
USAF Research Colleagues:	Ellsworth E. Hicks Donald A. Bush
Date:	August 20, 1979
Contract No:	F49620-79-C-0038

SPECIAL-PURPOSE PROCESSORS
FOR THE IMAGE-PROCESSING REQUIREMENTS
OF AUTOMATIC FEATURE EXTRACTION SYSTEMS

by

J.V. Oldfield

ABSTRACT

Image processing systems for feature extraction require complex operations on large quantities of image data. After considering these requirements in detail, the author has proposed a special-purpose computer system (PXP) for pixel processing and display. This employs vector operations on up to 9 pixels simultaneously, and should result in much faster execution of many feature extraction tasks, particularly those which affect the interactive user. The paper includes an outline of the system architecture and informal descriptions of typical algorithms. It discusses implementation possibilities using widely-available microprocessor components, and recommends that further development be undertaken with the aid of a high-level hardware description language (SMITE) and emulation system (QM-1), both of which will be available at Rome Air Development Center.

ACKNOWLEDGEMENTS

The author wishes to thank Mr E.E. Hicks and Mr D.A. Bush of the Image Exploitation Branch for the excellent facilities and support provided under the Summer Faculty Research Program at RADC. Mr J.L. Previte of the Information Sciences Division was most helpful regarding computer emulation facilities. He wishes also to thank Dr J. Lemmer and Mr D. Marks of the Pattern Analysis and Recognition Corporation for their cooperation in discussing pixel processing algorithms.

Finally he would like to thank the Air Force Systems Command, Air Force Office of Scientific Research, the Rome Air Development Center and the Southeastern Center for Electrical Engineering Education for the excellent opportunities and facilities made available to him.

I. INTRODUCTION

Map making has traditionally been a complex, time-consuming activity, involving ground-level surveying now supplemented or replaced by aerial and satellite imagery, followed by stages of analysis, map layout and the elaborate processes of high-quality multi-color printing. Sensor performance has improved dramatically in recent years and now covers wide spectral bands from infra-red to ultra-violet. This type of data is produced in such large volumes that only a small percentage can be processed extensively. At the other end of the map-making process, high-quality color printers are now available for both film and paper copy. The in-between stages of data analysis and map layout now form a serious bottleneck in map production.

A map has symbolic as well as metric aspects, and sometimes these are in conflict. For example in representing a highway and a railway track passing through a narrow valley, it may be necessary to displace either or both conventional symbols from their true position so as to clearly distinguish them. It is difficult to automate this in the design process. Again, the map-maker needs to bring together a variety of data in different forms to aid his analysis - previous maps, aerial and ground survey data, and more general intelligence information.

The Defense Mapping Agency is coordinating an effort to map the major part of the Earth's land surface, in the form of the Digital Landmass Simulation Data Base (1). The IRRE Branch of Rome Air Development Center is one of the collaborating agencies in this effort, and is particularly concerned with Feature Extraction Systems. These are computer-based image-processing and display systems which aid the map-maker by providing automatic and interactive means of classifying image data. For example, landscape features such as roads, forests, lakes, etc. can be distinguished automatically from their multi-band spectral

image data, due to characteristic spectral "signatures" i.e. the relative responses at different spectral frequencies. But it is virtually impossible to carry out such classifications automatically for images in general, especially when they contain many cultural features. Instead, the image analyst can design a classification scheme for a particular image or restricted set of images which will identify features of interest. Feature extraction systems make this possible by providing the following aids:

1. image input and output facilities for both optical and computer storage media.
2. pre-processing facilities e.g. contrast enhancement, picture noise reduction etc.
3. image statistics evaluation e.g. finding the mean intensity around each pixel.
4. classification scheme design, with transformations which make it easier to distinguish a small set of known objects selected by the analyst.
5. application of a classification scheme to a whole image or set of images.

The author has been extensively involved with interactive display systems for a number of years, particularly for computer-aided design of electronic systems. The Summer Faculty Research Program provided an excellent opportunity to explore a new but related area in which display technology was a limiting factor.

Image processing systems for feature extraction have extensive computing requirements, ranging from large data bases to advanced interaction with displays. This study is concerned with the algorithms employed in image processing for display, and how they may be speeded up with special-purpose computer hardware. In view of the dominance of raster-scan display technology, in which

picture element (pixel) data is stored in extensive semiconductor memory, it is now possible to consider a closely-coupled pixel processor (PXP) accessing pixels at high data rates.

It is interesting to observe the evolution in image storage for the experimental feature extraction systems developed by RADC:

1. disc-based systems which allowed TV-compatible data rates, but were subject to serious latency handicaps (2),
2. the PDP11/20 - Comtal system (3) in which the display memory is separate from computer memory. While computer access to pixel storage is at high speed, the method is very restrictive and so considerable buffering must be used,
3. the PDP11/34A - De Anza system (4,5), in which the display memory is directly accessible by the computer, but only in selected portions at a time i.e. by virtual addressing. The buffering requirements are much reduced. This is the display subsystem of the Automatic Feature Extraction System (AFES) being developed by the Pattern Analysis and Recognition Corporation under contract to RADC.

In this latest system, the role of the display processor is restricted to image generation from the refresh memory. The De Anza unit has a digital video processor capable of image processing operations as distinct from display, e.g. image differencing, spatial convolution etc. but advantage will not be taken of such facilities in the present system.

II. OBJECTIVES OF THE RESEARCH EFFORT

The dedication of a computer such as the PDP11/34A to an individual work station indicates the importance of fast response for the AFES user and I was encouraged to look for further means of improving response. At the same time consideration had to be

given to the overall cost of the work station, and here developments in microprocessor technology are very significant, since they give the systems designer of a special-purpose, low-volume computer system much more freedom of choice than previously. In summary, the objectives were as follows:

1. to become familiar with the image-processing and feature extraction methods currently employed,
2. to explore any possibilities of improving the real-time performance, in particular with novel forms of computer architecture.

III. DISPLAY AND PIXEL PROCESSING REQUIREMENTS

It is clear that the display requires extensive RAM storage, of the order of a megabyte e.g. for 4 512x512 8-bit color images as in the AFES display subsystem (De Anza IP5532). Future systems could well have even higher resolution and indeed the present system allows for a pair of 1024x1024 monochrome images. The algorithms employed in image processing access the same data, and once the decision has been made to store image data in semiconductor RAMs, it becomes feasible to consider dedicated processors for algorithm execution. The PDP11/34A-De Anza system is restricted by the 56k byte instruction address space and 256k byte bus address limitation of PDP11 systems and consequently memory mapping techniques are employed. With recent microprocessors a larger address space is available e.g. the 1 megabyte bus limit of the Intel 8086 (6). While such an address space is insufficient to contain the image memory (2 megabytes), the latter can be configured as four 512x512 8-byte images, with any one of the four selected as in the address space at any instant. Switching between images would be virtually

simultaneous, and would be little handicap to either display or image processing requirements.

Image processing algorithms require two-dimensional access to pixel data, and when implemented on conventional computers suffer some overhead in memory address computation i.e. forming a single store address from an x-y pixel address. Moreover they frequently require access to the immediate neighbors of a given pixel. The following are examples:

1. in collecting statistics for pixel classification it is common to evaluate an $n \times n$ box around a given pixel. Typically n is 3 or 5. Statistics include: average intensity, standard deviation, lowest, highest, range and mean.
2. in region-growing, the neighbors of a given seed pixel already labelled as belonging to a region are considered for inclusion in the same region, based on a threshold level.

Other algorithms include edge detection, thinning, line following and noise-point fill-in.

IV. ALTERNATIVE COMPUTER CONFIGURATIONS

In the search for improved performance, there are a number of alternative computer configurations to consider (7,8) :

IV.1 Multi-microprocessor computers

It is now feasible to construct such a system, typically with 8 or 16 processors sharing a common memory as well as having individual private memories. The major problem is to organize a computing task into parallel activities. Some AFES tasks e.g. collection of pixel classification statistics, can be subdivided on a rectangular area basis, and allocated to separate processors operating in parallel. Others, such as region-growing, cannot be readily subdivided due to overlap of the regions as they develop.

Considerable overhead would be involved in inter-process communication. It would also be necessary to provide memory protection, allowing one processor read/write access to its area, while neighboring processors are allowed read-only access, or even at times no access at all while a critical marking operation takes place. These difficulties and complications, coupled with the limited speed of typical microprocessors, would probably restrict the overall performance to less than that of a single powerful minicomputer equipped with cache memory and comprehensive hardware arithmetic facilities. Moreover the high data rates required for display generation would call for a special-purpose display processor, with further complications such as memory subdivision, control and timing.

IV.2 Vector arithmetic computers

These fall in the general classification as single-instruction path, multiple-data path (SIMD) computers (9). Examples include the Illiac IV, designed for floating-point operations on large matrices, and the STARAN with its 256 processors each obeying the same elementary instruction simultaneously. The general concept is relevant to image processing, since many operations involve identical computations for the 4 or 8 immediate neighbors of a pixel. Reference (10) discusses such applications further. The STARAN itself could be employed for some AFES functions, such as clustering in hyperspaces of large dimension, but in view of its cost it could obviously only serve as a central facility rather than as part of a work station. An important problem is the overhead in setting up a problem for STARAN from a conventional computer and the time required for array input and output.

It is interesting to apply the SIMD concept on a much smaller scale i.e. as an adjunct to a conventional central processor,

paying particular attention to the two-dimensional character of images. I have proposed a SIMD computer with a vector arithmetic unit of 9 elements. This number is sufficient for simultaneous pixel statistic evaluation with 3x3 boxes, and it appears very suitable for some otherwise time-consuming operations of region-growing. In proposing a novel computer configuration, one needs to evaluate its computational gains against drawbacks such as added programming complexity and the need for special system software. A useful example in which the payoff is worthwhile is an array processor as an adjunct to a minicomputer, e.g. the Floating Point Systems AP120B. While the array processor is difficult to program, the resulting speed-up in matrix operations may well justify the hardware cost and reorganization required. For AFES, the parallel example is a special-purpose computer for both display refresh and certain standard operations which require access to the same display data.

Subsequent sections of this paper consider the organization of a SIMD system for pixel processing (PXP) and its possible advantages as part of an AFES work station.

IV.2.1 Outline of Pixel Processor (PXP) Organization

The PXP would operate in close association with the host processor of an AFES work station. Figure 1 shows the overall arrangement. The PXP would drive the display monitor(s) and also carry out specialized functions such as statistics evaluation or region-labelling, at the command of the host processor. The PXP operates within the address space of the host, the latter having access to all the image memories. The console input devices (keyboard, tracker balls etc) would be serviced directly by the host computer. In designing the PXP, particular attention is required to the following aspects:

1. rapid access to image memory for both display and pixel

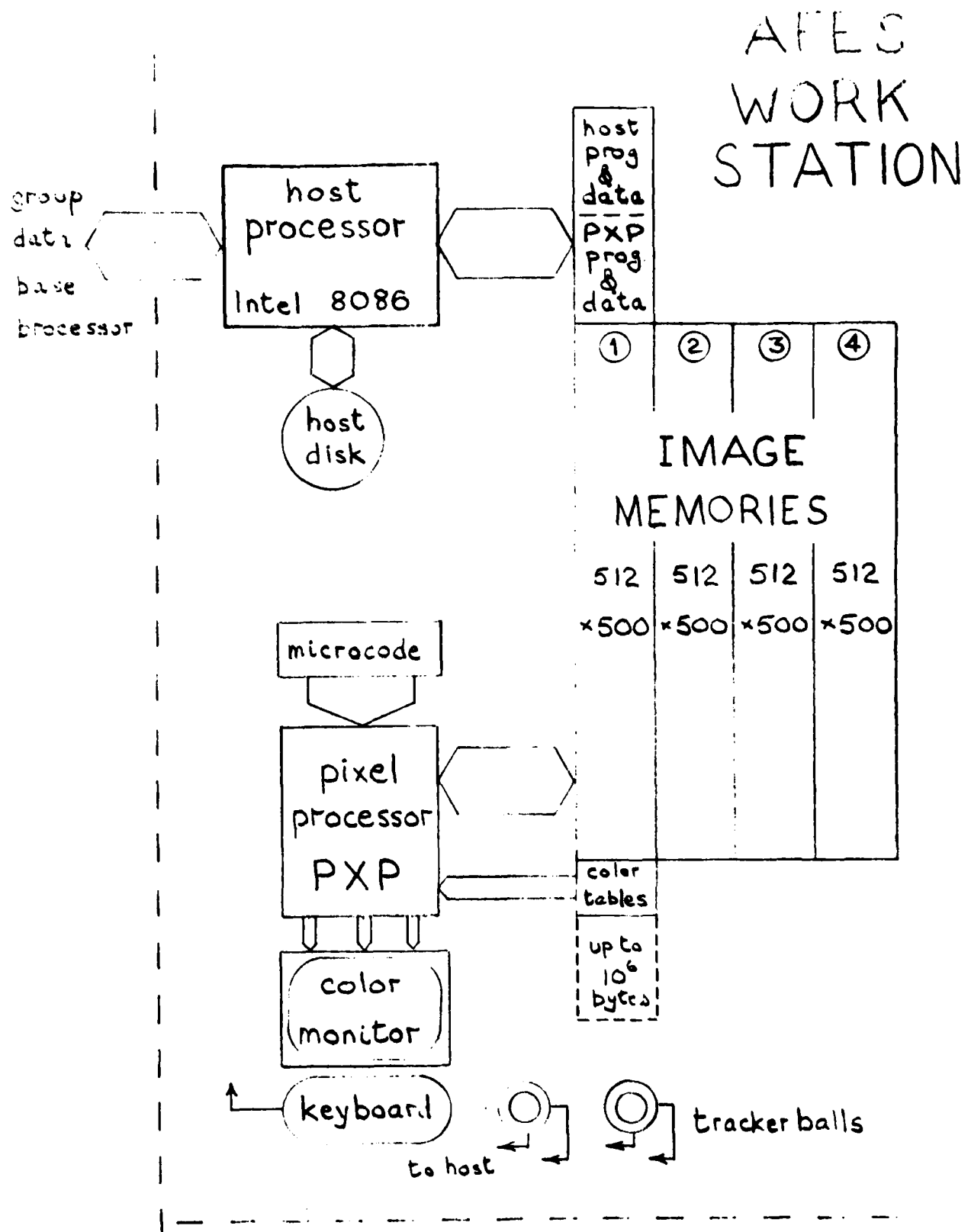


Figure 1. Overall arrangement of Work Station

processing,

2. means of controlling the individual elements of the arithmetic vector unit and the logical operations required,
3. automatic provision for image boundaries.

V. PXP MEMORY ORGANIZATION

PXP requires high-speed memory access to:

1. drive the display monitors at TV rates i.e. retrieving the red, green and blue components for each pixel on a TV line at very high speed (e.g. 39 microseconds for all 1024 elements of a raster line of a 1024x1024 element scan)
2. to load or store the 9-element arithmetic vector simultaneously.

I have developed a suitable scheme which requires that the image memory be divided up into 16 separate modules numbered 0-15. For present purposes I have assumed that the image memory is the same size as in the De Anza IP5532 viz. 4 images of 512x512 8-bit pixels, but the idea could readily be extended to larger image memories. Each of the 16 modules would hold 16k 32-bit words, each word subdivided into 4 8-bit bytes, i.e. one byte for each of the 4 image "planes". The 16 modules operate simultaneously and thus allow any set of 16 sequential pixels to be read across a horizontal line viz:

0 1 2 3 12 13 14 15 0 1 2 3

By staggering the arrangement for successive image lines, simultaneous access can be obtained to any 4x4 group of pixels:

0	1	2	3	12	13	14	15	0	1	2	3
4	5	6	7	0	1	2	3	4	5	6	7
8	9	10	11	4	5	6	7	8	9	10	11
12	13	14	15	8	9	10	11	12	13	14	15
0	1	2	3	12	13	14	15	0	1	2	3

.
.
etc

A simple address transformation is obtained, which allows one to transform a specified $x(\text{row})$, $y(\text{column})$ address into image memory module(m) and word(w) address. This can be described in FORTRAN as:

```

m = mod(4*mod(x,4) + mod(y,16),16)
w = 32*x + int(y/16)

```

or more significantly as the logical operations shown in Figure 2. Thus the address transformation is simple, fast and economic. As a result, the vector processor described in section (VI) can have simultaneous access to any set of 9 elements in a row or any set of 3x3 pixels. Note that simultaneous access does not extend to columns, but this does not seem a serious drawback. There are 4 distinct access modes, allowing simultaneous loading of all vector elements from the same pixel, from the sequence of nine to the right, nine to the left, and the 3x3 array around a given pixel. A scheme with fewer memory modules is feasible, but the address arithmetic is more complex and in any event the 16-way interleaving is desirable for TV data rates.

To simplify operations on boundary pixels, either at absolute boundaries or prescribed ones within an image, a 9-bit status register, the pixel access register (par), is associated with memory control. In reading, each bit is set to 1 or 0, depending

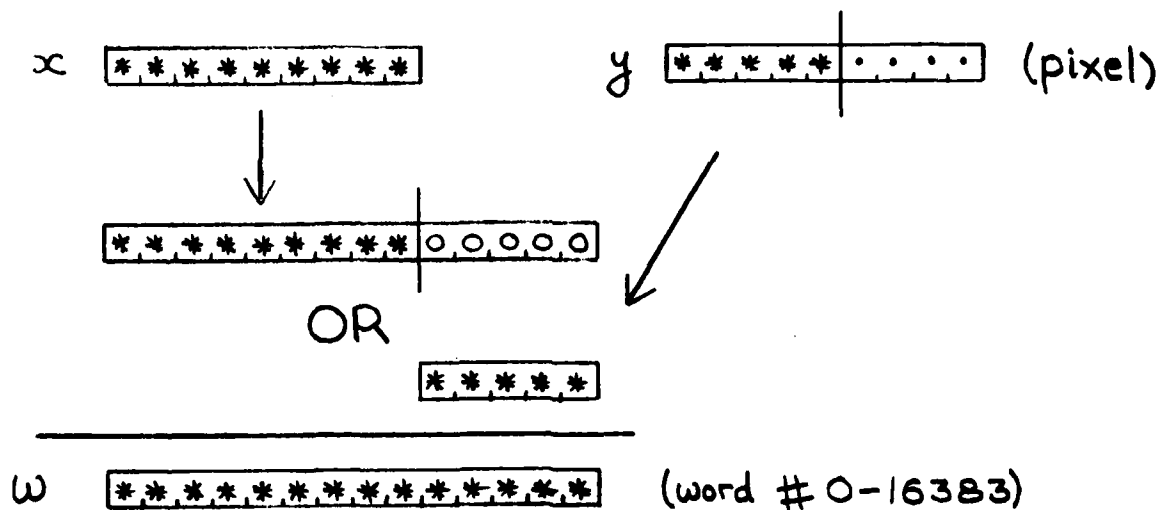
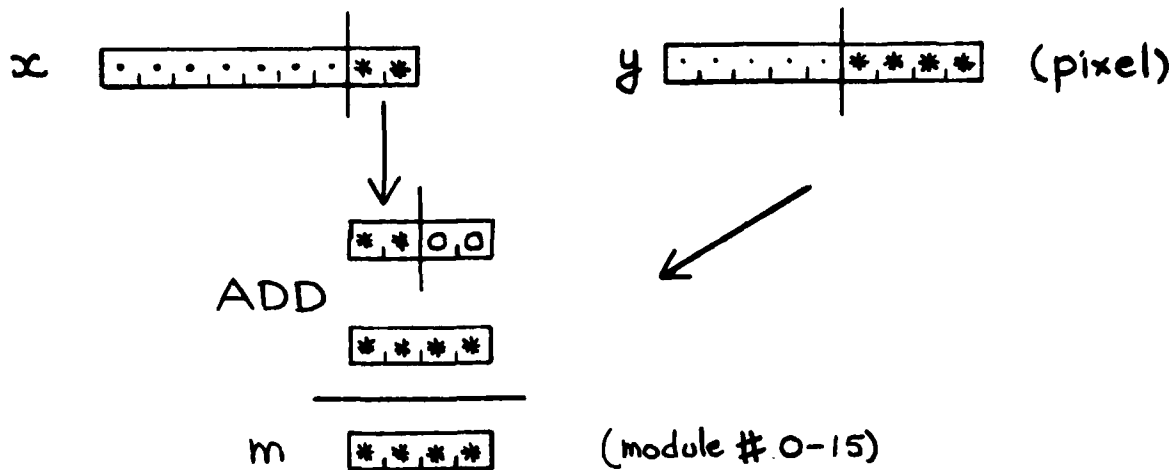


Figure 2. Logic for address transformation

on whether the pixel data is valid or not. On writing to memory, the register not only prevents writing to non-existent memory, but also allows selective write operations to be carried out, depending on arithmetic results. The pixel access register is set up only when the pixel x,y address is changed, and not when the particular byte (of the 4 stored for a given coordinate) is changed. The address logic uses limits xlow,ylow,xhigh,yhigh which can be changed by the PXP to suit requirements. Figure 3 shows the general arrangement. The address logic can be implemented by hardware or microprogram operations, depending on the speed required.

It is useful to carry out the same operation, stepping along rows and down columns, and so indexed addressing is provided, with separate x and y index registers associated with an instruction. This is discussed further in section (VIII).

VI. VECTOR ARITHMETIC UNIT

This unit can carry out 9 simultaneous arithmetic or logical operations on a 9-element vector, each element being 8-bits long. Figure 4 shows the general arrangement. The vector control register (vcr) allows individual elements to be disabled (0) or enabled (1). It is automatically loaded from the pixel access register when reading to disable operation for non-existent memory. It can also be changed directly by program, and it is important to see this as distinct from the pixel access register association.

There is a set of condition bits (zero,minus,carry) associated with each element of the array, reflecting the result of the latest vector arithmetic or logical operation. These are similar to the condition bits of a typical microprocessor, but are available collectively as 9-bit words. It is envisaged that most

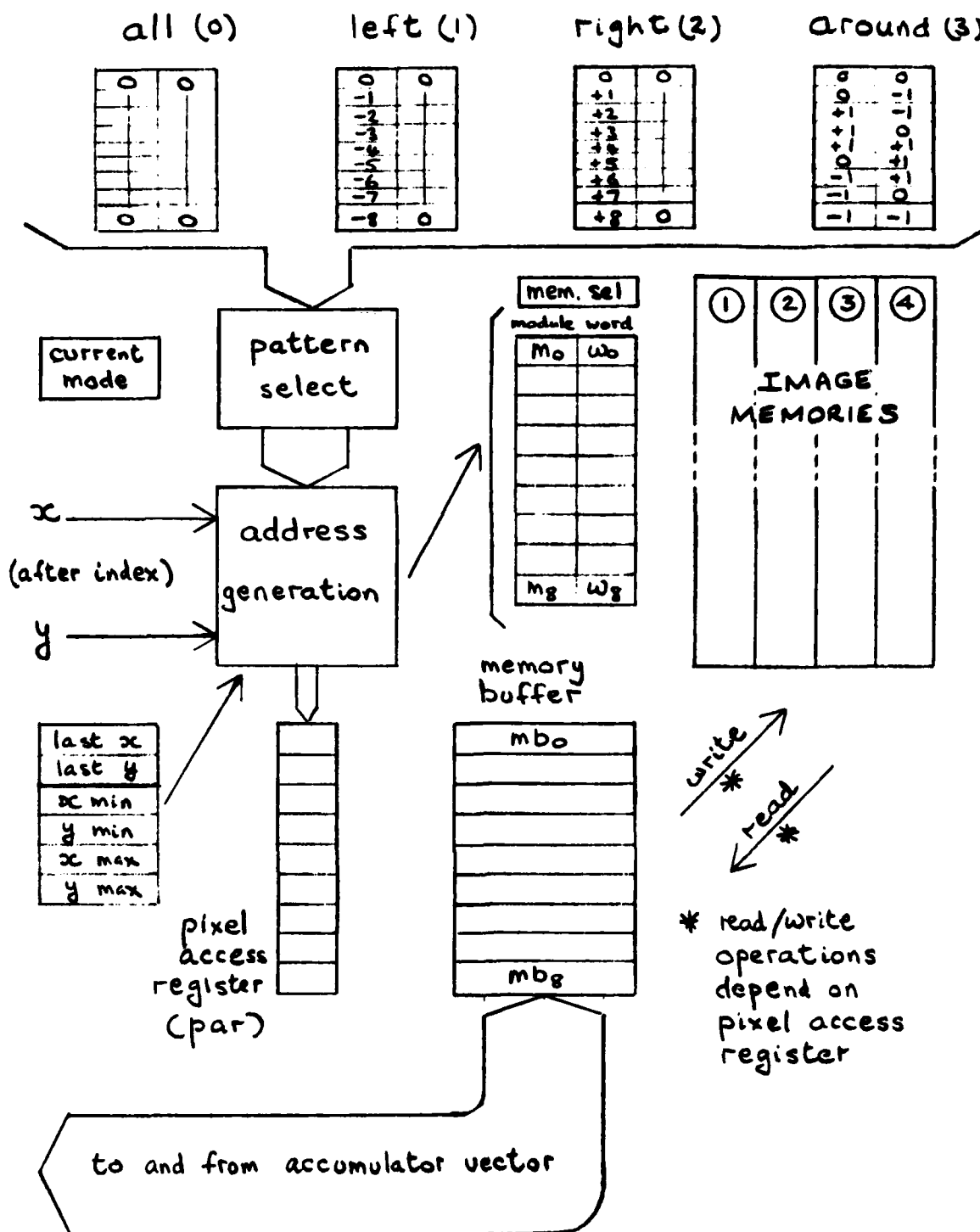


Figure 3. Memory access and control

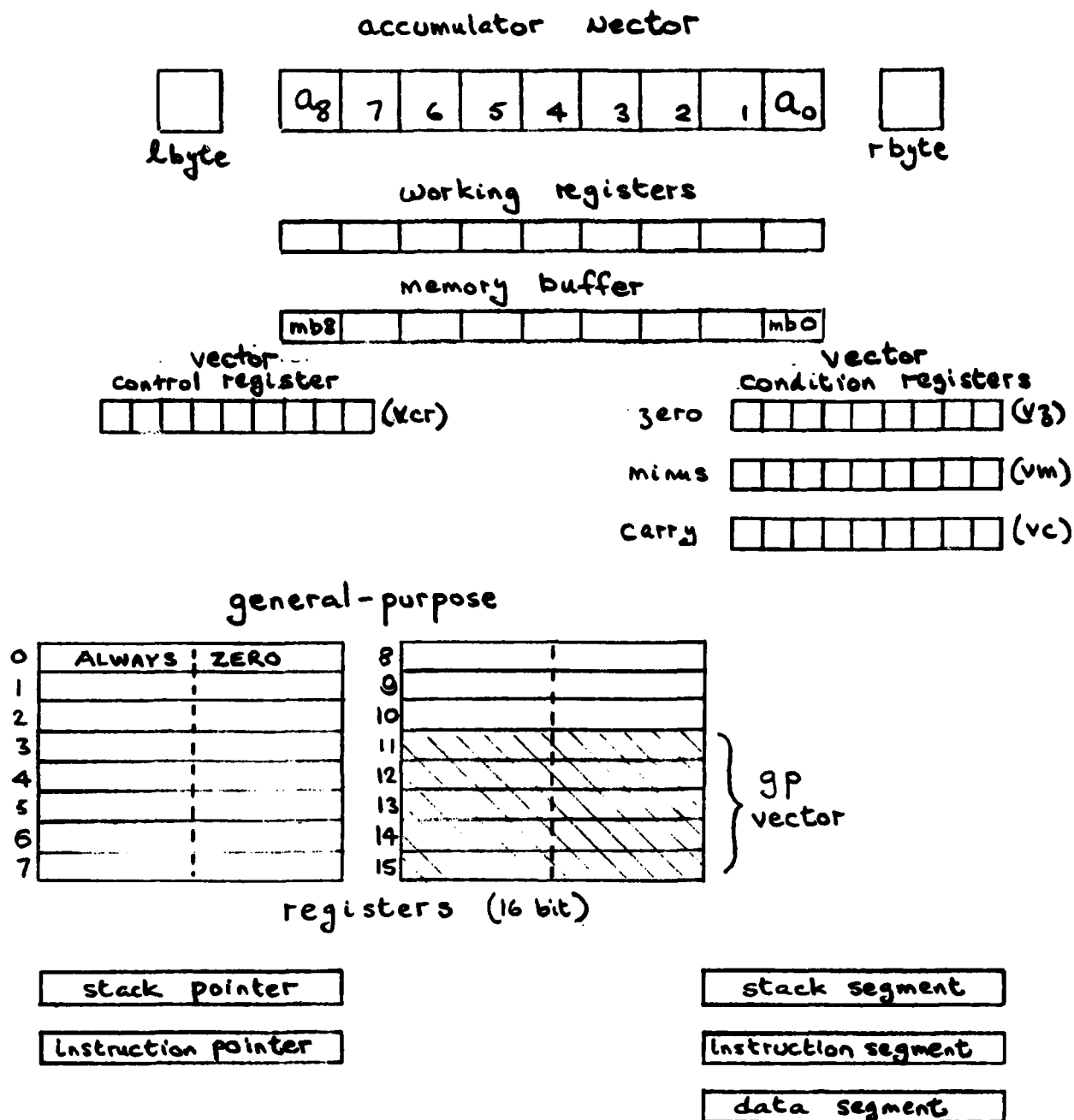


Figure 4. Accumulator vector and registers

operations would be on unsigned integers, and so an overflow register has not been included. However, signed arithmetic (ones or twos complement) would still be feasible by software.

A fairly restricted set of arithmetic and logical operations is proposed:

1. Load vector from:
image memory / main memory / gp register /
instruction(literal)
2. Store vector in image memory/main memory/gp register
3. add/subtract element contents to/from:
image memory / main memory / gp register / literal
4. shift element contents up/down 1 place
5. shift element contents to neighbor left/right (note
lbyte, rbyte)
6. swap element contents with neighbor left/right
7. add neighbor left/right to element contents
8. subtract element contents from neighbor left/right
9. compare element contents with neighbor left/right
10. zero, set to 1 or complement vector contents.

Note that these functions, and others, are readily available in chip form e.g. the 74181 4-bit arithmetic/logic unit chip. Most of the arithmetic operations will be distinct i.e. the data from one element will not affect another, but it will still be possible to carry out multi-byte arithmetic, or even say two pairs of multi-byte operations with the aid of the accumulator control register.

VII. CONVENTIONAL ARITHMETIC UNIT

As well as the vector arithmetic unit, a more conventional unit is required which provides for index arithmetic, logical operations to set up the accumulator control register, counting,

etc. This has been organized as a set of 32 16-bit registers, of which 16 have specific purposes, and the remainder are general. Not all the special-purpose registers hold the full 16 bits. The general purpose registers are numbered from 0 to 15, with register 0 always containing the constant zero.

special-purpose registers

accumulator vector	(9 x 8 bits)
lbyte, rbyte	(1 x 16)
vector control(vcr)	(1 x 9)
vector zero(vz)	(1 x 9)
vector minus(vm)	(1 x 9)
vector carry(vc)	(1 x 9)
pixel access(par)	(1 x 9)
stack pointer	(1 x 16)

The following facilities are provided for all registers, whether special-purpose or general:

- load from main memory/instruction (literal)
- store to main memory
- shift left/right (circular/logical)
- special shifts (8-bit circular, 9-bit etc.)
- logical (and/or/exclusive or/complement)
- increment/decrement
- add/subtract

Again, these facilities are readily available in chip form.

Note that as well as the 32 registers described here, other specific registers e.g. xlow, xhigh can be set by PXP program. Other registers include code, data and stack segment registers (16 bit), maintained by the host processor and not available to PXP programs. The 32 registers can be individually tested and there are condition bits (zero, minus, carry) indicating the result of the latest arithmetic or logical operation.

VIII. CONTROL UNIT

The control unit takes instructions from the main memory (shared with the host) and arranges for the associated memory or arithmetic/logical operations to be carried out in sequence. In view of available microprocessor technology, and for ease of adjustment, it would be advantageous to use microprogramming techniques. The memory reference instructions will allow separate index registers to be specified for row (x) and column (y) coordinates. It is not proposed to specify the instruction format in detail at this stage. Note that it may be an advantage to use a pipeline for instruction fetch, since the time for each instruction will vary e.g. vector and register operations will be faster than memory reference instructions. An advantage of the SIMD architecture in this context should be the relative infrequency of conditional jump instructions, which would require the pipeline to be purged and re-loaded. A stack will be maintained for subroutine linkage, and it will also be used to save and retrieve data using POP/PUSH instructions.

To avoid inessential complexity, it is not proposed to include interrupt facilities in the PXP itself, although it may well be useful for it to be able to interrupt the host. It might be feasible to be able to time-share the PXP between display refresh and image processing, but it is assumed that users would be content with a blank display while image processing is in progress.

IX. APPLICATION OF PXP TO SOME TYPICAL TASKS

It is important to evaluate the computational advantage of the PXP by estimating the time it would take to perform some of the pixel processing tasks associated with feature extraction which

are presently time-consuming. Since the instruction set has not been completely specified and detailed aspects of implementation have yet to be considered, only rough estimates can be made at this stage. Another uncertainty is the allocation of tasks between the PXP and the host. However it is hoped that the examples will give sufficient indication to merit further study.

In the absence of a formal instruction set, PXP programs will be described informally in English.

IX.1 Pixel statistics - 3x3 box

Assume that the pixel intensity data is already stored in an image memory. Also assume that the following analysis is required, and that it is to be sent to the host computer:

1. mean intensity
2. standard deviation
3. lowest intensity
4. highest intensity
5. range
6. median intensity.

The following procedure seems to be most efficient:

1. sort the pixel intensities in descending order
2. send lowest, highest and median to the host
3. use median as an approximation to the mean and refine it.
Find differences between each pixel and the median, then sum them, divide by 9 and add result to median
4. find differences between each pixel and the mean and square them
5. sum the squares of the differences, divide by 9 and take the square root to give the standard deviation.

The PXP organization is highly suitable for fast sorting since every pixel can be compared with its neighbor simultaneously, and then swapped if necessary. Appendix A.1 discusses the choice of

algorithm and shows how it can be turned into a PXP program. Procedure steps (3) and (4) exploit vector arithmetic and in (5) the 9-element summation can be commenced as 4 simultaneous pairs, then 2 pairs etc. Appendix A.2 shows that this is roughly twice as fast as a cyclic method.

IX.2 Pixel statistics for larger boxes

The vector arithmetic unit allows the PXP to be used effectively for boxes up to 9 pixels wide. This is more than required for a typical feature extraction system.

IX.3 Region growing

This is a process which is clearly required for AFES, but which is still at an experimental stage. A region is a contiguous area of an image in which all the pixels are associated by some common rule, typically that immediate-neighbor intensity differences lie within a threshold. Regions are grown from a single "seed" pixel and there may be considerable intensity differences between extreme pixels of a region. The work described here is based on studies at the PAR Corporation undertaken by Taenzer (11) and Marks (12). The algorithm is divided into 3 main stages:

1. grow regions, labelling pixels as region or edge. If the region is too small, its pixels are re-labelled as "reject"
2. grow regions out of reject pixels, so adjacent reject regions may be merged and become viable regions
3. assign any remaining reject regions to the neighboring region of nearest average intensity.

Stage 1 is particularly time-consuming. It involves examining each of the 8 neighbors of a seed (i.e. already labelled) pixel to see if the intensity difference is within a given threshold. If not, the neighbor is labelled as an edge pixel. If so and

neither of its immediate neighbors (in a circular sense) are already edge pixels, it will be labelled as being in the same region and then added to the seed list. Already-labelled pixels are not re-labelled.

The PXP is ideally suited to this task since it can handle all 8 neighboring cells simultaneously. Appendix A.3 outlines a suitable algorithm.

X. IMPLEMENTATION

An experimental prototype of the pixel processor could be implemented in a variety of forms, depending on the speed required and cost limitations. Important aspects are the display processor timing to keep up with high-resolution TV rates, color look-up tables, etc., and the speed advantage of vector, as distinct from single-accumulator arithmetic. In view of the novelty of the architecture, the instruction set should be easily alterable.

These requirements appear to be satisfied by the following choices:

1. The image memory should be in MOS form and follow trends in raster scan display systems generally e.g. using the largest capacity dynamic RAMs available (64-kilobit presently) with cycle times of the order of 400 nS.
2. The vector itself should comprise pairs of 4-bit arithmetic/logical chips such as the 74181, which provides all of the functions required. It would not be necessary to use carry-look-ahead logic, since the word length is only 8 bits. The SN74S181 Schottky version can perform an 8-bit add in only 18 nS. It is important that data transfers to and from the vector elements can take place in parallel i.e. simultaneously.

3. Some of the general-purpose registers should be distinct e.g. the general-purpose register vector used to save the contents of the accumulator vector. This would permit high-speed multi-byte copying.
4. The remaining registers could be implemented with 4-bit bi-polar bit-slice logic, such as the Am2901, which contains a 16-word RAM as well as being able to perform arithmetic and logical functions. Reference (13) gives an interesting example of an 8080 microprocessor emulated in this way.
5. The control part of the PXP could also use bit-slice logic, using a "wide" type micro-instruction format. Again reference (13) gives a useful example with a 56-bit micro-instruction word.

All the above devices could be readily modelled in the SMITE language. In summary, the design should be evaluated for readily-obtainable standard components, and this should be entirely feasible.

Some consideration must be given to software. In view of the novel architecture, good debugging aids are essential. Since the system includes a host processor and a display, it would be easy to show the state of the PXP in terms of the current instruction and register contents.

XI. RECOMMENDATIONS

This study has shown that the real-time performance of a feature extraction system could be improved by exploiting concurrent computer operations in the form of a single-instruction multiple-data path (SIMD) image processor. This could combine both image-processing and display functions. I recommend that this concept be investigated further.

An overall evaluation of the effectiveness of the proposed PXP system requires answers to the following questions:

1. How fast could typical feature extraction algorithms be executed, in comparison with the existing system ?
2. How easily could such algorithms be implemented e.g. would the complexities of vector processing be serious obstacles, would PXP programs be difficult to debug, how easily could tasks be divided between host processor and PXP, etc. ?
3. How complex would the PXP hardware be, and what would it cost to produce a prototype system ?

Answers to these questions could be obtained by defining the system in high-level terms i.e. using standard MSI and LSI components, with known cost and performance, and by emulating actual programs with the aid of suitable software. SMITE (14,15) is a computer description language for specifying a digital system (the target system) at a register-transfer level, including component timing information. It can represent systems in which activities take place in parallel, and which need to be synchronized with one another. The formal specification can be compiled on a host computer system such as MULTICS and used to set up the Nanodata QM-1 computer emulation system. This is a very flexible high-speed computer which can be microprogrammed at both the "nano-instruction" (80 nS per operation) level, using 360-bit wide nano-instructions which control register-to-register transfers, ALU operations etc., as well as at a more conventional micro-instruction level. It is an excellent tool for emulating proposed computers, since it can emulate a system both realistically and efficiently. The SMITE emulation facility has execution-time monitoring, statement-level stepping, symbol display and other aids for debugging target computer programs.

In summary, SMITE would demand a sufficiently-detailed description of the PXP system to answer question 3 (cost),

provide accurate timing estimates for question 1 (speed) and a test bed for somewhat subjective answers to question 2 (software). The vector arithmetic facilities of the proposed system would represent a significant step forward in AFES processing power. The ability to carry out up to nine simultaneous arithmetic or logical operations, coupled with the availability of data in high-speed registers, should lead to speed ups of at least an order of magnitude over the PDP11/34 - De Anza system, for those tasks which can exploit vector arithmetic. The increase in facilities and speed of microprocessors such as the Intel 8086, along with the availability of standard bit-sliced processors and LSI components should result in a powerful overall system at lower cost. The development of improved operating systems and high-level languages for microprocessors should make it easier to implement complex system software such as a feature extraction system during the timescale of any hardware development of PXP.

While these benefits seem evident, it is important to get more accurate estimates, along with the possible drawbacks, such as added programming complexity. The SMITE system would provide an excellent vehicle for this purpose.

REFERENCES

1. M.B. Faintich "DMA Concept of Image Analysis for Feature Extraction", unpublished memo, Defense Mapping Agency, December 1978.
2. Operations and maintenance manual for 5400 series Parallel Disc Memory, Data Disc Inc., 1973.
3. J.C. Lietz et al "Advanced Multi-spectral Image Descriptor System (AMIDS)", Final Report RADC -TR-74-346, February 1975.
4. "Mapping, Charting and Geodetic Features", PAR Report No. 78-50, Contract F30602-78-C-0080, December 1978.
5. "AFES Design Plan", P.A.R., Contract F30602-78-C-0080, April/May 1978.
6. MCS - 86 User's Manual, Intel Corp., July 1978.
7. D.J. Kuck "A Survey of Parallel Machine Organization and Programming", Computing Surveys, Vol. 9, no. 1, March 1977, p.29-59.
8. H.J. Siegel et al "A SIMD/MIMD multiprocessor system for image processing and pattern recognition", IEEE Computer Society Conference on Pattern Recognition and Image Processing, Chicago 1979, p.214-224.
9. M.J. Flynn "Some computer organizations and their effectiveness", IEEE Trans. on Computers, C-21, no. 9, September 1972, p.948-960.
10. N.S. Ramesh, K.S. Fu "A Survey of Computer Architectures for Image Processing and Pattern Recognition", Report TR-EE77-38, Purdue University, Contract AFOSR 74-2661, October 1977.
11. D.H. Taenzer "Interim Report on Region Growing", Technical Memorandum (unpublished), P.A.R., Contract F30602-78-C-0017, April 1978.
12. D. Marks (PAR Corporation), Private Communication. June 1979.
13. M. Shavit "An Emulation of the Am9080A: an example of a microprogrammed machine", Advanced Micro Systems, Sunnyvale 1978.
14. "SMITE Reference Manual" (TRW Defense and Space Systems Group), RADC-TR-77-364, November 1977.

15. B. Press, L.A. Prentice "SMITE Installation and Analysis",
(TRW), RADC-TR-78-212, December 1978.

APPENDIX

A.1 Sorting 9 pixel intensities

The sorting algorithms proposed here exploit the element pair swop instruction of the PXP. They assume the pixel intensities are already loaded to the accumulator vector.

A1.1 Simple sort

<u>instruction</u>	<u>comment</u>
1. lbyte<- 255	for comparison later
2. rbyte<- 0	" " " "
3. select a0 - a8	activate whole vector
4. compare right	
5. examine vm	check result of (4)
6. if (=0) -> 14	
7. gp reg <- vm	
8. compl. vm	
9. shift vm left	
10. vm <- vm & gp reg	
11. vcr <- vm	activate some elements
12. swop right	vector swop
13. -> 3	repeat till ordered
14. (finished)	pixels ordered
13 instructions	
167 instruction times (worst-case)	

A 1.2 Faster sort

This has a few more instructions but is faster.

1. lbyte <- 255	
2. rbyte <- 0	
3. select a0 - a8	
4. compare right	
5. examine vm	
6. if (=0) -> 18	
7. gp reg1 <- vm	
8. gp reg2 <- vm	
9. shift gp2 right	
10. compl. gp2	
11. gp2 <- gp1 & gp2	
12. if (=0) -> 3	
13. vcr <- gp2	
14. swop right	
15. shift gp2 right	for further swops
16. gp2 <- gp1 & gp2	
17. -> 11	till no more swops
18. (finished)	pixels ordered

instructioncommentA.2 Summation of vector elementsA 2.1 Cyclic method

1. gp reg <- 8	counter
2. rbyte <- 0	to hold m.s. result
3. select a0	activate a0 only
4. add left	a0<- a0 + a1 etc
5. examine vc	look at carry
6. if (=0) -> 8	jump if no carry
7. rbyte<-rbyte + 1	
8. gp <- gp -1	decrement count
9. if (=0) -> 13	
10. select a2 - a8	ready to shift
11. shift right	shift elements
12. -> 3	loop back
13. (finished)	

12 instructions

71 instruction times (worst-case)

A 2.2 Pairwise method

1. select a1,a3,a5,a7	
2. add left	4 pair adds (8bit)
3. shift vc left	deal with carry
4. gp reg <- vc	save carries
5. select a2,a4,a6,a8	
6. clear vector	ready for carries
7. examine gp reg	
8. if (=0) -> 11	
9. vcr <- gp reg	ready the vector
10. add 1 to vector	
11. select a1 - a8	
12. gp reg vec <- vector	save vector
13. shift vector right	
14. shift vector right	
15. select a1,a2,a5,a6	
16. add gp reg vector	2 pair adds (16 bit)
17. shift vc left	
18. gp reg n <- vc	save vc register
19. if (=0) ->22	check carry
20. acr <- gp reg n	set up vector
21. add 1 to vector	
22. gp reg vector <- vector	
23. shift vector right	
24. shift vector right	
25. shift vector right	
26. shift vector right	
27. select a1,a2	
28. add gp reg vector	pair add (16-bit)
29. examine vc	check carry

instructioncomment

```
30. if (no carry) -> 32
31. a2 <- a2 + 1
32. a1 <- a1 + a0
33. if (no carry) -> 35
34. a2 <- a2 + 1
35. (finished)                                result in a2, a1
```

35 instructions
35 instruction times (worst-case)

A 3. Region-labelling algorithm

1. select label image	i.e. region names
2. load (around) vector	pixel labels to vector
3. select a0 - a8	activate all elements
4. compare all: "unlabelled"	unlabelled pixels
5. gp reg <- vz	vz : unlabelled
6. vz0 <- 1	set vz bit 0 to 1
7. par <- vz	set up pixel access
8. select intensity image	pixel image proper
9. load(around) vector	unlab. pix. inten.
10. subtract center pixel	a0 available as gp reg
11. vcr <- vm	set up vec. cntrl.
12. compl. vector	moduli of int diffs.
13. vcr <- par	unlab. pix. & cent.
14. subtract threshold	
15. par <- vm	ready for edge labels
16. select label image	
17. load vector with "edge"	label edge pixels
18. store vector to image	
19. select a1 - a8	labels
20. load (around) vector	vz=1 for edge
21. compare "edge"	
22. compl. vz	ls for potential seeds
23. gp1 <- gp1 & vz	
24. gp2 <- vz	
25. 8-type circ shift left on vz	
26. gp2 <- gp2 or vz	
27. 8-type circ shift left on vz	
28. gp2 <- gp2 or vz	
29. 8-type circ shift right on vz	
30. ditto	
31. ditto	
32. gp2 <- gp2 or vz	
33. 8-type circ shift right on vz	0s for new seeds
34. gp2 <- gp2 or vz	
35. compl. gp2	new seeds
36. gp2 <- gp1 & gp2	set up pixel access
37. par <- gp2	set center pixel
38. par0 <- 1	

instruction

comment

39. load(around)vector
40. store vector
41. (finished)

get reg. label
label new seeds

40 instructions
40 instruction times

1979 USAF - SCEEE SUMMER FACULTY RESEARCH PROGRAM

Sponsored by the

AIR FORCE OFFICE OF SCIENTIFIC RESEARCH

Conducted by the

SOUTHEASTERN CENTER FOR ELECTRICAL ENGINEERING EDUCATION

FINAL REPORT

Prepared by:	John M. Owens, Ph.D
Academic Rank:	Professor
Department and University:	Dept. of Electrical Engineering, University of Texas, Arlington
Research Location:	Rome Air Development Center, Hanscom AFB, MA
USAF Research Colleagues:	J.C. Sethares
Date:	September 24, 1979
Contract No:	F49620-79-C-0038

MAGNETOSTATIC WAVE DECAY AND FILTER DEVICES

J.M. Owens

ABSTRACT

Magnetostatic waves (MSW) propagating in epitaxial yttrium iron garnet have been under serious investigation as complex signal processing elements for the past 3 years. This report presents the results of a study in two areas of MSW signal processing technology. First, the use of MSW delay lines as electronically variable time devices, with possible application in phased array antennas. Second, evaluation of element weighting techniques applicable to transversal filter implementation in MSW. The first area of study has yielded a number of simple MSW delay lines with delays adjustable from < 10 n sec to >100 n sec, insertion losses of less than 4 dB and bandwidth of >200 MHz. The second area of study has shown that width weighting is an effective transversal filter weighting technique.

ACKNOWLEDGEMENTS

The author would like to thank the Air Force Systems Command, Air Force Office of Scientific Research and Rome Air Development Center, Hanscom Air Force Base for the opportunity to spend a most interesting and worthwhile summer at Hanscom Air Force Base. In particular, he would like to thank Mr. J.C. Sethares, Mr. M. Stiglitz and Dr. P. Carr of RADC for the numerous helpful discussions, guidance and for helping with local arrangements which made the stay at RADC a most enjoyable and productive one for me.

I. INTRODUCTION

A military need exists for a microwave (1-20 GHz) analog signal processing technology with processing capabilities complementary to those developed over the past ten years with surface acoustic waves (SAW) at VHF/UHF frequencies. In particular tunable, matched filters and adjustable dispersive and non dispersive delay lines would find significant applications in military microwave systems. A new technology, with the potential to realize these requirements, has been developing over the past 3 years. This technology is based on magnetostatic wave (MSW) propagation in epitaxial YIG (yttrium iron garnet) and utilizes the concept of transversal filtering which has been so effectively utilized in SAW devices.

The object of this AFOSR Summer Faculty Research Program is the mutual interaction, of research efforts in the area of magnetostatic wave signal processing between the University of Texas at Arlington and Rome Air Development Center, Hanscom AFB. In particular two areas will be investigated, first the use of MSW delay lines as variable phase shifters for S-Band Phased Array Antennas, and second, the evaluation of weighting techniques applicable to MSW filters.

II. OBJECTIVES

The objectives of the project were:

- (1) To evaluate MSW delay lines for possible use in phased array antenna systems as electronically variable time delay elements.
- (2) To evaluate "width weighting" as a technique to provide amplitude weighting for MSW transducer transversal filters.

III. PHASED ARRAY ANTENNAS

Electronically scanned phased array antennas have been finding wider and wider application in military systems. For a pair of

radiating elements such a system (see Fig. 1) with element spacing d , maximum scan angle θ , and wavelength λ the required phase shift between elements ϕ is (1);

$$\phi_n - \phi_{n-1} = 2\pi \frac{d}{\lambda} \sin \theta$$

A beamwidth of 1° would require, as an example, 60 such elements spaced by $.9\lambda$. For a 60° scan the required interelement phase shift $\phi_n - \phi_{n-1}$ is $\approx 280^\circ$. As long as the signal being processed is constant and of long duration the phase shifters need only provide a variable differential phase shift of from $-(\phi_n - \phi_{n-1})$ to $+(\phi_n - \phi_{n-1})$. But, if the signal is not constant then, in order to preserve proper time relations appropriate group delay must also be present in the phase shifters and in this case the phase shift for the n^{th} element must be $n(\phi_n - \phi_{n-1})$ which would be a maximum of $14,400^\circ$ of phase shift or 13.2 nsec. at 3 GHz. The first type of phase shift is readily provided by ferrite, or diode phase shifters. Group delay shifts are at present provided by electronically switched sections of coaxial cable. This technique limits the effectiveness of scanned array systems due to significant cable and switch losses and the finite step size of discrete delay lines used. What is desired, ideally, is a transmission media which has an electronically adjustable propagation velocity, low loss, and is non dispersive over a significant bandwidth. At present, no devices satisfying all these requirements exist, but magnetostatic waves propagating in yttrium iron garnet offer an excellent possibility of ultimately satisfying these requirements.

IV. MAGNETOSTATIC WAVES

Magnetostatic waves are slow, magnetically dominated electromagnetic waves propagating in a magnetically biased ferrite (2).

Figure 2 shows the bias field orientation and dispersion diagram for

the 3 principle magnetostatic modes, propagating in a free yig slab. The addition of ground planes in proximity of the yig slab alters the dispersion characteristics somewhat but the basic form of the modes remain the same. (3)

Of the three basic modes, two are forward modes (v_{group} in the same direction as v_{phase}) and one backward mode (v_{group} opposite to v_{phase}). All are dispersive, and all have a finite pass band, whose position is adjustable by the D.C. bias field H_0 (3). The waves are easily coupled to (from an electromagnetic source) through the use of shorted fine wire couplers. (3) Propagation losses of as low as 12 dB/ μ sec at X-band have been achieved, (4) and thus low insertion loss variable delay lines are feasible. Figure 3 shows theoretical and experimental response characteristics of an MSSW surface wave delay line formed from a 30 μ m thick epitaxial YIG layer with 1 cm between 50 μ m wide 5 μ m thick shorted aluminum microstrip couplers (5). The sample was 3 mm wide. The minimum insertion loss for this line was 9 dB at 3.0 GHz.

V. VARIABLE PHASE SHIFTERS FROM SIMPLE MSSW DELAY LINES

From the preceeding section it can be seen that the basic requirement of a low loss, adjustable time delay element can be provided by a simple MSSW delay line. The variable delay can be provided at a single frequency by bias field adjustment. While the delay is adjustable at a single frequency, it is dispersive, that is the delay is a function of frequency. This kind of device would allow the fabrication of phased arrays with the appropriate adjustable "real time" delays but with narrow instantaneous bandwidths (of the order of a few MHz).

In order to demonstrate the delay characteristics of MSSW lines, 4 delay lines were fabricated, three of different lengths, and a fourth was matched at input and output to minimize insertion loss. Figure 4

shows the construction of the lines. An epitaxial yig film is flipped on an Al_2O_3 microstrip substrate on which the microstrip couplers are defined. Input and output are provided through OSM co-nectors, and a permanent magnet below provides the D.C. bias field. All devices are fabricated utilizing 30 μm yig films grown on 250 μm Gadolinium Gallium Garnet substrates, 3mm wide. The couplers defined on 250 μm Al_2O_3 substrates were 50 μm wide formed in 4 μm Al with spacing between the transducers of .25, .5 and 1 cm. The amplitude and phase response as measured with an HP 8410 network analyzer are shown in Figs. 3,5 and 6. As can be seen from these figures a wide range of delays can be achieved by choice of sample length and magnetic bias field. Figure 7 shows the response characteristics of a delay line with a parallel resonant matching network on both the input and output couplers. This line is optimized for a lower center frequency than those shown in Figs. 3 and 5, but, is still tunable over a 1 GHz bandwidth with a minimum insertion loss of 4 dB.

In order to demonstrate the tunable of these delay lines, a line identical to that shown in Fig. 3 had a 40 turn tuning coil added as shown in Figure 8. At 3.0 GHz this coil produced phase tuning of $0.75^\circ/\text{MA}$ or 810 MA/nsec. The power required was .22 W/nsec.

V1. ADJUSTABLE NON DISPERSIVE TIME DELAY SYSTEM

Figure 9 shows a system which has been conceived and tested to provide a non dispersive adjustable time delay system. It utilizes two MSW waves with opposite dispersion characteristics (MSSW and MSBVW) in series to realize this device. The system utilizes a 1 cm MSSW delay line with fixed bias (see Fig. 3) and a 1.25 cm MSBVW delay line with adjustable bias. (See Fig. 10). The amplitude and time delay responses are shown in Figure 11. Both lines are unmatched and thus the insertion loss is high (35 dB). As can be seen a 25 gauss adjustment of bias field produces a 15 nsec differential time delay with an approximately 200 MHz

bandwidth. The accuracy of the time delay measurement is limited by the measurement system to ~ 1 nsec, and clearly must be improved before the total applicability of the system can be judged, and improved as required.

VII. WEIGHTED ARRAY TRANSDUCER RESPONSE

Arrays of shorted microstrip transducer elements have been shown to provide limited control of the band pass characteristics of MSW delay lines. (6) This control is essential to realization of high quality MSW transversal filters. Essential to the realization of these filters is the development of techniques for amplitude weighting of transducer elements. One technique which shows promise for realizing weighting is that of varying the width of the transducer elements. As a step toward evaluating this technique, three devices have been fabricated, tested and compared with a super-position theory (7). The devices utilize two transducers 1 cm apart with 15 parallel bars in each. The individual bars are spaced 300 μm apart. The first device is a uniform width structure with 150 μm wide bars. The second has bars which vary linearly from 30 μm in width for the end bars to 240 μm in width at the center of the transducer. The third device has outside bars 240 μm in width with a linear variation to 30 μm for the center bar. The theoretical and experimental amplitude responses for these devices are shown in Figures 12, 13 and 14 respectively. As can be seen, the position of the primary filter response at ~ 3.1 GHz is well predicted. The uniform structure shows near in side lobe levels in reasonable agreement with theory, and Fig. 13 shows significant suppression of near in sidelobes. The theory, however, based on the superposition of independent conducting strips, does not predict the low frequency responses. Refinement of the theory to account for interacting bars and metal loading should prove useful in this respect. The weighting technique shows promise for control of the fundamental passband.

VIII. CONCLUSIONS/RECOMMENDATIONS

This study has demonstrated that magnetostatic wave delay lines offer, what is at present, the only continuously electronically variable low loss, microwave frequency time delay system applicable to phased array antenna systems. Simple delay lines with adjustable delays of from a few to > 100 n sec and insertion losses at 3 GHz of less than 4 dB have been demonstrated. A non-dispersive variable delay system with a 200 MHz bandwidth at 3GHz and time delay variation of 15 N sec has also been demonstrated. While these devices do not meet all the performance requirements desired by systems engineers, they do offer the only system available which meet the electronically variable time delay requirements. Considering the very limited time devoted to exploring these devices the results are most encouraging. Further work in the areas of input/output matching, dispersion control and optimization and the improvement of measurement techniques should result in significant improvement in device performance.

Initial evaluation of width weighting has shown the need for an improved theoretical model and further experiments to verify these improvements. Initial results are encouraging.

REFERENCES

1. Ramo, Whinnery and Van Duzer, "Fields and Waves In Communication Electronics" John Wiley and Sons, Inc., New York, 1965, pp 689.
2. R.W. Damon, J.R. Eschback, J Phys. Chem. Solids 19, 308-320, 1961.
3. J.D. Adams, J.H. Collins, J.M. Owens, The Radio and Electronic engineer, 45, pp 738-748, 1975.
4. Sessions 1 & 5, 20 September 1978, IEEE ISCAS Conf. Proc. IEEE Cat. No. 78CH 1358-1 CAS, May 1978.
5. J.H. Collins and J.M. Owens, 1978 Ultrasonics Symposium Proceedings, #CH 1358-1/78/000/0536 1978, pp 536-540.
6. H.J. WU, C.V. Smith and J.M. Owens, JAP So PP 2455-57, 1979.
7. J. Sethares, Personal Communications.

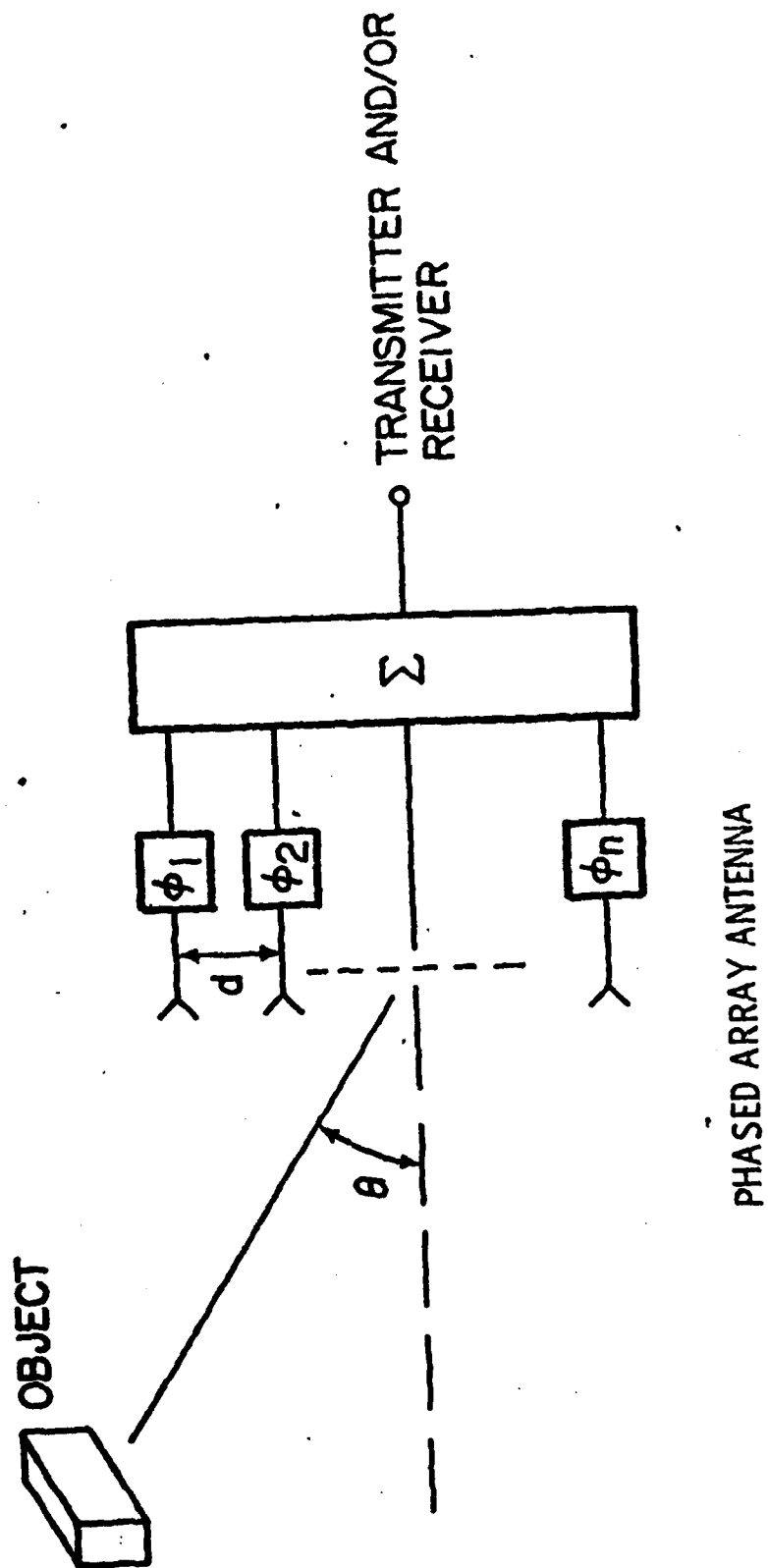


Figure 1 Phased Array Antenna.

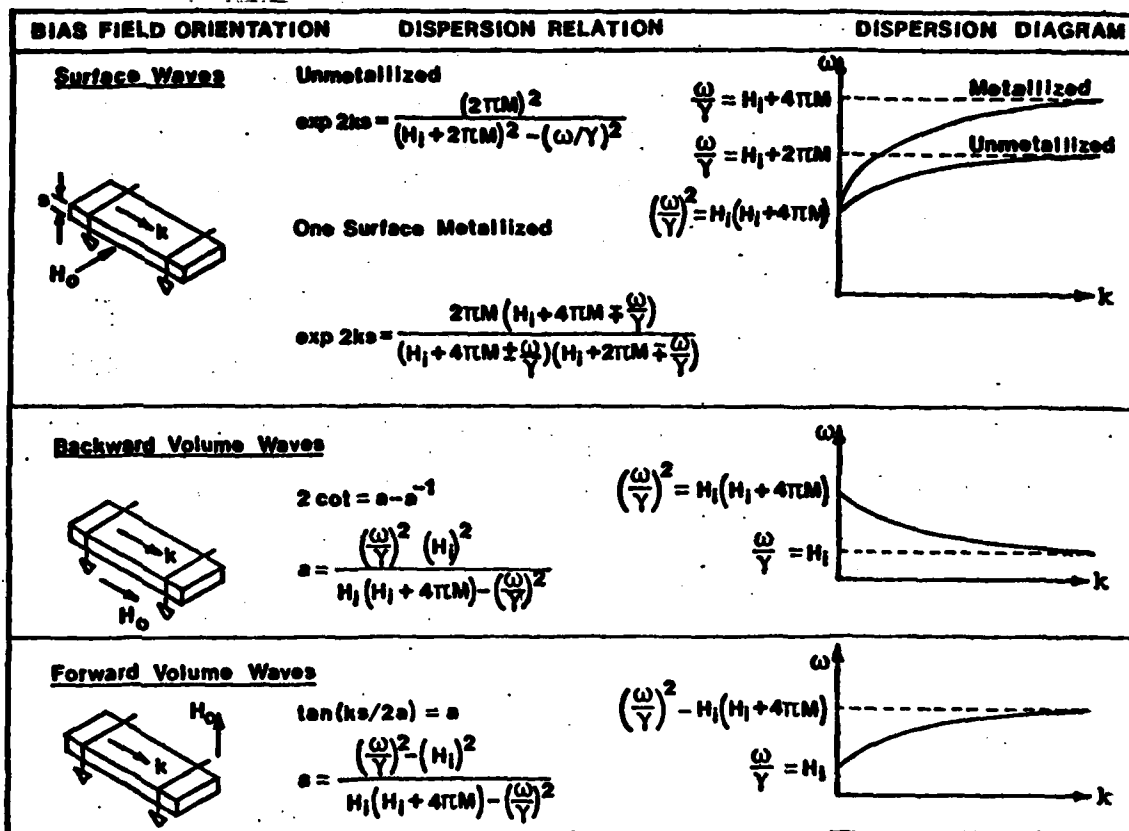
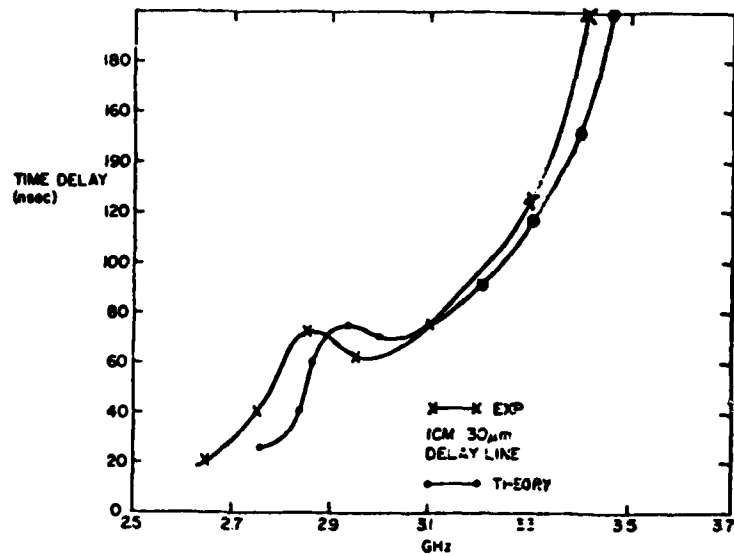
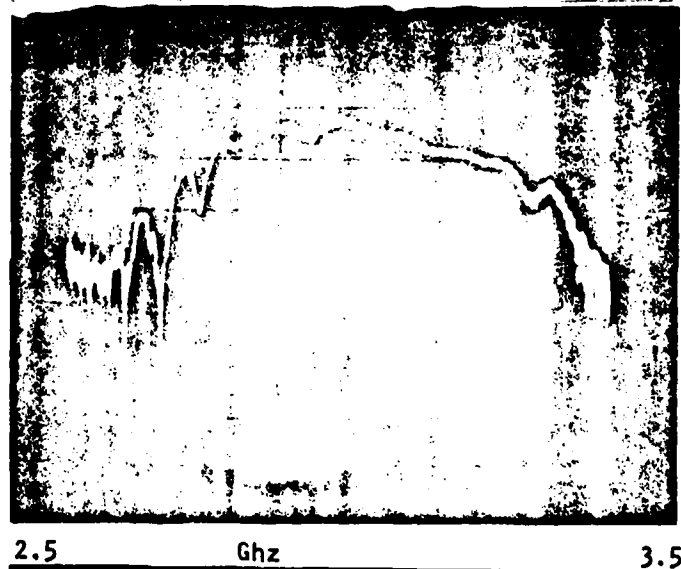


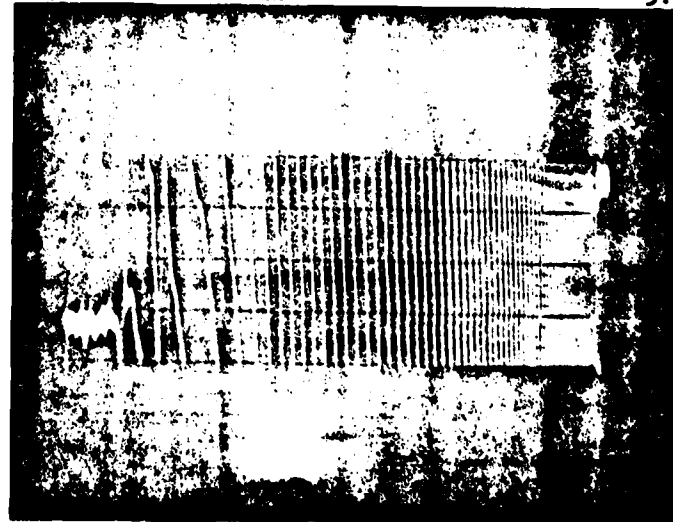
Figure 2- Dispersion Characteristics of Magnetostatic Waves in YIG Plates.



10 db/ Div.



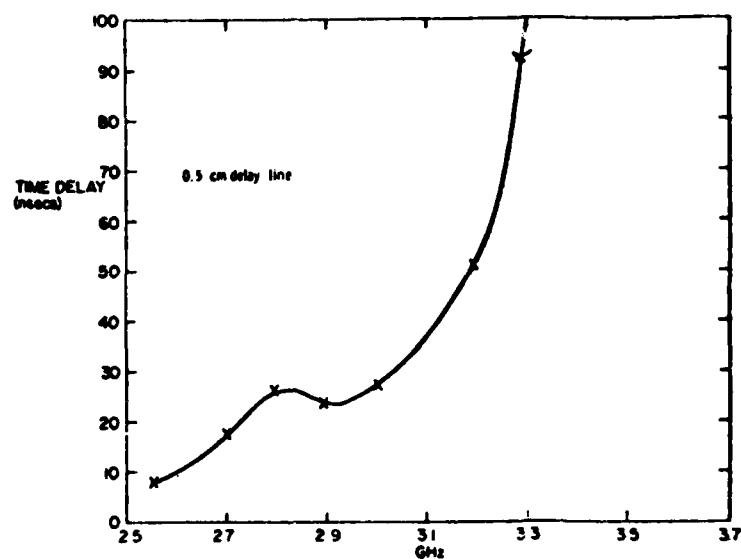
90 deg/div



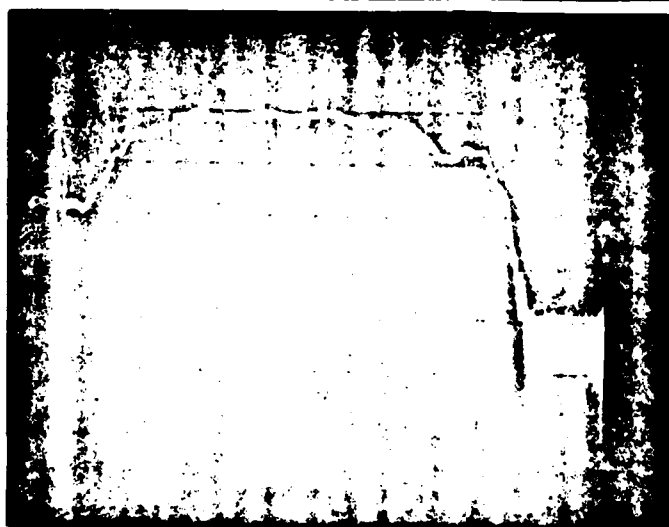
3. Experimental and Theoretical Group Delay Characteristics for a One Centimeter 30 μ m Thick YIG Delay Line. 49-13



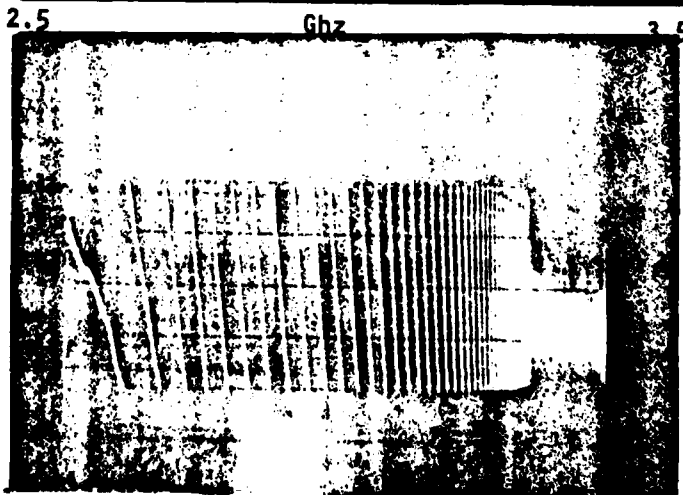
Figure 4 - One Centimeter MSSW Delay Line -
30 μ m YIG Film.



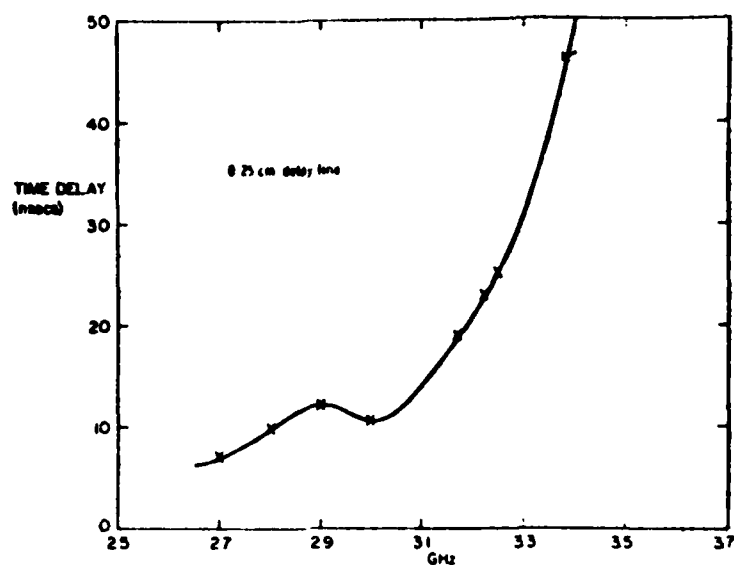
10 db / div



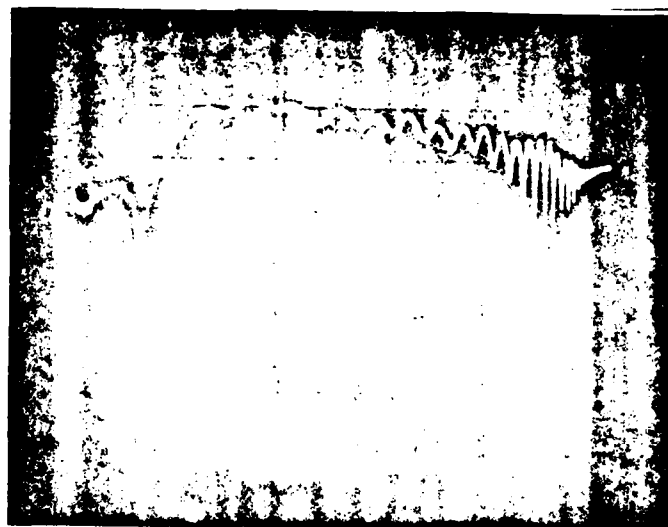
90 deg / div



5. Experimental Group Delay Characteristics for a 0.5 Centimeter Delay Line.

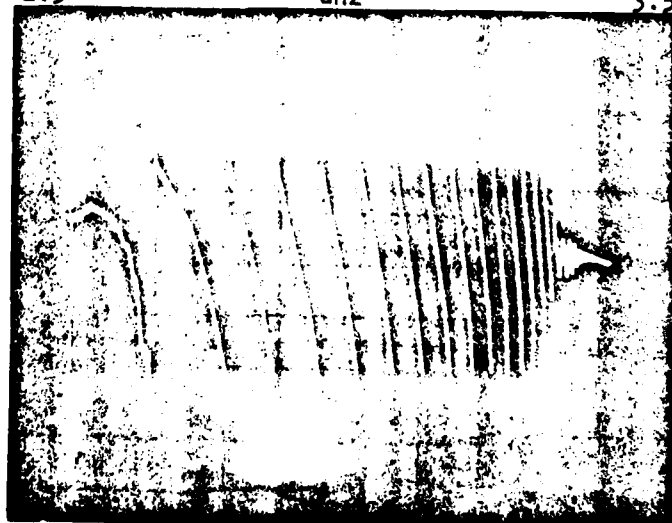


10 db/div

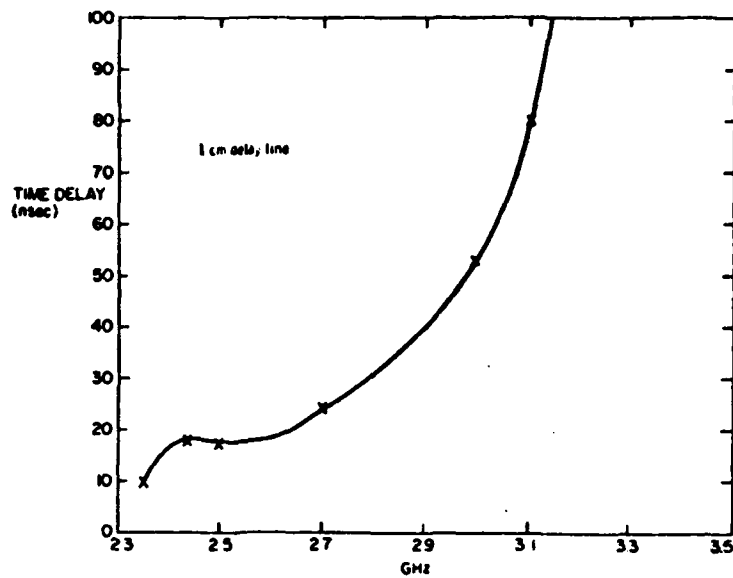


2.5 GHz 3.5

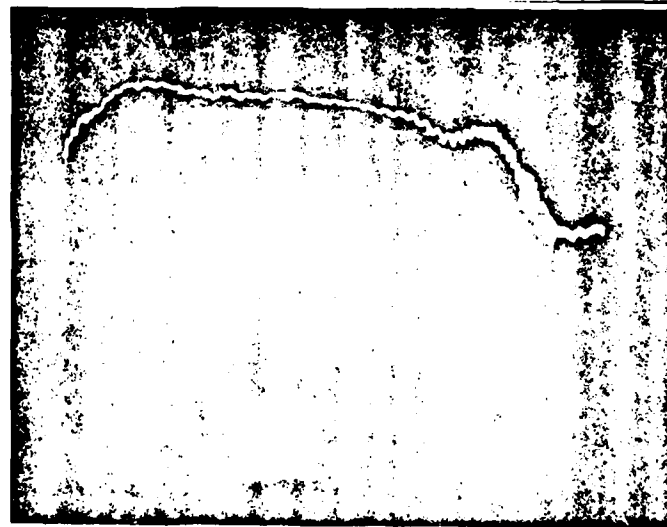
90 deg / div



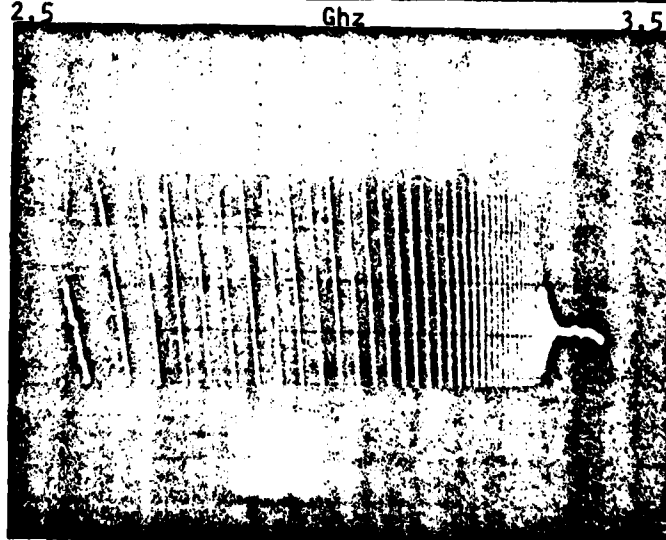
6. Experimental Group Delay Characteristics for a .25 Centimeter Delay Line.



10 db/div



90 deg/div



7. Experimental Group Delay for a One Centimeter Matched Delay Line.

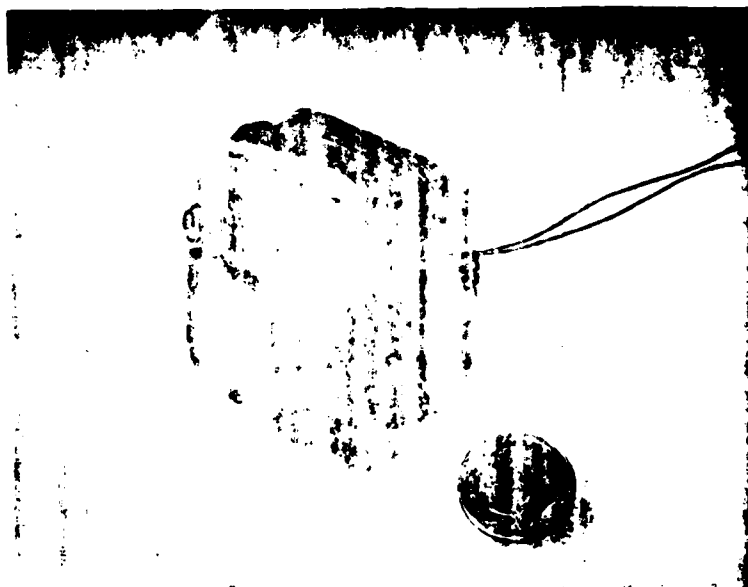


Figure 8 - One Centimeter MSSW Delay Line with a 40 Turn
Tuning Coll.

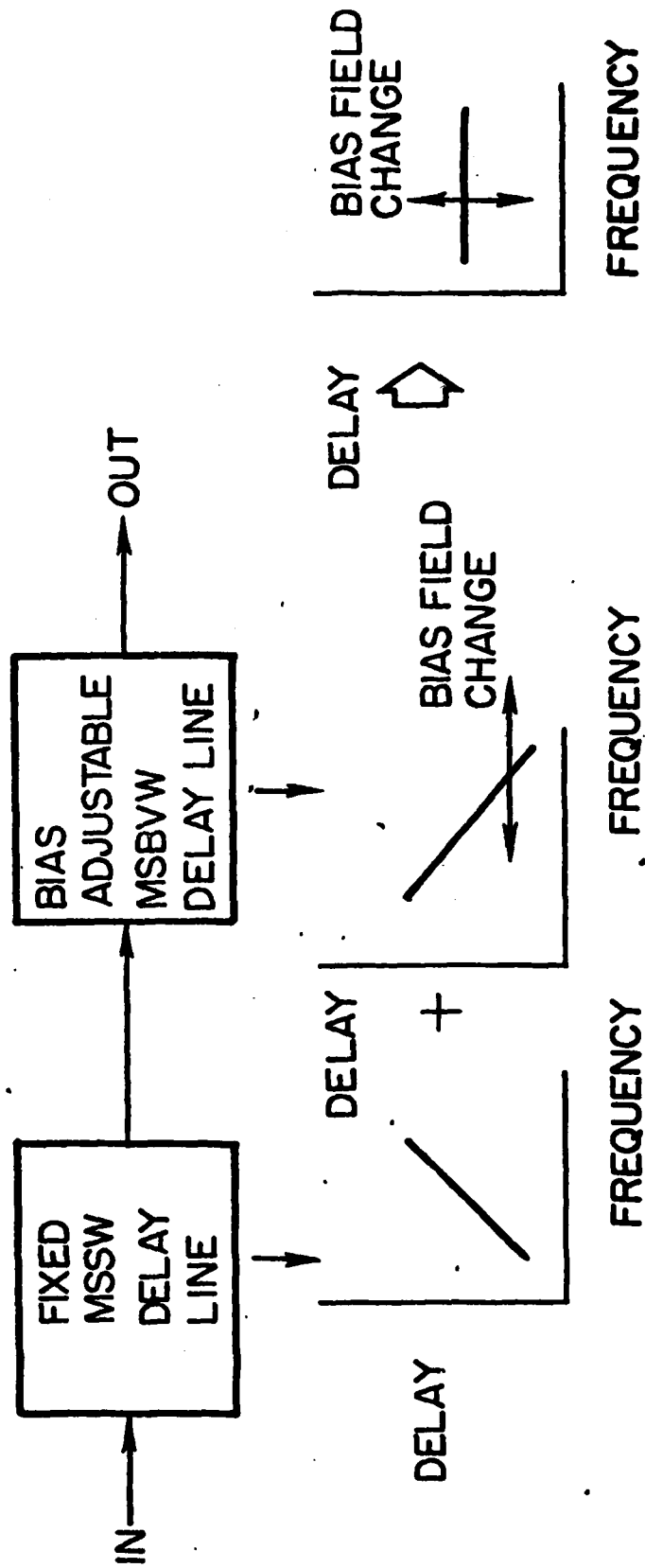
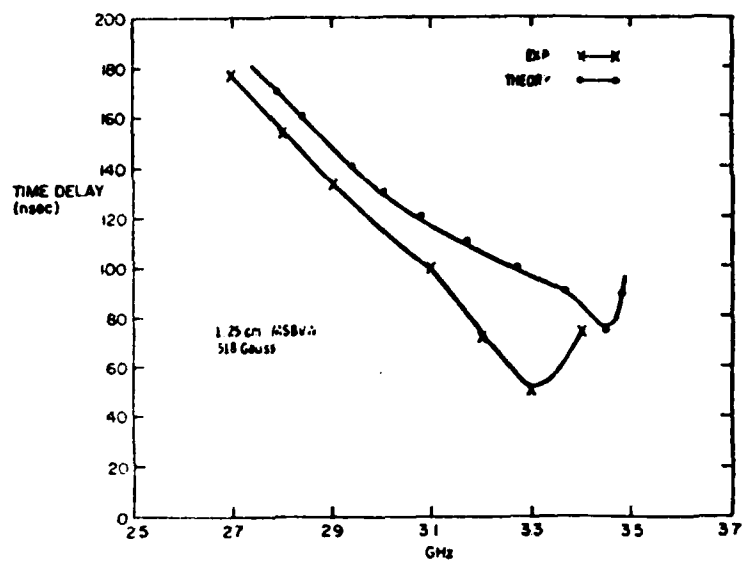
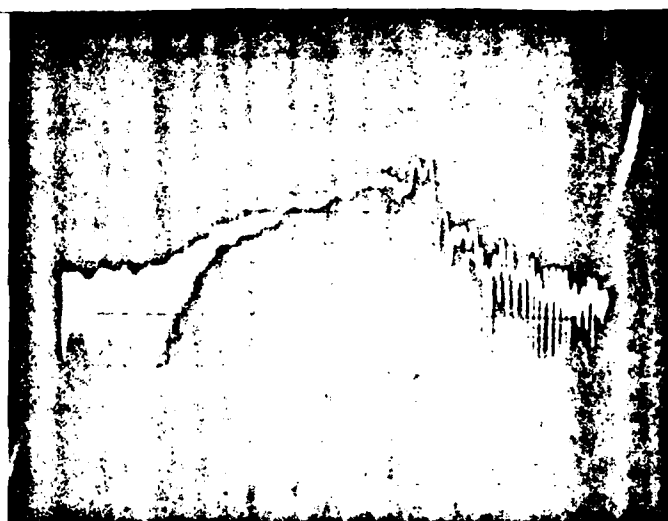


Figure 9 - Adjustable Non-Dispersive Time Delay System.

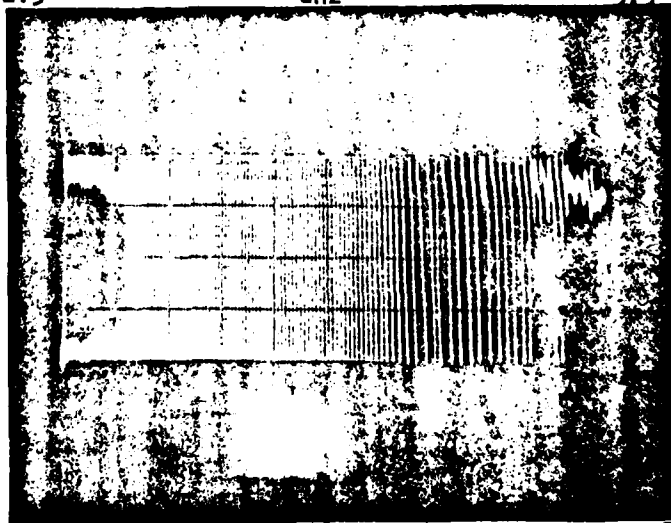


10 db/ div

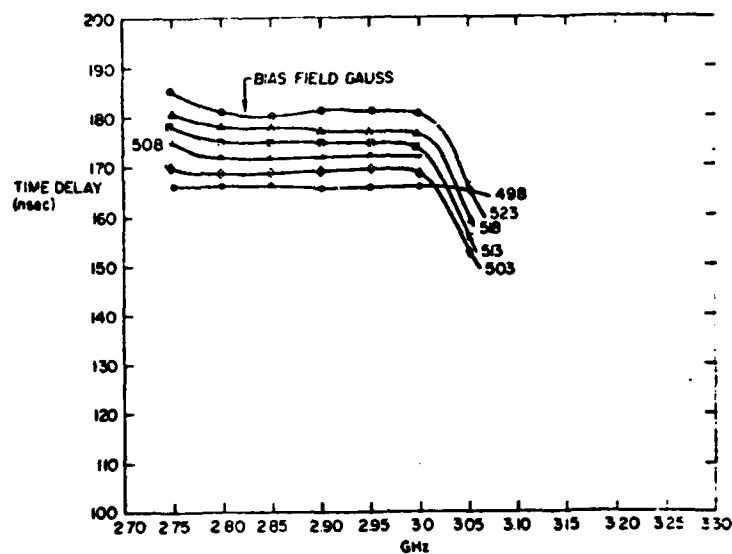


2.5 GHz 3.5

90 deg / div

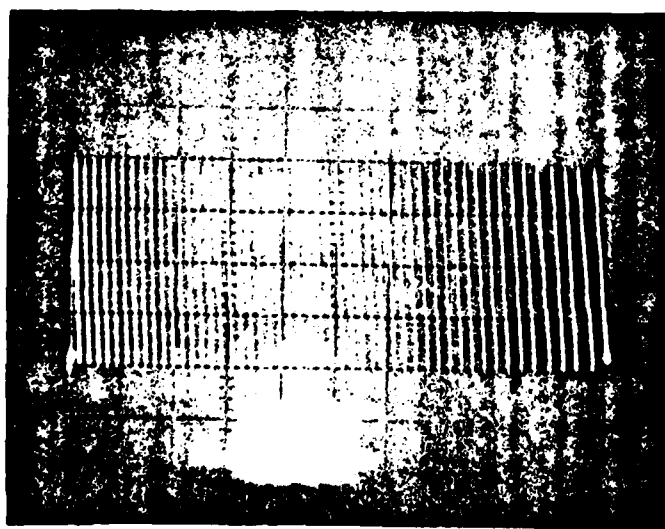
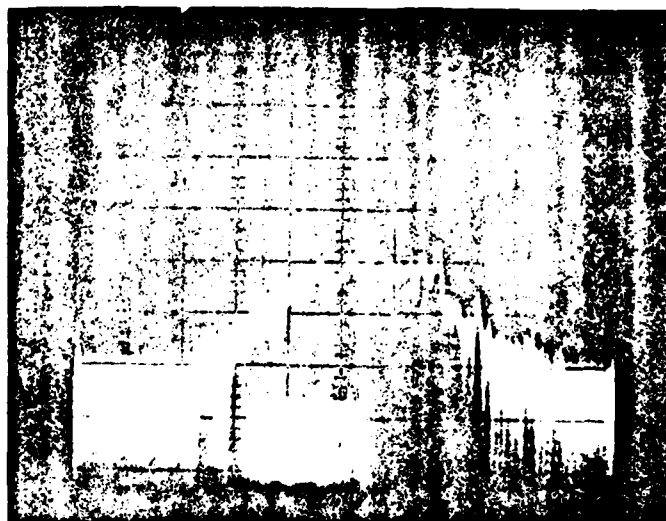


10. 1.25 Centimeter MSBW Delay Line with 518 Gauss Biasing Field.



10. 11 / 100

2.5-3.5 GHz



(c) 90 deg / div

2.5-3.5 GHz

11. Experimental Group Delay of an Adjustable Non-Dispersive Time Delay System.

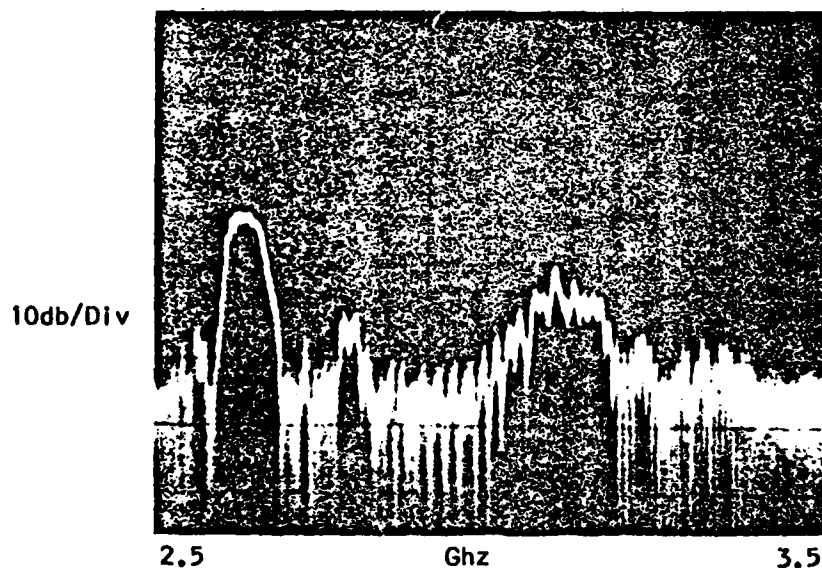
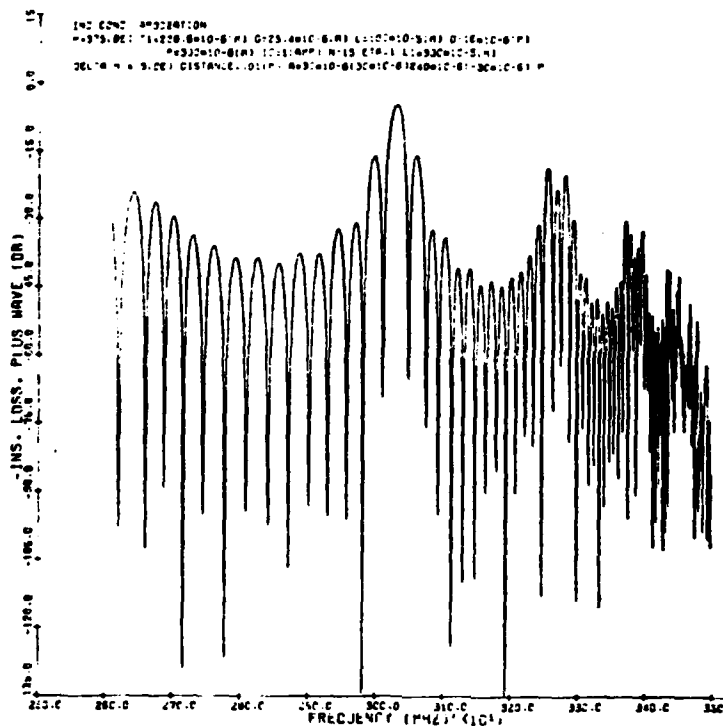


Figure 13 - Theoretical (Superposition Theory with Uniform Current Distribution) and Experimental Response of a Graded Width 15 Bar Transducer Array, 300 μ m Periodicity, 30 μ m Width on Ends, 240 μ m in Center, 16.5 μ m Film on a 250 μ m Substrate.

1979 USAF - SCEE SUMMER FACULTY RESEARCH PROGRAM

Sponsored by the

AIR FORCE OFFICE OF SCIENTIFIC RESEARCH

Conducted by the

SOUTHEASTERN CENTER FOR ELECTRICAL ENGINEERING EDUCATION

FINAL REPORT

IMPROVED METHODS FOR LARGE SCALE STRUCTURAL SYNTHESIS

Prepared by:	M. Pappas
Academic Rank:	Associate Professor
Department and University:	Department of Mechanical Engineering New Jersey Institute of Technology
Research Location:	AFFDL/FBR
USAF Research Colleague:	V.B. Venkayya
Date:	September 21, 1979
Contract No:	F49620-79-C-0038

IMPROVED METHODS FOR LARGE SCALE STRUCTURAL SYNTHESIS

by

M. Pappas

ABSTRACT

The report describes two potential improvements in techniques for large scale structural synthesis; methods for control of oscillation found to occur in many optimality criteria procedures and a primal mathematical programming algorithm. The central idea for oscillation control is the use of the gradients of a potentially active constraint set to prevent serious violation of one of the set when a move is made on the basis of only the active constraints. The mathematical programming procedure uses a modified feasible directions method.

Results of numerical experiments using these methods on two classical ten bar truss examples are very encouraging. Serious oscillations using earlier optimality criteria procedures were eliminated in all cases. The mathematical programming method was found to be comparable in effectiveness to the optimality criteria procedures.

Further research is required to refine these methods and substantiate the initial successes.

ACKNOWLEDGMENTS

The author wishes to express his gratitude to Dr. V.B. Venkayya, other personnel at AFFDL/FBR and in particular to Dr. N.S. Khot for their help and encouragement on this research and to the Air Force Systems Command, Air Force Office of Scientific Research and AFFDL/FBR at WPAFB Dayton, Ohio for their support of this effort.

I. INTRODUCTION

The structural optimization problem may be posed by the following:¹

Find

$$\min f(x_i) \quad i = 1, 2, \dots, I \quad (1)$$

subject to the conditions

$$g(x_j) \leq 0 \quad j = 1, 2, \dots, J \quad (2)$$

and

$$x_i^L \leq x_i \leq x_i^U \quad (3)$$

For the minimum weight design of structures modeled by bar and membrane plate elements the equations may be given by:²

$$f(x)_i = \sum_{j=1}^n A_{ij} x_j \quad (4)$$

$$g_j(x) = [\sum_{i=1}^n E_{ij}/x_i - U_j]/U_j \leq 0. \quad (5)$$

Optimality criteria (OC) methods resize the structure based on a solution of the problem

$$f_{,i} + \sum_{j \in J_A} \lambda_j g_{j,i} = 0 \quad (6)$$

by methods of successive substitutions where

$$x_i^{r+1} = x_i^r S_i(\eta_i, \lambda_j) \quad j \in J_A. \quad (7)$$

Here η is "resizing parameter" and J_A is a set of "active" constraints. For this report the meaning of the η parameter is that of the similar symbol of Ref. 5. Procedures which compute the values of the λ set considering the equations for λ as coupled will be referred to as "generalized" OC methods^{3,4} and those where the λ are assumed uncoupled as "simple" OC methods².

II. OBJECTIVES

There are two distinct projects associated with this research. These are:

1. A preliminary investigation of the effectiveness of a strategy to reduce divergence and oscillation in Optimality Criteria structural synthesis procedures.

2. The development of a primal Mathematical Programming (MP) procedure suitable for large scale structural synthesis.

III. OSCILLATION AND DIVERGENCE CONTROL

III.1 Background. All Optimality Criteria based methods require the selection of a constraint set for inclusion into the resizing problem of Eq. (6). This is usually done by including all those constraints where^{2,3,5}

$$g_j \geq -e_j \quad (8)$$

Here e_j will be referred to as the constraint "band width". The inclusion of too many constraints in the general OC procedures, result in an unnecessary increase in the computational effort required for the solution of the resizing problem. This effort can be substantial and may greatly exceed the reanalysis effort⁶. Excess constraints in simple OC procedures "overconstrain" the problem producing heavier designs⁷.

On the otherhand selection of band widths that are too small may lead to the major violation of a constraint that was not included in the resizing problem resulting in an increase in weight after scaling².

A major difficulty with OC procedures is that no rigorous or even reasonably reliable efficient procedure has been formulated for band width selection. The desire to reduce the computational effort in generalized OC procedures and the avoidance of the overconstraint problem in simple OC procedures usually results in selection of narrow band widths and thus in occasional, or even frequent, problems with oscillation or divergence^{5,8}.

Oscillation or divergence resulting from such problems will be referred to here as "primary oscillation". In addition to this mode oscillation can result from too large a value of the resizing parameter. Such oscillation will be referred to as "secondary oscillation".

III.2 Procedure for dealing with primary oscillation. The basic concept here is to introduce a potentially active constraint set J_p where $j \in J_p$ if

$$-e_{1j} \geq g_j \geq -e_{2j} \quad (9)$$

$$e_{2j} > e_{1j} \quad (10)$$

These constraints are not included directly in the resizing problem. However, if after resizing it appears, based on the gradient information associated with these constraints, that any of them may be violated the resizing step is shortened in an attempt to avoid this violation.

Where

$$\Delta x_1^r = x_1^{r+1} - x_1^r \quad (11)$$

the estimated value of g_j^{r+1} is given by

$$g_j^{r+1} = g_j^r + \sum_i g_{j,i}^r \Delta x_i^r \quad (12)$$

If any

$$g_1^{r+1} > 0 \quad (13)$$

compute a step shortening quantity K_j such that a move would produce a value of $g_j^{r+1} = 0$ for these constraints. Thus

$$K_j = -g_j^r / \sum_i g_{j,i}^r x_i^r \quad (14)$$

Call the smallest of these K^* and redefine x_1^{r+1} as

$$x_1^{r+1} = K^*(x_1^r + \Delta x_1^r) \quad (15)$$

III.3 Procedure for dealing with secondary oscillation. If a weight increase results after resizing and the sets J_A^{r+1} and J_P^{r+1} contain no constraints that were not in either J_A^r or J_P^r then it is assumed that the resizing parameter is too large. Design $r+1$ then discarded and a new resizing move made where

$$\eta^{r+1} = \eta^r / 2. \quad (16)$$

III.4 Termination Procedure. The resizing process is terminated if

$$|f(x^{r+1}) - f(x^r)| / f(x^r) \leq C_1 \quad (17)$$

where C_1 is a convergence criteria or if

$$\eta < C_2 \quad (18)$$

where C_2 is the minimum resizing parameter size.

III.5 Added Storage Requirements and Computational Effort. Once a step reduction value K_j is computed all the gradient information associated with that constraint may be discarded. Thus it is only necessary to store one set of constraint gradient components rather than the gradients of all constraints in the potentially active set. Furthermore, in most procedures once the quantities associated the determination of λ set are computed the gradients of the active set are no longer needed. Some part of the active constraint gradient storage may therefore be used for the particular potentially active constraint being considered. Thus, no additional storage is required for the primary oscillation control procedure.

In the case of the secondary oscillation control procedure if one is to formulate, a new resizing problem at a point x_1^T using a smaller n one can save computational effort if some information associated with the former resizing problem, that was destroyed during its solution, is saved. This information is derived from the gradients of the active constraint set. Since active set gradient storage usually requires much more space than the resizing problem information it may be stored in place of the active set gradient data along with the gradient components of one of the potentially active set. Thus, with appropriate information storage these procedures should normally not require any significant increase storage capacity.

The calculation of the additional potentially active constraint gradients requires additional computational effort at each redesign cycle. This additional effort is however usually small compared to the total computational effort and much smaller than the effort wasted by bad moves resulting from failure to consider, at all, these potentially active constraints.

IV. MATHEMATICAL PROGRAMMING (MP) ALGORITHM

IV.1 Background. Mathematical procedures are considered to be the most general and easily applied of the various optimization procedures. They avoid many of the difficulties associated with OC procedures⁹. MP procedures are however generally considered to be poorly suited to large structural synthesis problems without use of approximation techniques, at least in their primal form, due to the relatively large number of reanalysis typically required for most procedures⁴.

It has been the feeling of this writer that although the view that MP procedures are too inefficient for large scale structural synthesis may have some justification in the case of most existing methods it should be relatively easy to construct a procedure based on the method of feasible directions¹⁰ which will on the basis of total computational effort be competitive with OC procedures while still providing the flexibility to treat problems poorly suited to OC methods⁹. An attempt at such a procedure is presented here.

IV.2 The Feasible Direction (FD) MP Procedure. The feasible direction problem is usually formulated:¹ Find S_1 and σ so as to

Maximize σ

(19)

where

$$S^T f(x_1) + \sigma \leq 0 \quad (20)$$

and

$$S^T g_j(x_1) + W_j \sigma \leq 0 \quad j \in J_A \quad (21)$$

$$-1 \leq S_1 \leq 1 \quad (22)$$

where S consisting of components S_1 is the "feasible direction" of movement.

Equations (19) and (20) state that on the basis of the linearized functions the solution to this problem will produce a maximum possible improvement in $f(x_1)$. Equations (19) and (21) state for $W_j = 0$ that there will be no movement toward constraint violation and where $W_j > 0$ there will be movement away from violation. Equation (22) is used to eliminate unbounded solutions. This is a linear programming problem and may efficiently be solved by one of many well developed procedures.

Resizing is accomplished by letting

$$x_1^{r+1} = x_1^r + \alpha^r S_1^r \quad (23)$$

where α^r is selected arbitrarily. Here again one has the problem of determining an appropriate active set to include in Eqn. (21). Too large a band width will overconstrain the problem by forcing movement essentially parallel or away from a constraint that may not be critical. Too small a band width may produce serious violation of a constraint that was not considered in the direction finding problem Eqns. (19-22).

The overconstraining effect of too large a band width can be eliminated by replacing the $W_j \sigma$ term in (21) with a term producing movement toward the constraint. Thus replace Eq. (21) by

$$\alpha^r S^T \nabla g_j^r(x_1) < g_j^r \quad (24)$$

It may be seen that left hand side will produce an estimated change at most equal to the constraint value. Thus after resizing the value of the constraint will move toward zero or even near zero if the constraint is critical. In other words, if movement toward violation of the constraint improves the design, Eq. (24) will limit that movement only to the extent required to avoid violating the constraint. Thus, the redesign move will be influenced only by constraints expected to be critical.

It should be noted this procedure will also produce oscillation or divergence resulting from deficiencies in band width or η selection and that the same procedures for control of oscillation and divergence may be used here.

The value for α^r for this study is given by

$$\alpha^r = \eta^r |S^{r-1}|_{Vf}^r \quad (25)$$

where $|S_1^0| = \sqrt{I}$ and η^0 is arbitrarily selected. Such a value of η will tend to produce a change in the objective function of approximately 100 η^r percent if an S move, similar to S^{r-1} , is made in the Vf direction. Thus $\eta = .5$ would tend to produce about a 50% change in weight if one moved in the Vf direction. Since such a move would be deflected by the constraints the change after an actual move would be substantially less than that produced by a move in the Vf direction particularly during the later stages of the search where the design is highly constrained.

If a redesign move fails to produce a weight reduction η^r is reduced and design x^{r+1} is discarded as in Section III.3. A new design is then generated using

$$\eta^{r+1} = \eta^r / 2. \quad (26)$$

When this occurs the band width is also narrowed by setting

$$e_j^{r+1} = e_j^r / 2 \quad (27)$$

The e_j^0 are arbitrarily selected. Similarly these cuts are made if $S = 0$ is the solution¹⁰.

The design is scaled as in Ref. 2 after the move and reanalysis to produce a critical but feasible design.

Termination is accomplished by the procedure of Section III.4.

V. EXAMPLES

V.1 Problems. The two ten bar truss problems posed by Venkayya et al² are repeated in this preliminary study using the parameters of Ref. 5. The stress "constrained" problem involves the minimum weight design of the indeterminate structure under a single loading condition where the stress in all members must be held at or below one of two specified values. The optimal design in this structure weighs 1,497.60 lbs. In the displacement constrained problem two additional constraints are placed on the deflection of two joints. Side constraints [eqn (3)] are used for all variables.

The stresses and deflections are determined by a finite element analysis the results of which may be used to develop the constraint gradient information by means of the virtual unit load method².

These are now classic benchwork problems and represent a moderately difficult challenge for any proposed structural optimization scheme. The stress constrained problem has 9 (of 10) active stress constraints in addition to several active side constraints. The displacement constrained problem has two local minima one of which is constrained by the two displacement constraints (this design weighs 5,077.6 lbs) and one by a stress and one displacement constraint (this design weighs 5,061 lbs). Several side constraints are critical in both local optima.

V.2. Procedures. The generalized OC procedures described by Khot et al⁵ as the exponential [eq (7) of Ref. 5], and linear [eq (9) of Ref. 5] recursion forms was modified to use the oscillation control techniques described here in. In addition this procedure was also adapted to use the multiple iteration Newton Raphson procedure described by Khot et al in Ref. 8. The procedure from Ref. 8 is remarkably similar in that of Ref. 4 except for the method of solution of the λ problem. The oscillation control methods were added to the experimental program used to obtain the results given in Ref. 5 and 8 to generate the results contained herein.

The MP program used here was also developed from this same experimental program by replacing the resizing portions of the program.

VI. RESULTS OF USE OF OSCILLATION AND DIVERGENCE CONTROL PROCEDURE

VI.1 Primary Oscillation Control. Table 1 illustrates the application of this procedure to two cases where serious oscillation was experienced using earlier OC procedures^{5,8}. Both involve the stress constrained problem. In the first case the exponential recursion form with multiple iterations solution for the λ set was employed and in the other the exponential form with single solution for the λ set is used. It may be seen that the use of this procedure did infact control primary oscillation.

Two other test cases were used in which OC the procedures described in Ref. 5 and 8 were induced to oscillate badly by use of an excessively large resizing parameter ($\eta = 1$). The use of the primary oscillation control again suppressed this oscillation mode.

TABLE 1. Design Sequence, Stress Constrained 10 Bar Truss Problem With and Without Primary Oscillation Control. $\eta = 0.5$, Weight in lbs.

Design No.	Linear Form Multiple λ Iterations		Exponential Form Single λ Solution	
	No. Control	Control	No. Control	Control
1	3,435	3,435	3,435	3,435
2	4,452	2,059	3,118	2,169
3	2,342	1,959	4,870	1,991
4	7,221	1,801	2,809	2,292
5	8,576	1,664	2,746	1,838
6	2,689	1,654	4,854	1,876
7	1,662	1,540	2,840	1,683
8	2,229	1,532	2,169	1,656
9	1,704	1,526	2,219	1,597
10	1,626	1,521	2,976	1,574
11	23,992	1,516	3,871	1,558
12	11,185	1,512	2,969	1,548
13	4,694	1,508	3,370	1,539
14	9,542	1,505	2,796	1,532
15	4,948	1,502	4,340	1,525
16	14,146	1,499	2,496	1,520
17	6,914	1,498	3,880	1,515
18	6,998	1,532	2,701	1,510
19	10,665	1,497.60	4,125	1,507
20	5,667	1,498	2,3122	1,504
21		1,497.60		1,501
22		1,498		1,678
23		1,497.60		1,595
24		1,497.62		1,640
25		1,497.60		1,674

TABLE 2. Design Sequence, Stress Constrained 10 Bar Truss Problem Single Solution, Linear Form $\eta = 0.5$ at Start, Weight in lbs.

<u>Design No.</u>	<u>Primary Control Only</u>	<u>Both Controls</u>
1	3,435	3,435
2	2,444	2,444
3	1,836	1,836
4	2,294	2,294*
5	1,863	1,726
6	2,061	1,653
7	1,727	1,586
8	1,718	1,556
9	1,569	1,539
10	1,541	1,529
11	1,524	1,523
12	1,518	1,518
13	1,513	1,513
14	1,509	1,093
15	1,506	1,506
16	1,503	1,523
17	1,501	1,501
18	1,499	1,499
19	1,497.6	1,497.74
20	1,656	1,656*
21	1,685	1,572*
22	1,681	1,534*
23	1,677	1,516
24	1,677	1,497.67
25	1,678	1,506*
26		1,497.63
27		1,502*
28		1,497.61*

*Halved resizing parameter at this redesign cycle.

VI.2 Secondary Oscillation Control. Table 2 illustrates the application of the secondary procedure. With only primary control one sees here secondary oscillation at design number 4-6 and divergence at design number 20. It may be seen that the reduction in the resizing parameter produces convergence to the optimal design.

This procedure was found satisfactory only with the linear recursion forms. It was found unsatisfactory for the exponential form since the assumption that the λ problem formulated on the basis of the linear recursion relation may be used with the exponential form was not valid at small λ values. Because of this all subsequent numerical experiments are based on the linear recursion forms.

All runs used $e_{2j} = 2 e_{1j}$ to define the potentially active constraints. The quantities e_{1j} for the active constraints are defined by the procedure of Ref. 5. Termination constraints used for all runs were $C_1 = 10^{-6}$, $C_2 = 0.01$.

VI.3 Use of a Large Initial Resizing Parameter. Since the early experiments indicated that these controls would inhibit oscillation that would usually occur with excessive value of η an experiment was performed to investigate the possibility of using a large initial value of this parameter so as to speed convergence. The result is shown in Tables 3 and 4. These results fail to support the hypothesis that a large initial η is advantageous.

VI.4 Convergence of Multiple and Single λ Problem Solutions Procedures. It may also be seen from Tables 3 and 4 that the multiple λ iteration procedure possesses much better convergence properties than the single λ solution procedure. In fact the single λ solution procedure fails on the displacement constrained problem. It also fails on this problem when no oscillation controls are used.

An oscillation control procedure is important in allowing exploitation of the multiple λ iteration approach because of the oscillation problems with this method encountered in earlier studies. It is interesting to note that although Ref. 8 mentions the potential of this procedure it is not used in the later study of OC methods⁵.

VI.5 Comparison of Ordinary and Inverse Variables. The results of this study are shown in Table 5. There is no apparent advantage associated with the use of inverse variables.

TABLE 3. Comparison of Design Sequences Using Different Initial Resizing Parameters, Stress Constraints 10 Bar Truss, Weight in lbs.

Design No.	Multiple λ Iterations		Single λ Solution	
	$\eta=1$ at Start	$\eta=0.5$ at Start	$\eta=1$ at Start	$\eta=0.5$ at Start
1	3,435	3,435	3,435	3,435
2	2,128	2,059	2,740	2,444
3	1,915	1,959	1,825	1,836
4	1,772	1,801	1,719	2.294*
5	1,638	1,664	1,628	1,726
6	1,593	1,654	1,580	1,653
7	1,532	1,540	1,548	1,586
8	1,527	1,532	1,531	1,555
9	1,521	1,526	1,519	1,539
10	1,512	1,521	1,509	1,529
11	1,508	1,516	1,499	1,523
12	1,505	1,512	1,517*	1,518
13	1,502	1,508	1,638*	1,513
14	1,500	1,505	1,497.9	1,509
15	1,558*	1,502	1,572*	1,506
16	1,497.62	1,499	1,502	1,503
17	1,497.60	1,498	1,497.7	1,501
18	1,497.60†	1,532*	1,516*	1,499
19		1,497.63	1,506**	1,498
20		1,497.60		1,656*
21		1,497.60†		1,572*
22				1,534*
23				1,516*
24				1,497.67
25				1,506*
				(28)1,497.61†

*Halved resizing parameter.

†Terminated by convergence specification.

**Terminated by minimum resizing parameter specification.

TABLE 4. Comparison of Design Sequences Using Different Initial Resizing Parameters, Displacement Constrained 10 Bar Truss, Weight in lbs.

Design No.	Multiple λ Iterations		Single λ Solution	
	$\eta=1$ at Start	$\eta=0.5$ at Start	$\eta=1$ at Start	$\eta=0.5$ at Start
1	8,266	8,266	8,266	8,266
2	6,893	6,646	7,146	6,667
3	5,816	5,824	6,932	6,196
4	5,593	5,703	6,641	5,947
5	5,466	5,597	5,376	5,759
6	5,327	5,471	5,221	5,628
7	5,358	5,353	5,216	5,516
8	5,505*	5,195	5,162	5,401
9	5,200	5,079.6	5,179	5,280
10	5,094	5,078.9	5,129	5,187
11	5,076	5,084.4*	5,118	5,143
12	5,066	5,077.0	5,115	5,115
13	5,061.0	5,076.7	5,113	5,108
14	5,060.87	5,076.7	5,112	5,090.4
15	5,060.85		5,117	5,104.4*
16	5,060.85		5,111.5	5,094.2
17			5,111.35	5,089.4
18			5,111.31	5,088.0
19			5,111.253	5,086.9
20			5,111.247	5,086.0
25			5,098.7*	5,083.6*
30			5,094.6	5,082.9†
35			5,093.4	
50			5,093.3	

*Halved resizing parameter.

†Terminated by convergence specification.

TABLE 5. Comparison of Inverse and Ordinary Variables Using Multiple Iteration Linear Form Procedure, $n = 0.5$ at Start, Weight in lbs.
10 Bar Truss

<u>Design No.</u>	<u>Inverse</u>	<u>Ordinary</u>	<u>Inverse</u>	<u>Ordinary</u>
1	3,435	3,435	8,266	8,266
2	2,098	2,059	6,912	6,645
3	1,903	1,959	6,438	5,824
4	1,662	1,801	6,194	5,703
5	1,624	1,664	6,019	5,597
6	1,537	1,654	5,877	5,471
7	1,518	1,540	5,750	5,353
8	1,513	1,532	5,628	5,195
9	1,509	1,526	5,511	5,080
10	1,503	1,521	5,402	5,078.9
11	1,501	1,516	5,307	5,084*
12	1,593*	1,512	5,182	5,077.0
13	1,497.67	1,508	5,101	5,076.7
14	1,497.60	1,505	5,094	5,076.7
15	1,565*	1,502	5,081	
16	1,497.60	1,498.8	5,094	
17		1,497.9	5,081	
18		1,532*	5,0770	
19		1,497.63	5,076.7	
20		1,497.60	5,107*	
21		1,497.60	5,076.7	

*Halved resizing parameter.

TABLE 6. Design Sequences for Feasible Directions Algorithm Using Different Resizing Parameters, Weight in lbs. 10 Bar Truss.

<u>Design No.</u>	<u>Stress Constrained</u>			<u>Displacement Constrained</u>			
	0.1	0.2	0.5	0.1	0.2	0.5	0.5
1	3,435	3,435	3,435	8,266	8,266	8,266	8,266
2	3,166	2,885	2,224	7,770	7,394	7,006	7,006
3	2,884	2,455	2,722	7,040	6,837	7,642	6,610
4	2,641	2,096	1,818	6,801	6,629	7,608	6,385
5	2,448	1,817	2,300	6,615	6,402	6,331	6,171
6	2,279	2,006	1,787	6,466	6,097	6,217	5,976
7	2,125	1,703	1,677	6,309	5,826	5,796	5,854
8	1,854	1,693	1,604	6,150	5,668	5,492	5,564
9	1,736	1,623	1,557	6,002	6,358	5,225	5,398
10	1,792	1,571	1,528	5,827	5,512	5,164	5,176
11	1,671	1,535	1,507.6	5,637	5,172	5,281	5,115
12	1,644	1,516	1,501.4	5,396	5,114	6,225	5,739
13	1,624	1,742	1,737	5,178	5,090	5,175	5,066.9
14	1,606	1,506	1,498.3	5,112	5,088	5,125	5,126
15	1,585	1,737	1,498.4	5,169	5,090	5,108	5,091
16	1,567	1,501	1,497.9	5,082	5,081	5,099	5,067.6
17	1,549	1,725	1,498.5	5,079	5,084	5,095	
18	1,524	1,498	1,497.7	5,077	5,079.6	5,088	
19	1,515	1,725	1,498.4	5,078	5,079.6	5,085	
20	1,505	1,549	1,497.6	5,077.0	5,079.4	5,081	
25	1,506	1,497.6		5,077.6	5,078.6	5,077.1	
30	1,497.6			5,076.7	5,077.9	5,076.7	
35					5,077.6		
50					5,076.7		

†Modified Algorithm.

VII. PERFORMANCE OF THE FEASIBLE DIRECTIONS ALGORITHM

The results of this algorithm on the example problems using various values of η^0 are shown in Table 6. In all cases $e_j^0 = 0.5$. A small η^0 produces small changes in the initial designs. A large η^0 on the other-hand produces early oscillation associated with the need for step size reduction. This of course is similar to the situation in OC procedures.

Further development can undoubtedly substantially improve performance. For example the algorithm described in section V was modified such that; 1) the equations (21) and (28) are invoked (step size is reduced) after the change in weight on scaling is greater than the net decrease in weight after redesign and scaling; 2) the S^{r-1} in eq. (25) replaced by S^* where S^* is obtained after iterative solution of the feasible direction problem [eqns. (19-25)] until $|S^*| = |S^r|$. This modification produced a dramatic improvement in performance (see Table 6) on the sole problem on which it was tested.

VIII. COMPARISON OF THE OC AND FD PROCEDURES

On the basis of this limited study if one uses similar values of the resizing parameter it appears that the MP procedure requires fewer iterations for convergence than the single λ solution OC procedure even after the oscillation control improvements are made to the latter. The multiple λ iteration approach seems to possess superior convergence properties when these controls are used. It appears, however, that it may be relatively simple to greatly improve the performance of the MP procedure to the point where it is comparable to the multiple λ iteration OC procedure.

On the basis of computational effort required for convergence the picture is somewhat different. Analysis and resizing times are shown in Table 7. The analysis time is the CPU time required to do the finite element analysis. The resizing time includes the time required to compute the necessary derivatives and set up and solve either the λ or the feasible direction problem.

It may be seen that the resizing time required for the MP procedure is similar to the single λ solution OC method which is much less than the multiple λ iteration approach. Furthermore, it is the resizing effort that dominates. On larger problems one would expect a similar situation.

TABLE 7. Typical Analysis and Resizing Times, CPU Sec CYBER 74

	<u>Multiple λ Iteration</u>		<u>Single λ Solution</u>		<u>Feasible Direction</u>	
	<u>Analysis</u>	<u>Resizing</u>	<u>Analysis</u>	<u>Resizing</u>	<u>Analysis</u>	<u>Resizing</u>
Ten Bar Truss Stress Constrained	.022	1.996	.022	.1330	.073	.274
Ten Bar Truss Displacement Constrained	.021	.379	.022	.071	.022	.112
Two Hundred Bar Truss	2.351	17.44	2.341	.708	-	-

Furthermore, on large problems a more efficient but more complex linear programming procedure which ignores zero matrix entries rather than the simple procedure used here should substantially reduce the resizing effort making the MP procedure more attractive.

IX. CONCLUSION

Much more work needs to be done to verify the preliminary results developed here after further refinement of the concepts presented. The results of this work, however, supports the initial assumptions that oscillation problems associated with OC methods may easily be greatly reduced. Further the hypothesis that a simple primal MP procedure without approximations can be competitive with OC procedures for finite element based structural synthesis is also reinforced.

On the basis of this preliminary study the MP procedure seems more attractive than the OC procedures on large problems with many active constraints due to the large effort required to set up the λ problem⁶. On problems with very few active constraints the ability of the OC procedures to produce very large initial weight reductions makes these procedures attractive. Additional work needs to be done however to reduce the resizing computation effort of the multiple λ iteration approach to allow exploitation of its superior convergence properties.

The importance of these preliminary findings justifies expanded research in the area.

X. RECOMMENDATIONS

The preliminary results of this early research are quite encouraging and justify further study since these methods, if successful, represent major advances. The following additional research is therefore recommended:

1. Application of the oscillation control techniques to a simple OC procedure.
2. Refinement of the techniques. For example the development or improvement in the methods of band width and step size determination or specification.
3. Treatment of additional static problem examples.
4. Treatment of dynamic problem examples.
5. Treatment of example problems with local buckling constraints.

6. Comparison of the procedures developed as the result of this research with important large scale synthesis capabilities such as the ACCESS3 and OPTSTAT codes.
7. If justified, the incorporation of successful new methods into a formal structural synthesis program for general distribution.

REFERENCES

1. Mangasarian, O.L., "Techniques of Optimization", Transactions of the ASME, Journal of Engrg. for Industry, Vol. 94, Series B, No. 2, pp. 365-372, May 1972.
2. Venkayya, V.B., Khot, N.S., and Berke, L., "Application of Optimality Criteria Approaches to Automated Design of Large Practical Structures", AGARD Second Symposium on Structural Optimization, Milan, Italy, April 1973, pp. 3-1, 3-20.
3. Rizzi, P., "Optimization of Multi-Constrained Structures Based on Optimality Criteria", Proceedings of the 17th AIAA/ASME/SAE, Structures, Structural Dynamics and Materials Conference, King of Prussia, Pennsylvania, May 1976.
4. Schmit, L.A., and Fleury, C., "An Improved Analysis/Synthesis Capability Based on Dual Methods - ACCESS3", Proceedings of the 20th AIAA/ASME/SAE, Structures, Structural Dynamics and Materials Conference.
5. Khot, N.S., Berke, L., and Venkayya, V.B., "Minimum Weight Design of Structures by the Optimality Criterion and Projection Method", Proceedings of the 20th AIAA/ASME/SAE, Structures, Structural Dynamics and Materials Conference.
6. Khot, N.S., Private Communication.
7. Venkayya, V.B., Private Communication.
8. Khot, N.S., Berke, L., and Venkayya, V.B., "Comparison of Optimality Criteria Algorithms for Minimum Weight Design of Structures", Proceedings of the 19th AIAA/ASME/SAE Structures, Structural Dynamics and Materials Conference, held at Bethesda, Maryland, April 1978.
9. Pappas, M., and Venkayya, V.B., "Methods for Large Scale Structural Synthesis", AFFDL/FBR Technical Memo, in preparation.
10. Moradi, J.Y., and Pappas, M., "A Boundary Tracking Optimization Algorithm for Constrained Nonlinear Problems", Transactions of the ASME, Journal of Mechanical Design, Vol. 100, No. 2, pp. 292-296, April 1978.

1979 USAF - SCEEE SUMMER FACUTLY RESEARCH PROGRAM

Sponsored by the

AIR FORCE OFFICE OF SCIENTIFIC RESEARCH

Conducted by the

SOUTHEASTERN CENTER FOR ELECTRICAL ENGINEERING EDUCATION

FINAL REPORT

EDUCATIONAL IMPLICATIONS OF COGNITIVE RESEARCH ON IMAGERY

Prepared by:	Steven E. Poltrock
Academic Rank:	Assistant Professor
Department and University:	Psychology Department University of Denver
Research Location:	Human Resources Laboratory/Technical Training Lowry Air Force Base
USAF Research Colleague:	Larry G. Harding
Date:	September 12, 1979
Contract No.:	F49620-79-C-0038

EDUCATIONAL IMPLICATIONS OF COGNITIVE RESEARCH ON IMAGERY

by

Steven E. Poltrock

ABSTRACT

The current research and goals of the Human Resources Laboratory Technical Training Division are reviewed. Mental imagery is identified as an area of research with potential contributions to these goals. The cognitive research on mental imagery is extensively reviewed, with emphasis on three questions: (1) How does imagery function? (2) What situations are appropriate for imagery strategies? (3) Who can effectively use imagery in learning situations? The effectiveness of mental imagery as a strategy for learning is established. The report concludes with recommendations for applications of mental imagery in educational or training situations and recommendations for further research.

ACKNOWLEDGEMENTS

The author would like to thank the Air Force Systems Command, Air Force Office of Scientific Research for providing the opportunity to conduct this research. Special acknowledgement is due to the staff of the Human Resources Laboratory/Technical Training Division, particular Drs. Larry Harding and Marty Rockway, for their helpful guidance and discussions.

Finally, thanks are due to Dr. Lydia Hooke whose criticisms of earlier drafts greatly improved this manuscript.

I. INTRODUCTION:

The goal of the Technical Training Division of the Human Resources Laboratory is to improve technical training in the Air Force. This goal is addressed by conducting research on all aspects of the training process. Thus, to appreciate the directions of current research it is helpful to consider the nature and demands of technical training in the Air Force.

Group training is primarily conducted at Lowry Air Force Base under the control of the Air Training Command, which is the customer for the Human Resources Laboratory. The technical training courses at Lowry are intensive, requiring a full time effort for a period of weeks or months. Ideally, students should complete their courses as quickly as possible with competency in their technical field. Thus, the goals of the Air Training Command are twofold: (1) to reach a required level of competency, and (2) to reach this level in the minimum amount of time. Thus, much of the research sponsored by the Technical Training Division is intended to (1) improve the procedures for assessment of student progress, and (2) accelerate the learning process. Only the second of these two goals is considered here.

Acceleration of the learning process is a very broad goal, permitting a wide range of approaches. The most direct approach would be to conduct research leading to improved training procedures. Alternatively, the research could focus on the student rather than the teacher, and develop methods of improving the student's preparation for the course. A third approach would combine these two areas of focus by developing alternative training procedures that match characteristics of the students. In fact, research has been done or is in progress in each of these areas. A brief review of this research is presented.

Improvements in Training Procedures

A large literature exists on alternative training procedures and their efficacy. The research strategy is generally to compare a traditional classroom environment with an alternative approach. Alternatives that have been investigated include programmed instruction, computer-assisted instruction, and alternative instructional modalities. Currently, the Advanced Instructional System, developed by the Human Resources Laboratory, uses programmed texts, video terminals, film strips, slides, taped audio presentations, as well as lectures and technical manuals. The system includes the capability to conduct computer-assisted instruction, but this capability is not currently utilized.

Much of the recent research in the Human Resources Laboratory has been directed toward improving training procedures. Several projects have focused on computer-assisted instruction (CAI). Procedures for authoring a CAI course were developed for implementation in the Advanced Instructional System. In an earlier project, CAI lessons were compared with both lecture and self-paced methods of instruction in Air Force medical courses. The CAI lessons were found to be more efficient than the lectures, and slightly more efficient than self-paced instruction. Other research has investigated the use of knowledge-based intelligent CAI systems. These systems are capable of interacting with the student regarding the subject matter. The student can query the computer or receive hints during a problem-solving task, and the computer will develop a model of the student's strategies.

Preparatory Student Training

The development of improved training procedures requires attention to the learning stimulus. This work has been influenced by Behaviorism and its emphasis on the stimulus. Indeed, the programmed texts originated from considerations of behaviorist principles. Cognitive psychology has shifted the emphasis to the student. The cognitive psychologist is interested in the relationship between environmental variables and the strategies and processes available to the student. This section describes some approaches to developing these strategies.

The procedure for assigning students to courses followed at Lowry AFB ensures that all but a few students will be prepared for the course material. Those few who are not prepared may benefit from remedial courses designed to correct their particular deficiency. However, even those students who have the necessary abilities and aptitudes may benefit from instruction and practice with efficient methods for reading and studying. The Human Resources Laboratory is conducting research relevant to these problems.

A project has been completed to develop reading material for reading-improvement courses. A self-paced workbook based on job-related technical material was written to teach the use of imagery, paraphrasing, flowcharting, and methods for improving reading speed. Current research has explored the literacy gap (ie., the difference between the reading level of Airmen and the material they are required to read).

Study skills have been, and are currently, the object of research at the Human Resources Laboratory. In previous research, the effectiveness of several comprehension strategies was tested.^{6,7} The students who were

taught strategies achieved a higher level of performance and reported reduced test anxiety and better attitudes toward study. Current research is directed toward identifying student requirements through analysis of the Advanced Instructional System preassessment test battery, and devising skill training materials suitable for the individual student. This research seems particularly promising in the computer-managed environment of the Advanced Instructional System. The preassessment test battery provides an opportunity to obtain a description of the cognitive skills of a student, and this description can be the basis for a prescription of matching study skills.

Training Adapted to Students

The relation between a student's cognitive skills and the material to be learned continues to be important after the course has begun. The Advanced Instructional System was designed to recognize and respond to this relationship. Courses in the system include alternative modules designed to fit the needs of students with different learning strategies and abilities. The assignment of students to modules can be based on a number of criteria such as student preference, test performance, or the decision of an instructor. So far, little has been done to explore the relationship between a particular choice of criteria and performance in the modules.

Conceptually, matching training procedures to student characteristics seems promising. However, research in the area has not been promising. Perhaps the failures of this research stem from inappropriate choices of characteristics or training procedures. Much of this research has used personality variables such as learning style or psychometrically measured aptitude as the characteristic of interest. These measures are generally theoretically vacuous. A view of individual learning characteristics based on a cognitive model may provide a clearer rationale for selecting learning strategies. In fact, some limited success has been achieved by considering cognitive strategies. For example, instructions to use imagery as a learning aid have been found to be most effective with individuals who have developed imagery skills.

II. OBJECTIVES:

The objectives of this project were:

- (1) To identify an area of cognitive psychology with potential application to technical training.
- (2) To survey the research literature in the identified area, with particular attention to educational and training implications.
- (3) To develop a tutorial review of this area, identifying both potential applications to education and areas requiring additional research.

Due to space limitations, this report condenses a review which is furnished as a separate report.²⁸

III. MENTAL IMAGERY:

The criteria that guided selection of an area for further research were (1) demonstrated applicability to training, and (2) active cognitive research in the area. Mental imagery satisfies both criteria. Research sponsored by the Technical Training Division of the Human Resources Laboratory has demonstrated the effectiveness of imagery as a learning aid.^{6,7} Furthermore, the use of imagery as a learning aid has been recognized and studied by psychologists for many years. Currently, psychologists are investigating the mechanisms underlying imagery and individual differences in imagery ability. Theoretical developments in these areas offer promise for techniques to further enhance the positive effects of imagery on learning.

IV. REVIEW OF MENTAL IMAGERY RESEARCH:

The development of effective imagery strategies for educational settings is analogous to an engineering problem. Engineering solutions are derived by creatively applying scientific principles induced from research. However, the principles which have guided educational research on imagery are those specified by the ancient Greeks. Indeed, much of the recent psychological research has investigated the validity of those ancient principles. However, recent research has moved in several directions that hold promise for development of new principles. These researchers are addressing three questions: (1) how imagery functions, (2) what situations are appropriate for the use of imagery, and (3) who will benefit most from imagery strategies. Each of these directions is elaborated below.

How Imagery Functions

Semantic-Image Theory

Perhaps the broadest definition of mental imagery was suggested by Hunt,¹⁴ who states that an image is "an amalgamation of inputs from external perception and aroused memories." Thus, the image is not restricted to any one sensory modality. Indeed, it can include all modalities, emotional responses, and beliefs. Hunt proposed a semantic-image theory of thought in which pattern recognizers operate on both images and sensory inputs to activate a new set of memories and thereby generate a new image. This theory is relatively rigorous and is demonstrated to account for some qualitative aspects of human cognition. For the present purposes the most interesting aspects of the theory are the broad definition of an image and the central role images play in thought. Within this theory verbal processes, such as rehearsal, produce another form of imagery, ie., verbal imagery. With this broad definition one can quickly see that all conscious thought can be conceptualized as imagery in one or more modalities.

Kosslyn's Model of Visual Imagery

Stephen Kosslyn has systematically studied the functional properties of visual imagery and developed a model of the visual imagery processes.^{16,17,18,19,20,21,27} The model of imagery has been instantiated in a computer simulation. According to this model, images are represented on a two-dimensional surface such as a cathode ray tube (CRT). This CRT has fine resolution in the center, and becomes increasingly coarse as the boundaries are approached. Images are generated on the CRT and manipulated by means of some basic processes. These processes can rotate, scan, shrink, or expand an image or part of an image. Other processes find particular parts of an image and add additional detail.

Kosslyn's model differs from Hunt's theory in several ways. First, Kosslyn is working only with visual imagery. Second, images are generated according to a plan in Kosslyn's model, whereas Hunt suggests that images are the result of memory activations caused by input stimuli. The other differences are less interesting than some of the similarities. In both theories pattern recognition processes operate on images to interpret the generated image. Kosslyn's theory requires additional processes which transform the image by shrinking, expanding, rotating, or scanning it. Hunt's theory includes a class of change operations that can manipulate images, but does not specify the nature of these operations.

Kosslyn has pursued an active program of research to test and expand his theory and model. The CRT model was motivated by findings that more time is required to answer detailed questions about small images than big images.¹⁶ In addition, subjectively larger images take longer to generate than small images.¹⁶ Differential resolution on the CRT was motivated by findings that enlarging an image causes it to become too big to be seen, and the point at which the image becomes too big depends on the subject's criterion.¹⁸ The role of pattern recognition processes operating on images was confirmed by the finding that the time required to verify that an animal has a certain body part increases as the size of the part decreases. Furthermore, this finding holds only if subjects use an imagery strategy. When subjects were not instructed to use an imagery strategy the size of the body part did not influence response time, but the strength of the association between the animal and body part did influence response time.¹⁷

Paivio's Dual-Coding Theory

Allan Paivio deserves much of the credit for the current interest in imagery. He is primarily interested in the facilitative effects of imagery on memory, and has just briefly addressed how images are generated or manipulated. Paivio has extensively investigated the kinds of situations in which imagery is effective.²⁵ This issue will be addressed in the next section.

According to Paivio's dual-coding theory a stimulus may be encoded both verbally and as an image, yielding two independent memory codes. The existence of two codes increases the probability that the stimulus will be remembered. The quality of a code influences the probability that particular code will be remembered.

Paivio's theory has motivated a great deal of research attempting to test the dual-coding explanation of the facilitative effects of imagery. For example, Wittrock and Lumsdaine³⁷ cite several studies supporting the dual-coding theory. However, the theory remains controversial, and other explanations are frequently offered.

Effective Use of Imagery

The theoretical positions reviewed above suggest several factors that may influence the effectiveness of imagery as a learning aid. Some of these factors have been explored experimentally; others have not.

Interactive images. First, when imagery is used to associate two or more objects, the objects should be imaged as interacting with one another.

Indeed, Bower⁴ found that interactive images are much more effective than noninteractive images in a paired-associate learning task. Considerable research remains to be done in this area. It is not clear how one part of an image reintegrates the remainder or what kinds of interactions are helpful. For example, will an image of a man looking at a ball be as effective as an image of a man hitting a ball? Should the interactions be visible or dynamic? These issues have both practical and theoretical significance.

Multi-modal images. Hunt's theory asserts that images can be composed of many sensory modalities, emotions, and beliefs. Perhaps more memorable images can be created by including other modalities in the image. Indeed, in Hunt's theory dual-coding arises from generating both verbal and visual aspects of the image. To my knowledge, the effect on memory of adding modalities to an image has not been explored. However, some research has explored imagery in other modalities. Cartwright, Marks, and Durrent⁵ distinguished between three types of imagery, one of which included attitudes or feelings associated with the stimulus. Furthermore, Aylwin¹ instructed subjects to use kinesthetic imagery and obtained systematic results suggesting that subjects could readily follow these instructions.

Bizarre images. The ancient Greeks stated that bizarre images are more memorable,³⁸ and this advice has been followed by professional mnemonists. Research on the effectiveness of bizarre images has produced equivocal results. Much of this research is reviewed by Weber and Marshall³⁵ who concluded that most studies do not find an effect of bizarreness. Weber and Marshall investigated bizarreness by presenting bizarre or common pictures and testing memory in immediate and delayed tests. Bizarre pictures facilitated memory slightly in the delayed test but not in the immediate test. Thus, if bizarreness has an effect, it is small and is manifested over a delay. It is probably not helpful to instruct students to create bizarre images. However, the effect of bizarreness on memory may be different for created images than for memory images such as those studied by Weber and Marshall.

Dynamic images. Images can be constructed that involve movement that occurs in time. In a dynamic image an interaction between elements can be greatly elaborated and may increase the memorability and reintegrative powers of the image.

Most researchers have treated images as static, like a snapshot. Indeed, I know of no research investigating the effects of this dimension. However, the research by Aylwin¹ suggests that dynamic images can be readily constructed.

Situations Appropriate for Imagery Strategies

Despite the effectiveness of imagery as a learning aid, it is rarely recommended or taught in educational or training environments. Perhaps imagery is not recommended because it is not considered an effective strategy for the material to be learned. This section addresses the problems associated with applying imagery to a variety of learning tasks. First, those situations are considered for which imagery is well-suited. Then mnemonic devices which extend the usefulness of imagery are examined. Finally, the obstacles to development of new mnemonic devices are considered.

Imageful Ideas

One of Palvio's major contributions was to establish that memory performance for a word is largely determined by how easily the word's referent can be imaged²⁵. Concrete words are more easily represented in an image than are abstract words, and concrete words are remembered better than abstract words. Furthermore, abstract words which readily elicit an image (eg., religion) are more memorable than words which are difficult to image (eg., quality). Pictures are remembered even better than concrete words, presumably because pictures are the best possible stimulus for generating a visual image. These findings have been extended to show that more complex stimuli such as word triads,²⁶ sentences,⁸ and connected discourse³⁹ are more memorable if the ideas represented are more concrete. Thus imagery is an effective learning strategy when the material to be learned involves concrete objects, and if the relationships between objects are concrete. It would probably not be effective in a philosophy course dealing with abstract issues. However, it could be very helpful in engineering, physical sciences, or technical courses which teach relationships among concrete objects. Even the abstract ideas in a physics course can often be translated into concrete examples. These examples do not trivialize the material; they make it more memorable.

Concrete ideas often are expressed in the form Actor-Action-Object, and this form is rarely appropriate for abstract ideas. Thus, imagery is an appropriate strategy for learning material expressed in this form. However, this form cannot express all concrete ideas. For example, the

spatial relationships among objects are concrete and are readily learned through imagery. Thus, imagery is an effective strategy for learning a map. Furthermore, the transformational properties of images permit cognitive manipulations that are very helpful in using a map.

Much of the psychological research has examined the effectiveness of imagery in paired-associate learning.²⁵ This research has confirmed the importance of concreteness in this task also. Interestingly, the concreteness of the stimulus term is much more important than the concreteness of the response. Apparently, presentation of the stimulus term during a test elicits retrieval of an image when the stimulus is concrete. When an image is retrieved, the response term can be obtained by examination of the image.

Mnemonic Devices

Some of the limitations of imagery have been overcome by the development of mnemonic devices. These methods take advantage of the effectiveness of imagery for associating concrete stimuli. The mnemonic devices combine imagery with a memory structure to facilitate learning relationships which are not readily imaged. For example, suppose an ordered list of words is to be remembered. One could attempt to image the objects represented by the words standing in a line. However, this is not an interactive image and may not be readily learned. Alternatively, one could generate an image associating the first and second words, then another image to associate the second and third words, and so on. In fact this strategy is effective, but not as effective as the pegword system or the method of loci. These two methods are similar, so only the method of loci is considered here.

Before using the method of loci, a mnemonist must learn a sequence of locations that, preferably, are near one another and are easily imagined. For example, the rooms in one's home would be appropriate. As each word is presented, the mnemonist simply imagines the second object in a room, then advances to the next room. The words can be recalled in order by simply imagining a walk from room to room, recalling the objects from the image of the room.

This mnemonic technique deserves more careful examination to discover how it works. Imagery is used to associate two or more items; in this case, the rooms and objects. The mnemonic device provides a structure that is well known and is analogous to the structure to be learned. In this instance, the mnemonist wants to learn an ordered list of words, so a linear

ordering of rooms is connected to the words in the corresponding order.

Development of New Mnemonics

An imagery mnemonic is a means for learning an organization among elements that cannot be easily imaged. The mnemonic requires a known structure that is analogous to the organization to be learned. When this structure is established, imagery can be readily used to link the elements of the two structures.

In many cases a mnemonic is unnecessary. When the organization involves concrete relationships among elements, the entire organization can be learned via imagery. Thus, mnemonic devices are most appropriate for abstract relationships such as linear orderings or corporate organizations. Even in these situations the development of a mnemonic is valuable only if similar structures are frequently learned. Otherwise, the time and effort required to create an artificial structure may not be repaid.

When a mnemonic device is created it is important to construct a memorable structure of distinct, imageable elements. Other suggestions were offered by the Greek mnemonists. They recommended creating elements that are neither very big nor very small, well lit so the objects can be seen, and in a place where there is not much traffic.³⁸ The reason for the last suggestion is unknown.

Who Benefits from Imagery Strategies?

What aspects of imagery ability influence the effectiveness of an imagery learning strategy? This section briefly reviews current literature relevant to this question. Thoughtful and extensive reviews of this area have recently been prepared by White, Sheehan, and Ashton³⁶ and by Ernest.⁹

Self-Report Measures

Questionnaires remain the most frequently used method of assessing individual differences in imagery ability. These questionnaires have been designed to assess imagery vividness, imagery control, or preference to use visual versus verbal strategies. Numerous studies have verified the validity and reliability of these tests.³⁶ However, psychometric studies have questioned whether tests of vividness and tests of control really measure different processes. The correlations of these tests with learning measures presented below suggest that vividness and control really are distinct.⁹

Vividness measures. Betts³ introduced the Questionnaire upon Mental Imagery which included 15 questions. This test was later shortened to 35 questions by Sheehan,³¹

and is known in this shortened form as the QMI. The QMI remains the most widely used measure of imagery vividness. It measures vividness in seven sensory modalities, and factor analyses suggest these measures are partly independent.³¹ Recently, Marks²³ devised a 16 item questionnaire of visual vividness called the Vividness of Visual Imagery Questionnaire (VVIQ). The VVIQ has received wide usage only for the last few years.

Self ratings on these tests of vividness have been compared with performance in paired-associate learning, recognition memory, free recall, the speed to generate an image, speed to mentally rotate a figure, and speed to discriminate between two slightly different pictures. For the most part, vividness is unrelated to performance in these tasks. Vividness is apparently related to memory performance for verbal stimuli only when the memory test is unexpected.^{15,32} Perhaps individuals with vivid imagery are more likely to encode the stimuli in images when no test is expected.

Marks²³ found a relationship between vividness measured with the VVIQ and recall of pictures, but no relationship was found with the QMI.³³ Gur and Hilgard¹³ found that vividness measured with the VVIQ correlated with the speed to discriminate between pictures, but Berger and Gaunitz² disconfirmed this finding and attributed the original result to demand characteristics. Finally, Snyder³⁴ found no relation between speed of mental rotation and vividness.

In contrast to these negative findings, Ernest and Paivio¹⁰ found that people with vivid imagery are quicker to generate an image, particularly for abstract words. However, the research relevant to learning consistently finds little or no relationship to vividness.

Imagery control. The test used in virtually all studies of imagery control is the Gordon Test of Visual Imagery Control (TVIC).¹² This test was modified slightly by Richardson²⁹ to include 12 questions. The brevity of this test and the low variability in ratings prompted Lane²² to develop a new questionnaire which has not been widely used thus far.

Imagery control, as measured by the TVIC, and vividness have been compared with many of the same measures. However, much stronger relationships were found with imagery control. Control was correlated with paired-associate learning,²⁴ speed of mental rotation, speed of spatial problem solving, and performance on other spatial tasks.³⁴ The TVIC has not been widely used in studies of learning or memory, but the existing research appears promising.

Visual preference. Paivio²⁵ developed a test to discriminate between visualizers and verbalizers called the Individual Differences Questionnaire (IDQ). Recently, Richardson³⁰ has modified the IDQ to produce a shorter test containing 15 questions called the Verbalizer-Visualizer Questionnaire. The tests have not been widely used, and most studies with these tests have examined their psychometric properties.

Objective Measures

The use of questionnaires and self ratings is troubling to many experimental psychologists who have searched for an objective means for assessing imagery ability. Tests of spatial ability have frequently been adopted as an objective assessment. Tests that are frequently used include Flags, the Minnesota Paper Form Board, Space Relations, and the Primary Mental Abilities Space Test. Interestingly, these objective tests appear related to Gordon's test of imagery control.⁹ Spatial test scores were correlated with performance in each task that correlated with imagery control. In addition, spatial test scores are correlated with learning performance under many conditions.⁹ However, performance is unrelated to spatial test scores when stimuli are verbal and subjects use a verbal strategy.

Models and Theories

The study of individual differences in imagery ability has a long history, but not a particularly glorious one. Despite the volume of research, few interesting relationships have been observed. Researchers remain strongly interested in imagery vividness despite consistent failures to find significant correlations with vividness. Indeed, why should vividness be related to any cognitive processes involving imagery? To assume such a relationship exists is to assume a certain class of theories, and these theories consistently have been refuted. Marks²³ found that people who report little or no imagery can effectively use imagery mnemonic strategies. Thus, imagery vividness is not an important part of the function of imagery. This aspect of imagery may represent an epiphenomenon.

The theories and models presented in a previous section are the natural source for hypotheses regarding individual differences in imagery ability. In particular, Kosslyn's theory provides the level of description required to generate hypotheses. His theory emphasizes the role of image generation, scanning, rotation, shrinking, and enlarging. Furthermore, Kosslyn

distinguishes between transformations of an entire image and part of an image. These processes are reasonable candidates for the source of important individual differences. Indeed, the relationships found with imagery control and spatial ability are a partial confirmation of these hypotheses. Obviously, both imagery control and spatial ability depend on the ability to generate and manipulate parts or all of an image.

V. RECOMMENDATIONS:

Implications for Education

Imagery could serve as a very effective learning strategy, but it must be taught. Many people have little or no experience of imagery and, therefore, doubt that imagery will be effective. In fact, imagery mnemonic devices work for people who report no experience of imagery. Vividness is not related to memory performance.

Ability to control and manipulate mental images is related to learning. Thus, a program to teach imagery should emphasize exercises requiring mental transformations. Of course, it is unknown at present whether these skills are trainable, and a reasonable first step would be to examine this issue.

An exclusive emphasis on visual imagery is clearly unwarranted. Students should be encouraged to experience an image in several modalities. Even the usual verbal processes such as rote rehearsal may be considered a form of imagery.

It is particularly important that students learn to construct dynamic, interactive images. The interactions in the image will permit one portion of the image to reintegrate the entire image. The dynamic quality may assist in involving kinesthesia in the imagery and thereby add to its memorability.

Imagery is not effective for abstract material. Thus, students must learn when it is appropriate and when it is not. In many cases the abstract material can be expressed in concrete examples that are memorable and can be used to infer the abstract idea. When translation to a concrete idea is difficult the student must rely on the verbal strategies we all know and love.

Implications for Research

Several of the educational implications suggested above call for research. In particular, the effect on memory of generating multi-modal images or dynamic images requires investigation. In addition, the stability of individual differences deserves investigation. Can people be trained to improve their imagery? Dansereau's work clearly indicates that people can learn to use imagery more effectively, but whether imagery can be improved is unknown.

The current theories of imagery have important implications for research on individual differences. These theories suggest that individual differences in the effectiveness of imagery could be due to facility in generating or transforming images. Kosslyn's theory suggests specific transformations which deserve investigation. Alternatively, the important individual differences may exist at a meta-level that involves selecting an appropriate transformation.

REFERENCES

1. S. Aylwin, "The Structure of Visual and Kinaesthetic Imagery: A Free Association Study," British Journal of Psychology, 1977, 68, 353-360.
2. G. H. Berger & S. C. B. Gaunitz, "Self-Rated Imagery and Vividness of Task Pictures in Relation to Visual Imagery," British Journal of Psychology, 1977, 68, 283-288.
3. G. H. Betts, The Distribution and Functions of Mental Imagery. New York: Teachers College, Columbia University, 1909.
4. G. H. Bower, "Mental Imagery and Associative Learning," In L. W. Gregg (Ed.), Cognition in Learning and Memory. New York, Wiley, 1972.
5. D. S. Cartwright, M. E. Marks, & J. H. Durrett, Jr., "Definition and Measurement of Three Processes of Imagery Representation: Exploratory Studies of Verbally Stimulated Imagery," Program on Cognitive Factors in Human Learning and Memory Report No. 72, University of Colorado, 1977.
6. D. F. Dansereau, D. W. Collins, B. A. McDonald, G. Diekhoff, J. Garland, C. S. Holley, S. H. Evans, D. Irons, G. Long, C. Walker, T. Hilton, D. Lehman, M. Halemanu, A. M. Ellis & R. M. Fenker, "Systematic Training Program for Enhancing Learning Strategies and Skills: Further Development," AFHRL-TR-78-63. Lowry AFB, CO: Technical Training Division, Air Force Human Resources Laboratory, September, 1978.
7. D. F. Dansereau, G. L. Long, B. A. McDonald, T. R. Actkinson, A. M. Ellis, K. Collins, S. Williams & S. H. Evans, "Effective Learning Strategy Training Program: Development and Assessment," AFHRL-TR-75-41. Lowry AFB, CO: Technical Training Division, Air Force Human Resources Laboratory, June, 1975.
8. G. Davies & J. Proctor, "The Recall of Concrete and Abstract Sentences as a Function of Interpolated Task," British Journal of Psychology, 1976, 67, 63-72.
9. C. H. Ernest, "Mental Imagery and Cognition: A Critical Review," Journal of Mental Imagery, 1977, 1, 181-216.
10. C. H. Ernest & A. Paivio, "Imagery Ability in Paired-Associate and Incidental Learning," Psychonomic Science, 1969, 15, 181-182.
11. F. Galton, "Statistics of Mental Imagery," Mind, 1880, 5, 301-318.
12. R. Gordon, "An Investigation into Some of the Factors that Favour the Formation of Stereotyped Images," British Journal of Psychology, 1949, 39, 156-167.
13. R. C. Gur & E. R. Hilgard, "Visual Imagery and the Discrimination of Differences Between Altered Pictures Simultaneously and Successively Presented," British Journal of Psychology, 1975, 66, 341-345.

14. E. B. Hunt, "Imageful Thought," In J. W. Cotton & R. L. Klatsky (Eds.), Semantic Factors in Cognition. Hillsdale, NJ: Erlbaum, 1978.
15. W. H. Janssen, "Selective Interference in Paired-Associate and Free Recall Learning: Messing up the Image," Acta Psychologica, 1976, 40, 35-48.
16. S. M. Kosslyn, "Information Representation in Visual Images," Cognitive Psychology, 1975, 7, 341-370.
17. S. M. Kosslyn, "Can Imagery be Distinguished from other Forms of Internal Representation: Evidence from Studies of Information Retrieval Time," Memory & Cognition, 1976, 4, 291-297.
18. S. M. Kosslyn, "Measuring the Visual Angle of the Mind's Eye," Cognitive Psychology, 1978, 10, 356-389.
19. S. M. Kosslyn, "On the Demystification of Mental Imagery," In press.
20. S. M. Kosslyn, T. M. Ball, & B. J. Reiser, "Visual Images Preserve Metric Spatial Enformation: Evidence from Studies of Image Scanning," Journal of Experimental Psychology: Human Perception and Performance, 1978, 4, 47-60.
21. S. M. Kosslyn & J. R. Pomerantz, "Imagery, Propositions, and the form of Internal Representations," Cognitive Psychology, 1977, 9, 524-76.
22. J. B. Lane, "Problems in Assessment of Vividness and Control of Imagery," Perceptual and Motor Skills, 1977, 45, 363-368.
23. D. F. Marks, "Visual Imagery Differences in the Recall of Pictures," British Journal of Psychology, 1973, 64, 17-24.
24. G. Morelli & D. Lang, "Rated Imagery and Pictures in Paired-Associate Learning," Perceptual and Motor Skills, 1971, 33, 1247-1250.
25. A. Paivio, Imagery and Verbal Process, New York: Holt, Rinehart, & Winston, 1971.
26. A. Paivio & I. Begg, "Imagery and Associative Overlap in Short-Term Memory," Journal of Experimental Psychology, 1971, 89, 40-45.
27. S. Pinker & S. M. Kosslyn, "The Representation and Manipulation of Three-Dimensional Space in Mental Images," Journal of Mental Imagery, 1978, 2, 69-84.
28. S. E. Poltrock, "Educational Implications of Cognitive Imagery Research: A Tutorial Review," Technical Report to Human Resources Laboratory, Technical Training Division, Lowry AFB, Denver, CO.
29. A. Richardson, Mental Imagery, London: Routledge & Kegan Paul, 1969.
30. A. Richardson, "Verbalizer-Visualizer: A Cognitive Style Dimension," Journal of Mental Imagery, 1977, 1, 109-126.

31. P. W. Sheehan, "A Shortened Form of Betts' Questionnaire upon Mental Imagery," Journal of Clinical Psychology, 1967, 23, 386-389.
32. P. W. Sheehan, "Stimulus Imagery Effect and the Role of Imagery in Incidental Learning," Australian Journal of Psychology, 1973, 25, 93-102.
33. P. W. Sheehan & U. Neisser, "Some Variables Affecting the Vividness of Imagery in Recall," British Journal of Psychology, 1969, 60, 71-80.
34. C. R. Snyder, Individual Differences in Imagery and Thought, Unpublished doctoral dissertation, University of Oregon, 1972.
35. S. M. Weber & P. H. Marshall, "Bizarreness Effects in Imagery as a Function of Processing Level and Delay," Journal of Mental Imagery, 1978, 2, 291-300.
36. K. White, P. W. Sheehan & R. Ashton, "Imagery Assessment: A Survey of Self-Report Measures," Journal of Mental Imagery, 1977, 1, 145-170.
37. M. C. Wittrock & A. A. Lumsdaine, "Instructional Psychology," Annual Review of Psychology, 1977, 28, 417-459.
38. F. A. Yates, The Art of Memory, London: Routledge and Kegan Paul, 1966.
39. J. C. Yailie & A. Paivio, "Abstractness and Recall of Connected Discourse," Journal of Experimental Psychology, 1969, 82, 467-471.

1979 USAF - SCEEE SUMMER FACULTY RESEARCH PROGRAM

Sponsored by the

AIR FORCE OFFICE OF SCIENTIFIC RESEARCH

Conducted by the

SOUTHEASTERN CENTER FOR ELECTRICAL ENGINEERING EDUCATION

FINAL REPORT

ADAPTIVE SIGNAL PROCESSING FOR ARRAY ANTENNAS

Prepared by:	Douglas Preis, Ph.D.
Academic Rank:	Assistant Professor
Department and University:	Department of Electrical Engineering Tufts University
Research Location:	Electronic Systems Division (ESD), Development Plans (XR), Hanscom Field, Massachusetts
USAF Research Colleague:	Donald Brick, Ph.D., Technical Director Deputy for Development Plans
Date:	17 August 1979
Contract No:	F49620-79-C-0038

ADAPTIVE SIGNAL PROCESSING FOR ARRAY ANTENNAS

by

D. Preis

ABSTRACT

This report presents an overview of signal processing for array antennas. Included is a convenient chronological literature survey. These references are discussed by category. The following topics are considered: introductory review and survey articles, adaptive filtering, array antennas, benchmark papers and fundamental contributions in the field, algorithms, optimal and suboptimal processing, partially adaptive arrays, experimental studies and sensitivity considerations. The generalized adaptive array is discussed as a multivariable system and basic processing architectures are summarized. Key features, research trends, and deficiencies are discussed. Also included are recommendations for future research and development.

ACKNOWLEDGMENTS

The author acknowledges the sponsorship of the Air Force Systems Command and the Air Force Office of Scientific Research. Administrative direction and assistance from Dr. Dick Miller of the Southeast Center for Electrical Engineering Education as well as use of facilities at the Electronic Systems Division/Hanscom are acknowledged also. Especial thanks are extended to Dr. Don Brick for his good advice.

I. INTRODUCTION

An adaptive receiving array is a system capable of a certain combination of spatial, spectral, statistical and temporal discrimination of incoming signals which depends on the total signal environment. This selectivity is attained first by processing individual received signals from members of the array and then combining them to form an output signal which meets some prescribed performance criteria. Conceptually, an adaptive array is either a generalized antenna or a generalized filter which has signal-dependent parameters. When fully adapted or adjusted the complete receiving system is linear, however, during adaptation the system generally is nonlinear. Combined and adjustable diversity in space, time, and frequency coupled with parallel processing of received signals are, in theory, distinct advantages of the adaptive array. In practice, a decision in favor of an adaptive array subsequently confronts the system designer with a large number of difficult and interactive choices, each of which requires considerable expertise in disciplines as diverse as: electromagnetics and antenna array theory, modern spectral analysis, optimal filtering and control, adaptive signal processing, statistical communication theory, as well as many practical aspects of the capabilities, limitations and costs of both hardware and software.

II. OBJECTIVES

The first research objective was to review the open technical literature indicating significant developments in adaptive array signal processing during the past twenty years. A secondary goal was to provide a chronological list of technical publications (papers, books, technical reports and conference proceedings) on the subject and briefly discuss its contents by category. Assessment of the present state of the art, including identification of trends and deficiencies within the discipline, was the third research objective. The fourth research goal was to consider both advantages and disadvantages of adaptive signal processing when used in conjunction with array antennas.

The final objective was to provide recommendations for future research and development in the general field of adaptive array signal processing.

III. LITERATURE SURVEY

Several authors have written perceptively on the subject of adaptive antennas. There are quite a few worthwhile introductory and survey works available. CHAPMAN's article in the Microwave Journal [63] gives a good but not overly technical introduction to the many facets of this technology. In March 1964 and September 1976, special issues of the IEEE Transactions on Antennas and Propagation were devoted to adaptive antennas, the former edited by HANSEN [2] and the latter by GABRIEL [51]. GABRIEL [47] also has presented a comprehensive tutorial introduction to the subject. The books edited by GRIFFITHS [26] and TACCONI [39], containing the 1973 and 1976 NATO Conference papers, provide an excellent overview of array signal processing. Current reports by WIDROW et al. [59,74] include brief summaries of their pioneering works as well as new results and ideas from contemporary research. VURAL [61] has provided a comparative study of adaptive array processors. Very recently, WIDROW [80] has presented a concise review which intercompares popular adaptive array algorithms.

Trends in conventional (i.e. non-adaptive) array antenna research have been summarized and reviewed by MAILLOUX [62]. Mathematical procedures for array antenna "null steering" and "gain maximization" are given, for example, in DAVIES [7], chapter 10 of HARRINGTON [12], and DRANE and McILVENNA [15,17] where further references are available. HILDEBRAND's book [38] contains the necessary matrix theory background for this general approach. Recently, KRAFT et al. [83] have applied methods of digital filter design to the minimax optimization of arrays.

Fundamental to the study of adaptive antennas is the subject of adaptive filtering. Three works by WIDROW et al. [6,19,60], published at 5 year intervals, provide tutorial information and summaries of significant advances in adaptive filtering. Important issues on convergence properties of adaptive filters have been investigated by UNGERBOECK [18] and, recently, by MAZO [78]. Adaptive noise subtracting and noise cancelling studies are available in KAUNITZ and WIDROW [25] and in the comprehensive review by WIDROW et al. [37]. Statistical aspects of adaptive filtering are considered by WIDROW et al. [50]. Time-domain and frequency-domain studies are reported by GAURINO [77] and DENTINO et al. [73], respectively.

About twenty years ago the technology of adaptive signal processing for array antennas began with studies of techniques for antenna sidelobe cancellation. In US Patent 3,202,990 filed in 1959, HOWELLS proposed a novel scheme to cancel an array sidelobe which was receiving an interfering signal. This was accomplished by subtracting the output of a small secondary beam, positioned near the undesired sidelobe, from the array output. Superposition of array beams was used to modify the existing sidelobe structure of an array antenna. Some extension of this fundamental idea is embodied in most contemporary work on adaptive arrays.

In 1962 BYRN considered the problem of optimum signal processing for a sonar array designed to detect low intensity plane wave signals contaminated with noise and found that it was necessary to apply frequency-dependent complex weighting networks to the outputs of the array elements. Properties of these networks were determined by evaluating certain correlation matrices. The concept of separately filtering the output of each array element for optimal utilization of the array was proposed by MERMOZ [3]. The fundamental notion was that the signal-to-noise ratio of the array could be improved if the noise received by one element was correlated with that received by another. In 1964, SHOR [4] extended this idea by proposing and demonstrating the efficacy of an adaptive technique to adjust the filters, known as the method of steepest descent, in order to discriminate against coherent noise in a receiving array. In a significant report, APPLEBAUM [5] presented a systematic method for adaptively optimizing the signal-to-noise ratio of an array antenna and showed how this optimization was related to the earlier concept of sidelobe cancellation. WIDROW et al. [8,10] applied their own early work on adaptive filtering to the array problem by proposing an adaptive processor, connected to the array elements, for combined filtering in the spatial and frequency domains. The variable weights of the adaptive signal processor were adjusted using a least-mean-squares algorithm and an external pilot signal was required to "train" the processor. LACOSS [11] has intercompared adaptive processors in connection with seismic array processing. WIDROW et al. [16] have considered both analysis and synthesis of adaptive array processors comprised of tapped delay lines. A significant advance

was made in 1972 by FROST [20] who suggested that the adaptive array processor also satisfy certain linear constraints. With such constraints, fixed frequency response and directivity can be maintained for desired incoming signals while total noise power is minimized. OWSLEY [31] and APPLEBAUM and CHAPMAN [57] have presented further developments in constrained adaptation. BRENNAN and REED [21] have applied adaptive processing to radar systems to maximize the probability of detection. ZAHM [23] investigated the possibility of using an adaptive array to acquire a weak, desired signal in the presence of strong interference and found that the original signal-to-noise ratio could be inverted with adaptive processing. This notion of signal-to-noise inversion was an unforeseen but very useful processing advantage. REED et al. [35] have considered important questions on convergence rates for array adaptation and generally prefer direct matrix inversion to iterative techniques. Matrix processing is recommended by MERMOZ [43] also. GRIFFITHS [45] suggested implementing constraints using a conventional array in conjunction with an adaptive array. APPLEBAUM and KAPLAN [49] have considered array sidelobe suppression using sum and difference beams. GRIFFITHS [53] studied time-domain adaptive beamforming and reported a 10-15 dB signal-to-noise improvement with adaptive processing. WHITE [58] recommended the use of adaptive preprocessing networks to improve convergence rates of conventional adaptive processors. MAYHAN [66] has discussed a variety of techniques to improve the dynamic performance of adaptive multibeam antennas. PELLETIER et al. [88] proposed adaptive processing using a nonlinear control loop. Applications of adaptive arrays to spread spectrum and broadband communications have been discussed by COMPTON [68] and AUTREY [29]. WHITE [69,70] has proposed improved adaptive processing using artificial white noise and suggested the use of cascaded networks for deep nulling.

In more recent research, MAYHAN [76,85] evaluated effective bandwidth of adaptive nulling systems, MOLES and ANDREWS [81] have devised a novel array optimization technique which selectively excludes array elements. HODGKISS considered tradeoffs between time and frequency domain array processing. BURROWS [89] investigated element placement tradeoffs for adaptive arrays. GABRIEL [87] applied maximum entropy spectral analysis to the general study of adaptive array processing.

Algorithms for adaptive array processing have been investigated by GRIFFITHS [9,14], FROST [20], GITLIN et al. [22], WIDROW et al. [36], LUNDE [41], WIDROW and McCOOL [58] and AL KHATIB and COMPTON [67].

Results from experimental studies are available. RIEGLER and COMPTON [24] studied a two-element adaptive array. COMPTON [54] reported results on a four-element adaptive array. Recently, HOROWITZ et al. [79] implemented the sample matrix inversion algorithm for adaptive processing.

Questions of optimal versus sub-optimal processing and partial adaptivity have been considered by GIRAUDON [28,40], BANGS and SCHULTHEISS [30], BIENVENU and VERNET [32], CHAPMAN [55], MORGAN [72] and MENDELOVITZ and OESTREICH [86].

Several workers have addressed important issues on sensitivity and limitations of adaptive arrays. GILCHRIST [27] investigated practical limitations of time-processing for sonar arrays. COX [33] has provided a general mathematical sensitivity analysis for adaptive beamforming. HUDSON [42] has studied the effects of weight quantization in adaptive array processors. McCOOL [44] reported results on a constrained adaptive beamformer which was tolerant of gain and phase errors. NITZBERG [48] investigated the effects of errors on adaptive weights. TAHERI and STEINBERG [52] studied tolerances in adaptive arrays. BLUESTEIN [65] and RAU [64] have considered some practical aspects of adaptive arrays. QUAZI and NUTALL [84] investigated effects of errors and element failures on beampatterns.

IV. SIGNAL PROCESSING ARCHITECTURES FOR ADAPTIVE ARRAY ANTENNAS

Figure 1 is a block diagram of a generalized adaptive array which is represented as a multivariable system. Input signals to this system are either outputs from individual array sensing elements or outputs from a number of fixed antenna beams (performed from the sensing elements). These input signals are filtered separated but simultaneously (i.e. parallel processed) before being weighted and combined to form the processed output signal(s). At any instant in time, the processed output is a linear combination of these specially filtered input signals. The filters themselves are either tapped delay lines or spectrum

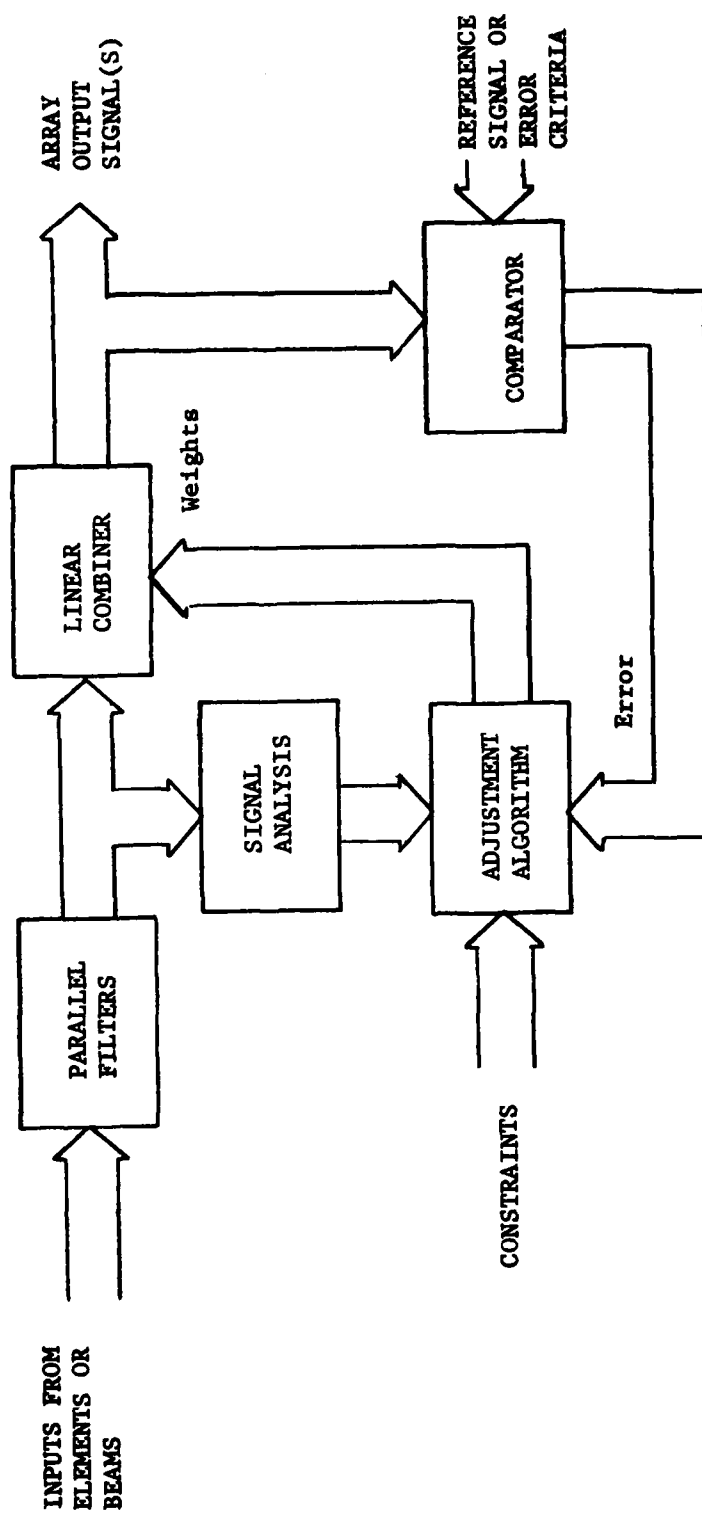


Figure 1. Generalized adaptive array as a multivariable filter

analyzers. In the former case, a section in time of each input signal (equal to delay line length) is continuously available. In the latter case, spectral estimates (in contiguous bands) of each input are continuously available. In this way, input signals appear in a form suitable for signal analysis (e.g. correlation, cross-power estimates). The outputs from each of these filters are also fed to a linear combiner where each output is weighted, as prescribed by the adjustment algorithm, then added (combined) to form the adaptive array output signal(s). The specific weighting used depends on an analysis of each filter's outputs, the error signal produced by comparing the processed output to a reference signal or performance criteria, imposed constraints, and the chosen adjustment algorithm.

It is convenient to define two spaces and two processing domains. Since inputs are signals from either spatially deployed elements or signals from a number of preformed beams fixed in space, the corresponding space external to the processor is termed element-space or beam-space. Filtering is considered to be performed either in the time domain (tapped delay line) or frequency domain (spectrum analyzers). With this terminology there are four separate combinations or choices of space and processing domain for an adaptive antenna system. Older system classifications were simply either narrow-band or broad-band.

In Figure 1, the signal analysis and adjustment algorithm blocks constitute the central and most complicated parts of the system. In practice, it is in these two areas that most diversity occurs. A major issue is the choice between gradient methods for optimization (which require frequent updating and can converge slowly but are implemented easily) and matrix inversion techniques (which require very accurate signal analysis of inputs and are more complicated to implement).

Common processing constraints are maintenance of a specified mainbeam and frequency response. The usual processing criteria are minimization of noise power or minimization of square-error between the output signal and a known reference signal.

V. CURRENT TRENDS

Adaptive signal processing for array antennas was proposed and developed originally as a means to prevent performance degradation in communication systems by suppressing directional interference and minimizing ambient noise. Emphasis has been placed on eliminating all signals that were uncorrelated with the desired signal. To this end, processing has become increasingly sophisticated and control very elaborate. Owing to the diminishing returns in system performance associated with extremely complex processing and the high costs of such processing, two current trends are: partial adaptivity and sub-optimal processing. A related concept is use of a small, auxiliary adaptive array in combination with a conventional array. Another trend is the search for methods to increase adaptation speeds for the entire system so that the overall transient response is faster. Preprocessing element or beam signals prior to adaptation is popular also. This is a form of data conditioning that can improve the performance of the control algorithm. Multiple constraints are currently a high priority. Some flexibility (or adaptability) is exchanged for better beamforming and frequency response, for example. The implication of such constraints is that, while good signal-to-noise ratio is important, it should not be obtained at the expense of signal distortion. There is considerable interest in applying modern spectral analysis, specifically, estimation theory, to the signal analysis portion of an adaptive array processor. A number of workers are concerned with the sensitivity of an adaptive array to element failures, tolerances and processing errors.

VI. DEFICIENCIES

The theory of adaptive signal processing for array antennas is extensive. There is not, however, a commensurate amount of experimental work on its practical implementation available in the open literature. In this connection, it is difficult to assess the current state of the art for practical systems. Generally, there has been a disproportionate interest in eliminating signal uncorrelated interference (e.g. directional noise) and little attention given to reduction of signal-correlated interference (e.g. multipath, scattering, reflections, clutter) which

also can corrupt desired signals. In analyses, array sensing elements (or beams) are assumed ideal, identical and accurate. Calculated processing advantages are based on this assumption which itself is subject to question. Signal-processing analysts prefer to form an antenna array using ideal isotropic elements which yield accurate samples of the spatial field for subsequent elaborate filtering and processing. They generally do not avail themselves of current antenna technology. On the other hand, antenna analysts design sophisticated arrays comprised of state-of-the-art elements but use only the most rudimentary signal processing in the form of phase shifters and weights. More interaction between these two communities is required for optimum system design.

No attention has been given to modeling the actual in situ performance of adaptive array systems where there may be nearby metallic objects or scatterers as well as an interface between two media, for example, an air-sea or air-earth interface. The proximity of such materials may degrade the performance of an adaptive antenna system significantly.

VII. RECOMMENDATIONS

A major advantage of signal processing for array antennas is the capability of parallel processing array element or beam signals. This advantage should be exploited not only for directional noise reduction but also for equalization of desired incoming signals which may be corrupted by multipath and proximity effects of metallic scatters or material interfaces. Matrix inversion optimization techniques are becoming the method of choice for small-scale adaptive processing because they are fast and do not require frequent updating. It seems reasonable to develop standardized hardware for matrix processing. More research is needed on efficient acquisition of accurate statistical estimates of incoming signals. A coordinated effort between specialists in signal processing and specialists in antenna array theory would be mutually advantageous and should be encouraged. There is a need for more experimental work. From their inception, future array antenna systems should be designed with some provisions for adaptive processing. Current research trends in the direction of simplified processing,

including partial adaptivity and sub-optimal processing, should be supported. More research is needed in modeling and measuring in situ performance proposed adaptive systems. Research in sensitivity to element failures, tolerances, and errors should continue.

REFERENCES

- [1] F. Bryn, "Optimum signal processing of three-dimensional arrays operating on Gaussian signals and noise," J. Acoust. Soc. of Amer., Vol. 34, No. 3, pp. 289-297, March 1962.
- [2] R. C. Hansen (ed.), "Special Issue on Active and Adaptive Antennas," IEEE Trans. Antennas and Propagation, Vol. AP-12, March 1964.
- [3] H. Mermoz, "Filtrage adapté et utilisation optimale d'une antenne," Proc. NATO Advanced Study Institute, Grenoble, France, pp. 163-294, 1964.
- [4] S. W. W. Shor, "Adaptive technique to discriminate against coherent noise in a narrow-band system," J. Acoust. Soc. of Amer., Vol. 39, pp. 74-78, January 1966.
- [5] S. P. Applebaum, "Adaptive Arrays," Syracuse University Research Corporation, Syracuse, N. Y., Technical Report SURC TR-66-001, August, 1966 (also in IEEE Trans. on Antennas and Propagation, Vol. AP-24, No. 5, pp. 585-598, September 1976).
- [6] B. Widrow, "Adaptive filters 1: fundamentals," Stanford University, Systems Theory Laboratory, Technical Report 6764-6, December 1966.
- [7] D. E. N. Davies, "Independent angular steering for each zero of the directional pattern for a linear array," IEEE Trans. Antennas and propagation, Vol. AP-15, No. 2, pp. 296-298, March 1967.
- [8] B. Widrow, L. Griffiths, P. E. Mantey, B. Goode, "Adaptive antenna systems," Stanford University, Systems Theory Laboratory Technical Report 6778-3, September 1967.
- [9] L. J. Griffiths, "A comparison of multidimensional Wiener and maximum-likelihood filters for antenna arrays," Proc. IEEE (Letters), Vol. 55, No. 11, pp. 2045-2047, November 1967.
- [10] B. Widrow, P. E. Mantey, L. J. Griffiths, and B. B. Goode, "Adaptive antenna systems," Proc. IEEE, Vol. 55, No. 12, pp. 2143-2159, December 1967.
- [11] R. T. Lacoss, "Adaptive combining of wideband array data for optimal reception," IEEE Trans. on Geoscience Electronics, Vol. GE-6, No. 2, pp. 78-86, May 1968.
- [12] R. F. Harrington, Field Computation by Moment Methods, Chapter 10, Macmillan, New York, 1968.
- [13] G. M. Jenkins and D. G. Watts, "Spectral Analysis and Its Applications, Holden-Day, San Francisco, 1968.
- [14] L. J. Griffiths, "A Simple adaptive algorithm for real-time processing in antenna arrays," Proc. IEEE, Vol. 57, pp. 1696-1704, October 1969.

- [15] C. Drane, Jr. and J. McIlvenna, "Gain maximization and controlled null placement simultaneously achieved in aerial array patterns," Radio and Electronic Engineer, Vol. 39, No. 1, pp. 49-57, January 1970.
- [16] B. Widrow, O. L. Frost, III, J.E. Brown, III, "Synthesis and analysis of adaptive array processors," Stanford University, Information Systems Laboratory, AD-726190, January 1971.
- [17] J. F. McIlvenna and C. J. Drane, Jr., "Maximum gain, mutual coupling and pattern control in array antennas," Radio and Electronic Engineer, Vol. 41, No. 12, pp. 569-572, December 1971.
- [18] G. Ungerboeck, "Theory on the speed of convergence in adaptive equalizers for digital communication," IBM Journal of Research and Development, Vol. 16, No. 6, pp. 546-555, November 1972.
- [19] B. Widrow, "Adaptive filters," from Part IV of Aspects of Network and System Theory edited by R. E. Kalman and N. DeClaris; Holt, Rinehart and Winston, New York, 1971
- [20] O. L. Frost, III, "An algorithm for linearly constrained adaptive array processing," Proc. IEEE, Vol. 60, No. 8, pp. 926-935, August 1972.
- [21] L. E. Brennan and I. S. Reed, "Theory of adaptive radar," IEEE Trans. Aerosp. Electron. Syst., Vol. AES-9, pp. 237-252, March 1973.
- [22] R. D. Gitlin, J. E. Mayo, and M. G. Taylor, "On the design of gradient algorithms for digitally implemented adaptive filters," IEEE Trans. on Circuit Theory, Vol. CT-20, No. 2, pp. 125-136, March 1973.
- [23] C. L. Zahn, "Application of adaptive arrays to suppress strong jammers in the presence of weak signals," IEEE Trans. on Aerospace and Electronic Systems, Vol. AES-9, No. 2, pp. 260-271, March 1973.
- [24] R. L. Riegler and R. T. Compton, Jr., "An adaptive array for interference rejection," Proc. IEEE, Vol. 61, No. 6, p. 748-758, June 1973.
- [25] J. Kaunitz and B. Widrow, "Noise subtracting filter study," Stanford University, Information Systems Laboratory, AD-767 717, October 1973.
- [26] J. W. R. Griffiths, P. L. Stoklin and C. Van Schooneveld (eds.), Signal Processing, Proceeding of the NATO Advanced Study Institute, Loughborough, England, Academic Press, New York, 1973.
- [27] R. B. Gilchrist, "Practical limits of time processing," pp. 357-362, in Signal Processing, J. W. R. Griffiths, et al. (eds.), Academic Press, New York, 1973.

- [28] C. Giraudon, "Results on active sonar optimum array processing," pp. 495-506, in Signal Processing, J. W. R. Griffiths, et al. (eds.), Academic Press, New York, 1973.
- [29] S. W. Autrey, "Design of arrays to achieve specified spatial characteristics over broad bands," pp. 507-524, in Signal Processing, J. W. R. Griffiths, et al. (eds.), Academic Press, New York, 1973.
- [30] W. J. Bangs and P. M. Schultheiss, "Space-time processing for optimal parameter estimation," pp. 577-590, in Signal Processing, J. W. R. Griffiths, et al. (eds.), Academic Press, New York, 1973.
- [31] M. L. Owsley, "A recent trend in adaptive spatial processing for sensor arrays: constrained adaptation," pp. 591-604, in Signal Processing, J. W. R. Griffiths et al. (eds.), Academic Press, New York, 1973.
- [32] G. Bienvenu and J. L. Vernet, "Enhancement of antenna performance by adaptive processing," pp. 605-618, in Signal Processing, J. W. R. Griffiths, et al. (eds.), Academic Press, New York, 1973.
- [33] H. Cox, "Sensitivity considerations in adaptive beamforming," pp. 619-646, in Signal Processing, J. W. R. Griffiths, et al. (eds.), Academic Press, New York, 1973.
- [34] L. W. Nolte, "Adaptive processing: time-varying parameters," pp. 647-656, in Signal Processing, J. W. R. Griffiths, et al. (eds.), Academic Press, New York, 1973.
- [35] I. S. Reed, J. D. Mallett, L. E. Brennan, "Rapid Convergence Rate in Adaptive Arrays," IEEE Trans. on Aerospace and Electronic Systems, Vol. AES-10, No. 6, pp. 853-863, November 1974.
- [36] B. Widrow, J. McCool and M. Ball, "The complex LMS algorithm," Proc. IEEE (Letters), Vol. 64, No. 4, pp. 719-720, April 1975.
- [37] B. Widrow, et al., "Adaptive noise cancelling: principles and applications," Proc. IEEE, Vol. 63, pp. 1692-1716, December 1975.
- [38] F. B. Hildebrand, Methods of Applied Mathematics, Chapter 1, Prentice-Hall, New Jersey, 1965.
- [39] G. Tacconi (ed.), Aspects of Signal Processing, Proceedings of the NATO Advanced Study Institute, La Spezia, Italy, D. Reidel Pub. Co., Boston, 1976.
- [40] C. Giraudon, "Optimum antenna processing: a modular approach," pp. 401-410, in Aspects of Signal Processing, G. Tacconi (ed.), D. Reidel Pub. Co., Boston, 1976.
- [41] E. B. Lunde, "The forgotten algorithm in adaptive beamforming," pp. 411-422, in Aspects of Signal Processing, G. Tacconi (ed.), D. Reidel Pub. Co., Boston, 1976.

- [42] J. E. Hudson, "The effects of signal and weight coefficient quantization in adaptive array processors," pp. 423-428, in Aspects of Signal Processing, G. Tacconi (ed.), D. Reidel Pub. Co., Boston, 1976.
- [43] H. Mermoz, "Complementarity of propagation model design with array processing," pp. 463-468, in Aspects of Signal Processing, G. Tacconi (ed.), D. Reidel Pub. Co., Boston, 1976.
- [44] J. M. McCool, "A constrained adaptive beamformer tolerant of gain and phase errors," pp. 477-484, in Aspects of Signal Processing, G. Tacconi (ed.), D. Reidel Pub. Co., Boston, 1976.
- [45] L. J. Griffiths, "An adaptive beamformer which implements constraints using an auxiliary array preprocessor," pp. 517-522, in Aspects of Signal Processing, G. Tacconi (ed.), D. Reidel Pub. Co., Boston, 1976.
- [46] N. L. Owsley, "Adaptive array processing," pp. 777-779, in Aspects of Signal Processing, G. Tacconi (ed.), D. Reidel Pub. Co., Boston, 1976.
- [47] W. F. Gabriel, "Adaptive arrays — an introduction," Proc. IEEE, Vol. 64, No. 2, pp. 239-272, February 1976.
- [48] R. Nitzberg, "Effects of errors on adaptive weights," IEEE Trans. on Aerospace and Electronic Systems, Vol. AES-12, No. 3, pp. 369-373, May 1976.
- [49] A. J. Applebaum and L. J. Kaplan, "Sidelobe suppression consideration in the design of electronically steered IFF antenna," IEEE Trans. on Antennas and Propagation, Vol. AP-24, No. 4, pp. 425-432, July 1976.
- [50] B. Widrow, J. M. McCool, M. G. Larimore and C. R. Johnson, Jr., "Stationary and nonstationary learning characteristics of the LMS adaptive filter," Proc. IEEE, pp. 1151-1162, August 1976.
- [51] W. F. Gabriel (ed.), "Special Issue on Adaptive Antennas," IEEE Trans. on Antennas and Propagation, Vol. AP-24, No. 5, September 1976.
- [52] S. H. Taheri and B. D. Steinberg, "Tolerances in self-cohering arrays of arbitrary geometry," IEEE Trans. on Antennas and Propagation, Vol. AP-24, No. 5, pp. 733-739, September 1976.
- [53] L. G. Griffiths, "Time-domain adaptive beamforming of HF backscatter radar signals," IEEE Trans. on Antennas and Propagation, Vol. AP-24, No. 5, pp. 707-720, September 1976.
- [54] R. T. Compton, Jr., "An experimental four-element adaptive array," IEEE Trans. on Antennas and Propagation, Vol. AP-24, No. 5, pp. 697-706, September 1976.

- [55] D. J. Chapman, "Partial adaptivity for the large array," IEEE Trans. on Antennas and Propagation, Vol. AP-24, No. 5, pp. 685-696, September 1976.
- [56] W. D. White, "Cascade preprocessor for adaptive arrays," IEEE Trans. on Antennas and Propagation, Vol. AP-24, No. 5, pp. 670-684, September 1976.
- [57] S. P. Applebaum, D. J. Chapman, "Adaptive arrays with mainbeam constraints," IEEE Trans. on Antennas and Propagation, Vol. AP-24, No. 5, pp. 650-661, September 1976.
- [58] B. Widrow and J. M. McCool, "A Comparison of adaptive algorithms based on the methods of steepest descent and random search," IEEE Trans. on Antennas and Propagation, Vol. AP-24, No. 5, pp. 615-637, September 1976.
- [59] B. Widrow, R. Chestek, J. R. Treichler, "Research on adaptive antenna techniques: final report," Stanford University, Information Systems Laboratory, AD-B019329, February 1977.
- [60] J. M. McCool and B. Widrow, "Principles and applications of adaptive filters: a tutorial review," AD-A037755, March 1977.
- [61] A. M. Vural, "A comparative performance study of adaptive array processors," IEEE Conference Record, International Conference on Acoustics, Speech, and Signal Processing, pp. 695-700, April 1977.
- [62] R. J. Mailloux, "Trends in array antenna research," RADC-TR-77-195, June 1977.
- [63] D. J. Chapman, "Adaptive arrays and sidelobe cancellers: a perspective," Microwave Journal, pp. 43-46, August 1977.
- [64] K. W. Rau, "Scattering effects upon adaptive antenna nulling," MITRE Corp. - WP-21437, September 1977.
- [65] L. I. Bluestein, "Issues in tactical satellite communications," MITRE Corp. - WP-21512, December 1977.
- [66] J. T. Mayhan, "Adaptive nulling with multiple beam antennas," IEEE Trans. on Antennas and Propagation, Vol. AP-26, No. 2, pp. 267-273, March 1978.
- [67] H. H. Al-Khatib and R. T. Compton, Jr., "A gain optimizing algorithm for adaptive arrays," IEEE Trans. on Antennas and Propagation, Vol. AP-26, No. 2, pp. 228-235, March 1978.
- [68] R. T. Compton, "An adaptive array in a spread-spectrum communication system," Proc. IEEE, Vol. 66, No. 3, pp. 289-298, March 1978.
- [69] W. D. White, "Artificial Noise in Adaptive Arrays," IEEE Trans. on Aerospace and Electronic Systems, Vol. AES-14, No. 2, pp. 380-384, March 1978.

- [70] W. D. White, "Adaptive cascade networks for deep nulling," IEEE Trans. on Antennas and Propagation, Vol. AP-26, No. 3, pp. 396-402, May 1978.
- [71] S. M. Sussman, L. G. Darian, K. W. Rau, "A survivable network of ground relays for tactical data communication," MITRE Corp. - MTR-3647, September 1978.
- [72] D. R. Morgan, "Partially adaptive arrays," IEEE Trans. on Antennas and Propagation, Vol. AP-26, No. 6, pp. 823-833, November 1978.
- [73] M. Dentino, J. McCool and B. Widrow, "Adaptive filtering in the frequency domain," Proc. IEEE (Letters), Vol. 66, No. 12, pp. 1658-1659, December 1978.
- [74] B. Widrow, R. Chestek, T. Saxe, "Research on adaptive antenna techniques III, final report," Stanford University, Information Systems Laboratory, AD-A068660, January 1979.
- [75] S. J. Caprio, "Applicability of MIL-STD 449D and MIL-STD-469 to modern radar systems," IEEE Trans. on Electromagnetic Compatibility, Vol. EMC-21, No. 2, May 1979.
- [76] J. T. Mayhan, "Some techniques for evaluating the bandwidth characteristics of adaptive nulling systems" IEEE Trans. on Antennas and Propagation, Vol. AP-27, No. 3, pp. 363-373, May 1979.
- [77] C. R. Guarino, "Adaptive signal processing using FIR and IIR filters," Proc. IEEE (Letters), Vol. 67, No. 6, pp. 957-958, June 1979.
- [78] J. E. Mazo, "On the independence theory of equalizer convergence," Bell System Technical Journal, Vol. 58, No. 5, pp. 963-993, May - June 1979.
- [79] L. L. Horowitz, W. G. Brodsky, H. Blatt, K. D. Senne, "Implementation of the sample matrix inversion algorithm for controlling adaptive antenna arrays," Electro-Professional Program, New York, New York, April 1979.
- [80] B. Widrow, "A review of adaptive antennas," IEEE Conference Record, International Conference on Acoustics, Speech and Signal Processing, pp. 273-278, April 1979.
- [81] L. A. Mole and F. A. Andrews, "An array optimization technique," IEEE Conference Record, International Conference on Acoustics, Speech, and Signal Processing, pp. 279-281, April 1979.
- [82] W. S. Hodgkiss, "Adaptive array processing: time vs. frequency domain," IEEE Conference Record, International Conference on Acoustics, Speech, and Signal Processing, pp. 282-285, April 1979.

- [83] R. P. Kraft, J. F. McDonald, and F. Ahlgren, "Minimax optimization of two-dimensional focused nonuniformly spaced arrays," IEEE Conference Record, International Conference on Acoustics, Speech, and Signal Processing, pp. 286-289, April 1979.
- [84] A. H. Quazi and A. H. Nuttall, "Effects of random shading, phasing errors and element failures on the beam patterns of line and planar arrays," IEEE Conference Record, International Conference on Acoustics, Speech, and Signal Processing, pp. 290-293, April 1979.
- [85] J. T. Mayhan, "A technique for measuring the bandwidth characteristics of adaptive nulling antennas," IEEE Conference on Antennas and Propagation, International Symposium Digest, pp. 190-192, June 1979.
- [86] E. Mendelovitz and E. T. Oestreich, "Phase only adaptive nulling with discrete values," IEEE Conference on Antennas and Propagation, International Symposium Digest, pp. 193-198, June 1979.
- [87] W. F. Gabriel, "Maximum entropy spatial resolution adaptive array," IEEE Conference on Antennas and Propagation, International Symposium Digest, pp. 203-206, June 1979.
- [88] M. Pelletier, G. Y. Delisle, and J. A. Cummins, "An experimental nonlinear adaptive array," IEEE Conference on Antennas and Propagation, International Symposium Digest, pp. 212-215, June 1979.
- [89] M. L. Burrows, "Element placement for adaptive satellite array antennas," IEEE Conference on Antennas and Propagation, International Symposium Digest, pp. 186-189, June 1979.

1979 USAF - SCEE SUMMER FACULTY RESEARCH PROGRAM

Sponsored by the

AIR FORCE OFFICE OF SCIENTIFIC RESEARCH

Conducted by the

SOUTHEASTERN CENTER FOR ELECTRICAL ENGINEERING EDUCATION

FINAL REPORT

DEEP LEVELS IN $\text{Al}_x\text{Ga}_{1-x}\text{As}$

Prepared by:	Dr. Rangaiya A. Rao
Academic Rank:	Associate Professor
Department and University:	Electrical Engineering Department San Jose State University
Research Location:	AFAL/DHR Wright-Patterson AFB, Ohio
USAF Research Colleague:	Dr. Dietrich W. Langer
Date:	August 10, 1979
Contract No:	F49620-79-C-0038

DEEP LEVELS IN $\text{Al}_x\text{Ga}_{1-x}\text{As}$

by

Dr. Rangaiya A. Rao

ABSTRACT

Deep levels in Fe-doped $\text{Al}_x\text{Ga}_{1-x}\text{As}$ layers were investigated by using the photoluminescence and the Deep Level Transient Spectroscopy techniques. Sharp photoluminescence bands around 0.37 eV were measured in $\text{Al}_2\text{Ga}_{1-x}\text{As:Fe}$ samples grown on undoped and Cr-doped GaAs Substrates. The x-values ranged from 0.06 to 0.47. The 0.37 eV emission was very weak or absent in $\text{Al}_x\text{Ga}_{1-x}\text{As:Fe}$ layers grown on GaAs:Te substrates. These layers showed broad bands near the band edge. DLTS peaks were observed in three samples with carrier densities in the range $10^{15} - 10^{16} \text{ cm}^{-3}$. One such peak for $\text{Al}_{0.71}\text{Ga}_{0.29}\text{As:Fe}$ has been analyzed and is found to be a hole trap at 0.75 eV above the valence band edge.

ACKNOWLEDGMENTS

The author would like to thank the Air Force Systems Command, Air Force Office of Scientific Research, and the South Eastern Center for Electrical Engineering Education for providing him with the opportunity to do some stimulating work at the Avionics Laboratory at the Wright-Patterson Air Force Base.

The author is especially grateful to Major Robert Almassy, Dr. D. C. Reynolds, and Dr. D. W. Langer for their guidance and to Dr. Elward Rodine and Phil WonYu for their invaluable assistance in conducting the research.

The many discussions with the scientists in the Electronic Research Laboratory were very helpful.

I. INTRODUCTION

The $\text{Al}_x\text{Ga}_{1-x}\text{As}/\text{GaAs}$ system has important applications in solar cells, heterojunction lasers and field effect transistors. $\text{Al}_x\text{Ga}_{1-x}\text{As}/\text{GaAs}$ solar cells have been operated at 1735 suns with 19% efficiency and a power output of 240 KW/m^2 of cell area. The $\text{Al}_x\text{Ga}_{1-x}\text{As}/\text{GaAs}$ heterojunction laser is one of the important components of the emerging field of optical communications. GaAs FETs operate at x-band and GaAs Integrated Circuits have been demonstrated. GaAs microwave devices have cornered a large share of the low to medium power microwave oscillator market.

Deep levels are energy levels in the band gap which are at least a few kT away from the band edges. They could be due to

- a. Chemical impurities (Au in Si; Cr in GaAs)
- b. Native defects (vacancies etc., caused by crystal growth, processing steps and radiation.
- c. Complexes (Te-V_{Ga} Complex in GaAs)
- d. Surfaces and interfaces.

They affect device performance in many ways.

(i) Device gain and speed are affected by carrier lifetime, carrier compensation, and carrier mobility which depend on deep levels.

(ii) The wavelength and the efficiency of optical emitters are affected gainfully and adversely by the presence of deep defect levels.

(iii) Device degradation and failure can often be traced to the presence of certain deep levels. Deep levels like those due to Cr are essential in obtaining semi-insulating substrates for device fabrication.

In this project deep levels in $\text{Al}_x\text{Ga}_{1-x}\text{As:Fe}$ were investigated. We wish to give a brief background of the work done by others in this field. Iron is a transitional metal with a ground state configuration of $3d^6 4s^2$ with stable charge states of $+3(3d^5)$ and $+2(3d^6)$. Iron enters Ga sites in GaAs and is a deep acceptor with a relatively large capture cross-section for holes. Available data on GaAs:Fe indicate relatively high solid solubility of Fe in GaAs for LPE layers grown at 850°C , iron deep level concentration of $5 \times 10^{14} \text{ cm}^{-3}$ are typical. The thermal activation energy of the deep levels of iron in GaAs around room temperature is 0.52 eV from Hall measurements [1] and also from DLTS measurements on LPE GaAs:Fe [2]. DLTS measurements of $\text{Al}_x\text{Ga}_{1-x}\text{As:Fe}$ for a limited range of values of x ($x = 0$ to $x = 0.2$) have been reported by Lang et al [2]. They found that the thermal activation energy increases from 0.52 eV for $x = 0$ to about 0.61 eV for $x = 0.2$ around room temperature while the bandgap varies from 1.42 eV to 1.65 eV. The deep level of Fe in $\text{Al}_x\text{Ga}_{1-x}\text{As}$ maintains the same relative position in the bandgap as x is varied.

A 0.37 eV level when measured from the valence band has been reported from resistivity measurements on GaAs:Fe around 300°K [3]. The zero phonon photoluminescence line of Fe in GaAs is 0.37 eV when measured at 6°K [4]. It has been attributed to the crystal field transitions from the 5_{T_2} excited state to the 5_E ground state of Fe^{2+} in the tetrahedral coordination. On the basis of this explanation, the 0.37 eV photoluminescence line of Fe in $\text{Al}_x\text{Ga}_{1-x}\text{As:Fe}$ should be nearly independent of aluminum composition x .

II. OBJECTIVES OF THE RESEARCH EFFORT

We set out to study the optical and thermal activation energies of Fe and some native defects in $\text{Al}_x\text{Ga}_{1-x}\text{As:Fe}$ as a function of aluminum composition x by photoluminescence and by DLTS techniques.

III. PREVIOUS WORK BY AUTHOR

Some $\text{Al}_x\text{Ga}_{1-x}\text{As:Fe}$ LPE layers were grown on Te-doped, Cr-doped, and undoped substrates. The layer thicknesses were determined by cleaving and staining in PA solution to range from 3 μm to 10 μm . Aluminum Composition was determined for $x < 0.4$ by bandedge photoluminescence and for $x > 0.4$ by microprobe analysis. Ohmic contacts were made on $\text{p-Al}_x\text{Ga}_{1-x}\text{As:Fe}/\text{n}^+\text{GaAs:Te}$ heterojunctions by evaporating and alloying Au-Zn on the p-side and Au-Ge on the n^+ -side.

IV. PRESENT WORK

The diodes were scribed to approximately 1 mm x 1 mm in area, mounted on TO-5 headers and wire bonded. I-V characteristics were measured to determine forward drop and to breakdown voltage. C-V characteristics were measured to determine the carrier concentration.

a. DLTS Measurements (with Dr. Elward Rodine)

A schematic of the DLTS experiment is shown in Fig. 1. A typical quiescent reverse bias on the diode was 1 volt for 150 ms with a +2 volt, 500 μs pulse bringing the diode briefly into forward bias to load the traps with holes. The typical DLTS spectrum for diode 706x-1 ($x = 0.71$) and the capacitance transient (see inset) signal are shown in Fig. 2. Fig. 3 shows the high temperature peak (centered around 350°K) obtained at rate windows ranging from 17.3 sec^{-1} to 115.5 sec^{-1} (top to bottom). Fig. 14 shows a plot of \ln (emission rate) Vs $1/kT$. The thermal activation energy measured this way is 0.75 eV.

DLTS data were taken on several other samples and will be analyzed in the future.

b. Photoluminescence Measurements (with Dr. Phil WonYu)

Photoluminescence measurements were made on several samples

at liquid He temperature. A photomultiplier detection system was used for near bandedge measurements (Fig. 5) and a cooled PbS detector was used for near infrared measurements up to $3.5 \mu\text{m}$ (Fig. 6). Layers grown on undoped or Cr-doped GaAs substrates showed the sharp photoluminescence peak at about 0.37 eV which is believed to be characteristic of Fe in GaAs. Layers grown on Te-doped GaAs substrates did not show the 0.37 eV band. However these samples showed broad peaks in the range of 8000 to $11,000 \text{ \AA}$.

V. CONCLUSIONS

The results obtained so far are preliminary results. A large bulk of the data still remains to be analyzed and some more data needs to be taken before final conclusions can be drawn. Suffice is to say that the results are interesting and the project should be continued.

VI. RECOMMENDATIONS

(i) Recommendations for improving the DLTS system have been given in a oral conversation with the acting director of the laboratory, Dr. D. W. Langer.

(ii) The project should be continued with the immediate emphasis on analysis of the data already obtained. The author will apply for a mini-grant to do this.

(iii) Samples that showed interesting results should be re-analyzed by microprobe analysis to be certain of the composition. If possible experiments should be done on samples which showed strong 0.37 eV peaks to determine if the luminescence observed is indeed from the layer and not from the substrate.

(iv) The author will try to obtain funding to grow $\text{Al}_x\text{Ga}_{1-x}\text{As}$ layers more suitable for DLTS and photoluminescence studies.

REFERENCES

1. P. L. Hayt and R. W. Haisty, J. Electrochem. Soc. 113, p. 296 (1966).
2. D. V. Lang, R. A. Logan, and L. C. Kimmerling, Phys. Rev. B, 15, p. 4874, 15 May 1977.
3. F. A. Cunnell, J. T. Edmond, and W. R. Harding, Solid State Electronics, 1, p. 97, 1960.
4. W. H. Koschel, V. Kaufmann, and S. G. Bishop, Solid State Comm., 21, p. 1069, 1977.

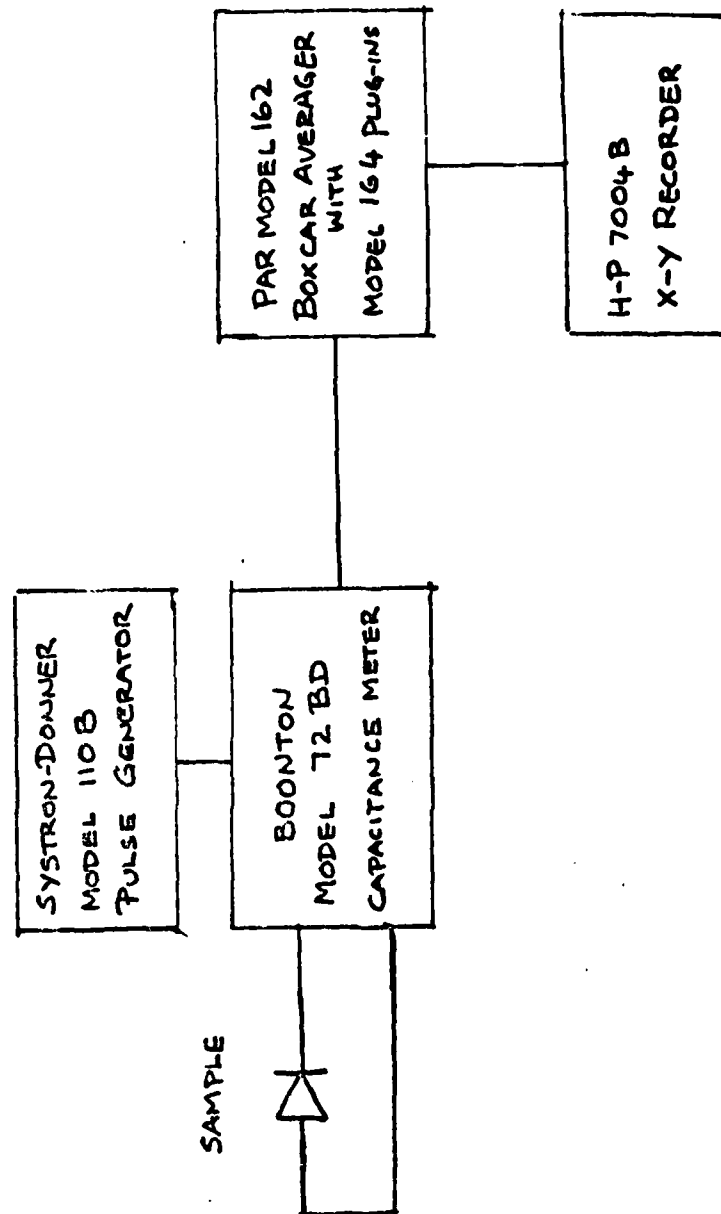


Fig. 1: Schematic of DLTS Experiment

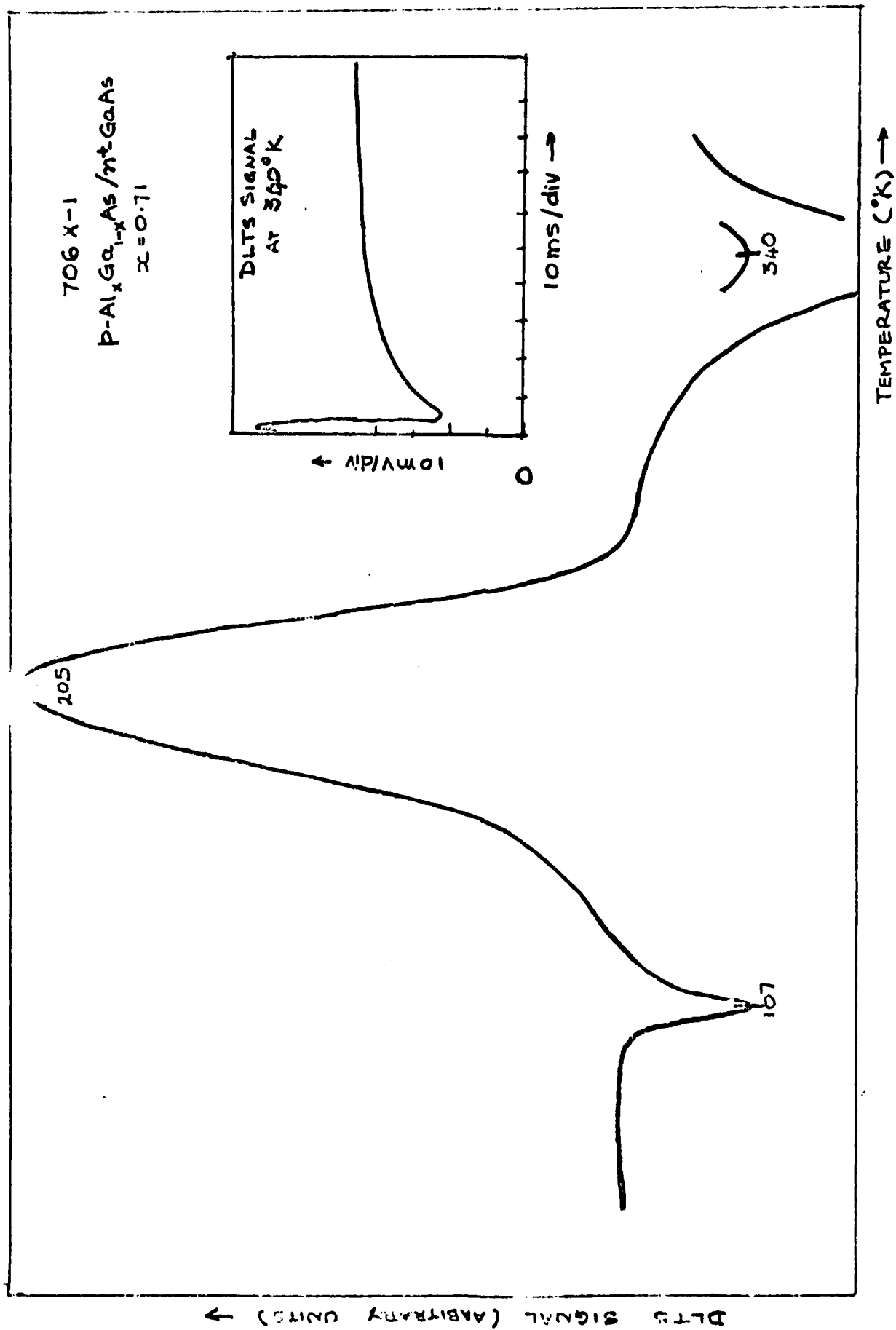


Fig. 2: A Typical DLTS Scan (Approximately 3 Hours)

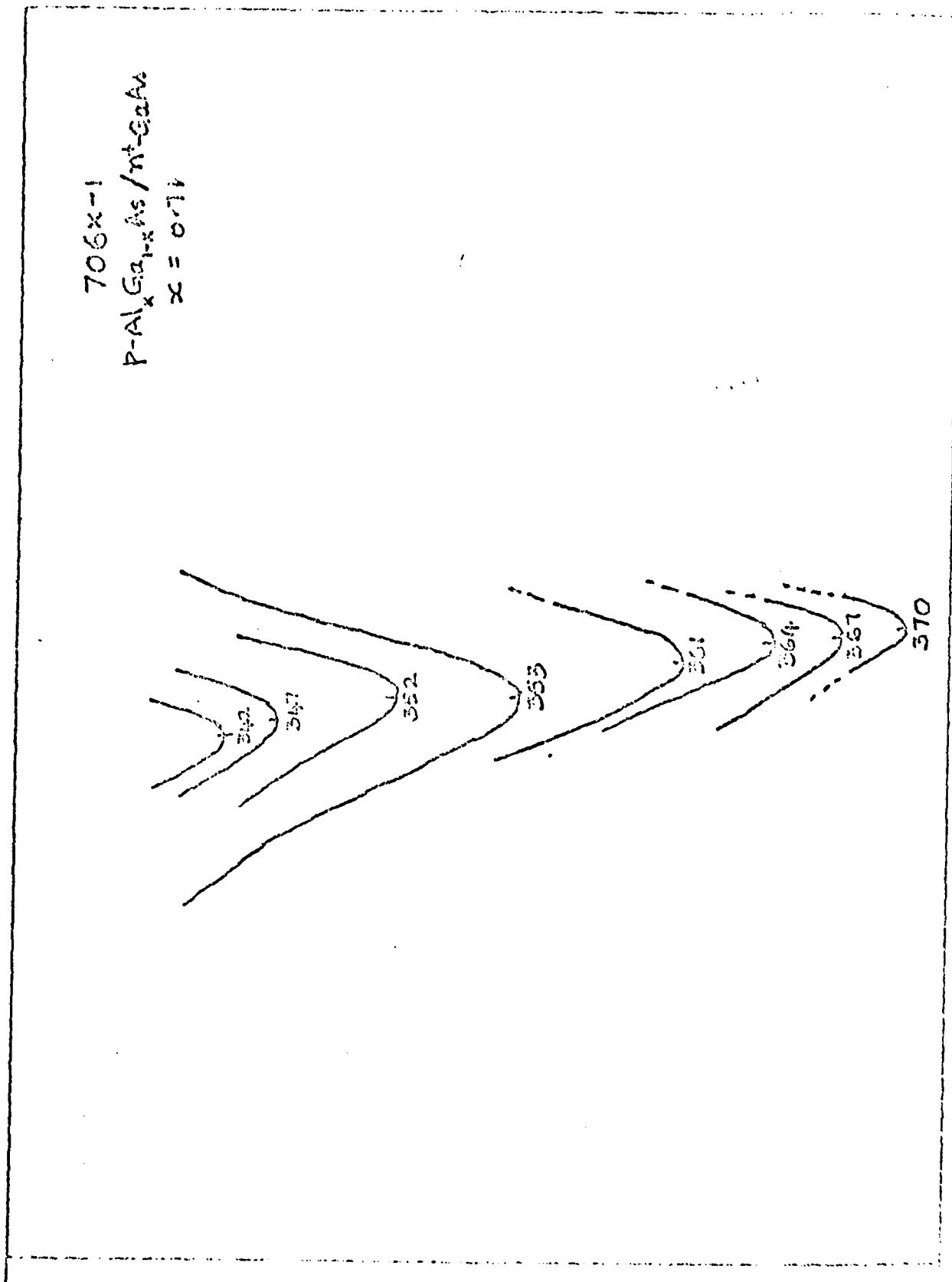


Fig. 3: Detailed Measurements on the High Temperature Peak (Approximately 30 min. each)

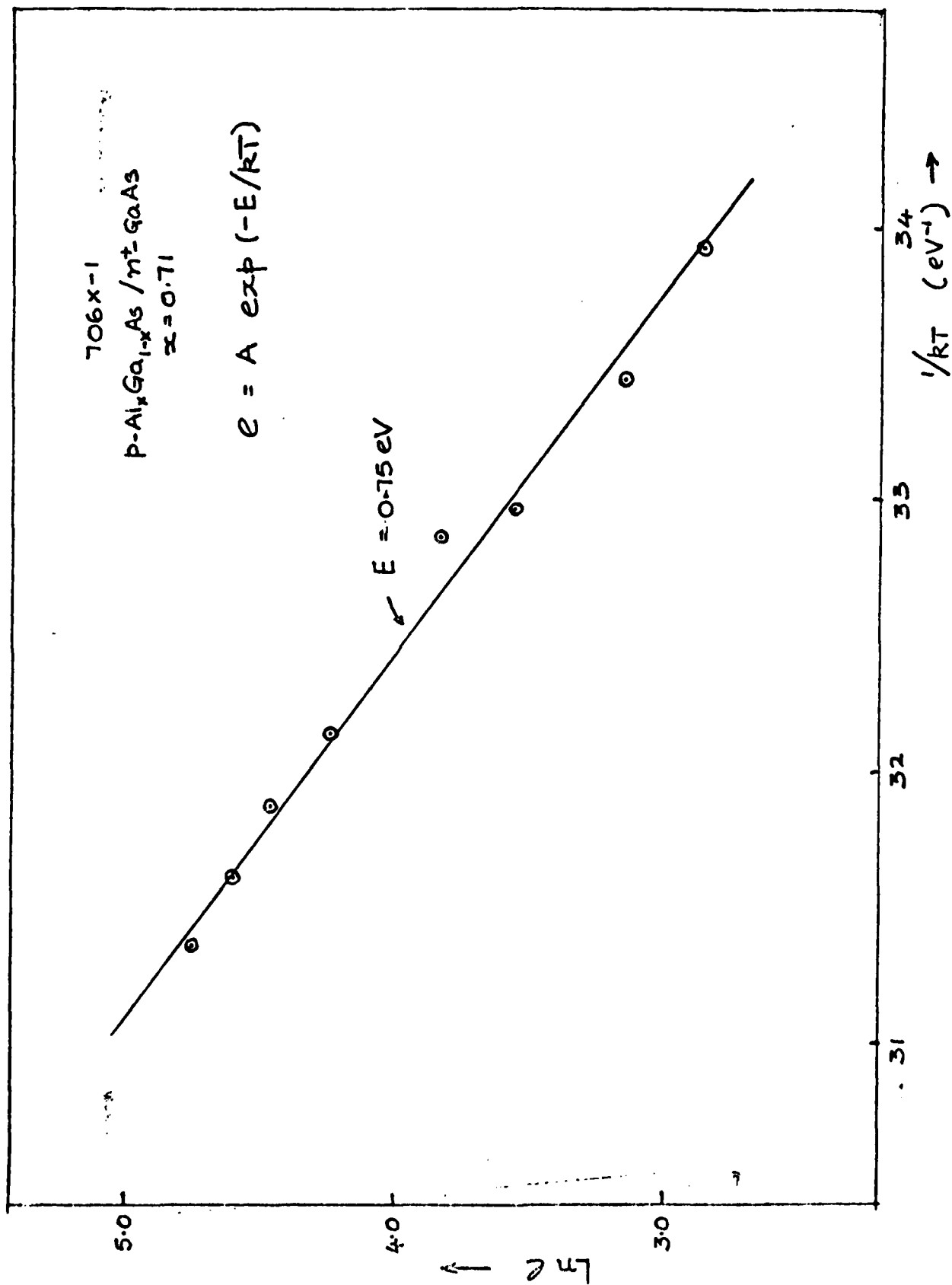


Fig. 4: $\ln j$ vs $1/kT$ for the High Temperature Peaks.

NEAR BAND EDGE PHOTOLUMINESCENCE
 $\text{Al}_x\text{Ga}_{1-x}\text{As:Fe/CrAs:Te}$

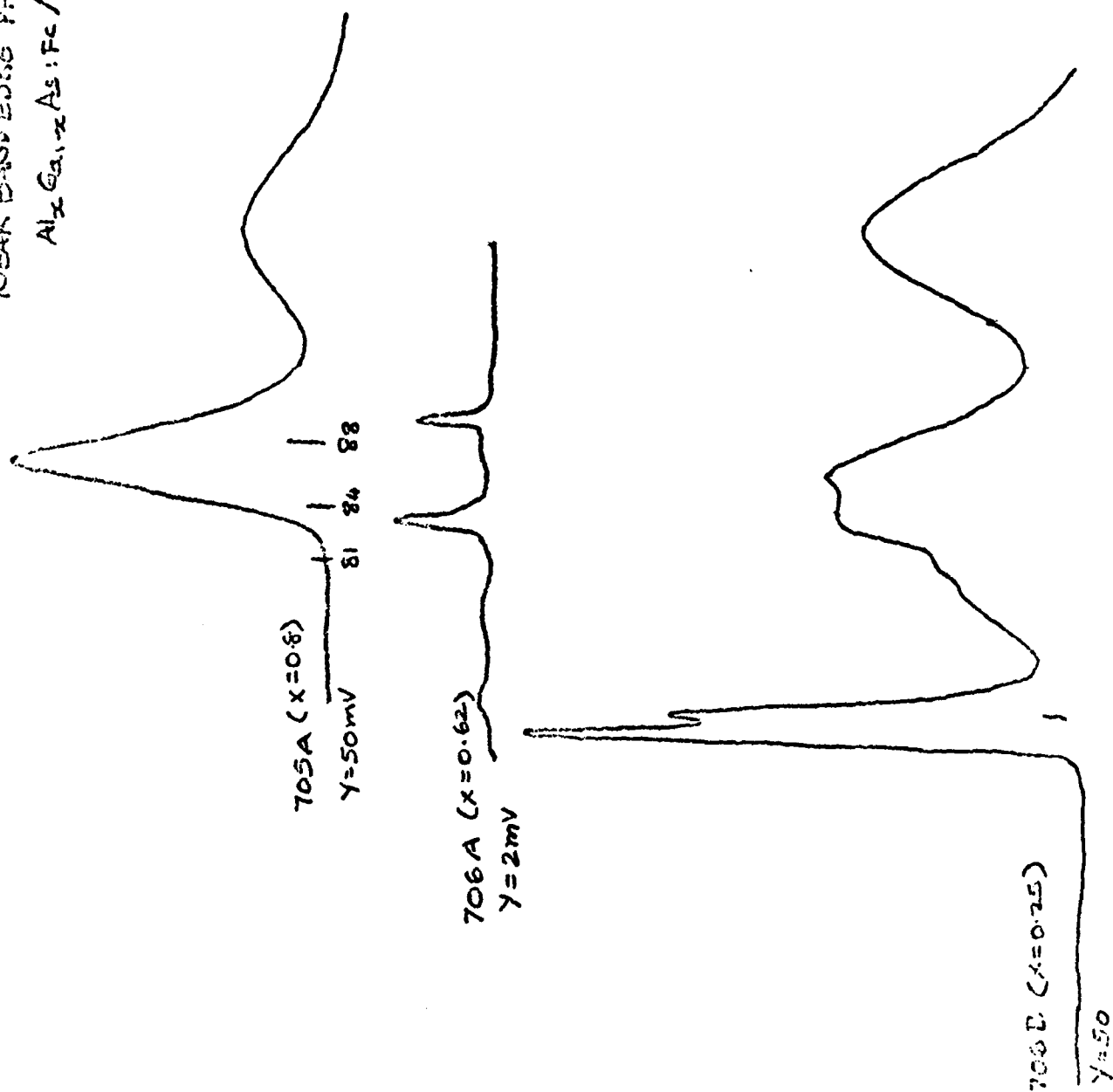


Fig. 5: Near Bandedge Photoluminescence

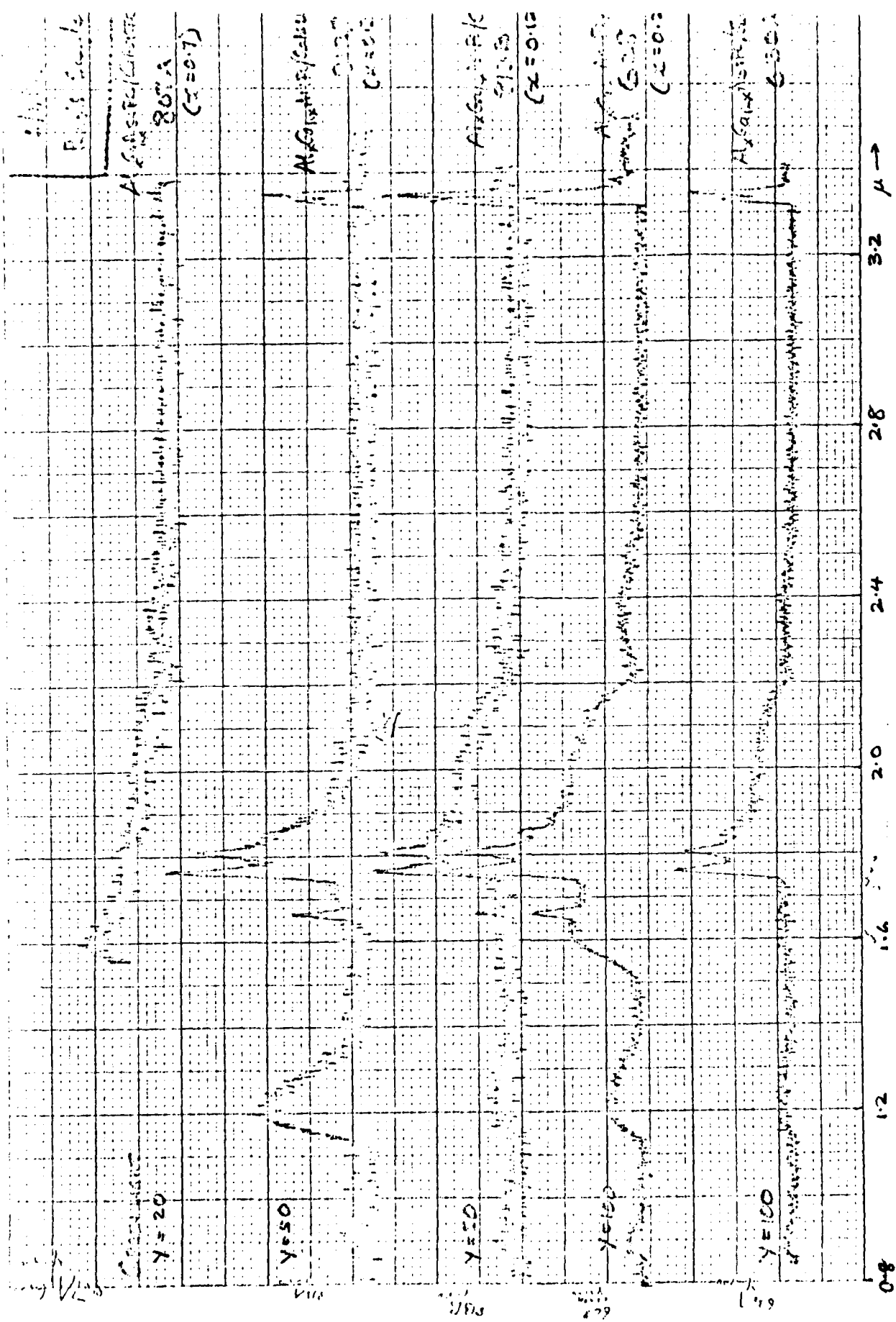


Fig. 6: Photoluminescence Measurements using Cooled-PBS Detector

THIS PAGE IS BEST QUALITY PRACTICABLE
FROM COPY FURNISHED TO EOD

1979 USAF-SCEEE SUMMER FACULTY RESEARCH PROGRAM

Sponsored by the

AIR FORCE OFFICE OF SCIENTIFIC RESEARCH

Conducted by the

SOUTHEASTERN CENTER FOR ELECTRICAL ENGINEERING EDUCATION

FINAL REPORT

DEVELOPMENT OF AN AIR-SAMPLING AND ANALYTICAL

METHOD FOR DIISOCYANATES

Prepared by: Stephen M. Rappaport, Ph.D.

Academic Rank: Assistant Professor

Department and University:

Department of Biomedical and Environmental Health Sciences
University of California, Berkeley

Research Location: USAF School of Aerospace Medicine

Crew Protection Branch

Brooks AFB, Texas

USAF Research Colleagues: Dr. Richard Miller, Major James Rock.

Contract No.: F 49620-79-C-0038

DEVELOPMENT OF AIR-SAMPLING AND ANALYTICAL METHOD
FOR DIISOCYANATES

ABSTRACT

Stephen M. Rappaport

A method has been developed for the collection and analysis of diisocyanates in air. Air is drawn through a filter impregnated with 1-naphthylenemethylamine (NMA) which reacts with the diisocyanate to produce a stable urea. The method should be suitable for the collection of diisocyanates in either vapor or aerosol form. The urea is dissolved in methanol and analyzed by high performance liquid chromatography (HPLC). The method was evaluated with 1,6-hexamethylene diisocyanate (HDI). Results indicated HDI vapor to be efficiently trapped by the filter. Analysis gave a quantitation limit of ~2ng/ injection which allows airborne HDI to be measured at 0.002ppm in a 10-L air sample. Additional development should reduce the limit of quantitation and simplify the analysis.

ACKNOWLEDGEMENTS

The author would like to thank the Air Force Systems Command, the Air Force Office of Scientific Research, the School of Aerospace Medicine, and the Southeastern Center for Electrical Engineering Education for the opportunity to perform this research. Special thanks is also due to Maj. James Rock, Dr. Richard Miller and Dr. Harry Hughes for their suggestions and support.

I. INTRODUCTION

Diisocyanates are used in the production of polyurethane products. They are extremely toxic compounds, producing lung effects and respiratory sensitization in man at air concentrations below 1 ppm. The Air Force uses large quantities of diisocyanates in two operations, aircraft painting (polyurethane paint) and in-place packaging (polyurethane foam). In both operations, diisocyanates are mixed with alcohols to form the polyurethane products as needed; thus, the possibility exists that unreacted diisocyanates will enter the worker's breathing zones.

The purpose of this research project has been the development of an air-sampling and analytical procedure which can be used by Air Force personnel in evaluating airborne exposures to diisocyanates. This method is needed since existing procedures are subject to numerous errors in both air sampling and analysis. A brief discussion of these procedures and their shortcomings follows.

Several methods are based upon conversion of aromatic diisocyanates to the corresponding diamines in a fritted bubbler (1-4). The diamines are diazotized, coupled with a chromophore, and the products measured spectrophotometrically. These methods do not measure aliphatic diisocyanates because of lower reactivities of these compounds. Since many polyurethane paints employ aliphatic diisocyanates, this is a serious shortcoming. Furthermore, the use of a fritted bubbler for sampling is undesirable because it has capricious collection characteristics for aerosols, a physical form often encountered with airborne diisocyanates, and it is subject to breakage and spillage of the liquid contents. The analytical procedure cannot differentiate among the diamines produced during sampling, the amines already present from the reaction of the diisocyanate and water vapor (prior to sampling), and the other amines present in the air (Amines are often used in polyurethane systems as catalysts.).

More recent methods react diisocyanates with chromaphore-containing amines in a bubbler followed by chromatographic analysis of the ureas produced (5-7). These procedures measure aliphatic as well as aromatic diisocyanates and, because a separation step is included, the product ureas can be differentiated from amines and other potentially interfering compounds. However, since bubblers are still used to collect the diisocyanates, these methods are subject to the sampling pitfalls listed above.

The research problem, as envisioned, has four components. First, a method must be developed which can collect either aromatic or aliphatic diisocyanates. Second, the sampler must efficiently collect either aerosols (produced by dispersion processes such as paint spraying, foam injection, etc.) or vapors (generated by vaporization or sublimation of diisocyanates from uncured systems). Third, the analytical method must be extremely sensitive since exposure must be measured at low levels (<0.01 ppm as vapors). Finally, the analysis must be specific for the diisocyanates investigated, i.e., not subject to interfering compounds.

The proposed collection method draws air through a high-efficiency filter which has been impregnated with a chromaphore-containing amine. Diisocyanate vapors react with the amine to produce a nonvolatile, unreactive urea. Diisocyanate aerosols are efficiently trapped by the filter. Any vapors released from trapped particles also react with the amine.

The proposed analytical method employs high performance liquid chromatography (HPLC) to separate the product urea from the amine used as the reagent and from other potentially interfering compounds. Detection employs UV photometry at the absorption maximum of the urea to ensure sensitive analysis.

II. OBJECTIVES

Clearly, it was impossible to develop and evaluate a method for all of the diisocyanates used by the Air Force in 10 weeks. Thus, one compound, 1,6-hexamethylene diisocyanate (HDI) was selected for study. This diisocyanate is used by the Air Force in the largest quantity (paint systems). Furthermore, because it is an aliphatic diisocyanate, a successful method would also be applicable to aromatic diisocyanates which are much more reactive, and therefore easier to collect by the proposed sampling procedure.

The objectives of this project were:

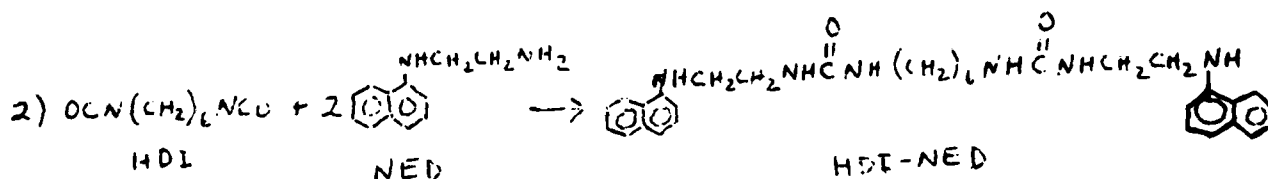
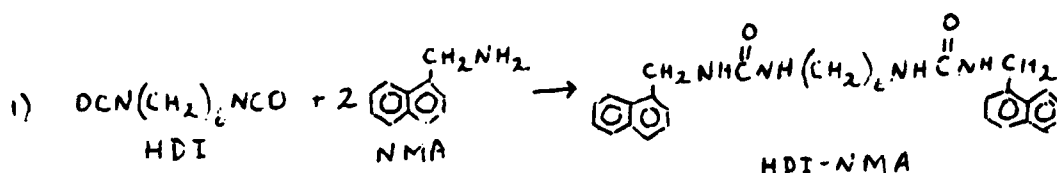
- 1) To select a chromophore-containing amine(s) which reacts rapidly with HDI at room temperature and produces a urea which can be sensitively detected by UV photometry,
- 2) To characterize the urea(s) produced by reaction between HDI and the amine(s),
- 3) To develop a HPLC procedure which separates the urea from the amine and impurities,
- 4) To collect HDI vapors from an airstream by an amine-impregnated filter and recover the product urea in high yield.

III. SELECTION OF THE REAGENT AMINE

In order to collect diisocyanate vapors from air successfully, the reagent amine must react very rapidly with these compounds. Whereas secondary amines will react with aromatic diisocyanates, only primary amines react rapidly with aliphatic diisocyanates (8-10). For instance, the reaction between HDI and nitro reagent, a secondary amine (N-4-nitrobenzyl-N-n-propylamine), required over 40 min. in liquid solution to go to completion (10).

Reactions between nitro reagent and several aromatic amines were virtually instantaneous (10). The reaction rate is also influenced by steric effects; thus, the carbon adjacent to the amino group should not contain substituent groups (8,9). In addition, the amine molecule must contain a strong UV chromophore ($\epsilon_{\text{max}} > 10^4$) to allow detection of small amounts of the urea.

Two amines were selected for study, 1-naphthalenemethylamine (NMA) previously used by Levine et al. for collecting airborne diisocyanates in bubblers (7), and N-1-naphthyl-ethylenediamine (NED). Structures of these compounds and the product ureas are shown in the following reactions:



Both of these amines absorb very strongly in the UV. Absorption spectra are shown in Figures 1 and 2. The maximum absorbance for NMA is at 223 nm ($\epsilon_{\text{max}} = 8.8 \times 10^4$) while the maximum absorbance for NED is at 210 nm ($\epsilon_{\text{max}} = 5.0 \times 10^4$).

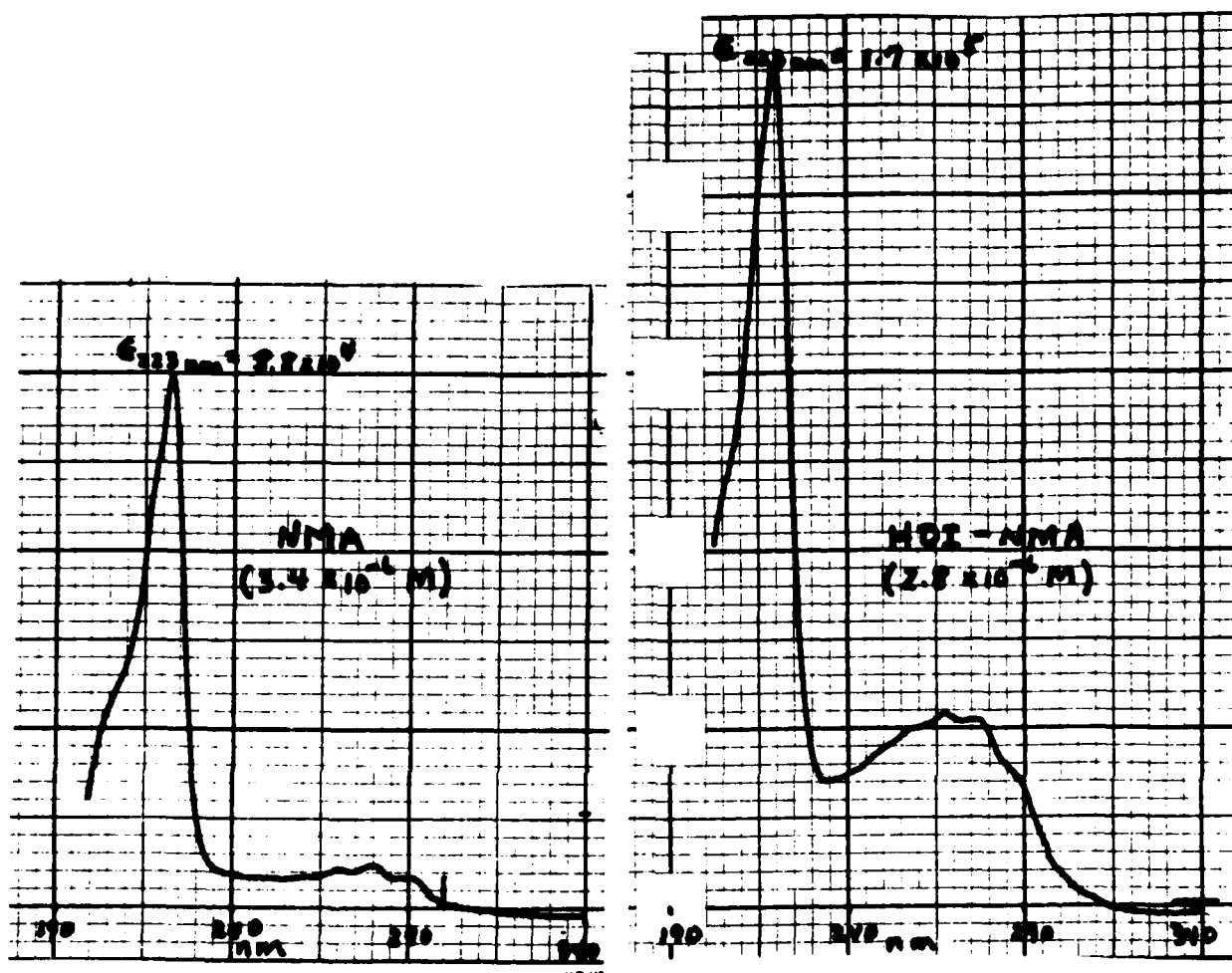


Figure 1. UV Absorption Spectra of NMA and HDI-NMA

Conditions:

Instrument - Beckman Acta III Spectrophotometer

Scan Rate - 0.2 nm/sec, 50 nm/inch

Slit Width - Programmed 0.6 nm at 340 nm, 1.5 nm at 190 nm

Range - 1 AUFS; Path Length - 1 cm; Solvent - CH₃OH

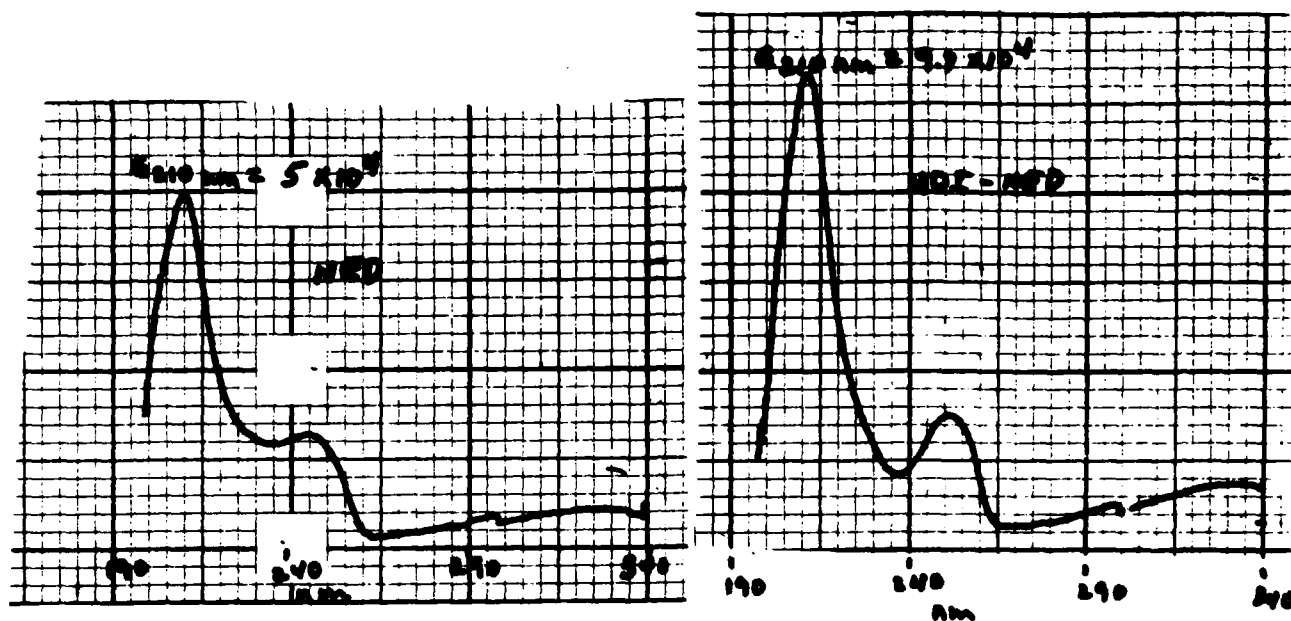


Figure 2. UV Absorption Spectra of NED and HDI-NED
(Conditions same as given in Figure 1)

IV. PREPARATION AND CHARACTERIZATION OF UREAS

Ureas were prepared by reacting HDI with either NMA or NED in methylene chloride solution. 1.2 mmoles of NMA and 0.31 mmoles of NED were dissolved in 2 ml of methylene chloride in separate test tubes. HDI was injected directly into these solutions with a microliter syringe; 0.43 μ moles were added to the NMA and 0.13 μ moles were added to the NED. White precipitates were formed immediately. After standing for five minutes at 60°C, the methylene chloride was removed by evaporation under nitrogen. The products were filtered with glass-fiber filters, washed with methylene chloride to remove the excess amine, dried in a vacuum oven at 50°C and weighed. Recoveries were 0.40 μ moles of HDI-NMA (92% yield) and 0.10 μ moles of HDI-NED (77% yield).

The ureas were dissolved in methanol and the UV absorption spectra obtained. These compounds were soluble only at concentrations $< \sim 10^{-6}$ M in methanol. Solubilities in other solvents (hexane, methylene chloride, acetonitrile, ethanol, water) were even lower. The absorption spectra are shown in Figures 1 and 2. They are qualitatively identical to the spectra of NMA and NED. However, the molar extinction coefficients (HDI-NMA $\epsilon_{223\text{nm}} = 1.7 \times 10^5$; HDI-NED $\epsilon_{210\text{nm}} = 9.7 \times 10^4$) are twice the values of the corresponding amines. This indicates that each molecule of the product does, indeed, contain two chromophore groups.

The melting points of the ureas were also measured. The melting range of HDI-NMA was from 245-248°C and of HDI-NED was from 189-191.5°C.

V. HPLC of HDI-NMA

Aliquots of HDI-NMA solutions were injected into an HPLC system, employing a variable-wavelength detector at the absorption maximum of 223 nm. The column was 30 cm x 4 mm-i.d. μ Bondapak-C₁₈ (Waters Assoc.) with a guard column containing Corasil-C₁₈ (Waters Assoc.). The mobile phase, consisting of 25% water/methanol, flowed through the column at 1.0 mL/min. Injections of 50 μ L were made with a loop injector.

Typical chromatograms are shown in Figure 3. HDI-NMA eluted at 6.2 min, well before NMA which eluted at 40 min. When the detector was operated at a range of 0.05 AUFS, the minimum amount of HDI-NMA which could be quantitated was ~ 2 ng corresponding to a solution concentration of 0.04 $\mu\text{g}/\text{mL}$.

VI. COLLECTION OF HDI IN AIR BY FILTERS IMPREGNATED WITH NMA

A. Impregnation of Filters

Glass-fiber filters (Millipore Type AP, 37 mm) were dipped into a 0.396 mg/mL solution of NMA in methylene chloride. Preliminary trials showed that 1 mL was absorbed; thus, each filter contained 396 μg of NMA. Filters were hung by metal clips to dry and stored at 0°C prior to use.

B. Challenge of Filters with HDI Vapor

Impregnated filters were placed in standard 37-mm plastic, in-line holders. A glass tube was connected to the inlet of each holder so that air did not come in contact with the plastic as it entered. The outlet of the holder was connected to the inlet of a standard glass midget impinger containing 10 mL of 10^{-4} M NMA in methylene chloride. Air was drawn through each sampling train at 0.3-0.4 L/min.

The experiment involved the addition of 6.13 μg of HDI in methylene chloride solution to the interior of the glass inlet tubes of three samplers as air was drawn through them. Two control samplers were not spiked with HDI. Air was drawn through each train for 10 min. Subsequent analysis of the filters and impinger solutions for HDI-NMA would show whether or not all of the HDI had been trapped by the filter.

C. Analysis of Filters and Impinger Solutions

Filters were removed from the holders and placed in 10-mL glass test tubes to which were added 6 mL of methylene chloride. Impinger

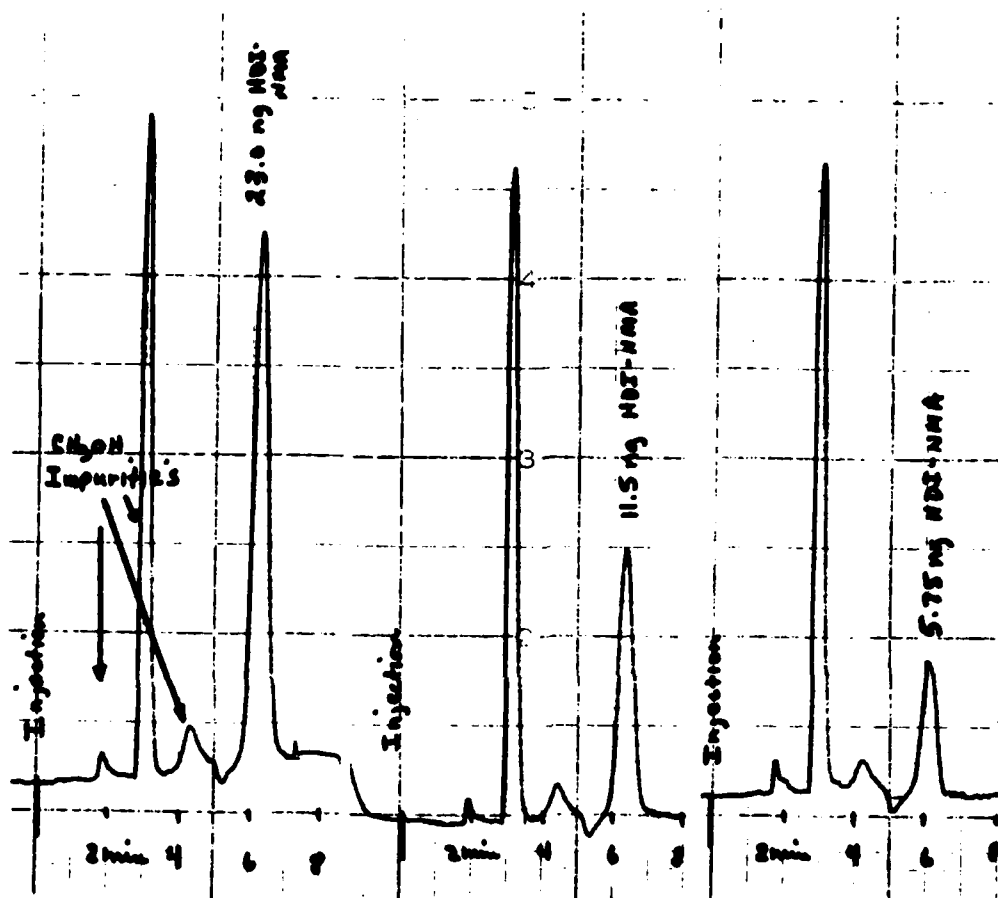


Figure 3. HPLC Chromatograms of HDI-NMA

Conditions:

Pump - Altex Model 100; Column - Waters μ Bondapak C₁₈
 Detector - Altex/Hitachi Model 100-10 at 223 nm, 0.05 AUFS
 Mobile Phase - 25% H₂O/CH₃OH at 1.0 mL/min
 Injection Volume - 50 μ L; Solvent - CH₃OH

solutions were also placed in test tubes. The solvent was removed from all samples at 40°C under nitrogen. Eight mL of methanol were added to each tube which was then capped and placed in an ultrasonic bath for 2 hr to dissolve the HDI-NMA. Aliquots of each sample were injected into the HPLC as previously described at a detector range of 0.05 AUFS.

D. Results

Data are shown in Table 1. HDI-NMA was found on the filters only; none was observed in downstream impingers. The mean recovery from the three filters in the experimental group was 18.0 µg. Since 6.13 µg of HDI produces 17.6 µg of HDI-NMA ($6.13 \text{ µg HDI} \times \frac{482.6 = \text{M.W. of HDI-NMA}}{168.2 = \text{M.W. of HDI}}$) upon reaction with

NMA, the mean recovery was 102%. This indicates that the filters quantitatively trapped the HDI vapors and that the urea was subsequently recovered without loss.

The quantitation limit at a detector range of 0.05 AUFS was 2 ng of HDI-NMA. If the HDI-NMA was dissolved in 4 mL of methanol, then the sensitivity of the method would be 0.16 µg/sample. This corresponds to an air concentration of 0.016 mg/m³ or 0.0023 ppm in a 10 L air sample. This is well below the 1978 Threshold Limit Value for 2,4-toluene diisocyanate (TDI), the most toxic of the diisocyanates, which is 0.02 ppm. Relatively straightforward improvements in analytical procedures should further reduce the quantitation limit by a factor of 10.

VI. RECOMMENDATIONS

This research has clearly shown the viability of the proposed sampling technique for diisocyanates. With additional development a valuable monitoring method should emerge which allows the evaluation of airborne exposures to personnel working with diisocyanates. To reiterate, the advantages of the proposed technique with respect to existing methods are:

TABLE 1
HDI-NMA RECOVERED FROM IMPREGNATED FILTERS
AND IMPINGER SOLUTIONS (ND = not detected, <0.1 µg)

<u>No</u>	<u>Sample Type</u>	<u>HDI-NMA Found (µg)</u>	<u>% Recovery</u>
1	Filter	19.3	110
	Impinger	ND	
2	Filter	17.8	101
	Impinger	ND	
3	Filter	17.0	96.6
	Impinger	ND	
4*	Filter	ND	
	Impinger	ND	
5*	Filter	ND	
	Impinger	ND	

*Control

- 1) The method should be appropriate for either aliphatic or aromatic diisocyanates,
- 2) The method should collect the airborne diisocyanates as either aerosols or vapors,
- 3) The method can differentiate the urea formed in the sampler from amines and other potentially interfering compounds, and
- 4) The sampler is simple, employs no liquids and is compatible with existing personal sampling equipment.

Additional research should be performed to validate the proposed method for HDI and other isocyanates used by the Air Force. Points which should be included in this validation program are:

- 1) Further evaluation of the method with HDI:
 - a) Test the sampling method with dynamic test atmospheres of HDI for both long and short-term sampling intervals,
 - b) Determine whether humidity influences the collection characteristics of the sampler,
 - c) Determine the storage stability of the samplers and the ureas after collection,
 - d) Determine the absolute sensitivity of the analytical procedure,
 - e) Streamline the chromatographic analysis to reduce the time required to elute NMA from the column, and
 - f) Collect samples during actual exposures to ensure that compounds present in the environment do not interfere with the method.
- 2) Evaluation of the method for other diisocyanates:
 - a) Synthesize and characterize the ureas produced upon reaction of the diisocyanates with NMA,
 - b) Evaluate the procedure with each compound as suggested for HDI (above), and
 - c) Determine whether those diisocyanates which are predominantly present as aerosols behave as predicted upon collection.

REFERENCES

- 1) K. Marcali, "Microdetermination of Toluene diisocyanates in Atmosphere," Anal. Chem., Vol 29, pp 552-558, 1957.
- 2) K.E. Grim and A.L. Lynch, "Recent Isocyanate-In-Air Analysis Studies," Am. Ind. Hyg. Assoc. J., vol 25, pp 285-290, 1964.
- 3) D.W. Meddle and R. Wood, "Apparatus for Preparing Standard Aerosol Atmospheres," Chem. and Ind., vol 47, pp 1635-1637, 1968.
- 4) D.W. Meddle and R. Wood, "A Method for the Determination of Aromatic Isocyanates in Air in the Presence of Primary Aromatic Amines," Analyst, vol 95, pp 402-407, 1970.
- 5) J. Keller, K.L. Dunlap and R.L. Sandridge, "Determination of Isocyanates in the Working Atmosphere by Thin-Layer Chromatography," Anal. Chem., vol 46, pp 1845-1846, 1974.
- 6) K.L. Dunlap, R.L. Sandridge and J. Keller, "Determination of Isocyanates in Working Atmospheres by High Speed Liquid Chromatography," Anal. Chem., vol 48, pp 497-499, 1976.
- 7) S.P. Levine, J.H. Hoggatt, E. Chladek, G. Jungclaus and J.L. Gerlock, "Determination of Aliphatic Isocyanates in Air by a Liquid Chromatographic-Fluorescence Technique," Anal. Chem., vol 51, pp 1106-1109, 1979.
- 8) D.J. David and H.B. Staley, Analytical Chemistry of the Polyurethanes, vol XVI, Part 3, New York (Wiley-Interscience, 1969), pp 215-217.
- 9) J.H. Saunders and K.C. Frisch, Polyurethanes Chemistry and Technology Part I Chemistry, New York (Interscience, 1962), pp 173-180.
- 10) C.R. Hastings-Vogt, C.Y. Ko and T.R. Ryan, "Simple Ureas Derived from Diisocyanates and their Liquid Chromatography on a 5-cm Column," J. Chromatog., vol 134, pp 451-458, 1977.

1979 USAF - SCEEE SUMMER FACULTY RESEARCH PROGRAM

Sponsored by the

AIR FORCE OFFICE OF SCIENTIFIC RESEARCH

Conducted by the

SOUTHEASTERN CENTER FOR ELECTRICAL ENGINEERING EDUCATION

FINAL REPORT

CIVILIAN APPRAISAL SYSTEM

Prepared by:	Jane Ann Rysberg
Academic Rank:	Assistant Professor
Department and University:	Psychology, The Ohio State University
Research Location:	Human Resources Laboratory Brooks Air Force Base, Texas
USAF Research Colleague:	Lt. Col. F. Ratliff Capt. J. Guerrieri
Date:	August 31, 1979
Contract No:	F49620-79-C-0038

CIVILIAN APPRAISAL SYSTEM

BY

JANE A. RYSBERG

ABSTRACT

The Civilian Appraisal System was conceived by the Civil Service Reform Act of 1978. Its birth place for the Air Force's Civil Service population is the Human Resources Laboratory, Brooks AFB. Appraisal has come to mean an objective description of performance which can be used for evaluations promotion actions, and recommendations for bonuses or specialized training. The creation of the Appraisal System requires the combined talents of educators, psychologists and human factors engineers, as well as the support and technical expertise of mathematicians, and computer and media specialists. The labors of this diverse population have been divided into modules based on the purpose of a specific aspect of the System. As the Civilian Appraisal project is ongoing, the following report is composed of a brief introduction to the need for the project, its present structure, and a specific look at the integrated work of the Appraisal personnel as it provided a basis for work done under the Summer Fellowship.

ACKNOWLEDGEMENTS

The author would like to thank the Air Force Systems Command and the Air Force Office Of Scientific Research for providing her the opportunity to spend a most worthwhile and interesting summer at Brooks Air Force Base. Special acknowledgement is also due to the Southeastern Center for Electrical Engineering Education and Dr. R.N. Miller for a well-organized program.

Finally, she would like to thank Col. T. Newton, Col. F. Ratliff, Capt. J. Guerrieri and Mr. T. Watson for numerous helpful discussions and guidance, and for providing a working atmosphere which enabled the author to expand her horizons considerably.

I. INTRODUCTION:

The Civil Service Reform Act of 1978 mandated a change in the philosophy and methodology of the evaluation of civilian job performance. The need for change in Civil Service job appraisals was multiply determined, but the major impetuses appear to be:

- a) a failure of past systems of evaluation to discriminate good and poor employees.
- b) a general inflation of evaluations caused by/due to the lack of discriminability.
- c) a reliance on subjective judgements in the evaluation process.

The new system of evaluation will provide an accurate assessment of job performance which can be used as a referent for both positive and negative personnel actions. This new system will be implemented on a staggered basis, with divisions based on purpose. First to be on line will be job appraisals for the Senior Executive Service (GS 16 to 18 and Executive levels IV and V), in October 1979. October 1981, performance appraisals will be workable for all other Civil Service employees. The system of monetary rewards, Merit Pay, will be implemented in the evaluation mode six to twelve months prior to the latter date.

The Human Resources Laboratory (HRL), Brooks Air Force Base was charged with the creation of this system for civil servants employed by the Air Force. The project was divided into four modules, EBO, POT, OT and E, and Merit Pay.

EBO (Evaluation By Objectives)

Module one dealt with the creation of the performance appraisal system. The underlying assumptions of the appraisal system were defined by the Reform Act. The embodiment of the demand for objectivity and interaction was called a work plan. A work plan

would result from a meeting between an individual and his/her supervisor to establish on-the-job-objectives. This would begin a rating cycle. The termination of the cycle would be marked by a performance appraisal based on work plans, and supported by an interview and possibly a written evaluation. As this work plan was more than a new rating form, the appraisal module also included planning for training to use the system.

POT (Potential and Promotion)

Another aspect of a work situation is vertical movement. How could the new kind of information about job performance be used in promotion decisions? As the work plan system is an ipsative one, what other types of information must be gathered to predict performance in a higher level job? What weightings should be given to these various types of information? Would a single promotion formula be appropriate across the job families, and levels of Civil Service or would different variables describe promotion potentials for file clerks as opposed to middle level managers? These were the types of questions addressed under module two.

OT and E (Operational Testing and Evaluation)

Module three was charged with measuring the impact and the validity of the entire appraisal system on the Civil Service population. As the system will be implemented in layers, OT and E will be the last module to be activated. It is still unsettled as to whether testing should occur on a modular basis, or on the basis of the whole implemented system, or should proceed using simulation techniques.

Merit Pay

The system of distributing monetary bonuses based on performance evaluations will be called Merit Pay. This bonus system is faced with some definitional problems, a major one being what level of work plan evaluation should be considered "meritorious"? Module four also appears to be facing problems with the receptivity of the target population.

Under past methods of dispensing incentives, significant percentages of individuals received bonuses. This is unlikely to continue under the Merit Pay System. How can the possible problem of demotivation be handled?

II. OBJECTIVES:

During the pre-summer visit it was determined that I would work on the statistical analyses of data from a pilot study. The study had used as stimuli the Job-Worker-Characteristic Survey. This would have placed me in the POT module.

By the time of my arrival at Brooks Air Force Base for my summer tenure, there had been a large increase in the share of the responsibility for implementation of the Civilian Appraisal System to be borne by HRL. It was therefore decided that I would rotate through the modules. The objectives were unique within each module.

Module One

- 1) to suggest methods of evaluating the performance appraisal system as it applied to the Senior Executive Service (SES)
- 2) to develop a set of questions addressing the impact of implementing the workplan system for non-SES civil servants

Module Two

- 1) to broaden the data base concerning the acceptance of certain possible measures of potential by the Civil Service population.

Module Three

- 1) to consider the possible impact of presently uncontrolled variables after full implementation of the appraisal system

Module Four

- 1) to suggest techniques for evaluating the impact of the new bonus system

III. Module One - A

There are several problems implicit in an assignment to evaluate the Senior Executive Service. First, what is the definition of "to evaluate"? A multiple definition of evaluation was adopted. This necessitated a research package which would measure the impact of the new appraisal system, as well as the accuracy of the use of the system.

Second, who is the target population of this attempt to evaluate the appraisal system? Although the workers supervisor dyad is the focus of the creation and usage of a work plan, a Review Board will also be involved in the evaluation process. A plan to evaluate the usage of the appraisal system for SES, must assay the participation of workers, supervisors and members of the Review Board. When attempting to measure the impact of the system one assumption must be kept in mind; work performance of a target individual is likely to be modified due to two by-products of the work plan system. These by-products are clarification of responsibility and presentation of a method of self-collecting job performance data. Will modifications in performance be obvious to supervisors? Will work relations between a worker and supervisor, or a supervisor and his/her peer be altered? Will the output of an executive's organization change in association with hypothesized changes in work style? In view of these possibilities, measures must be taken of the Senior Executives themselves, their supervisors and their work force.

The research package as it was finally envisioned included a series of questionnaires tapping creation and use of the work plan as well as assessment of the work climate. Specific questionnaires were written for the Senior Executives, their staff members and members of the Review Boards. In addition, it was suggested that pre- and post- output be collected. The draft questionnaires, a list of possible variables of interest, and a suggested analysis plan for the questionnaires can be

found in Attachment I.

Module I - B

A member of the EBO work group once declared that one of his goals was to create "the perfect appraisal system". This did summarize the focus of the group - the system.

A system, must however, interface in some areas with the population it is to serve. A set of pilot studies were needed which could point to aspects of system implementation which might be problematic. My reading of work to the summer indicated that needed areas of investigation were:

- 1) a test of non-theoretical aspects of the system, for example, the time to be allowed if completed work plans are to be mailed into a central grading site.
- 2) a collection of validity variables against which to grade the final evaluations
- 3) a method of grading work plans
- 4) a method of assessing system acceptance prior to implementation as a strongly negative attitude among the target population would imply a need for a public relations campaign prior to training
- 5) a method of evaluating the effectiveness of training, where effectiveness was defined both as retention of facts for a specified amount of time, and the ability to use this information as shown by creation of a work plan
- 6) a method of assessing the necessity of training all user of the system

Item One could be completed competently only by an economic analyst. Due to the diversity of jobs within the job families of Air Force Civil Service, data in response to Item Two should be gathered by job analysts.

A prototype method of grading work plans was created as a partial response to Item Three. Mildly trained graders found the work plan score sheet easy to use. Transfer of data to computer cards could also be smoothly accomplished using the prototype.

The question of acceptability was refined into questions on acceptabilities of the philosophy of the system, of the use of the

system, and of training to use the system. These points were addressed in a series of questionnaires designed to be administered at different points in the implementation process.

Items Five and Six were collapsed, and addressed in a single experimental design. The questionnaires, work plan score sheet and proposed research strategies are found in Attachment a.

IV. Module Two

In the POT module, one goal is creation of an algorithm predicting promotibility. This algorithm would be a regression formula which captured the relative importance given to specific variables by a promotion panel composed of experts from a particular job series. Prior to summoning job experts together, a flock of variables of possible interest are being collected. "Variables of Interest" are operationally defined as a source of information about job-relevant skills which is acceptable to members of the Civil Service community. For example, it might be discovered that personality trait x is very predictive of success in a particular job, however, if most workers objected to providing this personality data, trait x would not be considered as a variable of interest.

One method of gathering variables is to interview samples from the Civil Service population. This can be an efficient methodology, as workers are assumed to have simultaneous knowledge of job skills, and of their willingness to provide certain types of information.

Interviews were carried out at McClelland, Norton, and Patrick Air Force Bases. Most interviewees also took a pilot version of a job knowledge test (Civilian Personnel Exam, CPE) and a survey of job-related attitudes (Job Worker Characteristics Survey).

I was asked to go to Patrick AFB, as one of two interviewers. The use of two interviewers, one of them female was only the first of a set of changes made in this data gathering as opposed to previous attempts.

All changes reflect a desire for more rigorous quantification of the data.

Other changes in the methodology were:

- 1) a structured interview; open-ended interviews had been used previously
- 2) an attempt to control for possible age, sex, and status effects
- 3) a different technique for creating the subject groups

Also novel was the use of numerical presentations for the results of the interviews, and the comparisons of present to previous data. The trip report from the Patrick effort is Attachment 3. This researcher was responsible for the Methods, Discussion and Attachment sections.

V. Module Three

Operational Testing and Evaluation, and Merit Pay are the two modules which have received the least energy. In the case of OT & E this is partly due to its place in the chronology of implementation. Also, both OT & E and Merit Pay are awaiting certain policy decisions from within the Air Force hierarchy which will effect the structure of these two modules when implemented.

Although the physical labor on OT & E has been slowed, there is still some activity in the module. As in the beginning of any research project, this is the "activity of initiation", or a review of the literature. It is safe to assume that there have been no job performance appraisal systems as large as the Civil Service Appraisal System, much less an evaluation and testing of such a system. However, other large measurement systems exist which could serve as models both in methods of evaluation as well as in impact of the system on its target population. The problem was to select measurement systems with analogies in form or function to the Civilian Appraisal System, and to study the planned and unplanned changes in these existing systems. It was then possible to speculate on the future of the implemented Civil Service evaluation system, by looking at the

longitudinal changes in the models. The possible outcomes, as suggested by this investigation, are described in Attachment 4.

VI. Module Four

Whereas the previous modules were significant opportunities to manipulate research designs, the Merit Pay module is the greatest intellectual challenge. Modules one through three used skills possessed by psychologists, but module four is what psychologists do. Psychology is a science which treats organisms and their activities, especially in relation to a physical and social environment. Merit Pay has the potential to change the work environment of the managers/supervisors in the Civil Service population. This environmental change would not be the result of physical manipulations, but of modifications of the work attitudes and perceptions of the target individuals.

Merit Pay could be used as a motivational system by making the tie between performance and reinforcement more apparent. This more strengthened linkage is all but built into the Civilian Appraisal System due to the ipsative nature of the work plans. Further, subject anticipation could be gained by active involvement in creation of a reinforcement selection plan. This would be an expedient use of a bonus distribution plan, as Merit Pay is, as it could serve two purposes.

- 1) Motivational. Work by Premack and associates (1969) has demonstrated increased motivation, as measured by, for example, increases in total numbers of completed work products, when Ss were allowed to select reinforcers and/or the reinforcement schedule.
- 2) Perceptual. Some research has demonstrated changes in perceptions of the work place, such that workers see themselves as having more control over their environment. Correlational analyses suggested a relationship between a perception of control and active participation at work (white, 1960).

This perceptual-motivational combination could hallmark a change in the profile of Civil Servants' work attitudes. However, the focus of a

Merit Pay process has not been determined. Merit Pay could be used as a measurement system, similar to other aspects of the Civilian Appraisal System. In Attachment five the measurement vs. motivational prospects of Merit Pay are briefly described; different evaluation of impact studies methodologies are also sketched.

VII. Recommendations

My research designs and analogies for modules one through three are basically completed; they await modifications necessitated by the particular point in the Civilian Appraisal System at which they are used. Module four is still in a sufficient state of flux that more input is possible here than in the previous modules. My major recommendation must be to define the purpose of the Merit Pay System according to a consciously selected outcome among the population. Once the purpose has been described the structure of the Merit Pay System can be created based on literature available in areas such as work attitudes, and reinforcement and motivational theory, and pilot research designed specifically for the unique position of the Air Forces Civil Servants. A mini-grant proposal will shortly be submitted to AFOSR that addresses the motivational possibilities of subject involvement in an incentive system, which Merit Pay is.

My second major recommendation must be for the continued support and even enlargement of the Summer Fellowship program because of the tremendous enrichment received by this summer Fellow by her experiences at the Human Resources Laboratory.

REFERENCES

1. Good, T.L. & Brophy, J.E. Teacher-student relationships. New York: Holt, Rinehart and Winston, 1974.
2. Premack, D. Toward empirical behavioral laws:
I. Positive reinforcement, Psychological Review 1969, 66, 219-233.
3. Rist, R.C. Student social class and teacher expectations: The self-fulfilling prophecy in ghetto education. Harvard Educational Review, 1970, 40, 411-451.
4. White, R.W. Competence and psychological stages. In M.R. Jones, ed., Nebraska Symposium on Motivation, 1960. Lincoln: University of Nebraska Press, pp. 97-141.

Possible Organizational Variables of Interest:

Person hrs// persons directly employed

Phases completed in ongoing projects

projects completed

projects initiated

Computer time used

Outside consultants utilized

Office supply count (i.e., reams of paper, typewriter ribbons, xerox #)

Project sites visited

Presentations (professional) given

Implements: created, redesigned, new use

Techniques: created, refined, new use

Forms: shortened, created

Combined # of committee appointments

Meetings sponsored

Outside agents entertained

"Campaigns" initiated/completed

Tonnage of waste products

Obtained funding/approval for a new program

Wrote/implemented/passed new regulation

**THIS PAGE IS BEST QUALITY PRACTICABLE
FROM COPY FURNISHED TO DDC**

QUESTIONNAIRES -

Areas Tapped:

Format

Aid to review?

"Fair"

"Valuable" - serves purposes of -
Individual difference observed.

Scorability

Validity

Training impact.

Analyses -

- 1) Pearson Product Moment - 1) internal consistency
2) reliability

- 2) Canonical Correlation - condensation

Worker

Creation/dissemination of goals

1, 3, 4, 8, 9, 11, 13, 14

Implementation

2, 5, 6, 7, 10, 12

Affect

15

Reliability

Neg - 2, 4, 5, 8, 11, 13, 15

Pos - 1, 3, 6, 7, 9, 10, 12, 14

Executive

Creation/dissemination of goals

1, 5, 11, 7, 15

Implementation

3, 14, 8, 12, 4

Training

2

Format

10, 6

Scoring

9, 13

Reliability - Neg - 5, 11, 2, 9

Review Board

THIS PAGE IS NO QUALITY PRACTICABLE
FROM COPY FURNISHED TO DDG

Format

G: 1, 5, 10; S 2, 3

Scoring

G 6, 7, 8, 3, 16, 12; S 6, 9

Training

G 2, 11, 14; S 13

Goals

G 4, 9, 15, 13; S 8, 10, 11, 15

Validity

S 1, 4, 7, 12

Reliability - Neg -

G 10, 8, 11, 3, 14, 9, 13

S 7, 11, 5, 9, 12

WORKERS' QUESTIONNAIRE

The rating scale to be used in responding -

never seldom sometimes usually always

1. My supervisor makes work goals clear to the staff.
 - a. never
 - b. seldom
 - c. sometimes
 - d. usually
 - e. always
2. My supervisor does not criticize poor work (i.e. work not up to set standards; work not conforming with work plans).
3. My supervisor assigns staff members to particular tasks.
4. My supervisor works without a plan.
5. My supervisor does not maintain definite standards of (acceptable) performance.
6. My supervisor emphasizes the meeting of deadlines.
7. My supervisor encourages the use of uniform standards (of performance).
8. My supervisor presents work plans which are difficult to understand.
9. My supervisor makes sure that my part in the organization is understood by all members.
10. My supervisor asks that staff members follow standard rules and regulations.
11. My supervisor does not let staff members know what is expected of them.
12. My supervisor sees to it that staff members are working up to capacity.
13. My supervisor refuses to explain the work plan.
14. My supervisor sees to it that the work of staff members is coordinated.
15. It is unpleasant to be a member of this staff.

Demographics -

sex

age - blocked

race

yrs in CS

yrs in this job

worker X supervisor

SES QUESTIONNAIRE PART I

AGREE/DISAGREE FORMAT

1. I make work goals clear to the staff.
2. I have been penalized by inadequate training in the use of SESAP.
3. I criticize poor work (work not up to set standards; not conforming with work plans).
4. I ask that staff members follow standard rules and regulations.
5. I do not assign staff members to particular tasks.
6. Use of the work plan system has made visualization of my job requirements easier.
7. I let staff members know what is expected of them.
8. I emphasize the meeting of deadlines.
9. The scoring of the SESPA would be more subject to personal biases than other appraisal systems.
10. The format of the SESPA made it easy to describe my job.
11. It is unlikely that everyone's part in the organization is understood by all members.
12. I encourage the use of uniform standards.
13. The system of work plans is a better method of performance appraisal than past methods.
14. I maintain definite standards of (acceptable) performance.
15. I see to it that the work of staff members is coordinated.

SES QUESTIONNAIRE PART II - BEHAVIORAL

Format - check those that apply

Included on my SESPA were my:

- 1) Name
- 2) Title
- 3) Rating official
- 4) SS#
- 5) Organization

On the function/program performance subsection of my SESPA there was

- 1) a priority weight assigned
- 2) at least one performance requirement

On the individual performance subsection of my SESPA there was

- 1) a priority weight assigned
- 2) at least one performance requirement

Yes/No

Do the priority weights of the three areas sum to 100?

Have you assigned at least one critical element?

Does each performance requirement contain a

- 1) quantifier
- 2) action
- 3) date
- 4) . . .

ALL INFORMATION CONTAINED
HEREIN IS UNCLASSIFIED
DATE 10-10-2001 BY 1043

**QUESTIONNAIRE - REVIEW BOARD - GENERAL
AGREE/DISAGREE FORMAT**

1. The format of the SESPA makes it easy to read.
2. There has not been a great difference in the quality of the work plans I have read.
3. I could envision a superior method of job appraisal than the work plan system.
4. The SESAP is a good vehicle for comparing the performance of one executive with another.
5. Use of the SESPA makes it easy to visualize jobs with which I am unfamiliar.
6. The format of the SESPA makes it easy to score.
7. The scoring of the SESPA is less subject to personal biases than other rating forms I have used.
8. Individuals with poor writing skills but good job performance may be penalized by the use of SESPA.
9. The SESAP is not suitable for setting future pay rates.
10. The use of the SESPA has not made it easy to visualize jobs with which I am unfamiliar.
11. Errors in completion of the SESPA result from the inadequate training the writer received.
12. The SESAP is a time efficient method of performance appraisal.
13. The SESAP is not a suitable basis for initiating personal actions.
14. The SESAP would be an efficient method of performance appraisal if I, as a reviewer had received more (better?) training in the use of the system.
15. The SESAP provides a vehicle for the expression of management performance goals.
16. The system of work plans is a better method of performance appraisal than past methods.

WHEN PREPARED BY QUALITY PRACTICABLE
FROM COPY FURNISHED TO BDC

**QUESTIONNAIRE - REVIEW BOARD - SPECIFIC
AGREE/DISAGREE FORMAT**

1. This individual's score on the SESPA corroborated other available evidence.
2. This individual used quantified terms in the job description.
3. This individual's work plan appeared attainable yet challenging.
4. This individual's score on the SESPA corroborated my general impression of this person's performance.
5. This individual's SESAP does not provide the information needed to initiate a personnel action.
6. It was easy for the Review Board to achieve consensus on this individual's performance appraisal.
7. This work plan did not describe the job as I know it.
8. This individual's work plan provided the necessary information to compare this performance with that of another executive.
9. The performance appraisals take place at too infrequent intervals to be a good job evaluation/feedback system.
10. The individual's SESAP provided the type of information needed to set future pay rates.
11. This individual's SESAP did not express management performance goals.
12. A focus on organizational results is not a valid method of assessing an executives individual performance.
13. The construction of this work plan indicated that the executive fully understood the new appraisal system.

THIS PAGE IS BEST QUALITY PRACTICABLE
FROM COPY FURNISHED TO DDC

ATTACHMENT 2

PILOT TESTS

To accomplish:

- 1) Test of system: i.e., cost, goodness of forms used, type of snags/questions likely to occur, # of personnel needed, time consumption body movements...**
- 2) To Evaluate Method of Grading Work Plans: time consumption, goodness of proposed grading method, # of persons needed, amount of time needed to achieve desired level of inter-rater reliability, ease of data transfer to computer storage**
- 3) Collection of Validity Variables: for eventual "grading" of system check existence of proposed variables, feasibility of collecting same**
- 4) Acceptance of System: Casual data from pre-test situations suggested that initial acceptance of the appraisal system was low. These negative sentiments were apparently spread throughout the ranks of supervisors and employees. A new aspect of the project must be "selling the system". Need to judge the impact of this huckstering**
- 5) Training of employees: The question has arisen; as creation of work plans is a joint supervisor-worker venture, is the supervisor a trainer for his/her group of workers, making the training of these employees redundant? Test.**
- 6) Efficiency of Training: Is transmission of desired/central information being accomplished with present training techniques?**

Introduction

Employees outnumber supervisors by an estimated 15 to 1. This means that the training of the employee population is

comparatively more expensive than that of the supervisor population in terms of real money, work hours and fringe educational costs (duplicating, etc.) In addition, it is possible that employees will transfer a reliance on a supervisor from the work place to the educational situation making their attention to training in the appraisal system cursory. If this is the case, training of employees is expensive indeed.

A l'autre main, if training of both an employee and supervisor produces more than an additive effect (i.e., a trained supervisor-worker pair produces a work plan which is more than twice as good as that produced by an untrained pair), then measures should be taken to maximize the opportunity for all supervisors and employees to attend all aspects of training.

In addition to the question of relevance to specific subpopulations, there is the issue of the efficiency of the training for all populations. Efficiency will be defined as the transmission of desired/central information as measured by use and/or testing. Information pertinent to both questions can be addressed by a set of two interlocking studies.

Subjects

Experiment I

A representative sample of WG and CS employees will be assigned in a predetermined random order to one of four experimental groups. Equal age and sex distributions among groups probably cannot be achieved, but the distributions will be noted for possible statistical partialling.

The groups created will be:

Group	<u>n</u>	Time 1	Time 2
TT	100	received training	tested
NT	100	did not receive training	tested
NN	100	did not receive training	not tested
TN	100	received training	not tested

The dependent measure for all groups will be the goodness of the work plans created. In addition, all employee subjects will be asked to fill out a personal description checklist upon handing in the completed workplan (i.e., time on job, time under present supervisor, desire for promotion).

Experiment II

Two representative groups of supervisors will be assembled, including a variety of CS levels. Each group ($n = 75$) will be self-contained on non-adjacent bases.

Group I will receive a knowledge questionnaire on the appraisal system two weeks prior to the training session. A knowledge test will also be administered at the close of training, prior to the creation of a work plan.

Group II will receive the pre- and post-questionnaire on the same time schedule as Group I. No training will be given.

Materials

To create the questionnaire, a large pool of recognition items tapping knowledge of the appraisal system will be created. The items will be divided into four equal sized groups, so that two alternate forms of both pre and post test result. The split-half technique or KR-20 will be used to assess reliability of alternate forms.

The alternate forms of both pre and post tests will be given to randomly predetermined halves of Group I and II. The alternate forms of the post

test will also be administered to randomly predetermined halves of groups TT, and NT, experiment I.

Analyses

An ANOVA will be computed on the group means from experiment I as the a priori measure. The Scheffe' will be used a posteriori.

The relative mean performances of trained vs. untrained employees is the comparison of major interest, however, other variables may effect the creation of a suitable work plan. For example, the ability of individuals to benefit from any training, or the supervisor-employee relationship are possible variables of interest. Therefore, groups will be collapsed and a Pearson-Product Moment will be run between work plan scores, and the personal description measures.

To examine the efficiency of training, the mean knowledge test performances of groups TT and NT, experiment I will be examined, as well as the mean difference scores of groups I and II, experiment II. Knowledge test scores will not be compared between experiments I and II, although identical testing and training procedures were used, as different standards of knowledge might be regarded as adequate for employees and for supervisors.

Comments

It may seem that this design has been constructed on a philosophy of needless expense, particularly if one ponders the inclusion of group NT, experiment I. The strong suggestion from mathemagenic literature, however, is that testing, is a learning experience. In a situation in which the efficiency of training will ultimately be measured in a life situation, it would seem prudent to "err" on the side of design conservatism

Work Plan Checklist

Please mark 0 or 1, indicating absence or presence, except where otherwise indicated

Introductory Materials

____ Name
____ SSN
____ Job Title
____ AFSC
____ Org

Closing Materials

____ Signatures: Ratte
____ Rater
____ Reviewer
____ Dated: Ratte
____ Rater
____ Reviewer

Dominant Elements

____ Total number of Dominant Elements
____ Dominant Element number
____ Total number of Performance Standards at present Dominant Element
____ Performance Standard number
____ Verb, active=1, passive=0
____ Verb, observable=1, unobservable=0
____ Quantifier
____ Anchor Noun
____ Single behavior described
____ Priority points assigned
____ Method of testing employed
____ Performance Standard related to Del, year 1, 1990

____ Dominant Element number
____ Performance Standard number
____ Verb, active=1, passive=0
____ Verb, observable=1, unobservable=0
____ Quantifier
____ Anchor noun
____ Single behavior described
____ Priority points assigned
____ Method of testing employed
____ Performance Standard related to Del, year 1, 1990

____ Dominant Element number
____ Performance Standard number
____ Verb, active=1, passive=0
____ Verb, observable=1, unobservable=0
____ Quantifier
____ Anchor noun
____ Single behavior described
____ Priority Points assigned
____ Method of testing employed
____ Performance Standard related to Del, year 1, 1990

____ Priority points sum to 100
____ At least one Critical Element identified

THIS PAGE IS BEST QUALITY PRACTICES
FROM COPY FURNISHED TO DDC

INTRODUCTION

Every postal person knows that over-coming rain, snow and dead of night does not ensure swift completion of the appointed route. There are also angry dogs, cracks in the sidewalk and amorous housewives. Analogously, the perfect Civilian Appraisal System (CAS) is not enough; one must consider the perceptions of the system as held by the designated population. Particularly important to the successful implementation of the CAS might be its acceptability and credibility among potential users. Acceptability will be defined as an attitude indicating willingness to use the system as it stands. Credibility will define an attitude of trust in the system; do workers and supervisors believe the CAS to be capable of accomplishing its goals and only its goals (i.e., no hidden uses). Not to be forewarned of the direction of these attitudes prior to implementation might result in a Rosenthal and Jacobson-type (1968) "expecting^{ancy} effect" (the acting out of certain preconceptions to the detriment of the process).

Investigations in this area have specialized requirements:

- 1) objective scoring of subjective events (attitudes)
- 2) sampling techniques which will give as broad an opinion base as possible
- 3) capability of longitudinal usage, so trends can be detected
- 4) capacity for comparing responses of various subpopulations
- 5) simplicity of collection, tabulation and analyses. These

requirements are best met by the use of a questionnaire. A further refinement on the solution would be use of a series of questionnaires, as this would shorten the length of forms encountered by a simple S, and would ease the collection of

comparative data.

Acceptance

Acceptance could refer to either acceptance of content or acceptance of structure ("Well, S/he's got a great personality "vs. "S/he's beautiful but dumb"). We are interested in both aspects.

Subjects

Representative samples of WG and CS employees will be identified. Diversity in age and sex will be sought in the samples. Self-contained samples should be on non-adjacent bases. Samples will be divided into two groups based on past experience with CAS. One group will be composed of naive Se, while group two will consist of individuals who received CAS training.

Materials

Both groups one and two will receive questionnaire B, CAS acceptance and credibility. Only group two will receive questionnaire A, CAS training acceptance.

Analyses

Frequencies will be run for the responses to both questionnaires A and B. Questions from questionnaire A will be grouped according to area (i.e., course effectiveness, media effectiveness, study environment etc.) and a multiple R calculated between each cluster and the omnibus acceptance score. Omnibus acceptance scores will also be compared for subpopulations (ex. workers vs. supervisors, males vs. females, etc.).

For each individual receiving questionnaire B, a mean attitude score will be created. A negative number will indicate a basically negative attitude, whereas a positive score will indicate a positive attitude. The relative weight of scores will not be considered (i.e., a +3 will

not be one erg more positive than a score of +2) as no attempt will be made to ensure that the agree-disagree response format is cognitively anchored to an absolute zero point. The ratio of number of negative scores to the number of positive scores will be compared between the previously trained, and the naive groups. This will, of course, settle the debate as to the veracity of the adages, "To know him is to love him" "vs." "Absence makes the heart grow fonder" in relation to CAS ~~training~~ ^{training}.

A comment section will be included on questionnaire B. Three independent raters, blind to the purpose of the survey will categorize the free comments. If inter-rater agreement is less than 2/3, comment category placement will be settled by a fourth, non-blind rater.

THIS PAGE IS BEST QUALITY PRACTICABLE
FROM COPY FURNISHED TO EDC

COURSE ACCEPTANCE

Agree - Disagree Format

1. During the course, I learned everything about the civilian appraisal system that I will need to know.
2. The materials used in the course were so simple that they were an insult to my intelligence.
3. Too many technical (unexplained) terms were used in the course.
4. I have no understanding of why I should use the civilian appraisal system.
5. I think others of my general background will benefit from taking this course.
6. The objectives of the course were clearly stated.
7. The language used in instruction was so difficult that I was unable to understand much of the course.
8. The learning strategy used in this course (rule-example-practice?) is a good way to teach about the civilian appraisal system.
9. This course was given at a bad time of day.
10. The classroom ventilation was about right.
11. I found the slide presentations (films, video tape presentations, etc) entertaining and enjoyable.
12. The way the instructional content was presented was not appropriate for this kind of subject matter.
13. I do not feel that the course achieved its objectives.
14. This course made me feel confident about using the civilian appraisal system.
15. This course was full of useless details.
16. The course objectives were appropriate.
17. Seating arrangements allowed me an unobstructed view of the instructor.
18. I think the course was a waste of time.
19. The slide presentations (films, video tape presentations, etc) used in this course were effective in getting the material across.

20. The noise level around the classroom distracted me from the program.
21. I liked the type of presentation used in this course.
22. The room was not dark enough for audio-visual presentations.

THIS PAGE IS BEST QUALITY PRACTICABLE
FROM COPY FURNISHED TO EDC

COURSE ACCEPTANCE (Continued)

- 1) The amount of time provided for responding to practice work plans was
 - a. Far too short
 - b. Too short
 - c. Just about right
 - d. Too long
 - e. Far too long
- 2) The depth of coverage in this course was
 - a. Far too little
 - b. Too little
 - c. Just about right
 - d. Too much
 - e. Far too much
- 3) The number of concrete examples given during instruction was
 - a. Far too few
 - b. Too few
 - c. Just about right
 - d. Too many
 - e. Far too many
- 4) The amount of time spent covering the material was
 - a. Far too short
 - b. Too short
 - c. Just about right
 - d. Too long
 - e. Far too long

THIS PAGE IS BEST QUALITY PRACTICABLE
FROM COPY FURNISHED TO DDC

5) The amount of material covered in the time period was

- a. Far too short
- b. Too short
- c. Just about right
- d. Too long
- e. Far too long

THIS PAGE IS BEST QUALITY COPY AVAILABLE
FROM GPO. FORD BELL 20-220

Rating against a scale

THE INSTRUCTOR

Effective	_____	Ineffective
Knowledgeable	_____	Ignorant
Boring	_____	Interesting
Organized	_____	Disorganized
Unsure	_____	Confident
Convincing	_____	Unconvincing
Unprepared	_____	Prepared
Encouraged	_____	Discouraged
Criticized	_____	Praised
Patient	_____	Impatient
Considerate	_____	Inconsiderate
Hinders	_____	Helps
Friendly	_____	Unfriendly
Fair	_____	Unfair
Humorless	_____	Humorous

(Handouts, A-V Presentations, Books taken as a whole)

COURSE MATERIALS

Ineffective	_____	Effective
Boring	_____	Interesting
Concise	_____	Repetitious
Organized	_____	Disorganized,
Convincing	_____	Unconvincing
Hinders	_____	Helps
Clear	_____	Unclear
Efficient	_____	Inefficient
Understandable	_____	Confusing
Comprehensive	_____	Scanty

ACCEPTANCE: CREDIBILITY.

Select 3 items which you feel are most descriptive of the writing of work plans; Place a check mark (✓) before these 3 items.
The writing of work plans will:

- _____ generate a new paperwork burden
- _____ take up little time
- _____ be unfair if there is no work unit to which to charge the time
- _____ have to be done/revised infrequently
- _____ be impossible for jobs with no clear product
- _____ be difficult for supervisors and workers who do not have a close relationship.
- _____ be easy because workers and supervisors are well trained in the system

Select 4 items which you feel are most descriptive of the use of work plans in rating employees; place a check mark (✓) before these 4 items.
The use of work plans for rating:

- _____ will be difficult as the system can be "gamed" quickly (substantially)
- _____ will assist in the removal of poor workers
- _____ does not provide advantages over past evaluation systems
- _____ will assist in the reward of good workers
- _____ will probably not be acceptable to unions.
- _____ is less subject to supervisor biases than other appraisal systems
- _____ will stifle good workers
- _____ is unnecessary as adequate means exist to reward superior workers
- _____ will necessitate record keeping by both supervisors and workers

THIS PAGE IS BEST QUALITY PRACTICABLE
FROM COPY FURNISHED TO DDC

CIVILIAN APPRAISAL SYSTEM - CAS

Agree - Disagree format

1. I do not understand the CAS.
2. The CAS is a fair system of promotion and rating.
3. A supervisor will give workers feedback about their job performance under CAS.
4. The performance ratings in the CAS cannot be influenced by personality factors.
5. It is not possible for supervisors to know how well workers are performing their job.
6. The CAS is not acceptable to me.
7. I had the opportunity to become informed about the CAS and its uses.
8. The CAS can be used by supervisors to produce accurate ratings of performance.
9. A supervisor can use the CAS to show favoritism for certain employees.
10. The use of CAS will make it more difficult to obtain a promotion.
11. Under CAS, supervisors will be held accountable for their ratings.
12. The use of CAS will make it easier to obtain a transfer to a different job.
13. The CAS will provide more objective criteria for evaluating job performance.
14. Under CAS, outstanding performance ratings will only be given to the most deserving employees.
15. The CAS will not reduce the emphasis on subjective supervisory judgments.

disagree disagree NA/ agree agree
strongly no opinion strongly

- a. disagree strongly
- b. disagree
- c. NA and/or no opinion
- d. agree
- e. agree strongly

THIS PAGE IS BEST QUALITY PRACTICABLE
FROM COPY FURNISHED TO DDC

a structured interview; second, the addition of a questionnaire (both attempts at more rigorous quantification); and third, an attempt was made to control for possible sex or status effects on Ss willingness to respond in the interview. A female E was introduced to conduct 50% of the worker sessions. This was done as 86% of the female Ss were workers. The male E conducted all supervisor sessions to ensure ascribed status to the group leader. Fourthly, aware of the effects of a set to respond, the Es were careful to request personal opinions and experiences, as opposed to indicating that Ss were to respond as spokespersons for their occupational group. That Ss adopted the set to respond as individuals is evidenced by the frequency of personal versus collective statements. Statements of the form "a worker..." occurred less than 13% of the time, from a total of 774 statements.

Before proceeding to a discussion of data, some comments on the sample itself must be noted. The mean age of Civil Service employees at Patrick AFB is 49.4 years; therefore, the present attitudes might not be representative of Air Force Base populations, but are representative of the attitudes of civil servants of a particular age and seniority. Also, the original experimental design called for analyses by quadrads (worker, supervisor, co-worker, associate). However, a non-random loss of subjects from co-worker and associate groups precluded this type of analyses. Therefore, only group-by-group comparisons will be described.

Information from this study can be divided into two types: (a) produced by comparison to previous work in the area (Norton and McClellan studies), and (b) unique to this study.

The Norton and McClellan studies were basically descriptive, rather than quantitative, and these descriptions were basically negative. Group sentiments expressed in the McClellan trip report include 29 negative statements, as opposed to eight positive statements. From Norton, a total of 130 statements were collected; twenty-one of these were positive, 33 neutral. If the Patrick AFB data is examined only on negative-positive-neutral splits, in a total of 25 statement areas, (collapsing across Ss) three negative attitudes, nine neutral, and 13 positive were expressed. Could it be that in allowing Norton and McClellan Ss to perceive themselves as spokespersons, they expressed all permutations of possible problems, not their own attitudes, toward the system?

Although the McClellan data can be considered neutral to positive, in comparison of earlier investigations, the negative attitudes must be scrutinized as possible hinderances to system implementation in the Civil Service population. Examination of comments given with negative responses suggests that problems with the system lie in credibility, not acceptance; acceptance refers to a belief that the system can work, that an individual can use the system. Credibility refers to the belief that all individuals can/will use the system. Consider the differences in workers' responses to the question, "Can co-workers accurately rate performance?" versus "Can you accurately rate performance?" The responses were, respectively, 56% Yes, 32% No, 12% no response; 88% Yes, 5% No, 7% no response.

THIS PAGE IS BEST QUALITY PRACTICABLE
NOT TO BE REPRODUCED TO DDC

In perusing the data as provided in Atchs 5 - 7, one observation should be kept in mind: although the opening briefing stressed the use of the appraisal system in promotion, selection for training/retraining, and transfer, Ss overwhelmingly responded to the questionnaire and in the interviews on the promotion aspect. Out of 168 verbal responses across all interview sessions, three non-promotion references were made. Four non-promotion responses were made out of the 744 statements made on the questionnaires. Further research should be conducted to isolate attitudes vis a vis the system and attitudes toward selection for training, etc.

IV. RECOMMENDATIONS

The recommendations in this report are based on evaluation of the test program at Patrick AFB and should be considered for inclusion in any follow-on studies or implementation of an operational system:

A. An advanced publicity campaign should precede any future test program. Articles should be placed in the command and base newspapers citing the need for the research program and an explanation of how personnel selected to participate in the test will be affected.

B. Sample letters, such as the one used at Patrick AFB, should be furnished the Civilian Personnel Office to notify people of their selection and instruct them in their activities.

C. The daily bulletin should be used to remind participants of deadlines and strengthen efforts to have test materials returned to the program manager.

D. Additional announcements from key personnel in upper levels of Air Force management would assist in participant cooperation.

E. Future interviews should be constructed in a formal format with opportunity given for both oral and written responses. The feedback mechanism should permit statistical compilation of the data to clearly establish firm trends in acceptance/rejection of the instruments under study.

F. The Patrick AFB test suggests that approximately one manhour of CPC time was needed for each test subject involved in the experiment. This includes clerical and administrative time. This figure should be used in helping estimate manhours for CPC's involved in future testing.

G. This piece of research specifically addressed acceptance of the new system. Inferences from the data point to problems in credibility. A new research plan could be created to examine this potential problem, as well as other inferential area (i.e., employee age effects and non-promotion acceptance).

THIS COPY IS BEST QUALITY PRACTICABLE
FROM COPY FURNISHED TO DDC

ATTACHMENT 3

Assessment of Attitudes Toward Proposed Civilian Appraisal System

Major John C. Quebe
Dr. Jane A. Rysberg

I. INTRODUCTION

Background

Under Work Unit 7719 14 08, a pilot test program of the instruments under study for a revision of the Civil Service Promotion Potential Module, was conducted at Patrick AFB, Florida. In this test program, a Civilian Personnel Exam (CPE) was administered to 110 Civil Service workers. A Job-Worker Characteristic Rating was completed on each worker by his supervisor, his supervisor's associate, and a co-worker.

Group interviews were held in the Civilian Personnel Offices at Patrick AFB, Florida, on 23 and 24 July 1979 to obtain feedback from the subjects involved in the test program. Major John Quebe (PES) and Dr. Jane Rysberg (PEP) conducted the interviews.

II. METHODS

Subject

The subjects in this study numbered 89, 45 of which were male. The mean age of the Patrick AFB Civil Service population is 49.4 years. As this was an unencumbered random sample, the mean age of the group should approximate this statistic. The subjects were divided into four unequal size groups (workers, co-workers, supervisors, and associates) based on position in the work force. The size and sex distribution of each group is described in Atchs 1 - 4.

Materials

Individuals were interviewed in same rank groups of between six and ten persons. All sessions followed a standard format. A brief history of the Civil Service Reform Act and resultant programs in AFHRL were given in a slide presentation. A questionnaire was administered and a structured interview conducted. The questionnaire is available in Atchs 1 - 4. The data collected were written questionnaires and transcriptions of the interviews.

III. DISCUSSION

Two previous data-gathering ventures for the Promotion Potential Module used free-form interviews. The Patrick AFB project was initially conceived as another attempt to broaden the data base. Changes were made in the method of the data gathering, which has changed the type of data obtained. These changes were, first, movement from a free-form to

THIS PAGE IS BEST QUALITY PRACTITIONER
FROM COPY FURNISHED TO DDG

In perusing the data as provided in Atch's 5 - 7, one observation should be kept in mind: although the opening briefing stressed the use of the appraisal system in promotion, selection for training/retraining, and transfer, Ss overwhelmingly responded to the questionnaire and in the interviews on the promotion aspect. Out of 168 verbal responses across all interview sessions, three non-promotion references were made. Four non-promotion responses were made out of the 744 statements made on the questionnaires. Further research should be conducted to isolate attitudes vis a vis the system and attitudes toward selection for training, etc.

IV. RECOMMENDATIONS

The recommendations in this report are based on evaluation of the test program at Patrick AFB and should be considered for inclusion in any follow-on studies or implementation of an operational system:

A. An advanced publicity campaign should precede any future test program. Articles should be placed in the command and base newspapers citing the need for the research program and an explanation of how personnel selected to participate in the test will be affected.

B. Sample letters, such as the one used at Patrick AFB, should be furnished the Civilian Personnel Office to notify people of their selection and instruct them in their activities.

C. The daily bulletin should be used to remind participants of deadlines and strengthen efforts to have test materials returned to the program manager.

D. Additional announcements from key personnel in upper levels of Air Force management would assist in participant cooperation.

E. Future interviews should be constructed in a formal format with opportunity given for both oral and written responses. The feedback mechanism should permit statistical compilation of the data to clearly establish firm trends in acceptance/rejection of the instruments under study.

F. The Patrick AFB test suggests that approximately one manhour of CPO time was needed for each test subject involved in the experiment. This includes clerical and administrative time. This figure should be used in helping estimate manhours for CPO's involved in future testing.

G. This piece of research specifically addressed acceptance of the new system. Inferences from the data point to problems in credibility. A new research plan could be created to examine this potential problem, as well as other inferential area (i.e., employee age effects and non-promotion acceptance).

RECEIVED
AIR FORCE PERSONNEL
1964 JUN 10 10 10 AM

a structured interview; second, the addition of a questionnaire (both attempts at more rigorous quantification); and third, an attempt was made to control for possible sex or status effects on Ss willingness to respond in the interview. A female E was introduced to conduct 50% of the worker sessions. This was done as 86% of the female Ss were workers. The male E conducted all supervisor sessions to ensure ascribed status to the group leader. Fourthly, aware of the effects of a set to respond, the Es were careful to request personal opinions and experiences, as opposed to indicating that Ss were to respond as spokespersons for their occupational group. That Ss adopted the set to respond as individuals is evidenced by the frequency of personal versus collective statements. Statements of the form "a worker..." occurred less than 13% of the time, from a total of 774 statements.

Before proceeding to a discussion of data, some comments on the sample itself must be noted. The mean age of Civil Service employees at Patrick AFB is 49.4 years; therefore, the present attitudes might not be representative of Air Force Base populations, but are representative of the attitudes of civil servants of a particular age and seniority. Also, the original experimental design called for analyses by quadrads (worker, supervisor, co-worker, associate). However, a non-random loss of subjects from co-worker and associate groups precluded this type of analyses. Therefore, only group-by-group comparisons will be described.

Information from this study can be divided into two types: (a) produced by comparison to previous work in the area (Norton and McClellan studies), and (b) unique to this study.

The Norton and McClellan studies were basically descriptive, rather than quantitative, and these descriptions were basically negative. Group sentiments expressed in the McClellan trip report include 29 negative statements, as opposed to eight positive statements. From Norton, a total of 130 statements were collected; twenty-one of these were positive, 33 neutral. If the Patrick AFB data is examined only on negative-positive-neutral splits, in a total of 25 statement areas, (collapsing across Ss) three negative attitudes, nine neutral, and 13 positive were expressed. Could it be that in allowing Norton and McClellan Ss to perceive themselves as spokespersons, they expressed all permutations of possible problems, not their own attitudes, toward the system?

Although the McClellan data can be considered neutral to positive, in comparison of earlier investigations, the negative attitudes must be scrutinized as possible hinderances to system implementation in the Civil Service population. Examination of comments given with negative responses suggests that problems with the system lie in credibility, not acceptance; acceptance refers to a belief that the system can work, that an individual will use the system. Credibility refers to the belief that all individuals will use the system. Consider the differences in workers' responses to question, "Can co-workers accurately rate performance?" versus "Can you accurately rate performance?" The responses were, respectively, 56% Yes, 12% no response; 88% Yes, 5% No, 7% no response.

THIS PAGE IS BEST QUALITY PRACTICABLE
FOR THE RECORDING OF DATA

Participant Follow-up Questionnaire
(Ratee)

YOUR NAME Response to this Questionnaire by percent

YOUR RATER'S NAME Sample n = 43 M = 16 F = 24 T = 3
(SUPERVISOR)

1. Do you feel co-workers would accurately rate you if promotions/
selections were based in part on these ratings?

Yes	No	(Circle one)
56%	32%	No response 12%

Comment:

2. Would you accurately rate your co-workers under the same circumstances
in Question 1?

Yes	No	(Circle one)
88%	5%	No response 7%

Comment:

3. Who would be more able to accurately rate you?

Your Supervisor's Alternate	Your Supervisor's Associate	(Circle one)
61%	23%	No response 16%

Comment:

4. Is your supervisor's associate capable of rating you?

Yes	No	(Circle one)
47%	39%	No response 14%

Comment:

THIS PAGE IS BEST QUALITY PRACTICABLE
FROM COPY FURNISHED TO DDC

5. Would the Civilian Personnel Exam (CPE) help to accurately distinguish who in your shop would be most qualified for advancement?

Yes	No	(Circle one)
41%	47%	No response 12%

Comment:

6. Did the Civilian Personnel Exam challenge your abilities?

Yes	No	(Circle one)
63%	30%	No response 7%

Comment:

7. Were there any questions in the exam you found offensive?

Yes	No	(Circle one)
9%	89%	No response 2%

If yes, list the question number and why:

8. Which subtests from this examination are relevant to your job?

9. Are there any other methods that should be used to select workers for advancement?

Yes	No	
60%	12%	No response 28%

Comment:

THIS PAGE IS BEST QUALITY PRACTICABLE.
FROM COPY FURNISHED TO DDC

10. From the methods used in this experiment (supervisor, associate, co-worker ratings, and CPE), are there any you would eliminate if this became an operational system?

Yes
48%

No (Circle one)
40% No response 12%

If yes, which?

11. If only the supervisor's ratings in the test booklet and the Civilian Personnel Exam were added to the present system, do you think the new system would be an improvement over the current system?

Yes
61%

No (Circle one)
30% No response 9%

Comment:

THIS PAGE IS BEST QUALITY COPY AVAILABLE
FROM COPY FURNISHED TO EEO

Participant Follow-up Questionnaire
(Supervisors)

YOUR NAME Response to this Questionnaire by percent

RATED INDIVIDUAL'S NAME Sample, M = 10 M = 18 F = 4 T = 4

1. Would you expect the Civilian Personnel Exam (CPE) test scores on workers under your supervision to accurately reflect their advancement potential?

Yes No (Circle one)
50% 50%

Comment:

2. If the CPE test scores were combined with an effectiveness rating, would you expect this total to accurately reflect promotion/ performance potential of your workers?

Yes No (Circle one)
57% 35% No response 8%

Comment:

3. Is there another evaluation/measurement tool you would like to see used in selecting which of your employees should be selected for advancement?

Yes No (Circle one)
84% 12% No response 4%

Comment:

4. Do you feel your associate(s) could accurately rate your employees?

Yes No (Circle one)
54% 46%

Comment:

RECEIVED
FBI - NEW YORK
JAN 10 1964

5. Is your alternate capable of accurately rating your workers?

Yes No (Circle one)
77% 19% No response 4%

Comment:

6. Which do you feel would more accurately rate your employees?

Your alternate Your associate (Circle one)
69% 23% No response 8%

Comment:

7. Was there any section of the rating booklet you found difficult to complete?

Yes No (Circle one)
50% 50%

Comment:

8. Did the rating booklet give you a tool to accurately rate the promotion potential of your workers?

Yes No (Circle one)
54% 46%

Comment:

9. Would you be able to objectively and accurately discuss your ratings from this booklet with your workers face to face?

Yes No (Circle one)
69% 31%

Comment:

10. How many people do you supervise and rate? Range 4 - 18

Average 7
X 9.3

THIS PAGE IS FOR QUALITY PRACTICABLE
COPY FURNISHED TO DDC

Participant Follow-up Questionnaire
(Co-worker)

YOUR NAME Response to this Questionnaire by percept

RATED INDIVIDUAL'S NAME Sample n = 10 M = 3 F = 6 ? = 1

1. Were you aware that these co-worker ratings were a research tool only and would not be used in any current promotion or selection system?

Yes
100%

No (Circle one)

Comment:

2. With this understanding, were you able to give an accurate rating of your co-worker?

Yes
70%

No (Circle one)
30%

Comment:

3. If you answered no, why?

4. Would you be able to give an accurate co-worker rating if you knew it would be used, along with their rating of you, in a promotion/selection system?

Yes
60%

No (Circle one)
40%

Comment:

THIS PAGE IS BEST QUALITY REPRODUCTION
FROM COPY FURNISHED TO DDC

3. If co-workers were used for selection/promotion, do you feel other co-workers would rate you accurately?

Yes
60%

No (Circle one)
30% No response 10%

Comment:

6. Were there any sections in the booklet you found difficult to complete?

Yes
20%

No (Circle one)
80%

If yes, what were they?

THIS PAGE IS BEST QUALITY PRACTICABLE
FROM COPY FURNISHED TO DDC

Participant Follow-up Questionnaire
(Associate)

YOUR NAME Responses to this Questionnaire by percent

RATED INDIVIDUAL'S NAME Sample - n=10 M=6 F=1 ?=1

1. Did you know the ratee and his job performance well enough to give what you feel is an accurate rating?

Yes No (Circle one)

Comment: 70% 30%

2. Would inter-shop rivalry hinder your giving an accurate rating?

Yes No (Circle one)

Comment: 100%

3. Based on your personal experience, how frequently would associates be able to accurately rate workers?

10% of the time 20%	25% of the time 20%	50% of the time 20%	75% of the time 40%	90% of the time 0%
---------------------------	---------------------------	---------------------------	---------------------------	--------------------------

(Circle one)

Comment:

4. How many people do you rate? Range 1-13

Mode 6

\bar{X} 6.5

5. Were there any sections of the rating booklet you found difficult to complete?

Yes No (Circle one)

40% 50% No response 10%

If yes, what section and why?

THIS PAGE IS BEST QUALITY PRACTICAL
WHICH WAS FURNISHED TO DDC

A Comparison of Responses Across Groups on Key Questions

	n = 26 Supervisors	n = 10 Associates	n = 43 Workers	n = 10 Co-Workers
1. Would the CPE (Civilian Personnel Exam) help to accurately distinguish those most qualified for advancement?	YES 50 NO 50 NR		41 47 12	
2. Would co-workers accurately rate if promotions/selections were based on these ratings?	YES NO NR		56 32 12	60 30 10
3. Would you accurately rate co-workers if promotions/selections were based on these ratings?	YES NO NR		88 5 7	60 40
4. Is a supervisor's associate capable of rating workers?	YES NO NR	54 46	70 30	47 39 14
5. Is a supervisor's alternate capable of rating workers?	YES NO NR	69 23 8		61 23 16
6. Was the job-worker-characteristics booklet difficult to use?	YES NO NR	50 50	40 50 10	20 80
7. Are there methods aside from testing and effectiveness ratings which you would like to see used in selecting employees for advancement?	YES NO NR	84 12 4		60 12 28

THIS PAGE IS BEST QUALITY PRACTICABLE
FROM COPY FURNISHED TO DDC

Comparison of Identified Concerns Across Groups

Concerns with the use of the CPE in a promotional selection formula.

<u>Supervisors</u>	<u>Workers</u>
<ol style="list-style-type: none"> 1. Objection to test as only source of information 2. Concern that CPE will not be job relevant 3. Concern that test score will most strongly reflect test-taking ability 4. Desire for tests to identify additional variables, such as motivation, N Ach 	<ol style="list-style-type: none"> 1. Objection to test as only source of information 2. Concern that CPE will not be job relevant 3. Concern that test score will most strongly reflect test-taking ability . 4. Demand for practice tests

Concern with the use of co-worker ratings in a promotion-selection formula

<u>Co-Workers</u>	<u>Workers</u>
<ol style="list-style-type: none"> 1. Objectivity clouded by personality factors 2. Objectivity clouded by intra-office competition 3. Accuracy of rating effected by knowledge of job/length of acquaintance 4. Individual variation in ability to rate 	<ol style="list-style-type: none"> 1. Objectivity clouded by personality factors 2. Objectivity clouded by intra-office competition 3. Accuracy of rating effected by knowledge of job/length of acquaintance 4. Individual variation in ability to rate 5. Possibility of a sex effect 6. Desire for rating training and use of defined standards 7. Desire for input in co-worker rater selection

Concerns with the use of a supervisor's associate as a rater

<u>Supervisor</u>	<u>Associate</u>	<u>Worker</u>
<ol style="list-style-type: none"> 1. Lack of access to data due to time or geographic constraints 2. No associate exists 3. Not seen as responsibility 4. Objection to associate as only rating source 5. Possibility of timing such a system 6. Individual variation in ability to rate 	<ol style="list-style-type: none"> 1. Lack of access to data due to time or geographic constraints 	<ol style="list-style-type: none"> 1. Lack of access to data due to time or geographic constraints 2. No associate exists

THIS PAGE IS BEST QUALITY PRACTICABLE
FROM COPY FURNISHED TO DDC

Concerns with the use of the supervisor's alternate as a rater

Supervisor

1. Lack of access to data due to time or geographic constraints
2. An alternate does not exist
3. Not seen as responsibility of an alternate
4. Alternate is the associate

Worker

1. Lack of access to data due to time or geographic constraints
2. An alternate does not exist
3. Not seen as responsibility of an alternate
4. Individual variation in ability to rate

Concerns with the use of the Job-Worker-Characteristics Booklet

Supervisor

1. Difficult to rate areas which were not job appropriate
2. Objection to booklet as only source of information
3. Not detailed enough
4. Too detailed
5. Forces a ranking of employees
6. System more difficult to use than present system

Associate

1. Difficult to rate areas which were not job appropriate

Co-Worker

1. Difficult to rate areas which were not job appropriate

THIS PAGE IS BEST QUALITY PRINTING
FROM 1971 EDITION OF 10-20-200

ATTACHMENT 4

One hundred years ago, tradition tells us, an anonymous minister of the French government had a conversation with Alfred Binet.

"What does your test do?"

"It measures intelligence."

"Well, what is intelligence?"

"What my test measures," responded Binet. If the historical impetus to the construction of the original test is examined, it can be seen that the function of the Simon-Binet was to quantify and validate teachers' opinions of their students, particularly their less academically able students. Study of the uses of the Stanford-Binet, from the first form in 1905 to its most recent norming in 1978, suggests that the test has acquired a life of its own. Studies (Good & Brophy, 1974; Risk, 1970) show that teachers use classroom observations to validate the omnibus intelligence score. Also, the test itself has been sued in the courts of San Francisco County (1975) by a group of non-native speaking children. The charge-mistreatment at the hands (pages?) of the Stanford-Binet.

This implied organicity is not unique to systems evaluating intelligence. Think of the power yielded by measurement systems such as the MMPI, the GRE, even the lowly report card. When a system is large, automated, produces an evaluation on a delayed basis from the evaluated behavior, and has "consequences" (i.e., pay, placement, etc.), the involved individuals may cease to view the evaluation system as a reflection of their own behavior. They may react to it as having the power to direct their behavior, rather than their behavior directing it.

It is not enough then to create an evaluation system, such as work plans, and monitor it for accuracy of usage. The question must be considered, "What

will be the relation between the system of evaluation, and the evaluated in five, ten or fifty years?"

Various scenarios can be envisioned.

1) Standardization - Group basis.

After a number of rating cycles, a certain consistency is observed in work plans by occupational groups. In the interest of efficiency of creating plans, equity of work distribution, ease of training supervisors in observing to-be-rated behaviors and/or universality of expectancy about particular job classes, standardization is demanded. This could be a rigid program of a previously determined group of dominant elements (DELS) and performance standards (PS) for every job much as PDs exist today. A flexible type of standardization is also possible; a "menu" of possible DELs and PS is accumulated for each job. A worker-supervisor pair selects an appropriate subgroup of task descriptions for a particular rating cycle.

2) Standardization - Individual Basis

The first type of standardization is imposed from above. It is possible that a more informal, but equally pervasive type of standardization could grow from "below", rooted in either worker or supervisor.

a) An individual working holding a specific job for X number of rating cycles, choses to recycle his/her work plan unchanged.

b) A supervisor develops a work plan and simply provides it, perhaps with minor modifications, to employees who successively fill a particular work slot. While these uncharted changes might be desirable in terms of efficiency, they are undesirable in terms of the original philosophy of the Civilian Appraisal System.

1) Loss of worker-supervisor interaction. Standardization of either a formal or informal sort will mean a failure to maintain the interactive

aspects of the system. The face-to-face exchange mandated by the Civil Service Reform Act of 1978 will become a rubber stamping of previously created work plans. This supervisor-worker discussion might be a particularly vulnerable component, in the face of attempts at standardization, and many person's initial unwillingness to engage in novel, possibly stressful behaviors.

2) Normative approaches.

As the end product of the Civilian Appraisal System is an evaluation of a worker's performance a move toward some standardization of work plans might be seen as a step toward a more reliable end; all Ss in the same job could be rated on the same DELs and PS. Would this produce normalized data? The argument could be made that whereas jobs may be standardized people seldom are.

a) People start jobs at different points in time. It has often been observed that behavior changes as a result of exposure to a particular stimulus, otherwise known as practice, subjective fatigue, etc. What about accounting for the variance implicit in a time effect? Couldn't an S who has occupied job Y for six years be expected to be performing the job differently than an S who has held the job for six months? This performance differential might be observed both on the job, and on the work plan.

b) People bring different backgrounds to the job. Is the job of clerk-typist performed identically by a former librarian and a former lumberjack? Is the job of file clerk performed identically by an individual who is a philatelist and one who plays scrum-half for a rugby team in his/her free time? Interview subjects from a recent data gathering foray to Patrick AFB indicated a desire for information about personal development (i.e., courses, hobbies, etc.) and kinds (as opposed to durations) of work experiences. In situations in which employees must be compared, greater rating accuracy,

might be obtained by blocking candidates on experiential factors, both on the job and off. Category weighting systems could be devised to provide job comparisons across disparate work plans.

In summary:

1. Creation of the Civilian Appraisal System, (CAS) will continue after its implementation to guard against its becoming an idio-system.

2. At the heart of the CAS is individual performance. Jobs, as represented by work plans probably cannot be standardized. Creation of uniform work plans would violate the interactive components described by the Civil Service Reform Act of 1978, would ultimately stagnate the system, and would likely be impossible in the face of an almost infinite variation in work climates, worker-supervisor relations, unexpected job demands, etc.

3. The CAS in relation to individuals is an ipsative system; however, there are levels in the system when individuals must be compared (i.e., the "best" individual for a new job; the "most outstanding performer.") This calls for groups of Ss to be rated in the face of diverse work plans. An equitable approach might be to create behavior categories for the particular job. Score the dissimilar work plans for the presence/absence of the categories. Compare work plans of Ss, grouped according to similarity of external factors.

4. The most appropriate place for the commingling of work plans and other sources of information would be at the level of the performance review board.

THIS PAGE IS BEST QUALITY PRACTICABLE
FROM COPY FURNISHED TO EDC

ATTACHMENT 5

Essay: If there was a merit pay system, what could be done to evaluate it?

[Experts disagree. There are those who say that it is impolite to respond to a question with a question. These nay-sayers are primarily of the Emily Post-persuasion. There are, however, those individuals who claim that to begin a piece of prose with a query heightens the reader's interest. The proponents are primarily confined to the English 101 TA-type].

What does one mean by evaluation of merit pay? Does one wish to examine the degree of discrimination within the system, such that the concern is that "good" workers always receive the reward, and "poor" workers never do? Three types of investigations exist here.

1) Examination of the Merit Pay instrument.

Pretend that this instrument is a questionnaire. Is this questionnaire structured so that all good workers will respond "yes" to items to which poor workers will respond "no" and vice versa. The fly in the instrumental ointment is whereas everyone claims to recognize good work, no one has yet defined it.

2) Reliability.

Skipping rapidly away from topic 1, one could make a different assumption: that qualifies are fairly stable entities. Therefore, a Merit Pay System is identifying good workers if the same persons are offered the increments each year.

3) Longitudinal data collection.

An assumption, related to #2, would be that good and poor workers are mutually exclusive groups; the consequences which befall poor workers do not befall good workers. A set of "poor worker consequences" might be compiled, and compared to the activities of good workers. A Merit Pay system might be evaluated positively if it never predicted an increment for an individual who was fired within ten days of the award, for example.

There are several problems with the above methods of evaluation.

1) They are based on a circular definition. "Merit Pay is awarded to good workers. A good worker is someone who receives Merit Pay."

2) The analyses of the evaluation techniques are only correlational.

3) It is assumed that Merit Pay is an end product of something known as good work. What happens to the evaluation system if Merit Pay is viewed as a beginning - if the terminology becomes "reinforced" not rewarded. By definition, a reinforcer has the power to drive behavior. An evaluation of the Merit Pay system could be built on detecting

motivated changes in behavior and/or attitudes. For example,

1) Work plan change.

Pre-Merit Pay dispersal, all eligible individuals must write work plans describing activities during a defined period. Post reinforcement, samples of Ss receiving Merit Pay, and those not awarded would be asked to complete new work plans, those receiving Merit Pay might be expected to write second work plans reflecting increased motivational levels (i.e. greater number of work items, higher standards for old items, etc.)

2) Use of trained observers.

It is possible that a second writing of work plans would load more heavily on memory than motivation. To counteract this possibility, work plans might be written for Ss by trained observers. Blocks of behavior would be observed by the Os in the same format as #1 (pre-post; award receivers vs. non-receivers), but also balancing location, duration, etc. of initial and secondary observations. (if one is in a fault-finding mood, it is obvious that the success or failure of this evaluation method would hinge on the skill of the observer. There are few completely housebroken Os walking around loose, and the cost of training a feral O would be prohibitive).

3) Use of subordinates as observers.

Untrained Os might be used to take observations of behavior if they were provided with a clear format for gathering information. This format could be as simple as journal pages, divided into categories of behavior with instructions for scoring for durations or discrete instances of previously specified events. This type of data could be collected based on the assumption that the behavior change of an S with a significant responsibility in the area of management would be reflected in the directed activities of his/her subordinates. (Format pre-post; award receivers vs. non-receivers).

4) Use of S and/or associates as observers.

An attempt to broaden the data base of #3 might include the use of a behavioral check list by Merit Pay possibles, and their associates. The behavior check list might be created by simple arm-chairing, factor analysis of earlier work plans, or a brief use of trained Os. Again, increased motivation post-receipt of a Merit Pay goodie might be reflected in changes in numbers of behaviors, or behavior topography, while non-reinforced Ss could be expected to be more consistent.

5) Attitude questionnaires.

It has been found (in areas too unrelated to mention) that attitude changes are associated with behavior changes. A questionnaire might be composed to tap attitudes toward work. Items would cover attitudes (I derive much satisfaction from my work) as well as behavioral estimates (I would be willing to put in _____ hours of overtime on a particularly important project). If data was measured on an ordinal scale, attitude change could be shown by unit movement.

[Notice that the direction of movement is not predicted. Who would want to predict in the face of data that suggests

a. Previously high frequency behaviors decline in the face of reinforcement.

b. Strong attitudes become less strongly held in the face of reinforcement.

c. Freely chosen activities become less novel/creative when reinforced.

d. Correctly Chosen tangible extrinsic reinforcement is associated with increases in intangible intrinsic reinforcement.]

THIS PAGE IS BEST QUALITY PRACTICABLE
FROM COPY FURNISHED TO DDC

1979 USAF-SCEEE SUMMARY FACULTY RESEARCH PROGRAM
Sponsored by the
AIR FORCE OFFICE OF SCIENTIFIC RESEARCH
Conducted by the
SOUTHEASTERN CENTER FOR ELECTRICAL ENGINEERING EDUCATION

FINAL REPORT

A STUDY OF OPPORTUNISTIC MAINTENANCE POLICIES
FOR THE F100PW100 AIRCRAFT ENGINE

Prepared by: Michael C. Smith, Ph.D.
Academic Rank: Assistant Professor
Department and University: Department of Industrial
Engineering
University of Missouri - Columbia

Research Location: Directorate, Management Sciences
Office of DCS/Plans and Programs
Headquarters, Air Force Logistics Command
Wright-Patterson Air Force Base, Ohio

USAF Research Colleague: Mr. John L. Madden

Date: August 23, 1979

Contract No: F49620-79-C-0038

A STUDY OF OPPORTUNISTIC MAINTENANCE
POLICIES FOR THE F100PW100 AIRCRAFT ENGINE

BY

MICHAEL C. SMITH, Ph.D.

ABSTRACT

Application of carefully selected part level screening intervals to components of the F100PW100 engine can result in substantial economic and tactical benefits without introducing complex base level maintenance procedures. This report describes three approaches to developing an optimal screening policy: (1) single screens, (2) a computed screen, and (3) multiple screens. The multiple screen approach which uses base and depot level part screens is recommended as a short run maintenance policy while further refinement of the computed screen approach and a supporting information system are recommended for long run consideration. Examples of each approach are presented using data available at the time the research was done. Recommendations for future investigations are included.

ACKNOWLEDGMENTS

The author would like to thank the Air Force Systems Command, Air Force Office of Scientific Research and the Directorate of Management Sciences, Air Force Logistics Command for the opportunity to spend an interesting and rewarding summer at Wright-Patterson Air Force Base. In particular, special thanks are due Mr. John L. Madden for his continued direction and support throughout the summer. Ms. Virginia Williamson and Mr. Robert Novak were most helpful in resolving questions concerning the project and this help is appreciated.

In addition to those directly involved in this project, the author would like to thank Col. David H. Schweigerdt, Director, AFLC/XRS; Mr. Dan Danishek and Ms. Roz Vera, SCEE coordinators at WPAFB; and Dr. Richard N. Miller, SFRP Director for the parts they played in making this program possible and profitable.

CONTENTS

	ABSTRACT
	ACKNOWLEDGMENT
I.	INTRODUCTION
II.	OBJECTIVES
III.	MODEL FORMULATION
IV.	SINGLE SCREEN APPROACHES
V.	COMPUTED SCREEN APPROACH
VI.	MULTIPLE SCREEN APPROACH
VII.	RECOMMENDATIONS
VIII.	RECOMMENDED FURTHER RESEARCH
IX.	CONCLUSIONS
	TABLES AND FIGURES
	REFERENCES

I. INTRODUCTION:

The United States Air Force is currently engaged in a program through which a fleet of fighter aircraft will be procured over a period of several years. The aircraft comprising this fleet are known as the F-15 Eagle, built by McDonnell Douglas, and the F-16, built by General Dynamics. Both of these aircraft are powered by the F100PW100 engine manufactured by Pratt and Whitney.

The maintenance concept employed in the design and manufacture of the F100PW100 engine has been labeled On Condition Maintenance (OCM). An OCM policy allows engine maintenance actions only when the condition of the engine requires such action. Under this policy no scheduled inspections or overhauls based solely on time based criteria are performed. Maintenance actions are initiated for one of two reasons: (1) the maximum operating time (MOT) on a life limited component is reached, or (2) an engine component fails prematurely. A strict OCM policy allows only repair or replacement of the affected component(s) with no action taken on other engine components at the time of engine removal.

In August of 1976, the Directorate of Propulsion Systems, AFLC/LOP, requested a study concerning maintenance procedures for the F100PW100 engine. The motivation for this request was the desire to identify a maintenance policy which minimizes the long run maintenance cost of these engines. The project was undertaken by the Directorate of Management Sciences, AFLC/XRS and, under the direction of Mr. John L. Madden, has resulted in the development of a comprehensive and detailed computer simulation model of the F100PW100 life cycle. This model is currently being used to investigate the effects of various maintenance policy decisions on the life cycle cost of the F100PW100 engine.

The maintenance concepts now under study are called "opportunistic" maintenance policies. The term "opportunistic" is used because the policies direct that certain maintenance actions take place at times when the engine is out of service for the other repairs. This approach is designed to minimize the number of times the engine must be removed from the aircraft. The nature of the F100PW100 engine makes this approach particularly attractive. This engine employs a modular design concept in which the major engine components are classified into one of several relatively independent modules. This relationship can best be illustrated by the diagram in Figure 1. The engine consists of several modules which each contain several different parts. Maintenance actions can take place at the part, module, or engine level.

The opportunistic maintenance policies which have been investigated consider all levels of the engine hierarchy. The approaches used so far have centered on two primary decision criteria. The first criterion is a screening policy expressed in either flying hours, cycles, or operating hours. Screens are assigned to each module and applied to each part in the module. The effect of the screening policy is that a given part is replaced whenever the engine has been removed for maintenance and the remaining life on the part is less than the screening interval specified for all parts in the module in which the part of interest is located. The second criterion is a rule which specifies the conditions under which the entire engine should be sent to a higher level maintenance facility. This rule is used to determine whether individual modules are sent from the base, where they are removed, to the depot, where they are repaired or the entire engine with modules intact is sent to the depot for repair. This rule is intended to provide base maintenance personnel with a specific criterion for determining the appropriate disposition of engines requiring maintenance actions.

Although application of an opportunistic maintenance policy using these criteria appears to offer substantial reductions in life cycle maintenance cost, the investigators believed that further reductions in this cost might be achieved by developing and applying individual screens at the part level rather than at the module level only. This report documents the approach, the results, the current status, and remaining questions related to identifying and evaluating a part level screening policy. Following this introduction is a specific statement of the objectives of this project; next, a variety of approaches are described and the result of each is presented; recommendations for both short run and long run policies are presented in the following section; and, last, several areas requiring further research are identified and discussed.

II. OBJECTIVES:

The objectives of this project were:

A. To study and understand the mechanics of the computer model used to simulate maintenance actions on the F100PW100 engine and to develop an alternative model with similar logic but which would accommodate a screening policy in which individual part screens are applied.

B. To develop an optimization procedure in which individual part screens can be identified which minimize life cycle maintenance cost for the F100PW100 engine.

C. To generalize the optimization procedure developed in response to objective (B) above so that appropriate part level screens can be identified in an environment of changing operating characteristics and changing costs.

This report focuses primarily on these objectives but, where appropriate, identifies other products of the investigation which proved useful in the larger study concerned with the F100PW100 maintenance policy.

III. MODEL FORMULATION:

In order to adequately address the problem of identifying an optimal set of screens at the part level, a computer model which could be used to assess alternative part level screening policies was developed. The logic of this model mirrored that of the model used to apply module level screens except for the screening policy itself. (See reference 1 for a description of the original model).

The objective function of both models includes cost related to (1) parts replacement, (2) base and depot module maintenance activities, (3) base and depot engine maintenance activities, (4) transportation cost for both module and engine shipments to depot, and (5) base and depot pipeline (spares) cost for both the engine and individual modules. The objective function can be expressed as a linear combination of the events that cause these costs to be incurred and the costs themselves. The objective of the modeling process, then, is to identify a screening policy which minimizes the following function:

$$Z = \sum_{i=1}^2 a_i E_i + \sum_{k=1}^3 \sum_{j=1}^8 b_{jk} M_{jk} + \sum_{i=1}^{49} c_i P_i + dB \quad (1)$$

Where

- Z = total life cycle maintenance cost
- E_1 = the number of base reparable engines
- E_2 = the number of depot reparable engines
- M_{j1} = the number of times module j is base reparable
- M_{j2} = the number of times module j is sent to the depot alone for repair
- M_{j3} = the number of times module j is sent to the depot with the engine for repair
- P_i = the number of times part i is replaced
- B = the number of base manhours required for removing and replacing engines

The parameters a_j , b_{jk} , c_i and d are cost coefficients which include all of the maintenance cost described previously. As this objective function indicates, the life cycle maintenance cost is a function of the number of base and depot engine removals, the number of base and depot module removals, and the number of parts replaced. The number of base manhours required is listed as a separate output variable because it is affected by the specific combination of modules removed from an engine and is therefore affected by the screening policy in effect. Different versions of the model are designed to accommodate several types of screening policies and to operate under several different initialization procedures. The types of screening policies are:

A. A single but unique screen set for each part prior to running the model and not changed throughout the simulation run;

B. A screening policy which allows part screens to be computed at each removal based on the specific condition of the engine at the time of removal;

C. Separate base and depot level screens for each part set prior to running the model and not changed throughout the simulation run.

The initialization procedures incorporated into the model versions are:

A. A "warm up" procedure in which the time to life limit and time to failure for each part are set randomly based on input parameters and the engine is not reinitialized throughout the entire simulation run;

B. A "no warm up" procedure in which the time to life limit and time to failure for each part are set at their initial values and the engine is reinitialized by this procedure at the end of each life cycle until the simulation run is completed;

C. A "modified warm up" procedure in which the time to life limit and time to failure is set similar to (A) above but the engine is reinitialized by this procedure at the end of each life cycle until the simulation run is completed.

The various versions of this model allow all nine combinations of these patterns to be explored so that the appropriate screening policy for each initialization procedure can be identified. The result of experiments with these approaches is described in the remainder of this paper.

IV. SINGLE SCREEN APPROACHES:

Screening policies in which a screening interval is assigned to each part prior to the simulation run and not changed throughout the run are labeled single screen approaches. Three different single screen approaches as well

as some slight variations of these were investigated under the different initialization procedures. The three basic approaches are (1) a constant screen across all parts expressed in the natural operating units of each part, (2) individual part screens set inversely proportional to the replacement cost of the parts but limited to a specified proportion of part life, and (3) individual part screens set inversely proportional to the cost per unit time of the parts but limited to some proportion of the part life. The latter two types of screens discourage early replacement of parts which have high replacement cost or which have high cost per unit of part life.

Each of these approaches was tested under the "warm up" initialization procedure and an assumed fifteen year engine life cycle. The results of these experiments showed that, under the assumptions of the model, the minimum life cycle maintenance cost for each of the three single screening approaches is approximately equal. The minimum cost policy using a constant screening approach lies around 400 in the natural operating units of each part. This result was determined in the original study (see ref. 2) and is used as a benchmark for other policies. Table 1 provides typical results from a constant screening policy of 400 applied to all modules and parts. Since constant screens are much easier to apply than screens based on cost, one would tend to choose the constant screen over either approach involving part costs.

When the constant screening approach is used under the "no warm up" initialization procedure several of the output variables are changed. In general, compared to the "warm up" approach, engine and module removal rates are reduced, the number of manhours per base engine removal is reduced, and the maintenance cost per engine flying hour is reduced. Table 2 provides typical results for this policy using a constant

screen of 400. The reason for the reduction in these measures is that the engine is assumed to be equipped with new (zero time) parts at the beginning of each life cycle and, therefore, requires maintenance actions later in the life cycle than in the pure "warm up" approach.

The "modified warm up" policy randomly assigns part life remaining at the beginning of each new life cycle and produces the results shown in Table 3 when a constant screen of 400 is used. Under this assumption, measures of interest have slightly higher values than under either of the other initialization procedures. This occurs because the engine has neither new parts at the beginning of the life cycle (as in the "no warm up" model) nor does it start in the condition of the pure "warm up" model. Hence, the condition of the engine in this model does not reflect either a new engine or an engine in which the screening policy has been applied over a number of life cycles.

The conclusion which can be drawn from investigating single screen approaches is that, if a single screen for each part is to be employed, a constant screen across all parts will probably produce results as good as other policies which use single screens for each part. Furthermore, previous studies (ref.2) have shown that the screening constant selected is relatively insensitive to reasonable changes in the model assumptions and that the optimal screening interval under this policy is actually an optimal range and can be adjusted somewhat at the discretion of maintenance personnel.

V. COMPUTED SCREEN APPROACH:

The computed screen approach operates under the premise that the optimal screening decision (i.e., minimum cost decision) is a function of the condition of an engine when it

is removed from the aircraft. This approach involves comparing the cost of replacing a particular part to the expected cost of not replacing the part given that the engine has been removed for some other cause. The approach is motivated by the fact that screening decisions have an immediate economic impact and if this impact can be adequately described, a screening policy which optimizes the impact can be identified. This screening policy assumes that the optimal screening policy is dynamic in nature rather than a static policy which remains fixed throughout the engine life cycle. This process can best be characterized by the schematic model shown in Figure 2.

In order to implement the computed screen approach both the cost replacing a part and the expected cost of not replacing a part must be known at the time of engine removal. The procedure used in the model developed in this study computes the cost of replacing as the sum of module maintenance cost incurred due to replacing the part and the value of the remaining life of the part at the time it is replaced. The expected cost of not replacing the part is dependent upon the probability that the part in question will cause the next removal of the module in which the part resides and the cost of such removal. If a module is likely to be removed prior to reaching the life limit of the part in question then replacement of the part should be delayed. This economic trade-off can be expressed as follows:

Replace part i when

$$f_j(M'_j) + L_i(P_i/T_i) < (E + M_j)Pr(t_j > L_i) \quad (2)$$

Where

$$f_j \begin{cases} = 1/n_j & \text{for } n_j > 0 \\ = 0, & \text{otherwise} \end{cases}$$

n_j $\left\{ \begin{array}{l} = \text{number of parts screened in module } j \text{ when no} \\ \text{MOT's or failures occur in module } j; \\ = 0, \text{ otherwise} \end{array} \right.$
 L_i = time until life limit for part i
 P_i = replacement cost of part i
 T_i = maximum operating time of part i
 E = base engine removal cost
 M_j = total depot cost for module j including maintenance,
transportation, and pipeline
 M'_j $\left\{ \begin{array}{l} = (M_j - (\text{total base module maintenance cost})) \\ \text{when module } j \text{ is base reparable;} \\ = M_j, \text{ otherwise} \end{array} \right.$
 t_j = time until next removal of module j

$\Pr(t_j > L_i)$ = probability that the time until the next removal
of module j is greater than the remaining life on
part i

Since $\Pr(t_j > L_i)$ is actually the survival probability for
module j and is computed from the distribution of the time
until the next removal, it is affected by the screening policy
decision. This probability is also a part of the replacement
rule which determines whether or not a part should be replaced.
Since one quantity must be known before the other can be
obtained, an iterative approach must be used in order to
identify the appropriate survivor probabilities. That is, a
distribution is first assumed, then the rule is applied; the
resulting module removal distribution is observed, the module
survival probabilities are adjusted and the process is
repeated. When the actual module removal distributions are
approximately the same as those used in the decision rules,
then the interactive process stops and the final survival
probabilities are accepted.

One exception to this process exist. If a module has only one part and it has a life limit which is much less than the expected time to failure, the removal distribution generated by the above process does not adequately describe the module removal process. This is true because the single part MOT must, in this case, drive all or most of the module removals. Therefore, any assumed distribution with non-zero variance which is derived from the module removal distribution will bias the replacement rule toward early replacement. This bias can be overcome by determining $Pr(t_j > L_1)$ from the engine removal distribution rather than from the module distribution when the module has one part only.

In order to test the computed screen approach a set of module time until removal distributions was assumed. The exact probability that a module removal will occur later than some time L_1 is, of course, dependent upon part i . That is, since module removals are caused by part failures and life limits, the next removal must be caused some part. As the number of parts in a module increases, the effect of the particular part in question on the module removal distribution decreases. In testing this part replacement policy, the removal distribution of the module was assumed to be independent of the replacement decision for the part in question. The module removal distribution was further assumed to take the form of a two parameter Weibull distribution (location parameter set at zero) with shape and scale parameters derived from the observed removal distribution. The survival probabilities were computed from the complementary cumulative of the time until removal distribution as follows:

$$\begin{aligned} Pr(t_j > L_1) &= 1 - F(L_1) = 1 - \{1 - \exp[-(L_1/b_j)^{a_j}]\} \\ &= \exp[-(L_1/b_j)^{a_j}] \end{aligned} \quad (3)$$

Where a_j = shape parameter for module j
 b_j = scale parameter for module j

The Weibull parameters, a_j and b_j , were computed from the mean and variance of the time until removal distribution using the following relationships:

$$E(t_j) = b_j \Gamma(1 + 1/a_j)$$

$$V(t_j) = b_j^2 \{ \Gamma(1 + 2/a_j) - [\Gamma(1 + 1/a_j)]^2 \}$$

Where $E(t_j)$ = mean time until module removal
 $V(t_j)$ = variance of time until module removal
 $\Gamma(\cdot)$ = Gamma function

The results of testing this model using the Weibull assumption and the three different model initialization procedures are shown in Tables 4, 5 and 6. The pattern of the results among the initialization procedures is identical to that of the single screening approach. The results themselves, however, are considerably different. In every case, the factor of interest is improved using computed screens over that of any of the single screen approaches tested. The cost per engine flying hour is about 10% lower in the warm up and modified warm up models and the engine removal rate is about 10% lower in all three models. The major reason for these reductions is the fact that the computed screen approach discourages sending a module to depot (i.e., replacing parts) when the sole cause for module removal is a single part being screened. The computed screen approach sets much lower screens when a module has no MOT's or failures than when these events occur. Consequently,

part replacements are encouraged when the module has other causes for removal and discouraged when no other cause exists. The impact of this policy on the percentage of module removals for only one part screened is shown in Tables 1 through 6.

A major disadvantage of the computed screen approach is that decision must be made in a dynamic fashion. The decision maker must know the condition of the engine and, with this information, compute costs for replacing and not replacing each part. To assist in this procedure, a FORTRAN program was developed to determine the optimal screening intervals for each part under the assumptions mentioned previously. For a given set of costs and module removal distributions these optimal part screens were computed for a variety of module removal conditions. Table 7 provides a typical set of these screens computed using cost and removal data presently available. Table 7 is divided into three sections: (1) NRTS screens (for parts in depot bound modules), (2) RTS screens (for parts in modules with base repairable usage failures), and (3) No cause screens (for parts in modules with no MOT's or failures). The table is used by entering the section which describes the module in question, locating the rows which identify the parts in that module, and applying the appropriate screens to these parts. When the module is NRTS (non repairable this station), a single set of screens applies. When the module is RTS (repairable this station) or has no cause for removal, the set of applicable screens depends on the number of parts screened. The application of these screens is recursive in nature in that, first, the number of parts screened is assumed and the screens in the column under this assumed number are applied. If the actual number of parts screened equals the assumed number of parts screened, stop the process and send the module to depot where the NRTS screens are applied to all parts. If the actual number does not equal the assumed number, set the assumed number at the actual number and repeat the process.

If, at any point, the actual number screened equals zero (i.e., no parts screened), stop the process and do not send the module to depot unless the entire engine is sent to depot. If for any reason (MOT, failure, screening, or engine NRTS) the module goes to depot, the NRTS screens are applied.

Although this process can be applied manually it is quite complex and is likely to create confusion unless it is automated to the extent that the base level decision process is simplified. Consequently, unless data processing support is available or can be justified, a less complex screening rule must be provided. The section which follows provides a screening policy which capitalizes on the economic benefit of this model but retains the simplicity of the single screen approaches.

VI. MULTIPLE SCREEN APPROACH:

The multiple screen approach is similar to the computed screen approach because part screens are chosen based on the condition of the module. It is like the single screen approach because base level maintenance personnel have only to deal with a single set of part screens. Each part is assigned a pair of part screens, one applicable at the base level, the other applicable at the depot level. If a module has no cause for removal or is repairable at the base level, the base level screens are applied; if the module must go to the depot for any reason, the depot level screens are applied. Reasons for sending a module to depot include engine NRTS, MOTs, failures, and the fact that one or more parts meet the base level screen.

This approach has the built in capability of setting base and depot level part screens such that part replacements in modules which have no cause for removal is delayed while part

replacement in depot bound modules is done earlier than base screen would allow. This feature is the major economic benefit of the computed screens discussed earlier. The problem now becomes that of identifying the optimal combination of base and depot level screens.

The computed screen approach and the table of conditional part level screens (Table 7) provide the necessary information for selecting optimal base and depot level screens. The information provided by the computed screen models includes for each module, the distribution of the number of parts screened when no MOTs or useage failures occurs. From this information, the expected number of parts screened when no MOTs or failures occur can be obtained. Base level part screens can be selected from Table 7 which represent the screens applied when the expected number of parts is screened. Depot level screens should be identical to those computed (in Table 7) for NRTS modules. Further simplification of the screen can be achieved by grouping screens which are approximately equal (e.g., optimal depot level screens for core module parts are all approximately 1000 engine flying hours or 2200 cycles).

The multiple screen approach was tested under the three initialization procedures using the base and depot level screens shown in Table 8. The results of these tests are shown in Tables 9, 10 and 11. Again, considerable improvement over the single screen approaches was experienced. Cost and engine removal rates were approximately equal to that resulting from the computed screen approach. Evidently, maintenance policy costs are no more sensitive to the base/depot level screen simplification than to the Weibull removal distribution assumptions of the computed screen approach. In fact, as Tables 9, 10, and 11 show, the base/depot level screens produced better results than the computed screens in some cases.

The multiple screen approach is very attractive for several reasons:

A. It is simple because it requires only one set of screens at the base level and one set of screens at the depot level;

B. It can be applied manually -- no need for computer-aided decision logic;

C. It achieves the economic benefits of the optimal screening policy determined through the computed screen approach;

D. The large depot level screens applied to most parts at the depot provide a large "guarantee" for the remaining life of the module;

E. The average number of base manhours required per base engine removal is much less than that experienced under single screen approaches; and

F. Modules are, in general, sent to depot less frequently, and, when they are sent to depot, are eligible for a greater number of maintenance actions thus delaying the time until the next module removal is required.

VII. RECOMMENDATIONS:

The results of this investigation have both short and long run implications. For the short run (three to five years) the results of the study lead to the following recommendations:

Use the computed screen logic to assist in developing a near optimal set of base and depot level screens. Provide these screening rules to base and depot level maintenance personnel for use until such time as the long range recommendation can be implemented. Base and depot level screens will require updating as operating conditions and relevant costs change.

The long run recommendation resulting from this project is:

Continue to refine the computed screen approach particularly in the area of determining the appropriate module removal distribution. Investigate the possibility of implementing an on-line, real-time, base level maintenance information system which can compute screens based on engine status at the time of removal and provide immediate feedback to base personnel regarding appropriate part and module disposition. If the economic and tactical benefits of such a system justify its cost, then work toward implementation of such a system.

VIII. RECOMMENDED FURTHER RESEARCH:

In addition to the research implications of the long run recommendations, several specific areas merit further investigation.

A. What is the impact of a parts (module) inventory in which parts (modules) have a known age distribution? How can parts (modules) be selected from such an inventory and matched to modules (engines) in a manner which minimizes maintenance cost over a fleet of engines?

B. Is a module (engine) inspection plan desirable? What is the tactical and economic impact of such inspections and how should they be conducted (i.e., scheduled or opportunistic)?

C. What is the impact of an opportunistic maintenance policy at the fleet level? Will rules which minimize costs for a single engine also minimize costs for a fleet of engines?

IX. CONCLUSION:

The research effort described in this report provides guidance for developing maintenance policies for the F100PW100 engine. One word of caution must be offered: The specific results presented here are based on a particular combination of MOTs, failure parameters, and cost data and will change as these data change. Fortunately, the base/depot screening policy is relatively insensitive to small changes in these factors and should result in screens which are applicable over a broad range of model input values. The approaches presented and the results achieved provide a basis for both short run and long run maintenance policy decisions and suggest areas where further research is needed or may prove fruitful.

TABLE 1
MAINTENANCE SYSTEM RESULT FOR
A CONSTANT PART SCREENING POLICY

Screening Constant: 400 part operating unit
Engine Life Cycle: 15 years
Simulation Length: 2000 years (133 life cycles)
Initialization Procedure: Warm-Up

<u>Component</u>	<u>Removals/KFH*</u>	<u>% Removal With One Part Screened Only</u>
Engine	6.84	-
Module 1	1.09	0%
Module 2	3.73	45%
Module 3	2.61	57%
Module 4	3.34	39%
Module 5	2.03	15%
Module 6	1.73	69%
Module 7	.91	92%
Module 8	3.08	0%

*KFH = 1000 engine flying hours

Base manhours per engine removal: 178 hours
Cost per 15 year life cycle: \$661,319
Cost per engine flying hour: \$216

TABLE 2
MAINTENANCE SYSTEM RESULT FOR
A CONSTANT PART SCREENING POLICY

Screening Constant: 400 part operating unit
Engine Life Cycle: 20 years
Simulation Length: 2000 years (100 life cycles)
Initialization Procedures: No Warm-Up

<u>Component</u>	<u>Removals/RFH*</u>	<u>% Removals With One Part Screened Only</u>
Engine	5.85	-
Module 1	.98	0%
Module 2	3.06	46%
Module 3	1.38	53%
Module 4	1.24	26%
Module 5	1.59	7%
Module 6	1.21	69%
Module 7	.75	87%
Module 8	2.96	0%

*KFH = 1000 engine flying hours

Base manhours per engine removal: 140 hours
Cost per 20 year life cycle: \$579,890
Cost per engine flying hour: \$142

TABLE 3
MAINTENANCE SYSTEM RESULT FOR
A CONSTANT PART SCREENING POLICY

Screening Constant: 400 part operating units
Engine Life Cycle: 20 years
Simulation Length: 2000 years (100 life cycles)
Initialization Procedure: Modified Warm-Up

<u>Component</u>	<u>Removals/KFH*</u>	<u>% Removals With One Part Screened Only</u>
Engine	7.11	-
Module 1	1.08	0%
Module 2	4.04	50%
Module 3	2.66	59%
Module 4	3.40	48%
Module 5	3.36	47%
Module 6	1.66	69%
Module 7	.90	94%
Module 8	3.12	0%

*KFH = 1000 engine flying hours

Base manhours per engine removal: 185 hours
Cost per 20 year life cycle: \$890,246
Cost per engine flying hour: \$218

TABLE 4
MAINTENANCE SYSTEM RESULTS FOR
A COMPUTED SCREEN POLICY

Engine Life Cycle: 15 years
Simulation Length: 2000 years (133 life cycles)
Initialization Procedure: Warm-Up

<u>Component</u>	<u>Removals/KFH*</u>	<u>% Removals With One Part Screened Only</u>
Engine	6.08	-
Module 1	1.10	0%
Module 2	3.16	17%
Module 3	1.69	17%
Module 4	1.44	1%
Module 5	2.61	19%
Module 6	1.14	5%
Module 7	1.05	97%
Module 8	3.13	0%

*KFH = 1000 engine flying hours

Base manhours per engine removal: 155 hours
Cost per 15 year life cycle: \$604,056
Cost per engine flying hour: \$197

TABLE 5
MAINTENANCE SYSTEM RESULTS FOR
A COMPUTED SCREEN POLICY

Engine Life Cycle: 20 years
Simulation Length: 2000 years (100 life cycles)
Initialization Procedure: No Warm-Up

<u>Component</u>	<u>Removals/KFH*</u>	<u>% Removals With One Part Screened Only</u>
Engine	5.34	-
Module 1	0.99	0%
Module 2	2.69	11%
Module 3	0.88	2%
Module 4	0.84	2%
Module 5	2.08	17%
Module 6	0.79	1%
Module 7	0.81	96%
Module 8	3.10	0%

*KFH = 1000 engine flying hours

Base manhours per engine removal: 133 hours
Cost per 20 year life cycle: \$573,473
Cost per engine flying hour: \$141

TABLE 6
MAINTENANCE SYSTEM RESULTS FOR
A COMPUTED SCREEN POLICY

Engine Life Cycle: 20 years
Simulation Length: 2000 years (100 life cycles)
Initialization Procedure: Modified Warm-Up

<u>Components</u>	<u>Removals/KFH*</u>	<u>% Removals With One Part Screened Only</u>
Engine	6.08	-
Module 1	1.11	0%
Module 2	3.27	20%
Module 3	1.75	18%
Module 4	1.53	4%
Module 5	2.65	19%
Module 6	1.27	17%
Module 7	0.86	79%
Module 8	3.16	0%

*KFH = 1000 engine flying hours

Base manhours per engine removal: 154 hours
Cost per 20 year life cycle: \$798,584
Cost per engine flying hour: \$196

TABLE 7
BREAKEVEN PART SCREENS BY MODULE CONDITIONS

PART NO.	NRTS SCRN	RTS						NO CAUSE					
		1	2	3	4	5	6	1	2	3	4	5	6
1	0	0	0	0	0	0	0	0	0	0	0	0	0
2	0	0	0	0	0	0	0	0	0	0	0	0	0
3	280	279	280	280	280	280	280	236	258	265	269	271	273
4	237	236	237	237	237	237	237	200	219	225	228	230	231
5	308	306	307	307	308	308	308	258	283	291	295	298	299
6	481	477	479	479	480	480	480	369	417	436	446	453	457
7	0	0	0	0	0	0	0	0	0	0	0	0	0
8	591	390	487	521	538	548	555	331	458	500	522	536	545
9	621	407	510	545	563	575	582	346	478	523	547	561	571
10	638	417	522	559	578	590	597	354	489	536	561	575	585
11	997	532	694	765	808	836	857	449	639	720	767	802	826
12	1069	540	708	785	832	864	888	455	650	736	789	825	853
13	1041	537	704	778	824	855	878	453	647	731	782	817	844
14	1122	544	716	796	845	880	906	459	656	745	800	838	867
15	982	530	690	761	802	830	850	448	636	716	764	796	820
16	0	0	0	0	0	0	0	0	0	0	0	0	0
17	1242	393	646	753	819	865	901	315	602	717	787	836	873
18	1305	395	649	758	825	873	910	316	605	721	792	842	881
19	1185	391	642	747	811	856	890	313	599	711	780	827	863
20	1255	394	647	754	820	867	903	315	603	718	788	837	875
21	1098	386	632	733	793	835	865	309	590	699	764	808	841
22	1165	390	640	744	807	852	885	312	597	709	777	823	859
23	998	376	613	707	761	798	824	300	574	676	735	775	803
24	997	376	613	707	761	797	824	300	574	676	735	774	803
25	994	376	612	706	760	796	822	300	573	675	734	773	802
26	1079	384	629	729	788	829	858	307	588	696	757	803	835
27	1097	386	632	733	793	834	865	309	590	699	763	808	841
28	1104	386	633	734	795	836	867	309	591	700	765	810	843
29	1064	383	627	725	784	824	853	306	585	693	756	798	830
30	872	354	576	658	703	732	752	281	540	631	681	714	736
31	996	376	613	707	761	797	823	300	573	676	735	774	803
32	903	361	587	672	720	750	772	287	550	644	697	731	755
33	1111	387	634	735	796	838	869	309	592	701	767	811	845
34	993	375	612	706	760	796	822	299	573	675	734	773	801
35	1043	381	623	720	778	816	845	305	582	688	750	792	822
36	987	375	611	704	757	793	819	299	571	673	731	770	798
37	986	374	611	703	757	792	818	299	571	673	731	770	798
38	0	0	0	0	0	0	0	0	0	0	0	0	0
39	418	316	364	381	390	395	399	267	337	363	376	384	389
40	456	337	392	412	422	429	433	284	362	390	406	415	422
41	277	216	246	256	261	264	266	182	230	245	253	258	261
42	391	299	343	359	367	372	375	254	319	342	354	361	366
43	490	354	414	437	449	456	462	297	380	412	429	440	448
44	0	0	0	0	0	0	0	0	0	0	0	0	0
45	721	437	579	626	649	664	673	386	555	610	637	654	665
46	753	456	603	653	677	692	702	404	578	636	665	682	694
47	853	511	676	732	761	779	791	454	647	713	746	767	781
48	621	445	514	544	560	571	578	411	491	526	545	558	567
49	0	0	0	0	0	0	0	0	0	0	0	0	0

TABLE 8
TYPICAL "GOOD" BASE AND DEPOT LEVEL
PART SCREENS FOR USE ON MULTIPLE
SCREEN MAINTENANCE POLICY
(All Screens in Engine Flying Hours)

Part No.	Base Screen	Depot Screen	Part No.	Base Screen	Depot Screen
1	0	0	26	300	1000
2	0	0	27	300	1000
3	250	250	28	300	1000
4	250	250	29	300	1000
5	250	250	30	300	1000
6	450	450	31	300	1000
7	0	0	32	300	1000
8	350	600	33	300	1000
9	350	600	34	300	1000
10	350	600	35	300	1000
11	450	1000	36	300	1000
12	450	1000	37	300	1000
13	450	1000	38	0	0
14	450	1000	39	400	400
15	450	1000	40	400	400
16	0	0	41	275	275
17	300	1000	42	350	350
18	300	1000	43	500	750
19	300	1000	44	0	0
20	300	1000	45	400	750
21	300	1000	46	400	750
22	300	1000	47	450	850
23	300	1000	48	400	620
24	300	1000	49	0	0
25	300	1000			

TABLE 9
MAINTENANCE SYSTEM RESULTS FOR
A MULTIPLE SCREEN POLICY

Engine Life Cycle: 15 years
Simulation Length: 2000 years (133 life cycles)
Initialization Procedure: Warm-Up

<u>Component</u>	<u>Removals/KFH*</u>	<u>% Removals With One Part Screened Only</u>
Engine	5.94	-
Module 1	1.08	0%
Module 2	3.66	36%
Module 3	1.36	12%
Module 4	1.22	2%
Module 5	3.46	17%
Module 6	1.12	3%
Module 7	1.03	96%
Module 8	3.13	0%

*KFH = 1000 engine flying hours

Base manhours per engine removals: 164 hours
Cost per 15 year life cycle: \$602,406
Cost per engine flying hour: \$197

NOTE: Base and depot screens are given in Table 8.

TABLE 10
MAINTENANCE SYSTEM RESULTS FOR
A MULTIPLE SCREEN POLICY

Engine Life Cycle: 20 years
Simulation Length: 2000 years (100 life cycles)
Initialization Procedure: No Warm-Up

<u>Component</u>	<u>Removals/KFH*</u>	<u>% Removals With One Part Screened Only</u>
Engine	5.41	-
Module 1	1.00	0%
Module 2	3.26	35%
Module 3	0.88	1%
Module 4	0.79	1%
Module 5	2.97	26%
Module 6	0.81	0%
Module 7	0.81	97%
Module 8	3.07	0%

*KFH = 1000 engine flying hours

Base manhours per engine removal: 147 hours
Cost per 20 year life cycle: \$592,397
Cost per engine flying hours: \$145

NOTE: Base and depot screens are given in Table 8.

TABLE 11
MAINTENANCE SYSTEM RESULTS FOR
A MULTIPLE SCREEN APPROACH

Engine Life Cycle: 20 years
Simulation Length: 2000 years (100 life cycle)
Initialization Procedure: Modified Warm-Up

<u>Component</u>	<u>Removals/KFH*</u>	<u>% Removals With One Part Screened Only</u>
Engine	6.14	-
Module	1.13	0%
Module 2	3.93	41%
Module 3	1.57	15%
Module 4	1.34	3%
Module 5	3.45	40%
Module 6	1.08	14%
Module 7	1.00	95%
Module 8	3.23	0%

*KFH = 1000 engine flying hours

Base manhours per engine removals: 163 hours
Cost per 20 year life cycle: \$773,820
Cost per engine flying hours: \$190

NOTE: Base and depot screens are given in Table 8.

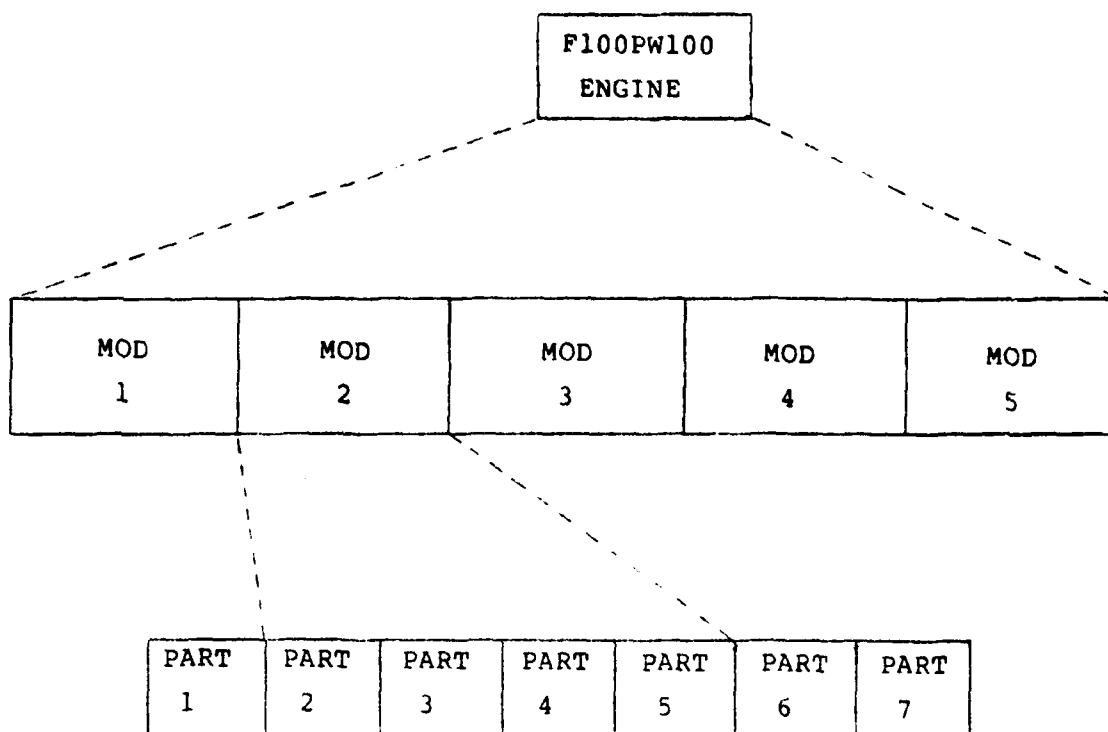
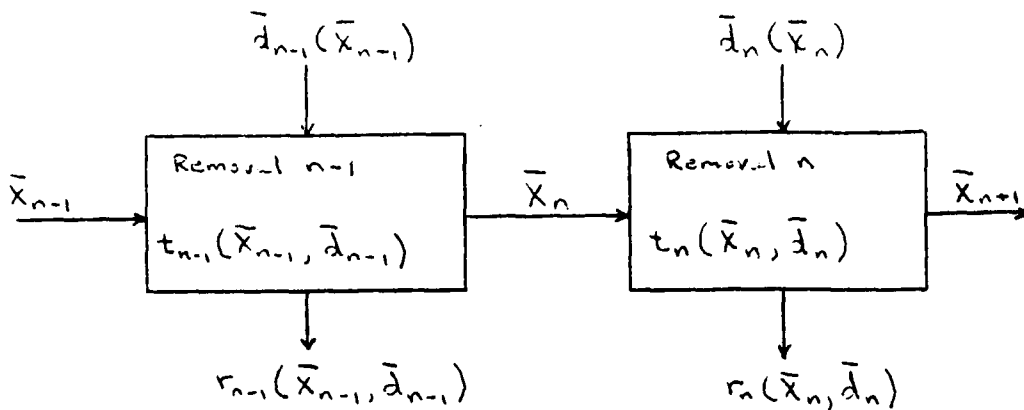


FIGURE 1.
F100PW100 ENGINE/MODULE/PART RELATIONSHIPS



Each box represents an engine removal. The vector \bar{x}_n represents the condition of engine parts when a removal occurs. The vector $\bar{d}_n(\bar{x}_n)$ is the decision vector and depends on the condition of the parts, \bar{x}_n . The function $t_n(\bar{x}_n, \bar{d}_n)$ transforms the condition of the engine at removal n into the condition of the engine at removal $n+1$ and depends on the condition of the engine when removal n occurs, \bar{x}_n , and the decisions made at the removal, \bar{d}_n . The return function $r_n(\bar{x}_n, \bar{d}_n)$ determines the economic impact of decisions made at removal n given the condition of the engine at removal n . The objective of a dynamic maintenance policy is to make decisions at each removal which optimize the sum of the return functions at each removal.

FIGURE 2.
SCHEMATIC REPRESENTATION OF A
DYNAMIC MAINTENANCE POLICY

REFERENCES

1. Madden, J.L., Persensky, P.A., Williamson, V.L., and Niklas, M.R., Opportunistic Maintenance Engine Simulation Model - OMENS, Working Paper Number XRS-77-7-10, Logistics Systems Laboratory Division, Directorate at Management Sciences, AFLC, WPAFB, Ohio, May 1979.
2. Madden, J.L., F-100 Opportunistic Maintenance Policy Analysis, Working Note Number XRS-77-7-12, Logistics Systems Laboratory Division, Directorate of Management Sciences, AFLC, WPAFB, Ohio, July 1979.

1979 USAF - SCEE SUMMER FACULTY RESEARCH PROGRAM

Sponsored by the

AIR FORCE OFFICE OF SCIENTIFIC RESEARCH

Conducted by the

SOUTHEASTERN CENTER FOR ELECTRICAL ENGINEERING EDUCATION

FINAL REPORT

ERROR ANALYSIS FOR A RADIO-FREQUENCY SYSTEMS SIMULATION FACILITY

Prepared by:	Walter D. Stanaland
Academic Rank:	Assistant Professor
Department and University:	Systems Science, University of West Florida
Research Location:	ADTC/AFATL/DLMA, Eglin AFB, FL
USAF Research Colleague:	Larry Lewis
Date:	28 August 1979
Contract No:	F49620-79-C-0038

ERROR ANALYSIS FOR A RADIO-FREQUENCY SYSTEMS SIMULATION FACILITY

by

(Walter D. Stanaland)

ABSTRACT

Error analysis associated with radio-frequency simulation facilities must consider error determination methods as well as error reduction designs. This study effort is devoted to both considerations. For error identification, the mean-square error, which occurs between transmitter and receiver detector output, is identified and computer modeling has been started. For design improvements, a time domain sensitivity comparison function has been defined for the first time.

The mean-square error definition includes a computer program which defines the input auto-correlation function, output auto-correlation function, crosscorrelation function, and convolution integral. The summation of terms remains unfinished.

ACKNOWLEDGMENT

The Author would like to thank the Air Force Armament Laboratory and the Southeastern Center of Electrical Engineering Education for providing him the opportunity to spend a most worthwhile and interesting summer at Eglin Air Force Base. Special Acknowledgment is also due to the welcome received from personnel within the Radio-Frequency Simulation Branch of the Armament Laboratory.

Finally, he would like to thank Mr. Larry Lewis of the Radio-Frequency Simulation Branch for instruction and guidance during the summer activity. His efforts were both helpful and appreciated.

I. INTRODUCTION

The problems addressed in this report are related to operations of simulated radio-frequency systems. The simulations require very special analysis to assure their proper calibration and operational performance. In particular, systems such as pulsed radar have repeated transmissions and return signals. In addition, noise is usually present in the signals. To obtain signal information from composite noise/signal waveforms special waveform processing is required. From the 1930's to the present time many authors have addressed this problem. Some of the important authors are Weiner (1), Rice (2, 3, 4) North (5) and others.

In 1943 North defined the matched filter which is usually associated with radar receivers. In 1949 Weiner defined a filter which minimizes the mean-square error in the output from the filter. In most cases the authors have used the characteristics of stationary random processes as a basis for analysis of waveforms. And in general, the mean-square error was used as a performance indicator. Hence, finding filters or systems which minimize the effect of the mean-square error was the objective of most design problems.

Because the pulse repetition rate of pulsed radar is normally much greater than the dynamic frequencies of desired returned signals, stationary statistics are a natural assumption for the pulsed radar analysis problem. To utilize previously defined methods, such as the mean-square error, the mechanics of convolution integrals, auto-correlation functions, and crosscorrelation functions must be defined and computerized. This computer definition has been a major part of my summer effort at the Armament Laboratory at Eglin AFB.

Although analysis methods are required for proper calibration and operations of equipment, such methods do not provide a capability to reduce the effects of system parameter changes. Historically, the effects of system parameter changes have been reduced by feedback methods. In fact, sensitivity comparison functions have been defined in the frequency domain by Cruz and Perkins (6). The functions compare the open-loop errors to the closed-loop errors and provide a functional matrix for feedback system mechanization. However, the time domain sensitivity comparison function has never been defined. A large part of my summer effort has been to define a time domain sensitivity comparison function.

II OBJECTIVES

The objectives of this project are:

(1) Begin computerization of the functions required to define the mean-square error. This included convolution integral, input auto-correlation function, output auto-correlation function and crosscorrelation function.

(2) Define the form of a time domain sensitivity comparison function. This function is the relationship between output error for open and closed-loop systems.

III Mean-Square Error Equation

A facility which simulates rf signals is usually involved in repetitive transmissions of a specific signal. If such a signal does not change in amplitude, phase, polarization or frequency with time, it will appear to be stationary in time to an observer who is observing at the transmission repetition frequency. Most repetitive natural signals vary with time, but if the change is relatively small over several repeated transmissions, the signals may appear stationary for observations over several transmission cycles. Therefore, it is worthwhile to investigate measurement errors involved with stationary random processes.

Simulation of rf signals requires apriori knowledge of the characteristics of the signal to be simulated. Hence, the input signal to a receiver system, which detects a simulated transmission, is known. Let the input to a receiver be $f_i(t)$. The output from the receiver can be computed if the receiver response characteristics are known. If the input simulation is perfect and the receiver is operating properly, the receiver output is the desired signal $f_d(t)$. In general, the receiver output is not $f_d(t)$, but instead is a signal $f_o(t)$. The difference between $f_d(t)$ and $f_o(t)$ is the output error. The mean-square output error \bar{e}^2 is given by,

$$(1) \quad \bar{e}^2 = \lim_{T \rightarrow \infty} \frac{1}{2T} \int_{-T}^T [f_o(t) - f_d(t)]^2 dt$$

But $f_o(t)$ can be defined in terms of the convolution integral as,

$$(2) \quad f_o(t) = \int_{-\infty}^{\infty} h(\tau) f_i(t-\tau) d\tau$$

By substituting equation (2) into equation (1) and expanding the square term one has [],

$$(3) \quad \bar{e}^2 = \lim_{T \rightarrow \infty} \frac{1}{2T} \int_{-T}^T \left[\int_{-\infty}^{\infty} h(\tau) f_i(t-\tau) d\tau \int_{-\infty}^{\infty} h(\sigma) f_i(t-\sigma) d\sigma \right. \\ \left. - 2f_d(t) \int_{-\infty}^{\infty} h(\tau) f_i(t-\tau) d\tau + f_d^2(t) \right]$$

The variable σ is used in the second integrand of the first term of the expansion simply to denote that a variable of integration other than τ is used.

If the order of integration and the processes of integrating and taking limits are interchanged [], the expression for \bar{e}^2 can be written as,

$$(4) \quad \bar{e}^2 = \int_{-\infty}^{\infty} h(\tau) d\tau \int_{-\infty}^{\infty} h(\sigma) d\sigma \lim_{T \rightarrow \infty} \frac{1}{2T} \int_{-T}^T f_i(t-\tau) f_i(t-\sigma) dt \\ - 2 \int_{-\infty}^{\infty} h(\tau) d\tau \lim_{T \rightarrow \infty} \frac{1}{2T} \int_{-T}^T f_i(t-\tau) f_d(t) dt \\ + \lim_{T \rightarrow \infty} \frac{1}{2T} \int_{-T}^T f_d^2(t) dt$$

Inspection of equation (4) reveals that the input signal function $f_i(t)$ and the desired output signal $f_d(t)$ enter the mean-square-error expression only in the form of an averaging of the product of two time functions. The significance of this is made clearer as a function $\phi_{ab}(\tau)$ is defined.

$$(5) \quad \phi_{ab}(\tau) = \lim_{T \rightarrow \infty} \frac{1}{2T} \int_{-T}^T f_a(t) f_b(t+\tau) dt$$

By substituting for $\phi(\tau)$ in equation (4), the mean-error-squared equation can be written as,

$$(6) \quad \bar{e}^2 = \int_{-\infty}^{\infty} h(\tau) d\tau \int_{-\infty}^{\infty} h(\sigma) d\sigma \phi_{ii}(\tau-\sigma) \\ - 2 \int_{-\infty}^{\infty} h(\tau) d\tau \phi_{id}(\tau) + \phi_{dd}(0)$$

The function $\phi(\tau)$ is the correlation function of statistics. $\phi_{ii}(\tau)$ is the autocorrelation function of the input signal, $f_i(t)$. $\phi_{dd}(\tau)$ is the autocorrelation function of the desired output, and $\phi_{id}(\tau)$ is the crosscorrelation function between the input signal and the desired output. This means the mean-square-error can be determined entirely by the system characteristics described by the unit-impulse response $h(t)$ and by the correlation functions of the input and desired output. Hence, it is important to identify the input, desired output, and input-output correlation functions.

In Equation (6) the mean-square error will be zero if $h(\tau)$ is exactly the designed impulse response function so that $f_o(t) = f_d(t)$. Hence for \bar{e}^2 to be other than zero $h(\tau)$ cannot be the designed value. In fact, the actual impulse response function with perturbed system parameters is not known and the actual impulse response cannot be computed. Therefore, it is important to work with design values.

d

Let the desired output be,

$$f_d(t) = \int_{-\infty}^{\infty} g(\tau) f_i(t-\tau) d\tau$$

Then substitute into Equation (1) and expand as accomplished for Equation (3).

Then

$$\bar{e}^2 = \lim_{T \rightarrow \infty} \frac{1}{2T} \int_{-T}^T \left[\int_{-\infty}^{\infty} g(\tau) f_i(t-\tau) d\tau \int_{-\infty}^{\infty} g(\sigma) f_i(t-\sigma) d\sigma \right. \\ \left. - 2 f_i(t) \int_{-\infty}^{\infty} g(\tau) f_i(t-\tau) d\tau + f_i^2(t) \right] dt$$

By completing the manipulations required for definition of Equation (6) one has

$$\bar{e}^2 = \int_{-\infty}^{\infty} g(\tau) d\tau \int_{-\infty}^{\infty} g(\sigma) d\sigma \phi_{ii}(\tau-\sigma) \\ - 2 \int_{-\infty}^{\infty} g(\tau) d\tau \phi_{io}(\tau) + \phi_{oo}(0)$$

This equation allows use of online computation of $\phi_{oo}(0)$ and $\phi_{io}(\tau)$ and at the same time using the designed value of unit impulse response $g(\tau)$. This equation can be mechanized online.

The system being considered is specified in Figure (1). There are three basic parts

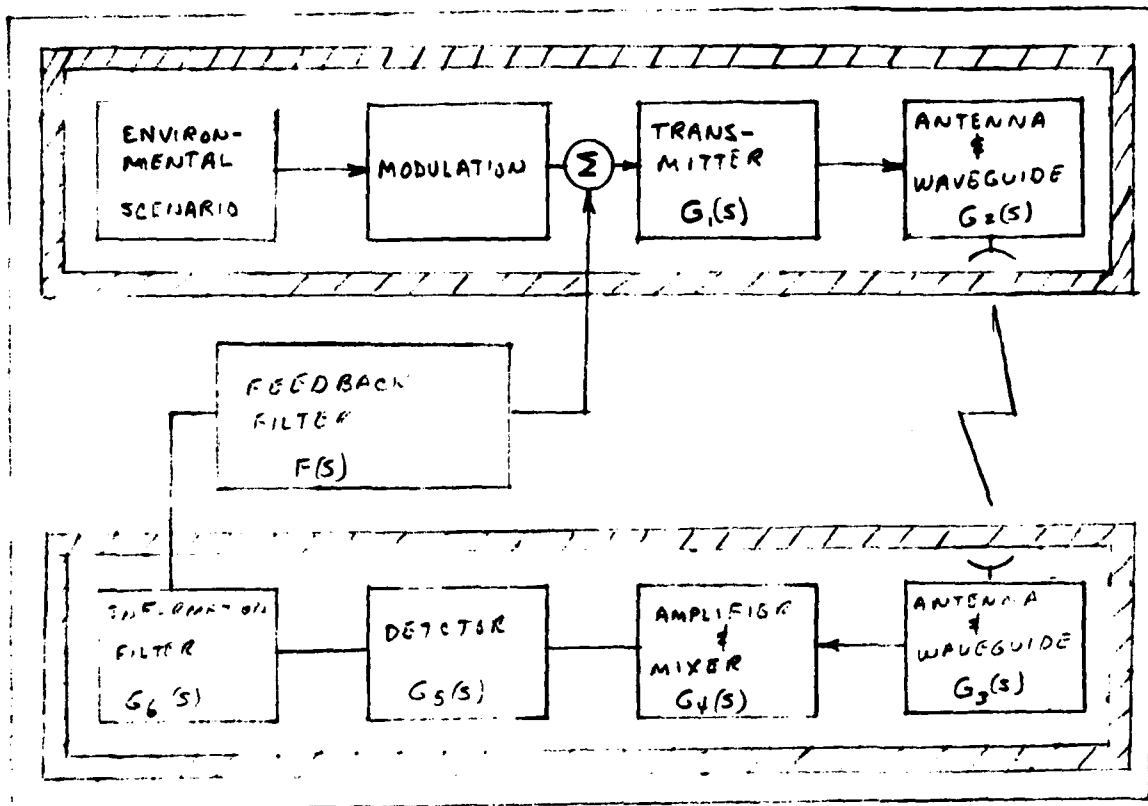


Figure (1) Radio frequency simulator with receiving system and possible feedback path

to the diagram. They are simulated transmission system, receiving system, and feedback system. It should be mentioned that the feedback system will not be implemented unless it is justified. However, the simulated transmission system is real, along with many possible receiver systems.

To apply Equation (3) to this system, the impulse response function $h(\tau)$ must be defined. By proper selection of $h(\tau)$ the input auto-correlation function can be simplified. Let the impulse response function represent the system between transmitter input and receiving system detector output. Then

$$(7) \quad H(s) = G_1(s)G_2(s)G_3(s)G_4(s)G_5(s)$$

Equation (7) represents transfer function provided the blocks in Figure (1) are isolatable and laplace transformable. Then by taking the inverse laplace transform $h(\tau)$ is defined. Then with

$$(8) \quad h(\tau) = \mathcal{F}^{-1}[H(s)]$$

$h(\tau)$ known the output of the receiver detector is given as:

$$(9) \quad y(t) = \int_0^+ h(\tau) x(t-\tau) d\tau$$

The variable $x(t-\tau)$ is the folded and shifted input signal which is the amplitude modulation waveform directed from the environmental definition. Then the output waveform is known, $h(\tau)$ is known and the output can be solved by convolution. In addition, the auto-correlation function can be determined, the output auto-correlation function can be determined and the crosscorrelation function can be determined. The computer program for determining the correlation functions and the convolution integral results has been developed during this summer project. These are all required before the mean-square error can be determined.

IV Time Domain Sensitivity Comparison Function

The time domain sensitivity comparison was first defined by Cruz and Perkins (6). This function compares the system output errors caused by system plant parameter changes for open and closed-loop conditions. The system used to define the sensitivity comparison function is shown in Figure (2).

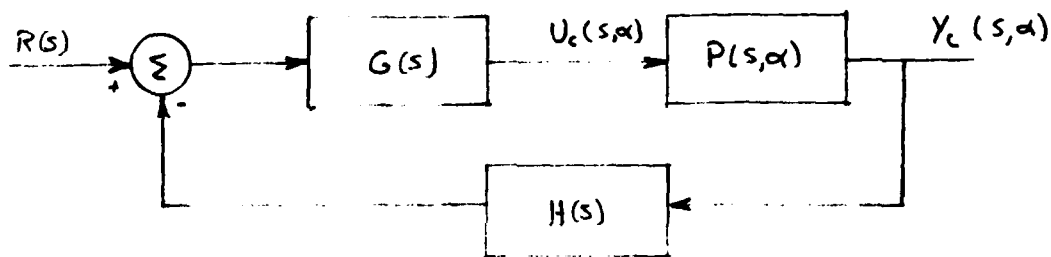


Figure (2) Closed-loop system with plant transfer function $P(s, \alpha)$, feedback transfer function $H(s)$ and forward path transfer function $G(s)$

To compare open and closed-loop conditions the following constraints are imposed:

(1) The plant parameters (α_i) are nominally the designed values and are prespecified.

(2) For nominal values of α_i the control function $U_c(s, \alpha)$ the output function $Y_c(s, \alpha)$ and the input function $R(s)$ must be equal whether the feedback path ($H(s)$) is closed or not. This implies that the value of $G(s)$ is different for open and closed loop systems. When the values of α_i depart from their nominal values, for unknown or unrecognized conditions, the errors produced in the output will generally be different for the open and closed-loop system. Cruz and Perkins developed the sensitivity comparison function which compares these different sets of errors provided the changes in the parameters, α , are sufficiently small to maintain linearity. The error comparison is defined by Equation (10). The sensitivity comparison

$$(10) \quad E_c = S E_o$$

$$S = [I + P_n G H]^{-1}$$

where: \underline{E}_c = output errors in closed-loop system

\underline{E}_o = output errors in open-loop system

P_n = nominal plant transfer function = $P_n(s, \alpha)$

$GH = G(s) H(s)$

function $S(s)$ is basically a complex plane function and can be related to the frequency domain (6).

With time domain waveforms it would be convenient to work with a sensitivity comparison function in the time domain. However, such a function does not exist in the literature. For this reason, the remainder of this discussion is devoted to developing a time domain sensitivity comparison function.

To begin development of the time domain sensitivity comparison function, consider Figure (3). The important Equations are:

$$\begin{aligned}
 (11) \quad \dot{\underline{X}}_o(t) &= F \underline{X}_o(t) + T \underline{u}_o(t) && \text{nx1 vector, state differentiated with respect to time} \\
 \underline{u}_o(t) &= G_o(t) r(t) && \text{control vector qx1} \\
 \underline{Y}_o(t) &= C \underline{X}_o(t) && \text{output vector px1}
 \end{aligned}$$

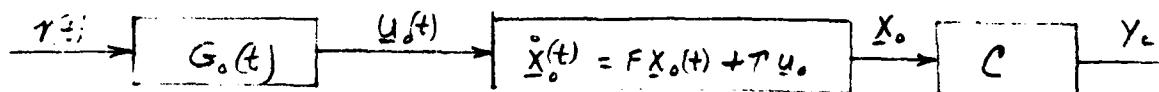


Figure (3) Open-Loop Diagram of System With Plant Matrix, F

The control variable $\underline{u}_o(t)$ can be eliminated from Equations (11) and the result is Equations (12).

$$\begin{aligned}
 (12) \quad \dot{\underline{X}}_o &= F \underline{X}_o(t) + T G_o(t) r(t) \\
 \underline{Y}_o &= C \underline{X}_o(t)
 \end{aligned}$$

A closed-loop diagram can also represent the system as shown in Figure (4)

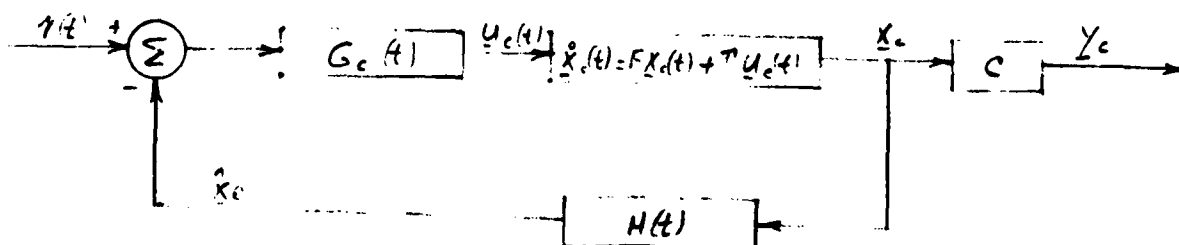


Figure (4) Closed-loop diagram of system with plant matrix, F

The important equations of the system defined in Figure (4) are:

$$\begin{aligned}
 (13) \quad \dot{\underline{X}}_o(t) &= F \underline{X}_o(t) + T \underline{u}_c(t) && \text{plant equation nx1} \\
 \underline{u}_c(t) &= G_c [\tau(t) - \underline{X}_c] && \text{control vector qx1} \\
 \underline{Y}_c(t) &= C \underline{X}_c && \text{output vector px1} \\
 \hat{\underline{X}}_c(t) &= H(t) \underline{X}_c && \text{state observation vector nx1}
 \end{aligned}$$

By eliminating $\hat{\underline{X}}_c(t)$ and the control vector, the equations become,

$$\begin{aligned}
 (14) \quad \dot{\underline{X}}_c(t) &= [F - T G_c H] \underline{X}_c(t) + T G_c \tau(t) \\
 \underline{Y}_c(t) &= C \underline{X}_c(t)
 \end{aligned}$$

The zero state solutions for the state vector in Equations (12) and (14) are,

$$\begin{aligned}
 (15) \quad \underline{X}_c(t) &= \int_0^t e^{[F - T G_c H](t-\tau)} T G_c \tau(\tau) d\tau = \int_0^t \Phi_c(t, \tau) T G_c(\tau) \tau(\tau) d\tau \\
 \underline{X}_o(t) &= \int_0^t e^{F(t-\tau)} T G_o(\tau) \tau(\tau) d\tau = \int_0^t \Phi_o(t, \tau) T G_o(\tau) \tau(\tau) d\tau
 \end{aligned}$$

where: $\Phi_c(t, \tau)$ = state transition matrix for the closed-loop system between τ and t .
 $= e^{[F - T G_c H](t-\tau)}$

$\Phi_o(t, \tau)$ = state transition matrix for the open-loop system between τ and t .
 $= e^{F(t-\tau)}$

and the outputs are:

$$\begin{aligned}
 (16) \quad Y_c &= C \underline{X}_c \\
 Y_o &= C \underline{X}_o
 \end{aligned}$$

If the outputs for the open and closed-loop systems are to be nominally equal, then:

$$(17) \quad Y_c - Y_o = 0 = C [\underline{X}_c - \underline{X}_o]$$

For Equation (17) to be satisfied for arbitrary C , then $\underline{X}_c - \underline{X}_o$ must be zero. Or

$$(18) \quad \int_0^t \Phi_c(t, \tau) T G_c(\tau) \tau(\tau) d\tau - \int_0^t \Phi_o(t, \tau) T G_o(\tau) \tau(\tau) d\tau = 0$$

Since the variables of integration and the limits of integration are the same in Equation (18), a single integral can be used.

$$(19) \quad \int_0^t [\Phi_c(t, \tau) T G_c(\tau) - \Phi_o(t, \tau) T G_o(\tau)] \tau(\tau) d\tau = 0$$

For Equation (19) to be satisfied for arbitrary $\tau(\tau)$, the terms inside the bracket must have a rank of zero. Then

$$(20) \quad \Phi_c(t, \tau) T G_c(\tau) \Phi_c(\tau, 0) T G_c(0) = 0$$

By solving for $T G_c(\tau)$ one has,

$$(21) \quad T G_c(\tau) = \Phi_c(\tau, t) \Phi_c(t, 0) T G_c(0)$$

Equation (21) is a well known equivalence relationship [].

When the plant parameters are perturbed, the state, output and derivatives are also perturbed. Since superposition holds for linear systems, Equation (12) can be written for the perturbed plant parameter condition as,

$$(22) \quad \dot{\underline{X}}_{on} - \delta \dot{\underline{X}}_o = [F + \Delta F] (\underline{X}_{on} - \delta \underline{X}_o) + T G_o(t) \gamma(t)$$

where: $\delta \dot{\underline{X}}_o$ = perturbed open-loop state derivative

$\dot{\underline{X}}_{on}$ = nominal open-loop state derivative.

ΔF = perturbed plant matrix

$\delta \underline{X}_o$ = perturbed open-loop state

\underline{X}_{on} = nominal open-loop state.

By rearranging Equation (22) one has,

$$(23) \quad [\dot{\underline{X}}_{on} - F \underline{X}_{on} - T G_o(t) \gamma(t)] - \delta \dot{\underline{X}}_o = \Delta F \underline{X}_{on} - [F + \Delta F] \delta \underline{X}_o$$

The bracketed term on the left side of Equation (23) is a null vector, according to Equation (12). Then

$$(24) \quad \delta \dot{\underline{X}}_o = -\Delta F \underline{X}_{on} + [F + \Delta F] \delta \underline{X}_o$$

The solution to Equation (24) is given from linear system theory as,

$$(25) \quad \delta \underline{X}_o(t) = e^{[F + \Delta F](t-t_0)} \delta \underline{X}_o(t_0) - \int_{t_0}^t e^{[F + \Delta F](t-\tau)} \Delta F \underline{X}_{on}(\tau) d\tau$$

Assuming that the initial error in $\delta \underline{X}_o$ is equal to zero, one has

$$(26) \quad \delta \underline{X}_o(t) = - \int_{t_0}^t e^{[F + \Delta F](t-\tau)} \Delta F \underline{X}_{on}(\tau) d\tau$$

This is the error in the open-loop system at t caused by system plant parameter changes.

An equivalent equation for errors can be written for the closed-loop system. It is given as,

$$(27) \quad \delta \underline{X}_c(t) = - \int_{t_0}^t e^{[F + \Delta F - T G_c H](t-\tau)} \Delta F \underline{X}_{on}(\tau) d\tau$$

The state error can be compared by use of Equations (26) and (27). Let

$$(28) \quad \delta \underline{X}_c(t) = \int_t \delta \underline{X}_o(t)$$

where: S_t = Time domain sensitivity comparison function.

By substitution into Equation (28) one has,

$$(29) \quad - \int_{t_0}^t \Phi_{\Delta F_c}(t, \tau) \Delta F \underline{x}_{cn}(\tau) d\tau = - S_t \int_{t_0}^t \Phi_{\Delta F_o}(t, \tau) \Delta F \underline{x}_{on}(\tau) d\tau$$

Now $\underline{x}_{cn}(\tau) = \underline{x}_{on}(\tau)$ because of the nominally equivalent condition between the open and closed-loop system. To further simplify Equation (29), assume that S_t is not a function of τ so that it can be brought under the integral. This assumption must be justified later. Then Equation (29) can be rearranged to become,

$$(30) \quad 0 = \int_{t_0}^t [S_t \Phi_{\Delta F_o}(t, \tau) - \Phi_{\Delta F_c}(t, \tau)] \Delta F \underline{x}_{on}(\tau) d\tau$$

For arbitrary ΔF and $\underline{x}_{on}(\tau)$ the integral is null if and only if the bracketed terms in the integral have rank of zero. Then the bracketed terms can be set equal to the null matrix, and by rearrangement the solution for the time domain sensitivity comparison function is,

$$(31) \quad S_t = \Phi_{\Delta F_c}(t, \tau) \Phi_{\Delta F_o}(\tau, t)$$

Equation (31) can be rewritten as,

$$(32) \quad S_t = \left[e^{[F + \Delta F - \tau G_c H](t-\tau)} \cdot e^{[F + \Delta F](\tau-t)} \right]$$

From Equation (32) it is obvious that S_t is only a function of $(t-\tau)$ and not τ by itself. Hence, the previous assumption is justified.

The sensitivity comparison function defined by Equations (31) and (32) is valid for all values of ΔF provided the system remains linear. However, the actual values of ΔF are unknown and Equation (31) and (32) are not computable. But when ΔF approaches a null matrix S_t approaches a computable form. Define,

$$(33) \quad S_t = \lim_{\Delta F \rightarrow 0} e^{[F + \Delta F - \tau G_c H](t-\tau)} \cdot e^{[F + \Delta F](\tau-t)} \\ = \Phi_c(t, \tau) \Phi_o(\tau, t)$$

The values of $\Phi_c(t, \tau)$ and $\Phi_o(\tau, t)$ can be computed and used to relate open and closed-loop state-errors as described by Equation (28). Then,

$$(34) \quad \delta \underline{x}_c(t) = \Phi_c(t, \tau) \Phi_o(\tau, t) \delta \underline{x}_o(t)$$

The last two terms on the right side of Equation (34) has the form,

$$(35) \quad \delta \underline{x}_o(\tau) = \Phi_o(\tau, t) \delta \underline{x}_o(t)$$

Then the closed-loop error at t is equal to,

$$(36) \quad \delta \underline{X}_c(t) = \Phi_c(t, \tau) \delta \underline{X}_o(\tau) = \Phi_c(t, \tau) \delta \underline{X}_o(\tau)$$

Hence, the time domain sensitivity comparison function for small perturbations assumes that $\delta \underline{X}_o(\tau) \approx \delta \underline{X}_c(\tau)$. Therefore, the closer τ is to t the smaller the difference between closed and open-loop errors. This realization of the time domain sensitivity comparison function and the fact that $\delta \underline{X}_c(t) = \Phi_c(t, \tau) \delta \underline{X}_o(\tau)$ leads to another comparison function.

$$(37) \quad [\delta \underline{X}_c(t) - \delta \underline{X}_o(t)] = [\Phi_c(t, \tau) - \Phi_o(t, \tau)] \delta \underline{X}(\tau)$$

In general, one is interested in a criteria for deciding whether a closed-loop system reduces errors due to plant parameter changes. Historically, performance indices, such as least square error, have been used. Since it is desired to keep closed-loop errors smaller than open-loop error, the difference between their squared errors can indicate the desirability of a specific system. Consider Equations (35) and (36) and the resulting square errors.

$$(38) \quad \sum_{i=1}^N \delta X_{o,i}^2(t) = \delta \underline{X}_o^T(t) \cdot \delta \underline{X}_o(t) = \delta \underline{X}_o^T(\tau) \Phi_o^T(t, \tau) \Phi_o(t, \tau) \delta \underline{X}_o(\tau)$$

$$\sum_{i=1}^N \delta X_{c,i}^2 = \delta \underline{X}_c^T(t) \cdot \delta \underline{X}_c(t) = \delta \underline{X}_o^T(\tau) \Phi_c^T(t, \tau) \Phi_c(t, \tau) \delta \underline{X}_o(\tau)$$

From Equations (38), the difference between the sum of errors squared is,

$$(39) \quad \delta \underline{X}_c^T(t) \cdot \delta \underline{X}_c(t) - \delta \underline{X}_o^T(t) \cdot \delta \underline{X}_o(t) = \delta \underline{X}_o^T(\tau) [\Phi_c^T(t, \tau) \Phi_c(t, \tau) - \Phi_o^T(t, \tau) \Phi_o(t, \tau)] \delta \underline{X}_o(\tau)$$

If the left side of Equation (39) is negative, the matrix within the brackets on the right must be negative definite. This is a criteria which can be used to test the validity for using feedback.

To obtain an elementary concept of the meaning of the criteria, consider a system plant matrix, F , which has all distinct eigen values $\lambda_1, \lambda_2, \lambda_3, \dots, \lambda_n$ and uncoupled equations. Then the state transition matrix ($\Phi_o(t, \tau)$) for the open-loop system is,

$$(40) \quad \Phi_o(t, \tau) = e^{F(t-\tau)}$$

Since the states of $\Phi_o(t, \tau)$ are uncoupled one can write Equation (40) as,

$$(41) \quad \Phi_o(t, \tau) = \begin{bmatrix} e^{\lambda_1(t-\tau)} & & \\ & e^{\lambda_2(t-\tau)} & \\ & & \ddots \\ & & & e^{\lambda_n(t-\tau)} \end{bmatrix}$$

and by premultiplying $\Phi_o(t, \tau)$ by its transpose, one has,

$$(42) \quad \Phi_o^T(t, \tau) \Phi_o(t, \tau) = \begin{bmatrix} e^{2\lambda_1(t-\tau)} & & \\ & \ddots & \\ & & e^{2\lambda_n(t-\tau)} \end{bmatrix}$$

A corresponding matrix can also be written for the closed-loop system.

$$(43) \quad \Phi_c^T(t, \tau) \Phi_c(t, \tau) = \begin{bmatrix} e^{2\lambda_{c1}(t-\tau)} & & \\ & e^{2\lambda_{c2}(t-\tau)} & \\ & & \ddots & \\ & & & e^{2\lambda_{cn}(t-\tau)} \end{bmatrix}$$

Observe that the eigen values of $\Phi^T(t, \tau) \Phi(t, \tau)$ are the square of the values for those associated with the $\Phi(t, \tau)$ matrix. Since the eigen values of $\Phi_o(t, \tau)$ and $\Phi_c(t, \tau)$ are all greater than zero, the matrices are positive definite. The closer the eigen values are to zero the smaller the positive value will become when evaluate using a quadratic form. Hence, the smaller or more negative (in the complex plane) the eigen values of the closed-loop system become the smaller the squared errors. Hence, the objective of the closed-loop system is to change the eigen values as defined by the open-loop system so that they have more negative real parts. If the feedback system can accomplish this, the closed-loop system can reduce the squared error.

V. Recommendations

The methods and concepts discussed in the preceeding sections were defined to improve analysis capability of an operational radio-frequency simulation and test facility. Such analysis should identify problems related to the operational facility. The basic areas of interest were identification of mean-square errors of unknown source and reduction of error caused by unknown changes in system parameters. The effort needed in both of these areas is not complete. Therefore, I recommend the effort in these areas be continued. To accomplish this, I recommend the following task:

(1) Identify the states of the RF system. The number of states may be large because modulation amplitude, modulation frequency, carrier amplitude, carrier frequency, carrier phase, carrier polarization, etc. must be defined. This is a difficult task.

(2) Define the transfer functions for the system as defined in Figure (1). Some of the blocks may not be linear. In which case, the transfer function of linear part should be obtained along with identification of the nonlinear mechanics.

(3) Complete the computer program for defining the mean-square error. This requires knowledge of the transfer relationships for each part of the operation system, the input auto-correlation function, desired output and auto-correlation function and the crosscorrelation function. The autocorrelation functions have been programmed by the efforts leading to this report.

(4) Continue to analyze open-loop systems with different types of state transition matrices. Such matrices should include ones with non-distinct eigen values with chains of lengths greater than one. In each case the significant impacts of the time domain sensitivity comparison function should be evaluated.

5. Design feedback systems for the RF simulation facility compatible with results obtained from the investigation in (4) above.

6. Change and/or mechanize systems as indicated by above analysis.

I cannot continue this effort for the remainder of this year because I expect to spend much of the year at the University of Florida doing other research.

REFERENCES

Conference and Journal Publications:

1. Rice, S.O., "Mathematical Analysis of Random Noise", Bell System Tech J., Vol 23, pp 282-332, July 1944; Vol 24, pp 46-156, January 1945.
2. Rice, S.O., "The Distribution of the Maxima of a Random Curve", Amer. J., Math., Vol 61, pp 409-416, April 1939.
3. Rice, S.O., "Two Lectures on Random Noise", Calif, Inst. of Technology, Pasadena, Calif, May 1952.
4. North, D.O., "Analysis of the Factors which Determine Signal/Noise Discrimination in Pulsed Carrier Systems", RCA Labs. Tech Report PTR-6C (June 25, 1943).

Textbooks:

5. Weiner, N., "The Interpolation, Extrapolation and Smoothing of Stationary Time Series", John Wiley and Sons, Inc., New York, 1949.
6. Cruz, J.B., "Feedback Systems", Inter-University Electronics Series, Volume 14, McGraw-Hill Book Company 1971.
7. Truxal, J.G., "Control System Synthesis", Electrical and Electronic Series, McGraw-Hill, 1955.

1979 USAF - SCEEE SUMMER FACULTY RESEARCH PROGRAM

Sponsored by the

AIR FORCE OFFICE OF SCIENTIFIC RESEARCH

Conducted by the

SOUTHEASTERN CENTER FOR ELECTRICAL ENGINEERING EDUCATION

FINAL REPORT

A HIGH ALTITUDE TETHERED AEROSTAT SYSTEM STUDY

Prepared by:	Dr. Edwin F. Strother
Academic Rank:	Associate Professor
Department and University:	Department of Physics and Space Sciences Florida Institute of Technology Melbourne, Florida
Research Location:	Air Force Geophysics Laboratory Aerospace Instrumentation Division Hanscom Air Force Base Massachusetts 01731
USAF Research Colleagues:	Mr. J. C. Payne and Mr. J. F. Dwyer
Date:	September 15, 1979
Contract No:	F49620-79-C-0038

A HIGH ALTITUDE TETHERED AEROSTAT SYSTEM STUDY

by

E. F. STROTHER

ABSTRACT

The advantages of a High Altitude Tethered Aerostat/Balloon system are discussed briefly. Since the tether itself is the single factor which will dominate the design of the balloon and performance of the system, a comparison and brief evaluation of various tether materials is given. Despite some handling problems, Kevlar, an aramid fiber with a specific tensile strength four to five times that of steel is the most promising tether material at the present time. The use of Kevlar cable makes it entirely feasible to operate a single natural shape balloon in the minimum wind field region which lies between 65,000 to 70,000 feet above MSL. Significant problems remain, however, associated with the deployment of a partially inflated tethered balloon through the lower altitude region of high dynamic pressure. Possible solutions to this deployment problem are given. Existing computer simulations of High Altitude Tethered Aerostat/Balloon systems are evaluated and recommendations for further work are presented. The list of 65 references at the end of this paper represents the most important contract reports and published papers relevant to high altitude tethered systems.

ACKNOWLEDGEMENT

The author would like to thank the Air Force Systems Command and the Air Force Office of Scientific Research for supporting his research at the Geophysics Laboratory, Hanscom Air Force Base. Special acknowledgement is due to Mr. James C. Payne and Mr. James F. Dwyer of the Air Force Geophysics Laboratory with whom the author worked and to the entire staff of the Aerospace Instrumentation Laboratory who, by their support and assistance, made his stay most worthwhile and interesting.

Special thanks are also due to Dr. Richard N. Miller, Managing Director of the Southeastern Center for Electrical Engineering Education, and to Dr. John N. Howard, Chief Scientist, AFGL, for their coordination of and assistance during the project.

I. INTRODUCTION

This study is based on earlier indications that high altitude (above 50,000 ft.) tethered balloons can be built and flown if certain problems are overcome. It is the purpose of this project, in part, to examine these problems and to make recommendations concerning possible solutions to them.

There are many applications, both civil and military, for stationary high altitude platforms. Most notably in the areas of communication and remote sensing, high altitude tethered balloon systems could be expected to provide cost-effective alternatives to orbiting satellites, aircraft, and free balloons.

The advantages of a high altitude tethered balloon system would be lower initial cost than satellites or aircraft and longer time on station than could be provided by aircraft or free balloons. Additionally, the tethered aerostate would have minimum operational manpower requirements and, assuming that satisfactory recovery techniques can be worked out, would be more accessible, hence more versatile than either a satellite or a free balloon. A final consideration is that they would be less energy intensive than any system requiring power for lift, propulsion, or station keeping.

The single factor which will dominate the design of a high altitude tethered system is the tether itself. A complex interaction exists between the tether and the balloon in that any increase in operational altitude results in a longer, hence heavier, cable. Therefore, in order to carry this extra weight the balloon size must be

increased with the resulting disadvantage of generating larger aerodynamic forces (lift and drag) which in turn require that a stronger (heavier) cable be used. Also, increasing the cable diameter increases the magnitude of the aerodynamic forces acting on the cable itself. Therefore, at high altitudes the cable weight penalty rapidly becomes severe with small additional increases in altitude.

The above problem can be alleviated by (1) employing cables with the highest possible strength-to-weight ratio, (2) tapering the cable, or (3) staging two or more aerostats with stepped cables interconnecting them.

Of the three solutions listed, the last is the least desirable from the standpoint of system complexity and cost. Indeed, with recent material science developments, it now seems entirely feasible to operate at very high altitudes with a single balloon and tether.

II. OBJECTIVES

The research objectives of this project were:

- (1) To review the body of literature associated with high altitude tethered balloon and aerostat systems.
- (2) To investigate various materials suitable for a high altitude tether.
- (3) To identify and evaluate existing analytical solutions of tether cable problems as they might apply to the deployment and operation of a high altitude tethered balloon system.

III. LITERATURE SEARCH RESULTS FOR HIGH ALTITUDE TETHERED AEROSTAT/BALLOON SYSTEMS

The list of references at the end of this paper represent the most important proposals, contracts, and published papers relevant to high-altitude tethered systems.

IV. TETHER MATERIALS AND PHYSICAL CHARACTERISTICS

The single most important parameter to characterize a cable is its strength to (specific) weight ratio*, which, having units of length, is also called the breaking length of the cable. This is the maximum length of cable which can support its own weight without breaking.

From Figure 1 it is seen that Kevlar 29 and Kevlar 49** have the highest breaking lengths, closely followed by a graphite composite. Compared to the more conventional tether materials like nylon, dacron, and steel, the "glass" cables consisting of bundles of fiberglass in an epoxy resin matrix, exhibit very high specific tensile strengths. For example, the glass-epoxy composite cable "Glastran" possesses three times the strength-to-weight ratio of steel cable of the same diameter yet has a tensile strength nearly equal to that of steel. More impressive still is a similar comparison of Kevlar with steel. While Kevlar, Glastran, and steel all have comparable tensile strengths, the low density of Kevlar (1.44 grams/cm^3) gives it a breaking length of four to five times greater than that of steel. The advantage of Kevlar is further illustrated when cable weight is plotted against breaking strength as is shown in Figure 2.

Another consideration in tether selection is the diameter of the cable. Under still air conditions cable size would be of relatively little concern; however, due to aerodynamic forces of the wind it is desirable to reduce the tether diameter as much as possible. Figure 3 shows for a given breaking strength there is little difference between

*The terms strength to weight ratio, specific tensile strength, and breaking length are all equivalent.

**Kevlar is a poly-p benzamide (aramid) available as low modulus type 29 or higher modulus 49. Both versions retain excellent modulus and strength up to 350°F while showing no degradation at -70°F .

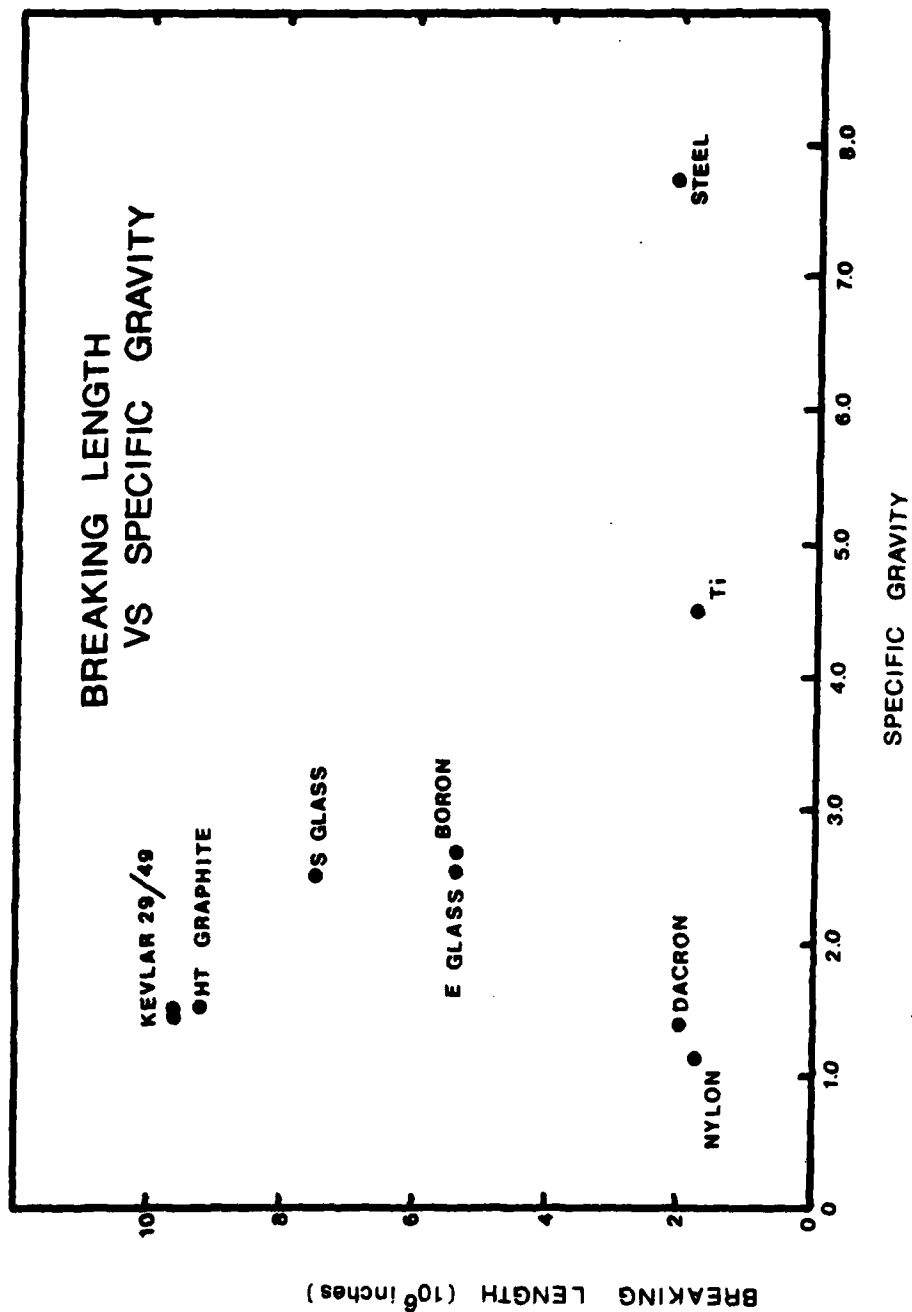


FIGURE 1: BREAKING LENGTH VS. SPECIFIC GRAVITY OF VARIOUS HIGH ALTITUDE TETHER CANDIDATE MATERIALS.

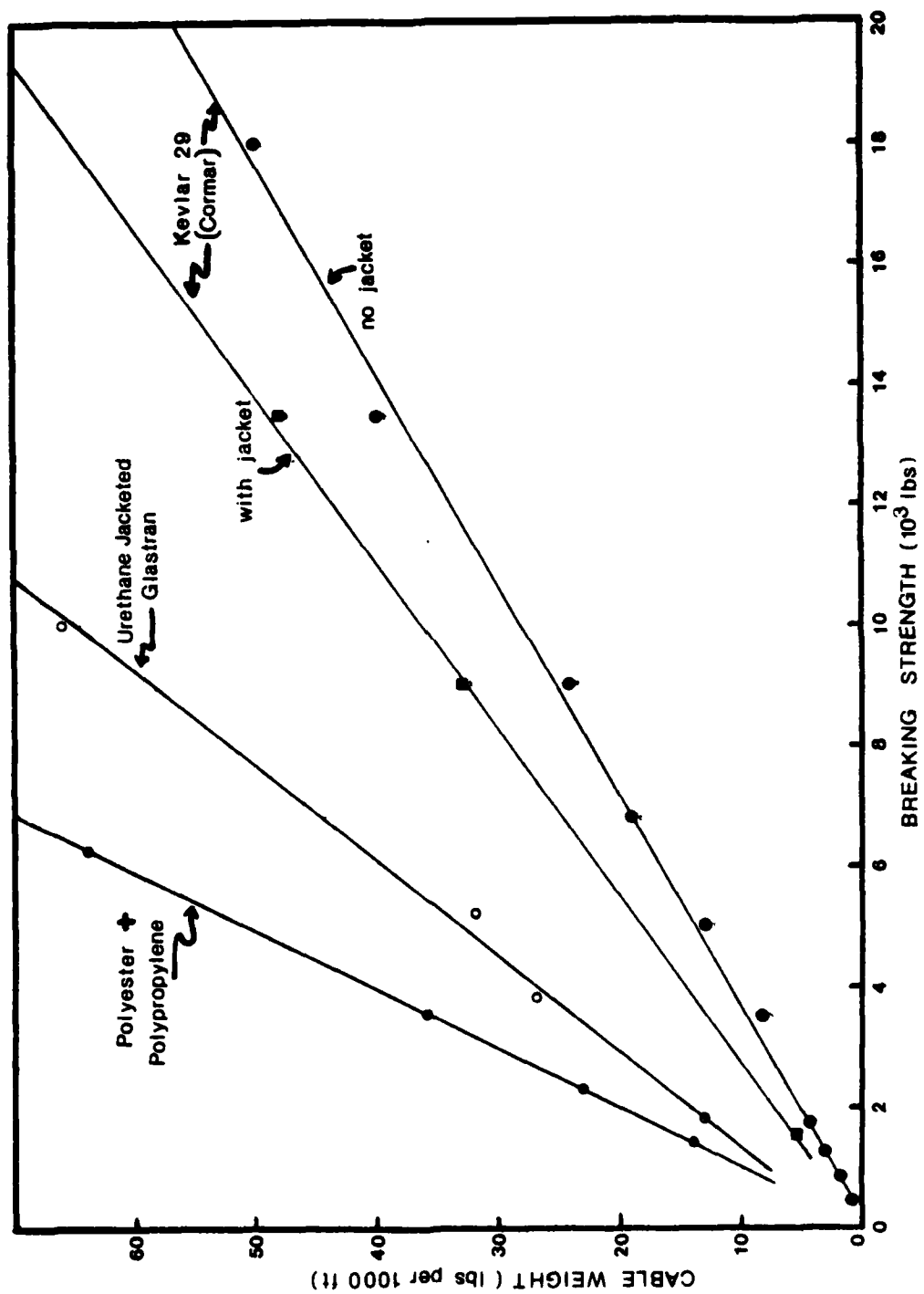


FIGURE 2: CABLE WEIGHT (LBS PER 1000 FT) VERSUS BREAKING STRENGTH IN THOUSANDS OF POUNDS.

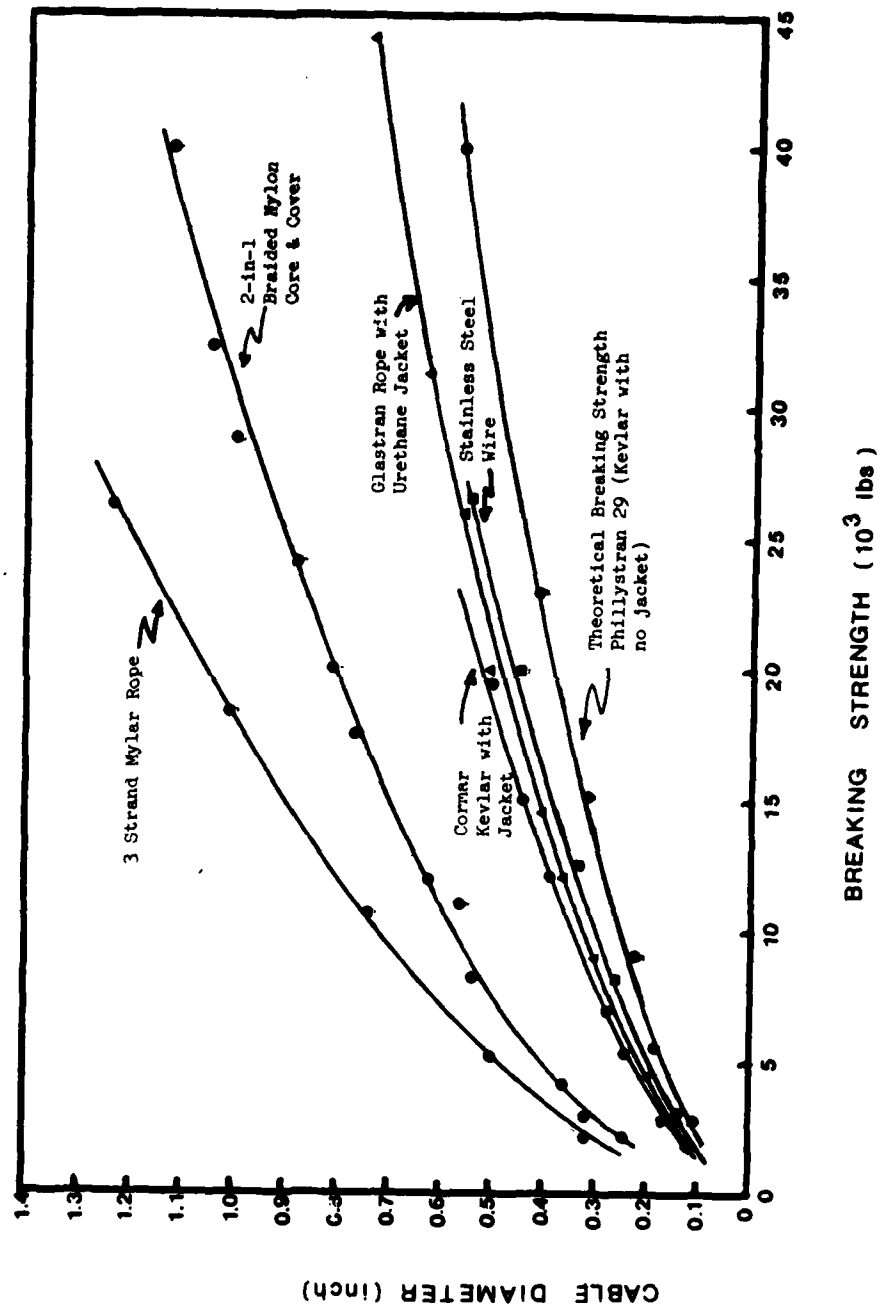


FIGURE 3: CABLE DIAMETER VERSUS BREAKING STRENGTH

the diameters of jacketed Kevlar and Glastran or steel wire rope. However, from weight considerations alone a system employing a steel tether will, even under ideal circumstances, require a balloon volume considerably larger than an equivalent system at the same design altitude using a Kevlar tether. This is illustrated in Figure 4. Here the minimum balloon volumes required for tethered flight at any given altitude up to 90,000 ft. are given for both steel and Kevlar tethers. It should be noted that in order to reach the minimum wind field altitude at approximately 65,000 feet the minimum balloon volume required with a steel tether would be approximately three times that required for an otherwise identical system employing a Kevlar tether having comparable breaking strength and diameter.

Other factors which must be considered in evaluating any tether material are:

- (1) Resistance to UV degradation
- (2) Abrasion resistance
- (3) Moisture and weathering resistance
- (4) Handling properties and winch compatibility
- (5) Cost

Kevlar lines are generally jacketed with a braided nylon or polyester and may be impregnated with neoprene or PVC. The jackets add abrasion resistance and ease of handling while providing UV protection to the Kevlar fibers. While largely unaffected by salt water, fuels, and many organic solvents, in order to prevent the absorption of moisture and minimize problems arising from icing loads, an impervious extruded

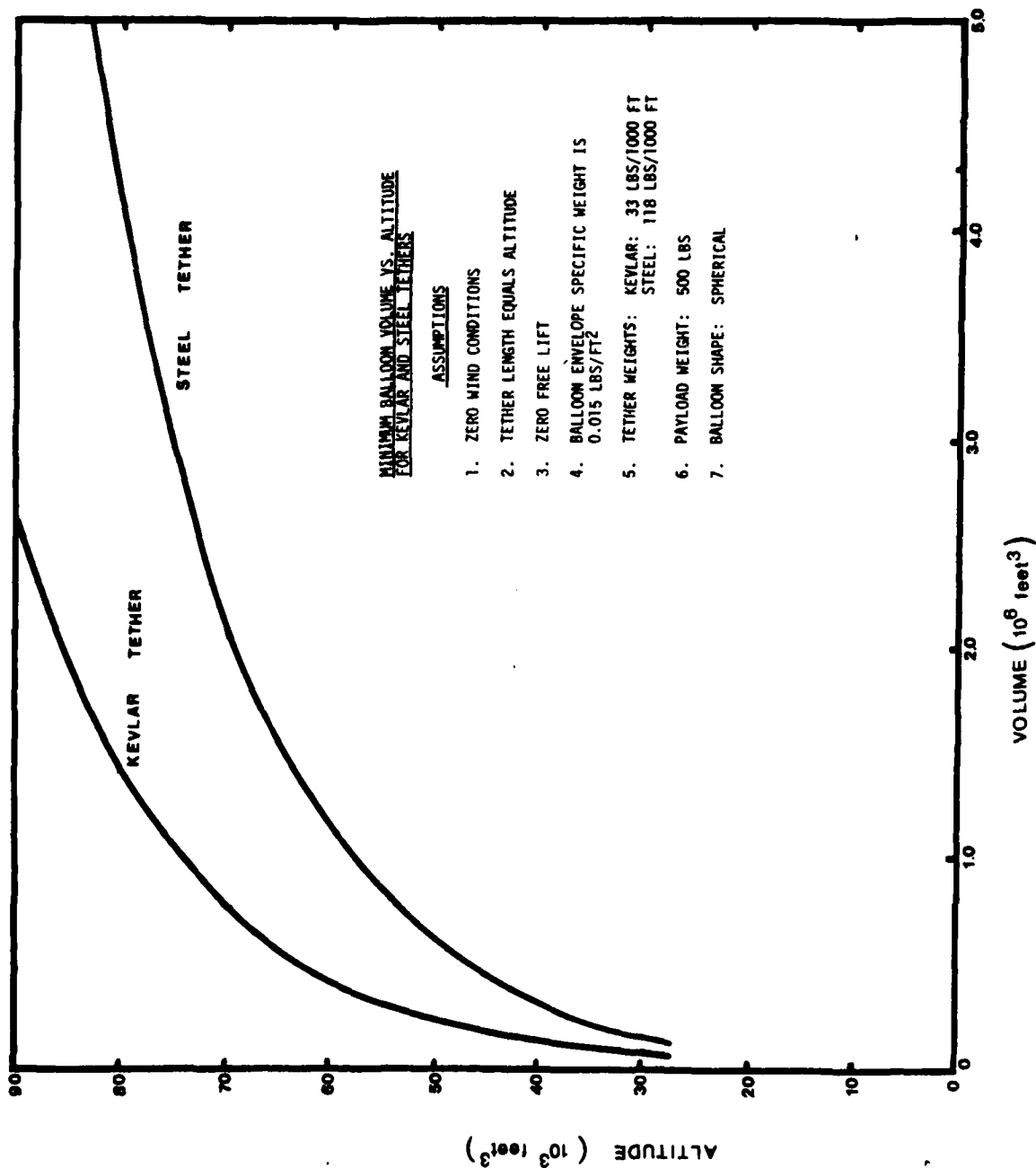


FIGURE 4:

sleeve of PVC, polyurethane, or polyethelyne should be considered in a high altitude tethered balloon system. It should be pointed out, however, that serious "hockling" problems may occur when the tension is suddenly removed from a Kevlar rope whose fibers are tightly jacketed with a material having a much lower elastic modulus.

Kevlar fibers can be braided to produce no-torque lines and ropes. However, recent AFGL experience with braided Kevlar indicates that the fibers can break on the friction drive due to torsion applied by the winch. That is, some fibers are loaded and some unloaded over a short length; this unequal loading causes failure of individual fibers. This observation is consistent with Kevlar's intrinsic elastic/nonplastic properties which make it much less forgiving than other rope and cable materials. Along the tether itself the torsional problem is not as severe as it is on the winch since the twist is distributed over a long cable length. A swivel joint at the confluence point can further reduce torsional problems in the tether.

V. EVALUATION OF COMPUTER SIMULATIONS

In the absence of wind and weather the tethered aerostat, independent of its design altitude, is a very simple system to analyze. Under this idealized situation, no phase of its flight mode, including deployment or recovery, is difficult to describe analytically. The next complication would be to treat a tethered system at equilibrium under the action of a constant two dimensional wind field. Of course, the deployment and recovery phases being dynamic processes require a more sophisticated analysis than does the system under steady state conditions at a fixed operational altitude.

During this project a detailed investigation was undertaken to identify and evaluate any existing programs which would provide computer simulation of the deployment of a high altitude tethered balloon or aerostat system. A series of programs were developed in 1976-77 at AFGL* for use in a Hewlett-Packard Model 9810A desk computer. The following is a brief summary of these programs which could be used in the design and performance of a tethered balloon system.

Program 76.001 (Basic Buoyancy) treats the most restricted static case of no wind conditions. This program can be used to determine the minimum balloon/aerostat volume required to operate at a given altitude with zero ballonnet volume. It also provides an option for multi-cable geometry. Program 76.002, also restricted to no wind conditions, locates the position of the balloon's center of gravity and center of buoyancy for a given trim angle at a given altitude. Programs 76.003, 004, and 005 generalize the system flight conditions to include the effects of a two dimensional wind field. They determine the balloon

*AFGL-TR-0195, John B. Wright, 26 August 1976; and AFGL-TR-77-0203, John B. Wright, 15 September 1977.

trim angle α , the total force F_T at the top of the tether, and θ , the tether angle at the balloon. While 76.003 is a general program for any tethered balloon, 76.004-5 are specialized to a 45,000 ft³ aerostat of the Family II design. Program 76.004 is in turn restricted to a single design altitude (for which case the ballonnet volume is zero) whereas 76.005 is more general in that it provides α , F_T , and θ for a Family II aerostat over a range of altitudes from ballonnet empty to full.

Program 76.006 determines tether cable parameters of a single cable in a two dimensional wind field. It provides the tension, angle, and space position of all points of the cable from balloon to surface. A limitation is that F_T and θ must be known at each altitude. Hence, either 76.003, 4, or 5 must be run before 76.006 in order to determine the net total force and its angle at the balloon when the balloon is at a given trim condition.

AFGL Program 77.007 retains many features of 76.006 but generalizes to three dimensions in that both the magnitude and azimuth of the wind up to twelve different altitudes are permitted. Program 77.007P, which includes a plotting subroutine, is essentially identical to 77.007. Both of these programs are based on solving the cable problem where the balloon altitude is fixed. Behavior of the balloon and tether during deployment or recovery can be done in steps by a restart option which allows the program to be rerun with the balloon relocated at a new altitude in the same wind field. Again, as in the case of 76.006, the parameters F_T and θ must be calculated by programs 76.003-5 and then used as inputs to the three dimensional programs.

Program 77.007 has two options; (1) a rerun with a different cable without having to re-enter a new wind profile, and (ii) the ability to hold the cable length just calculated constant, change the wind profile and find the balloon's new equilibrium altitude. This second option requires the use of program 77.007B. Both 77.007 and 77.007B are designed to be used together and therefore each can be used to call the other.

The AFGL programs are applicable up to an altitude of 20 kilometers (approximately 65,600 feet) altitude without modification. In principle, therefore, they can be used to simulate a high altitude tethered balloon system; however, they suffer from several major deficiencies. In particular, several programs must be run sequentially in order to accomplish a given deployment or recovery simulation. It should also be pointed out that a true real time deployment simulation is not possible with these programs. Rather, the simulation consists of starting the balloon at altitude and determining its equilibrium configuration under the action of a given wind profile. Then, a new set of input parameters are calculated (from another program) for a lower altitude; these in turn are fed into the main program to determine the new balloon/tether equilibrium configuration in the same wind field. Essentially this provides a quasi-static simulation in which the balloon and tether system move from one equilibrium position to the next. Therefore, it will approximate a real recovery or deployment only if the cable is winched in or out sufficiently slowly.

Another restriction is that these programs are written for balloons or aerostats with ballonets. Therefore, while it is fairly straightforward, if not tedious, to obtain a flight simulation of a Family II tethered aerostat in order to completely simulate the deployment of a reefed natural shaped balloon, certain program modifications would have

to be made. On the other hand, given the total force vector \vec{F}_T at the top of the tether, then the balloon space and type is irrelevant and for a given altitude the system simply reduces to a tether (no balloon) with a top force F_T acting at angle θ above the horizontal.

Also under evaluation during this study was a mathematical model and computer program developed by GAC* to simulate the ascent and descent of high altitude tethered aerostats through a three dimensional wind profile. The analytical approach used was to write the Lagrangian for the system from which Lagrange's equations of motion could be obtained; Runge-Kutta numerical integration was then used to solve the equations of motion for the tether/balloon system.

While the basic analytical approach is correct as it is applied to the system model, there are several deficiencies in the model itself. For example, the balloon is considered to be a thin spherical shell which expands as it rises. This, of course, is not a realistic model of an actual balloon during deployment. The tether modeling is more realistic in that it is simulated by N number of straight links which grow at the same rate as the tether is "paid out." However, the program lacks versatility by assuming the use of a stepped cable (rather than a tapered or constant diameter cable). Therefore, for the simple case of a uniform tether, the program still requires an unnecessarily complicated tether data input field and continues to determine the weight of each link by averaging the end conditions. On the other hand, if a continuously tapered tether is used, the

*Technical Report GER 13714 Task Report No. 4, ARPA Contract F19628-67-C-0145. Goodyear Aerospace Corp., 1 February, 1968.

tether diameter must be determined at thirty-three positions along its length and this information presented as input data.

While a detailed evaluation of this simulation was not possible by the end of this study, the program deck had been recovered (by manual keypunch) from the program listings which were available. Furthermore, the program has been documented and a duplicate deck produced. Mr. Jim Dwyer generated several subroutines which were entirely missing from the program listing itself. At the time of this writing the program has been run extensively for diagnostic purposes and should be ready for a production run very soon.

VI. RECOMMENDATIONS

At the present time the operation of a single natural shape tethered balloon in the minimum wind field region between 65,000 to 70,000 feet above mean sealevel seems entirely feasible. Kevlar, despite some handling problems is the tether of choice due to its high strength to weight ratio. In order for Kevlar to reach its full potential as a balloon tether material improvement needs to be made in the areas of covering (jacket) material and winch compatibility.

The problem of deploying a natural shape balloon through the region of maximum dynamic pressure which generally occurs between 30,000-50,000 feet has yet to be resolved. While the main requirements are to prevent the loose uninflated balloon material from acting like a sail during ascent, the following possible solutions exist:

- (1) Reefing the uninflated portion of the balloon such that the reefing points can be sequentially released allowing part of the excess material to be free for additional gas expansion during further ascent.

- (2) Providing the balloon with a ballonet/blower system.
- (3) Designing the partially inflated balloon to have an aerodynamical shape during ascent through the region of high wind velocities; as it continues to ascend into a region of lower wind speeds, the fully inflated shape would become more spherical.
- (4) Employing a tandem aerostat/balloon system in order to penetrate the high pressure region.
- (5) Top loading the balloon in order to maintain a tight balloon envelope during ascent.
- (6) Allowing free ascent of the balloon to an altitude above the region of high wind velocities where upon the tether would be deployed from the balloon, recovered and secured to a ground winch.

While several of these techniques have been attempted, none to date have been entirely successful. In the light of new materials development more work needs to be done before it will be possible to identify the best deployment technique.

Additional work also needs to be done in the area of computer simulation of both the ascent and the descent of a high altitude tethered balloon system. It is therefore recommended that the AFGL programs be used to simulate the deployment of various balloon types in a typical three dimensional wind field using the various deployment techniques described above. Even without modification, these programs will provide total cable length, the space configuration of the cable, and the horizontal "blow-down" distance of the balloon in a given wind field.

If it is intended that these programs be used extensively, then a beneficial step would be to convert them from the reversed polish language of the HP-9810A to Fortran IV. This would eliminate the program memory limitations of the HP-9810A and would allow a given simulation to be accomplished in a single rather than multiple runs.

It is also recommended that work continue on the program originally developed by Goodyear Aerospace Corporation. When completed, this program should provide a valuable real-time simulation of the deployment or recovery of a high altitude tethered balloon system. Unlike the AFGL programs, this program allows the investigator to vary the winching rate of the tether and to determine the effects this will have on the balloon/tether system.

REFERENCES

TETHERED BALLOON SYSTEMS/HIGH ALTITUDE CONCEPTS

FEASIBILITY STUDY FOR A HIGH-ALTITUDE TETHERED BALLOON SYSTEM (BALTOON) (U). Technical Report 2452. ARPA Contract SD-198, Electric Division of General Mills, Inc., St. Paul, Minnesota, 21 October 1963.

FEASIBILITY STUDY, HIGH-ALTITUDE TETHERED BALLOON SYSTEM FOR ADVANCED RESEARCH PROJECTS AGENCY. Technical Report GER 11287. ARPA Contract SD-199. Goodyear Aerospace Corporation, Akron, Ohio, 23 October 1963.

FINAL REPORT, FEASIBILITY STUDY (U). Technical Report 1724-TR1. ARPA Contract SD200 Minneapolis-Honeywell Regulator Company, Aeronautical Division, Minneapolis, Minnesota, 8 October 1963.

ONE-HUNDRED-THOUSAND FOOT TETHERED BALLOON FEASIBILITY STUDY (U). Technical Report TR01820.01-1. Prepared for Office of Secretary of Defense, Advanced Research Projects Agency. ARPA Contract SD-201. Vitro Laboratories Division of Vitro Corporation of America, 9 October 1963.

HIGH ALTITUDE TETHERED BALLOON SYSTEMS STUDY, TASK REPORTS, Goodyear Aerospace Corp Contract F19(628)-67-C-0145:

TASK REPORT 1, J. Menke, May 1967.

TASK REPORT 2, J. Vorachek, November 1967.

TASK REPORT 3, W. Conley, January 1968.

TASK REPORT 5, J. Vorachek, March 1968.

HIGH ALTITUDE TETHERED BALLOON SYSTEMS STUDY Technical Report GER 13260. AFCL Contract F 19628-67-C-0145, Goodyear Aerospace Corp., Akron, Ohio 23 Oct. 1963.

FEASIBILITY STUDY OF HIGH ALTITUDE BALLOON SUPPORTED STATIONARY PLATFORMS, Report No. MR 20,092, C. Kaplan, April 1960.

PROPOSAL FOR A TETHERED BALLOON SYSTEM FOR THE DEFENSE ATOMIC SUPPORT AGENCY, Honeywell Systems and Research Div., Revised 30 July 1965 as Document 5C-E-17-1.

TETHERED AEROLOGICAL BALLOON SYSTEM-Phase I, Contract N123-(60539) 38845A, Aerological Laboratories, 19 Sept. 1963.

TETHERED AEROLOGICAL BALLOON SYSTEM RESEARCH AND DEVELOPMENT PROGRAM, C. A. Smith, N 123 (60530)38845A, 15 Feb., 1965.

HIGH-ALTITUDE TETHERED BALLOON DESIGN, W. F. Conley, Proc., AFCL Tethered Balloon Workshop 1967, p. 43-59.

TETHER CABLE DYNAMICS

FORCES ON A CABLE-RESTRAINED BALLOON SYSTEM, J. Angevine et. al., NCAR TN-47, Jan., 1970.

THE OSCILLATORY MOTION OF CABLE TOWED BODIES, L. F. Whicker, Dissertation--University of California, July 16, 1957.

EQUILIBRIUM AND NATURAL FREQUENCIES OF CABLE STRUCTURES (A NONLINEAR FINITE ELEMENT APPROACH) W. M. Henghold; J. J. Russell (From: Computers and Structures, Vol. 6, 1976.)

THE STABILITY OF CAPTIVE BALLOONS FOR INSTRUMENT FLYING, (Includes Analysis of Multi-Cable Configurations,) R. Potter, Contract NA58-5384(6711729), 1965.

ANALYSIS OF AN ELASTIC CABLE WITH BALLOON IN WIND, D. Walker, AFCE Analog Section.

EQUILIBRIUM AND STABILITY OF A CIRCULATORY TOWED CABLE SUBJECT TO AERODYNAMIC DRAG, J. J. Russell; W. J. Anderson, From Journal of Aircraft, Vol. 14, July, 1977.

A FINITE ELEMENT ANALYSIS OF VORTEX-INDUCED CABLE OSCILLATIONS, J. J. Russell, Research Report, May 1979.

VIBRATION OF POWER LINES IN A STEADY WIND (Suppression of Vibrations By Tuned Dampers), R. Ruedy, Canadian Journal of Research, Vol. 13, Manuscript Received Oct. 11, 1935.

GALLOPING CONDUCTORS AND A METHOD FOR STUDYING THEM, E. L. Tornquist; C. Becker, From: AIEE Transactions, Vol. 66, 1947.

EQUILIBRIUM CONFIGURATIONS OF FLYING CABLES OF CAPTIVE BALLOONS, AND CABLE DERIVATIVES FOR STABILITY CALCULATIONS, S. Neumark, Report #AERO 2653, Ministry of Aviation, London, June 1961.

ON THE ACTION OF WIND OF FLEXIBLE CABLES, WITH APPLICATIONS TO CABLES TOWED BELOW AEROPLANES, AND BALLOON CABLES, A. R. McLeod, From: Advisory Committee for Aeronautics, London, October 1918.

STEADY STATE BEHAVIOUR OF A CABLE USED FOR SUSPENDING A SONAR BODY FROM A HELICOPTER, N. E. Gilbert, Department of Defense (Australia) Aerodynamic Report 149, AR-001-269, May 1978.

A THEORETICAL AND EXPERIMENTAL INVESTIGATION OF IMPACT LOADS IN STRANDED STEEL CABLES DURING LONGITUDINAL EXCITATION, J. F. Goeller, et. al. Themis Program N00014-68-0506-0001, April 1960.

PROPOGATION OF A LONGITUDINAL PULSE IN WIRE ROPES UNDER AXIAL LOADS, H. H. Vanderveldt, et al., Experimental Mechanics, Oct. 1970.

WIND INDUCED VIBRATIONS OF SKEWED CIRCULAR CYLINDERS, G. H. Koopman, Themis Program N00014-68-A-0506-0001, Report 70100, Nov. 1970.

DYNAMICAL STABILITY OF A TOWED THIN FLEXIBLE CYLINDER, H. P. Pao, Themix Program NO. 893(1968-71) N00014-68-A-0506, Report 69-11, Dec. 1969.

RESISTANCE OF STREAMLINE WIRES, G. Defoe, NACA TN 279, March 1928.

TABLES FOR COMPUTING THE EQUILIBRIUM CONFIGURATION OF A FLEXIBLE CABLE IN A UNIFORM STREAM, L. Pote, Department of the Navy, R&D Report, March, 1951.

A FIRST ORDER THEORY FOR PREDICTING THE STABILITY OF CABLE TOWED AND TETHERED BODIES WHERE THE CABLE HAS A GENERAL CURVATURE AND TENSION VARIATION, J. DeLaurier, Von Karman Inst., Fluid Dynamics, TN-68-1970.

A STABILITY ANALYSIS OF CABLE BODY SYSTEMS TOTALLY IMMERSED IN A FLUID STREAM, J. DeLaurier, NASA CR 2021m, 1972.

FORCES ON A CABLE -RESTRAINED BALLOON SYSTEM. J. Angevine et al., NCAR-TN-47, January 1970.

TETHER MATERIALS/EVALUATION

COMAR-KEVLAR ROPES AND CABLES, E. Scala, Sea Technology, July 1977, p. 13.

TETHER CABLE EVALUATION, Goodyear Aerospace Corp., Technical Report GER-12561.

AEROSPACE WIRE AND CABLES METHODS OF TESTING, Aerospace Standard, 15 July, 1971.

GLASS EPOXY COMPOSITE CABLES FOR TETHERED BALLOONS, G. Hanna, Proc. AFCRL Tethered Balloon Workshop, p. 129, 1967.

AEROSTRAND, J. Kane, Proc. AFCRL Tethered Balloon Workshop, p. 115, 1967.

REINFORCED FIBERGLASS AS A BALLOON TETHER, R. McKee, Proc. AFCRL Tethered Balloon Workshop, p. 163, 1967. AFCRL-68-0097, March, 1968.

TETHERED AEROLOGICAL BALLOON SYSTEM, S. Elliott, et al., NOTS TP 3830, Sept. 1965.

SOME ASPECTS OF HIGH-ALTITUDE TETHERED BALLOON FLIGHT, L. A. Speed, Proc., AFCRL Tethered Balloon Workshop, 1967, p. 95-104.

TETHERED BALLOONS: PRESENT AND FUTURE, E. Young, AIAA Paper 68-941, Sept. 1968.

TETHERED AEROLOGICAL BALLOON SYSTEM, S. D. Elliott, Proc., AFCRL SBS 1964, p. 1-26.

TETHERED BALLOON SYSTEMS/GENERAL CONCEPTS

BALLOONS ON A TETHER, Aerospace Instrumentation Laboratory, AFCRL, OAR Review, March-April, 1969, p. 6.

DEFINITION OF TETHERED BALLOON SYSTEMS, P. Myers et al., GAC, Contract FL9628071-C-0091, Scientific Report 1, (AD725708).

AFCRL TETHERED BALLOON PROGRAMS, W. Ferguson, Proc. AFCRL Scientific Balloon Workshop 1965, p. 77 (AD634765).

STATISTICS OF PARAMETERS AFFECTING TETHERED BALLOON FLIGHTS, J. Hess, AFCRL-66-480, July 1966 (AD637853).

CAPABILITIES OF CAPTIVE BALLOON SYSTEMS, J. A. Menke. Proc. AFCRL Sci. Ball. Systems, p. 183-202, Dec. 1963.

NEW FRENCH TETHERED BALLOONS OF LARGE VOLUME: DEVELOPMENT, HANDLING, AND SAFETY PROBLEMS, P. Perroud, et al. Proc., Sixth AFCRL, Scientific Balloon Systems, p. 423-438, Oct. 1970.

COMPUTER SIMULATIONS OF HIGH ALTITUDE TETHERED BALLOON SYSTEMS

COMPUTER PROGRAMS FOR TETHERED BALLOON SYSTEM DESIGN AND PERFORMANCE EVALUATION, J. B. Wright, AFGL-TR-76-0195, 26 Aug. 1976.

COMPUTER PROGRAMS FOR THREE-DIMENSIONAL CABLE PROBLEMS IN TETHERED BALLOON APPLICATIONS, J. B. Wright, AFGL-TR-770203, 15 Sept., 1977.

MATHEMATICAL MODEL AND COMPUTER PROGRAM FOR ASCENT AND DESCENT OF HIGH ALTITUDE TETHERED BALLOON SYSTEMS, G. Doyle, et al., Goodyear Aerospace Corp., Task Report 4, Contract F 19(628)-67-C-0145, Feb. 1968.

BALLOON MOTIONS

A DYNAMIC ANALYSIS OF A MOORED AERODYNAMICALLY SHAPED BALLOON SUBJECTED TO ATMOSPHERIC TURBULENCE, J. D. DeLaurier, Proc., Seventh AFCRL Scientific Balloon Symposium, p. 177-193.

INVESTIGATION OF STABILITY CHARACTERISTICS OF TETHERED BALLOON SYSTEMS, G. Doyle, et al. Goodyear Aerospace Corp., Contract F19628-71-C-0091, Scientific Report No. 2, July 1971, AFCRL-71-0406(AD731570).

INVESTIGATION OF DYNAMIC BEHAVIOR OF TETHERED BALLOON SYSTEMS, J. Vorachek, et al., Goodyear Aerospace Corp., Contract F 19628-71-C-0091, Final Report, Jan. 1972.

STABILITY AND DYNAMIC BEHAVIOR OF TWO TETHERED BALLOON SYSTEMS, G. Doyle, et al., Goodyear Aerospace Corp., Contract F 19628-73-C-0219, AFCRL-TR-73-0396.

COMPARISON OF ANALYTICALLY AND EXPERIMENTALLY DETERMINED DYNAMIC BEHAVIOR OF TETHERED BALLOONS, J. Vorachek, et al., GAC, Contract F19628-72-C-0219, Scientific Report No. 1, March 1973.

COMPUTER PROGRAMS FOR CALCULATING AND PLOTTING THE STABILITY CHARACTERISTICS OF A BALLOON TETHERED IN A WIND, R. Bennett et al., NASA TM X-2740, 1973.

STABILITY ANALYSIS AND TREND STUDY OF A BALLOON TETHERED IN A WIND, WITH EXPERIMENTAL COMPARISONS, L. T. Redd, et al., NASA TN-7272, 1973.

THE STABILITY OF CAPTIVE BALLOONS FOR INSTRUMENT FLYING, INCLUDING ANALYSIS OF MULTI-CABLE CONFIGURATIONS, Wyle Labs, R. Potter, Contract NAS 8-5384(6711729), 1965.

MISCELLANEOUS

ATMOSPHERIC ELECTRICAL HAZARDS RELATED TO TETHERED BALLOONS, R. Behn, Battelle Columbus Labs Tactical Tech Center, Contract No. F33657-710C-0893, May 1972.

LIGHTNING PROTECTION MEASURES FOR LOW-ALTITUDE TETHERED BALLOON SYSTEMS, P. E. eggers et al., Battelle Columbus Laboratories Tactical Technology Center Contract DAA H01-72-C-0982, May 1973. Report No. A-4038(LP) Task No. 1.

1979 USAF - SCEE SUMMER FACULTY RESEARCH PROGRAM

Sponsored by the

AIR FORCE OFFICE OF SCIENTIFIC RESEARCH

Conducted by the

SOUTHEASTERN CENTER FOR ELECTRICAL ENGINEERING EDUCATION

FINAL REPORT

PATTERN RECOGNITION/IMAGE PROCESSING IN OPTICAL TRACKING

Prepared by: Edgar C. Tacker

Academic Rank: Professor

Dept. & Univ.: Electrical Engineering Dept.
University of Houston
Houston, Texas 77004

Research
Location: The Frank J. Seiler Research Laboratory
USAF Academy, Colorado 80840

USAF Research
Colleague: Lt. Col. Joseph S. Ford II
Director of Aerospace - Mechanics Sciences

Date: September 17, 1979

Contract: F49620-79-C-0038

PATTERN RECOGNITION/IMAGE PROCESSING
IN OPTICAL TRACKING

by

Edgar C. Tacker

ABSTRACT

The availability of advanced microprocessor technology opens up new opportunities for exploring tracking schemes that up to now would not have been considered due to excessive computational complexity, weight, or cost. This report describes an approach that utilizes a particular method of image feature selection and decision analysis. Preliminary results are stated and a comprehensive set of recommendations for future research is given.

Also discussed is the progress made by this author in establishing a seminar series and workshop/conference on image processing and pattern recognition, to be held at the USAFA this coming year.

ACKNOWLEDGEMENT

First, the author wishes to express his appreciation to the Air Force Systems Command and the Air Force Office of Scientific Research for sponsoring the Summer Faculty Research Program. This program was expertly directed by Dr. Richard N. Miller of the Southeastern Center for Electrical Engineering Education.

The author especially appreciated the friendly professional research attitudes of the entire staff of the Frank J. Sellar Research Laboratory. Special thanks are due to Donna Weiss for her superb secretarial service. Finally, the author wishes to thank Lt. Col. Joseph S. Ford II for his unfailing enthusiasm and his wealth of original ideas that initiated and sustained my research efforts this past summer.

I INTRODUCTION

A great deal is known about optical tracking and quite sophisticated optical tracking systems have been designed and employed. One fundamental thesis of the work described herein was not to attempt to add refinements to well established tracking methods, but rather to strive to generate new ideas in this area. Another fundamental thesis was to concentrate on those ideas that promised to lead to tracker designs that feature extreme simplicity (and thus most likely low total costs) while meeting practicable constraints relative to required speed and accuracy.

It seemed clear that the summer of 1979 was an especially appropriate time for commencing to adopt these two fundamental theses. Just recently the intersection of two powerful forces has become a significant factor in R&D planning in the national defense sector. First, the increasingly rapid escalation of costs of producing armaments using available designs, together with the essentially flat-in-real-terms DOD allocations, has priced most of the available missile designs out of the defense market (at least with respect to any credible number being produced within these budgetary constraints). Secondly, microprocessor/microcomputer technology has finally come of age. In particular, it has been established that these devices can be mass produced with sufficient end-product reliability and, moreover, the true capabilities of these products (and their near-term successors) are clearly perceived. In short, the availability of this advanced microprocessor technology opens up new opportunities for exploring guidance and tracking schemes that up until now would not have been considered due to excessive computational complexity, weight, or cost.

II. OBJECTIVES OF THE RESEARCH EFFORT

There are of course numerous ways to utilize ten weeks of research effort by an individual. After quite a bit of thought it was decided that the most effective approach for our particular situation would be for me to spend this time assisting the FJSRL in initiating a research program of a considerably wider scope. As far as my personal efforts were concerned there were to be two primary components of research. One component involved formalizing and generalizing some ideas in optical tracking originally suggested by Lt. Col. Joseph S. Ford at FJSRL. The other component involved planning and organizing a research seminar series in the area of image processing and pattern recognition to be held at the USAFA over the next year. In the process of discussions with potential invited speakers it became apparent that there was great interest in the research community in developing more scientific interaction than could be afforded via the seminar series. For this reason a new objective was added to the list of objectives--that of initiating the organization of a culminating workshop/conference.*

III THE OPTICAL TRACKING PROBLEM

Consider the requirement of obtaining a sequence of images from some target object in a form appropriate for automatic processing and interpretation via a microcomputer system. For instance, these images could be obtained from a camera with an appropriate lensing subsystem and an appropriately thresholded and controlled CCD array. Whenever convenient we shall refer to this particular implementation means (which would, of course, also include an appropriate interface to the microcomputer system); however, the proposed research is not at all dependent upon using this particular type of

*Progress as of August, 1979 on the planning and organization of the seminar series and culminating workshop/conference will be given in Appendix I

camera system.

In the usual case the target will be imbedded within a field of clutter, and the unprocessed image will fail to adequately describe the target. This unprocessed image may be thought of as being composed of two images, one being closely related to the true target image, and one closely representing the total background within the field of view. The densities and relative motions of these hypothetical images would in general be expected to differ, thereby providing a means of discriminating between these two components. Thus, at least partial suppression of the clutter component should be possible, thereby enhancing the signal/noise ratio for target tracking purposes. These considerations formed the primary intuitive impetus for the research, while the challenge associated with the need for transforming such qualitative notions into scientifically sound methods formed the primary analytical impetus for the research.

Due to the aforementioned cost considerations it was decided to start at a very basic level of system complexity, adding additional sophistication only if a definite need for it could be demonstrated.

The most basic of picture functions are composed of pixels having a single gray level. During this initial research phase attention was restricted to the use of binary-valued picture functions having matrix representations of the form of an $n \times n$ matrix, $P = (P_{ij})$, wherein

- (a) $n = 2^k$, k a positive integer
 - (b) $P_{ij} = 0$ or 1 for $1 \leq i, j \leq n$.
- (1)

Thus, a given picture function is represented by one of the $2^{2^n} (= 2^{2^{2^k}})$ binary-valued $n \times n$ matrices of this form.

For our purposes* the object to be tracked will at each instant in time be

*Guidance and control problems were not explicitly considered in this research.

represented by a corresponding binary-valued picture function generically denoted by the symbol R . R will be a binary-valued $n \times n$ matrix of the form given in (1). At the initial time $k = 0^*$ the acquisition subsystem** furnishes the initial "reference" image (pattern) R_0 to the tracking subsystem, and it is the task of the tracking subsystem to track the future "motions" of this reference pattern. In a completely deterministic (and therefore completely unrealistic) setting only the position of R_0 would change; i.e., if we momentarily let $R(k)$ denote the binary-valued picture function representing the object to be tracked at time k , then $R(k) = R_0$ for all $k > 0$. If we now let $S(k)$ denote the output of our optical tracker at time k , then in this idealic deterministic setting we know that the optimum output should satisfy $S(k) = R(k) = R_0$ for all $k > 0$. In a non-deterministic setting the identity $R(k) = R_0$ no longer holds, and a reference-updating criterion must be devised. At each discrete time k , this would nominally involve determining the "search" pattern $S(k)^o$ that is "closest"*** to the reference pattern $R(k-1)$ and then updating according to

$$R(k) = S(k)^o. \quad (2)$$

Clearly, the effectiveness of a particular optical tracking algorithm depends crucially upon the particular reference-updating process utilized and the specific means used in the actual implementation.

A virtual prerequisite to developing an efficient reference-updating algorithm is to process only as much of the image data as is absolutely

* The discrete-time index k ($k=0,1,2,\dots$) is used for notational convenience.

** The acquisition problem per se was not considered in this research.

*** A wide variety of statistical measures are readily available for this purpose.

necessary to satisfy given performance requirements. This consideration strongly suggests that the feature selection problem should play an important role in this research, and, indeed, the remainder of this report will be concerned with this problem.

IV FEATURE SELECTION FOR BINARY-VALUED PICTURE FUNCTIONS

Consider a given binary-valued picture function, P , of the form of (1). Let us now pose the problem of selecting a single feature, F_1 , from the pattern of 0's and 1's that appears to give the best description of P . Here, we pick

$$F_1 = \text{The numbers of 1's in } P$$

$$= \sum_{i=1}^n \sum_{j=1}^n P_{ij}, \text{ where } n=2^k. \quad (3)$$

This selected feature partitions the patterns into classes; e.g., for $n = 4$ there are 17 distinct classes corresponding to the 17 possible values 0, 1, 2, . . . , 16 that F_1 can take on. As a basis for a decision function, d_1 , F_1 provides a reasonable measure of discrimination.

To obtain additional discrimination one may use d_2 , that utilizes two features instead of one. For instance, we may use the feature vector $F^{(2)} = (F_1, F_2)$ where F_1 is as before (see (3)) and

$$F_2 = \sum_{i=1}^{2^{k-1}} \sum_{j=1}^{2^{k-1}} P_{ij}. \quad (4)$$

For the $n = 4$ case this augmented feature vector partitions the patterns into 81 distinct classes, and thus the discriminating power of a decision function, d_2 , based upon (F_1, F_2) should be somewhat greater than that of d_1 .

More generally, this suggests the use of the feature vector $F^{(m)}(F_1, F_2, \dots, F_m)$.

where

$$F_q = \sum_{i=1}^{2^{k-q+1}} \sum_{j=1}^{2^{k-q+1}} P_{ij} \quad (5)$$

for $q = 1, 2, \dots, m$ and $m = 1, 2, \dots, k$,

together with associated decision functions $d_1, d_2, \dots, d_m, \dots, d_k$. Clearly, the discriminating power of d_m continues to increase relative to d_1, \dots, d_{m-1} as m increases.

Thus we have a sequence, $F^{(1)}, \dots, F^{(k)}$, of feature space transformations of successive refinement on the pattern space of binary picture functions, together with associated decision functions d_1, \dots, d_k . This is, of course, by no means the only way to select features for binary-valued picture functions, but it is the only one that has been analyzed thus far. Even then, only a partial analysis has been made. The completion of this analysis as well as analysis of other methods of feature selection are suggested as future research tasks.

V. RECOMMENDATIONS

As mentioned in Section II, my research activities this past summer were primarily concerned with initiating a longer term research program and associated research seminar series. For this reason this section will be somewhat lengthy. Some preliminary results were obtained during the latter portion of my stay at FJSRL. This preliminary work involved seeking effective means of testing the hypothesis that two binary-valued picture functions R and S originated from the same source. The approach used therein involved defining appropriate acceptance/rejection decision functions on the associated feature space of $R \times S$. Preliminary results were encouraging. When applied (analytically) to some simplified test cases, an expected error rate in the neighborhood of 10% resulted.

Further, algorithms of this type should be very easy to implement via the use of microprocessors. Such implementations would feature simplicity of structure, speed, and low cost.

Additional test cases and candidate feature space transformations need to be investigated and subjected to exact analysis. The results obtained herein should then form a solid foundation upon which to generalize to more realistic settings.

In particular, the following basic research tasks are suggested:

1. Complete the exact deterministic analysis of an additional selected set of test cases. This involves the following subtasks for each test case:
 - (a) Determine the ensemble of possible reference (R) and search (S) pattern classes and their associated distributions.
 - (b) Define an appropriate set of decision functions on $R \times S$ for each possible set of features.
 - (c) Determine a practicable performance measure for this decision subsystem of the tracker.
 - (d) Quantify, using exact analysis, the performance measure (over $R \times S$) of each feature vector defined in (b) above.
 - (e) Make a qualitative assessment of the results of (d) and suggest tradeoffs.
2. Generalize the methodology of 1 to apply for any $N \times N$ picture array where N is of the form $N = 2^K$, K being an arbitrary positive integer.

Generalized subtasks 2(a) and 2(b) will be formulated so that they immediately reduce to 1(a) and 1(b) when the value of K is appropriately selected.

Generalized subtasks 2(c) and 2(d) will require, among other things:

- i) specifying the desired range of parameters to be considered
 - ii) developing a computer program to perform the required analysis
 - iii) utilizing the test case results to validate the resulting computer program
 - iv) specifying the nature of the tradeoffs to be studied
3. Provide, at the block diagram level, microcomputer architectures appropriate

for the real-time generation of the decision functions as defined in generalized subtasks 2(b). A preliminary assessment of their relative merits should also be provided.

The next phase of the research would be to make greater use of digital simulation to generate and test new ideas. Some analytical work will be required in this phase as well, in order to adapt the formulations in the earlier phase to be compatible with the requirements of an operational real time decision-making system. In particular, theoretically-based prediction and search algorithms should be developed early in this phase of the research.

The candidate decision systems should then be tested and refined by simulating their performance when the image patterns experience various sorts of relative motion, starting with the simplest case of uniform rectilinear motion, progressing through the case of uniform rotational motion, and, finally, culminating with the case of general planar motion.

The analysis and simulation should then be broadened to include non-deterministic phenomena. In particular, methods developed in a deterministic setting should be evaluated for selected types of clutter as well as for some of the standard noise types.

An analysis of these results should provide information of value in developing an image-data preprocessor. This would essentially involve a parametric search over a suitably restricted range of possibilities.

The next phase of the research should involve formalizing the intuitively-based decomposition mentioned in Section III. In particular, the next step would be to model the background within the field of view by producing appropriate binary patterns, C_i , at each frame time, t_i . These patterns would then be appropriately "subtracted" from the unprocessed target image. The processed target image should then have a sufficiently improved signal/noise ratio that more conventional pattern recognition techniques based upon target geometries might be successfully employed.

The picture processor developed at this stage in the research should work reasonably well under a wide variety of conditions under which the scene changes little on a frame-to-frame basis. However, it seems reasonably certain that performance improvements could be obtained by introducing a peripheral field of view (with a somewhat coarser grid size) that would anticipate significant changes in background about to enter into the primary field of view. Schemes for coordinating the primary and peripheral field processors would be an important part of the research in this phase of the research.

Finally, an overall evaluation should be made, wherein the resulting tracking system is tested, via digital simulation, under as realistic conditions as possible.

REFERENCES

1. Rosenfeld, A. and Kak, A. C., Digital Picture Processing, Academic Press, New York, 1976.
2. Gonzales, R. C. and Wintz, P., Digital Image Processing, Addison-Wesley, Reading, Massachusetts, 1977.
3. Duda, R. O. and Hart, P. E., Pattern Classification and Scene Analysis, Wiley, New York, 1973.
4. Tou, J. T. and Gonzalez, R. C., Pattern Recognition Principles, Addison-Wesley, Reading, Massachusetts, 1974.

APPENDIX: STATUS ON THE DEVELOPMENT OF A SEMINAR SERIES AND
WORKSHOP/CONFERENCE ON IMAGING PROCESSING AND PATTERN RECOGNITION--
REAL-TIME AND ADAPTIVE ASPECTS.

The general plan is to develop a series of twelve monthly seminars at the USAFA to be given by selected invited speakers. The seminars would be comprised of both a formal and an informal segment. A workshop/conference would then be held at the conclusion of the seminar series. It would be planned to discuss cosponsorship with appropriate technical societies such as the IEEE Societies on Computers, Automatic Control, Information Theory, and Systems, Man and Cybernetics; as well as others such as the Pattern Recognition Society. The primary requirement to be made of these societies would be to endorse and advertise the workshop/conference, both by providing space in their publications and via providing us with their mailing lists.

The invited speakers will, both for the seminar series and the workshop/conference, be strongly encouraged to emphasize the recent and the new ideas that might potentially be useful in the future rather than giving "how to do it" expositions.

A preliminary survey of potential invited speakers has been made, and the response has been very enthusiastic. Represented in this sample survey have been active researchers in universities, at government laboratories, and in industry. Some of the persons surveyed have been internationally recognized authorities. As an example in this latter category, Professor Azriel Rosenfeld of the University of Maryland has agreed to participate as an invited speaker both in the seminar series and in the subsequent workshop/conference.

Within the general area suggested by the title of this section, the proposed range of topics is quite large, and the speaker backgrounds vary widely--from persons specializing in tracking research per se to persons specializing in biomodeling.

It is felt that such a seminar series, culminating with a workshop/conference, should stimulate the research community to generate new ideas that could provide useful insights into future designs of a wide variety of devices, including, in particular, optical trackers.

1979 USAF - SCEEE SUMMER FACULTY RESEARCH PROGRAM

Sponsored by the

AIR FORCE OFFICE OF SCIENTIFIC RESEARCH

Conducted by the

SOUTHEASTERN CENTER FOR ELECTRICAL ENGINEERING EDUCATION

FINAL REPORT

ATMOSPHERIC ABSORPTION OF RADIATION BY H₂O AND CO

Prepared by:	Richard H. Tipping
Academic Rank:	Associate Professor
Department and University:	Physics Department, University of Nebraska at Omaha
Research Location:	Air Force Geophysics Laboratory, Hanscom Air Force Base
USAF Research Colleague:	S. A. Clough
Date:	7 September, 1979
Contract No:	F49620 - 79 - C - 0038

ATMOSPHERIC ABSORPTION OF RADIATION BY H₂O AND CO

by

Richard H. Tipping

ABSTRACT

A theoretical investigation of the absorption of radiation by H₂O molecules in the earth's atmosphere was carried out. This was concerned primarily with an attempt to modify the usual Lorentzian line shape to obtain a more realistic description of the absorption in the far wings of spectral lines. The modified line shape was then used to investigate the continuum absorption in the 0 - 1200 cm⁻¹ region where the absorption is very sensitive to the assumed line shape. The importance of collision induced effects in the absorption spectrum of water was also estimated. While multipole - induced single transitions produce negligible effects, double transitions and the interference between the allowed and the induced dipole moments may lead to significant contributions to the continuum. The atmospheric absorption by carbon monoxide was also considered, and new line positions and strengths were determined for 574 lines belonging to four isotopic species. These should be accurate to 0.001 cm⁻¹ in position and to a few percent in strength. This data set includes all lines of CO whose strength exceeds 10⁻²⁴ molecules/cm² at the standard temperature of 296 K.

ACKNOWLEDGMENT

The author would like to thank Drs. S. A. Clough, L. S. Rothman, and F. X. Kneizys of the Optical Physics Division, Infrared Branch, at the Air Force Geophysics Laboratory for numerous discussions, and for providing a very stimulating environment in which this research was carried out. In addition, the author would also like to thank Dr. R. W. Davies of the Center for Atmospheric Research, University of Lowell, for many informative and fruitful discussions. Thanks are also extended to Dr. R. Gamache of the Center for Atmospheric Research, University of Lowell, for his programming assistance. Financial support from the Air Force Systems Command and the Air Force Office of Scientific Research, and office support from the Air Force Geophysics Laboratory, Hanscom Air Force Base are also gratefully acknowledged.

I. INTRODUCTION:

The absorption of microwave and infrared radiation by molecules in the earth's atmosphere is a problem of extreme practical importance in such diverse areas as meteorology, pollution control, satellite monitoring, etc. For this reason, about 10 years ago the Air Force Cambridge Research Laboratory (AFCRL), now the Air Force Geophysics Laboratory (AFGL), initiated a project with the aim of "providing a complete set of data for all vibration - rotation lines of all naturally occurring molecules of significance in the terrestrial atmosphere."¹ Up to now, the following molecules have been included in this compilation: water vapor, carbon dioxide, ozone, nitrous oxide, carbon monoxide, methane, and oxygen; this list is currently being expanded to include more trace molecules. The original compilation is continually revised as more accurate or more extensive data on these molecules becomes available. In Section VI of the present report, the updating and extension of the CO data base will be described.

One of the more interesting regions of the spectrum covered by the compilation is the window between 500 and 1200 cm^{-1} in which there are no strong bands centered. There is, however, a residual absorption due mostly to H_2O . Considerable controversy has been generated regarding the nature of this absorption; most of the discussion has centered on the question of whether this absorption is due to the far wings of allowed dipole lines, or to water dimers² or larger molecular complexes.³ These latter mechanisms have been invoked in an attempt to explain the quadratic pressure dependence and strong inverse temperature dependence⁴ (as the temperature increases, the absorption becomes significantly less), and were motivated in part by the failure of the widely used pressure broadened Lorentzian line shape. However, as will be discussed in Sections III

and IV of this report, the Lorentzian line shape is known from very general considerations to fail in the line wings. The question to be addressed is then: "can the continuum (residual) absorption of H_2O in the region out to 1200 cm^{-1} be accounted for by a linear superposition of suitably modified collision broadened line shapes due to transitions in individual molecules?" Closely related to this question is the role of collision induced effects in the observed spectrum. These effects will be considered in Section V.

II. OBJECTIVES:

There are two basic objectives of the current research effort related to the absorption of radiation in the earth's atmosphere by H_2O and by CO molecules, respectively. The absorption due to water is by far the more ambitious and difficult part and, accordingly, most time was spent on this problem. It is a difficult problem because the absorption which is of interest, the "water vapor continuum", takes place at frequencies far removed from the line centers. The standard pressure broadened line shape (Lorentzian) used to describe the centers of lines is not applicable in the wings, and other approaches had to be explored. There are quite general considerations, to be discussed in the following section, which provide some information on the adequacy of the approximations which have to be made in order to derive a tractable line shape, but a great deal of work is still necessary for a complete understanding of this problem. Another facet of the absorption due to H_2O concerns the importance of collision induced effects in the continuum. While this mechanism is known to play a significant role in the absorption of radiation by N_2 in the atmosphere, its relevance to the continuum absorption of water has not been investigated heretofore. Again it is found that there are some interesting tentative results which should be pursued further.

In contrast to the situation for H_2O , the absorption due to CO is relatively straightforward. In view of the recent experimental^{5,6} and theoretical^{7,8} advances, the accuracy of the positions and strengths of the CO lines important in atmospheric absorption could be improved and extended. The new data base for CO, which has already been incorporated in the AFGL tape compilation, is described in Section VI.

III. GENERAL PROPERTIES OF THE ABSORPTION COEFFICIENT:

In the non-saturated, linear optical regime, the absorption of radiation at frequency ω and position l is related to the incident intensity at $l=0$ by the Beer-Lambert law

$$I(\omega, l) = I(\omega, 0) e^{-\alpha(\omega) l} \quad (1)$$

where $\alpha(\omega)$ is the frequency dependent absorption coefficient per unit length. This can be written in terms of the molecular parameters

$$\alpha(\omega) = \frac{N}{V} \left(\frac{4\pi^2}{3k} \right) \omega \left(1 - e^{-\beta \hbar \omega} \right) \sum_{if} p_i |K_{if}|^2 \delta(\omega - \omega_{fi}) \quad (2)$$

where N is the number of absorbing molecules in the volume V , $\beta = (kT)^{-1}$, and p_i are the standard Boltzmann factors

$$p_i = \frac{e^{-\beta E_i}}{Z} \quad (3)$$

where Z is the partition function. One can define the spectral density, $\phi(\omega)$, according to

$$\phi(\omega) = \sum_{if} p_i |K_{if}|^2 \delta(\omega - \omega_{fi}) \quad (4)$$

This satisfies the condition of detailed balance, i.e.,

$$\phi(-\omega) = e^{-\beta \hbar \omega} \phi(\omega) \quad (5)$$

which assures that the system remains in thermodynamic equilibrium. Also, because the absorption coefficient is real, one can easily show that

$$\alpha(\omega) = \alpha(-\omega) \quad (6)$$

Thus the absorption coefficient must be an even function of ω .

In order to investigate the line shape, it is convenient to write the spectral density in terms of the Fourier transform of the dipole moment correlation function

$$\phi(\omega) = \frac{1}{2\pi} \int_{-\infty}^{\infty} dt e^{-i\omega t} \langle \vec{\mu}(0) \cdot \vec{\mu}(t) \rangle \quad (7)$$

where $\vec{\mu}(t)$ is the Heisenberg dipole operator for the system involving the Hamiltonian, \mathcal{H} ,

$$\vec{\mu}(t) = e^{i\mathcal{H}t/\hbar} \vec{\mu}(0) e^{-i\mathcal{H}t/\hbar} \quad (8)$$

and the angular brackets denote a canonical statistical average. Thus, one can write the absorption coefficient in the form

$$\alpha(\omega) = \frac{N}{V} \left(\frac{4\pi^2}{3\hbar c} \right) \omega (1 - e^{-\beta \hbar \omega}) \frac{1}{2\pi} \int_{-\infty}^{\infty} dt e^{-i\omega t} \langle \vec{\mu}(0) \cdot \vec{\mu}(t) \rangle \quad (9)$$

For some purposes, it is often convenient to rewrite the absorption coefficient in either of the following equivalent forms⁹:

$$\alpha(\omega) = \frac{N}{V} \left(\frac{4\pi^2}{3\hbar c} \right) \omega \frac{1}{2\pi} \int_{-\infty}^{\infty} dt e^{-i\omega t} \langle \vec{\mu}(0) \cdot \vec{\mu}(t) - \vec{\mu}(t) \cdot \vec{\mu}(0) \rangle \quad (10)$$

or

$$\alpha(\omega) = \frac{N}{V} \left(\frac{4\pi^2}{3\hbar c} \right) \omega \tanh \left(\frac{\beta \hbar \omega}{2} \right) \frac{1}{2\pi} \int_{-\infty}^{\infty} dt e^{-i\omega t} \langle \vec{\mu}(0) \cdot \vec{\mu}(t) + \vec{\mu}(t) \cdot \vec{\mu}(0) \rangle \quad (11)$$

Equations (10) and (11) are useful in establishing three general relations¹⁰ which must be satisfied by the "true" absorption coefficient. These are: the generalized Nyquist theorem, the Kramers-Kronig relation and the f-sum rule. These relations, which are discussed in detail in Ref. (10), are exact and, therefore, provide checks on the validity of the approximations which are usually made (e.g. density matrix is factorable into a perturber and an absorber part, the dipole operator for the system is additive, non-overlapping lines, etc.) in order to derive the absorption coefficient starting from Eq. (9), Eq. (10) or Eq. (11).

IV. THE LINE SHAPE PROBLEM FOR H₂O LINES:

One of the most difficult and as yet not completely solved aspects in the determination of the absorption of radiation by H₂O vapor is the calculation of the line shape

of an isolated line over all frequencies. In the standard impact theory of pressure broadening,¹¹ the time dependent correlation function, $C(t)$, is assumed to be an exponential

$$C(t) \equiv \frac{\langle \vec{\mu}(0) \cdot \vec{\mu}(t) \rangle}{|\vec{\mu}(0)|^2} = e^{i\omega_{fi}^{\circ} t} e^{-\Gamma|t|} \quad (12)$$

where Γ is a complex parameter, the real part Γ' of which is the pressure broadened width, and the imaginary part Γ'' is the shift from the unperturbed transition frequency ω_{fi}° . The Fourier transform of this function leads to a Lorentzian line shape centered about the shifted frequency $\omega_{fi} = \omega_{fi}^{\circ} - \Gamma''$; that is,

$$\frac{1}{2\pi} \int_{-\infty}^{\infty} dt e^{-i\omega t} C(t) = \frac{\Gamma'/\pi}{(\Gamma')^2 + (\omega - \omega_{fi})^2} \quad (13)$$

This form provides a good fit to experimental spectral lines near their centers ($\omega - \omega_{fi} \approx \Gamma'$). Because of the approximations implicit in the impact theory, the correlation function is not well represented for times of the order of or less than a typical collision duration. This is manifest in Eq. (12) through the appearance of the unphysical absolute value sign on t . This is included so as to force the exponential model to satisfy the general symmetry requirement that the real part of $C(t)$ be an even function of t . As a result, $C(t)$ as given by Eq. (12) has discontinuous derivatives at $t=0$ and leads to an incorrect representation of the line shape in the wings of the lines.

This is precisely the region of interest, however, for the continuum absorption problem of water.

The calculation of the true line shape based on a realistic microscopic model is not feasible at present. However, some progress can be made by adopting a model for the correlation function which avoids the small time problems discussed above. One such model has been proposed by Anderson¹² in conjunction with a different problem. This correlation function can be cast in the form

$$C(t) = e^{i\omega_{fi}t} \exp \left\{ -\Gamma t \int_0^{t/\tau_d} e^{-\frac{\pi x^2}{4}} dx + \frac{2\tau_d\Gamma}{\pi} \left[1 - e^{-\frac{\pi t^2}{4\tau_d^2}} \right] \right\} \quad (14)$$

where the parameter τ_d can be thought of as the duration of a collision. This form has several useful properties:

$$(i) \quad C(0) = 1 \quad (15)$$

$$(ii) \quad C(-t) = C(t) \quad (16)$$

$$(iii) \quad \lim_{\tau_d \rightarrow 0} C(t) \approx \exp \{ -\Gamma |t| \} \quad (17)$$

$$(iv) \quad \lim_{t \rightarrow 0} C(t) \approx \exp \left\{ -\frac{\Gamma t^2}{2\tau_d} \right\} \quad (18)$$

The first two conditions imply that the correlation function is properly normalized and satisfies the correct symmetry

relation, while the latter two lead to a line shape which is Lorentzian near the line center but Gaussian in the far wings. This is a reasonable result but it is by no means exact or even unique.¹³

In order to test the applicability of Eq. (14), we have computed its Fourier transform numerically for various values of τ_d . As expected, this model leads to less absorption than the Lorentzian shape in the wings. The pressure dependence is quadratic and the temperature dependence is at least qualitatively in the correct direction. More work is needed, however, before one can quantitatively assess the adequacy of Eq (14) as a realistic model.

V. COLLISION INDUCED EFFECTS IN THE WATER SPECTRUM:

In addition to the allowed dipole absorption discussed above, there is another mechanism which, in general, leads to absorption of radiation. This will be referred to as "collision induced absorption" and arises from transient dipoles created during binary collisions. The resulting spectral lines differ from those in the allowed spectrum in several ways: The lines are broader (typical half widths of 50 cm^{-1}); the lines can arise from transitions obeying different selection rules and thus appear at different frequencies; their intensity varies quadratically with the density in self absorption, or as the product of the densities in foreign gas mixtures.¹⁴ In order to assess the importance of this mechanism as a possible contributor to the continuum absorption, the ratio of the dipole induced dipole intensity (which has the same selection rules and matrix elements as the corresponding allowed transition) to that of the allowed line was estimated. This ratio turned out to be of the order of 10^{-5} , too weak to account for appreciable absorption in the far wing region of the pure rotational lines.

There are, however, several other collision induced

mechanisms which may also be considered:

(i) The quadrupole induced dipole spectrum, while it will be weaker in strength, will absorb at somewhat different frequencies. Even though the reduced strength can be offset by the change in transition frequency (in so far as the continuum absorption is concerned), it is felt that this contribution is also unlikely to be of much importance in the 300 - 1200 cm^{-1} region.

(ii) For molecules with an anisotropic polarizability (e.g. H_2O), the possibility exists for "double transitions"; that is, both molecules in a binary collision simultaneously undergo radiative transitions. Under certain circumstances, this can lead to significant absorption.¹⁵ Furthermore, the frequency involved would correspond to approximately twice that of the single transition. This absorption would thus occur in the wings of the allowed lines where the allowed absorption coefficient would have fallen off significantly, with the possible implication that this process may not be negligible in this region. This possibility should certainly be investigated in greater detail.

(iii) A third mechanism which also warrants further investigation is that due to the interference between the allowed and the induced dipoles.¹⁶ This effect will lead to absorption several orders of magnitude greater than that due to pure induced absorption and, consequently, may be of importance. This effect is also known to alter the shape of the lines.¹⁶

To summarize this section:

The pure collision induced absorption due to multipole-induced dipoles is too weak to contribute appreciably to the water continuum in the region 300 - 1200 cm^{-1} . On the other hand, dipole induced dipole double transitions, and the interference between the allowed and the induced dipoles

may play a significant role and bear further investigation.

VI. THE ABSORPTION SPECTRUM OF CO:

Carbon monoxide is present in the earth's atmosphere in sufficient quantity, and it absorbs radiation strongly enough in several regions of the infrared, to have been included among the seven molecules considered in the original AFCRL compilation¹ of atmospheric absorption line parameters. This work contained results from several of the lesser abundant isotopic species calculated from the parameters of the most abundant variant $^{12}\text{C}^{16}\text{O}$ through the usual isotopic relations of the spectroscopic constants, and included all lines whose strength exceeded 1.9×10^{-23} molecules/cm². It was felt appropriate to update this set of data at the present time for the following reasons:

(i) Improved experimental frequency measurements have been published recently^{5,6} which now extend to all the isotopes of interest. No uncertainties need to be introduced via the isotopic relations in order to determine the Dunham coefficients of the rarer isotopes. This permits a direct and more accurate calculation of the line positions. The best available frequency parameters are listed in Table I along with the most recent isotopic abundances and rotational partition functions used in the computations.

(ii) Higher overtone intensities ($3 - 0^{18}$ and $4 - 0^{19}$ bands) have been reported. These enable one to obtain a more accurate dipole moment function and, thus, more accurate line strengths. Using all the available experimental intensity data,⁸ the dipole moment function can be well represented by the power series

$$M(x) = -0.12230 + 3.5398 x - 0.3234 x^2 - 3.5626 x^3 \\ + 2.4491 x^4 + 5.7684 x^5$$

(19)

where $\chi \equiv \frac{R - R_e}{R_e}$ is the dimensionless displacement from the equilibrium internuclear separation, R_e .

(iii) Accurate vibration - rotation matrix elements

$\langle n'' J'' | \chi^2 | n' J' \rangle$ have been computed using a numerical solution of the Schrodinger equation for $J=0$ through 5 for all the transitions of interest.⁸ These can be used in conjunction with Eq. (19) in order to calculate accurate line strengths.

(iv) The pure rotational line strengths previously compiled on the tape were based on an incorrect theoretical treatment of vibration-rotation interaction.²⁰ While this did not affect the low J lines significantly, for the higher J lines the errors introduced were of the order of 10 to 20%..

The correct Herman-Wallis factor for the pure rotational band can be written in the form²¹

$$F(J) = \left[1 + \frac{8 B_e^2 M_1}{\omega_e^2 M_0} (J+1)^2 \right] \quad (20)$$

where B_e and ω_e are the usual rotational and vibrational constants. In the actual calculations, however, the numerical matrix elements were employed.

Using the data listed in Table I, new line positions and ground state energies were generated; these should be accurate to 0.001 cm^{-1} for all the lines. The cutoff strength was lowered to 1×10^{-24} molecules/cm² which includes a total of 574 lines (383 old lines plus 191 new ones). The information on the current CO data set is summarized in Table II. While it is hard to estimate the absolute accuracy of the line strengths, it is felt that the pure rotational lines are accurate to better than a percent, the fundamental lines to 2%, and the remaining overtone and hot band lines to approximately 10%. As mentioned previously, this new data

set has already been incorporated into the AFGL tape compilation.

VII. RECOMMENDATIONS:

As a result of the effort described herein, the following recommendations are made in regard to additional research:

(i) The importance of dipole induced dipole double transitions in water should be investigated, and a more quantitative estimate of their contribution to the continuum in the $300 - 1200 \text{ cm}^{-1}$ region should be made.

(ii) The modification of the allowed spectrum arising from the interference between the allowed and the collision induced dipoles should be studied.

(iii) Further investigation of the line shape of allowed spectral lines especially in the far wings is certainly needed. In this regard, the breakdown of the usual impact approximations has to be considered. The question of whether the continuum absorption can be accounted for by a hindered rotation-librational model to describe the effects of close binary collisions²² should be addressed.

(iv) The influence of line mixing on the spectrum has not been considered in the present study; it has been tacitly assumed that the total spectrum can be synthesized by the incoherent superposition of individual lines. A study of the importance of this approximation should be undertaken.

All of the above will involve a considerable amount of research effort. However, in view of the importance of the problem from both the theoretical and practical standpoints, it is felt that such an effort is very worthwhile.

No further effort on the absorption of radiation by CO is needed if one is only interested in absorption by gases at the standard temperature of 296K. However, in order to synthesize the spectrum of CO corresponding to considerably higher temperatures (for example, as would be observed in aircraft exhausts), one would have to include

additional hot bands in the analysis. This can be accomplished by a straight forward extension of the results of Section VI without any theoretical complications.

REFERENCES

1. R. A. McClatchey, W. S. Benedict, S. A. Clough, D. E. Burch, R. F. Calfee, K. Fox, L. S. Rothman, and J. S. Garing, "AFCRL Atmospheric Absorption Line Parameter Compilation", AFCRL - TR - 73 - 0096, Air Force Cambridge Research Laboratory, 1973.
2. P. Varansi, S. Chou, and S. S. Penner, "Absorption Coefficients for Water Vapor in the 600 - 1000 cm^{-1} Region", J. Quant. Spectrosc. Radiat. Transfer 8, 1537 (1968).
3. H. R. Carlon, "Ion Content and Infrared Absorption of Moist Atmospheres", J. Atm. Sci. 36, 832 (1979), and references contained therein.
4. D. E. Burch, and D. A. Gryvnak, "Method of Calculating H_2O Transmission between 333 and 633 cm^{-1} ", Final Report No. AFGL - TR - 79 - 0054, 1979.
5. R. M. Dale, M. Herman, J. W. C. Johns, A. R. W. McKellar, S. Nagler, and I. K. M. Strathy, "Improved Laser Frequencies and the Dunham Coefficients for Isotopically Substituted Carbon Monoxide", Can. J. Phys. 57, 677 (1979).
6. T. R. Todd, C. M. Clayton, W. B. Telfair, T. K. McCubbin, and J. Pliva, "CO Emission Spectrum", J. Mol. Spec. 62, 201 (1976).
7. R. H. Tipping, "Vibration - Rotation Intensities for 'Hot' Bands", J. Mol. Spec. 61, 272 (1976).
8. S. M. Kirshner, R. J. LeRoy, J. F. Ogilvie, and R. H. Tipping, "Radial Matrix Elements and Dipole Moment Function of CO", J. Mol. Spec. 65, 306 (1977).
9. R. W. Davis, "Theoretical Investigation of Continuum Absorption, Lineshapes, and Linewidths of Infrared transitions of H_2O and other Atmospheric Constituents", Quarterly Status Report No. 4, University of Lowell, Center for Atmospheric Research, (1977).
10. J. H. Van Vleck and D. L. Huber, "Absorption, Emission, and Linebreadths: A Semihistorical Perspective", Rev. Mod. Phys. 49, 939 (1977).
11. R. H. Tipping and R. M. Herman, "Impact Theory for the Noble Gas Pressure - Induced HCl Vibration - Rotation

and Pure Rotation Line Widths", J. Quant. Spectrosc. Radiat Transfer 10, 881 (1970).

12. P. W. Anderson, "A Mathematical Model for the Narrowing of Spectral Lines by Exchange of Motion", J. Phys. Soc. (Japan) 9, 316 (1954).
13. G. Birnbaum, "The Shape of Collision Broadened Lines from Resonance to the Far Wings", J. Quant. Spectrosc. Radiat. Transfer 21, 597 (1979).
14. N. H. Rich and A. R. W. McKellar, "A Bibliography on Collision - Induced Absorption", Can. J. Phys. 54, 486 (1976).
15. S. P. Reddy, G. Varghese and R. D. G. Prasad, "Overlap Parameters of $H_2 - H_2$ Molecular Pairs from the Absorption Spectra of the Collision - Induced Fundamental Band of H_2 ", Phys. Rev. A15, 975 (1977).
16. R. M. Herman, R. H. Tipping and J. D. Poll, "Shape of the R and P Lines in the Fundamental Band of Gaseous HD", Phys. Rev. A, Oct. 1979, to be published.
17. A. H. M. Ross, R. S. Eng, and H. Kildal, "Hetrodyne Measurements of $^{12}C^{18}O$, $^{13}C^{16}O$, and $^{13}C^{18}O$ Laser Frequencies: Mass Dependence of Dunham Coefficients", Opt. Commun. 12, 433 (1974).
18. R. A. Toth, R. H. Hunt, and E. K. Plyler, "Line Intensities in the 3 - 0 Band of CO and Dipole Moment Matrix Elements for the CO Molecule", J. Mol. Spec. 32, 85 (1969).
19. C. Chackerian and F. P. J. Valero, "Absolute Intensity Measurement of the 4 - 0 Vibration - Rotation Band of Carbon Monoxide", J. Mol. Spec. 62, 338 (1976).
20. M. Greenbaum, "Absorption Line Parameters for Carbon Monoxide Isotopes", Riverside Research Institute Report T - 3/306 - 3 - 14.
21. R. H. Tipping and J. F. Ogilvie, "The Influence of the Potential Function on Vibration - Rotation Wavefunctions and Matrix Elements of Diatomic Molecules", J. Mol. Struct. 35. 1 (1976).
22. R. M. Herman, private communication.

TABLE I: MOLECULAR PARAMETERS

Dunham Parameters (cm ⁻¹)	^a 12C16O	^a 13C16O	^a 12C18O	^b 12C17O
Y ₁₀	2169.81386	2121.44032	2117.39961	2142.16656
Y ₂₀	-13.288392	-12.702559	-12.654287	-12.952202
Y ₃₀ X 10 ²	1.05185	0.98317	0.97780	1.01352
Y ₄₀ X 10	0.5712	0.5219	0.5180	0.5341
Y ₅₀ X 10 ⁶	0.989	0.883	0.875	0.947
Y ₆₀ X 10 ⁷	-0.3168	-0.2767	-0.2736	-0.2950
Y ₀₁	1.93128090	1.84615169	1.83911378	1.88238458
Y ₁₁ X 10	-0.1750430	-0.1635961	-0.1626612	-0.1684370
Y ₂₁ X 10 ⁶	0.552	0.504	0.501	0.485
Y ₃₁ X 10 ⁷	0.273	0.244	0.241	0.255
Y ₀₂ X 10 ⁵	-0.612096	-0.559315	-0.555058	-0.581683
Y ₁₂ X 10 ⁹	1.075	0.960	0.952	1.068
Y ₂₂ X 10 ⁹	-0.1817	-0.1587	-0.1569	-0.1580
Y ₀₃ X 10 ¹¹	0.571	0.499	0.493	0.661
Y ₁₃ X 10 ¹²	-0.1634	-0.1395	-0.1377	-0.1986
B ₀	1.92252887	1.837972	1.80309808	1.87396286
D ₀ X 10 ⁶	-6.12023	-5.59271	-5.5014	-5.81634
H ₀ X 10 ¹²	5.63	4.92	4.86	6.51
R isotope	.986517	.011073	.002017	.000366
Q _{rotation}	107.4165	112.3429	112.7699	110.1917

a. Ref. 5.

b. Ref. 17.

TABLE II: SUMMARY OF CO DATA

BAND	LINES	ISOTOPE	NUMBER OF LINES	STRENGTH
0-0	R(0)-R(34)	26	35	1.828×10^{-20}
	R(3)-R(25)	36	23	1.957×10^{-22}
	R(6)-R(19)	28	14	3.551×10^{-23}
TOTAL			72	1.851×10^{-20}
0-1	R(0)-R(39)	26	40	5.415×10^{-18}
	P(1)-P(39)	26	39	4.398×10^{-18}
	R(0)-R(33)	36	34	5.812×10^{-20}
	P(1)-P(33)	36	33	4.712×10^{-20}
	R(0)-R(30)	28	31	1.054×10^{-20}
	P(1)-P(30)	28	30	8.550×10^{-21}
	R(0)-R(26)	27	27	1.957×10^{-21}
	P(1)-P(26)	27	26	1.585×10^{-21}
TOTAL			260	9.941×10^{-18}
0-2	R(0)-R(32)	26	33	4.286×10^{-20}
	P(1)-P(31)	26	31	3.237×10^{-20}
	R(0)-R(23)	36	24	4.446×10^{-22}
	P(1)-P(23)	36	23	3.368×10^{-22}
	R(0)-R(18)	28	19	7.772×10^{-23}
	P(1)-P(17)	28	17	5.795×10^{-23}
	R(4)-R(10)	27	7	8.034×10^{-24}
TOTAL			154	7.615×10^{-20}
0-3	R(0)-R(22)	26	23	2.889×10^{-22}
	P(1)-P(20)	26	20	1.938×10^{-22}
TOTAL			43	4.827×10^{-22}
1-2	R(0)-R(22)	26	23	3.193×10^{-22}
	P(1)-P(22)	26	22	2.596×10^{-22}
TOTAL			45	5.789×10^{-22}

1979 USAF - SCEE SUMMER FACULTY RESEARCH PROGRAM

Sponsored by the

AIR FORCE OFFICE OF SCIENTIFIC RESEARCH

Conducted by the

SOUTHEASTERN CENTER FOR ELECTRICAL ENGINEERING EDUCATION

FINAL REPORT

STUDY AND EVALUATION OF SIIDS AND ADPT SYSTEMS

Prepared by:	Pramod K. Varshney
Academic Rank:	Assistant Professor
Department and University:	Electrical and Computer Engineering Department Syracuse University
Research Location:	Rome Air Development Center (RADC/DCLF) Communications and Control Division Telecommunications Branch
USAF Research Colleague:	Joseph W. DeGroat
Date:	August 21, 1979
Contract No:	F49620-79-C-0038

STUDY AND EVALUATION OF SIIDS AND ADPT SYSTEMS

by

Pramod K. Varshney

ABSTRACT

In this report, findings based on the study of the Standard Integrated Information Distribution System (SIIDS) and the Automatic Data Processing Telecommunication (ADPT) system are presented. Two proposed designs of SIIDS are discussed and evaluated. ADPT testbed, which has recently been installed at the Rome Air Development Center, is described. An experimental plan for the ADPT testbed is suggested. The ADPT testbed can be employed to run simulation experiments which will provide useful information regarding integrated switching and other concepts related to packet communication networks.

ACKNOWLEDGMENTS

I would like to thank the Air Force Systems Command, Air Force Office of Scientific Research, and the Southeastern Center for Electrical Engineering Education for providing me the opportunity to spend the summer visiting the Rome Air Development Center, Griffiss Air Force Base.

I would also like to thank Capt J. DeGroat and Mr D. McAuliffe for many helpful discussions. Thanks are also due to the Communications and Control Division, Rome Air Development Center for providing me the necessary facilities.

I. INTRODUCTION:

The traditional telecommunication switching requirement has been to provide man-to-man voice communications by means of circuit switching. It was necessary to establish an end-to-end connection by means of a communication channel and no additional information processing was needed. The telecommunication environment is changing and is now characterized by an increasingly greater variety of data terminals and increasing man-machine and machine-machine communications in addition to the traditional man-man communication. For data communication, the concept of packet switching has been successfully demonstrated and implemented in many existing telecommunication networks. A comparative performance evaluation of switching methods has shown that packet switching is more efficient for traffic consisting of short messages, e.g., interactive traffic and circuit switching is more effective for long continuous messages, e.g., digitized voice traffic or bulk data traffic [22,30].

Future military telecommunication systems will be required to accommodate a wide variety of traffic requirements and will include the following:

- (i) a wide range of traffic rates from low speed teletype terminals requiring hundreds of bits/sec to wideband video and graphics requiring hundred of kilobits/sec.
- (ii) a wide range of transaction sizes from short interactive messages requiring several hundred bits to

bulk data transfers of millions of bits.

- (iii) a wide range of delivery time requirements ranging from continuous, near real time requirements of voice and video to intermittent operation of interactive or bulk data users which may be queued.

In light of these anticipated traffic requirements, one important issue in telecommunication network design is whether circuit switching and packet switching be provided by separate networks or they can be combined in an efficient fashion into a single network. An integrated approach to switching seems to be more attractive as it provides a more cost-effective utilization of communication resources, e.g., transmission and switching facilities. This approach provides a more flexible means of communication especially with changing traffic patterns. It also provides the possibility of interconnecting a broad community of user terminals.

The Communications and Control Division of the Rome Air Development Center (RADC) has been pursuing the integrated approach to telecommunications switching for quite some time. This approach has been employed by the RCA Corporation to develop a unified node. This integrated switching node, also known as the Automatic Data Processing Telecommunication (ADPT) system or testbed, has recently been installed at RADC. The summer research effort reported here was mainly concerned with a study of the ADPT testbed. Some effort was also devoted to an

evaluation of the Standard Integrated Information Distribution System (SIIDS), the findings of which are described in Section 8.

II. OBJECTIVES:

The objectives of the summer research effort were:

- (1) To review the philosophy, design and function of the ADPT system.
- (2) To formulate an extended experimentation plan for the ADPT testbed with applications to telecommunication network design in mind.
- (3) To review and evaluate the two proposed designs for the SIIDS.

III. INTEGRATED SWITCHING:

The concept of integrated switching which combines the features of circuit switching and packet switching has been introduced quite recently and is, in essence, a hybrid scheme. An integrated switching facility provides both packet and circuit switching service in that it supports a user community requiring either circuit switched service (e.g., telephones) or packet switched service (e.g., interactive traffic) or both. The high bandwidth transmission capacity is shared by the two types of traffic. The scheme is implemented in terms of a synchronous time-division multiplexed (TDM) frame structure. The channel is synchronously clocked and is divided into frames of fixed

duration. Each frame is further subdivided into slots. The slot duration is determined by the voice digitization rate and the frame duration. Circuit switched voice requires a single slot for transmission whereas packet switched data may require a multiple number of slots for transmission. The TDM frame is partitioned into two regions by means of a boundary. One region is dedicated to circuit switched traffic and the other to packet switched traffic. All circuit switched traffic which cannot seize channel capacity upon arrival is blocked. All packet switched traffic which cannot be transmitted is buffered and is serviced on a first-come-first-served basis. The boundary which partitions the TDM frame may be fixed which implies that there is no dynamic sharing of channel capacity. The boundary can also be movable which allows for the packet switched traffic to utilize any idle circuit switched slots. This movable boundary case is also known as the dynamic channel allocation scheme [21,29] and is further discussed in this report. Further refinements on this basic scheme have also been considered in the literature (e.g., [23,24]).

Kummerle [16] and Zafiropulo [37] first suggested the integration of circuit switching and packet switching. This concept was also proposed by Coviello and Vena [5] where they called it the slotted envelope network (SENET) concept. This SENET concept has been studied further and a system architecture has been proposed in [31,32]. Variations of the basic concept have been studied by Miyahara et al [23,24]. Network Analysis

Corporation has considered the design of integrated networks and this has resulted in a number of publications [9-11,25,26]. The performance of the basic scheme has been analyzed in [1,7,26,35]. So far the concept of integrated switching has been proposed, the performance evaluation has been considered and a limited amount of simulation has been performed. Thus far, experimentation with an actual switch has not been performed. This type of experimentation is expected to prove extremely valuable in gaining a better understanding of integrated switching. The ADPT testbed provides such an experimental facility where actual experiments can be performed. ADPT testbed and suggested experimentation on it are discussed further in this report.

IV. ADPT TESTBED:

The principal purpose of the ADPT system is to run meaningful experiments on the testbed which will provide useful data that can be used while designing telecommunication networks. The physical configuration of the ADPT testbed facility is shown in Figure 1. The implementation includes two specialized switching devices which were specifically designed for the ADPT testbed. The first is the interactive communication channel (ICC). The ICC terminates all packet formatted communication lines within the ADPT testbed. It performs all bit oriented data processing dictated by the ADCCP protocol and, thus, acts as a front end unit for the communications processor. The second is the buffer matrix (BMX). The BMX adaptively multiplexes and demultiplexes digitized voice and packet data on all internodal

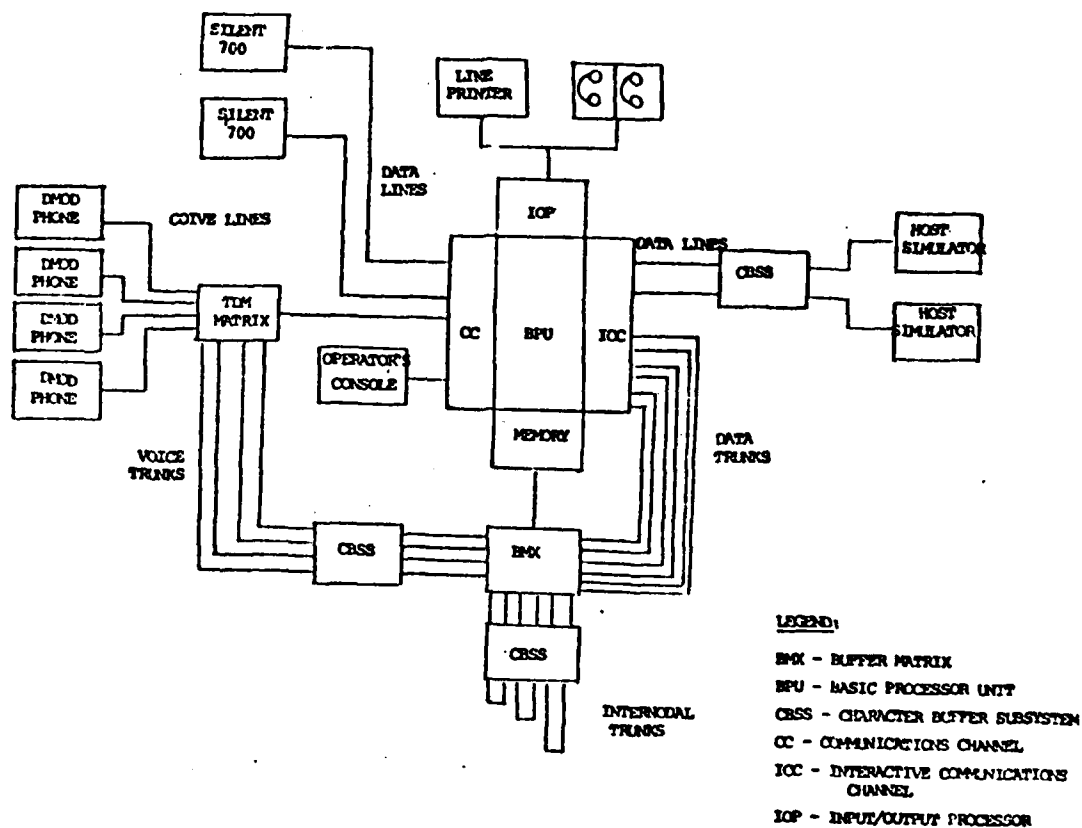


Figure 1 Physical Configuration of the ADPT testbed

trunks in the ADPT testbed. The mixing of voice and data is performed according to the dynamic channel allocation scheme.

The physical configuration of the ADPT testbed facility is shown in Figure 1. The system can be configured in two distinct configurations. The first is a three-node subnetwork simulator configuration. This configuration can be used to simulate integrated switching of voice and data traffic between integrated nodes employing dynamic channel allocation. The functional configuration along with the equipments acting as traffic sources and sinks is shown in Figure 2. Each node in the three node subnetwork simulator operates as an integrated node providing both local access and internodal trunking for a variety of digital subscribers. All internodal trunks in the three node subnetwork simulator employ dynamic channel allocation for the adaptive multiplexing of digitized voice and digital data onto common transmission facilities. Internodal trunks in the ADPT testbed facility operate at 96 kb/s. Digital information is transmitted on these trunks in TDM frames of length 5760 bits. Each TDM frame consists of three distinct regions as shown in Figure 3. There is a 96 bit synchronization pattern at the beginning of each frame. Next, rate-dependent slices of virtual connections are dynamically allocated to real-time (class I) users on a demand basis. There is a pre-determined limit beyond which class I users are blocked. Any unfilled portion of the TDM frame is filled with store and forward packet data (class II). If sufficient packet data is not present, the frame is filled

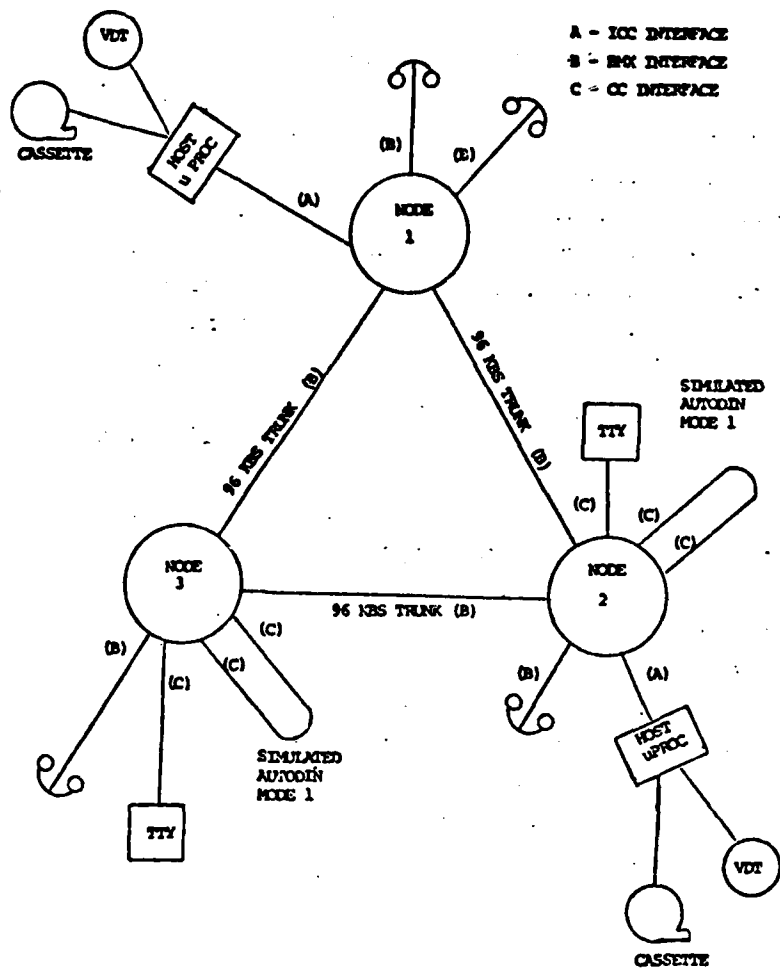


Figure 2 Three node subnetwork simulator configuration

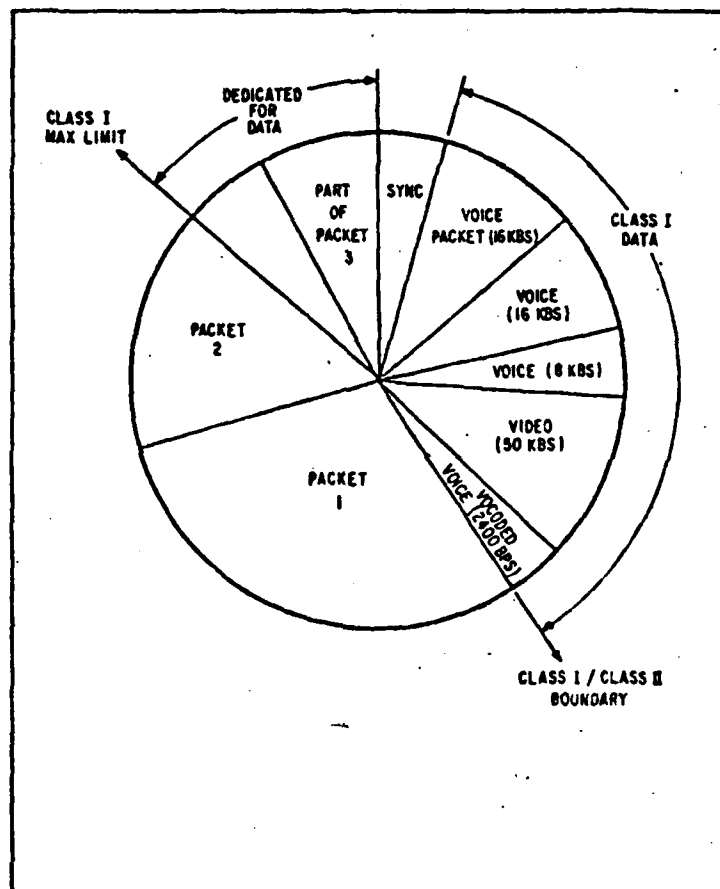


Figure 3 TDM frame for internodal trunks

with flag sequences.

The second configuration of the ADPT testbed facility is known as the test node simulator. This configuration can be employed to measure and analyze nodal performance parameters in an integrated network environment. This configuration is implemented by means of a sophisticated software package. The traffic is introduced by means of a prerecorded traffic tape containing compressed voice and data transactions. The tape is generated off-line by a discrete-event simulation program. The traffic tape contains intermixed voice and data transactions in order of the desired time of entry to the test node simulator. Network simulation software setup is as shown in Figure 4. The test node is surrounded by the network simulation software which provides a functional equivalent of a connected network environment. The simulator control unit coordinates the execution of the other network simulation modules and also manages buffer resources allocation to the network simulation software. Nodal performance parameters and statistics are collected on an output tape. A data reduction program is used off-line to produce desired nodal performance output for evaluation and analysis.

V. NODAL PERFORMANCE OUTPUT AND DATA REDUCTION PROGRAM:

The test node simulator can be used to determine nodal performance parameters in an integrated network environment. In order to determine nodal performance, relevant parameters are

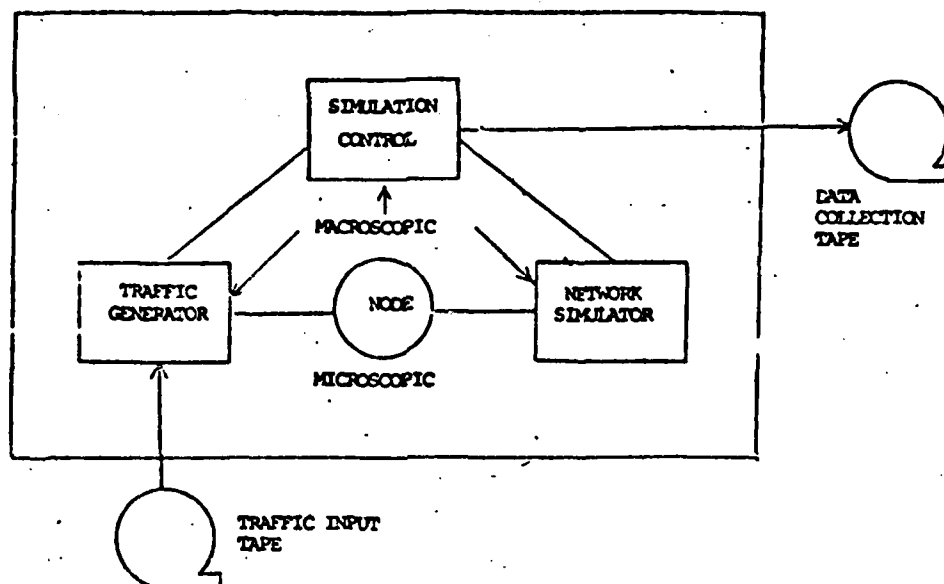


Figure 4 Test Node Simulator Software

recorded every second. The following parameters are recorded.

- (i) Incident traffic statistics (number of data and voice transactions in progress)
- (ii) Voice grade of service
- (iii) Acceptance and delivery delays
- (iv) Throughput (packets/sec into and out of the node)
- (v) Buffer utilization
- (vi) Trunk utilization (percent occupancy of trunk bandwidth)
- (vii) Presence of saturation conditions
- (viii) Queue lengths
- (ix) Packet nodal delays

In addition, information regarding completed data or voice call is gathered. All of the above is stored on a tape which is processed offline by a data reduction program. The data reduction program generates the following performance parameters and statistics:

- (i) Total number of packets.
- (ii) Mean and maximum tandem packet delay in milliseconds for each of the four data priorities: control (C), and priority 1-3 (P1, P2, P3).

- (iii) Mean and maximum nodal throughput in packets per second in and out.
- (iv) Mean and maximum queue size in number of packets for the trunk transmit queue (X) and the four associated backlog queues (control, and priority 1-3).
- (v) Mean and maximum trunk utilization in percent, for input, output and voice.
- (vi) Mean and maximum buffer utilization in percent.
- (vii) Average processor utilization in percent.

The data reduction program can also produce histograms, probability density functions and cumulative probability distribution functions of the desired performance parameters.

The principal measures which characterize the performance of an integrated node are the probability of blocking for the voice traffic, average delay for the data traffic, throughput of the node and trunk utilization. All of these parameters can be measured and their statistics generated by the existing facilities in the test node simulator and the data reduction program. One feature that can be added to the existing facilities is some additional plotting capability. The user will specify the graph that he wishes to obtain by specifying the parameter to be plotted on the horizontal axis and the parameter to be plotted on the vertical axis. As an example, one might want to plot average packet delay on the vertical axis and the

voice traffic intensity on the horizontal axis. This optional feature will enhance the capability of the system in that it will be able to provide a pictorial representation of the performance. The existing measurement facility also provides snapshot statistics in the form of a second-by-second account of the nodal parameters. This is a nice feature since it can be used to detect momentary congestions and queue buildups. A recent study [33] has indicated that the study of the transient behavior of the performance of an integrated node is important due to the disparity in the transaction duration of voice and data subscribers. Snapshot statistics are expected to be quite useful in the study of the transient behavior of the integrated node.

VI. EXPERIMENTATION WITH TEST NODE SIMULATOR:

The test node simulator configuration can be employed to determine the performance of a switching node operating in an integrated node environment. One simulation run involves setting up the nodal configuration and certain network parameters, introducing a specified mix and volume of data and voice traffic and finally measuring the desired performance parameters. The test node simulator is quite flexible in that by setting nodal parameters appropriately a wide range of situations can be produced. First we describe the possible variables for various simulation runs.

The first variable is the nodal configuration itself and the possible variables are

- (i) Number of lines and trunks.
- (ii) Rates of lines and trunks.
- (iii) Maximum voice bandwidth on trunks.
- (iv) Trunk routing algorithm.
- (v) Total buffers allotted for data.
- (vi) Throttling thresholds and rules.
- (vii) Preemption and priority rules.

The second variable is the modeling and parameter specification of the network response turnaround delay. This is a function of the number of nodes traversed and network congestion. The third variable is the traffic introduced. There are two types of traffics to be introduced namely voice traffic and data traffic. The variables for the two classes are listed separately. For the voice traffic, the variables are

- (i) Mean voice level node must accommodate (in Erlangs).
- (ii) Call types, e.g., local to local, tandem, incoming and outgoing.
- (iii) Call arrival rate distribution.
- (iv) Call mean holding time.
- (v) Call holding time distribution.

- (vi) Call bandwidth (digital bit rate of voice calls).
- (vii) Call bandwidth distribution.

For the data traffic, the variables are

- (i) Traffic volume (in transactions per hour).
- (ii) Transaction type, e.g., local, tandem, incoming or outgoing.
- (iii) Transaction arrival rate distribution.
- (iv) Transaction precedence distribution.
- (v) Mean transaction duration.
- (vi) Transaction duration distribution.

In the above we have discussed the possible variables that we can have for various simulations runs. The list is very large and all the variables cannot be changed as each simulation run involves a considerable amount of run time. Several meaningful experiments are suggested in the following. Traffic is introduced in the node by means of prerecorded tapes which are generated off-line by means of a simulation program. The first step should be to generate a library of traffic tapes which may be used in various simulation runs. There are two possible approaches which may be used to evaluate the nodal performance. The first is to keep the voice traffic fixed and vary the data traffic in steps to generate a number of traffic tapes. The

second is to keep the data traffic fixed and vary the voice traffic in steps during traffic tape generation. The following three sets of traffic tapes are expected to be useful.

- A. For a fixed moderate amount of voice traffic, increase data traffic ranging from light traffic to heavy traffic. This set of tapes will be useful in determining the nodal performance sensitivity to changing data traffic.
- B. For a fixed moderate amount of data traffic, increase voice traffic ranging from light traffic to heavy traffic. This set of tapes will be useful in determining the nodal performance sensitivity to changing voice traffic.
- C. Generate a traffic tape with a heavy voice traffic and a heavy data traffic. This tape will be useful in determining the nodal performance under heavy loading.

Some of the suggested experiments are now described.

- 1. Determine the nodal performance for the traffic tape set A. The nodal configuration should be kept fixed during this experiment. The turnaround delay should be assumed to be zero. This experiment will determine the effect of changing the data traffic on the nodal performance for a fixed voice traffic.

2. Keep the nodal configuration as in experiment 1. Assume the turnaround delay to be zero. Determine the nodal performance for the traffic tape set B. This experiment will yield information regarding the effect of changing voice traffic on the nodal performance for a fixed data traffic.
3. For the same experimental setup as in 1 and 2, gather nodal performance data for tape C which will represent the node performance under heavy loading.
4. Keep the nodal configuration as in experiment 1. Select an appropriate traffic tape from set A or B (tape with moderate data and voice traffic). Run the experiment for various models of the turnaround delay to determine its effect on the nodal performance. This will provide some information regarding the nodal performance as a function of the network size and complexity.
5. Same as 4 but with tape C which will mean a repetition of the fourth experiment under heavy loading conditions.
6. Fix the dummy voice bandwidth at the same level as in experiment 1. Keep the same nodal configuration and zero turnaround delay. Run the simulations for the same data traffic as in traffic tape set A. A comparison of the results obtained from experiment 1 and 6 will represent the comparative performance of the fixed boundary strategy and the movable boundary strategy.

7. Select a typical traffic tape from the set A or B (same tape as in 4, call it D). Assume zero turnaround delay. Run the simulations with tapes C and D. In this experiment, nodal configuration will be varied. Keep other nodal configuration parameters fixed and vary the trunk rate. This experiment will determine the effect of varying the trunk rate on the nodal performance under moderate loading and heavy loading.
8. Assume zero turnaround delay. In this experiment, vary the maximum voice bandwidth on trunks while keeping the other nodal configuration parameters fixed. Perform the simulation with tapes C and D. This experiment will determine the effect of varying the maximum voice bandwidth on trunks on the nodal performance under both moderate and heavy loading conditions.
9. The effect of varying the buffer size and buffer management strategies can also be studied. Appropriate nodal configuration parameters will be varied and simulation will be run for tapes C and D.
10. Keep the nodal configuration as in 1 and zero turnaround delay. Study the effect of changing the voice digitization rate. This will be accomplished by generating traffic tapes with various voice digitation rates and using these tapes to run the simulation experiment.

11. Keep the nodal configuration as in 1 and assume zero turnaround delay. Study the effect of changing the maximum packet length. The simulation runs can be performed using tapes A and C. It is expected that the results of this experiment will yield an optimum maximum packet size.

VII. ADDITIONAL EXPERIMENTAL POSSIBILITIES FOR ADPT TESTBED:

The main function of the test node simulator configuration is to measure and analyze the performance of a switching node in an integrated network environment. The three node subnetwork simulator was employed for the validation of the functional operation of the specialized switching hardware and applications software of the ADPT testbed facility. The three node subnetwork simulator can now be used for the demonstration of integrated switching concept using the dynamic channel allocation policy. In addition to the above stated goals, the ADPT testbed can be used in a variety of other experimentations. In this section, we briefly discuss some of the experimental possibilities.

Packet Voice Experimentation: Circuit switching has been used exclusively for voice transmission. However, there has been some recent effort on packetized voice transmission [8]. The test node simulator configuration provides a virtual circuit switching operation and cannot be used for packet voice experiments in its current form. However, it seems possible that the basic simulator can be modified to include the possibility of

packetized voice. Some form of flow control will be necessary to ensure a continuous voice transmission. It is anticipated that a software module will be necessary which will packetize the digitized voice and implement an appropriate packet voice protocol and flow control policy.

Packet Network Interconnection Experiments: The three node subnetwork simulator can be used in a variety of network interconnection experiments. An interconnection of the subnetwork with another network can be attempted. The first possibility is to try to connect the subnetwork to the ARPA network. The EISN network whose fifth node is expected to be located at RADC represents another network with which an interconnection of the subnetwork can be tried. The main issues that can be dealt with are protocols for network interconnection, gateway implementation and validation, data security considerations and interfaces.

Local Network Experimentation: Useful experience can be gained while attempting to connect a variety of computing resources located in a local area. The ADPT testbed facility represents one such resource which may be connected to other computing facilities of the RADC. This experiment will yield useful information in the area of local network design, e.g., distributed processing techniques, data base management, protocol design, interfacing and data security considerations.

Experimentation with Channel Simulators: Digital Communications

Experimental Facility (DICEF) has several channel simulators and it also has access to various real transmission media. These facilities can be used in conjunction with the ADPT testbed. The trunk provided with the testbed can be replaced by a real channel or a channel simulator. This experiment will provide some useful information regarding the effect of various channels on the performance of the integrated node. The three node subnetwork simulator configuration can also demonstrate the operation of the dynamic channel allocation concept on a subnetwork employing specific channel simulators.

Protocol Evaluation and Validation: The ADPT testbed can also be used to evaluate and validate protocols. By means of a specific software package, the protocol to be validated or evaluated can be implemented on the ADPT testbed. The correct functioning of the three node subnetwork simulator configuration will indicate the validity of the protocol. The efficiency of the protocol, which is mostly measured in terms of bandwidth, throughput or transit delay, can be measured from the test node simulator configuration.

Data Security Experimentation: The three node subnetwork simulator configuration can be used to run data security experiments. Messages and terminals can be assigned different security classifications. Data security procedure can be implemented by means of a software package and checked for adequacy by operating the three node subnetwork simulator.

Packet Radio and Satellite Network Experimentation: Additional software can be generated which will portray the packet radio network or satellite network environment. Appropriate protocols can be implemented. The ADPT testbed can then be employed to gather experimental data regarding the performance of a node employing the dynamic channel allocation policy in a packet radio or satellite network environment.

VIII. STANDARD INTEGRATED INFORMATION DISTRIBUTION SYSTEM:

The Standard Integrated Information Distribution System (SIIDS) is also known as the Flexible Intraconnect (FI) and we shall use the latter term in this section. The Flexible Intraconnect is a wideband cable-based communication system which integrates the control and distribution of digital and analog signals for Tactical Air Force C³ Centers. The FI provides as single standardized, architectural building block that is common to all types of C³ centers. It also provides configuration flexibility and potential for growth. The FI system is as shown in Figure 5. It consists of three major segments: the local intraconnect (LI), which is physically located within an individual shelter and which supports the internal information transfer requirement; the external intraconnect (EI), which physically connects groups of shelters and supports the inter-shelter information transfer requirements; and the shelter/shelter intraconnect capability (S/SIC), which provides a direct digital path between adjacent shelters. The proposed architecture for the FI is a star/bus hierarchial topology. Two

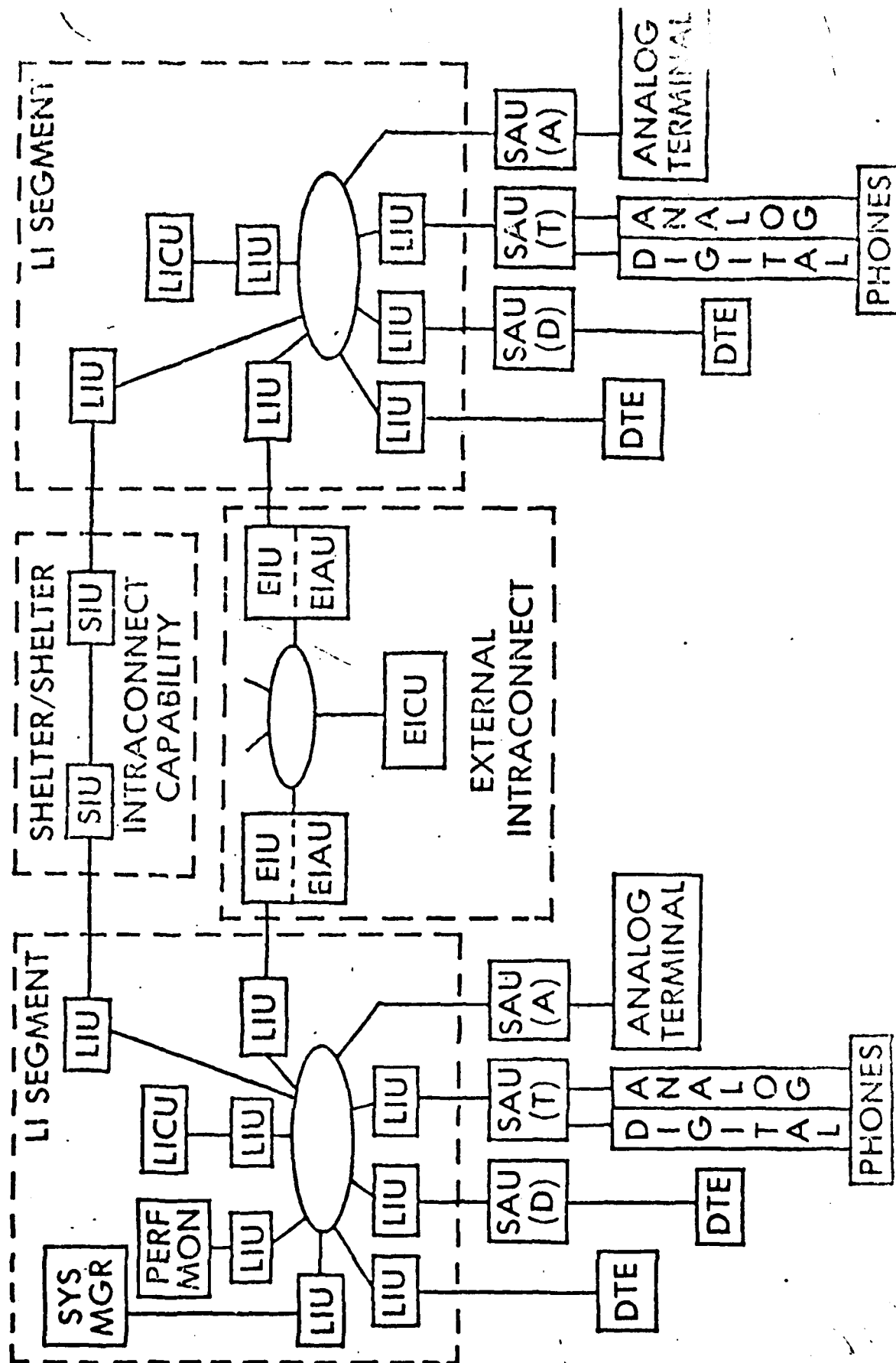


Figure 5 FI System

levels of intraconnect are provided. One level is for local (intrashelter) traffic and the other is for external (intracenter) traffic. Local intraconnect employs a conventional open-loop topology using twisted-pair ribbon cable for transmission. External intraconnect uses a star topology with multichannel fiber optic cable for transmission. The design criteria of the FI were the following:

- (i) To provide "positive control" of system operations in that it was highly disciplined, there was no lockup or runaway, it minimized unpredictableness and required simple operator actions.
- (ii) To exploit the technology by maximizing digital implementations and by using microprocessors, surface acoustic wave devices and fiber optic cables.
- (iii) To provide adequate system efficiency.

Four types of services are provided. First is the traditional point-to-point service. Second is the broadcast service where a subscriber can send a message to several other subscribers. Virtual bus and lazy susan bus capabilities are the other two types of specialized services which can be provided to communities of users. Two independent contractors designed the flexible intraconnect with the above criteria in mind. These two designs were reviewed and some comments regarding the basic design, system integrity and efficiency follow in this section.

In [12], the protocol for data transfer control on the local intraconnect and external intraconnect is a time slotted reservation system on a TDMA bus. Although the protocols are generally the same, there are differences between the local and external intraconnects based on their physical structures and control mechanisms. First, we discuss the local intraconnect operation. During local transmission, assigned slots are provided for the virtual bus and lazy susan messages. Prior to each block message transfer, the local intraconnect unit (LIU) makes reservations with the local intraconnect control unit (LICU) indicating destination addresses and message length. The control unit controls transmission via a transfer enable line and the data bus. Transmission handshakes are accomplished via memory status messages which each LIU reports to the LICU and ACK/NACK replies at the end of each message transfer. The LICU polls each LIU for possible reservations. The reservation consists of a three word interchange between the LICU and the LIU. The first word is placed on the bus by the LICU. It contains the address of the LIU that is being polled for reservation requests. The LIU transmits the second and third words indicating the destination address and the message length. Polling and transfer of messages is done during the time reserved for block messages. During the reservation process, the external intraconnect unit has priority. This seems like a good idea as it would prevent any possible congestion in the entire FI system.

In each external intraconnect cycle, assigned slots are

provided for virtual bus and lazy susan message transfers and a slot is also assigned to each EIU for short message transfers. For each block message transfer, a front-end handshake and an ACK/NACK of message transfer status occurs. This handshake procedure is performed via assigned handshake slots. Front-end handshake is achieved through a three-step process which is (a) transfer of message counts between EI's, (b) requests for transfer of messages, and (c) granting of such requests. In this process there is a propagation delay--time needed for the request to reach the destination EI and time needed for the granting of request to come to the sending EI. In the design, it has been proposed that this time be not wasted and utilized in transmitting short messages. This is a good idea but it requires an extremely precise synchronization and may not be worth the effort.

The FI design proposed by the Hughes Corporation [12] seems basically sound. The following good features are worth mentioning.

- (i) During the reservation process in the LI, EI has priority, i.e., external data that wishes to enter the local intraconnect has priority over the local data. This will minimize the possibility of congestions in the FI.
- (ii) An effort is made to utilize the propagation delay in the EI by sending short messages. This is a good idea

In [12], the protocol for data transfer control on the local intraconnect and external intraconnect is a time slotted reservation system on a TDMA bus. Although the protocols are generally the same, there are differences between the local and external intraconnects based on their physical structures and control mechanisms. First, we discuss the local intraconnect operation. During local transmission, assigned slots are provided for the virtual bus and lazy susan messages. Prior to each block message transfer, the local intraconnect unit (LIU) makes reservations with the local intraconnect control unit (LICU) indicating destination addresses and message length. The control unit controls transmission via a transfer enable line and the data bus. Transmission handshakes are accomplished via memory status messages which each LIU reports to the LICU and ACK/NACK replies at the end of each message transfer. The LICU polls each LIU for possible reservations. The reservation consists of a three word interchange between the LICU and the LIU. The first word is placed on the bus by the LICU. It contains the address of the LIU that is being polled for reservation requests. The LIU transmits the second and third words indicating the destination address and the message length. Polling and transfer of messages is done during the time reserved for block messages. During the reservation process, the external intraconnect unit has priority. This seems like a good idea as it would prevent any possible congestion in the entire FI system.

In each external intraconnect cycle, assigned slots are

provided for virtual bus and lazy susan message transfers and a slot is also assigned to each EIU for short message transfers. For each block message transfer, a front-end handshake and an ACK/NACK of message transfer status occurs. This handshake procedure is performed via assigned handshake slots. Front-end handshake is achieved through a three-step process which is (a) transfer of message counts between EI's, (b) requests for transfer of messages, and (c) granting of such requests. In this process there is a propagation delay--time needed for the request to reach the destination EI and time needed for the granting of request to come to the sending EI. In the design, it has been proposed that this time be not wasted and utilized in transmitting short messages. This is a good idea but it requires an extremely precise synchronization and may not be worth the effort.

The FI design proposed by the Hughes Corporation [12] seems basically sound. The following good features are worth mentioning.

- (i) During the reservation process in the LI, EI has priority, i.e., external data that wishes to enter the local intraconnect has priority over the local data. This will minimize the possibility of congestions in the FI.
- (ii) An effort is made to utilize the propagation delay in the EI by sending short messages. This is a good idea

but at the expense of added complexity.

On the negative side, the following should be noted.

- (i) In order to implement the scheme which utilizes the propagation delay, a sophisticated synchronization and measurement scheme is used. This adds complexity to the system. It may be possible that this added complexity does not improve the efficiency much and thus, may not be worth the effort. Efficiency of both the schemes, one without the propagation delay transmission and the other with the transmission should be compared before arriving at a meaningful conclusion.
- (ii) The LICU polls LIU's in a sequential fashion to make reservations. Wouldn't it be simpler if the LIU's transmitted their data when polled rather than making reservations and then starting their transmissions.
- (iii) No details of the polling algorithm are provided. It is not clear if any priority scheme is implemented. In any real C³ center environment, a priority structure will be highly desirable. Would the reservation scheme proposed provide a satisfactory performance under heavy loading?
- (iv) LIU's provide their memory status reports to the LICU frequently. It is not mentioned as to how frequent is this. If it is not done frequently enough, it may

result in lost messages. If the LICU thinks that a particular LIU is available and it sends a packet to the LIU, the packet may be lost if the LIU has filled up since the previous memory status report.

The FI proposed in [20] is also implemented in terms of a two-level bus system consisting of the LI and the EI. First, we shall discuss the LI operation. The LICU acts as the LI bus controller and performs the following three major functions. First, when there is no EI/LI bus data interchange, the LIU continually polls LIU's on the LI bus according to its polling algorithm. This allows for data interchange between devices within a shelter. Second, when data is to be transmitted to a device in another shelter, LICU buffers it and transfers it to the EI via the EIU. Third, LICU receives all EI data destined for the LI, it buffers it and then transmits over the LI. The LIU transfers the device's message into its buffer, formulates the network header for transmission control, packetizes the device message and network header, and when polled, transfers the packet onto the LI bus for transmission to its destination device. The data is transferred between the LIU's and LICU on a demand-response time division multiple access basis, with LI bus access provided on a polling basis. Each LIU and LICU monitors every packet transmitted over the bus. Each LIU analyzes the packet network header to determine if the packet is destined for itself and what, if any, action is to be taken. An LIU response depends upon the packet type. There are three types of packets.

The first is a poll packet. The LICU polls an LIU by sending a short poll packet containing the LIU's address and a poll message code. The addressed LIU responds with a data packet if it has to be transmitted. Otherwise, it sends an idle packet. After detecting the completion of the poll response packet, LICU polls the next LIU in the polling sequence. The second type of packet is the query response packet. This type of procedure is used for direct address messages. When the source LIU is polled, it sends a short query packet to the destination LIU to determine the availability of buffer space. If space is available, a response packet is sent to the source LIU which immediately transmits the data packet on the LI. If buffer space is not available, the source LIU must wait for a poll from the LICU which will also indicate buffer availability. Third type of packet is a data packet which is used for data transfers between LIU's.

Implementation of the virtual bus and lazy susan nets is performed by means of the polling algorithm. The local intraconnect system described appears to be good. The whole implementation is in terms of a polling scheme which is flexible and is to be designed with the specific system in mind.

The EI is the facility that allows users in different shelters to communicate with each other. It has a star topology. The EI consists of the EICU, a switched-active transponder, an EIU for every point of the star, and a full-duplex fiber optic transmission medium between each EIU and the transponder. The EI can support two types of services: digital TDMA transmission and

high speed analog transmission. Digital TDMA service is provided to transfer data packets generated in the LIU's between LI's in different shelters. The EI transmission system consists of two links between the transponder and each shelter. One uplink from the shelter to the transponder and a downlink from the transponder back to the shelter. The EICU polls one shelter at a time according to the polling algorithm stored in the EICU. A polling message which contains the address of the EIU to be polled is transmitted over every downlink in the star. Upon recognition of the address, the EIU transmits its response to the poll over the uplink to the transponder. The response packet is sent over the EI downlinks to every EIU in the system. Thus, each EIU receives all transmissions from every source on the EI but responds only to the packets addressed to it. The polling scheme can be designed so that it can be altered to satisfy the center requirements. Each EIU multiplexes the received data packets in a word and bit serial stream. At any time only one EIU transmits a data packet over its uplink and all the others transmit a long pseudorandom sequence. The transponder operates under the control of the EICU and switches its commutator depending upon selected EIU. Each EIU scans the received data. If a packet destined for the EIU is received, the EIU either passes it on to the LI or sends a response packet to the EICU. The analog transmission service of the EI is used to transfer unidirectional wideband analog signals like radar and video data between shelters on the EI. It consists of simplex links between the transponder and the shelters engaged in the EI analog

transmission. Frequency division multiplexing is employed for such transmission.

The FI design proposed by the Martin Marietta Corporation [20] seems pretty good. The two main features are its flexibility and conceptual simplicity.

(i) The design of the entire FI system is quite flexible. A system to suit a particular C³ center can be implemented by means of the polling algorithms. The polling algorithms can be altered on a dynamic basis for changing requirements.

(ii) The proposed design is conceptually simple. Implementation in terms of the polling scheme is easy to understand and intuitively appealing. Desired amount of complexity in terms of priority structure can be incorporated in the polling algorithm.

On the negative side,

(i) It is not very clear from the report [20] as to how Virtual Bus and Lazy Susan services are provided. It is not mentioned as to how it is implemented in the polling scheme.

(ii) Some efficiency is being sacrificed to gain conceptual simplicity.

(iii) If an adaptive polling scheme is designed, care will

have to be exercised to ensure accuracy of the algorithm. Also, control units will be more complex.

IX. RECOMMENDATIONS:

The ADPT testbed located at the RADC represents a major experimental tool. This facility should be employed to run simulation experiments in order to gain a better understanding of integrated switching. The testbed can also be used in a variety of packet communication network experimentations. An experimental plan for the ADPT testbed has been suggested in this report. This plan should be pursued by the RADC personnel to fully utilize the capability of the testbed. A theoretical study of integrated switching and related concepts should be performed in parallel with the experimental program. Close coordination between the two studies will be quite fruitful. In the SIIDS program, the FI design proposed in [20] seems more attractive mainly due to its flexibility and simplicity.

REFERENCES AND SELECTED BIBLIOGRAPHY

1. E. Arthurs and B.W. Stuck, "A Theoretical Traffic Performance Analysis of an Integrated Voice-Data Virtual Circuit Packet Switch," IEEE Trans Comm, Vol COM-27, pp 1104-1111, July 1979.
2. J.A. Blackman, "Integrated Switching of Voice and Non-Voice Traffic," Proc Int Comm Conf, 1976.
3. G.B. Cicchetti and A. Lubarsky, "Hybrid Integrated Digital Network," Proc World Telecommunication Forum, 1975.
4. G.J. Coviello, O.L. Lake and G.R. Redinbo, "System Design Implications of Packetized Voice," Proc Int Comm Conf, 1977.
5. G. Coviello and P. Vena, "Integration of Circuit/Packet Switching by a SENET (Slotted Network Envelope) Concept," Proc Nat Telecom Conf, 1975.
6. R. Esterling and P. Hahn, "A Comparison of Digital Data Network Switching Alternatives," Proc Nat Telecom Conf, 1975.
7. M.J. Fischer and T.C. Harris, "A Model for Evaluating the Performance of an Integrated Circuit and Packet Switched Multiplex Structure," IEEE Trans Comm, Vol COM-24, pp 195-202, February 1976.
8. J.W. Forgie and A.G. Nemeth, "An Efficient Packetized

Voice/Data Network Using Statistical Flow Control," Proc Int Comm Conf, 1977.

9. I. Gitman, H. Frank, B. Occhiogrosso and W. Hsieh, "Issues in Integrated Network Design," Proc Int Comm Conf, 1977.
10. I. Gitman and H. Frank, "Economic Analysis of Integrated Voice and Data Networks: A Case Study," Proc IEEE, Vol 66, pp 1549-1570, November 1978.
11. W. Hsieh, I. Gitman and B. Occhiogrosso, "Design of Hybrid-Switched Networks For Voice and Data," Proc Int Comm Conf, 1978.
12. Hughes Aircraft Company, "Modular C³ Interface Analysis, Volume II - Study Methodology and Results," Final Technical Report, F19628-77-C-0261, Rome Air Development Center, April 1979.
13. C. Jenny and K. Kuenmerle, "Distributed Processing within an Integrated Circuit/Packet Switching Node," IEEE Trans Comm, Vol COM-24, pp 1089-1100, October 1976.
14. P. Kermani and L. Kleinrock, "A Tradeoff Study of Switching Systems," Proc Int Comm Conf, 1979.
15. N. Keyes and M. Gerla, "Report on Experience in Developing a Hybrid Packet and Circuit Switched Network," Proc Int Comm Conf, 1978.

16. K. Kuemmerle, "Multiplexor Performance for Integrated Line and Packet Switched Traffic," Proc of Second Int Conf on Computer Communications, 1974.
17. K. Kuemmerle and H. Rudin, "Packet and Circuit Switching: A Comparison of Cost and Performance," Proc Nat Telecom Conf, 1976.
18. K. Kuemmerle and H. Rudin, "Packet and Circuit Switching: Cost/Performance Boundaries," Computer Networks, Vol 2, pp 3-17, February 1978.
19. B. Maglaris and M. Schwartz, "Optimal Bandwidth Allocation in Integrated Line- and Packet-Switched Channels," Proc Int Comm Conf, 1979.
20. Martin Marietta Corp, "Modular C³ Interface Analysis: Volume I," Final Technical Report, F19628-77-C-0262, Rome Air Development Center, April 1979.
21. D. McAuliffe, "An Integrated Approach to Communications Switching," Proc Int Comm Conf, 1978.
22. H. Miyahara, Y. Teshigawara and T. Hasegawa, "Delay and Throughput Evaluation of Switching Methods in Computer Communication Networks," IEEE Trans Comm, Vol COM-26, pp 337-344.
23. H. Miyahara and T. Hasegawa, "Integrated Switching with Variable Frame and Packet," Proc Int Comm Conf, 1978.

24. H. Miyahara and T. Hasegawa, "Performance Evaluation of Modified Multiplexing Technique with Two Types of Packet for Circuit and Packet Switched Traffic," Proc Int Comm Conf, 1979.
25. Network Analysis Corporation, "Economic Analysis of Integrated DOD Voice and Data Networks," Final Report, prepared for ARPA, September 1978.
26. B. Occhiogrosso, I. Gitman, W. Hsieh and H. Frank, "Performance Analysis of Integrated Switching Communication Systems," Proc Nat Telecom Conf, 1977.
27. L.H. Ozarow and J.K. DeRosa, "A Combined Packet and Circuit-Switched Processing Satellite System," Proc Int Comm Conf, 1979.
28. Proceedings of IEEE, Vol 66, No 11, November 1978.
29. RCA Corp, "Studies for Development of a Unified Node Employing Dynamic Channel Allocation," Final Report, RADC-TR-77-380, December 1977.
30. R.D. Rosner, "Packet Switching and Circuit Switching: A Comparison," Proc Nat Telecom Conf, 1975.
31. M.J. Ross, A.C. Tabbot and J.A. Waite, "Design Approaches and Performance Criteria for Integrated Voice/Data Switching," Proc IEEE, Vol 65, pp 1283-1295, September 1977.

32. M.J. Ross, "System Engineering of Integrated Voice and Data Switches," Proc Int Comm Conf, 1978.
33. H. Rudin, "Studies on the Integration of Circuit and Packet Switching," Proc Int Comm Conf, 1978.
34. D. Schutzer, "An Analysis of a Distributed Switching Network with Integrated Voice and Data in Support of Command and Control," IEEE Trans Comm, Vol COM-27, pp 1124-1130, July 1979.
35. J.T. Wang and M.T. Liu, "Analysis and Simulation of the Mixed Voice/Data Transmission System for Computer Communication," Proc Nat Telecom Conf, 1976.
36. C.J. Weinstein, M.L. Malpass and M.J. Fischer, "Data Traffic Performance of an Integrated Circuit- and Packet-Switched Multiplex Structure," Proc Int Comm Conf, 1979.
37. P. Zafiropulo, "Flexible Multiplexing for Networks Supporting Line-Switched and Packet-Switched Data Traffic," Proc Second Int Conf on Computer Comm, 1974.

1979 USAF - SCEE SUMMER FACULTY RESEARCH PROGRAM

Sponsored by the

AIR FORCE OFFICE OF SCIENTIFIC RESEARCH

Conducted by the

SOUTHEASTERN CENTER FOR ELECTRICAL ENGINEERING EDUCATION

FINAL REPORT

STABILITY ANALYSIS OF THE LOWER BRANCH
SOLUTIONS OF THE FALKNER-SKAN EQUATIONS

Prepared by:	Ghasi R. Verma
Academic Rank:	Associate Professor
Department and University:	Department of Mathematics University of Rhode Island Kingston, R.I. 02881
Research Location:	Air Force Flight Dynamics Laboratory Wright Patterson Air Force Base, Ohio
USAF Research Colleague:	Dr. W. L. Hankey
Date:	August 3, 1979
Contract No:	F49620-79-C-0038

STABILITY ANALYSIS OF THE LOWER
BRANCH SOLUTIONS OF THE FALKNER-SKAN EQUATIONS

BY

G. R. Verma

ABSTRACT

In this report a series of similar separated flows for different pressure gradient parameters are analysed. The amplification factors and propagation velocities in all these different cases are determined and the most significant modes are identified.

ACKNOWLEDGEMENT

The author would like to thank the Air Force Systems Command Air Force Office of Scientific Research and Southern Center for Electrical Engineering Education for providing him the opportunity to spend a most worthwhile and interesting summer at Wright-Patterson Air Force Base. Special acknowledgement is also due to Dr. W. L. Hankey of the Air Force Flight Dynamics Laboratory for numerous helpful discussions and guidance and for providing a very congenial working atmosphere which enabled the author to expand his horizons considerably in the area of computational fluid dynamics.

Finally he would like to thank Dr. Charles Jobe of AFFDL and Mr. Stephen Scherr of Michigan State University for helping him in programming.

LIST OF SYMBOLS

C	$= C_r + iC_i$, where C_r and C_i are real and $i = \sqrt{-1}$
C_r	propagation velocity
C_i	amplification factor
f	defined by $\frac{df}{d\eta} = \frac{U}{U_e}$; dimensionless velocity ratio
m	pressure gradient parameter (eqn 3.10)
p	pressure
U	longitudinal velocity component
V	transverse velocity component
α	wave number
$\bar{\alpha}$	$= \alpha \frac{dy}{d\eta}$
β	pressure gradient parameter (eqn 3.10)
δ	boundary layer thickness
δ^*	displacement thickness
ξ	transformed similarity variable (eqn 3.6)
η	transformed similarity variable (eqn 3.7)
$\phi(y)$	small perturbation variable for transverse velocity (eqn 4.2)
ν	kinematic viscosity

Subscripts

e	external flow
x	partial derivative with respect to x
y	partial derivative with respect to y
η	partial derivative with respect to η
\wedge	small perturbation variable function of y

LIST OF ILLUSTRATIONS

Figure

- 1 Graph of C_R versus $\alpha\delta^*$ for various β
- 2 Graph of C_I versus $\alpha\delta^*$ for various β
- 3 Graph of complex wave velocity in Howard's circle
- 4 Error reduction plot for the computer program
- 5a Graph of real eigenfunctions ϕ_r for $\beta = -.0001, -.0005, -.002$
and for maximum C_I values.
- 5b Graph of imaginary eigenfunction ϕ_i for $\beta = -.0001, -.0005, -.002$
and for maximum C_I values
- 5c Graph of real eigenfunction ϕ_r for $\beta = -.04, -.08, -.12, -.16,$
-.19884 and for maximum C_I values
- 5d Graph of imaginary eigenfunction ϕ_i for $\beta = -.04, -.08, -.12,$
-.16, -.19884 and for maximum C_I values

LIST OF TABLES

Table 1a-1h

Eigenvalues from stability analysis for reversed flow boundary layers for various β .

I	INTRODUCTION
II	OBJECTIVE OF RESEARCH EFFORT
III	MEAN FLOW EQUATIONS
IV	PERTURBATION EQUATIONS
V	SOLVING SCHEME
VI	RESULTS
VII	CONCLUSION
VIII	RECOMMENDATIONS

REFERENCES

1	APPENDIX	HOWARD CIRCLE THEORM
2	APPENDIX	TABULATED RESULTS
3	APPENDIX	COMPUTER PROGRAM

I. INTRODUCTION

Self excited oscillations have been experimentally observed in separated flows for over hundred years. Rayleigh [1] in 1880 proved that for inviscid, incompressible flow the unstable velocity profiles must have an inflection point. Tollmein [2] in 1935 showed that for symmetrical velocity distributions, or for velocity distributions of the boundary layer type, the existence of the inflection point implies instability.

Recently Hankey and Shang [3] have examined the self induced pressure oscillations in an open cavity. Their numerical computations compare very well with the previous experimental investigations. Roscoe and Hankey [4] have studied the stability of hyperbolic tangent velocity profile in a compressible fluid, while Hankey, Hunter and Harney [5] have examined the self-sustained oscillations (Buzz) on spiked tipped bodies for large Mach numbers. However, a systematic stability analysis of separated flows has not been undertaken. It is the purpose of this report to conduct a stability analysis of a general class of separated flows (i.e. reversed flow Falkner-Skan) in order to help shed light on the phenomenon of self-excited fluid flows.

II. OBJECTIVES OF THE RESEARCH EFFORT

The objective of this research effort was to analyze a series of similar separated flows for different values of β and to determine the amplification factors and propagation velocities in all these different cases. Eight cases of different β were identified to be analyzed. These cases were those with reversed flows which contained velocity profiles with inflection points.

III. MEAN FLOW EQUATIONS

In this report, incompressible flows will be analyzed. In subsequent work we plan to analyze the compressible flows.

The incompressible two-dimensional Navier-Stokes equations are as follows

$$U_t + UU_x + VU_y = -\frac{1}{\rho} P_x + \nu \nabla^2 U \quad (3.1)$$

$$V_t + UV_x + VV_y = -\frac{1}{\rho} P_y + \nu \nabla^2 V \quad (3.2)$$

$$U_x + V_y = 0 \quad (3.3)$$

Applying the boundary layer approximations to the above equations for steady flows results in the following:

$$UU_x + VU_y = U_e U_{ex} + \nu U_{yy} \quad (3.4)$$

$$U_x + V_y = 0 \quad (3.5)$$

These equations may be reduced to one ordinary differential equation for the case where $U_e = cx^m$ by transforming with similarity variables.

$$d\xi = \frac{U_e dx}{\nu} \quad (3.6)$$

$$d\eta = \frac{U_e dy}{\sqrt{2\xi} \nu} \quad (3.7)$$

Hence

$$f''' + ff'' = \beta(f'^2 - 1) \quad (3.8)$$

where

$$f'(\eta) = \frac{U}{U_e} \quad (3.9)$$

$$\text{and } \beta = \frac{\xi U_e f}{U_e} = \frac{2m}{m+1} = \text{constant} \quad (3.10)$$

with boundary conditions

$$f(0) = 0, f'(0) = 0, f'(\infty) = 1 \quad (3.11)$$

Falkner and Skan [6] originally derived this equation for attached flows however, Stewartson [7] discovered a lower branch to these solutions which represented reversed flows from incipient separation to the Chapman solution. Christian, Hankey and Petty [8] have tabulated these solutions for compressible and incompressible flows. It is this wide class of flows (which have inflection points) that are known to be unstable for which we shall now perform a stability analysis.

IV. PERTURBATION EQUATIONS

Let us assume small perturbations of the form

$$U = \bar{U}(y) + \hat{U}(y) e^{i\alpha(x - ct)} \quad (4.1)$$

$$V = \hat{\phi}(y) e^{i\alpha(x - ct)} \quad (4.2)$$

$$p = P_e(x) + \hat{P}(y) e^{i\alpha(x - ct)} \quad (4.3)$$

where $c = c_r + ic_i$ and \hat{U} , $\hat{\phi}$ and \hat{P} are small in comparison to the mean quantities. If we substitute these values of U , V , and P in equations (3.1), (3.2) and (3.3); retain only the first order terms and assume that Reynolds number Uex/ν is large then the equations (4.1), (4.2) and (4.3) reduce to one single equation

$$\phi'' - (\alpha^2 + \frac{\bar{U}''}{\bar{U} - c})\phi = 0 \quad (4.4)$$

The classical Rayleigh equation with the boundary conditions

$$\phi(0) = 0, \quad \phi(\infty) = 0 \quad (4.5a,b)$$

By transforming the equation from y to the η variable we obtain the following equation

$$\phi_{\eta\eta} - (\bar{\alpha}^2 + \frac{f'''}{f' - c})\phi = 0 \quad (4.6)$$

where

$$\bar{\alpha} = \alpha \frac{dy}{d\eta}$$

By inserting the values of $f'(\eta, \beta)$ into the Rayleigh equation $c(\bar{\alpha}, \beta)$ can be determined as an eigenvalue which satisfies the boundary conditions (4.5a,b).

V. SOLVING SCHEME

Eigenvalues were determined by a shooting method; starting with a given boundary condition, integrating over the range of η and comparing the result with the outer boundary condition, namely $\phi = 0$ at η_{\max} . The process involved minimization of the error in the outer boundary condition which was chosen to be the square of the norm of ϕ , $|\phi|^2 = \phi_R^2 + \phi_1^2 = \text{SSQ}$. (See Appendix 3). The integration was done using a fourth-order Runge-Kutta method.

The method of finding eigenvalues utilized a minimization routine written primarily by Roscoe [4]. Starting from a given guess the routine searched along a constant line of c_1 with increasing steps until it found a relative minimum of the error. It then used the last three calculated points to determine a parabola, with the c_1 value at the vertex used as the latest approximation. Then this value of c_1 was held constant and a search along a line of changing c_1 was carried out. After a new minimum was found, the quadratic approximation was again used to determine a new value for c_1 . The third step involved searching the line connecting the original guess and the new point. After finding a minimum and utilizing quadratic approximation, the error was checked to see if it was less than some preset limit. If not, the routine started again with the latest value used in place of the original guess.

Generally, the routine worked quite well. Most of the search time was attributable to bad guesses and finding the direction in which the search should be continued. An eigenvalue was usually located in a very

narrow region of the plane and even though the step size was continually reduced, it was frequently large enough to move the test point out of the acceptable region. For example, the initial guess in one case led to an error of 4.1×10^{13} , however, after only 128 new error computations, the error had been reduced 17 orders of magnitude to 1.9×10^{-4} , while c_r had been changed by 4.25% and c_i had been changed by 3.82%. Convergence was also retarded for small values of c_i , e.g. $|c_i| < .001$. This was concurrent with c_r approaching its limiting value.

The Howard semicircle theorem [9] was used as an aid in determining suitable initial guesses. If c_r is the propagation velocity, α is the wave number, c_i is the amplification factor, and U_{\max} and U_{\min} are the maximum and minimum values of the range of U , the theorem states

$$[c_r - 1/2(U_{\max} + U_{\min})]^2 + c_i^2 \leq [1/2(U_{\max} - U_{\min})]^2.$$

Thus, the complex wave velocity for an unstable mode lies inside the upper semi-circle which has the range of U as diameter.

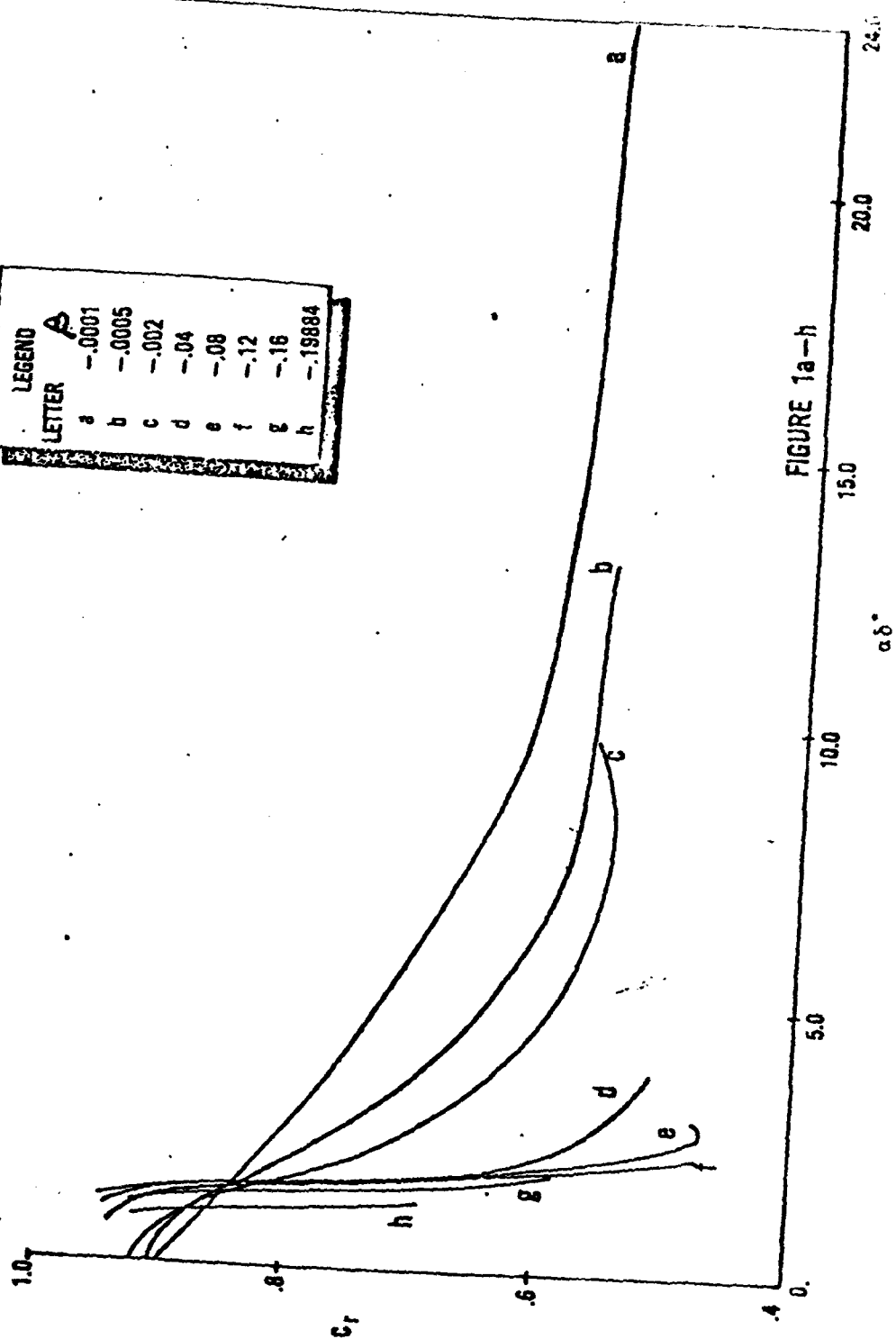
VI. RESULTS

Eight cases were computed for β values of $-.0001$, $-.0005$, $-.002$, $-.04$, $-.08$, $-.12$, $-.16$ and $-.19884$. For a wide range of $\bar{\alpha}$ values the eigenvalues were ascertained. These values are tabulated in tables 1a-1h in Appendix B. $\bar{\alpha}$ is related to α by the relation

$$\alpha\delta^* = \bar{\alpha}\delta^* \frac{d\eta}{dy} = \bar{\alpha} \int_0^{\infty} (1 - f') d\eta$$

The values of C_r and C_1 versus $\alpha\delta^*$ are plotted in figures 1a-1h and 2a-2h. Figure 3a-3h shows Howard's plot (9) for these solutions. Some typical eigenvalues for a series of solutions are also tabulated and plotted in Appendix B.

LEGEND	
LETTER	A
a	-.0001
b	-.0005
c	-.002
d	-.04
e	-.08
f	-.12
g	-.16
h	-.19884



LEGEND	
LETTER	β
a	-.0001
b	-.0005
c	-.002
d	-.04
e	-.08
f	-.12
g	-.16
h	-.19884

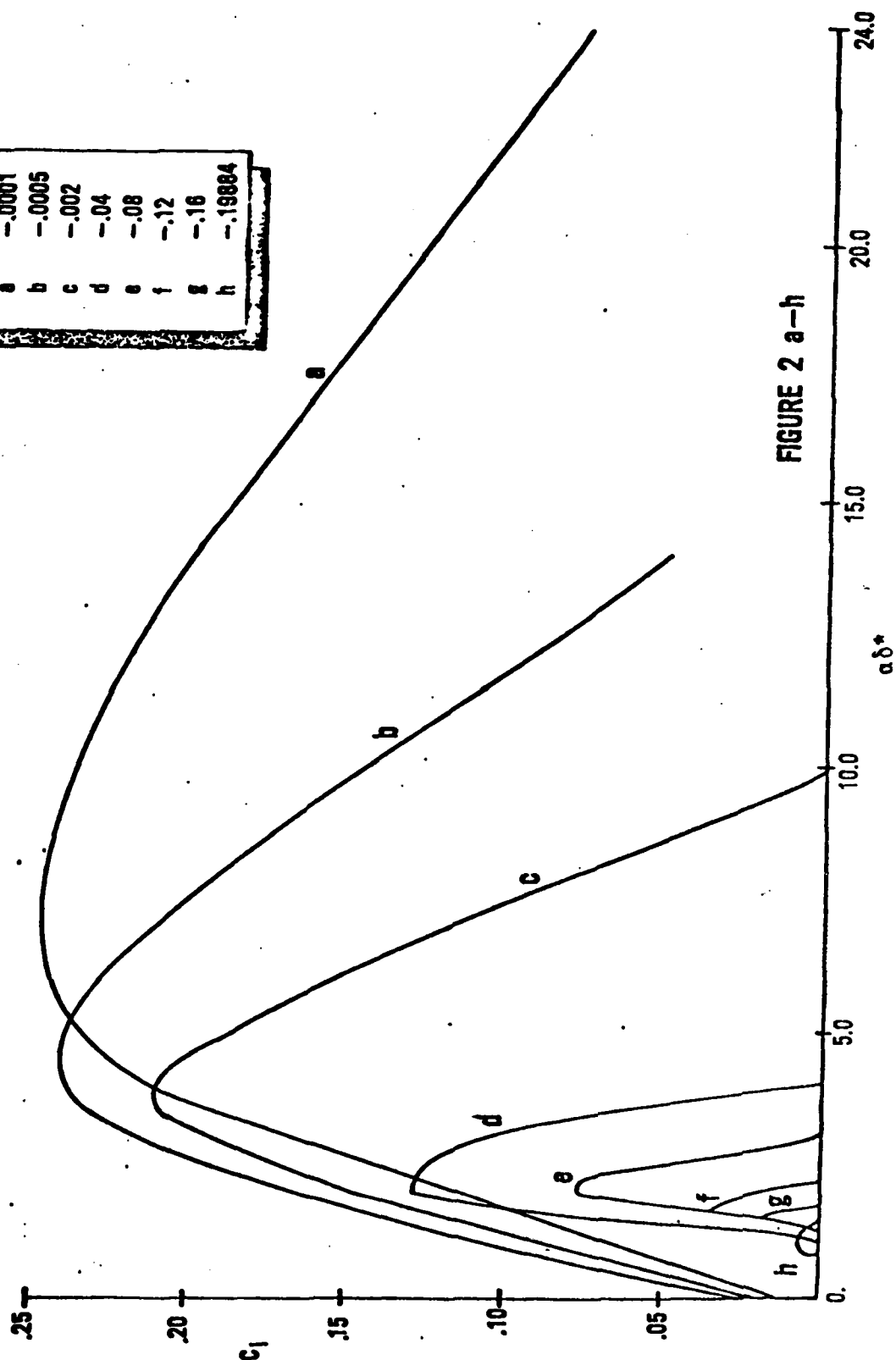


FIGURE 2 a-h

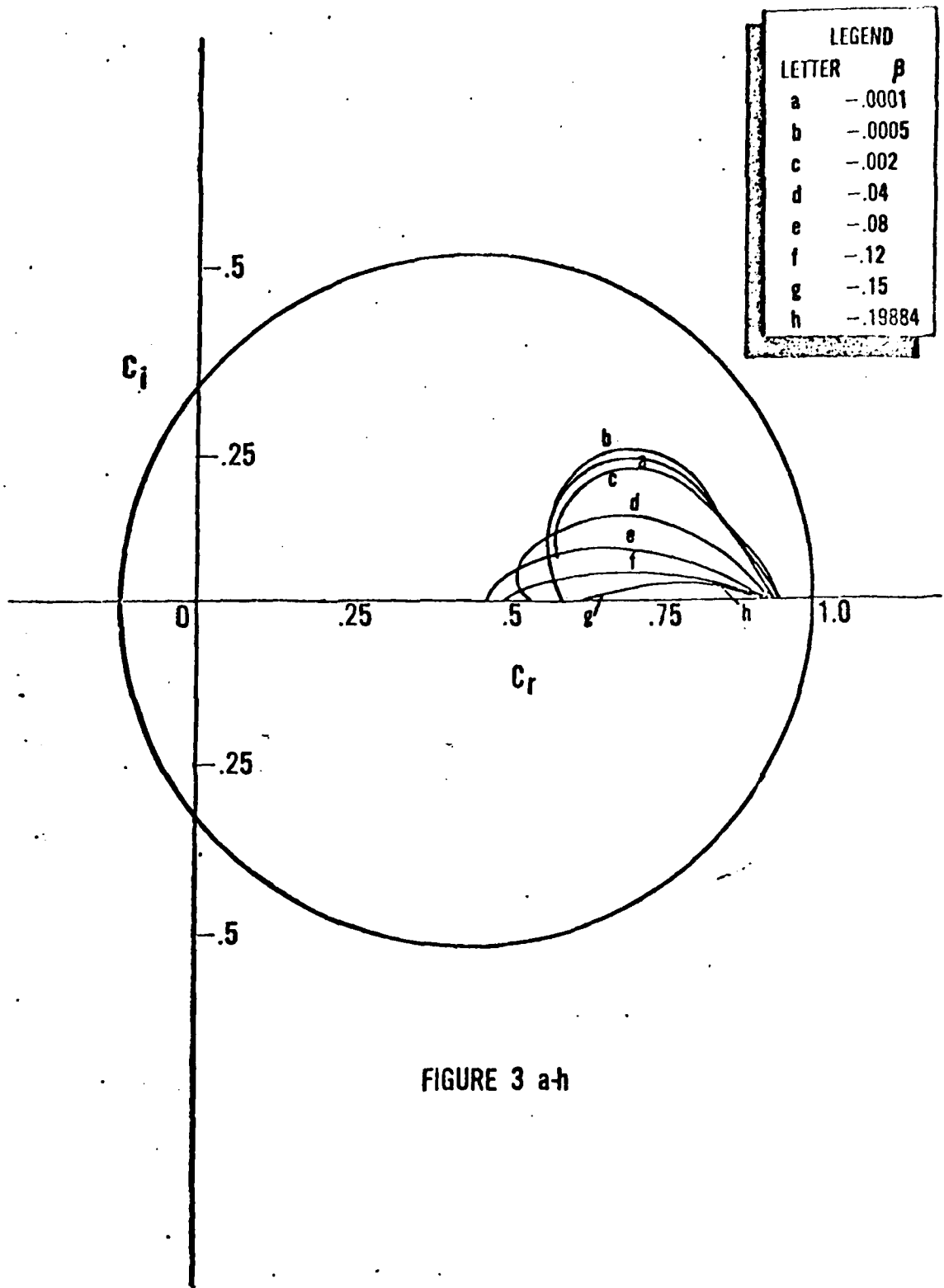


FIGURE 3 a-h

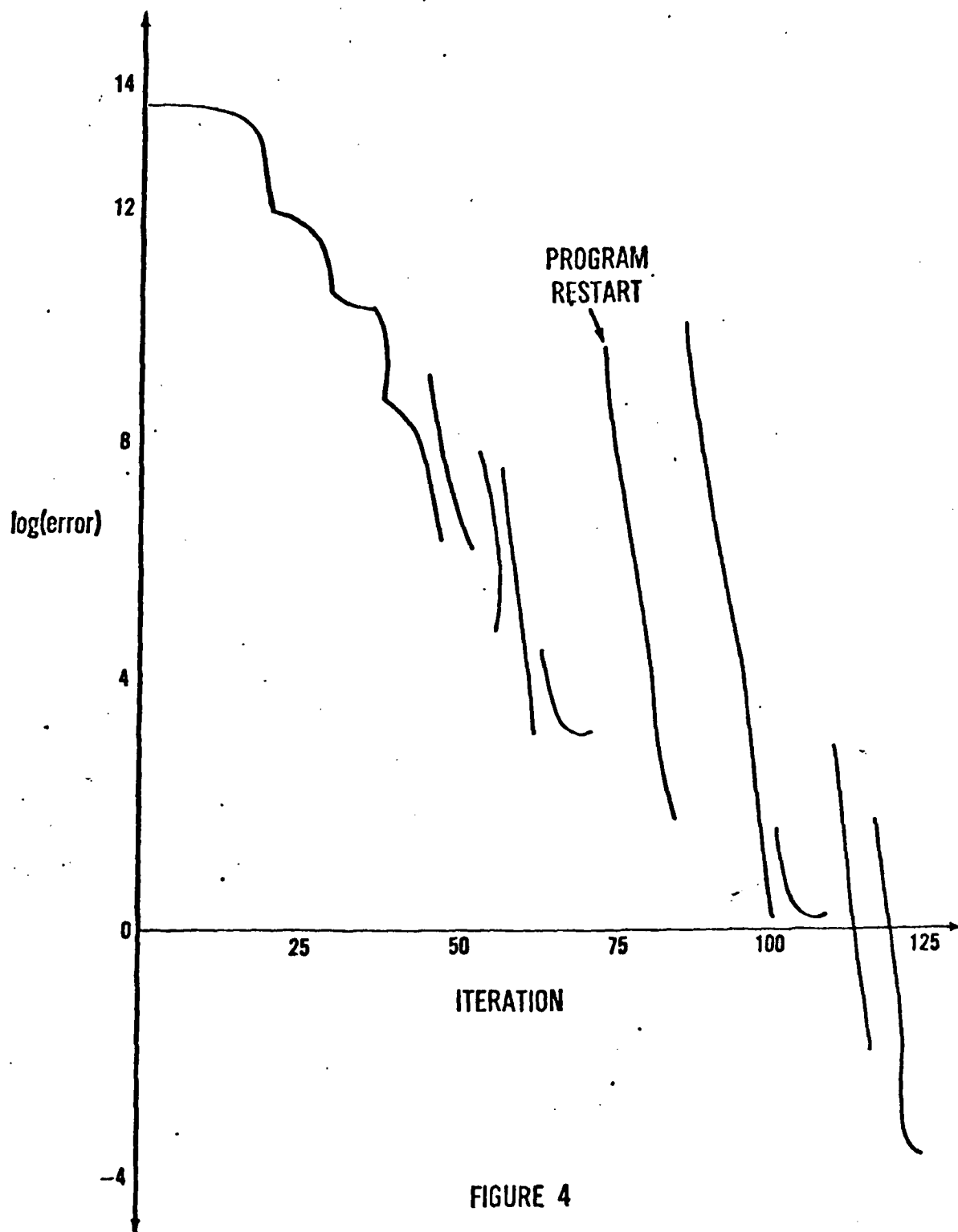


FIGURE 4

VII. CONCLUSIONS

The stability of a series of similar separated flows have been analyzed. Amplification factors and propagation velocities of the disturbances were determined. The results show that a small zone of instability does exist for these flows with inflexion points. The amplification factor increases as the extent of the reversed flow increases.

VIII. RECOMMENDATIONS

Suggestions for follow-on research: We would like to investigate the instability of laminar separated flows under the influence of compressibility. For a hyperbolic tangent velocity profile Roscoe (4) showed the instability to diminish with the increase of Mach number until the Rayleigh instability actually vanished at Mach number $M = 2.5$. The analysis should be repeated for the compressible, adiabatic, Falkner-Skan velocity profiles. We have completed $M = 0$ cases for various values of β , and would like to examine the influence of Mach number for the same values of β . It was observed that for $\beta = -.0001$ and $-.0005$ the convergence at the two ends of the spectrum was very slow. These cases should be analyzed somewhat more thoroughly.

REFERENCES

1. Raleigh, Lord (1880) "On the Stability or Instability of Certain Fluid Motions. Scientific Papers, Vol. 1, 474-87, Cambridge University Press.
2. Tollmien, W. Ein allgemeines Kriterium der Instabilität laminar Geschwindigkeitsverteilungen. Nachr. Ges. Wiss. Göttingen Math. Phys. Klasse, Fachgruppe I, 1 79-114 (1935); English translation in NACA TM No 792 (1936).
3. Hankey, W. L., Shang, J. S., "The Numerical Solution of Pressure Oscillations in an Open Cavity," AIAA Paper 79-0136, Jan 79.
4. Roscoe, D. F. and Hankey, W. L., "The Stability of a Compressible Free Shear Layer (To be published as an AFFDL-TR).
5. Hankey, W. L., Hunter, L. G., Harney, D., "Self Sustained Oscillations on Spiked Tipped Bodies at Mach 3." AFFDL-TM-79-23-FXM.
6. Falkner, V. M., Skan, S. W., "Some Approximate Solutions of the Boundary Layer Equations, Phil. Mag. 12 *65(1931) ARC R & M 1314 (1930).
7. Stewartson, K., "Further Solutions of the Falkner-Skan Equations. Proc. Camb. Phil. Soc. 50 454-465 (1954).
8. Christian, J. W., Hankey, W. L., Petty, J. S., "Similar Solutions of the Attached and Separated Compressible Laminar Boundary Layer with Heat Transfer and Pressure Gradient. ARL 70-0023, Feb 1970.
9. Howard, L. N., Note on a Paper of John W. Miles: Jour. Fluid Mech. 10 (1961) pp 509-512.

APPENDIX 1

THE HOWARD CIRCLE THEOREM

The Howard semicircle theorem [9] is an extension of the well known fact that if the amplification factor $C_1 > 0$ then the propagation velocity C_r must lie in the range of U . Howard was able to restrict the permissible values of C_r and C_1 so that the complex wave velocity C is confined to a semicircle which has the range of U as its diameter. If U_{\max} and U_{\min} are the extrema of the range of U , the theorem states

$$[C_r - 1/2(a + b)]^2 + C_1^2 \leq [1/2(a + b)]^2, \quad C_1 > 0$$

where $a = U_{\max}$, $b = U_{\min}$.

APPENDIX 2

EIGENVALUES FROM STABILITY ANALYSIS FOR REVERSED FLOW BOUNDARY LAYERS

EIGENVALUES FROM STABILITY ANALYSIS FOR
REVERSED FLOW BOUNDARY LAYERS

TABLE 1a

$\beta = -.0001$

α	c_r	c_i
0	.90538414741	.025680518247
.01	.91223794353	.071997946349
.02	.89422525454	.11766985541
.03	.87074750211	.12610731927
.04	.8412659309	.14572816584
.05	.80533205	.17071090
.07	.76425576	.21131732
.10	.72900063223	.23958792186
.15	.67639882435	.24398318931
.18	.651890026062	.23545393641
.20	.637998788145	.22696852817
.22	.62587353506	.21686502743
.25	.60392754004	.19700990613
.27	.60253175376	.18702547786
.29	.58908572761	.17144819857
.30	.58616022	.16481124
.31	.58992531643	.16063748234
.32	.58748966823	.15388430488
.35	.58168544052	.13349344451
.40	.57632116036	.099664728940
.41	.56994477164	.090751023415
.42	.56963082632391	.08414875686479

EIGENVALUES FROM STABILITY ANALYSIS FOR
REVERSED FLOW BOUNDARY LAYERS

TABLE 1b

$$\beta = -.0005$$

$\bar{\alpha}$	c_r	c_1
0	.91530377348	.02166761564
.01	.91372171557	.025240777143
.05	.85274628651	.13020125042
.10	.74360436406	.21320430557
.15	.67480093675282	.24234861164626
.20	.63120621598575	.23023864570417
.25	.60282728906963	.20264037260815
.30	.58491658821	.16939693499
.35	.57438769614	.13455531319
.40	.56967589511	.099924636095
.45	.56930353919	.066316584587
.46	.5696486522	.059749391713

**EIGENVALUES FROM STABILITY ANALYSIS FOR
REVERSED FLOW BOUNDARY LAYERS**

TABLE 1c

$\beta = -.002$

α	C_T	C_1
0	.9237409069	.0095488477066
.01	.92117830521	.010983058744
.05	.88971797	.091967207
.10	.78686024	.15214965
.15	.70466415	.20301679
.20	.64798726	.21161601
.25	.61069242	.19445403
.30	.58711391	.16596060
.35	.57311136	.13306074
.40	.56593472	.098968376
.45	.56371274	.065174535
.50	.56504181973	.032280308591
.55	.56865534872	.00023011047136
.56	.57775580181	.19174876005(10) ⁻¹⁰
.57	.58685371398	.61658214056(10) ⁻¹¹
.58	.58704040582	.34648626536(10) ⁻¹¹

EIGENVALUES FROM STABILITY ANALYSIS FOR
REVERSED FLOW BOUNDARY LAYERS

TABLE 1d

$$\beta = -.04$$

$\bar{\alpha}$	C_r	C_1
.12	.9462446953107	.00077598474441
.13	.94480294724055	.00092398603074
.14	.93834475353190	.0019712426475
.15	.92864533	.0041227836
.17	.91398636	.009481253
.20	.88234356	.031932225
.23	.78918067	.079558300
.25	.73325251	.10055163
.30	.63589654	.12879591
.35	.57744885	.12534423
.40	.54449017	.10193011
.42	.53642765	.089694409
.44	.53060095	.076599668
.46	.52663117	.062983805
.48	.52423199	.049089198
.50	.52306536	.035068680
.52	.52292271	.021022046
.54	.52356367	.0069847632
.55	.52416855	.34183573(10) ⁻⁶
.56	.53445687	.11840627(10) ⁻⁸

TABLE 1d (con't)

$$\beta = -.04$$

$\bar{\alpha}$	C_r	C_1
.57	.53445745	$.28132369(10)^{-9}$
.58	.53445776	$.10618506(10)^{-9}$
.59	.53445776	$-.16007328(10)^{-10}$
.60	.534457761505	$-.581878617(10)^{-10}$
.61	.53445776292	$-.75694864203(10)^{-10}$

EIGENVALUES FROM STABILITY ANALYSIS FOR
REVERSED FLOW BOUNDARY LAYERS

TABLE 1e

$\beta = -.08$

$\bar{\alpha}$	C_r	C_1
.20	.94462051904	.00060442053448
.22	.93168283195	.0023838799717
.25	.91152233835	.007171373662
.27	.89227578	.014429883
.30	.83585489	.036775313
.35	.68705498	.067058934
.40	.57949813	.076982790
.45	.51260920	.067262598
.47	.49694639	.057479918

EIGENVALUES FROM STABILITY ANALYSIS FOR
REVERSED FLOW BOUNDARY LAYERS

TABLE 1f

$\beta = -.12$

$\bar{\alpha}$	C_r	C_1
.28	.93771615513	.00057735106118
.30	.92267372951	.0025385188104
.32	.90428630103	.006241760255
.35	.86703422542955	.016184737774036
.37	.82518601942224	.025407066978775
.40	.74110563666309	.033621469860405
.42	.68545236670957	.034160709745084
.45	.60602465101	.029295418399
.47	.54979488217	.020797858572
.50	.47928620449	.17208372583(10) ⁻⁸
.51	.47900001254	.164119887(10) ⁻⁸
.52	.47900001195552	.2969542445(10) ⁻⁹

EIGENVALUES FROM STABILITY ANALYSIS FOR
REVERSED FLOW BOUNDARY LAYERS

TABLE 1g

$\beta = -.16$

$\bar{\alpha}$	C_r	C_i
.35	.92539848853	.00064674041646
.37	.90652445594	.0030732291515
.40	.87214263	.0087996030
.42	.839073304	.013608897
.45	.76943755	.016917978
.47	.71714018755	.014067976705
.50	.63945116	.0025996533
.52	.59255631588	-.0054550150066

EIGENVALUES FROM STABILITY ANALYSIS FOR
REVERSED FLOW BOUNDARY LAYERS

TABLE 1h

$$\beta = -.19884$$

α	C_r	C_1
.37	.92379057577	.00067331237442
.38	.91876397945	.00087323704317
.39	.91329400663	.001065562476
.40	.90688937	.0013915674
.42	.89032638669	.00295916137
.45	.85880806	.0055504066
.47	.83019514805718	.0066806913008495
.50	.77300900	.0043585794
.52	.7283639558	.48854083711(10) ⁻⁶
.53	.70401641	.28953714(10) ⁻⁷
.54	.70412941	-.19018251(10) ⁻⁷

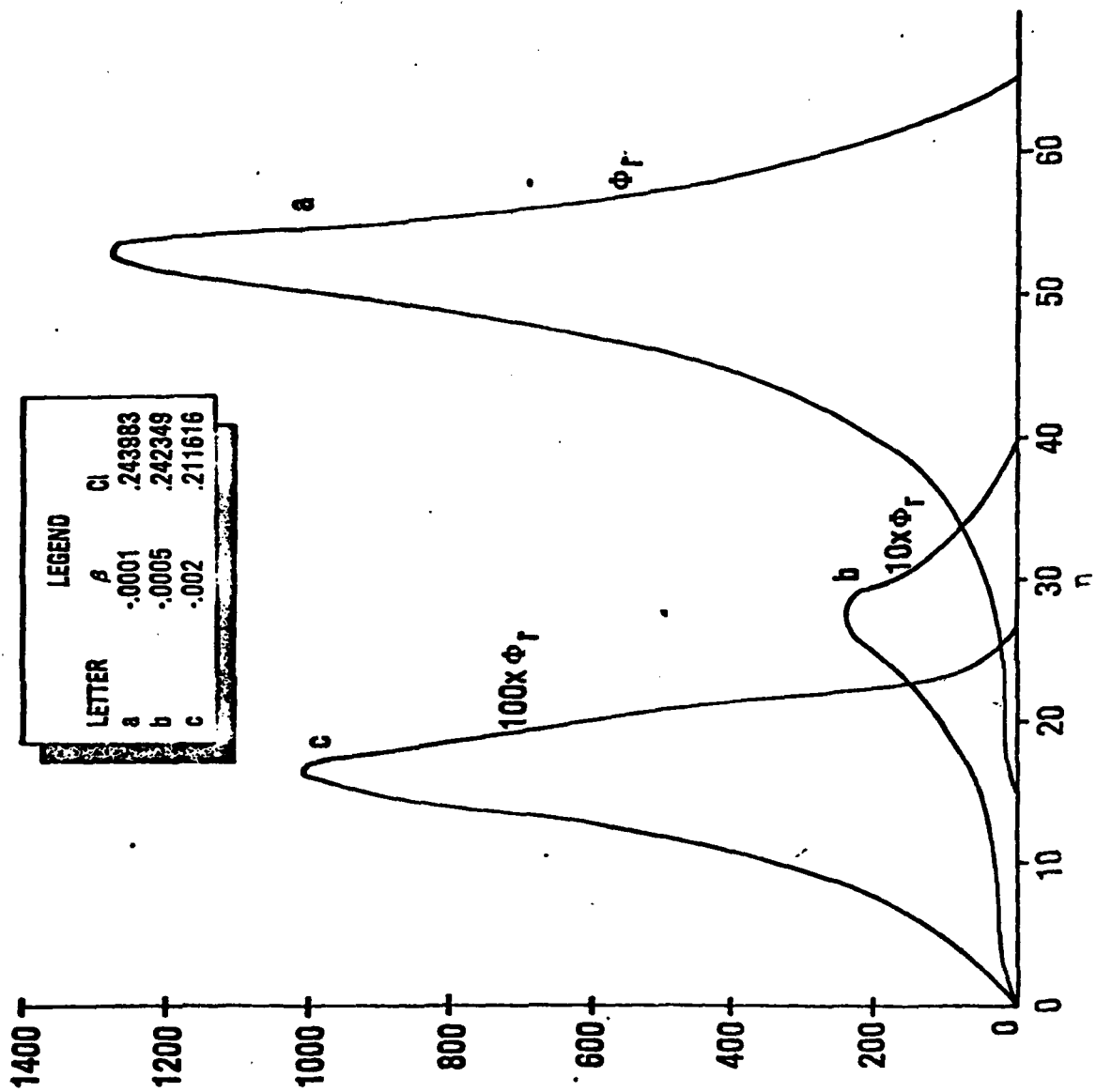


FIGURE 5a

LEGEND		
LETTER	δ	C_I
a	.0001	.243983
b	.0005	.242349
c	.002	.211616

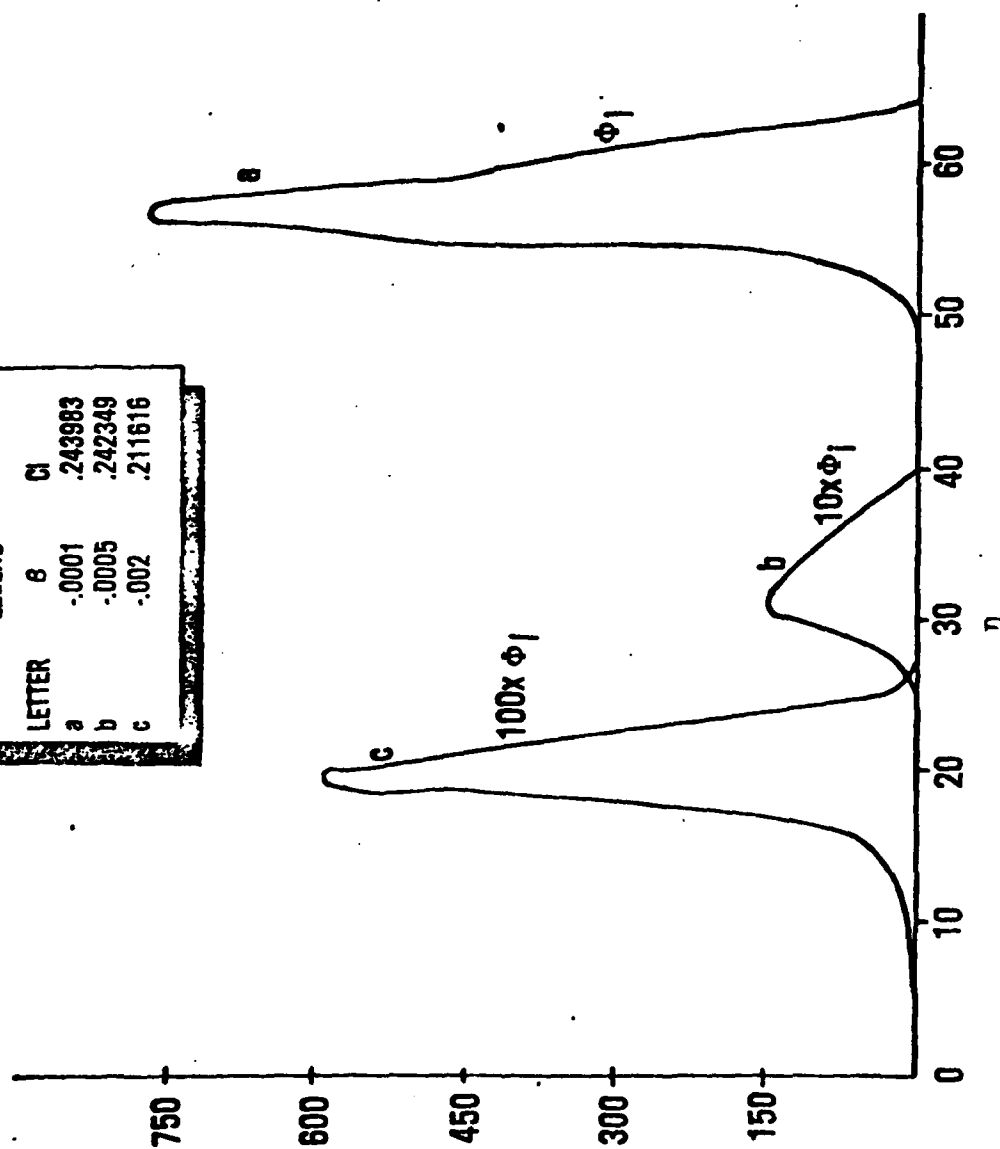


FIGURE 5b

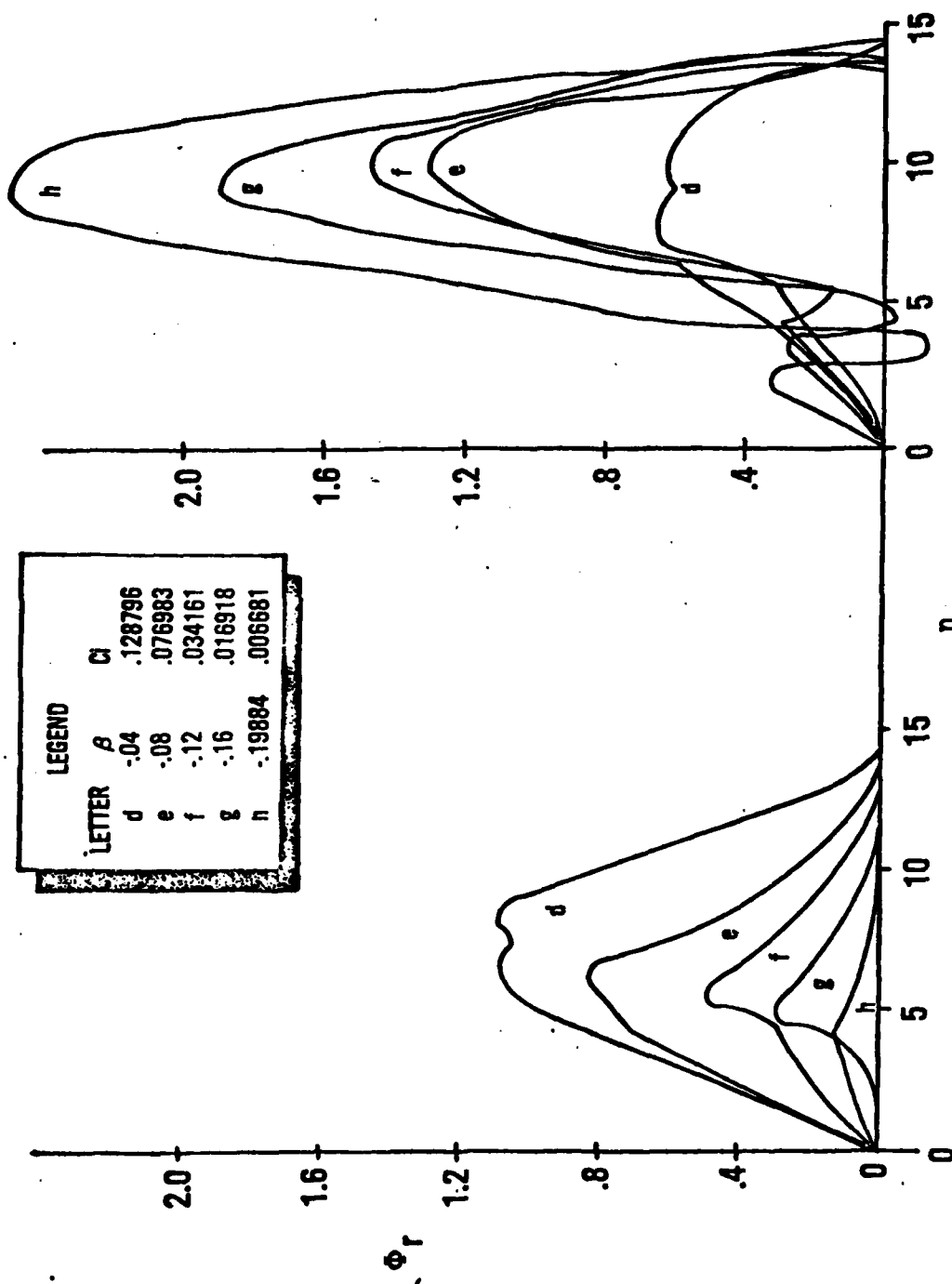


FIGURE 5c - d

APPENDIX 3

COMPUTER PROGRAM

The following FORTRAN program was used in the search for eigenvalues. The driver program FINDMIN gives the initial guesses for CREAL and CIM and then calls the minimization routine. The error is returned as SSQ. Subroutine MAINFCN does the integration using a system routine RKDF which uses a fourth order Runge-Kutta method. The arguments to RKDF are: X - the independent variable, Y - the dependent variables, N - the number of variables, DX - the step size, and IER - an error return. RKDF also requires a function F which computes the derivatives of the dependent variables and stores them in P.

The minimization routines are fairly general. The equivalence causes the minimization to be done with respect to CREAL and CIM. To minimize with respect to CIM and ALPHA the equivalence statement would be: "EQUIVALENCE (CIM, X(1)), (ALPHA, X(2))." Note that the two variables which are equivalenced with X(1) and X(2) must be stored consecutively in memory.

The array Y represents the following quantities. $Y(1) = f$, $Y(2) = f'$, $Y(3) = f''$, $Y(4) = \phi_R$, $Y(5) = \phi_I$, $Y(6) = \phi_R'$, $Y(7) = \phi_I'$. Convergence was generally achieved when minimization errors of 10^{-5} to 10^{-9} occurred for most cases.


```

C
C
C      PROGRAM FINDMIN(INPUT,OUTPUT,TAPE5=INPUT,TAPE2=OUTPUT)
C      COMMON CREAL,CIM,ALPHA,BETA,P3D
C      COMMON /92/SSQ
C      CREAL = .57194967522
C      CIM = .933942176531
C      ALPHA = .5
C      CALL MIN1
C      WRITE(2,1)ALPHA,BETA,CREAL,CIM,SSQ
C      1  FORMAT(50(2H*))/" ALPHA=",E14.6,5X,"BETA=",E14.6/" CREAL=",E14.8,5X
C      1X,"CIM=",E14.8,5X,"ERROR=",E14.5/50(2H*))
C      100  CONTINUE
C      END
C      SUBROUTINE MAINFCN
C      COMMON CREAL,CIM,ALPHA,BETA,P3D
C      COMMON /82/SSQ
C      DIMENSION Y(7),P(7)
C      BETA = -.0005
C      Y(3) = -.0051546
C      XEND = 40.
C      X = 00.0
C      Y(1) = 0.00
C      Y(2) = 0.0
C      Y(4) = 0.0
C      Y(5) = 0.0
C      CCBAR = CREAL*CREAL + CIM*CIM
C      BCC = BETA / CCBAR
C      FACT R = ALPHA*ALPHA + BCC*CREAL
C      R4 = FACTR*FACTR + BCC*BCC*CIM*CIM
C      R = SQRT(SQRT(R4))
C      GAMMA = 0.5*ATAN2(-BCC*CIM,FACT R)
C      Y(6) = R * COS(GAMMA)
C      Y(7) = R * SIN(GAMMA)
C      DX = 0.05
C      N = 7
C      CALL F(X,Y,P)
C      C*** *****INNER LOOP ***** INTEGRATION *****
C      2  CONTINUE
C      CALL RKDF(X,Y,N,DX,IER)
C      IF(X.LE.XEND) GO TO 2
C      C*** *****INNER LOOP ***** INTEGRATION *****
C      SSQ=Y(5)*Y(5)+Y(4)*Y(4)
C      RETURN
C      END
C      SUBROUTINE F(X,Y,P)
C      COMMON CREAL,CIM,ALPHA,BETA,P3D
C      DIMENSION Y(7),P(7)
C      P(1) = Y(2)
C      P(2) = Y(3)
C      P(3) = BETA*(Y(2) -1.)*(Y(2) + 1.) - Y(1)*Y(3)
C      P(4) = Y(6)
C      P(5) = Y(7)
C      U = Y(2)
C      UDB = P(3)
C      D = UDB/((U-CREAL)**2 + CIM**2)
C      B = D*CIM
C      A = ALPHA*ALPHA + D*(U-CREAL)
C      P(6) = A*Y(4) - 3*Y(5)
C      P(7) = B*Y(4) - A*Y(2)
C      RETURN
C      END
C      SUBROUTINE MIN1
C      COMMON CREAL,CIM,ALPHA,BETA,P3D

```

```

COMMON /B2/ SSQ
DIMENSION XEST(2,2),X(2),STEP(2)
EQUIVALENCE(CREAL,X(1)),(CIH,X(2))
STEP(1) = 1.E-10
STEP(2) = 1.E-4
ERSSQ=1.E-3
P3D=0.
2 CONTINUE
DY=STEP(1)
XEST(1,1)=X(1)
GRAD=1.E-30
C
C SEARCH ALONG X1-AXIS
C
CALL MIN2(X,DY,GRAD)
IF(SSQ.LT.ERSSQ)RETURN
XEST(1,2)=X(1)
STEP(1)=DY
XEST(2,1)=X(2)
DY=STEP(2)
GRAD=1.E+30
C
C SEARCH ALONG X2-AXIS
C
CALL MIN2(X,DY,GRAD)
IF(SSQ.LT.ERSSQ)RETURN
XEST(2,2)=X(2)
STEP(2)=DY
GRAD=(XEST(1,2)-XEST(1,1))/(XEST(2,2)-XEST(2,1))
C
C SEARCH ALONG LINE
C
CALL MIN2(X,DY,GRAD)
IF(SSQ.GT.ERSSQ)GOTO2
RETURN
END
SUBROUTINE MIN2(X,STEP,GRAD)
COMMON /B2/ SSQ
LOGICAL DIRP,DIRN
DIMENSION X(2),Y1(3),Y2(3),F(3)
ERSSQ=1.E-3
C
C FIND DIRECTION
C
WRITE(2,200)
200 FORMAT(11X,"FIND DIRECTION")
N=0
SGRAD=SIGN(1.,GRAD)
CALL MAINFCN
2 CONTINUE
DIRP=.FALSE.
DIRN=.FALSE.
X1STAR=X(1)
X2STAR=X(2)
F(1)=SSQ
Y1(1)=X(1)
Y2(1)=X(2)
WRITE(2,100) SSQ,X(1),X(2)
IF(SSQ.LT.ERSSQ)RETURN
100 FORMAT(10X,"ERR= ",E17.11,"GR= ",E17.11," CI= ",E17.11)
13 CONTINUE
C
C TRY POSITIVE INCREMENT
C
STEPX=STEP
OX=STEPX/SORT(1.+GRAD**2)

```

```

      X(1)=X1STAR+DX
      X(2)=X2STAR+SGRAD*SQRT(STEPX**2-DX**2)
      CALL MAINFCN
      F(2)=SSQ
      Y1(2)=X(1)
      Y2(2)=X(2)
      IF (F(2)-F(1)) 9,11,11
      9  CONTINUE
      C
      C  POSITIVE INCREMENT WORKED
      C
      DIRP=.TRUE.
      STEPX=2*STEP
      DX=STEPX/SQRT(1.+GRAD**2)
      X(1)=X1STAR+DX
      X(2)=X2STAR+SGRAD*SQRT(STEPX**2-DX**2)
      CALL MAINFCN
      F(3)=SSQ
      Y1(3)=X(1)
      Y2(3)=X(2)
      WRITE(2,100) SSQ,X(1),X(2)
      IF(SSQ.LT.ERSSQ) RETURN
      GOTO14
      11 CONTINUE
      C
      C  TRY NEGATIVE INCREMENT
      C
      STEPX=STEP
      DX=STEPX/SQRT(1.+GRAD**2)
      X(1)=X1STAR-DX
      X(2)=X2STAR-SGRAD*SQRT(STEPX**2-DX**2)
      CALL MAINFCN
      F(2)=SSQ
      Y1(2)=X(1)
      Y2(2)=X(2)
      WRITE(2,100) SSQ,X(1),X(2)
      IF(SSQ.LT.ERSSQ) RETURN
      IF (F(2)-F(1)) 10,12,12
      10 CONTINUE
      DIRN=.TRUE.
      C
      C  NEGATIVE INCREMENT WORKED
      C
      STEPX=2.*STEP
      DX=STEPX/SQRT(1.+GRAD**2)
      X(1)=X1STAR-DX
      X(2)=X2STAR-SGRAD*SQRT(STEPX**2-DX**2)
      CALL MAINFCN
      F(3)=SSQ
      Y1(3)=X(1)
      Y2(3)=X(2)
      WRITE(2,100) SSQ,X(1),X(2)
      IF(SSQ.LT.ERSSQ) RETURN
      GOTO14
      12 CONTINUE
      C
      C  NEITHER WORKED. HALVE STEP
      C
      STEP=STEP/2.
      GOTO13
      14 CONTINUE
      C
      C  DIRECTION FOUND
      C
      WRITE(2,201)
      201 FORMAT(10X,"BRACKET MINIMUM")

```

```

C      IF (DIRP) XSIGN=+1
C      IF (DIRN) XSIGN=-1
15     CONTINUE
C      IF (F(3)-F(2)) 16,17,17
16     CONTINUE
C      N=N+1
C      STEPX=N*STEP
C      DX=STEPX/SQRT(1.+GRAD**2)
C      X(1)=X(1)+XSIGN*DX
C      X(2)=X(2)+XSIGN*SGRAD*SQRT(STEPX**2-DX**2)
C      Y1(1)=Y1(2)
C      Y1(2)=Y1(3)
C      Y1(3)=X(1)
C      Y2(1)=Y2(2)
C      Y2(2)=Y2(3)
C      Y2(3)=X(2)
C      F(1)=F(2)
C      F(2)=F(3)
C      CALL MAINFCN
C      F(3)=SSQ
C      WRITE(2,100) SSQ,X(1),X(2)
C      IF(SSQ.LT.ERSSQ) RETURN
C      IF (F(3)-F(2)) 16,17,17
17     CONTINUE
C
C      MINIMUM BRACKETED
C
C      NOW FIT QUADRATIC
C
C      WRITE(2,202)
202    FORMAT(10X,"USE QUADRATIC APPROX FOR MINIMUM")
C      IF(ABS(GRAD).GT.0.5E+10) GOTO3
C      F1=Y1(1)-Y1(2)
C      F2=Y1(1)-Y1(3)
C      F3=Y1(2)-Y1(3)
C      BIT1=F(1)/F1/F2
C      BIT2=-F(2)/F1/F3
C      BIT3=F(3)/F2/F3
C      CIT1=Y1(1)*(BIT2+BIT3)
C      CIT2=Y1(2)*(BIT1+BIT3)
C      CIT3=Y1(3)*(BIT1+BIT2)
C      X(1)=(CIT1+CIT2+CIT3)/2./(BIT1+BIT2+BIT3)
C      IF(ABS(GRAD).LT.1.5E-10) GOTO4
3      CONTINUE
C      F1=Y2(1)-Y2(2)
C      F2=Y2(1)-Y2(3)
C      F3=Y2(2)-Y2(3)
C      BIT1=F(1)/F1/F2
C      BIT2=-F(2)/F1/F3
C      BIT3=F(3)/F2/F3
C      CIT1=Y2(1)*(BIT2+BIT3)
C      CIT2=Y2(2)*(BIT1+BIT3)
C      CIT3=Y2(3)*(BIT1+BIT2)
C      X(2)=(CIT1+CIT2+CIT3)/2./(BIT1+BIT2+BIT3)
4      CONTINUE
C      CALL MAINFCN
C      WRITE(2,100) SSQ,X(1),X(2)
C      IF(SSQ.LT.ERSSQ) RETURN
C      STEP=STEP/2.
1      CONTINUE
C      RETURN
C      END

```

1979 USAF - SCEEE SUMMER FACULTY RESEARCH PROGRAM

Sponsored by the

AIR FORCE OFFICE OF SCIENTIFIC RESEARCH

Conducted by the

SOUTHEASTERN CENTER FOR ELECTRICAL ENGINEERING EDUCATION

FINAL REPORT

INDUCTANCE MATRIX OF A PERMENENT MAGNET

ALTERNATOR

Prepared by:	Ta-hsien Wei
Academic Rank:	Assistant Professor
Department and University:	Electrical Engineering Department North Carolina A&T State University
Research Location:	AFAPL/POD Wright-Patterson Air Force Base Dayton, Ohio 45433
USAF Research Colleague:	Captain Frederick C. Brockhurst
Date:	August 6, 1979
Contract No:	F49620-79-C-0038

INDUCTANCE MATRIX OF A PERMANENT MAGNET ALTERNATOR

by

T. H. Wei

ABSTRACT

Different methods of getting the inductance matrix of an alternator are given. The inductance matrix is very important in the analysis and simulation of a pulsed power system. This report gives an approximate 6×6 inductance matrix for a permanent magnet alternator based on magnetic circuit analysis, which has traditionally been used for devices design. Each matrix element is an expression of machine geometry and construction materials. The inductance matrix can be implemented in a computer program, presumably with less memory space and shorter running time in comparison with the implementation of finite element method. Suggestions for further theoretical research in the inductance matrix are given.

ACKNOWLEDGEMENT

The author would like to thank the Air Force Systems Command, Air Force Office of Scientific Research, and the Southeastern Center for Electrical Engineering Education for providing him the opportunity to spend a most worthwhile summer at Wright-Patterson Air Force Base. Special acknowledgement is also due Dr. Richard N. Miller for a well-organized program.

He is grateful to Captain Frederick C. Brockhurst for suggesting the research topic. Numerous helpful discussions with Captain Brockhurst and Captain Hugh L. Southall are gratefully acknowledged.

I. INTRODUCTION:

The Air Force Aero Propulsion Laboratory (AFAPL) is presently developing a finite element computer analysis package¹ to improve the accuracy of the present alternator design computer programs. AFAPL is also developing a computer program to dynamically simulate the electrical characteristics of a complete pulsed power systems (pps). In a simulation program for pps or phase-controlled converters² a dynamical equivalent circuit of an alternator is needed and is not available at present. Finite element method applied to an alternator by minimizing a magnetic energy functional³ has been a new powerful numerical method since 1970 and now is being applied to find the dynamical equivalent circuit of an alternator.¹ This research is motivated to find a different algorithm based on magnetic circuit to establish the dynamical equivalent circuit of an alternator, so that the two results can be compared and improved. This approach has been used in device design⁴ for more than half a century. The magnetic circuit approach gives better physical insight and when implemented in computer program is likely to run faster than the finite element method. Towards the goal of a dynamical equivalent circuit this project restricts to a permanent magnet alternator⁵ and gets its inductance matrix with magnetic circuit saturation being considered.

An alternator can be represented⁶ by six windings as shown in Fig. 1. Three phase stator windings a, b, and c;

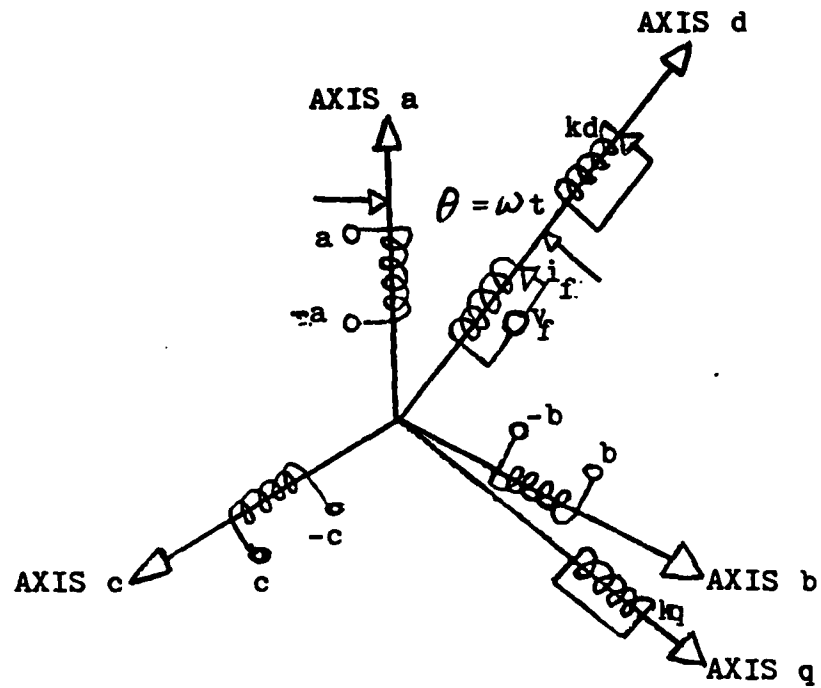


Figure 1
Schematic Representation of a Synchronous Machine

one rotor field winding f ; and two other rotor windings k_d , k_q which represent damping effects of the shield along the direct (k_d) and quadrature (k_q) axes, and which are permanently short-circuited. The field winding f represents permanent magnet. The vector equation of motion of the alternator has the form

$$v = R i + \frac{d}{dt}(M i) \quad (1)$$

Both v and i are 6×1 column matrix, R is 6×6 diagonal matrix, and M is the 6×6 inductance matrix being sought after. Each of the six equations corresponds to one of the six windings.

Using vector potential, of which only the axial component exists, the basic field equation in 2-dimensional cylindrical coordinates is

$$\frac{\partial^2 A}{\partial r^2} + \frac{1}{r} \frac{\partial A}{\partial r} + \frac{1}{r^2} \frac{\partial^2 A}{\partial \theta^2} = \mu \sigma \frac{\partial A}{\partial t} \quad (2)$$

μ = permeability, h/m

σ = conductivity, $1/\Omega m$

Considering ideal cylindrical geometry and neglecting damper windings White and Woodson⁷ found elements of M depending on μ , or saturation for sinusoidal current sheets distribution. Most recently⁸ equation (2) was solved for elements of M for round rotor and superconducting generator, again neglecting damper shield.

Garg derived M for utility synchronous machine,⁹ trans-

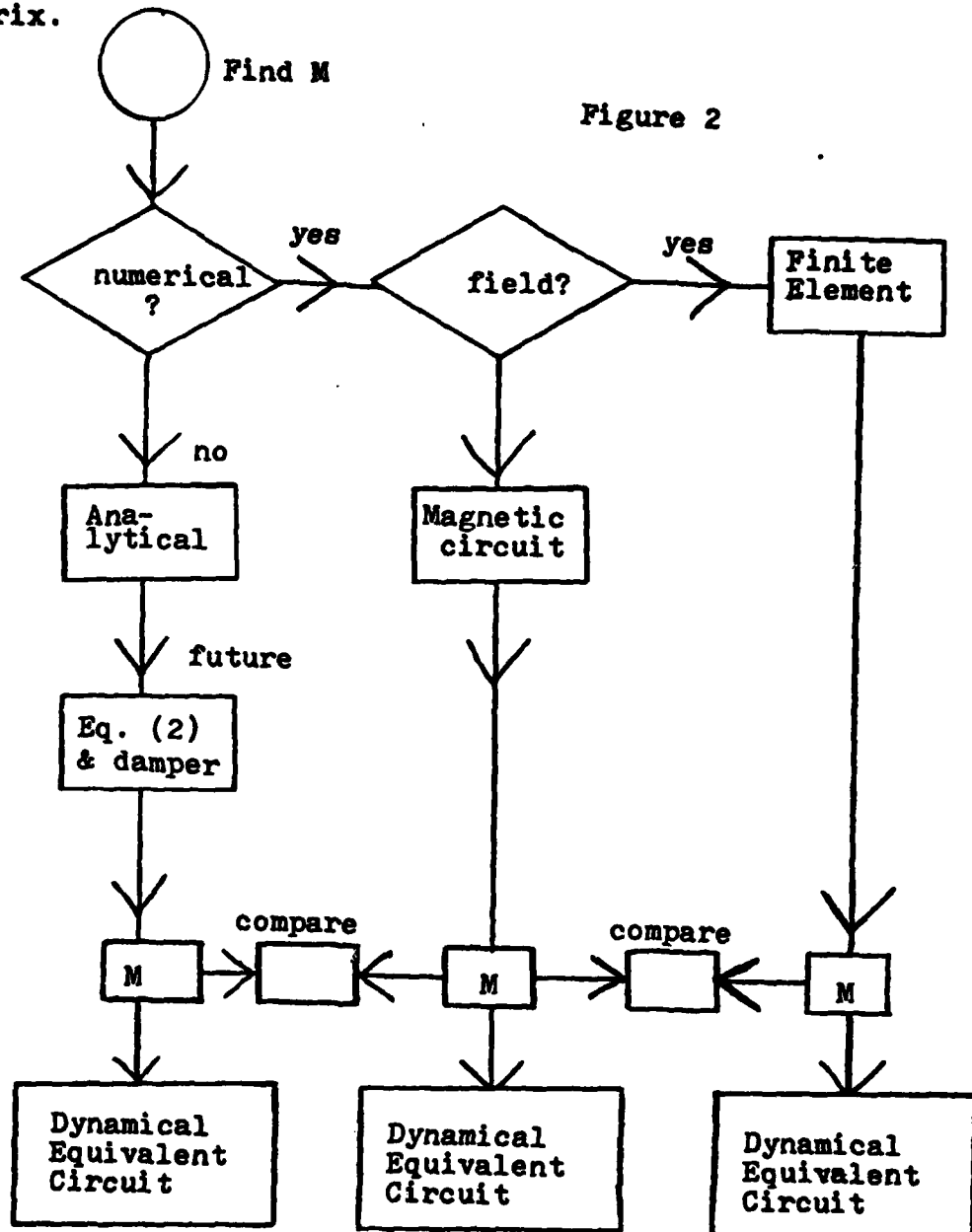
formed M into dqo representation, and analyzed a machine in terms of sampled dqo state variables. Since Park transformation¹⁰ is valid for linear machine, how much effect introduced by considering the non-linear magnetic saturation in the transformation is not clear.

A 3-dimensional cylindrical damper shield and the permanent magnetic excitation make the inductance matrix for a tangential permanent magnet alternator a new problem. The damper shield is rigidly on the rotor, whereas a similar electromagnetic shield of a superconducting generator can oscillate during severe faults. If oscillation of the shield is ignored, an ideal shield screens the fault stator armature magnetic field from being seen by the permanent magnet or the superconducting field coil. Under such assumption one can assume that the shields are equivalent although permanent magnet shield is iron-cored and the superconducting shield is air-cored. At present the self inductance of the electromagnetic shield of a superconducting generator has not been solved satisfactorily.¹¹ The calculations of self inductances and mutual inductances of armature and field for a superconducting generator are more reliable. One expects similar situation in the permanent magnet alternator.

In solving the inductance matrix it is assumed that the machine is symmetrical in 3-phases, the inductance matrix will be 3-phase symmetrical. In simulation in a case one phase is in conduction and the other two phases are open-circuited, the differential equation (1) is still valid by setting two

phase currents zero. In dealing directly with equation (1), corresponding to real situation, the linear Park transformation is not needed.

Fig. 2 shows different ways finding M , the inductance matrix.



II. OBJECTIVES:

The objectives of this project were:

(1) Using saturable magnetic circuit theory find the inductance matrix of a permanent magnet alternator in terms of design parameters or machine geometry and properties of machine materials.

(2) Implement the inductance matrix into computer program, so that the future simulation executive can call the complete pps and fine adjust machine parameters or system components.

(3) Compare the inductance matrices gotten by finite element method and magnetic circuit method so that one can fine tune both methods.

It turns out that this is a research and development program. In this summer only (1) is completed. (2) has been started. Since both finite element method and magnetic circuit method for inductance matrix are being developed, (3) is for 1980.

III. ASSUMPTIONS:

The following assumptions are made in the development of inductance expressions:

(1) Saturation in magnetic circuits is taken into account. Hysteresis and eddy currents in these circuits are ignored.

(2) Although superposition principle is true only

for linear machine, it is being used. Hence Park transformation is permissible.

(3) The flux densities and mmf are Fourier analyzed. Only fundamental quantities are considered.

(4) Leakage flux path for field and armature windings are defined when flux from one winding is not linking the other winding.

(5) Damper currents flow like currents in a damper cage.

(6) The permanent magnet operates near the neighborhood of maximum energy point¹² in the second quadrant of the B-H curve.

IV. SATURABLE MAGNETIC CIRCUIT¹³ AND INDUCTANCES¹⁴:

Figure 3 shows both a d-flux line and a q-flux line. The q-flux line is due to the armature current only. d-flux line is either due to the permanent magnet or due to the armature current. From Figure 3 one sees immediately that synchronous reactances satisfy $x_d < x_q$ because $R_d > R_q$.

R_d is the direct axis reluctance, R_q is the quadrature reluctance.

$$R_d = \frac{g_d}{\mu_0 A_d} + \frac{l_{ip}}{\mu_{ip} A_{ip}} + \frac{l_{is}}{\mu_{is} A_{is}} + \frac{l_{pm}}{\mu_0 A_{pm}}$$

R_q has similar expression. A is the cross section area, l is path length. ip stands for iron pole, is iron stator, pm permanent magnet.

All the magnetic properties of construction are in the

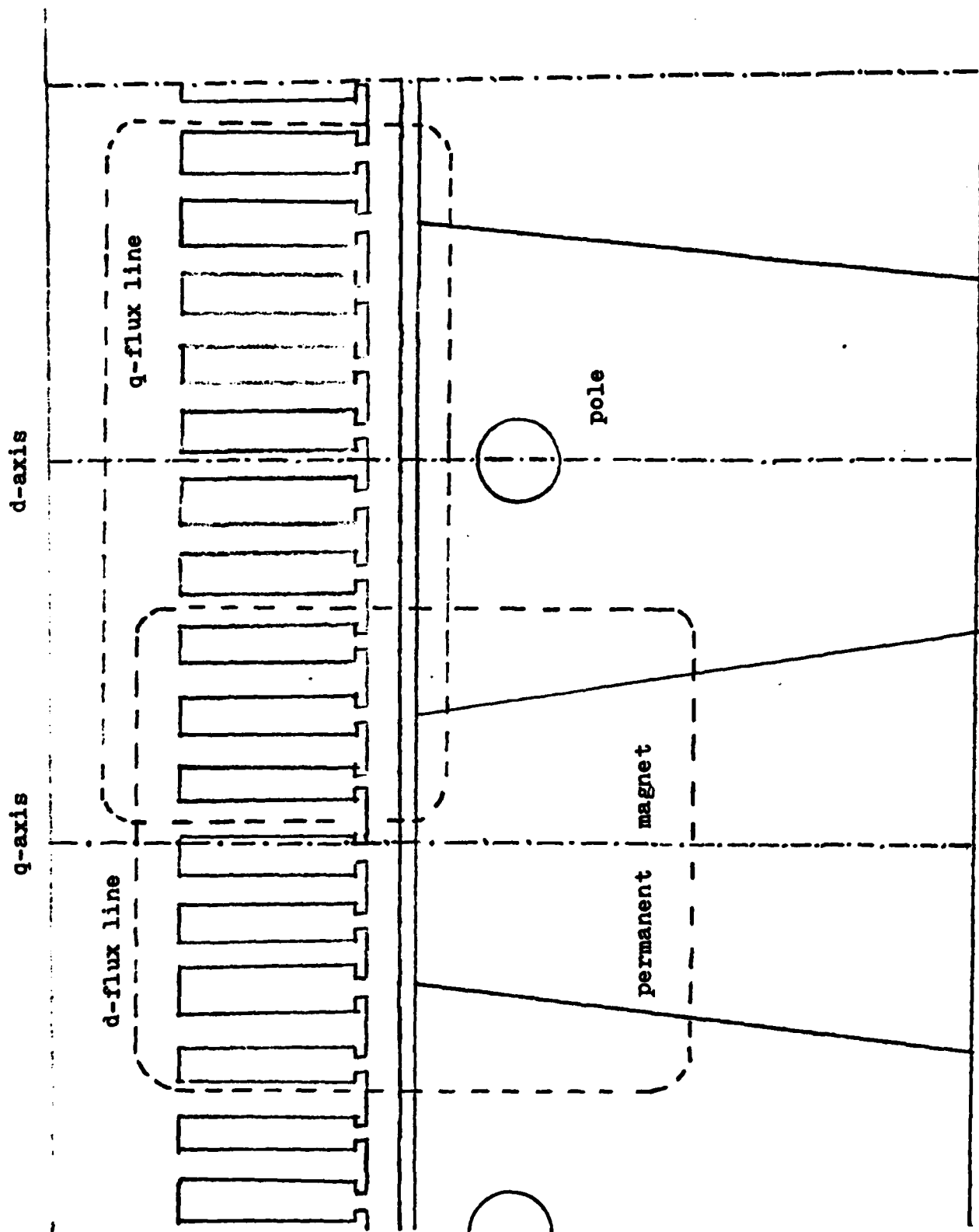


Figure 3

expressions for reluctances. Saturation of the magnetic circuit is being accounted for in the denominator of R_d and R_q by μ . It is essential to fit the B-H curves of stator and pole materials into curves with an accuracy of 5%. Some preliminary work is done in B-H curve fitting by piecewise curves.

The q-flux line is reasonably assumed. The accuracy of R_q depends on the path length and cross section in the permanent magnet and air gap. There is no ambiguity in R_d . The d-flux line crosses the air gap perpendicular to the pole and traverses the permanent magnet along its axis.

In general an inductance can be expressed in the form¹⁵

$$L_{ij} = M_{ij} = \frac{N_i N_j}{R_{ij}} \quad (3)$$

This form is arrived at in the following manner: First consider mmf $N_j I_j$ in coil j, take fundamental wave of Fourier series; project the fundamental mmf along d and q axes; R_d and R_q come into play when B_{id} and B_{iq} , the flux densities linking coil i are obtained; take fundamentals B_{mid} and B_{miq} because B_{id} and B_{iq} are not sinusoidal due to R_d and R_q ; combine these fundamentals vectorially into B_{mi} ; from B_{mi} get ψ_i ; from ψ_i get M_{ij} , the ijth element of M by dividing I_j . Recall that $L = \psi / I$.

V. KNOWN INDUCTANCE MATRIX ELEMENT:⁹

$M_{46} = M_{64} = 0$, $M_{56} = M_{65} = 0$. This is because coil kq is perpendicular to coils f and kd.

Applying the recipe described after equation (3), and adding the appropriate leakage inductance to equation (3) when $i = j$, the armature inductances have the form

$$M_{11} = L_{sa} + L_v \cos(2\omega t)$$

$$M_{22} = L_{sa} + L_v \cos(2\omega t + 2\pi/3)$$

$$M_{33} = L_{sa} + L_v \cos(2\omega t - 2\pi/3)$$

L_{sa} contains the armature leakage inductance per phase. L_{sa} , L_v and other L symbols in this section and next section are functions of machine geometry and construction materials.

By definition the mutual inductance has no leakage contribution. The armature mutual inductances are of the form.

$$M_{12} = M_{21} = L_{ma} + L_v \cos(2\omega t - 2\pi/3)$$

$$M_{23} = M_{32} = -L_{ma} + L_v \cos(2\omega t)$$

$$M_{31} = M_{13} = -L_{ma} + L_v \cos(2\omega t + 2\pi/3)$$

VI. NEW INDUCTANCE MATRIX ELEMENTS,⁹

The permanent magnet self inductance can be gotten by assuming that it has N_f number of turns, and a current I_f consistent with the maximum energy neighborhood. After the field inductance L_{ff} is reflected to the stator side, $N_f I_f$ disappears from L_{ff} . Then L_{ff} has to be corrected by the leakage inductance of the permanent magnet,

$$M_{44} = K_1 L_{ff}$$

K_1 is the leakage coefficient of the permanent magnet. The leakage flux contains end leakage, hub leakage and air gap leakage. It is estimated that K_1 ranges from 1.10 when more

than one small circular cooling holes are used to 1.24 when a big hexagonal cooling hole¹ is used.

The mutual inductances between the permanent magnet and the armature has the form

$$M_{14} = M_{41} = L_{af} \cos \omega t$$

$$M_{24} = M_{42} = L_{af} \cos(\omega t - 2\pi/3)$$

$$M_{34} = M_{43} = L_{af} \cos(\omega t + 2\pi/3)$$

Based on assumption (5), the mutual inductances between damper shield and armature have the form

$$M_{15} = M_{51} = L_{akd} \cos \omega t$$

$$M_{25} = M_{52} = L_{akd} \cos(\omega t - 2\pi/3)$$

$$M_{35} = M_{53} = L_{akd} \cos(\omega t + 2\pi/3)$$

$$M_{16} = M_{61} = L_{akq} \cos(\omega t + \pi/2)$$

$$M_{26} = M_{62} = L_{akq} \cos(\omega t + \pi/2 - 2\pi/3)$$

$$M_{36} = M_{63} = L_{akq} \cos(\omega t + \pi/2 + 2\pi/3)$$

The mutual inductances between damper and field are

$$M_{45} = M_{54} = L_{akd}$$

$$M_{46} = M_{64} = L_{akq}$$

Finally the inductances of kd and kq are obtained from damper shield constraint,¹⁶

$$M_{55} = \frac{L_{akd}^2}{L_{af}}$$

$$M_{66} = \frac{L_{akq}^2}{L_{af}}$$

VII. RECOMMENDATIONS:

Two recommendations A and B:

(A) Use analytic method to solve equation (2) for the ideal geometry with cylindrical damper included. Compare the results of inductance matrix from other two methods (see Fig. 2). At present the solution of a damper problem is not realistic. The assumption (5) that the currents flow like a cage damper is obviously not true.

The equation of motion (1) depends on the diagonal matrix R . The resistance of the damper not only includes the skin effect, but presumably includes the effect of higher current harmonics in the alternator. It seems to be an attractive problem to get damper resistance R_{kd} , R_{kq} analytically.

(B) The inductance matrix gotten by the magnetic circuit method can be implemented into a computer program. Implementation has two stages. First stage: (1) Write the computer program as a main program. (2) Fit the B-H curve. (3) Hold the permanent magnet at normal working point, change the μ , say at 8 points up to region of saturation, put in the dimension of the machine, get the inductance matrix elements in terms of a trigonometric and time function. (4) Fit the inductances into curves of polynomials in $\mu = \frac{B}{H}$. The nominal machine operating point is a natural check point. (5) Vary the permanent magnet operating point, repeat the process. (6) Compare results with finite element

program, change the magnetic circuit program to improve accuracy if necessary.

Second stage: (1) Integrate the inductance matrix program with the design program. (2) Integrate the inductance matrix program into the pps simulation package.

Establishing the inductance matrix by the alternative method of magnetic circuit other than the more accurate method of finite element approach would give better physical insight. With the flux plot from finite element method as guidance the magnetic circuit method is expected to have good accuracy. The speed of the computer program based on magnetic circuit is likely faster than that from the finite element method. The author is making a proposal for mini grant to carry out part of the recommendation (B), namely implementing the inductance matrix only.

REFERENCES

1. N. A. Demerdash, T. W. Nehl and F. A. Fouad, "Finite Element Analysis of Non-linear Electromagnetic Devices", VPI and S.U., Electrical Engineering, Blacksburg, Va. 24061, Nov. 1978
2. B. R. Pelly, "Thyristor Phase-Controlled Converters and Cycloconverters", Wiley-Interscience, New York, 1971
3. J. R. Brauer, "Saturated Magnetic Energy Functional for Finite Element Analysis of Electric Machines", Paper C75-151-6, IEEE Winter Power Meeting, Jan. 1975
4. H. Roters, "Electromagnetic Devices", John Wiley & Sons, Inc., New York, 1944
5. "User Manual for BIGMAG Computer Program", Prepared for US AF Air Force Systems Command, Wright-Patterson AFB, Ohio 45433, Garrett Research Manufacturing Co. of California, March, 1978
6. C. Concordia, "Synchronous Machines", John Wiley & Sons, Inc., New York, 1951
7. D. C. White and H. H. Woodson, "Electromechanical Energy Conversion", John Wiley & Sons, Inc., New York, 1959
8. A. Hughes, T. J. E. Miller, "Analysis of Fields and Inductances in Air-cored and Iron-cored Synchronous Machines", Proc. IEE, Vol. 124, pp. 121-126, 1977
9. V. Garg, "A Model of Saturated Synchronous Machines for Dynamic Analysis and Control Purposes", Ph.D. Thesis, VPI. and S.U., Blacksburg, Va., 1975
10. R. H. Park, "Two Reaction Theory of Synchronous Machines: Generalized Method of Analysis-Pt. I", Trans. of AIEE, Vol. 48, pp. 716-736, 1929
11. "Superconducting Generator Design", Vol. 2, Prepared for EPRI, General Electric Co., Schenectady, N. Y., March, 1978
12. M. McCaig, "Permanent Magnets in Theory and Practices", John Wiley & Sons, New York, 1977
13. A. E. Fitzgerald, C. Kingsley, Jr., A. Kusko, "Electric Machinery", Third Ed., McGraw-Hill, New York, 1971
14. E. W. Kimbark, "Power System Stability: Synchronous Machines", Dover, New York, 1968
15. P. W. Franklin, "The Inductance Matrix of the Three Phase Salient Pole and Turbo Type Synchronous Machine", A75-405-1, IEEE PES Summer Meeting, San Francisco, Calif., July, 1975
16. D. L. Luck, "Electromechanical and Thermal Effects of Faults upon Superconducting Generator", MIT Thesis, Cambridge, Mass., 1971

1979 USAF - SCEEE SUMMER FACULTY RESEARCH PROGRAM

Sponsored by the

AIR FORCE OFFICE OF SCIENTIFIC RESEARCH

Conducted by the

SOUTHEASTERN CENTER FOR ELECTRICAL ENGINEERING EDUCATION

FINAL REPORT

Analysis for Coherent Anti-Stokes Raman Spectroscopy (CARS)

Prepared by:	Herschel Weil
Academic Rank:	Professor
Department and University:	Electrical and Computer Engineering, University of Michigan
Research Location:	AFAPL/POE-3
USAF Research Colleague:	Paul W. Schreiber
Date:	28 August 1979
Contract No:	F49620-79-C-0038

Analysis for Coherent Anti-Stokes Raman Spectroscopy (CARS)

by

Herschel Weil

ABSTRACT

Equations have been formulated to describe the generation of CARS spectra under physical assumptions corresponding to experimental work being conducted at AFAPL to develop CARS as a diagnostic tool for the evaluation of combustion processes. A number of physical effects including competing scattering processes have been included to improve the quantitative linkage between the directly measurable spectral parameters and the quantities of primary interest, namely molecular concentrations and temperatures. The resulting equations are a set of coupled nonlinear differential equations. These have been solved numerically for one set of conditions to study saturation effects for the CARS intensity due to depletion of the vibrational ground state population by a strong pump wave.

ACKNOWLEDGEMENT

The author would like to thank the USAF-SCEEE Summer Faculty Research Program for the opportunity to do this research.

He is particularly grateful to Mr. Paul W. Schreiber who is the originator and project monitor for the AFAPL program on CARS spectroscopy for introducing him to the subject and his continuing helpful discussions and guidance.

He is also grateful to Dr. Won Roh of AFIT who had been collaborating with Mr. Schreiber for providing his notes and a preliminary computing program for a first try at generating the type of analytic-numerical results presented herein.

I. INTRODUCTION:

Coherent anti-Stokes Raman Spectroscopy is a form of Raman spectroscopy which has developed with the advent of laser light. In it the medium -usually gas or liquid- is irradiated by two waves, the pump and Stokes waves whose frequency difference matches a vibrational frequency characteristic of the molecule. The result is coherent generation of a new wave at the anti-Stokes frequency associated with the vibrational frequency. For collinearly phase-matched beams the intensity or power per unit area, I_a , in the new wave is roughly proportional to the pump intensity, I_p , squared times the Stokes intensity, I_s , and also is proportional to the square of the distance over which the phase matched interaction occurs. Thus a very intense anti-Stokes output can be generated, orders of magnitude greater than spontaneous Raman scattering. Furthermore, unlike spontaneous Raman scattering, it is directional so that all the anti-Stokes radiation can be readily collected. Because of these two properties as well as others the generation of CARS spectra offers a potentially very practical tool for the measurement of molecular species concentrations and temperature in gases, in particular combustion gases. These commonly contain many particulates which can scatter incident radiation and also radiate due to laser heating so strongly they cause relatively weak spontaneous Raman radiation to be lost in the particle generated "noise" while the far stronger CARS scattering would not be. Even with no particles in the gas ordinary spontaneous Raman scattering is in fact much weaker than the Rayleigh scattering which arises from the gas molecules and there is also interference due to fluorescent radiation. Because of these considerations AFAPL is actively laying the ground work for the use of CARS as an eventually routine diagnostic tool for combustion systems.^{1,2,3}

The connection between measured CARS spectra for gases and the desired quantities; molecular species concentrations and temperature must be made on the basis of theory taking into account both the particular experimental set-up as well as quantum mechanical or quasi-classical theory of modification of the internal molecular structure of the constituent molecules by the applied and internally generated electromagnetic fields. The experimental

designs and data interpretations have been based on theory which has been strictly limited to the most essential physical factors which explain CARS. In this way a convenient analytical formula for the CARS intensity was obtained which gives the proportionalities discussed above. While the formula has clearly been of great value in a general understanding of CARS it is inadequate for the accurate quantitative prediction of the CARS spectra under certain conditions. In particular it is quite inadequate to predict saturation effects which occur as I_p is increased. Furthermore, the CARS spectrum as a whole, taking into account relative line strengths, is what is needed for temperature determination and this too requires a more complete theory. Among the physical factors which are omitted in obtaining the analytic formula for CARS intensity are the following:

- (a) Decrease in pump and Stokes intensities as the waves propagate through the gas.
- (b) Time variation of the population of the vibrational levels.
- (c) Coupling between vibrational levels through populations interchanges and non-resonant contributions to the wave fields.
- (d) Scattering processes which occur simultaneously with CARS; i.e, stimulated Stokes, anti-Stokes and inverse Raman or pump; coherent Stokes and pump and coherent secondary Stokes (CSSRS).
- (e) Laser pulse shape (deviation from rectangular shape)

As soon as factors such as these are accounted for the mechanical model consists of three or more non-linear coupled partial differential equations which can be solved only by numerical techniques.

II. OBJECTIVES OF THE RESEARCH EFFORT:

The overall objective was to study the effects on CARS spectra of physical factors such as (a) through (d) listed in the INTRODUCTION.

When the author began his summer stay at AFAPL this work had in fact been initiated by Dr Roh and Mr. Schreiber, then put aside because Dr. Roh had to concentrate his efforts elsewhere. Dr. Roh had in fact derived and programmed equations governing CARS and most of the processes listed in (d) and including effect (a). Dr. Roh had a working program for the solution of this set of equations. He had also formulated but not programmed an approach to handling (b) for one vibrational level plus ground state. Effects (c) and (e) were not included nor were rotational effects. Thus the specific objectives were to

- (1) First modify the existing program to take into account effect (b) and use it to study, as a function of various parameters, CARS saturation effects which occur when ground level population depletion makes the difference in population between one vibrational and ground level tend toward zero.
- (2) Determine what further physical effects of interest could easily be incorporated into the code and incorporate them.

This led to incorporating (e) and studying numerically the effect of a pulse shape which was a Gaussian times a rectangle function. Also Raman scattering, which had been neglected, was taken into account.

- (3) Determine what additional effects would likely be most important in determining the CARS line strengths and shapes without the constraint that they could be simply incorporated into the existing code. Write out the appropriate equation set. If time remains program these and obtain numerical results for study.

This led to formulation of the equations taking into account all effects (a) through (e) for two vibrational levels plus ground state and taking account of the rotational levels in an approximate way. There was no time remaining for programming these equations.

III. PHYSICAL BASIS FOR CARS

To describe the generation of CARS spectra we consider the vibrational energy level diagram, Fig 1.

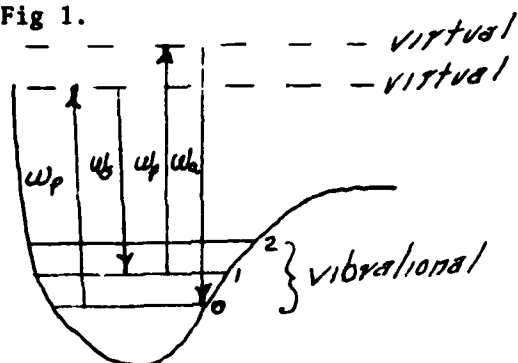


Figure 1: CARS

showing the ground state and two higher levels for a diatomic molecule. When a gas of such molecules is pumped by intense laser radiation of circular frequency ω_p , the set of simultaneous coherent photon-molecule interactions illustrated in Fig. 1 can be set-up; loss of two pump photons, scattering of a photon at ω_s , the Stokes frequency and at ω_a , the anti-Stokes frequency. This process occurs when the gas is also irradiated by an external source at the Stokes frequency. The process is maximized when the vectors satisfy the condition $2\vec{k}_p - \vec{k}_s = \vec{k}_a$. For gases this condition is almost satisfied when the vectors lie in a straight line. In the CARS experimental systems at AFAPL, the gas is irradiated by collinear pump and Stokes laser beams of the same polarization. These are focussed into a small region in the gas so as to obtain a high resolution as well as a high intensity. In the focal region the beams "neck down" to a short cylindrical region in which they may be considered to have plane phase fronts.

Along with CARS there are other coherent Raman processes which take place; inverse CARS and coherent secondary Stokes Raman (leading to CSSRS spectroscopy) and its inverse. These are illustrated by the diagram in Fig 2 where it is seen that the CSSRS frequency $\omega_c = 2\omega_s - \omega_p = \omega_p - 2\omega_s$. There are also stimulated emissions which occur independantly of one another and do not combine coherently as in CARS. These are shown in Fig 3.

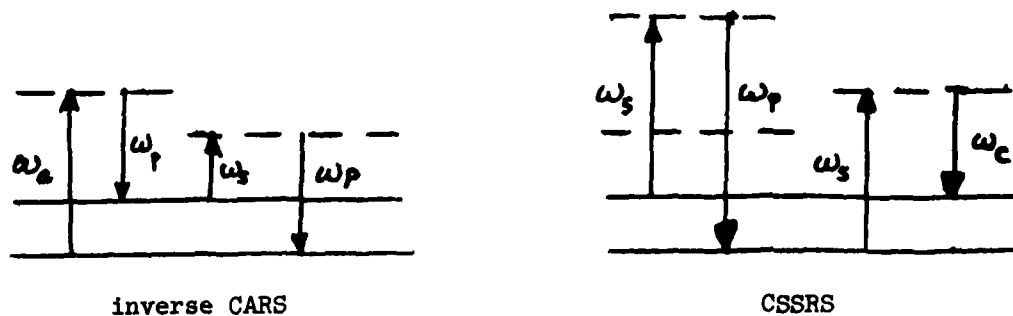


Figure 2: COHERENT RAMAN PROCESSES

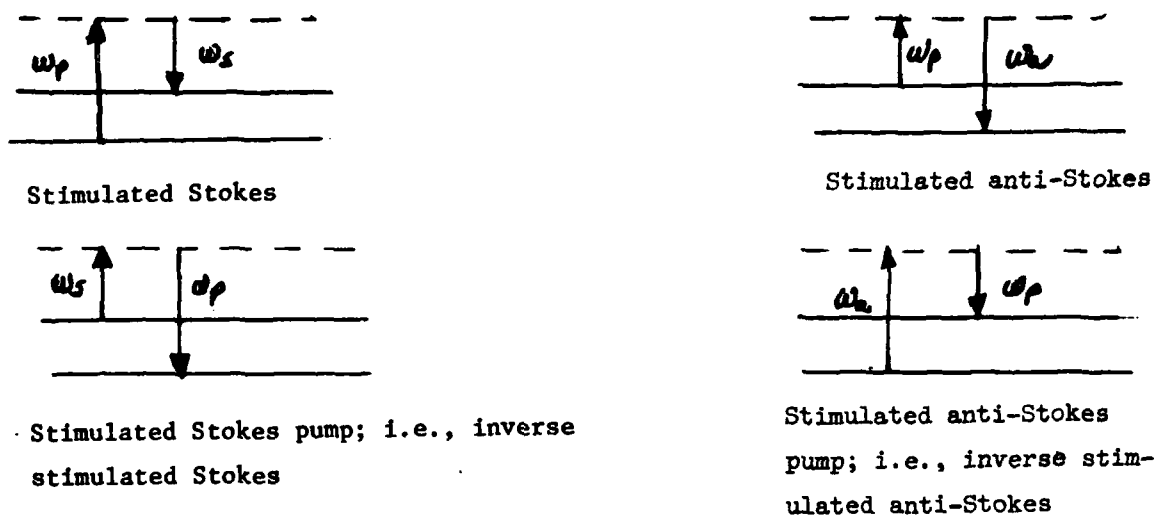


Figure 3: STIMULATED RAMAN SCATTERING

These processes are all induced by the third order electric field dependant -hence non-linear- term in the susceptibility of the gas. In this point of view the induced molecular polarization may be written as

$$\underline{P}(t) = \underline{P}^{(1)}(t) + \underline{P}^{(3)}(t)$$

or in terms of the electric field \underline{E} and susceptibility tensors, $\chi^{(1)}, \chi^{(3)}$ (1)

$$P_i(t) = \chi_i^{(1)} E_i(t) + \chi_{\alpha\beta\gamma}^{(3)} E_\alpha E_\beta E_\gamma$$

The vector \underline{E} in the AFAPL experiment may be considered to be made of the sum of pump, Stokes and anti-Stokes components all with the same direction of propagation and same linear wave polarization.

If more energy levels or more processes such as CSSRS are considered additional wave components at the appropriate frequencies will also contribute. The Stokes component may include not only the strictly Stokes frequency $\omega_s = 2\omega_p - \omega_j$ of the internally generated radiation but a frequency band centered at ω_s and corresponding to the frequency band of the incident Stokes laser radiation.

For the present we ignore the last complication and assume pulsed quasimonochromatic waves.

$$E(x, t) = E_p(x, t) \exp(i\omega_p t - i k_p x) + E_s(x, t) \exp(i\omega_s t - i k_s x) + E_a(x, t) \exp(i\omega_a t - i k_a x) + c.c. \quad (2)$$

within the laser pulse duration. In Eq. 2 $E_p(x, t)$, $E_s(x, t)$ and $E_a(x, t)$ are considered to be slowly varying function of both x and t relative to the oscillatory exponentials and c.c. stands for complex conjugate. We will also use the notation $f^*(t)$ to represent the complex conjugate of any function $f(t)$.

The polarization given by (1) is induced by vibrational displacement q forced by the field $E(t)$. The forcing function is proportional to E^2 and $P^{(3)}$ is proportional to qE , namely

$$P_j^{(3)} = N_j \frac{c^4}{\omega_s^4} \frac{2m\omega_j'}{\hbar} \left[\frac{d\sigma}{d\Omega} \right]_j qE \quad (3)$$

where m is the reduced mass, $\left[\frac{d\sigma}{d\Omega} \right]_j$ the Raman scattering cross-section, ω_j' is the vibrational frequency for the j 'th level, N_j is the population density of the j 'th level relative to that of the zero'th level, c the velocity of light in vacuo and \hbar is Planck's constant/ 2π .

The equation governing the forced vibrations associated with the j 'th energy level is

$$\frac{\partial^2 q}{\partial t^2} + \Gamma_j \frac{\partial q}{\partial t} + \omega_j'^2 q = \frac{1}{2m} \left[\frac{c^4}{\omega_s^4} \frac{2m\omega_j'}{\hbar} \left[\frac{d\sigma}{d\Omega} \right]_j \right]^{\frac{1}{2}} E^2 \quad (4)$$

The solution of this equation is to be substituted into (3) to obtain $P^{(3)}$.

To express the result concisely let E_j and ω_j represent any one of the quantities $E_p, E_s, E_a, E_p^*, E_s^*, E_a^*$ and the associated frequencies $\omega_p, \omega_s, \omega_a, -\omega_p, -\omega_s$ and $-\omega_a$ respectively. Then $P^{(3)}$ for the energy level j is.

$$P_j^{(3)} = \frac{N_j E}{2m} \left[\frac{e^4}{\omega_j^4} \frac{2m\omega_j}{\hbar} \left[\frac{d\sigma}{d\Omega} \right]_j \right] \sum_{\alpha, \beta} \frac{E_\alpha E_\beta \exp[-i(k_\alpha + k_\beta)x + i(\omega_\alpha + \omega_\beta)t]}{\omega_j^2 - (\omega_\alpha + \omega_\beta)^2 + i(\omega_\alpha + \omega_\beta)\Gamma} \quad (5)$$

When more than one vibration level is taken into account not only must the index j be summed over but, for each vibrational level, one must include in E contributions from the Stokes and anti-Stokes lines due to that level.

Examination of (5) shows that the dominant terms in the sums will correspond to the resonant terms, those for which $\omega_j^2 = (\omega_\alpha + \omega_\beta)^2$ while the next largest terms will be those for which $\omega_j^2 = (\omega_\alpha + \omega_\beta)^2 / \dots$.

The electric fields are all solutions of the inhomogeneous wave equation

$$\frac{\partial^2 E}{\partial x^2} - \frac{n^2}{c^2} \frac{\partial^2 E}{\partial t^2} = \frac{4\pi}{c^2} \frac{\partial^2}{\partial t^2} P^{(3)}(x, t) \quad (6)$$

where the refractive index "n" arises because of the linear polarization term $P^{(1)}$.

When (5) is substituted into (6) the result is a set of ordinary differential equations for the E_α coupled with each other by the differentiated $P^{(3)}$ term.

The term

$$\frac{\partial^2 E_\alpha \exp(i\omega_\alpha t - i k_\alpha x)}{\partial x^2} = \frac{\partial^2 E_\alpha}{\partial x^2} - 2i k_\alpha \frac{\partial E_\alpha}{\partial x} - k_\alpha^2 E_\alpha \quad (7)$$

In accord with the slowly varying assumption of $E_\alpha(x, t)$ in past work and most of the present work, the term $\frac{\partial^2 E_\alpha}{\partial x^2}$ has been neglected in comparison with $2k_\alpha \frac{\partial E_\alpha}{\partial x}$. In fact this assumption is not necessarily true for the

anti-Stokes wave at the boundary of the gas (if the boundary is taken as sharply defined, as by an enclosure) and unless care is taken in the problem formulation one experiences difficulty in starting the integration of the full equations at the boundary.* This difficulty is avoided, the number of integrations halved and the computations greatly speeded up by dropping the second derivative term. Numerical comparison of results obtained with and without the second derivative term showed that, except for the field very close to the boundary, little relative numerical error is made by this simplification.

With the second derivatives dropped the set of equations which results for a system in which two vibrational levels plus ground state are considered is as follows.

$$K'_j = -i \left(\frac{4\pi c^4}{h} \right) (N_j - N_{j-1}) \left(\frac{d\sigma}{d\Omega} \right)_j, \quad j=1, 2$$

$$D_k(\pm\omega_p, \omega) = \omega_{sj}^{-4} (\omega_k \mp \omega_p + \omega + i\Gamma_k/2)^{-1} \quad (8)$$

$$k=1, 2$$

$$\frac{\partial E_{aj}}{\partial x} = k_{aj} K_j \left\{ [D_1(\omega_p - \omega_{sj}) + D_2(\omega_p - \omega_{sj})] E_{sj}^* E_p^2 e^{i\Delta k_j x} \right. \\ \left. + 2 [D_1(-\omega_p, \omega_a) + D_2(-\omega_p, \omega_a)] |E_p|^2 E_{aj} \right\} \quad (9)$$

$$\text{where } \Delta k_j = 2k_p - k_s - k_{aj}$$

* For the analytic approximate CARS term $\text{Re}(\frac{\partial^2 E_x}{\partial x^2}) / \text{Re}(k_x \frac{\partial E_x}{\partial x})$ is proportional to $(A' \Delta k_x - A'')^{-1}$ for small x where $A' = \text{Re}(E_p^2 E_s)$, $A'' = \text{Im}(E_p^2 E_s)$. If the phase of either the incident pump or Stokes wave is zero the approximate solution's second derivative is in fact singular and the true solution almost certainly has a non-negligible second derivative. The incident waves phase however does not however affect the magnitude of the generated CARS. One would not expect it to, and we have verified by numerical example that it does not.

$$\frac{\partial E_{sj}}{\partial x} = \hbar_{sj} K_j \left\{ 2 [D_1^*(\omega_p, -\omega_{sj}) + D_2^*(\omega_p, -\omega_{sj})] |E_p|^2 E_{sj} + [D_1^*(-\omega_p, \omega_{sj}) + D_2^*(-\omega_p, \omega_{sj})] E_p^2 E_{sj}^* e^{i\Delta k_j x} \right\} \quad (10)$$

$$\frac{\partial E_p}{\partial x} = 2 \hbar_p \sum_{j=1}^2 K_j \left\{ [D_1(\omega_p, -\omega_{sj}) + D_2(\omega_p, -\omega_{sj})] |E_{sj}|^2 E_p + [D_1^*(-\omega_p, \omega_{sj}) + D_2^*(-\omega_p, \omega_{sj})] |E_{sj}|^2 E_p + [D_1^*(\omega_p, -\omega_{sj}) + D_2^*(\omega_p, -\omega_{sj})] E_s E_a E_p^* e^{-i\Delta k_j x} \right\} \quad (11)$$

In these equations we must bear in mind that the N_j are variable in time because of a combination of stimulated Raman scattering induced population changes at each energy level plus thermal relaxation. The two Raman processes are indicated in Fig (4). Where they

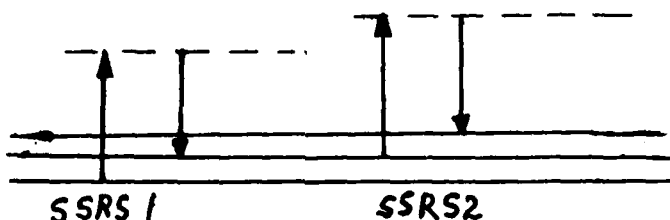


Figure 4: STIMULATED RAMAN PROCESSES AND ENERGY LEVEL POPULATIONS

are labelled SSRS1 and SSRS2. To derive the equations governing the time variability of the N_j one considers the Stokes photon densities in the two Stokes beams which irradiate the gas sample; Entering the sample these are n_{sj} and leaving they are $n_s + \frac{\partial n_s}{\partial x} dx$. Finally we introduce relaxation times denoted by subscripted τ 's such as τ_2 , which represents the rate of decay from N_2 to the equilibrium value N_{20} for level 2 due to thermal decay from energy level 2 to energy level 1. Appropriate equilibrium values are determined by Maxwellian distributions. With some further approximation (assuming no vibrational rotation interaction and much

more rapid equilibration of rotational levels than vibrational levels) the effect of the rotational levels can be taken account by determining suitable mean equilibrium levels.

In any case the general set of equations becomes

$$I_{sj} \equiv \frac{c}{2\pi} E_{sj} E_{sj}^* = m_{sj} \hbar \omega_{sj} \quad (12)$$

so that

$$\frac{\partial m_{sj}}{\partial x} = \frac{c}{2\pi \hbar \omega_{sj}} \left(E_{sj} \frac{\partial E_{sj}^*}{\partial x} + E_{sj}^* \frac{\partial E_{sj}}{\partial x} \right) \quad (13)$$

where the electric field derivatives are given by (10). With the help of Fig (4) we have

$$\frac{dN_1}{dt} = \left. \frac{dN_1}{dt} \right]_{SSRS} - \frac{N_2 - N_{20}}{\tau_{21}} - \frac{N_1 - N_{10}}{\tau_{10}} \quad (14)$$

where the contribution due to the level one stimulated Stokes Raman scattering term $\left. \frac{dN_1}{dt} \right]_{SSRS}$ is related to the intensities by (13) and

$$\left. \frac{dN_1}{dt} \right]_{SSRS} = c \left(\frac{\partial m_{s1}}{\partial x} - \frac{\partial m_{s2}}{\partial x} \right) \quad (15)$$

Similarly

$$\frac{dN_2}{dt} = \left. \frac{dN_2}{dt} \right]_{SSRS} - \frac{N_2 - N_{20}}{\tau_{210}}, \quad \left. \frac{dN_2}{dt} \right]_{SSRS} = c \frac{\partial m_{s2}}{\partial x} \quad (16)$$

$$\frac{dN_0}{dt} = \left. \frac{dN_0}{dt} \right]_{SSRS} + \frac{N_2 - N_{20}}{\tau_{20}} + \frac{N_1 - N_{10}}{\tau_{10}} \quad (17)$$

$$\left. \frac{dN_0}{dt} \right]_{SSRS} = -c \frac{\partial m_{s1}}{\partial x} \quad (18)$$

$$\frac{d}{dt} (N_0 + N_1 + N_2) = 0. \quad (19)$$

IV Computations

Our numerical work to date has been confined to the case of one level plus ground level only. The numerical procedure was based on the fact that time of propagation of an e-m wave through the sample (\sim sample dimension/c) is much smaller than the time over which there is an appreciable change in the vibration level populations. The equations for E_a were solved at the initial time $t=0$ with $N_0 - N_1$ fixed at its initial value giving E throughout the gas and hence the intensities I_p , I_s and I_a as functions of x . With these values $N_0 - N_1$ at a later time $t = t$ was computed as a function of x and the equations (8) - (11) re-solved for $E_a(x)$ using this x dependent function for $(N_0 - N_1)$. This process was repeated for the duration of the pulse. To compare results with the experimental data measurements the anti-Stokes energy $E_a = \int I_a dt$ from the gas sample was computed.

Since only levels 0 and 1 were included the quantity $N_0 - N_1$ was incorporated into the ratio $\Delta(t) = (N_0 - N_1)/(N_0 + N_1)$ and $\Delta(t + \delta t)$ computed from

$$\Delta(t + \delta t) \approx \Delta(t) + \frac{\partial \Delta(t)}{\partial t} \delta t \quad (21)$$

The explicit form of $\frac{\partial \Delta(t)}{\partial t}$ can be derived from the previous equations to be

$$\frac{\partial \Delta}{\partial t} = \frac{\Delta_0 - \Delta}{\tau_{10}} - \Delta \cdot \frac{4}{\pi^2 k_s^2} \frac{d\sigma}{d\Omega} |E_p|^2 |E_s|^2 \frac{\Gamma/2}{[\omega_1 - (\omega_s - \omega_p)]^2 + \Gamma^2/4} \quad (22)$$

A suitable value for δt was chosen by numerical experimentation

In Fig. (5) we show plots of E_a vs, $I = |E_p|^4 |E_s|^4$. Based on the analytic approximate CARS theory this curve should be a straight line and independent of the individual values of $|E_p|$ and $|E_s|$ for a given value of I . Our results which are computed for quite large E_p show how the output E_a falls below a straight line extrapolation of the values for smaller I . This is the saturation effect which was referred to in the introduction and which is due to a lessening of the fraction $\Delta(t)$ as I_p increases. Furthermore, two such curves are shown, one with $E_s = 1000$ and one with $E_s = 250$. In the latter case larger E_p values are used to generate the same value of $|E_p|^4 |E_s|^2$. The outputs are clearly different in the two cases contrary to the prediction of the approximate analytic theory. An example of pulse shaping effects is also illustrated in Fig. (5).

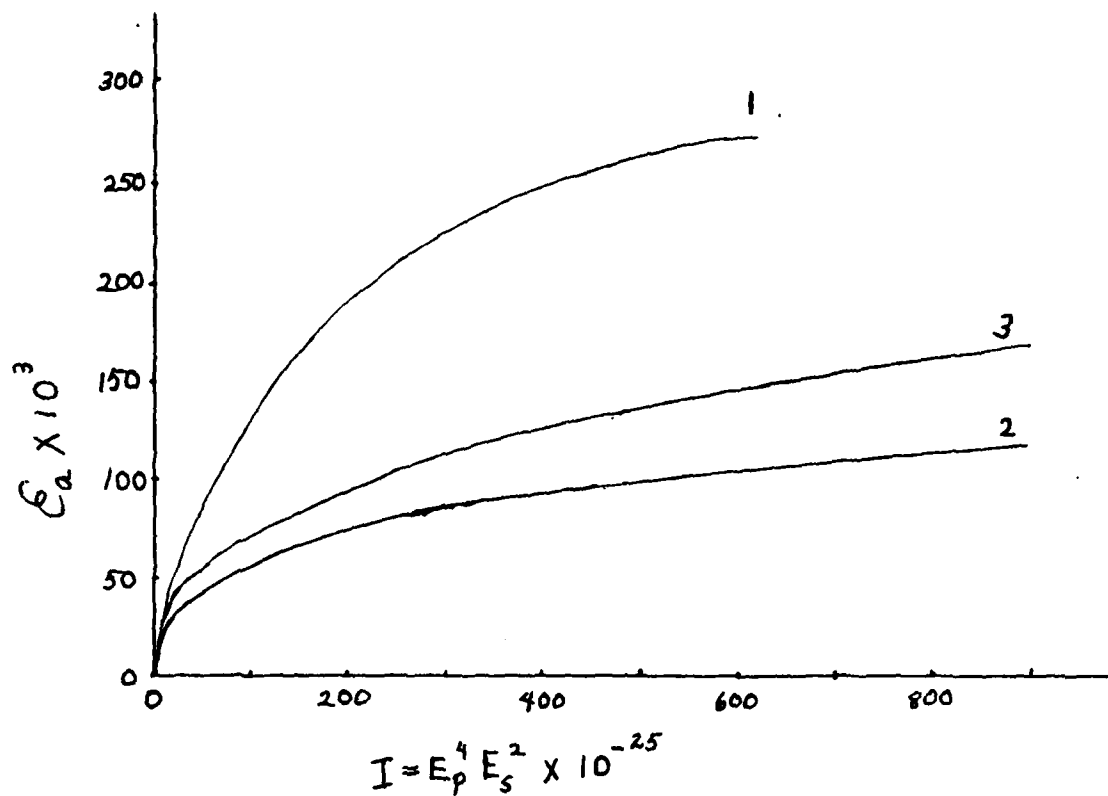


Figure 4. Energy vs. Parameter I

Energy in the anti-Stokes beam at the end of the interaction region as a function of parameter I. All units are Gaussian units.

1 and 2 Gaussian shaped pump and Stokes pulses cut off at the half power points.

1. $E_s = 250$, 2. $E_s = 1000$
3. Rectangular pulses with same peak values and durations as the Gaussian pulses; $E_s = 1000$.

Other results which we do not reproduce here concerned limited numerical exploration of the sensitivity of the computed anti-Stokes energy to the Stokes cross-section $\left[\frac{d\sigma}{d\Omega}\right]$ and the time constants τ , quantities for which there is considerable uncertainty regarding the correct numerical values. Some exploration was also made of the effects of the d^2E_s/dx^2 terms on accuracy and on computing time.

V RECOMMENDATIONS FOR FURTHER RESEARCH.

(a) Further numerical work should be carried out at AFAPL using the present program (for one excited energy level) and the results compared with experiments. This will indicate how well the present theory explains observations and perhaps indicate important improvements which need to be made.

(b) The more complete theory given by Eqs (8) through (20) should be programmed for computation and further numerical studies and comparison with experiment made. Relatively minor modifications and additions can add in CSSRS and also permit rotational levels to be taken into account approximately.

In this regard we recommend that the program be written in Fortran unlike the existing work which was done in MIMIC, a computer language and compiler developed at WPAFB about 1962. MIMIC is no longer supported by the WPAFB Computer Center, and (although this is not documented there) certain operations and procedures regarding logic functions and the use of subprograms no longer work. In addition there is inadequate flexibility in the output; there is no way to avoid printing out a vastly excessive amount of data not needed for our work and there is no provision to use any solution method for the differential equations other than fourth order Runge-Kutta. The writer believes that, for the equations involved, predictor-corrector methods would be better.

(c) Further research is needed to better model the theoretical set-up; particularly in taking into account focussing of the pump and Stokes beams, finite Stokes bandwidth, and the fact that for some of the experimental set-ups anti-Stokes radiation is being generated outside of the test region as well as in it.

(d) Study the effect of orthogonal instead of parallel pump and Stokes radiation.

REFERENCES

1. Schreiber, P. W., R. Gupta, W. B. Roh, "Application of Lasers of Combustion Diagnostics," SPIE Proceedings, Vol. 158 Laser Spectroscopy-Applications and Techniques 1978.
2. Switzer, G. L., W. M. Roquemore, R. P. Bradely, P. W. Schreiber, W. B. Roh, "CARS Measurements in a Bluff-Body Stabilized-Diffusion Flames," Applied Optics 18, No. 14, pp. 2343-2345, July 15, 1979.
3. Eckbreth, A. C., P. W. Schreiber, "Coherent Anti-Stokes Raman Spectroscopy Application Combustion and Gas Phase Diagnostics," Chemical Applications of Nonlinear Spectroscopy, Academic Press, Chapt. 2 (to be published).

1979 USAF - SCEE SUMMER FACULTY RESEARCH PROGR.

Sponsored by the

AIR FORCE OFFICE OF SCIENTIFIC RESEARCH

Conducted by the

SOUTHEASTERN CENTER FOR ELECTRICAL ENGINEERING EDUCATION

FINAL REPORT

An Investigation of One and Three Parameter Item
Response Models with Implications for Computerized
Adaptive Testing

Prepared by:	Bronel R. Whelchel, Ph.D.
Academic Rank:	Associate Professor of Computer Science and Statistics
Department and University:	Department of Sociology, Tennessee State University, Nashville, Tennessee
Research Location:	AFHRL/PEP Brooks AFB, TX 78235
USAF Research Colleague:	Dr. Malcolm Rhee
Date:	August 8, 1979
Contract No.:	F49620-79-C-0038

AN INVESTIGATION OF ONE AND THREE PARAMETER
ITEM RESPONSE MODELS WITH IMPLICATIONS FOR
COMPUTERIZED ADAPTIVE TESTING

by

Brone! R. Whelchel

ABSTRACT

"Adaptive" testing is one of a number of terms used to describe a procedure whereby the test items that comprise an individual's test are selected during the test itself. Some of the other terms used interchangeably with adaptive testing include tailored testing, branched testing, programmed testing, and individualized testing. The term "adaptive" was chosen because these tests adapt themselves to the examinee; different persons answer different items, with the items chosen sequentially to suit the individual examinee's performance.

The general objective of computer driver adaptive testing is to accurately estimate an individual's position on the underlying trait the test purports to measure. Conventional paper-and-pencil test administration typically suffers from several sources of error in the measurement of an individual's ability. Conventional peaked tests are designed to discriminate most effectively at a single ability level and thus assume that most individuals taking the test fall into this category. When they do not, the accuracy of estimation of their status on the trait becomes progressively more inaccurate as their ability deviates from this point.

The result of this lower precision of measurement is lower overall reliability, and lower validity as well (Weiss, 1974). Lord (1970, 1971a, 1971c, 1971d, 1971e) and Hick (1951) have concluded that a test score most accurately reflects an individual's ability when the probability of a correct response to an item is .5 for that individual. Conventional tests obviously cannot meet the requirements of .5 probability for all examinees as all items must be given to all examinees.

A second source of error results from not extracting all the information contained in an examinee's answers to questions. Conventional tests typically use number or proportion of items correct or some transformation of total test score and disregard item discrimination. Two recent developments have enabled the psychometrician to more accurately assess the status of individuals on measureable traits: Adaptive testing and latent trait test theory. Adaptive testing enables adapting each test to fit characteristics of each individual test. Thus, it allows the presentation of the most informative items to an examinee to be used as the basis of that individual's test score. Latent trait test theory allows the calculation of ability estimates in the same metric for each examinee and permits comparisons among scores even though each may have taken a different subset of items (Lord, 1970; Wood, 1973).

The following contractors to the Office of Naval Research are engaged in adaptive testing studies: The Psychometric Methods Program, University of Minnesota, the Tailored Testing Research Laboratory University of Missouri, Department of Psychology, University of Southern California. The AFOSR and AFHRL have adaptive testing contracts with Professors Ron Hambleton and Hariharan Swaminathan at the University of Massachusetts. The proposed study does not duplicate other efforts but rather is complimentary. Results of the proposed effort will advance the state of knowledge in this important area.

As was evident from paper presented at the 1979 adaptive testing conference (CAT' 79) there is an interest in real data comparisons of one and three parameter item response models. It is possible that adaptive testing procedures might have a high utility for small groups when the one parameter model is used. The proposed efforts would compare one and three parameter models in a student population. The independent variables would be one and three parameter item calibration procedures and the dependent variables would be test scores and correlation with an external criterion. Hopefully, computer adaptive testing will from a military standpoint reduce test taking time 25% therefore, reducing the cost of such efforts by 30%.

ACKNOWLEDGEMENTS

This research was accomplished under the contract number F49620-79-C-0038, 1979 USAF-SCEE Summer Faculty Research Program, Air Force Office of Scientific Research. The research in Adaptive Testing is one of the many research areas in which AFHRL, Brooks Air Force Base, Texas is engaged. I am pleased to have been a member of such an outstanding research team and to have been involved in I consider a very worthwhile endeavor. Recognition must be given Colonel Tyree H. Newton, HRL, Personnel Research Division, Brooks AFB and LtColonel Forrest R. Ratliff, HRL, Manpower Development and Evaluation Branch also of Brooks AFB for their instrumental roles in directing research conducted in this area.

The author is further indebted to Dr. Malcolm Rhee who not only guided my research during my summer Faculty summer research program but has consented to provide guidance and supervision to further research to be conducted during the academic year 1979-1980 at Tennessee State University in Nashville under a mini grant proposal.

I further wish to acknowledge Dr. Richard N. Miller, Ph.D., SFRP Director who so expertly directed, supervised and counseled me into the appropriate area where my research expertise could be utilized to the benefit of the U.S. Air Force and the U.S. at large.

Lastly, I wish to acknowledge the Air Force Systems Command and the Air Force Office of Scientific Research for making such a worthwhile program available to University faculty members who otherwise would not have the opportunity to contribute.

I. INTRODUCTION: "Adaptive" testing is one of a number of terms used to describe a procedure whereby the test items that comprise an individual's test are selected during the test itself. Some of the other terms used interchangeably with adaptive testing include tailored testing, branched testing, programmed testing, and individualized testing. The term "adaptive" was chosen because these tests adapt themselves to the examinee; different persons answer different items, with the items chosen sequentially to suit the individual examinee's performance.

Differential selection of test items may be accomplished in any number of ways. But, generally, in adaptive tests a more difficult item is administered following each correct answer, and an easier item following an incorrect one. Some methods of adaptive testing have been implemented in paper-and-pencil mode; for example, Lord's (1971) flexilevel adaptive test was designed specifically for paper-and-pencil administration. However, experience has shown that the instructions for paper-and-pencil adaptive tests are too complex for some examinees to follow successfully (Weiss & Betz, 1973, p. 23). A more satisfactory mode of administration is through use of an interactive computer terminal or similar device. Thus, Weiss (1976) chose to administer adaptive tests at a cathode-ray terminal (CRT); Bayroff, Ross and Fischl (1974) reported the Army's development of a computer-controlled slide projection terminal for adaptive testing; Waters (1977) designed and built a micro-processor terminal which directs the examinee through an adaptive sequence of test items read from a printed booklet.

Item selection strategies. Because adaptive tests are quite different from conventional tests in which all examinees must answer the same set of test items, adaptive testing poses some new psychometric problems. One problem is how to choose successive items from the pool of available items. This problem can be solved through an item selection strategy, which defines a formalized rule for item choice.

Numerous item selection strategies are possible. They vary from very simple two-branch rules to rules based on the optimization of rather complex mathematical functions (Weiss, 1974). Obviously, computerizing the item-selection process, facilitates the use of the mathematical optimization procedures.

Scoring adaptive tests. Since different examinees take sets of test items which may differ in number, difficulty, and discriminating power, the traditional number correct score will not suffice to order people on most adaptive tests. Some scoring procedure is required which will consider not only how many items were answered correctly, but also which items were taken, and the pattern of right and wrong answers to those items. The scoring procedures most widely used in adaptive testing are based on various formulations of latent trait theory (e.g., Birnbaum, 1968; Lord, 1952, 1974; Rasch, 1960). All of these formulations provide statistical methods for locating examinees on a common scale, even though they responded

to different sets of test items.

Item response theory. Because of the unique characteristics of adaptive tests--tailoring each test to the individual and locating all examinees on a common scale despite the different items constituting each test--traditional test theory is inadequate for use in adaptive testing. "Latent trait" or "item response" theory (Lord, 1952, 1976) provides an adequate theory (Lord, 1952, 1976) provides an adequate theoretical basis for the development of adaptive testing.

Item response theory, also known as item characteristic curve theory, is a general term for theoretical formulations which account for examinees' responses to test items in terms of their status on an underlying attribute. In ability (or achievement) testing, the higher the attribute status, the larger is the probability of a correct response to any given item which measures the trait in question. Through appropriate scaling procedures, a response curve can be constructed for every such test item. This item characteristic curve (ICC) expresses the probability of a correct response as a mathematical function of the scaled trait and the item characteristics.

Every person can be characterized by his/her location on this scale. Every test item also has a location parameter (its threshold, or "difficulty") and perhaps its own rate parameter (proportional to the steepness of the ICC), analogous to its discriminating power. Some items also have a lower asymptote, or guessing parameter.

Knowing which items a person has answered; the difficulty, discrimination, and guessing parameters of those items; and whether the answers were correct or incorrect permits the use of the statistical techniques of item response theory to estimate the examinee's ability. The resulting ability estimate is a "test score" of sorts which has an error component like any other observed score. Unlike classical test theory, item response theory makes no assumption that measurement errors are independent of "true score", which is appropriate because this central assumption of classical test theory is untenable (Lumsden, 1976). Whether ability is defined as "true score" or as location on a latent continuum, errors of measurement can vary at different levels of the trait, reflecting in part the discrepancy between examinee trait level and the difficulties of the test items.

Information. Item response theory permits the evaluation of something closely akin to the standard error of measurement as a function of underlying ability, if the test item parameters are known. This is called the test information function (Birnbaum, 1968) which is inversely proportional to the standard error of estimating an examinee's location on the trait scale. If the information function of a typical peaked conventional test (one whose items are all about equal in difficulty) were plotted, its test information function would likewise be peaked--very high over a narrow range of the trait, but diminishing in magnitude elsewhere. Such a test will discriminate very well over a narrow interval of the trait range; it will not discriminate as well outside that interval. The ability level at which the test information function is highest can be referred to as the test "center".

The information function of a "rectangular" conventional test (one whose item difficulties are uniformly distributed over a wide range) is fairly flat, but low over a broad interval on the trait scale around the test center. This test would measure about equally well over a much wider range than the peaked test, but other things being equal, would not discriminate nearly as effectively as does the peaked test at its center.

The design of conventional tests. A test measures best (most precisely) where its information function is highest (and hence its standard error is lowest). It is frequently desirable to have high measurement precision over most of the normal range of the attribute we seek to measure. This is tantamount to a high, flat information function. Conventional testing, however, presents a dilemma. A peaked test can be constructed which yields an information function with a high peak; or at the other extreme, a rectangular test can be built which has a low, flat information function. A test with a high, flat information function cannot be constructed for conventional test administration unless it is extremely long.

This problem can be referred to as a "bandwidth-fidelity dilemma", with apologies to Cronbach (1961), who described a different "bandwidth-fidelity dilemma". The designer of a conventional test can construct it to have high "fidelity"--high precision, low measurement error--over a narrow range of ability; or to have a broad "bandwidth"--equiprecision of measurement over a wide range of ability, at the expense of fidelity. In designing a conventional test, there is a tradeoff between broad bandwidth and high fidelity; the designer cannot have both.

II. OBJECTIVES: Herein resides the most attractive feature of adaptive tests from a psychometric point of view: Because the test is adapted to the individual, the discrepancy between trait level and item difficulty can be made both small and fairly constant across the trait range. The result is a flat information function which is also generally high. Adaptive tests--and only adaptive tests--are capable of accurate, equiprecise measurement over a wide ability range. This should pay dividends in test reliability, criterion-related validity, and in the general utility of the test for a broad range of measurement and decision applications.

A properly designed adaptive test will have higher reliability than a conventional test of the same length. As a corollary to that, an adaptive test can achieve a specified level of reliability in substantially fewer items than can a conventional test, thus permitting the measurement of additional attributes in the time saved. Both improved reliability and additional measurements should result in an increment in predictive validity over that obtained using conventional tests.

In addition to the psychometric benefits accruing from the use of adaptive tests, there are psychological benefits to the examinees. Adaptive tests can have positive effects on the test-taking motivation of examinees (Betz & Weiss, 1976b) and, for some testees, on their measured ability levels (Betz & Weiss, 1976a). By tailoring test difficulty to examinee

III, IV, V. Interim Conclusions: Ree (1978b) demonstrated the feasibility of computer item banking and item manipulation in a military test construction environment. A computer-based system comprised of an item editor for entry and modification of items was designed as was an interactive procedure for item pool and test construction. This allowed estimates of number-right score mean, variance, reliability, and percentile equivalents to be estimated and printed. Several printing options permit the ordering of items to suit the user. The accuracy of the estimation procedures was tested by computing item parameters in one group and estimating the test parameters in a hold-out group. These estimates were found to be quite good.

Another research objective is to recognize the consequences of errors in item calibration. Past research (Ree, 1979) indicates that, as long as errors are normally distributed, the b parameter has the greatest effect on scores, followed by the a parameter and then the c parameter, even in low ability groups. The item parameter that appears to be the most influential, b, is also the item parameter which can be estimated with the most accuracy in practice, while the c parameter, generally the least influential, is the item parameter which is the most difficult to estimate.

A simulation study (Ree, 1978c) of the effectiveness of four-item characteristic curve parameter estimation program was conducted. Using the three parameter logistic model, three dissimilar groups (data sets) of 2,000 simulated subjects were administered 80-item tests. These simulated test responses were then calibrated using the four programs. The estimated item parameters were compared to the known item parameters in four analyses for each program in all of the three data sets. It was concluded that the selection of an item calibration procedure should be dependent on the distribution of ability in the calibration sample, the planned uses of the item parameters, and the computer resources available.

Because it will be necessary to develop item pools of from about 150 to 450 items, special techniques have been developed to link separately administered subsets of items at the item level. Ree and Jensen (1979) studies one of these procedures which uses a set of common anchor items in each subset of items in order to offer operational procedures. To establish large item pools, it is necessary to try out several hundred items for possible inclusion. Because it is impractical to administer several hundred items to the same several thousand people, the invariance properties of Item Characteristic Curve parameters are used to equate test items. A simulation study was conducted in order to investigate the effects of errors in estimated ICC parameters on equated parameters. Four samples of simulated examinees, ranging from 250 to 2,000 subjects, were administered a test for estimation of "anchor" ICC parameters to be used in equating. An additional four samples of examinees, also ranging from 250 to 2,000 subjects, were administered a different test containing

the identical 20 anchor items, plus 60 additional items. The effectiveness of the equating procedures was studied through analysis of summed absolute deviation from the known item parameters of the estimated item parameters and the equated item parameters for the various combinations of "anchor" item calibration sample size and equating sample size.

It was determined that the b parameter could be accurately estimated with as few as 500 subjects, but the a parameter required at least twice as many subjects for accurate estimation. Operationally, this means that large numbers (say, 2,000) of subjects will be needed for development of the required item pools when calibrated with the three parameter model.

It is expected that the Tennessee State research will further be sharing this knowledge in this field which is new by assessing the effects of item characteristic curve models in a field setting. This will contribute materially to the efforts on going at AFHRL. It will also provide some of the answers to psychometric problems which must be overcome prior to operational implementation of computer driver adaptive testing.

ability, adaptive tests can reduce the effects of guessing among low-ability examinees and make any remaining effects relatively constant across ability levels.

As was evident from paper presented at the 1979 adaptive testing conference (CAT' 79) there is an interest in real data comparisons of one and three parameter item response models. It is possible that adaptive testing procedures might have a high utility for small groups when the one parameter model is used. The proposed efforts would compare one and three parameter models in a student population. The independent variables would be one and three parameter item calibration procedures and the dependent variables would be test scores and correlation with an external criterion. Hopefully, computer adaptive testing will from a military standpoint reduce test taking time 25% therefore, reducing the cost of such efforts by 30%.

The fact that TSU hosts the only Air Force ROTC unit in Middle Tennessee is a plus. It fosters an understanding and appreciation of the atmosphere that most of the thousands of college students in this area miss. This is possible because there are eight schools in the Nashville Area that have crosstown agreements with Tennessee State. These crosstown agreements enable students at these eight schools to pursue their academic careers at the school of their choice while pursuing an Air Force commission through Tennessee State's program.

The impact is great, for each student must enroll with the Office of Admissions and Records, each student receives grades from TSU, and each student must attend classes on TSU's campus. Such requirements ensure that Tennessee State's "Touch of Greatness" is filtered throughout the academic community.

Since its establishment at TSU in 1953, AFROTC Det 790 has been a major source of black officers for the U.S. Air Force. More than 98 percent of the 356 commissionees have been black. Many of them remain in active service to the Air Force, and two are currently ROTC instructors at TSU.

The research involved in this study will continue under a mini grant will hopefully provide insight and meaning to the whole area of computerized adaptive testing by providing data from a segment of the population that heretofore has not contributed as a unit.

The physical equipment and the software is a duplicate of the hardware and software at Brooks AFB, TX. The approach to be taken will be to continue the collection, synthesis and analysis of data.

VI Recommendations: Guidance for implementing the results of this research will be directly related to the efforts of AFHRL, Brooks AFB, TX, in that research involved in this study is not a repeat study but hopefully it will convey some conception of what adaptive testing is and the rudiments of the test theory supporting it.

Several procedures for estimating latent trait status have been presented. It has also been suggested that adaptive testing procedure often can provide more accurate estimates of latent trait status than conventional tests. Though there is no necessary connection between latent trait theory and adaptive testing, there is a strong natural impetus toward their joint application. Latent trait theory provides adaptive testing with a coherent theoretical foundation. It is a guide to procedures for designing and scoring adaptive tests. On the other hand, adaptive testing offers the opportunity to take maximum advantage of the potentialities of latent trait theory. At this point in time, both a new type of test theory and a new type of testing technology are available. Their joint effect might possibly exceed the sum of the two parts.

REFERENCES

Conference and journal publications:

1. Cleary, T. A. Test bias: prediction of grades of Negro and White students in integrated colleges. *Journal of Educational Measurement*, 1968, 5, 115-124.
2. Darlington, R. B. Another look at "cultural fairness." *Journal of Educational Measurement*, 1973, 10, 237-255.
3. Gugel, J. F., Schmidt, F. L., and Urry, V. W. Effectiveness of the ancillary estimation procedure. Proceedings of the First Conference on Computerized Adaptive Testing, U.S. Civil Service Commission, Bureau of Policies and Standards. Professional Series, 75-6, 1975, 103-106.
4. Hambleton, R. K. and Cook, L. Latent trait models and their use in the analysis of educational test data. *Journal of Educational Measurement*, 1977, 14, 75-96.
5. Meredith, J. B. Jr., and Dion, R. J. Utilization of differential proficiency levels for criterion-referenced training system assessment. Proceedings of a Symposium presented at the 19th Annual convention of the Military Testing Association, 1977, 1258-1269.
6. Pine, S. M. Applications of item characteristic curve theory to the problem of test bias, in Weiss, D. J. (ed) Proceedings of a Symposium presented at the 18th Annual Convention of the Military Testing Association Research Report 77-1, Psychometric Methods Program, Dept. of Psychology, Univ. of Minn., Mar. 1977, 37-43.
7. Ree, M.J. Implementation of a model adaptive testing system at an AFEES. Paper presented at a symposium of the Eighteenth Annual Conference of the Military Testing Association, San Antonio, TX., 1977a.
8. Rudner, L.M. An evaluation of select approaches for biased item identification. Proceedings of a Symposium presented at the 19th Annual Convention of the Military Testing Association, 1977.
9. Scheuneman, J. Validating a procedure for assessing bias in test items in the absence of an outside criterion. Paper presented at the American Educational Research Association, San Francisco, April 1976.
10. Simpson, J. B. Estimation of latent trait status in adaptive testing procedures. Proceedings of a Symposium presented at the 18th Annual Convention of the Military Testing Association, Research Report 77-1, March 1977, Psychometric Methods Program, Dept. of Psychology, Univ. of Minn., 5-23.
11. Thorndike, R. L. Concepts of culture-fairness. *Journal of Educational Measurement*, 1971, 8, 63-70.

12. Urry, V. W. Tailored testing: a successful application of latent trait theory. *Journal of Educational Measurement*, 1977, 14, 181-196.
13. Weiss, D. J. Adaptive testing research at Minnesota - overview, recent results and future directions. *Proceedings of the First Conference on Computerized Adaptive Testing*. U. S. Civil Service Commission. Professional Series 75-6, March 1976, pp. 24-25.
14. Wright, B. D. Solving measurement problems with the Rasch model. *Journal of Educational Measurement*, 1977, 14, 97-116.

REFERENCES

Textbooks:

1. Baker, F. B. Advances in item analysis. Review of Educational Research, Winter 1977, vol. 47, No. 1, 151-178.
2. Bejar, I. I. An application of the continuous response level model to personality measurement. Applied Psychological Measurement, vol. 1, No. 4, Fall 1977(a), 509-521.
3. Bejar, I. I., Wiess, D. J., and Kingsbury, G. G. Calibration of an item pool for the adaptive measurement of achievement. Research report 77-5, Psychometric Methods Program, Dept. of Psychology, Univ. of Minnesota, Sep 1977(b).
4. Birnbaum, A. "Some latent trait models and their use in inferring an examinee's ability." In Lord, F. M. & Novick, M. R., Statistical Theories of Mental Test Scores; Addison-Wesley, Reading, Mass.; 1968; Chpts. 17-20.
5. Bock, R. D., and Lieberman, M. Fitting a response model for N dichotomously scored items. Psychometrika, 1970, 35, 179-197.
6. Brogden, H. Variation in Test Validity with Variation in the Distribution of Item Difficulties, Number of Items, and Degree of their Intercorrelation. Psychometrika, 1946, 11, 197-214.
7. Brown, J. B. and Weiss, D. J. An adaptive testing strategy for achievement test batteries. Research Report 77-6, Oct 1977. Psychometric Methods Program, Dept. of Psychology, Univ. of Minnesota.
8. Carroll, J. B. Problems in the factor analysis of tests varying difficulty. Amer. Psychologist, 1950, 5, 369. (Abstract).
9. Cleary, T. A. Test bias: prediction of grades of Negro and White students in integrated colleges. Journal of Educational Measurement, 1968, 5, 115-124.
10. Christofferson, A. Factor analysis of dichotomized variables. Psychometrika, 1975, 40, 5-32.
11. Cronbach, L. J. Essentials of Psychological Testing, Harper and Row, New York, 1960.
12. Cronbach, L. J. and Warrington, W. G. Efficiency of multiple-choice test as a function of spread of item difficulties. Psychometrika, 1952, 17.
13. Durovic, J. J. Use of the Rasch model in assessing item bias. Paper presented a part of a symposium entitled "What's Happening in Measurement: The Use of Rasch and other Latent Trait Models," Eastern Educational Research Association, Williamsburg, Va, March, 1978.

14. Ferguson, G. A. Item selection by the constant process. *Psychometrika*, 1942, 7, 19-29.
15. Gorman, S. Computerized adaptive testing with a military population. Paper presented at the Computerized Adaptive Testing '77 Conference, Univ. of Minnesota, July 1977.
16. Green, S. B., Lissitz, R. W., Mulaik, S. A. Limitations of coefficient alpha as an index of test unidimensionality. *Education and Psychological Measurement*, 1977, 37, 827-838.
17. Gugel, J. F. A multiple-choice biserial correlation adjustment for guessing. Unpublished.
18. Gulliksen, H. *Theory of mental tests*, John Wiley & Sons, Inc., New York, 1950.
19. Hoffman, B. *The Tyranny of Testing*, Collier, 1962.
20. Hunter, J. E. and Schmidt, F. L. A critical analysis of the statistical and ethical implications of various definitions of "test bias." *Psych. Bulletin*, vol. 83, #6, Nov. 1976, 1053-1071.
21. Lord, F. M. An empirical study of item-test regression, *Psychometrika*, 1965, 30, 373-376.
22. Tucker, L. R. Maximum validity of a test with equivalent items. *Psychometrika*, 1946, 11, 1-13.
23. Wood, R. L., Wingersky- M. S., and Lord, F. M. LOGIST: A computer program for estimating examinee ability and item characteristic curve parameters. Research Memorandum 76-6. Princeton, NJ: Educational Testing Service, 1976.

1979 USAF-SCEEE SUMMER FACULTY RESEARCH PROGRAM

Sponsored by

THE AIR FORCE OFFICE OF SCIENTIFIC RESEARCH

Conducted by the

SOUTHEASTERN CENTER FOR ELECTRICAL ENGINEERING EDUCATION

PARTICIPANT'S FINAL REPORT

MODULATED SPONTANEOUS RAMAN EFFECT FOR

LASER ALL-OPTICAL FREQUENCY STANDARDS

Prepared by:	Charles R. Willis
Academic Rank:	Professor
Department and University	Physics Department Boston University
Assignment	Rome Air Development Center Hanscom AFB, MA 01731
RADC Research Colleague:	Dr. C. Leiby
Date:	July 18, 1979
Contract No:	F49620-79-0038

MODULATED SPONTANEOUS RAMAN EFFECT FOR
LASER ALL-OPTICAL FREQUENCY STANDARDS

by

C. R. WILLIS

ABSTRACT

The purpose of this report is to investigate the feasibility of using the Modulated Raman Effect in laser all-optical frequency standards. After a brief review of all-optical frequency standard programs at the Electro-optical Device Technology Branch, we derive the equations of motion for the density matrix of the hyperfine levels of the ground state for atoms undergoing a modulated Raman effect. We show that the spectrum of the modulated Raman effect is the same as the unmodulated Raman effect. Consequently, for stationary atoms the spectrum depends only on the narrow lines of the ground hyperfine states and is independent of the broad excited state line-shape. We conclude with a list of remaining extensions of the present work that are needed to establish the viability of Raman effect for all-optical frequency standards.

ACKNOWLEDGEMENT

The author would like to thank AFOSR and SCHEE for providing me the opportunity to spend an interesting and profitable summer at RADC, Hanscom Field. Also, I would like to thank Dr. A. Yang, Electro-Optic Device Technology Branch Chief. I am especially indebted to Drs. Clare Leiby and Richard Picard who by their many and useful high quality interactions made my stay very pleasant as well as scientifically profitable.

I. Introduction

The purpose of the present work is to determine the spectra of the spontaneous Raman effect when the optical beam is coherently modulated at the hyperfine transition. In particular, does the spectra depend on both the lifetimes of the ground and the excited atomic states, or does it depend on only the lifetimes of the long-lived ground hyperfine states? The answer to the preceding question is important for the possible use of the Raman or Resonant Raman Effect in All-Optical Frequency standard schemes being carried out at ESO. To provide motivation for the present research, we will first describe the frequency standard program at ESO, then we will derive the spectral of the modulated Raman effect.

Proposed optically pumped atomic beam frequency standards have typically employed lasers or resonance discharge tubes and photodetectors to replace the dipole magnets and hot wire detector of a standard Rabi resonance apparatus both for state selection in the A region and for detection of transitions in the B region while still using a Ramsey type microwave cavity to induce transitions in the resonance or C region. (For example, see Refs. (1,2,3)). Various advantages including some size and weight reductions are potentially achievable by the elimination of the magnets required for state selection and analysis. However, such standards would still require a large L-branch cavity within the atomic beam vacuum chamber to induce transitions between hyperfine levels of the ground state. The frequency standard group at ESO have proposed two schemes for eliminating the requirement for microwaves within the C region and hence achieving all-optical standards.

The first scheme is laser-induced fluorescence for state inversion. The first step is state selection by optical pumping with a dye laser of frequency ν_0 which in the case of Na pumps all the atoms from the $F=2$

level into the $F=1$ hyperfine level of the $3^2S_{1/2}$ ground states. If the laser frequency could be shifted by the hyperfine frequency ν_{hf} (i.e. from ν_0 to $\nu_0 + \nu_{hf}$) one could repopulate level $F=2$ by absorption of shifted laser radiation $\nu_1 = \nu_0 + \nu_{hf}$ followed by fluorescence. In addition to eliminating the necessity for a microwave cavity in the resonance region, this scheme also eliminates completely the need for a separate B region for state detection. Instead, the fluorescence signal in the C region can be used as a measure of the rate at which state $^3S_{1/2}$ ($F=2$) is being repopulated and may be used to derive a clock signal. The shifting of the laser radiation by a microwave frequency ν_{hf} can be accomplished by amplitude or frequency modulating the laser light with a LiNbO₃ microwave-driven acousto-optic modulator. The modulator acts as a thick diffraction grating; consequently the modulated light emerges at the Bragg angle and is spatially separated from the unmodulated light which is not deflected. By varying the microwave drive power the ratio of the powers at ν_0 and at ν_1 can be controlled.

A clock based on laser induced fluorescence will tend to be inherently less stable than one operating directly on the hyperfine transition because of the great disparity in widths between the optical and hyperfine transitions (typically of the order of megahertz for the optical transition and kilohertz for the hyperfine transition). However, since the frequency stability of a clock is proportional to the optical line width Γ and inversely proportional to the square root of the number of collected photons, it is possible to compensate for the large optical line width by a sufficiently high fluorescent flux. In the present case, the fluorescent flux can be made sufficiently large that frequency standards of remarkably high stability are possible.

The second scheme process for eliminating the requirement for micro-waves and hence achieving all-optical frequency standard is the use of stimulated Raman processes for state inversion. This scheme developed out of my interaction with Dr. C. Leiby and Dr. R.H. Picard of ESO while I was a summer faculty research associate. In this scheme the $^2S_{1/2}$ (F=1) state is selected by laser pumping followed by fluorescence as in the previous section. However, the inversion in the B region is accomplished by a two-photon resonance involving an absorbed photon of frequency $\nu_1 = \nu_0 + \nu_{\mu w}$ and an emitted photon of frequency ν_0 . When the microwave frequency $\nu_{\mu w} = \nu_{hf}$ a difference-frequency crossing resonance⁴ occurs and there is a sharp maximum in the gain at the Stokes frequency $\nu_s = \nu_0$. This resonant Raman process is enhanced by the presence of the resonant $^2P_{3/2}$ (F'=1) intermediate state. The bandwidth of the Raman gain is independent of the width of the optical $^2P_{3/2}$ (F'=1) level and depends only on the sum of the narrow hyperfine $^2S_{1/2}$ levels for stationary atoms or for beams which are perpendicular to the direction of the laser beam. Consequently, by use of the resonant Raman effect it is possible with the use of atomic beams to arrange the geometry such that the megahertz line width of the laser induced scheme is replaced by the long-level hyperfine level linewidths which are only of the order of kilohertz. One advantage of the present scheme is that the fluctuations in ν_0 do not directly affect the frequency stability since both pump and Stokes frequencies fluctuate in the same way. Hence, the current scheme is relatively insensitive to laser frequency jitter. There are some potential drawbacks of the current scheme. In the next section we derive the equations of motion of the density matrix for the hyperfine levels of an atom undergoing the spontaneous Raman effect.

The Raman Effect

We start with the quantum mechanical Liouville equation for ρ

$$i \hbar \dot{\rho} = [H_0 + \lambda V, \rho] \quad (1.1)$$

After a transformation to the interaction representation we iterate the resultant equation four times, starting from the density matrix at time $t = 0$. The result is

$$\tilde{\rho}(t) - \tilde{\rho}(0) = \hbar^{-4} \int_0^t dt_4 \int_0^{t_4} dt_3 \int_0^{t_3} dt_2 \int_0^{t_2} dt_1 [V(t_4), [V(t_3), [V(t_2), [V(t_1), \tilde{\rho}(0)]]]] \quad (1.2)$$

where the tilde indicates the interaction representation. If the interaction time exists and is small compared with the relaxation time then the right hand side of Eq. (1.2) is proportional to t . Dividing by t we obtain

$$\frac{d\tilde{\rho}}{dt} = K\tilde{\rho}$$

where

$$K\tilde{\rho} \equiv \lim_{t \rightarrow \infty} t^{-1} \hbar^{-4} \int_0^t dt_4 \int_0^{t_4} dt_3 \int_0^{t_3} dt_2 \int_0^{t_2} dt_1 [V(t_4), [V(t_3), [V(t_2), [V(t_1), \tilde{\rho}(0)]]]] \quad (1.3)$$

Eq. (1.5) is true at $t = 0$. We assume it is true for all times t . The rigorous derivation does not change the form of K but proves Eq. (1.3) is true not just at $t = 0$ but for all times. We will derive Eq. (1.3) by explicit calculation of the operator K .

The equations of motion for the density matrix for the spontaneous Raman effect are

$$\dot{\rho}_{\mu\mu} = K_{\mu\nu}\rho_{\nu\nu} - K_{\nu\mu}\rho_{\mu\mu} \approx T^{-1}(a_{\mu\nu}\rho_{\nu\nu} - a_{\nu\mu}\rho_{\mu\mu}) \quad (1.4a)$$

$$\dot{\rho}_{\mu\nu} = -i\Delta_{\mu\nu}\rho_{\mu\nu} - \frac{1}{2}(K_{\mu\nu} + K_{\nu\mu})\rho_{\mu\nu} \approx -i\Delta_{\mu\nu}\rho_{\mu\nu} - T^{-1}(a_{\mu\nu} + a_{\nu\mu})\rho_{\mu\nu} \quad (1.4b)$$

where ρ is in the interaction representation and for convenience we have dropped the tilde. The explicit expressions for $K_{\mu\nu}$, $a_{\mu\nu}$, $\Delta_{\mu\nu}$, and T are given later in this section. The $a_{\mu\nu}$ are purely angular factors. The reason

for the approximate equality signs in Eqs. (1.4a) and (1.4b) is that the magnitude of the probability per unit time of going from state ν to state μ differ by terms of order $(\Omega_{\mu\nu}/\Omega_0)$ where Ω_0 is optical atomic resonant frequency. We are using the optical pumping convention of using Greek letters to label the Zeeman levels of the ground state and Latin letters for the Zeeman levels of the atomic excited states. Although the results will apply to any number of levels in the ground state, for convenience we will consider just two ground state levels μ and ν .

One might conjecture Eq. (1.4a) from Fermi's golden rule, however there are two fundamental reasons and one practical reason why a derivation of Eqs. (1.4a) and (1.4b) are necessary. First it is necessary to show there are no additional terms in Eq. (1.4a) coupling $\dot{\rho}_{\mu\mu}$ $\rho_{\mu\nu}$ which is a distinct a priori possibility unanswerable by a simple appeal to Fermi's golden rule. Second, Fermi's golden rule does not tell you how to get the equations of motion for the off-diagonal matrix elements of the density matrix. Finally, the effect of modulation is easily introduced into the derivation of the equations of motion for the density matrix of atoms undergoing the Raman effect.

In order to evaluate the kernel K defined in Eq. (1.3) we must introduce an explicit representation of the interaction $P \cdot E$. We need a quantum mechanical description of the beam for two reasons. First, the thermal beams used in optical pumping have approximately 10^{-7} photons per mode so the concept of a phase is not very well defined; second, spontaneous emission of a quantized matter system requires the radiation field to be quantized. The definition of $E(\underline{r}, t)$ is

$$\underline{E}(\underline{r}, t) = i(2V)^{-1} \sum_{\underline{k}} (\hbar \Omega_{\underline{k}})^{1/2} (\underline{\epsilon}_{\underline{k}} \underline{a}_{\underline{k}} \exp i(\underline{k} \cdot \underline{r} - \omega t) - \underline{\epsilon}_{\underline{k}}^{\dagger} \underline{a}_{\underline{k}}^{\dagger} \exp - i(\underline{k} \cdot \underline{r} - \omega t)) \quad (1.5)$$

where V is the volume of the system, ϵ_k is the polarization of the photons of wave vector k and frequency Ω_k , and a_k and a_k^\dagger are the usual annihilation and creation operators which satisfy the commutation relations

$$[a_k, a_k^\dagger] = \delta_{kk'}, \quad [a_k, a_{k'}] = [a_k^\dagger, a_{k'}^\dagger] = 0.$$

We are using real polarization vectors. For complex polarization vectors the second term on the right hand side of Eq. (1.5) would be ϵ_k . At the end of the calculation we go over to a continuous density of states. In the beginning of the calculation, however, it is convenient formally to treat the radiation states as discrete. The integral of the dipole moment of the atom over the electric field in the dipole approximation is

$$\int \underline{P}(\underline{r}) \cdot \underline{E}(\underline{r}) d\underline{r} = i(2V)^{-1/2} \sum_k (\hbar \Omega_k)^{1/2} p(a_k e^{i\mathbf{k} \cdot \underline{X}} \underline{\epsilon}_k \cdot \underline{D} + a_k^\dagger e^{-i\mathbf{k} \cdot \underline{X}} \underline{\epsilon}_k \cdot \underline{D}) \equiv \sum_k a_k \phi_k + a_k^\dagger \phi_k^\dagger \quad (1.6)$$

where p is the matrix element of the electron dipole operator between the electron radial ground and excited states, \underline{X} is the center of mass of the atom, and \underline{D} is the unit vector ($\underline{r}/|\underline{r}|$) in the direction of the dipole moment. The definition of the ϕ_k is

$$\phi_k \equiv ip(\hbar \omega_k)^{1/2} (2V)^{-1/2} \exp(i\mathbf{k} \cdot \underline{X}) \underline{\epsilon}_k \cdot \underline{D}$$

with matrix elements in the interaction representation

$$\langle \mu | \phi_k(t) | m \rangle = C_k \langle \mu | \epsilon_k \cdot \underline{D} | m \rangle \exp(-i\Omega_{\mu m} t)$$

where

$$C_k \equiv ip(\hbar \Omega_k)^{1/2} (2V)^{-1/2} \exp i\mathbf{k} \cdot \underline{X}$$

and where

$$\hbar \Omega_{\mu m} \equiv E_\mu - E_m.$$

In the definition of K in Eq. (1.3) we have products over all possible sets of four operators. However when we average K over the thermal beam the only possible products which survive are of the form $\langle a_{\mathbf{k}}^\dagger a_{\mathbf{k}} a_{\mathbf{k}'}^\dagger a_{\mathbf{k}'} \rangle$ or $\langle a_{\mathbf{k}}^\dagger a_{\mathbf{k}'} a_{\mathbf{k}} a_{\mathbf{k}'}^\dagger \rangle$ where $\langle \dots \rangle$ denotes an average over the density matrix of the thermal optical radiation beam. We are using the term thermal to indicate that the density matrix for the optical beam is diagonal in the photon number representation; and modes of different wave number are uncorrelated. Secondly only those terms with time dependence $\exp i(\Omega_{\mathbf{k}} - \Omega_{\mathbf{m}\mu})t$ contribute those of the form $\exp i(\Omega_{\mathbf{k}} + \Omega_{\mathbf{m}\mu})t$ are smaller by a factor of 10^{14} . This is just the familiar rotating wave approximation which corresponds in the Raman effect to neglecting the diagrams where the final photon is first emitted, then the incident photon is absorbed.

When we substitute Eq. (1.6) for V in Eq. (1.3) for K and use the definitions for $\phi_{\mathbf{k}}$ and $C_{\mathbf{k}}$ we obtain after a very lengthy calculation the following result for K,

$$K_{\mu\nu} = (2\pi)^{-5} c^{-6} h^{-2} p^4 \int \int d\Omega_{\mathbf{k}} d\Omega_{\mathbf{k}'} \Omega_{\mathbf{k}} \Omega_{\mathbf{k}'} n(\Omega_{\mathbf{k}}) \delta[\Omega_{\mathbf{k}'} - (\Omega_{\mathbf{k}} - \Omega_{\mu\nu})] (\omega_{\nu\mathbf{k}} \omega_{\mu\mathbf{k}})^{-1} \sum_{\mathbf{m}} \left| \langle \mu | \epsilon_{\mathbf{k}} \cdot \underline{\mathbf{D}} | \mathbf{m} \rangle \right|^2 \left| \langle \nu | \epsilon_{\mathbf{k}'} \cdot \underline{\mathbf{D}} | \mathbf{m} \rangle \right|^2 \quad (1.7)$$

where $n(\Omega_{\mathbf{k}}) \equiv \langle a_{\mathbf{k}}^\dagger a_{\mathbf{k}} \rangle$

and where

$$V^{-1} \sum_{\mathbf{k}} (\dots) \rightarrow (2\pi)^{-3} \int d\mathbf{k} (\dots) = (2\pi c)^{-3} \int d\Omega_{\mathbf{k}} (\dots)$$

The result of the integration over $d\Omega_{\mathbf{k}}$, is

$$K_{\mu\nu} = \frac{N}{V} 4p^4 3^{-1} c^{-3} h^{-1} dv_{\mathbf{k}} v_{\mathbf{k}}^3 (v_{\mathbf{k}} - v_{\mu\nu})^3 n(v_{\mathbf{k}}) v_{\nu\mathbf{k}}^{-2} (3/4) \{ |\langle \mu | \epsilon_{\mathbf{k}} \cdot \underline{\mathbf{D}} | \mathbf{m} \rangle|^2 \}_{\text{avg}} |\langle \nu | \epsilon_{\mathbf{k}} \cdot \underline{\mathbf{D}} | \mathbf{m} \rangle|^2$$

$$= \frac{N \Gamma}{V} p^2 \hbar^{-1} dv_k v_k^3 n(v_k) (v_k - v_{\mu\nu})^3 v_0^{-3} v_{\nu k}^{-2} a_{\mu\nu} \quad (1.8)$$

where $2\pi v_{kv} = \Omega_{kv}$, $2\pi v_{kv} = \omega_{kv}$ and v_0 is the frequency difference between the electronic ground state and its degenerate excited state. The angular factor $a_{\mu\nu}$ and the inverse of the spontaneous emission lifetime Γ are

$$a_{\mu\nu} \equiv (3/4) \sum_m (|\langle \mu | \underline{\epsilon}_k \cdot \underline{D} | m \rangle|^2)_{\text{avg}} |\langle \nu | \underline{\epsilon}_k \cdot \underline{D} | m \rangle|^2$$

$$\text{and } \Gamma \equiv 4\pi^2 v_0^3 (3c^3 \hbar)^{-1}$$

where $\{....\}_{\text{avg}}$ is the average over the angles of polarization of spontaneous emission. The expression $(v_k - v_{\mu\nu})^3$ differs from v_k^3 by less than one part in 10^3 . Consequently Eq. (1.8) for $K_{\mu\nu}$ reduces to the following expression

$$K_{\mu\nu} \approx \frac{N \Gamma}{V} p^2 \hbar^{-1} dv_k v_k^3 n(v_k) v_{kv}^{-2} a_{\mu\nu} \equiv T^{-1} a_{\mu\nu}.$$

The relaxation time is essentially independent of the states μ and ν , because the expression for $K_{\nu\mu}$ differs in magnitude from $K_{\mu\nu}$ only in the replacement of $(v_k - v_{\mu\nu})^3$ which is a difference of the order of 10^{-3} and thus $K_{\nu\mu}$ is equal to $T^{-1} a_{\nu\mu}$.

We obtain the expression for $i\Delta_{\mu\nu}$ in continuous variables in the same manner and the resulting

$$i\Delta_{\mu\nu} = \frac{p^4 i}{(2\pi c)^6 \hbar^2} \iint \frac{d\Omega_k d\Omega_{k'}}{\omega_{\nu k} \omega_{\mu k'}} \Omega_k \Omega_{k'} n(\Omega_k) \mathcal{P} \frac{1}{\Omega_{k'} - \Omega_k + \Omega_{\mu\nu}} \sum_m |\langle \mu | \underline{\epsilon}_k \cdot \underline{D} | m \rangle|^2 |\langle \nu | \underline{\epsilon}_{k'} \cdot \underline{D} | m \rangle|^2 \quad (1.9)$$

$$= \frac{i \Gamma p^2 a_{\mu\nu}}{\hbar c^3 (2\pi)^6} \iint \frac{d\Omega_k d\Omega_{k'} \Omega_k^3 \Omega_{k'}^3 n(\Omega_k)}{\omega_{\nu k} \omega_{\mu k'}} \mathcal{P} \frac{1}{\Omega_{k'} - \Omega_k + \Omega_{\mu\nu}}.$$

Accurate estimates of $\Delta_{\mu\nu}$ probably requires machine computation.

We have shown the spectrum for the Raman effect is proportional to

$$\int d\Omega_k' \Omega_k \Omega_k' \delta \Omega_k - (\Omega_k' - \Omega_{\mu\nu}) (\omega_{\nu k} \omega_{\nu k})^{-1}$$

which is independent of the lifetime of the excited atomic states as far as the resonant frequency condition is concerned. In the next section we will determine the modifications in the Raman effect when we modulate the optical frequency at the hyperfine frequency $\Omega_{\mu\nu}$.

III Externally Modulated Raman Effect

In Sec. II we found in the absence of modulation that the equations of motion for the diagonal and the off-diagonal density matrix elements were not coupled to each other. As a result the steady state transverse magnetization vanished. We now show if the thermal beam is modulated at the frequency $\Omega_{\mu\nu}$ then the equations of motion for the diagonal and off-diagonal matrix elements are coupled to each other and consequently as we now show the density matrix for the hyperfine levels behave as if they were driven directly by a coherent hyperfine frequency field rather than a coherently modulated optical field.

We give only the results of the calculations since they are tedious and differ from those of the unmodulated Raman effect in only two ways, namely $\langle a_k^\dagger a_k \rangle$ is replaced by $\langle a_k^\dagger a_{k+k} \rangle$ and $|\langle \nu | \epsilon_k \cdot D | m \rangle|^2$ is replaced by $\langle \mu | \epsilon_k \cdot D | m \rangle \langle m | \epsilon_k \cdot D | \nu \rangle$. The full equation for $\dot{\rho}_{\mu\nu}$ is

$$\dot{\rho}_{\mu\nu} + i \Delta_{\mu\nu} \rho_{\mu\nu} + T^{-1} a_{\mu\nu} \rho_{\mu\nu} = d D_{\mu\nu} (\rho_{\mu\mu} - \rho_{\nu\nu})$$

where

$$D_{\mu\nu} \equiv A_{\mu\nu} + iB_{\mu\nu} \equiv (2T)^{-1} (c_{\nu\mu} - c_{\mu\nu}) + i(2T_p)^{-1} (c_{\mu\nu} + c_{\nu\mu})$$

$$c_{\mu\nu} \equiv \sum_m (|\langle \mu | \epsilon_k \cdot D | m \rangle|^2)_{\text{avg}} \langle \mu | \epsilon_k \cdot D | m \rangle \langle m | \epsilon_k \cdot D | \nu \rangle$$

and where

$$T_p^{-1} = \frac{2\pi p^4}{(2\pi c)^6 \hbar^2} \iint \frac{d\Omega_k, d\Omega_k \Omega_k^3 \Omega_{k'}^3, n(\Omega_k)}{\omega_{\mu k} \omega_{\nu k'}} \rho \frac{1}{\Omega_{k'} - \Omega_k - \Omega_{\mu\nu}}.$$

We use the results of Ref. 5, to replace $\langle a_k a_{k+k} \rangle$ by $d \langle a_k a_k \rangle$ where $\Omega_{k+k} = \Omega_k + \Omega_{\mu\nu}$ and d , the depth of the modulation, varies between zero and one. The relaxation time T_p differs from T only in that the delta function of $\Omega_{k'} - \Omega_k - \Omega_{\mu\nu}$

is replaced by the "Principal part" of the same argument. As a consequence of their definitions the coefficients A , B , and D satisfy the following symmetry relations: $D_{\mu\nu} = -D_{\nu\mu}^*$, $B_{\mu\nu} = B_{\nu\mu}^*$, and $A_{\nu\mu}^* = -A_{\mu\nu}$,

which guarantee the preservation of the hermiticity of the density matrix ρ . For some polarizations such as linear polarization the $A_{\mu\nu}$ vanish and the $D_{\mu\nu}$ is purely imaginary. In order that $D_{\mu\nu}$ does not vanish the polarization must be coherent in the sense of Cohen-Tannoudji⁶; i.e. the polarization must be a linear combination of two or more of the three states of polarization σ^+ , σ , and π .

The modulation produces a contribution from the off-diagonal density matrix elements to the equations of motion for the diagonal density matrix elements in exactly the same manner as the diagonal elements contribute to the equations of motion of the off-diagonal elements. The equation of motion for the population difference is

$$[\partial(\rho_{\mu\mu} - \rho_{\nu\nu})/\partial t] + T^{-1} (a_{\nu\mu} \rho_{\mu\mu} - a_{\mu\nu} \rho_{\nu\nu}) = -2d(D_{\mu\nu} \rho_{\nu\mu} - D_{\nu\mu} \rho_{\mu\nu}) \quad (3.2)$$

The factor of two in the above equation is a consequence of the fact that $\dot{\rho}_{\nu\nu}$ is equal and opposite to $\dot{\rho}_{\mu\mu}$.

From Eqs. (3.1) and (3.2) we see that the spectrum of the modulated Raman effect is the same as the spectrum of the unmodulated spectra. The second important result is that the modulation represented by the term $-2dD_{\mu\nu}$

is equivalent to an external field $-i\hbar^{-1}\langle\mu|\mu.H_0|\mu\rangle$ where H_0 is a coherent external field of frequency $\Omega_{\mu\nu}$. Therefore we have proved that a coherently modulated external chaotic beam transfers the hyperfine coherent modulation directly to the hyperfine levels of the atom in exactly the same manner as an applied coherent hyperfine field.

IV Conclusions

We have accomplished the first step in the calculations needed to use the second scheme of Sec. I for all-optical frequency standards. Many more calculations remain to be performed before the viability of the record scheme is demonstrated. Future work must extend the present work to 1) resonant Raman, 2) to coherent optical beams, 3) to high intensity pump beams and 4) to determining the optimum approach to an error signal for the all optical frequency standards.

REFERENCES

1. A. Kastler, J. Phys. (Paris) II, 255 (1950).
2. J. L Picqué, Proceedings Second Frequency Standard and Meterology Symposium, (NBS, 1976), P.51.
3. P. Céréz and F. Hartmann, IEEE J. Quantum Elec. QE-13, 344 (1977).
4. H.R. Schlossberg and A. Javan, Phys. Rev. 150, 267 (1966).
5. C.R. Willis, J. Opt. Soc. 60, 921 (1970) and unpublished report.
6. C. Cohen-Tannondji, Ann. Phys. (Paris) 7, 423, 469 (1962).

1979 USAF-~~SCEE~~ SUMMER FACULTY RESEARCH PROGRAM

Sponsored by

THE AIR FORCE OFFICE OF SCIENTIFIC RESEARCH

Conducted by the

SOUTHEASTERN CENTER FOR ELECTRICAL ENGINEERING EDUCATION

PARTICIPANT'S FINAL REPORT

UNSTEADY LAMINAR BOUNDARY LAYERS DUE TO
TRANSVERSE CYLINDER & FREE STREAM OSCILATIONS

Prepared By:

Dennis E. Wilson

Academic Rank:

Assistant Professor

Department and
University:

Department of Mechanical
Engineering, University of SC

Assignment:

Arnold Air Force Station, TN
Arnold Engineering Development
Center

Research
Colleague:

Ching Lo

Date:

July 16, 1979

Contract No:

F49620-79-C-0038

UNSTEADY LAMINAR BOUNDARY LAYERS DUE TO
TRANSVERSE CYLINDER & FREE STREAM OSCILLATIONS

by

D. E. Wilson

ABSTRACT

The purpose of the present investigation is twofold: first, the response of a laminar boundary layer on a circular cylinder to small periodic transverse fluctuations of the free stream velocity is investigated. And secondly, the kinematically similar problem of a periodic transverse oscillation of the cylinder with respect to a steady uniform free stream is considered.

The solution is accomplished by first expanding the stream function in terms of ϵ , where ϵ is the ratio of the transverse velocity component to the undisturbed free stream velocity. The resulting equations are then solved by an asymptotic expansion in terms of the reduced frequency. Due to the singular nature of the perturbation problem, an inner and outer region are defined and the method of matched asymptotic expansions is employed. The result is compared to a numerical solution valid for all frequencies. In addition, an exact solution valid only in the stagnation point region is presented for comparison.

OBJECTIVES

The general objectives for the summer Faculty Research Program were as follows:

- 1.) Investigate the flow field in the neighborhood of cylinder undergoing transverse oscillations with respect to a steady uniform free stream. In addition, the flow field in the neighborhood of a fixed cylinder subjected to an unsteady free stream which contains an equivalent transverse periodic oscillation is investigated.
- 2.) An approximate analytical solution under reasonable restrictions, valid for any geometry should be obtained. This solution should then be checked with known solutions in the stagnation point region or numerical results.

ACKNOWLEDGEMENT

The author would like to thank the Air Force Systems Command, Air Force Office of Scientific Research, and the Southeastern Center for Electrical Engineering Education for providing him the opportunity to spend a most worthwhile and interesting summer at Arnold Air Force Station.

The author appreciates the efforts of Dr. C. F. Lo, of the Propulsion Wind Tunnel Facility for providing both an interesting problem and a pleasant research environment. In addition, the author is grateful for the numerical calculations provided by Dr. H. Burns of the Computational Support Branch.

1.0 INTRODUCTION

In unsteady flow, potential theory has been used quite successfully to describe many important aerodynamic characteristics such as flutter, inlet distortion, and helicopter blade loading. However, the inviscid approach is inadequate for describing detailed features and basic mechanisms present in many unsteady flows. Some examples are: dynamic stall, stall flutter and unsteady separation. In these cases, time-dependent boundary layer theory must be employed to describe a number of unsteady viscous effects such as temporal and spatial phase differences, non-linear streaming, separation delay and viscous damping.

Most studies of unsteady boundary layers have been concerned with the response of laminar incompressible boundary layers to small periodic fluctuations in the free stream. The first substantial effort in this area is due to Lighthill [1] and Lin [2]. With few exceptions, most analysis has concentrated either upon the stagnation point region [3], [4] or flow past a semi-infinite flat plate [5], [6]. In addition, most of these investigations consider the boundary layer response of an oscillating free stream near a fixed body. The statement is then usually made that for incompressible flow the problem is equivalent to one of an oscillating body in the presence of a steady uniform flow [4], [7]. It is the authors contention that this particular statement does not hold in general.

With these factors in mind, the purpose of the present investigation is twofold: first, the response of a laminar boundary layer on a circular cylinder to small periodic transverse fluctuations of the free-stream velocity is investigated. And secondly, the kinematically similar problem of a periodic transverse oscillation of the cylinder with respect to a steady uniform free stream is considered.

The solution is accomplished by first expanding the stream function in terms of ϵ , where ϵ is the ratio of the transverse

velocity component to the undisturbed free stream velocity. The resulting equations are then solved by an expansion in terms of the reduced frequency which is compared to a numerical solution of the same equation. In addition, an exact solution valid only in the stagnation point region is presented for comparison.

2.0 MATHEMATICAL FORMULATION

The basic problem considered in this investigation is that of an unsteady incompressible flow over an infinite circular cylinder. Two distinct situations, as shown in Figure 1, are responsible for the unsteady periodic nature of the flow. First, a uniform flow approaches the cylinder which is oscillating transversely with respect to the free stream, whereas in this second case, the cylinder is fixed in space and the free stream contains an oscillating transverse component.

For the case of an infinite cylinder, the flow will be two-dimensional. The usual boundary layer coordinates are adopted, where x denotes the coordinate parallel to the surface and y is the coordinate normal to the surface. Curvature can be neglected in the analysis through first order as discussed by Gersten [8] and Van Dyke [9].

Defining the stream function, ψ as

$$u \equiv \frac{\partial \psi}{\partial y} \quad \text{and} \quad v \equiv -\frac{\partial \psi}{\partial x}$$

We may write the boundary layer equations as

$$\frac{\partial^2 \psi}{\partial t \partial y} + \frac{\partial \psi}{\partial y} \frac{\partial^2 \psi}{\partial x \partial y} - \frac{\partial \psi}{\partial x} \frac{\partial^2 \psi}{\partial y^2} = \frac{\partial u_e}{\partial t} + u_e \frac{\partial u_e}{\partial x} + \nu \frac{\partial^3 \psi}{\partial y^3} \quad (1)$$

The boundary conditions are simply

$$\frac{\partial \psi}{\partial y} = \frac{\partial \psi}{\partial x} = 0 \quad \text{at} \quad y = 0 \quad (2)$$

and

$$\frac{\partial \psi}{\partial y} \rightarrow U_e(x, t) \quad \text{as} \quad y \rightarrow \infty \quad (3)$$

In Equation (1) and (3), U_e represents the velocity at the edge of the boundary layer which will be determined from potential theory.

2.1 POTENTIAL FLOW AND BOUNDARY CONDITIONS

It has long been recognized [10] that for compressible flow, the two problems: fixed bodies in oscillating flows and oscillating bodies in a steady uniform flow are not equivalent. The discrepancy is due to the inertia term introduced in the boundary layer equations when transforming from the fixed to the oscillating coordinate system. In one case the term is $\rho_\infty(\partial U_e/\partial t)$, whereas, in the other case it is $\rho(\partial U_e/\partial t)$.

A common misconception currently being propagated [4], [7] is that for incompressible flows, ie $\rho = \rho_\infty$, the two problems are equivalent. It is, however, correct to conclude that the equations are identical but the boundary condition for the two problems are not necessarily the same. The original conclusion that the effect of oscillating free stream vs oscillating body produces equivalent equations and, hence, equivalent flow can be traced to Lighthill [1] and Glauert [11]. For the specific problems that they considered both the equations and the boundary condition transform equivalently and, hence, both the mathematical description and the resulting fluid flow are identical. It cannot, however, be generalized to include all incompressible flow situations as will presently be shown.

First, consider the case of a cylinder oscillating transversely in a steady uniform flow. Using potential theory, the outer flow can be determined as follows: let (r, θ) be the polar coordinates of a point with respect to the axes through the center of the cylinder, and let (X_0, Y_0) be the coordinates

of this center with respect to the fixed coordinates, as shown in Figure 2.

The equation of motion for irrotational flow is simply

$$\nabla^2 \psi = 0 \quad (4)$$

The boundary condition is given by

$$-\frac{1}{r} \frac{\partial \psi}{\partial \theta} = \dot{x}_0 \cos \theta + \dot{y}_0 \sin \theta \quad (5)$$

where $v_r = -\partial \psi / \partial \theta$. Following the method described by G. I. Taylor [12] the solution is simply

$$\psi = \frac{R^2 \dot{y}_0}{r} \cos \theta - U_\infty \left(r - \frac{R^2}{r} \right) \sin \theta \quad (6)$$

The circumferential velocity at $r = R$ is then

$$v_\theta(R, \theta) = -\dot{y}_0 \cos \theta - 2U_\infty \sin \theta \quad (7)$$

Denoting this as the edge velocity, U_e , and letting

$\dot{y}_0 = V_0 \cos \omega t$ yields

$$U_e(x, t) = 2U_\infty \sin \phi - (V_0 \cos \phi) \cos \omega t \quad (8)$$

From this, we see that the velocity of the stagnation point is given by

$$U_{s.p.} = -\frac{\omega R}{4U_\infty} V_0 \sin \omega t \quad (9)$$

Next considering an oscillating free stream approaching a fixed cylinder the result is simply

$$U_e(x,t) = 2[U_\infty \sin \phi - (V_0 \cos \phi) \cos \omega t] \quad (10)$$

and the stagnation point velocity is given by

$$U_{s.p.} = - \frac{\omega D}{2U_\infty} V_0 \sin \omega t \quad (11)$$

It should be noted that in both Equations (9) and (10), the restriction of small stagnation point displacement was made so that $\tan^{-1} \phi_{s.p.} \approx \phi_{s.p.}$. This restriction is not included, however, in the expressions for $U_e(x, t)$.

2.2 NONDIMENSIONALIZATION

Before proceeding with the analysis, a set of nondimensional variables must be selected. Two important viscous length scales are involved in this problem. They are δ_S and δ_B , where $\delta_S \sim (\nu/\omega)^{1/2}$ is referred to as the Stokes layer and $\delta_B \sim (\nu/C)^{1/2}$ is the steady boundary layer thickness, or more precisely the Heimenz layer. If there were no steady layer present, the fluctuating part of the flow would extend a distance proportionate to $(\nu/\omega)^{1/2}$ away from the wall. When a steady flow is present and $\omega \sim C$ the two layers are of comparable magnitude and the resulting flow is quite complex. But if the frequency is high $\delta_S/\delta_B \ll 1$ and the fluctuations are confined to a thin Stokes layer near the wall and essentially exist independent of the steady flow. This feature will be exploited later in the high frequency perturbation analysis. For now, we will use δ_B as the characteristic length normal to the wall, and define the following non-dimensional variables.

$$\eta \equiv \frac{y}{(\nu/C)^{1/2}}, \quad \xi \equiv \frac{x}{R}, \quad \hat{t} \equiv \omega t$$

$$\hat{\psi} \equiv \frac{\psi}{(2\nu U_\infty R)^{1/2}}, \quad \hat{U}_e \equiv \frac{U_e}{2U_\infty}, \quad C \equiv \frac{4U_\infty}{D} \quad (12)$$

Substituting Equations (12) into Equation (2) yields

$$\alpha \frac{\partial^2 \hat{\psi}}{\partial \zeta \partial \eta} + \frac{\partial \hat{\psi}}{\partial \eta} \frac{\partial^2 \hat{\psi}}{\partial \zeta \partial \eta} - \frac{\partial \hat{\psi}}{\partial \zeta} \frac{\partial^2 \hat{\psi}}{\partial \eta^2} - \frac{\partial^3 \hat{\psi}}{\partial \eta^3} = \alpha \frac{\partial \hat{u}_e}{\partial \zeta} + \hat{u}_e \frac{\partial \hat{u}_e}{\partial \zeta} \quad (13)$$

with boundary conditions given by

$$\frac{\partial \hat{\psi}}{\partial \eta} = \frac{\partial \hat{\psi}}{\partial \zeta} = 0 \quad \text{at} \quad \eta = 0 \quad (14)$$

$$\frac{\partial \hat{\psi}}{\partial \eta} \rightarrow \hat{u}_e \quad \text{as} \quad \eta \rightarrow \infty \quad (15)$$

The edge velocity for the oscillating cylinder case is now written as

$$\hat{u}_e = \sin \zeta - \left(\frac{V_0}{2U_\infty} \cos \zeta \right) e^{i\tau} \quad (16)$$

In Equation (13) the new parameter, α , appears and is defined as $\alpha = (\omega D)/(4U_\infty)$, and is directly related to δ_B/δ_S .

2.3 SMALL FLUCTUATION EQUATIONS

From the definition of the problem, the fluctuations of the transverse free stream velocity or the cylinder velocity are considered small with respect to U_∞ . This ratio, which appears in Equation (16) is taken quite naturally as the perturbation parameter such that $\epsilon = (V_0)/2U_\infty \ll 1$. The velocity outside the boundary layer is then written as

$$\hat{u}_e(\zeta, \tau) = \hat{u}_0(\zeta) + \epsilon \hat{u}_1(\zeta, \tau) \quad (17)$$

where $\hat{u}_1(\zeta, \tau) = -(\cos \zeta) e^{i\tau}$ for the oscillating cylinder and $\hat{u}_1(\zeta, \tau) = -(2 \cos \zeta) e^{i\tau}$ for the fixed cylinder in an oscillating free stream.

Expanding the stream function as

$$\hat{\psi}(z, \eta, \epsilon; \alpha) = \hat{\psi}_0(z, \eta) + \epsilon \hat{\psi}_1(z, \eta, \epsilon; \alpha) + O[\epsilon^2]$$

we get the following two equations for $\hat{\psi}_0$ and $\hat{\psi}_1$:

$$\frac{\partial \hat{\psi}_0}{\partial \eta} \frac{\partial^2 \hat{\psi}_0}{\partial z \partial \eta} - \frac{\partial \hat{\psi}_0}{\partial z} \frac{\partial^2 \hat{\psi}_0}{\partial \eta^2} - \frac{\partial^3 \hat{\psi}_0}{\partial \eta^3} = \hat{v}_0 \frac{d \hat{v}_0}{dz} \quad (18)$$

and

$$\begin{aligned} \alpha \frac{\partial^2 \hat{\psi}_1}{\partial \eta \partial z} + \frac{\partial \hat{\psi}_0}{\partial \eta} \frac{\partial^2 \hat{\psi}_1}{\partial z \partial \eta} + \frac{\partial^2 \hat{\psi}_0}{\partial z \partial \eta} \frac{\partial \hat{\psi}_1}{\partial \eta} \\ - \frac{\partial \hat{\psi}_0}{\partial z} \frac{\partial^2 \hat{\psi}_1}{\partial \eta^2} - \frac{\partial^2 \hat{\psi}_0}{\partial \eta^2} \frac{\partial \hat{\psi}_1}{\partial z} - \frac{\partial^3 \hat{\psi}_1}{\partial \eta^3} = \\ \alpha \frac{\partial \hat{v}_1}{\partial z} + \hat{v}_0 \frac{\partial \hat{v}_1}{\partial z} + \hat{v}_1 \frac{d \hat{v}_0}{dz} \end{aligned} \quad (19)$$

In addition, the nonhomogeneous terms in Equation (19) imply that $\hat{\psi}_1$ can be written as

$$\hat{\psi}_1(z, \eta, \epsilon) = \chi_1(z, \eta) e^{\alpha \epsilon} \quad (20)$$

When $\epsilon = 0$, the problem reduces to steady uniform flow past a circular cylinder as expected. The solution is given by $\hat{\psi}_0(z, \eta)$ from Equation (18) subject to the following boundary conditions:

$$\begin{aligned} \frac{\partial \hat{\psi}_0}{\partial \eta} = \frac{\partial \hat{\psi}_0}{\partial z} = 0 \quad \text{at} \quad \eta = 0 \\ \frac{\partial \hat{\psi}_0}{\partial \eta} \rightarrow \hat{v}_0 \quad \text{as} \quad \eta \rightarrow \infty \end{aligned} \quad (21)$$

The fluctuating component ψ_1 can then be found by solving Equation (19) subject to the following boundary conditions

$$\begin{aligned} \frac{\partial \hat{\psi}_1}{\partial \eta} = \frac{\partial \hat{\psi}_1}{\partial \zeta} &= 0 & \text{at} & \quad \eta = 0 \\ \frac{\partial \hat{\psi}_1}{\partial \eta} &\rightarrow \hat{v}_1 & \text{as} & \quad \eta \rightarrow \infty \end{aligned} \quad (22)$$

At this point it is necessary to point out a somewhat subtle restriction on the problem to insure that the predominate perturbation to the problem is due to the small free-stream fluctuation, $v_0 e^{i\omega t}$ and not a higher order correction due to the steady streaming created in the boundary layer. Looking at the unsteady pressure term in Equation (13), the condition can be written as $\alpha\epsilon \ll 1$, which implies $U_\infty^2/\omega D \gg v_0$. The parameter $U_\infty^2/\omega D$ represents a characteristic streaming velocity in the boundary layer as first pointed out by Stuart [13]. Using this velocity along with the cylinder diameter to form a Reynolds number we find the usual requirement that

$$R_s = \frac{U_\infty^2}{\omega D} \gg 1 \quad (23)$$

where R_s is usually referred to as the streaming Reynolds number.

Before proceeding with the perturbation analysis, it will be useful to obtain a very elegant exact solution which is not dependent upon any of the parameter, ie α and ϵ , restrictions just enumerated. The solution is, however, limited to the stagnation point region only.

3.0 STAGNATION POINT SOLUTION

In the stagnation point region, ie $\zeta \ll 1$, the edge velocity for the oscillating cylinder case can be written as

$$U_e(\zeta, t) = \zeta - \epsilon e^{i\alpha t} + O[\zeta^2] \quad (24)$$

When $\epsilon = 0$, the solution becomes the classical Hiemenz flow, where $U = \zeta f'(\eta)$. When ϵ is arbitrary, an exact solution, first shown by Galuert [11] and independently by Rott [14] is possible. In this case the equation of motion can be decomposed into a steady nonlinear equation and an unsteady linear equation. The case under consideration is slightly different from that of either Glauert or Rott, but the method is identical.

We begin by writing the stream function as

$$\hat{\psi}(\zeta, \eta, t) = \zeta f'(\eta) - \epsilon \chi(\eta) e^{i\alpha t} \quad (25)$$

where ϵ is now arbitrary. Substituting this expression into Equation (13) we obtain

$$\zeta(f''' + ff' - f'^2 + 1) + \epsilon e^{i\alpha t}(\chi''' + f\chi'' - f'\chi' - i\alpha\chi' + i\alpha + 1) = 0 \quad (26)$$

The first group of terms equals zero so that the equation for χ is simply

$$\chi''' + f\chi'' - f'\chi' - i\alpha\chi' = -i\alpha - 1 \quad (27)$$

with boundary conditions given by

$$\chi(0) = \chi'(0) = 0 \quad \text{and} \quad \chi'(\infty) \rightarrow 1 \quad (28)$$

The solution to Equation (24) was obtained by numerical integration. An approximate solution is also possible for the case of small and large values of α . This is obtained by substituting

$$\chi'(\eta) = \frac{f' - i\alpha + i\alpha\phi}{1 - \alpha} \quad (29)$$

into Equation (24). This transformation gives the following equation for ϕ :

$$\phi'' + f\phi' - f'\phi - i\alpha\phi = 0 \quad (30)$$

$$\phi(0) = 1 \quad \text{and} \quad \phi(\infty) \rightarrow 0 \quad (31)$$

Equation (27) is now identical to Glauert's original equation and the solution is given by a series expansion. Results of the numerical integration are compared with Glauert's series solution in Figure 3 for the oscillating component of the wall shear stress, denoted as $\tau_{\omega,0}$. This is defined as $\tau_{\omega,0} = \mu(\partial U_0 / \partial y)$ where

$$U_0 = -V_0 \chi'(\eta) e^{i\omega t} \quad (32)$$

Using Equation (29), we find that $\tau_{\omega,0}$ is given by

$$\frac{\tau_{\omega,0}}{\rho V_0^2} = - \left(\frac{c_{\mu}}{V_0^2} \right)^{1/2} \chi''(0) e^{i\omega t} \quad (33)$$

Both the real and imaginary part of $\chi''(0)$ are shown in Figure 3 along with the phase angle. The phase angle is defined as the wall shear stress advance relative to the velocity and is the argument of $\chi''(0)$.

For the fixed cylinder placed in an oscillating free-stream, Equation (24) becomes simply

$$\hat{U}_e(s, t) = s - 2\epsilon e^{i\tau} + O[s^2] \quad (34)$$

The solution for $\chi'(u)$ is then identical and the oscillating component of the shear stress is simply twice as large.

4.0 HIGH FREQUENCY SOLUTION

Returning to the small fluctuation equations we seek solutions for $\alpha \gg 1$. For Equation (19) to be valid, we require that $\alpha\epsilon \ll 1$ which implies that $[(\omega D)/(V_0)]\epsilon \gg 1$. But $V_0 = \omega a$, where a is the oscillation amplitude. Using this we see that $(D/a)\epsilon \gg 1$, thus, for $\alpha \gg 1$ we require that the oscillation amplitude go to zero. Under these conditions, the high frequency form of Equation (19) becomes

$$\frac{\partial^2 \hat{\psi}_1}{\partial \eta \partial \tau} = \frac{\partial \hat{U}_1}{\partial \tau}$$

The solution subject to Equation (20) is

$$\hat{\psi}_1 = [-\gamma \cos s + C_2(s)] e^{i\tau}$$

and it is obvious that the boundary condition at the wall cannot be satisfied. This is a classical hallmark of singular perturbation problems and is due mathematically to the order of the differential equation being reduced by one. Physically, the situation is explained by the existence of a thin layer near the wall where the viscous effects are concentrated and the major part of the boundary layer reacts as if it were inviscid to the small fluctuations.

The method of matched asymptotic expansions will now be employed in order to obtain a solution to Equation (19) for $\alpha \gg 1$.

4.1 OUTER SOLUTION

Using Equation (20) in Equation (19) and the boundary conditions for the oscillating cylinder, we obtain the following equation:

$$\begin{aligned} \frac{\partial \hat{\chi}_1}{\partial \eta} = & -\cos \zeta - i\delta^2 \left\{ -\cos 2\zeta + \frac{\partial \hat{\chi}_0}{\partial \zeta} \frac{\partial^2 \hat{\chi}_1}{\partial \eta^2} \right. \\ & \left. + \frac{\partial^2 \hat{\chi}_0}{\partial \eta^2} \frac{\partial \hat{\chi}_1}{\partial \zeta} - \frac{\partial \hat{\chi}_0}{\partial \eta} \frac{\partial^2 \hat{\chi}_1}{\partial \zeta \partial \eta} - \frac{\partial^2 \hat{\chi}_0}{\partial \zeta \partial \eta} \frac{\partial \hat{\chi}_1}{\partial \eta} + \frac{\partial^3 \hat{\chi}_1}{\partial \eta^3} \right\} \quad (35) \end{aligned}$$

with boundary conditions

$$\frac{\partial \hat{\chi}_1}{\partial \eta} = \frac{\partial \hat{\chi}_1}{\partial \zeta} = 0 \quad \text{at} \quad \eta = 0 \quad (36)$$

$$\frac{\partial \hat{\chi}_1}{\partial \eta} \rightarrow -\cos \zeta \quad \text{as} \quad \eta \rightarrow \infty \quad (37)$$

In Equation (35), δ represents the ratio of the Stokes layer to the Hiemenz layer and is defined as

$$\delta \equiv \alpha^{-1/2} = \frac{(\nu/\omega)^{1/2}}{(\nu/c)^{1/2}} \quad (38)$$

Expanding $\hat{\chi}_1(\zeta, \eta)$ in powers of δ as

$$\hat{\chi}_1(\zeta, \eta) = \sum_{n=0}^{\infty} \delta^n \phi_n(\zeta, \eta) \quad (39)$$

and then substituting into Equation (35) we get the following equations for ϕ_n

$$\frac{\partial \phi_0}{\partial \eta} = -\cos \zeta \quad (40)$$

$$\frac{\partial \phi_1}{\partial \eta} = 0 \quad (41)$$

$$\begin{aligned} \frac{\partial \phi_2}{\partial \eta} = -i \left\{ -\cos 2\zeta + \frac{\partial \hat{\Lambda}_0}{\partial \zeta} \frac{\partial^2 \phi_0}{\partial \eta^2} + \frac{\partial^2 \hat{\Lambda}_0}{\partial \eta^2} \frac{\partial \phi_0}{\partial \zeta} \right. \\ \left. - \frac{\partial \hat{\Lambda}_0}{\partial \eta} \frac{\partial^2 \phi_0}{\partial \zeta \partial \eta} - \frac{\partial^2 \hat{\Lambda}_0}{\partial \zeta \partial \eta} \frac{\partial \phi_0}{\partial \eta} + \frac{\partial^3 \phi_0}{\partial \eta^3} \right\} \quad (42) \end{aligned}$$

$$\begin{aligned} \frac{\partial \phi_n}{\partial \eta} = -i \left\{ \frac{\partial \hat{\Lambda}_0}{\partial \zeta} \frac{\partial^2 \phi_{n-2}}{\partial \eta^2} + \frac{\partial \hat{\Lambda}_0}{\partial \eta^2} \frac{\partial \phi_{n-2}}{\partial \zeta} - \frac{\partial \hat{\Lambda}_0}{\partial \eta} \frac{\partial^2 \phi_{n-2}}{\partial \zeta \partial \eta} \right. \\ \left. - \frac{\partial^2 \hat{\Lambda}_0}{\partial \zeta \partial \eta} \frac{\partial \phi_{n-2}}{\partial \eta} + \frac{\partial^3 \phi_{n-2}}{\partial \eta^3} \right\} \quad (43) \\ n > 2 \end{aligned}$$

which are subject to the outer boundary conditions

$$\frac{\partial \phi_0}{\partial \eta} \rightarrow -\eta \cos \zeta \quad \text{as} \quad \eta \rightarrow \infty \quad (44)$$

$$\frac{\partial \phi_n}{\partial \eta} \rightarrow 0 \quad \text{as} \quad \eta \rightarrow \infty \quad (45)$$

The solutions to the first two equations are

$$\phi_0 = -\eta \cos \zeta + C_0(\zeta) \quad (46)$$

$$\phi_1 = C_1(\zeta) \quad (47)$$

Using these two solutions, the equations for ϕ_2 and ϕ_3 become

$$\frac{\partial \phi_2}{\partial \eta} = i \left\{ \sin \zeta (1 \hat{\psi}_{0,11} - \hat{\psi}_{0,1}) - \hat{\psi}_{0,31} \cos \zeta + \cos 2\zeta \right\} \quad (48)$$

$$\frac{\partial \phi_3}{\partial \eta} = -i \left\{ \hat{\psi}_{0,11} C'_1(\zeta) \right\} \quad (49)$$

The solutions are then

$$\phi_2 = i \left\{ \sin \zeta (1 \hat{\psi}_{0,11} - 2 \hat{\psi}_0) - \hat{\psi}_{0,31} \cos \zeta + 1 \cos 2\zeta + C_2(\zeta) \right\} \quad (50)$$

and

$$\phi_3 = -i \hat{\psi}_{0,11} C'_1(\zeta) + C_3(\zeta) \quad (51)$$

Higher order solutions are conceptually straightforward, however, they become quite lengthy, and only solutions through δ^3 are presented.

4.2 INNER SOLUTION

Both the dependent variable and the normal coordinate must be scaled differently in the inner region. Using the Stokes layer as the appropriate scale, we obtain the following:

$$\tilde{\eta} = \frac{\eta}{(2\nu/\omega)^{1/2}} = \eta \alpha^{1/2} = \frac{\eta}{\delta}, \quad \tilde{\zeta} = \zeta$$

$$\tilde{\psi} = \frac{\psi}{2\nu_\infty (\nu/\omega)^{1/2}} = \hat{\psi} \alpha^{1/2} = \frac{\hat{\psi}}{\delta}, \quad \tilde{e} = e, \quad \tilde{v}_e = \hat{v}_e \quad (52)$$

Transforming Equation (19), we get

$$\begin{aligned} \frac{\partial^2 \tilde{\Psi}}{\partial \eta \partial z} - \frac{\partial^3 \tilde{\Psi}}{\partial \eta^3} - \frac{\partial \tilde{U}}{\partial z} &= \delta \left\{ \hat{\Psi}_{0,3} \frac{\partial \tilde{\Psi}}{\partial \eta^2} \right\} \\ &+ \delta^2 \left\{ \tilde{U}_0 \frac{\partial \tilde{U}}{\partial z} + \tilde{U}_1 \frac{d\tilde{U}_0}{dz} - \hat{\Psi}_{0,1} \frac{\partial^2 \tilde{\Psi}}{\partial z \partial \eta} \right. \\ &\left. - \hat{\Psi}_{0,3\eta} \frac{\partial \tilde{\Psi}}{\partial \eta} \right\} + \delta^3 \left\{ \hat{\Psi}_{0,11} \frac{\partial \tilde{\Psi}}{\partial z} \right\} \end{aligned} \quad (53)$$

As before, the stream function may be written as

$$\tilde{\Psi}(z, \eta, z) = \tilde{\chi}(z, \eta) e^{iz} \quad (54)$$

and $\tilde{\chi}(z, \eta)$ can be expanded as

$$\tilde{\chi}(z, \eta) = \sum_{n=0}^{\infty} \delta^n \Phi_n(z, \eta) \quad (55)$$

Before these results are substituted into Equation (53), the coefficients, $\hat{\Psi}_{0,3}$ etc, must be rewritten in terms of the inner variables. In doing this, it is important to remember that the inner solution is obtained by letting $\delta \rightarrow 0$ with $\tilde{\eta}$ fixed. But the coefficients are functions of $\eta = \delta \tilde{\eta}$. Therefore the coefficients should be expanded for small η , and then rewritten in terms of $\delta \tilde{\eta}$. This procedure is outlined next.

The steady state solution, $\hat{\Psi}_0$, is expanded using the Howarth series as

$$\hat{\Psi}_0(z, \eta) = f_0 z + a_2 f_2 z^2 + (a_4 f_4 + a_2^2 f_{22}) z^3 + \dots$$

and the external velocity is written as

$$U_e(z) = z[1 + d_2 z^2 + d_4 z^4 + \dots]$$

Substituting these into Equation (18) yields a series of equations for the f 's similar to f_0 below.

$$f_0''' + f_0 f_0'' + 1 - f_0'^2 = 0$$

$$f(0) = f'(0) = 0, \quad f'(\infty) \rightarrow 1$$

Next expanding each f as $\eta \rightarrow 0$ yields expressions similar to the result for f_0 given below.

$$f_0 = a_1 \frac{\eta^2}{2!} - \frac{\eta^3}{3!} + a_1^2 \frac{\eta^5}{5!} + O[\eta^6]$$

where $a_1 = 1.23259$

The final result for $\hat{\psi}_0$ thru z^5 is then

$$\begin{aligned} \hat{\psi}_0(z, \eta) = & \frac{1}{2} \eta^2 \left[a_1 z + \frac{a_2}{3!} z^3 + \left(\frac{b_2}{5!} + \frac{c_2}{(3!)^2} z \right) z^5 + \dots \right] \\ & + \eta^3 \left[\frac{1}{3!} z + \frac{4}{4!} z^3 + \left(\frac{b}{4!} + \frac{3}{3!} \right) z^5 + \dots \right] \\ & + O[\eta^5] \end{aligned} \quad (56)$$

where $a_2 = 2.8978$, $b_2 = 3.8082$, $c_2 = 0.7150$

Returning to the inner variables, Equation (56) can be written as

$$\tilde{\psi}(z, \tilde{\eta}) = \delta^2 \tilde{\eta}^2 F_2(z) + \delta^3 \tilde{\eta}^3 F_3(z) + O[\delta^5] \quad (57)$$

where $F_2(z)$ and $F_3(z)$ are the terms in brackets.

Now using Equations (54) and (57), Equation (53) can be written as

$$\begin{aligned}
 i \frac{\partial \tilde{\chi}_1}{\partial \eta} - \frac{\partial^3 \tilde{\chi}_1}{\partial \eta^3} = & -i \cos \zeta - \delta^2 \{ \cos 2\zeta \} \\
 & + \delta^3 \left\{ 2F_2 \frac{\partial \tilde{\chi}_1}{\partial \zeta} + \tilde{\eta}^2 F_2' \frac{\partial \tilde{\chi}_1}{\partial \eta} \right. \\
 & \left. - 2\tilde{\eta} F_2 \frac{\partial^2 \tilde{\chi}_1}{\partial \zeta \partial \eta} - 2\tilde{\eta} F_2' \frac{\partial \tilde{\chi}_1}{\partial \eta} \right\}
 \end{aligned} \quad (58)$$

with boundary conditions given by

$$\frac{\partial \tilde{\chi}_1}{\partial \eta} = \frac{\partial \tilde{\chi}_1}{\partial \zeta} = 0 \quad (59)$$

and

$$\lim_{\tilde{\eta} \rightarrow \infty} \left[\frac{\partial \tilde{\chi}_1}{\partial \eta} \right] = \lim_{\eta \rightarrow 0} \left[\frac{\partial \hat{\chi}_1}{\partial \eta} \right] \quad (60)$$

Finally using Equation (55), we get the following equations for Φ_n through third order :

$$\frac{\partial^3 \Phi_0}{\partial \eta^3} - i \frac{\partial \Phi_0}{\partial \eta} = i \cos \zeta \quad (61)$$

$$\frac{\partial^3 \Phi_1}{\partial \eta^3} - i \frac{\partial \Phi_1}{\partial \eta} = 0 \quad (62)$$

$$\frac{\partial^3 \Phi_2}{\partial \eta^3} - i \frac{\partial \Phi_2}{\partial \eta} = \cos 2\zeta \quad (63)$$

$$\begin{aligned}
 \frac{\partial^3 \Phi_3}{\partial \eta^3} - i \frac{\partial \Phi_3}{\partial \eta} = & 2\tilde{\eta} F_2 \frac{\partial^2 \Phi_0}{\partial \zeta \partial \eta} + 2\tilde{\eta} F_2' \frac{\partial \Phi_0}{\partial \eta} \\
 & - 2F_2 \frac{\partial \Phi_0}{\partial \zeta} - \tilde{\eta}^2 F_2' \frac{\partial^2 \Phi_0}{\partial \eta^2}
 \end{aligned} \quad (64)$$

The solutions, subject to the boundary conditions are

$$\Phi_0 = \cos \zeta [-\tilde{\eta} + s^{-1}(1 - e^{-s\tilde{\eta}})] \quad (65)$$

$$\Phi_1 = 0 \quad (66)$$

$$\Phi_2 = \cos 2\zeta [i\tilde{\eta} - s(1 - e^{-s\tilde{\eta}})] \quad (67)$$

$$\begin{aligned} \Phi_3 = 2F_2 \sin \zeta \left[\frac{1}{4}(e^{-s\tilde{\eta}} - 1) - \frac{i}{s}\tilde{\eta} + (i\frac{\tilde{\eta}^2}{4} + s\frac{5}{4}\tilde{\eta})e^{-s\tilde{\eta}} \right] \\ + F_2' \cos \zeta \left[\frac{13}{4}(1 - e^{-s\tilde{\eta}}) - \tilde{\eta}^2 + (\frac{1}{6}s\tilde{\eta}^3 - i\frac{5}{4}\tilde{\eta}^2 - \frac{13s}{4}\tilde{\eta})e^{-s\tilde{\eta}} \right] \end{aligned} \quad (68)$$

where $S \equiv (i)^{1/2} = 1 + i/\sqrt{2}$. As expected, the first term in the expansion, ie, Φ_0 , represents a Stokes wave solution in response to the unsteady pressure term and the second term, Φ_2 , represents a Stokes wave solution to the quasi-steady pressure term.

4.3 COMPOSITE SOLUTION

To determine the unknown constants in the outer solution, we will use the matching principle below.

$$\lim_{\eta \rightarrow 0} X_i^0(\zeta, \eta) = \lim_{\tilde{\eta} \rightarrow \infty} X_i^i(\zeta, \tilde{\eta})$$

This simply states that the inner expansion of (the outer expansion) equals the outer expansion of (the inner expansion).

Neglecting exponentially small terms, the inner expansion can be written in outer variables as

$$\begin{aligned}
\chi^i(s, \eta) \sim & -\eta \cos \zeta + \delta(s^{-1} \cos \zeta) \\
& + \delta^2(i\eta \cos 2\zeta - i\eta^2 F_2' \cos \zeta) \\
& - \delta^3(s \cos 2\zeta + \frac{i}{s} \eta F_2 \sin \zeta) \\
& + O(\delta^4)
\end{aligned} \tag{69}$$

Similarly, the outer expansion can be expanded as $\eta \rightarrow 0$ as

$$\begin{aligned}
\chi^o(s, \eta) \sim & -\eta \cos 2\zeta + C_0(s) + \delta(C_1(s)) \\
& + \delta^2(i\eta^2 F_2 \cos \zeta + i\eta \cos 2\zeta + C_2(s)) \\
& + \delta^3(iC_1'(s) \eta F_2 + C_3(s)) \\
& + O(\delta^4)
\end{aligned} \tag{70}$$

Comparing equal powers of δ we obtain

$$C_0 = 0, C_1 = s^{-1} \cos \zeta, C_2 = 0, C_3 = -s \cos 2\zeta \tag{71}$$

The composite expansion can now be written as

$$\begin{aligned}
\chi^c &= \chi^i + \chi^o - (\chi^i)^o \\
&= \chi^i + \chi^o - (\chi^o)^i
\end{aligned} \tag{72}$$

where $(\chi^L)^0$ is given by Equation (69). The result is

$$\begin{aligned}
 \chi^L = & \delta \left[s^{-1} (1 - e^{-s\tilde{\eta}}) \cos \zeta \right] - \delta^3 \left[s (1 - e^{-s\tilde{\eta}}) \cos 2\zeta \right] \\
 & + \delta^4 \left[2F_2 \sin \zeta \left\{ \frac{1}{4} (e^{-s\tilde{\eta}}) + (i\frac{\tilde{\eta}^2}{4} + s\frac{5}{4}\tilde{\eta}) e^{-s\tilde{\eta}} \right\} \right. \\
 & + F_2' \cos \zeta \left\{ \frac{13}{4} (-e^{-s\tilde{\eta}}) + (\frac{1}{6s}\tilde{\eta}^3 - i\frac{5}{4}\tilde{\eta}^2 - \frac{13s}{4}\tilde{\eta}) e^{-s\tilde{\eta}} \right\} \left. \right] + O[\delta^5] \\
 & + \delta^2 \left[i \sin \zeta (\eta \hat{\psi}_{0,\eta} - 2\hat{\psi}_0) + \hat{\psi}_{0,\zeta} \cos \zeta \right] \\
 & + \delta^3 \left[\hat{\psi}_{0,\eta} \frac{1}{s} \cos \zeta \right] + O[\delta^4]
 \end{aligned} \tag{73}$$

Differentiating Equation (73) with respect to η will yield the ζ component of velocity. Recalling that $\delta(\partial/\partial\eta) = \partial/\partial\tilde{\eta}$, we obtain

$$\begin{aligned}
 u \sim \frac{\partial \chi^L}{\partial \eta} = & -(1 - e^{-s\tilde{\eta}}) \cos \zeta + i\delta^2 \left[(1 - e^{-s\tilde{\eta}}) \cos 2\zeta \right. \\
 & + \sin \zeta (\eta \hat{\psi}_{0,\eta} - \hat{\psi}_{0,\eta}) - \hat{\psi}_{0,\zeta} \cos \zeta \left. \right] \\
 & + \delta^3 \left[2F_2 \sin \zeta \left[(s - i\frac{3}{4}\tilde{\eta} - is\frac{1}{4}\tilde{\eta}^2) e^{-s\tilde{\eta}} - \frac{i}{s} \right] \right. \\
 & + F_2' \cos \zeta \left(-i\frac{3}{4}\tilde{\eta} + is\frac{3}{4}\tilde{\eta}^2 - \frac{1}{6}\tilde{\eta}^3 \right) e^{-s\tilde{\eta}} + i\hat{\psi}_{0,\eta} \cos \zeta \left. \right] + O[\delta^4]
 \end{aligned} \tag{74}$$

Notice in Equation (74) the order of terms neglected is δ^4 , whereas in Equation (73) it is δ^5 and δ^4 . This occurs due to the differentiation with respect to η in the inner region.

The nondimensional wall shear stress can also be obtained by differentiating Equation (74) with respect to η which yields

$$\begin{aligned} \hat{\tau}_0 = & -\frac{S}{8} \cos \zeta + i S \delta \cos 2\zeta \\ & + \delta^2 \left[i \frac{7}{2} F_2 \sin \zeta + i \frac{9}{4} F_2' \cos \zeta \right] + O[\delta^3] \end{aligned} \quad (75)$$

The first two terms can be rewritten using $S = (1 + i)/\sqrt{2}$ as

$$\hat{\tau}_0 = \frac{1}{\sqrt{2}} \left\{ \left(\frac{\cos \zeta}{8} - \delta \cos 2\zeta \right) + i \left(\frac{\cos \zeta}{8} + \delta \cos 2\zeta \right) \right\} + O[\delta^2] \quad (76)$$

Notice that at the stagnation point, $\zeta = 0$, we find that as $\delta \rightarrow 0$, ie $\alpha \rightarrow \infty$, we obtain a phase shift of 45° with respect to the velocity, which is in agreement with the stagnation point solution in Section 3.0. We also obtain the interesting result that at 45° from the stagnation point the phase shift becomes independent of the reduced frequency, at least to second order.

As with the stagnation point solution, the solution for the second case, namely a fixed cylinder placed in an oscillating flow is trivial. The factor of two can be absorbed in ϵ so that both the oscillating velocity and shear stress differ only in magnitude by a factor of two.

5.0 NUMERICAL SOLUTION

A solution of Equation (19) valid for arbitrary α can be accomplished in a variety of ways which fall basically into two categories. First, either a finite difference or finite element solution can be obtained by solving the equation directly. And secondly, a power series expansion in ζ which yields a set of ordinary differential equations in η can be employed.

The first approach is the most direct and in general the most accurate but suffers from large computer storage and time requirements. The second approach can yield accurate solutions for a certain class of problems. Specifically when applied to

boundary layers on blunt bodies, accurate solutions with a minimum of terms are possible. The problem under consideration falls into this category, consequently this approach is adopted for the solution of Equation (19) for $\zeta \leq 1$.

First, Equation (18) is solved by the Howarth series approach. The outer flow is expanded as

$$U_0(\zeta) = \zeta \left(1 - \frac{\zeta^2}{3!} + \frac{\zeta^4}{5!} - + \dots \right) \quad (77)$$

Similarly, the stream function is expanded as

$$\begin{aligned} \hat{\psi}_0(\zeta, \eta) = & f_0(\eta) \zeta + a_2 f_2(\eta) \zeta^3 \\ & + (a_4 f_4(\eta) + a_2^2 f_{22}(\eta)) \zeta^5 \\ & + (a_6 f_6(\eta) + a_2 a_4 f_{42}(\eta) + a_2^3 f_{222}(\eta)) \zeta^7 + \dots \end{aligned} \quad (78)$$

Substituting into Equation (18) yields a series of equations in η , of which the first two are listed below:

$$\begin{aligned} f_0''' + f_0 f_0'' - f_0'^2 + 1 &= 0 \\ f_2''' + f_0 f_2'' - 4 f_0' f_2' + 3 f_0'' f_2 &= 4 \end{aligned}$$

with boundary conditions

$$\begin{aligned} f_0(0) = f_0'(0) &= 0, \quad f_0'(\infty) \rightarrow 1 \\ f_2(0) = f_2'(0) &= 0, \quad f_2'(\infty) \rightarrow 1 \end{aligned}$$

Equation (19) is solved in a similar manner, by first using Equation (20). The right hand side of Equation (19) becomes

$$-i\alpha \cos \zeta + \cos 2\zeta = - \left[(1+i\alpha) - \left(\frac{\zeta^2+1}{2!} \right) \zeta^2 + \left(\frac{\zeta^4+1}{4!} \right) \zeta^4 - + \dots \right] \quad (79)$$

Thus, the stream function, $\chi_1(\zeta, \eta)$ can be written as

$$\chi_1(\zeta, \eta) = b_0 \phi_0(\eta) + b_2 \phi_2(\eta) \zeta^2 + b_4 \phi_4(\eta) \zeta^4 + \dots \quad (80)$$

From the outer boundary condition

$$\frac{\partial \chi_1}{\partial \eta} \rightarrow -\cos \zeta = - \left[1 - \frac{\zeta^2}{2!} + \frac{\zeta^4}{4!} - + \dots \right] \quad (81)$$

we see that

$$b_0 = -1, \quad b_2 = \frac{1}{2!}, \quad \text{etc.}$$

Substituting Equation (79) and (80) into Equation (19) we get for the first two equations

$$\phi_0''' + f_0 \phi_0'' - f_0 \phi_0' - i\alpha \phi_0' = -1 - i\alpha \quad (82)$$

$$\begin{aligned} \phi_2''' + f_0 \phi_2'' - 3f_0' \phi_2' - i\alpha \phi_2' + 2f_0'' \phi_2 = \\ -\zeta + f_2' \phi_0' + f_2 \phi_0'' \end{aligned} \quad (83)$$

with associated boundary conditions given by

$$\phi_0(0) = \phi_0'(0) = 0, \quad \phi_0'(\infty) \rightarrow 1 \quad (84)$$

$$\phi_2(0) = \phi_2'(0) = 0, \quad \phi_2'(\infty) \rightarrow 1 \quad (85)$$

The complete set of equations for ϕ_n was integrated by a Runge Kutta method and typical curves for $\partial\chi_1/\partial\eta$ accurate to $O(\zeta^8)$ are shown in Figure 4. The function $\partial\chi_1/\partial\eta$ is related to the ζ component of velocity by the relation

$$U_1(\zeta, \eta, t) = \frac{\partial\chi_1}{\partial\eta} e^{i\zeta}$$

The outer boundary condition given by Equation (81) represents the case of an oscillating cylinder in a steady uniform free stream. As with the other solutions, the results for the case of a fixed cylinder placed in a free stream with fluctuating flow angularity differs only by a factor of two in magnitude. All other behavior, such as phase shift for the wall shear stress is identical.

Notice that, as expected, the numerical results in this section as $\zeta \rightarrow 0$ agree with the exact stagnation point solution given in Section 3.0.

As a final comparison, Equation (74) can be written at the stagnation point as

$$\begin{aligned} \frac{\partial\chi^c}{\partial\eta} = & -(1 - e^{-1/\beta}) - \beta^2 \left[(1 - e^{-1/\beta}) - f_0' \right] \\ & - \beta^3 \frac{a_1}{2} \left[\frac{3}{4} \left(\frac{1}{\beta} \right) + \frac{3}{4} \left(\frac{1}{\beta} \right)^2 + \frac{1}{6} \left(\frac{1}{\beta} \right)^3 \right] e^{-1/\beta} \\ & + O[\beta^4] \end{aligned} \quad (86)$$

where $\beta \equiv (c/l\omega)^{1/2}$ and $f'_0(\eta)$ is the well known stagnation point solution. This expansion should be the same as the exact solution which is valid only at the stagnation point. It can easily be checked with the stagnation point solution using Equation (29) along with the following expansion for ϕ :

$$\phi = \sum_{n=0}^{\infty} \left(\frac{c}{l\omega}\right)^n \phi_n \quad (87)$$

Equation (87) is substituted into Equation (30) which yields a series of ϕ_n equations which can easily be solved.

The first two such solutions are

$$\phi_0 = e^{-(\frac{l\omega}{c})\eta} \quad (88)$$

$$\phi_3 = -a_1 e^{-\frac{l\omega}{c}\eta} \left[\frac{3}{8} \left(\frac{1}{\beta}\right) + \frac{3}{8} \left(\frac{1}{\beta}\right)^2 + \frac{1}{12} \left(\frac{1}{\beta}\right)^3 \right] \quad (89)$$

The remaining solutions are given by Glavert [11]. Finally expanding Equation (29) and substituting Equation (87) into this expansion yields

$$\chi'(\eta) = (1 - \phi_0) + \beta^2(1 - \phi_0 - f'_0) + \beta^3(-\phi_3) + o(\beta^4) \quad (90)$$

Now substituting Equations (88) and (89) into (90) yields a result that is in exact agreement with Equation (86).

6.0 SUMMARY OF RESULTS

The problem of determining the response of a laminar boundary layer on a circular cylinder to small periodic transverse oscillations of the free stream plus the counterpart, involving periodic transverse oscillations with respect to a steady uniform free stream has been solved. The method of solution involved three basic approaches. First, an exact analysis valid only at the stagnation point, i.e., $\zeta \ll 1$, was presented. Secondly, a high frequency analysis, i.e., $\frac{\omega D}{4V_\infty} \gg 1$, valid for $0 < \zeta < 1$ was presented. And finally, a numerical solution valid for all frequencies and $0 < \zeta < 1$ was conducted.

In all three approaches, the results were the same, namely the oscillating component of velocity and shear stress behaved the same for both cases. The only difference is that for the oscillating free stream-fixed cylinder case, the magnitude of both the oscillating component of wall shear stress and velocity were greater in magnitude by a factor of two. The oscillating component is denoted $\tau_{\omega 1}$, where the total shear stress τ_ω is defined as

$$\tau_\omega = \tau_{\omega 0} + \epsilon \tau_{\omega 1} + O[\epsilon^2].$$

Finally, as discussed in Section 4 and 5 the results for the high frequency solution are shown to be in exact agreement with the exact stagnation point solution when $\zeta \rightarrow 0$. Those results show that the phase shift of the wall shear goes to 45° as $\alpha \rightarrow \infty$.

REFERENCES

1. Lighthill, M. J. "The Response of Laminar Skin Friction and Heat Transfer to Fluctuations in the Stream Velocity." Proc. Royal Society, Vol. 224A, 1954, pp. 1-23.
2. Lin, C. C. "Motion in the Boundary Layer with a Rapidly Oscillating External Flow." Proc. 9th Int. Congress Applied Mechanics, Brussels, Vol. 4, 1956, pp. 155-169.
3. Ghoshal, A. and Ghoshal, S. "Thermal Boundary-Layer Theory Near the Stagnation Point in Three-Dimensional Fluctuating Flow." J. Fluid Mechanics, Vol. 43, Part 3, 1970, pp. 465-476.
4. Ishigaki, H. "Periodic Boundary Layer Near a Two-Dimensional Stagnation Point." J. Fluid Mechanics, Vol. 43, Part 3, 1970, pp. 477-486.
5. Ackerberg, R. C. and Phillips, J. H. "The Unsteady Laminar Boundary Layer on a Semi-Infinite Plate Due to Small Fluctuations in Magnitude of the Free-Stream Velocity." J. Fluid Mechanics, Vol. 51, Part 1, 1972, pp. 137-157.
6. Pedley, T. J. "Two-Dimensional Boundary Layers in a Free Stream which Oscillates without Reversing." J. Fluid Mechanics, Vol. 55, Part 2, 1972, pp. 359-383.
7. Telionis, D. P. "Review - Unsteady Boundary Layers, Separated and Attached." J. Fluid Engr., Vol. 101, 1979, pp. 29-43.
8. Gnersten, K. "Higher Order Boundary Layer Theory." Fluid Dyn. Trans., Vol. 7, Part II, Polish Acad Sci., pp. 7-36.
9. Van Dyke, M. "Higher Approximations in Boundary Layer Theory." Annual Review of Fluid Mech., Vol. 1, 1969, pp. 265-292.
10. Ostrach, S. "Compressible Laminar Boundary Layer and Heat Transfer for Unsteady Motions of a Flat Plate." NACA TN 3569, 1955.

11. Glauert, M. B. "The Laminar Boundary Layer on Oscillating Plates and Cylinders." J. Fluid Mechanics, Vol. 1, 1956, pp. 97-110.
12. Taylor, G. I. "Motion of Solids in Fluids when the Flow Is Not Irrotational." Proc. Roy. Soc., A93, 1917, pp. 99-113.
13. Stuart, J. T. "Double Boundary Layers in Oscillatory Viscous Flow." J. Fluid Mechanics, Vol. 24, Part 4, 1966, pp. 673-687.
14. Rott, N. "Unsteady Viscous Flow in the Vicinity of a Stagnation Point." Quart. Appl. Math., Vol. 13, 1956, pp. 444-451.

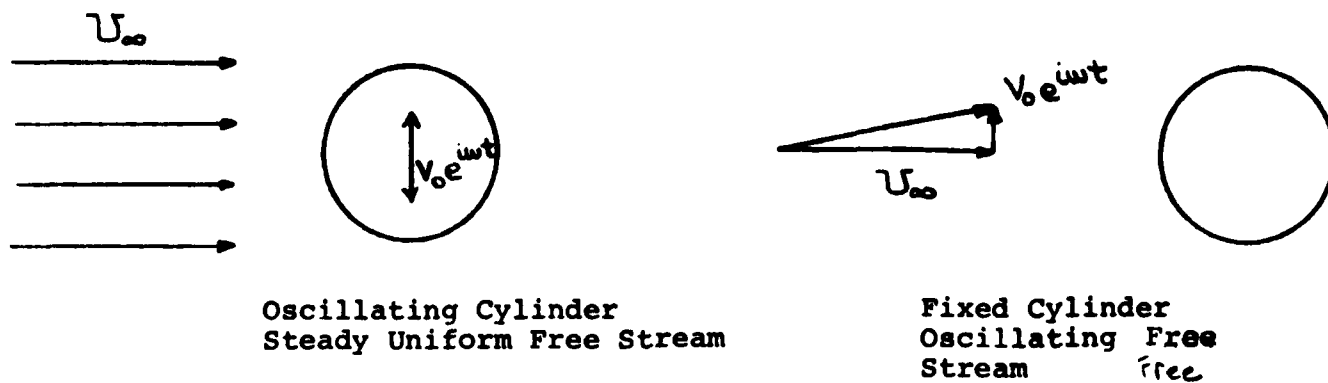


Figure 1

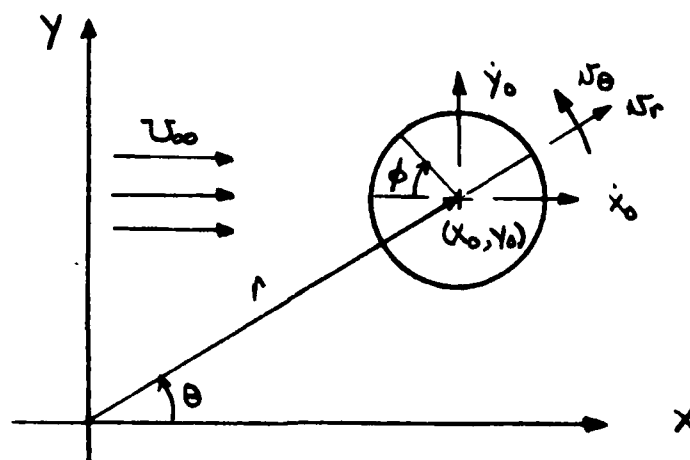


Figure 2. Oscillating Cylinder in Uniform Flow

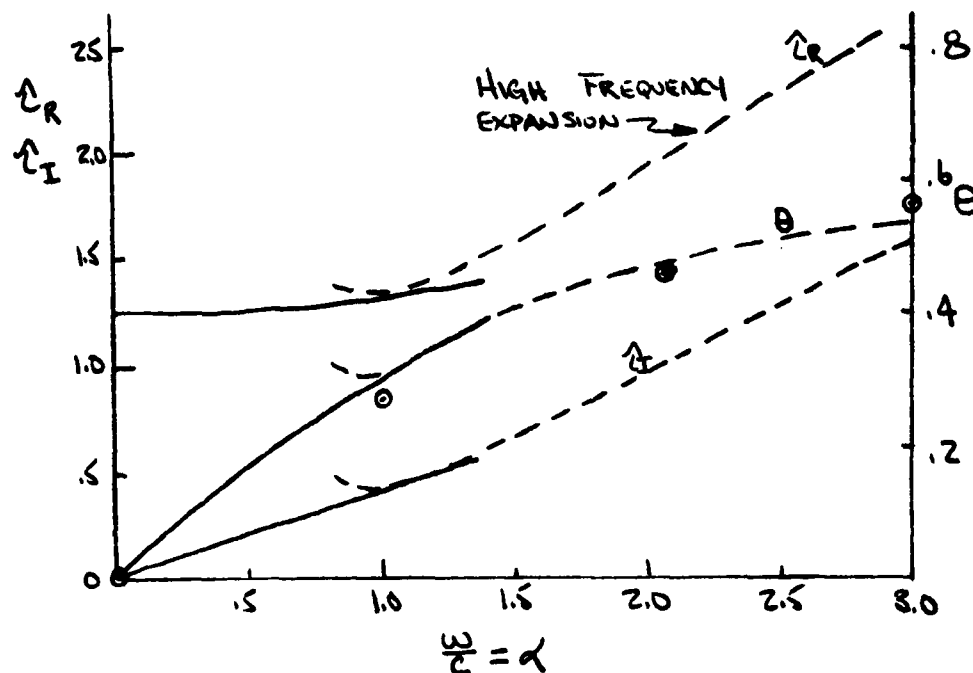


Figure 3. Variation with Frequency of the Real and Imaginary Shear Stress and the Phase Angle θ .

○ NUMERICAL RESULTS

--- HIGH FREQUENCY EXPANSION

— LOW FREQUENCY EXPANSION

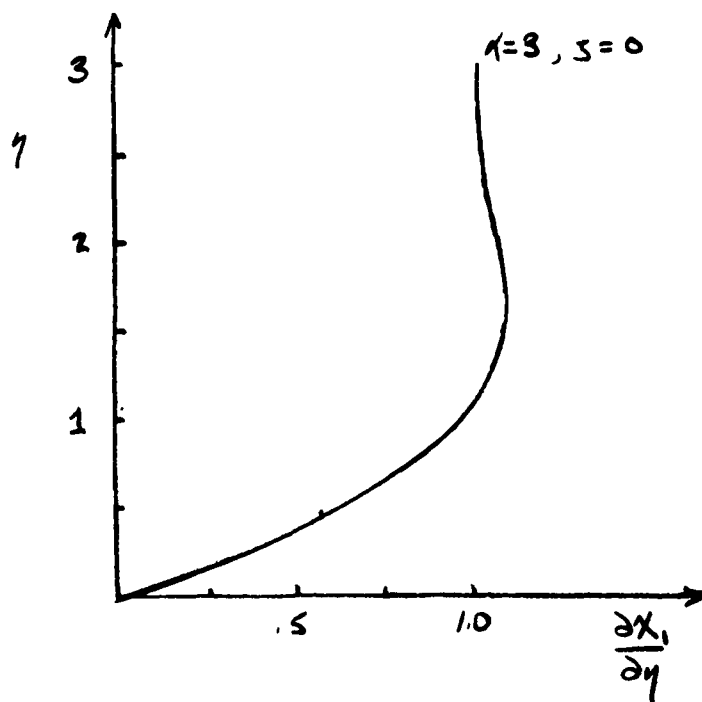


Figure 4. Typical Velocity Profiles.

1979 USAF - SCEEE SUMMER FACULTY RESEARCH PROGRAM

Sponsored by the

AIR FORCE OFFICE OF SCIENTIFIC RESEARCH

Conducted by the

SOUTHEASTERN CENTER FOR ELECTRICAL ENGINEERING EDUCATION

FINAL REPORT

RESPONSE OF AIRFIELD PAVEMENT TO LARGE MAGNITUDE DYNAMIC LOADS

Prepared by:	Gerald A. Woelfl
Academic Rank:	Assistant Professor
Department and University:	Department of Civil Engineering, Marquette University
Research Location:	Air Force Engineering and Services Center/RDCR, Rapid Runway Repair Branch, Tyndall AFB, Florida
USAF Research Colleague:	Robert Van Orman
Date:	September 10, 1979
Contract No:	F49620-79-C-0038

RESPONSE OF AIRFIELD PAVEMENT TO LARGE
MAGNITUDE DYNAMIC LOADS

by

Gerald A. Woelfl

ABSTRACT

The evaluation of rapidly repaired bomb damaged runways requires determining the dynamic response of pavement due to large dynamic loads. This report recommends using one of the sophisticated computer codes currently available for a conventional static analysis of airfield pavements, but with the use of appropriate dynamic material properties to predict the dynamic response of pavement. In order to select the appropriate dynamic material properties, the stress variation as a function of time is developed for pavements subjected to moving wheel loads. A review of the literature indicates that the elastic properties and fatigue strength of Portland Cement Concrete are relatively the same for dynamic as for static loading. The dynamic response of asphalt concrete, granular base and subbase material, and subgrade soil, however, is significantly improved relative to the response of these materials to static loads. Further, the dynamic behavior of granular material is time-independent, but for asphalt concrete and subgrade soils, especially cohesive soils, the dynamic properties vary with aircraft velocity, i.e., rate and duration of loading. Recommendations for further research in this area are also given.

ACKNOWLEDGEMENT

The author would like to thank the Air Force Systems Command and the Air Force Office of Scientific Research for providing him with the opportunity to spend a most worthwhile summer at Tyndall Air Force Base. The author would also like to thank the Southeastern Center for Electrical Engineering Education, and in particular Dr. Richard Miller, for a well organized program.

Special acknowledgement is also due those at the Air Force Engineering and Services Center at Tyndall for their cooperation and assistance, and for providing a pleasant working environment.

The author is especially indebted to Mr. Robert Van Orman, Lt Col Roger Caldwell, Capt Michael McNerney, and Phillip Nash for their continuous encouragement and guidance and for numerous helpful discussions.

Finally, the author would like to thank Marquette University, and in particular Prof. William Murphy, for encouragement and support in this rewarding endeavor.

I. INTRODUCTION:

The design and analysis of airport pavements is based on static wheel loads. But measurements of landing gear forces during various aircraft modes of operation have shown that pavements are subjected to dynamic loads of higher magnitude than the static load. Traditionally, because of the relatively slow response of pavement materials, these higher magnitude dynamic loads were neglected in pavement design. Field observations have reinforced the use of static load for pavement design. Areas of airfield pavements subjected to static and low speed modes of aircraft operation generally show more distress than areas of runways limited to medium and high-speed aircraft operations.

The objective of the Air Force's Rapid Runway Repair program is to repair a 50 ft. by 5,000 ft. section of bomb damaged runway as rapidly as possible. Because of the limited length of the repaired runway, it is unlikely that it will be subjected to static aircraft loadings. For this reason the structural design and analysis of rapid runway repairs are based on the results of field tests using an aircraft load cart at creep speeds of about 2 to 3 mph (1).

Because of the time constraints for rapid runway repair, the repaired runway section will have considerably more surface roughness than conventionally constructed airport pavements. This increased surface roughness will yield unusually high magnitude dynamic loads during various aircraft modes of operation - up to 2.5 times the static wheel load for main landing gears and even higher for the nose gear. Current research efforts in the Air Force Bomb Damage Repair program concentrate on the effects of these high magnitude dynamic loadings to the aircraft structure, aircraft payload, and pilot performance. The response of the pavement to these high magnitude dynamic loads, however, must also be investigated.

Specifically, the structural adequacy of the repaired runway subjected to medium and high speed aircraft taxi modes must be eval-

uated from the results of field tests using load carts at creep speeds.

The problem is: most field test programs conducted to evaluate the performance of airfield pavements have been limited to static and creep-speed loadings; field tests which have included higher aircraft speeds have been limited to relatively smooth surfaces and therefore high magnitude dynamic loads were not encountered; and, field testing on rough surfaces (bomb damaged repaired runways) has for the most part been limited to aircraft response.

II. OBJECTIVES

The purpose of this report is to develop an approach to predict the performance of rapid runway repairs subjected to high magnitude dynamic aircraft loads caused by the unusual surface roughness of rapidly repaired runways.

Because of time limitations and the broad scope of the topic, this study is confined to the following objectives:

1. Review the results of recent field tests addressing the response of airfield pavements to dynamic loads.
2. Define an analytical approach for evaluating the performance of airfield pavements subjected to high magnitude dynamic loading.
3. Describe pavement stresses as a function of time due to moving wheel loads.
4. Discuss the dynamic behavior of pavement materials.

III. RECENT FIELD TESTING

Because of growing concerns over detrimental effects of dynamic loads on airport pavements the Federal Aviation Administration (FAA) sponsored a study entitled "Aircraft Dynamic Wheel Load Effects on Airport Pavements" by Wignot, et al dated May 1970 (2). The study included analysis of both aircraft and pavement dynamic responses, and scaled pavement tests.

This initial FAA study raised many questions concerning the response of pavement to dynamic loads. As a result, the FAA sponsored an extensive experimental study conducted by the U.S. Army Engineer Waterways and Experiment Station (WES) during the period from May, 1971 to January, 1975 and described in a three volume report en-

titled "Pavement Response to Aircraft Dynamic Loads" (3,4,5). The purpose of this study was to determine the relationship between responses of flexible and rigid runway pavements to static and dynamic loads. The study used data from instrumented aircraft on instrumented sections of both flexible and rigid pavements.

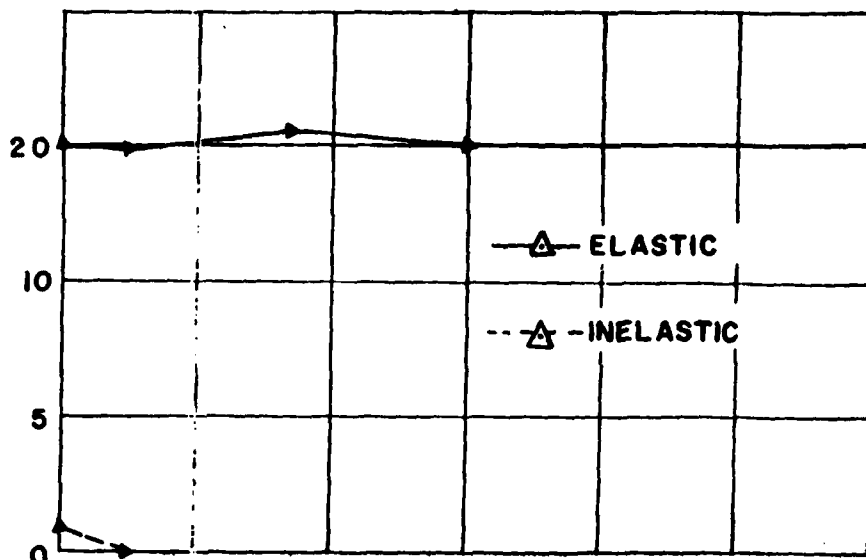
In addition to static tests, the WES investigation dealt with a number of aircraft modes of operation. Both aircraft and pavement measurements were recorded during creep-, slow-, medium-, and high-speed taxiing, high-speed breaking, high-speed breaking with reverse thrust, takeoff rotation, touch down, and turning.

For the study, gages were installed in flexible and rigid pavement test sections to measure pavement responses to dynamic loads in the form of relative displacements and pressures at various depths and locations within the pavement structure. A total of 162 gages were installed in the flexible test section and 153 gages were installed in the rigid pavement section. A series of tests were conducted on both pavement sections during cold weather when the pavement surface layer temperatures ranged from 35 to 55°F; an additional series of tests were conducted on the flexible pavement test section during hot weather when the pavement surface layer temperatures ranged from 84 to 116°F.

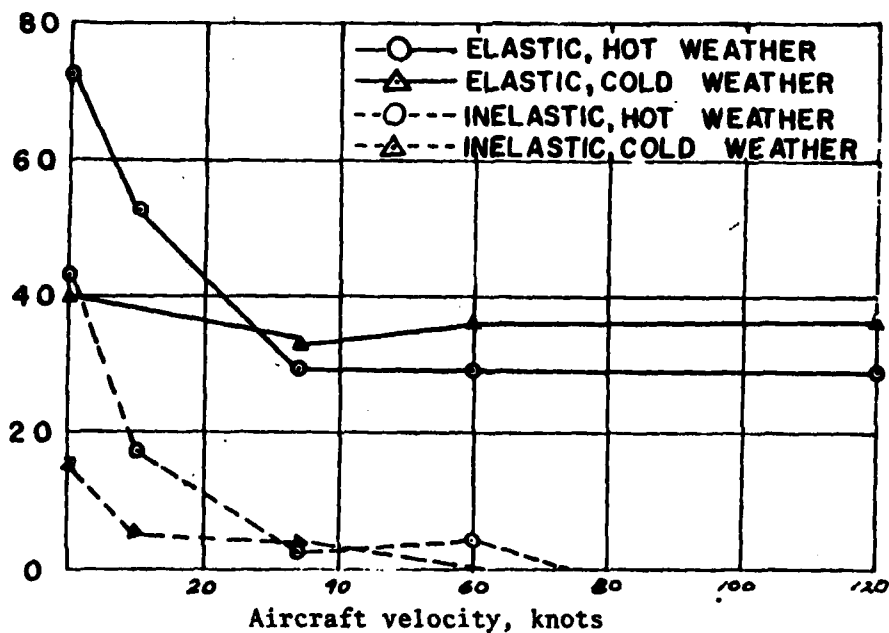
The interpretation of results relied on separating the data into an elastic phase and an inelastic phase. Inelastic displacements are residual displacements remaining after the wheel had passed. If loads were repeatedly applied on the same wheel path, the pavement would become "conditioned" and the inelastic displacements would be permanent after a few initial repeated loadings. However, aircraft traffic loading is randomly distributed, in actual use airfield pavements never become totally conditioned and therefore inelastic displacements are not permanent, but occur continuously throughout the life of the pavement. For this reason the WES tests used a distributed traffic pattern as does the rapid runway repair testing at Tyndall Air Force base.

Figure 1 summarizes results for the taxi tests at various air-

Displacement between 0 to 15 ft. depth, 10^{-3} in.



a. - rigid pavement



b. - flexible pavement

Figure 1. - Maximum elastic and inelastic vertical relative displacements between 0 to 15 ft. depth versus velocity.

craft velocities for both rigid and flexible pavements. The maximum elastic and inelastic surface displacements are shown separately.

The elastic displacements for rigid pavement and for flexible pavement at cold temperatures remained relatively constant, being independent of aircraft speed. Elastic displacements for the flexible pavement at higher temperatures, however, decreases considerably as aircraft velocity increases. This elastic response of pavements relative to aircraft speed, type of material, and for asphalt, material temperature, correlates well with elastic material properties. The modulus of elasticity of concrete changes little with rate of loading. The complex modulus of asphalt, however, varies with the frequency of the applied load (and therefore with rate and duration of loading); as the frequency increases, the modulus increases. For asphalt concrete at low temperatures, frequency has much less effect on the modulus whereas, at high temperatures, the modulus increases substantially with an increase in frequency. Material behavior is discussed in more detail in section VI of this report.

Figure 1 shows that the rigid pavement had little inelastic behavior. Therefore, predicting the response of rigid pavement to aircraft at various speeds from pavement response to creep-speed loads simplifies to an elastic analysis providing the proper elastic material properties are used in the analysis.

From figure 1, flexible pavement shows considerable inelastic behavior, especially at the higher temperature. However, since this inelastic behavior decreases rapidly with aircraft velocity, an elastic analysis, with appropriate material properties, can be used to predict the response of flexible pavements for various aircraft speeds based on the results of creep speed taxi tests. Heukelom and Klomp (6) states the Road Research Laboratory concluded that flexible roads behave elastically under vehicles moving at speeds exceeding 15 mph, and probably also at lower speeds.

The WES study showed that "... no basic aircraft ground operating mode induced pavement responses (elastic plus inelastic) greater than those occurring for static load conditions..." However, the

flexible and rigid runways used for the investigation were relatively smooth. The vertical gear loads varied from .45 to 1.25 times the static load for creep through high speed taxi modes for the flexible hot weather tests. For the cold weather tests, main and nose gear loads varied from .55 to 1.20 times the static load for flexible pavement and .35 to 1.25 times the static load for rigid pavement.

The Air Force is currently conducting an extensive field test program referred to as "Have Bounce" (7). The Have Bounce program utilizes instrumented aircraft operating at various speeds on runways repaired with various configurations of AM-2 mats. The repaired runway has unusually high surface roughness since the top surface of the mats are about 1 1/2 inches above the pavement surface. A short ramp is used for the transition from pavement surface to mat surface.

Preliminary data from the first phase of the Have-Bounce testing program indicates that the vertical dynamic main gear loads are as much as 2.5 times the static aircraft weight because of the increased surface roughness. Nose gear loads were as high as 3 times the static main gear loads, but since static nose gear loads are considerably less than main gear loads, main gear loads are the critical loads for design. Although the WES study did not investigate high magnitude dynamic loads, Ledbetter concludes:

"The larger than static load response that could occur should be entirely elastic and should not be detrimental to the pavement structure except by contributing to an increase in elastic fatigue damage."

But the above conclusion is based on test results of conventionally constructed airfield pavements. Rapid runway repairs differ from conventional pavements, however, in that repair techniques do not provide for sufficient compaction of the subgrade in the repaired area. Therefore, high magnitude loads at faster aircraft speeds may produce larger inelastic displacements than inelastic displacements resulting from creep-speed load cart tests.

The high magnitude dynamic loads resulting from surface roughness are not constant, but rather periodic. Preliminary data from

the Have Bounce investigation showed main gear loads had a frequency between 1.8 to about 2.03 Hz. The frequency varied with aircraft gross weight but was relatively independent of aircraft velocity.

A similar type of oscillation was noted by Yang during creep-speed load cart tests at Newark Airport (8). The instrumented test pavement consisted of asphalt concrete on various granular bases. The fundamental frequency of the loading vehicle simulating a Boeing 747 ranged from 1.6 to 2.0 Hz.

A frequency of about 2 Hz was visually observed for the F-4 load cart used for rapid runway repair field testing at Tyndall Air Force Base. The F-4 load cart used at Tyndall, as well as the load cart used for the Newark testing, had no shock absorber except the damping of the pneumatic tires.

IV. DYNAMIC ANALYSIS OF PAVEMENT

There are many failure criteria used in the evaluation of air-field pavements but for structural analysis of pavement systems, material failure is the only controlling factor. It must be emphasized, however, that material failure in itself does not constitute failure of the pavement system. Material failure as pavement failure criteria may be too conservative for conventionally constructed pavements since a cracked pavement may be acceptable to the user, provided the riding surface is satisfactory. Parker, et al (9) report that rigid pavements with high-strength foundations continued to satisfactorily carry loads after cracking, but that rigid pavements with low-strength foundations developed multiple cracking and differential displacements (increased surface roughness) soon after initial cracking. Because most rapid runway repair methods being considered involve low-strength foundations, the use of material failure is probably more realistic than for conventionally constructed pavements.

From the standpoint of structural analysis of pavements, the two material failure criteria currently used are rupture failure due to a few loads of excessive magnitude and fatigue failure due to repeated loads. Because of the unusual surface roughness of rapidly re-

paired runways, the pavement would be subjected to repeated high magnitude loads and therefore pavement evaluation should be based on fatigue failure rather than rupture failure. Specifically, stresses and strains within the pavement structure should be compared with limiting fatigue values which are based on the expected number of load repetitions. Assuming inelastic pavement response plays a minor role in the dynamic response of pavements, an elastic analysis can be used to determine the pavement stresses and strains.

The problem of computing dynamic stresses and strains due to a moving wheel load has been solved for a plate on a Winkler foundation and for a plate on an elastic halfspace (2). But even with the sophisticated computational techniques currently available, the solution of the problem requires a number of simplifying assumptions regarding structural behavior and material properties.

Another approach to determine dynamic pavement response is to simplify the dynamic load by treating it as a static load and using dynamic material properties for the analysis. With this approach, more realistic results are obtained since material properties and structural behavior can be more accurately modeled. The main objection to using a static analysis with appropriate dynamic material properties is that inertia effects are ignored. Mass and damping effects have generally been neglected in pavement design since only high speed or high frequency dynamic loads would cause inertia effects to influence dynamic pavement response.

Heukelom, Klomp, and Foster have studied the influence of mass and damping of pavement systems on the dynamic response of highway pavements (6,10,11). They found that mass and damping have hardly any influence on the stresses which are generated in a pavement on a good subgrade (i.e., excluding peat) under actual traffic loading. Consequently, they conclude that the application of static theories is justified provided that dynamic values of the material properties are used.

The FAA sponsored study (2) included an analysis of mass effects on airfield pavements which showed that inertia forces at taxi speeds

as high as 230 mph have little influence on dynamic pavement response. The study also concludes that if the dynamic load has a frequency below about 10 Hz (aircraft taxi mode loadings are limited to frequencies of 1 to 5 Hz), inertia effects are negligible.

Considering the approximations made for input data required for pavement analysis, it can be concluded that ignoring inertia effects has little influence on the accuracy of results.

In summary, the dynamic performance of pavements can be evaluated by using the expected maximum magnitudes of dynamic loads as static loads and performing a conventional static analysis using appropriate dynamic material properties. This approach makes use of finite element computer programs, such as the Air Force computer code PREDICT (12), which have been developed for pavement analysis (PREDICT has the potential for doing a complete dynamic analysis which includes inertia effects, but this part of the program has not been developed). The resulting stresses and strains from such an analysis would then be compared to limiting fatigue values which take into account dynamic loading.

V. PAVEMENT STRESS VARIATION AS A FUNCTION OF TIME FOR DYNAMIC LOADS

Although the response of pavement is not very sensitive to mass and damping effects, the response is sensitive to material properties which in turn depend on duration of load and rate of loading. Before material properties can be discussed, therefore, pavement stress as a function of time must be described for a pavement subjected to a moving wheel load of oscillating magnitude.

Pavement stress variation with time can be determined by visualizing the stress distribution due to a static load as moving through the pavement with time. For example, Figure 2b shows the stress distribution which would be expected for horizontal stress at the bottom of a rigid pavement slab due to a static wheel load. Assume the stress distribution can be approximated with a half cosine function:

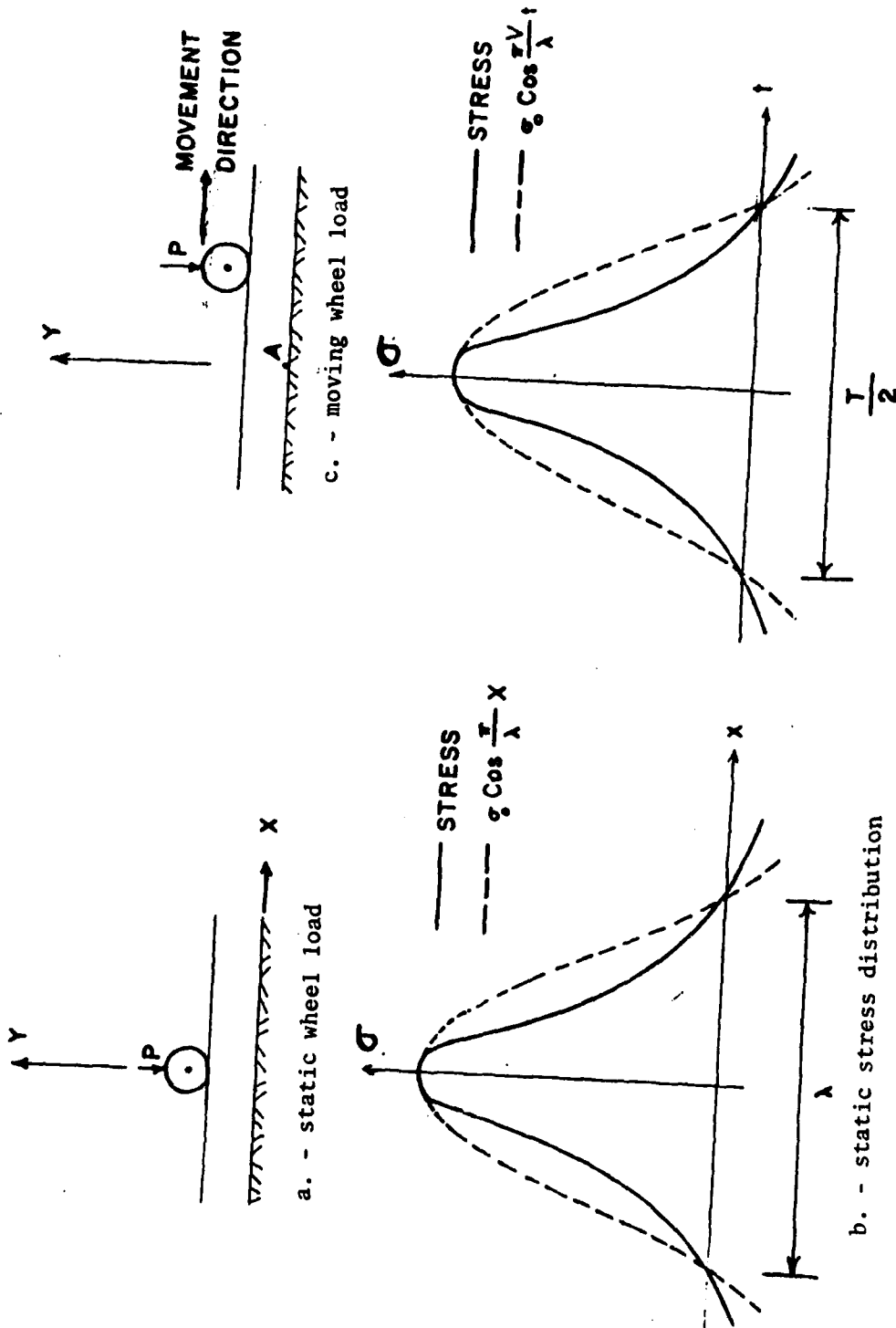


Figure 2. - The relationship between static stress distribution and stress as a function of time for a moving wheel load

$$\sigma_x = \sigma_0 \cos \frac{\pi}{\lambda} x \quad (1)$$

$$\text{for } -\frac{\lambda}{2} < x < +\frac{\lambda}{2}$$

where σ_0 = maximum stress directly under the wheel

λ = half the wave length (the distance between points of inflection of the slab)

The stress distribution could be more accurately described by a Fourier series, but for purposes of this report, the above approximation is sufficient.

The half-wavelength, as defined for this report, is the distance between points of inflection of the slab and is a function of the characteristic length (plate rigidity and subgrade stiffness (8,13)) of the plate and the dimensions of the tire footprint. Since the dynamic response of the tire is relatively instantaneous (tire pressure remains constant), the tire footprint dimensions will be a function of aircraft landing gear configuration and magnitude of the wheel load. Trial runs using the Air Force computer code PRE-DICT gave values for λ of between 2 and 20 ft. for an F-4 aircraft at various gross weights on an 8 inch thick concrete pavement on various subgrades. Yang (8) observed the distance between points of inflection to be 12 ft. for various thicknesses of asphalt concrete pavements on different bases. Ullidtz (22) approximates the half-wavelength for flexible pavement as the footprint length plus the thickness of asphalt concrete.

The important point is that the half-wavelength, λ , and the maximum stress, σ_0 , directly under the wheel can be determined from a static stress analysis of the pavement structure. As will be shown, this is all that is needed to describe the stress as a function of time.

For a moving wheel load, the static stress distribution can be visualized as moving through the pavement system with time; ie, for a given point, such as point A shown in figure 2c, the stress will vary with time as shown in figure 2d. Actually, because of horizon-

tal forces induced by moving wheel loads, the stress variation with time curve would be nonsymmetric; this effect is not included in this report. These horizontal forces could be included in a static stress analysis, but the problem is that the sophisticated computer codes currently available are limited to axisymmetric loading.

To transform stress as a function of distance to stress as a function of time, assume constant velocity (aircraft acceleration would cause negligible nonsymmetry in the stress as a function of time curve). Then

$$V = \frac{\lambda}{t} \quad (2)$$

where V = aircraft velocity in ft/sec

and

$$\sigma_t = \sigma_0 \cos \frac{\pi V}{\lambda} t \quad (3)$$

for

$$-\frac{\lambda}{2V} < t < +\frac{\lambda}{2V}$$

where σ_0 = maximum stress at $t = 0$, i.e., when the wheel load is directly over Point A

The duration of load (for this report, the duration of the main stress pulse will be referred to as the duration of load) is simply one-half the period, or

$$\frac{T}{2} = \frac{\lambda}{V} \quad (4)$$

So far a constant load has been used but as stated earlier, for rough surfaces the load is periodic. The stress under the wheel load, σ_0 , is a function of time as shown in figure 3a. For the critical case when the periodic load is a maximum at $t = 0$, ie, when the maximum wheel load is directly over point A, σ_0 can be expressed by

$$\sigma_0 = \sigma_s + \sigma' \cos 2\pi f t \quad (5)$$

where

σ_s = stress due to static aircraft load

σ' = additional increase or decrease of stress with time

f = frequency of wheel load

The stress variation with time for point A is then:

$$\sigma_t = (\sigma_s + \sigma' \cos 2\pi ft) \cos \frac{\pi V}{\lambda} t \quad (6)$$

for

$$-\frac{\lambda}{2V} < t < +\frac{\lambda}{2V}$$

Inspection of equation 6 shows that the duration of load is the same as for equation 3 and as calculated in equation 4. As shown in figure 3, the term in parenthesis in equation 6 merely alters the wave shape of the stress as a function of time curve. For medium and high aircraft speeds, $2\pi f$ will be less than $\frac{\pi V}{\lambda}$ and the change in wave shape becomes negligible. Therefore little error is introduced if equation 3 is used provided that the maximum stress resulting from the maximum magnitude dynamic load is used for σ_0 , ie,

$$\sigma_t \approx \sigma_0 \cos \frac{\pi V}{\lambda} t \quad (3)$$

where

$$\sigma_0 = \sigma_s + \sigma'$$

To determine the rate of loading, the first derivative of stress as expressed in equation 3 would be taken with respect to time. However, since the rate of stress application changes with time, this is not a good parameter to work with. If the wave-shape and duration of loading are used for determining material properties, then the rate of loading will automatically be incorporated.

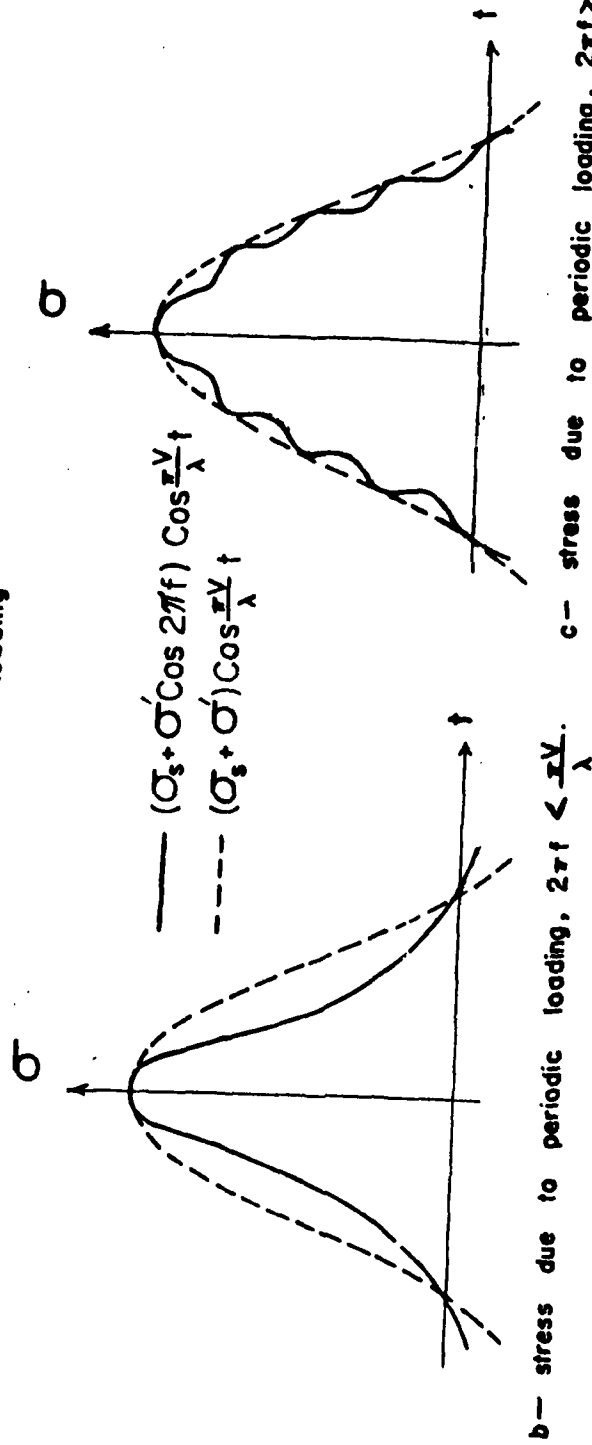
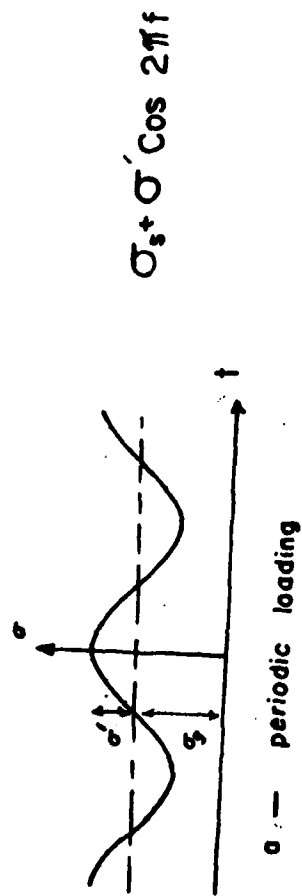


Figure 3. - Pavement stress as a function of time due to a periodic moving wheel load

VI. DYNAMIC RESPONSE OF PAVING MATERIALS

The structural adequacy of pavement subjected to high magnitude loads at medium and high aircraft speeds must be evaluated on the basis of results from creep-speed field tests. As aircraft speed increases, the average rate of loading increases and duration of load decreases. The purpose of this section is to determine the influence of rate of loading and duration of load on the elastic properties and the fatigue life of pavement materials.

There is an enormous amount of literature available on the dynamic behavior of pavement materials. This section is by no means a complete review of the literature, however it does provide a guide for selecting appropriate dynamic material properties for dynamic pavement evaluation.

Portland Cement Concrete

Most materials when loaded have a time-dependent response, and concrete is no exception. The work of several investigators on the effects of rate of loading on the behavior of concrete was reviewed by McHenry and Shideler (14). Figure 4 shows the influence of rate of

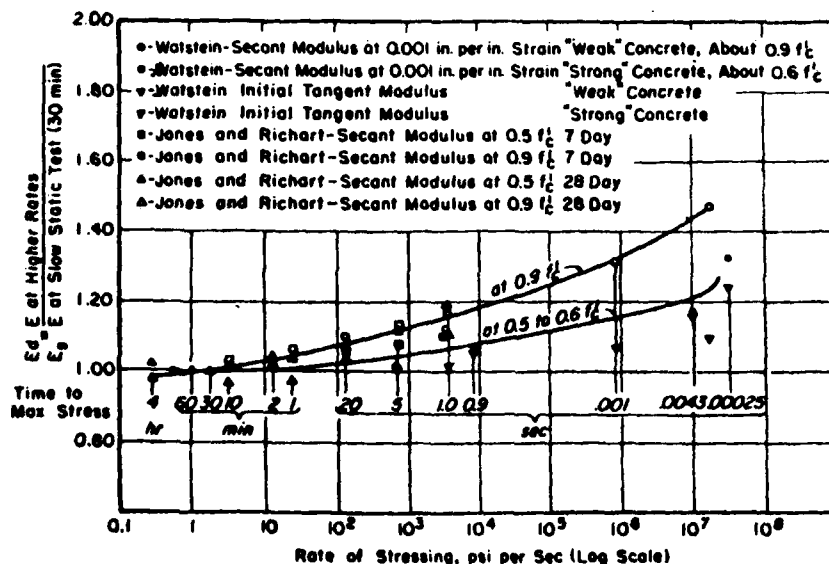


Figure 4 - Effect of Rate of Stressing on the Modulus of Elasticity of Concrete (after McHenry (14)).

loading on the modulus of elasticity and indicates that the modulus increases with an increasing rate of loading. The lower values of moduli at slower rates of loading were attributed to creep of the concrete.

For pavements subjected to moving wheel loads, the rate of loading varies as a function of time. If the average rate of loading is approximated from the maximum stress divided by half the duration of loading as expressed in equation 4, then the expected rate of loading due to a moving wheel load would range from about 200 to 100,000 psi/sec (assuming maximum stress equals 450 psi, the half-wavelength is 5 ft., and aircraft velocity varies from 3 to 150 mph). From figure 4, a 20% increase for the modulus of elasticity of PCC might be expected for high aircraft velocities. But since the rate of loading varies with time, and in fact approaches zero at the higher stress levels, the increase in modulus as aircraft velocity increases from creep to high speed would be considerably less than 20%. Considering the variation of modulus of elasticity with other factors (mix proportions, aggregate properties, type of test used to determine the modulus, etc.), the relatively small increase, perhaps 10%, in modulus which could be expected as a result of high speed wheel loads is negligible.

Chou's (15) review of pavement materials indicates that Poisson's ratio of PCC has a range of about 0.11 to 0.22 when determined from static tests, and the results of dynamic tests averaged about .24. Since Poisson's ratio of PCC has very little effect on the response of rigid pavements, using a value of .2, which is generally used for traditional static analysis, seems reasonable for dynamic analysis as well.

The compressive strength, tensile strength, and modulus of rupture of PCC increase with an increase in rate of loading. Cowell (16) found that for a rate of loading of 100,000 psi/sec, the compressive strength increase ranged from 10% to 30%, depending on mix proportions and maturity of the concrete, as compared with the static strength. Similarly the increase in tensile strength ranged from 30%

to 50% for a loading rate of 100,000 psi/sec. Results of impact tests on POC by Lundeen (17,18) showed an average ratio of dynamic to static strength of 1.36 for compression, 1.74 for tension, and 2.46 for the modulus of rupture. A rupture failure of concrete from high magnitude loads at medium and high aircraft speeds seems unlikely.

Since the compressive, tensile, and rupture strengths of concrete vary with rate of loading, it would seem that fatigue performance would also be time-dependent. Chou (15), summarizing the results of several studies, indicates that frequencies of the repeated load (and hence rate of loading) between 70 and 900 repetitions per minute had no effect on fatigue strength, but frequencies as low as 10 repetitions per minute may result in slightly lower fatigue lives. The load pulse associated with ten repetitions per minute corresponds to the load pulse of an aircraft at creep to slow taxi speeds.

The type of repeated loading used in fatigue tests may simulate traffic loading on highway pavements, but the type of repeated loading on airport pavements is quite different. For airport pavements subjected to aircraft taxi loads, loading is of short duration but very low frequency; ie, the loading cycle is made up of a short load pulse followed by a relatively long rest period. Chou (15) reports of fatigue testing which included periodic rest periods, ie, a rest period of 1, 5, 10, etc. minutes after every 4500 load repetitions. In general it was found that rest periods were beneficial. A five minute rest period resulted in a 10% increase in fatigue strength; longer rest periods did not yield any further increase in fatigue strength but shorter rest periods did show smaller increases.

Fatigue tests which include an appropriate rest period within each loading cycle were not found (at least by this author) in the literature. Fatigue performance may be quite different if a rest period were included in each load cycle.

In conclusion, the elastic constants for concrete to be used in an analysis of the response of pavement to moving wheel loads should be the same as those currently used for a traditional static analysis.

Also, based on the current literature, no increase in fatigue strength can be assumed for concrete pavements subjected to dynamic loads. Fatigue testing should be done, however, to determine if the fatigue performance of concrete is improved when the repeated load cycle includes an appropriate rest period.

Polymer Concrete

Since polymer concrete is a relatively new material, there is little literature available on the dynamic behavior of the material. Creep tests have shown that the behavior of polymer concrete is more time-dependent than PCC (19) and therefore the modulus of elasticity should be determined using dynamic methods. The effect of rate of loading on the modulus of rupture of polymer concrete is also needed as well as fatigue testing incorporating various load durations and rest periods.

Asphalt Concrete

Although asphalt concrete is not currently being considered for rapid runway repairs, runways which may have to be repaired are asphalt concrete or have asphalt concrete overlays. The undamaged portions of the runway surrounding the repairs will be subjected to high magnitude dynamic loads due to increased surface roughness.

Unlike PCC, the stiffness of asphalt concrete changes dramatically with dynamic loadings. The response of asphalt concrete can be separated into a time-dependent component and an instantaneous component. For short duration dynamic loads, the response is primarily elastic.

Green (20) reports of several studies which showed that the elastic modulus of asphalt concrete wearing surfaces is highly dependent on loading frequency. For example, at loading frequencies of 1, 4, and 16 Hz, the moduli were 370,000, 570,000, and 770,000 psi respectively. There are a number of nomographs available to determine the stiffness of asphalt concrete for various loading times (6, 15, 21).

No information could be found for the effects of rate and duration of loading on Poisson's ratio. However, Poisson's ratio of the asphalt concrete surface layer has little influence on the response

of flexible pavements.

The fatigue life of asphalt concrete depends on the rate of loading, duration of load, loading frequency, and the inclusion of a rest period in the loading cycle. These variables are interdependent and therefore it is difficult to discuss the effects of each of them individually. The most recent literature review on the fatigue life of asphalt concrete is that by Decker (21).

The loading waveform used for fatigue testing has an influence on fatigue life. Decker reports that specimens subjected to a square-waveform loading had less than half the fatigue life of identical specimens loaded sinusoidally, whereas the use of a triangular waveform loading resulted in a 45% increase in fatigue life as compared to sinusoidal loading. Frequency and maximum stress amplitude were held constant for the test. The square-waveform loading has the fastest rate of loading but the maximum stress is applied for the entire load cycle whereas the maximum stress is only applied for an instant for the triangular loading. The duration of the higher magnitude portion of the load apparently dominates the behavior.

As previously pointed out, actual loading of airport pavements includes a relatively long rest period as part of the loading cycle. Decker reports on a number of fatigue studies which included a rest period within each load cycle. In general, the longer the rest period, the higher the fatigue life until a maximum beneficial rest period is reached. Further lengthening of the rest period beyond this maximum beneficial period has no influence on fatigue life. This maximum beneficial rest period is a function of stress magnitude, load period, and temperature. In most cases the rest period included in actual aircraft loadings of airfield pavements probably exceeds the maximum beneficial rest period.

In a study to determine the effects of frequency of loading on the fatigue life of asphalt concrete, Decker reports of testing for which the ratio of load duration to rest period was held constant while the frequency varied from about 1 to 40 Hz. The fatigue life

for the loading frequency of 40 Hz was almost 200 times longer than the fatigue life at 1 Hz frequency loading. However, the rate of loading increased, while the duration of load and rest period decreased as frequency increased. Because of this interdependence of variables, frequency of loading is not a good parameter to use.

The most accurate representation of stresses due to a moving wheel load was made by Van Dijk, et al (as reported by Decker). The shape of the load pulse consisted of a large tensile pulse between two small compressive pulses followed by a rest period. The length of rest period was varied and as it increased, the fatigue life increased considerably. Again, the importance of rest periods was demonstrated.

However, to determine the influence of aircraft speed on fatigue life of asphalt concrete airfield pavements, what is needed is fatigue tests to determine the effect of load duration. The loading cycle should be similar to Van Dijk's with a constant rest period (equal or greater than the maximum beneficial rest period). This would best simulate actual field loadings.

In summary, there's reason to believe that the increased stiffness and fatigue life of asphalt concrete associated with medium and high aircraft speeds probably offset the higher magnitude loads due to surface roughness. However, this would have to be verified by a parametric study and possibly fatigue testing as described above.

Granular Material

The modulus of elasticity of granular materials determined from dynamic tests is generally higher than the modulus determined from static tests. This is perhaps best illustrated by the fact that the dynamic moduli measured for soils by the NDT van developed by the Air Force are "corrected" prior to using these values for static pavement evaluation (12). Specifically, the correction for flexible pavements consists of dividing the dynamic moduli of granular base and subgrade material by 2 to get equivalent static moduli. (The same correction is done for asphalt concrete, but for PCC the mea-

sured values are used directly since there is little difference between the dynamic and static moduli.)

Although the dynamic modulus is significantly higher than the static modulus, the dynamic modulus for clean sands and gravels appears to be independent of load duration and rate of loading. Apparently a slow deformation (creep phenomenon) develops in the course of a static test; once testing is in the dynamic range, however, the response of the material is no longer time-dependent. Allen (as reported by Chou (15)) found that the resilient response of well-graded granular materials is independent of stress duration, and concludes that any pulse duration in the range of those applied to pavements by wheel loads moving at speeds of 15 to 70 mph could be used for testing. Wignot, et al, (2) also conclude that the dynamic behavior of granular materials is relatively independent of duration and frequency of loading.

Parker, et al, (9) have developed a laboratory procedure for determining the resilient modulus and Poisson's ratio using a cyclic triaxial test. The procedure uses a repetitive stress state similar to that encountered in a base course layer in a pavement structure under a moving wheel load. The recommended load duration of 0.1 to 0.2 sec (haversine wave form) corresponds to aircraft speeds of about 30 to 120 mph (depending on λ); the recommended cycle duration of 3 sec. provides a rest period between stress pulses.

Since it is impossible to duplicate field conditions in the laboratory, field measurements for dynamic modulus and Poisson's ratio are preferred. (This is especially true for rapid runway repair since unconventional construction methods are used.) Field vibratory testing techniques for determining the dynamic modulus of elasticity and Poisson's ratio are referenced by Chou (15).

Vibratory testing does not directly simulate aircraft traffic loads since the latter are separate load pulses whereas the former uses a sustained vibration. Mass and damping effects have more influence for sustained vibration but become insignificant for single pulse loadings. However, Keukelom and Foster (11) have shown that

the modulus measured from sustained vibrations is equal to the modulus associated with traffic loadings within 20%. Several investigators have shown good correlations between field measured strains under moving wheel loads and computed strains using dynamic material properties measured from field vibratory testing techniques (15,20, 9).

Based on extensive field tests, Heukelom and Klomp (6) developed a correlation between the dynamic modulus and CBR as

$$E \text{ (in psi)} = 1500 \text{ CBR} \quad (7)$$

The use of equation 7 is not recommended however, since computed dynamics moduli can range from 50% to as high as 200% of the actual measured values. Chou (15) suggests that the poor correlations between dynamic modulus of elasticity and CBR is because the CBR test produces plastic as well as elastic responses. Similarly, static plate bearing test results cannot be used for dynamic evaluation of pavements.

In summary, the dynamic modulus of granular materials is relatively independent of rate and duration of loading. If possible, field testing should be used to determine the dynamic modulus and Poisson's ratio.

Subgrade Soils

The dynamic response of cohesive and cohesionless subgrade soils is similar to granular materials in that the dynamic modulus is considerably higher than the modulus measured from static tests. For example, Parker, et al, (9) reported static moduli of 1850 and 1600 psi as compared to resilient moduli of 7,500 and 13,000 psi for a high-plasticity clay and low-plasticity clay respectively.

But cohesive soils differ from granular soils in that dynamic moduli are sensitive to rate and duration of loading. Wignot, et al (2) reports test results for the complex modulus of a silty clay subgrade at different loading frequencies. At 90% saturation, the complex moduli of the soil were 2,000, 3,500 and 6,200 psi at frequencies of 0.16, 1.6, and 16 Hz respectively. For cohesionless soils, fre-

quency of loading has less influence on the modulus.

Parker, et al, (9) developed a laboratory test to determine the resilient modulus and Poisson's ratio for subgrade soils. The test is similar to the one briefly discussed for granular soils. Instead of using the load duration and frequency given by Parker, it is suggested that these be varied since subgrade soils are sensitive to frequency of loading. In this way, test results can be used to determine pavement response for different aircraft speeds.

Since the modulus and Poisson's ratio of the subgrade have such a strong influence on pavement response, field testing is preferred over laboratory testing. This is especially true for rapid runway repairs since the condition of the subgrade is so variable (uncompacted bomb damage debris). Field vibratory testing, as referenced by Chou (15) and briefly discussed for granular materials, can provide the dynamic modulus and Poisson's ratio.

VII. CONCLUSIONS

Based on the results of this investigation, the following conclusions are noted:

1. The response of stiff pavements, i.e., rigid pavements and flexible pavements at low temperatures, is primarily elastic; flexible pavement at higher temperatures exhibits significant inelastic as well as elastic behavior at slow aircraft speeds, but the inelastic behavior becomes insignificant at higher aircraft speeds. Large dynamic loads, however, may yield significant inelastic responses at higher aircraft velocities due to lack of compaction in the subgrade.
2. A static analysis can be used to obtain the response of pavement for dynamic loadings if appropriate dynamic moduli and limiting fatigue values corresponding to dynamic loading are used for material properties in the analysis. The mass and damping effects are not included using this method but it has been shown that these effects have little influence on dynamic pavement response.
3. Based on the literature cited, the modulus of elasticity, Poisson's ratio, and the fatigue strength of Portland Cement concrete are relatively independent of rate and duration of loading and therefore, the usual static values for these properties would be used for a dynamic analysis. However, since the modulus of rupture of concrete is substantially

higher for faster rates of loading, a rupture failure of concrete pavement due to large dynamic loads at medium and high aircraft speeds is unlikely.

4. The increased stiffness and longer fatigue life of asphalt concrete for medium and high aircraft speed loadings probably offset the larger magnitudes of these loadings occurring due to surface roughness. However, this should be verified by a dynamic evaluation of flexible pavement.
5. The properties of granular base and subbase materials should be determined from dynamic testing since static tests would yield values too low for dynamic pavement analysis. The dynamic properties, however, are relatively insensitive to rate and duration of loading; i.e., the response of these materials would not be dependent on aircraft velocity.
6. The response of subgrade soil, especially cohesive soils, depends on aircraft speed. Therefore, the elastic properties of the subgrade must be determined at various loading frequencies (i.e., various rates and durations of loading) to determine dynamic pavement response associated with various aircraft speeds.

VIII. RECOMMENDATIONS

1. A parametric study must be undertaken to determine the influence of dynamic loads of various magnitudes at various aircraft speeds on the response of pavements. Using the approach outlined in this report, one of the sophisticated computer codes (such as PREDICT) currently available can be used. Design curves must then be developed which would not only be useful for predicting pavement response for large dynamic loads but would also be of benefit in designing and analyzing rapid runway repairs for the creep-speed field test program.
2. Because of the unusual nature of the subgrade for rapid runway repairs (uncompacted bomb damage debris) and because the behavior of the subgrade plays such a dominant role in the response of pavement, field tests must be conducted to determine the dynamic properties of the subgrade. Dynamic properties of the subgrade are needed to determine the response of pavement to large dynamic loads at higher aircraft speeds, and also to provide for more accurate design and analysis for the creep-speed field test program. The literature survey must be continued before specific field testing can be recommended.

3. The dynamic properties and fatigue strength of polymer concrete must be determined. For fatigue testing, the load cycle should incorporate an appropriate rest period in order to accurately simulate traffic loading on airfield pavements. (Similarly, fatigue testing which includes a rest period in each loading cycle should also be done for Portland Cement Concrete.)
4. This report has not addressed the influence of horizontal loads on the dynamic response of pavements. Since the horizontal wheel loads increase with aircraft velocity, they probably have a strong influence on the dynamic response of pavement at higher aircraft speeds.

REFERENCES

1. Baker, J. E., et al., "Bomb Damage Repair New Concept Study," AFESC/RDCR, Tyndall AFB, Florida, June 1979.
2. Wignot, J. E., et al., "Aircraft Dynamic Wheel Load Effect on Airport Pavements," Report No. FAA-RD-70-19, Federal Aviation Administration, Washington, D. C., May 1970.
3. Horn, W. J. and Ledbetter, R. H., "Pavement Response to Aircraft Dynamic Loads; Volume I: Instrumentation Systems and Testing Program," Report No. FAA-RD-74-39-I, Federal Aviation Administration, Washington, D. C., June 1975.
4. Ledbetter, R. H., "Pavement Response to Aircraft Dynamic Loads; Presentation and Analysis of Data; Appendix B: Data," Report No. FAA-RD-74-39, Vol II, September 1975, Federal Aviation Administration, Washington, D. C., and Technical Report S-75-11, Vol II, U. S. Army Engineer Waterways Experiment Station, CE, Vicksburg, Miss., September 1975.
5. Ledbetter, R. H., "Pavement Response to Aircraft Dynamic Loads; Vol III; Compendium," Report No. FAA-RD-74-39-III, Federal Aviation Administration, Washington, D. C., November 1975.
6. Heukelom, W., and Klomp, A.J.G., "Road Design and Dynamic Loading," Proc. Assn. Asphalt Paving Tech., Vol. 33, 1964.
7. Redd, L. T., and Borowski, R., "Have Bounce Phase I Test Results," Report No. AFFTC-TR-79-1, April 1979.
8. Yang, N. C., "Design of Functional Pavements," McGraw-Hill Book Company, New York, 1972.
9. Parker, F., et al., "Development of a Structural Design Procedure for Rigid Airport Pavements," Report No. FAA-RD-77-81, Federal Aviation Administration, Washington, D. C., April 1979.
10. Heukelom, W., "Analysis of Dynamic Deflections of Soils and Pavements," Goetechnique 11, 1961.
11. Heukelom, W. and Foster, C. R., "Dynamic Testing of Pavements," Journal of the Structural Division, Proc. ASCE 86, February, 1960.
12. Nielsen, J. P. and Baird, G. T., "Pavement Evaluation System," Report No. CERF AP-20, Eric H. Wang Civil Engineering Research Facility, Albuquerque, New Mexico, August, 1976.
13. Timoshenko, S. and Woinowski-Krieger, S., "Theory of Plates and Shells," McGraw-Hill Book Company, New York, 1959.

14. McHenry, D. and Shideler, J., "Review of Data on Effect of Speed in Mechanical Testing of Concrete," Symposium on Speed of Testing of Non-Metallic Materials, ASTM Symposium Special Technical Publication No. 185, June 29, 1955.
15. Chou, Y. T., "Engineering Behavior of Pavement Materials; State of the Art," Report No. FAA-RD-77-37 (also designated TR S-77-9, U. S. Army Engineer Waterways Experiment Station), Federal Aviation Administration, Washington, D. C., February, 1977.
16. Cowell, W., "Dynamic Properties of Plain Portland Cement Concrete," Report No. R447, Naval Facilities Engineering Command, U. S. Naval Civil Engineering Laboratory, Port Hueneme, California, June 1966.
17. Lundeen, R. L., "Dynamic and Static Tests of Plain Concrete Specimens," Miscellaneous Paper 6-609, Report No. 1, U. S. Army Engineer Waterways Experiment Station, CE, Vicksburg, Miss., November, 1963
18. Lundeen, R. L., "Dynamic and Static Tests of Plain Concrete Specimens; Phase II: Flexure and Triaxial Compression," Miscellaneous Paper 6-609, Report No. 2, U. S. Army Engineer Waterways Experiment Station, CE, Vicksburg, Miss., November 1964.
19. McNerney, M., "An Investigation Into the Use of Polymer-Concrete for Rapid Repair of Airfield Pavements," Report No. CEEDO-TR-78-10, Air Force Systems Command, Tyndall Air Force Base, Florida, January, 1978.
20. Green, J., "Literature Review - Elastic Constants for Airport Pavement Materials," Report No. FAA-RD-76-138, Federal Aviation Administration, Washington, D. C., March 1978.
21. Decker, D. S., "Predicting the Fatigue Life of Flexible Airfield Pavements - A Recommended Approach," Report No. CEEDO-TR-79, Air Force Systems Command, Tyndall Air Force Base, Florida, June, 1979.
22. Ullidtz, P., "Computer Simulation of Pavement Performance," Report No. 18, The Institute of Roads, Transport and Town Planning, The Technical Institute of Denmark, Lyngby, Denmark, 1978.

1979 USAF - SCEE SUMMER FACULTY RESEARCH PROGRAM

Sponsored by the

AIR FORCE OFFICE OF SCIENTIFIC RESEARCH

Conducted by the

SOUTHEASTERN CENTER FOR ELECTRICAL ENGINEERING EDUCATION

FINAL REPORT

ANALYSIS OF THE ROLE OF HIGH BRIGHTNESS
ELECTRON GUNS IN LITHOGRAPHY

by

John Wolfe

Assistant Professor

Department of Electrical Engineering

University of Houston - Central Campus

Research Location

Air Force Avionics Lab/AFAL/DH, Wright Patterson AFB

USAF Research Colleague

John M. Blasingame

September 1, 1979

Contract No.: F49620-79-C-0038

ANALYSIS OF THE ROLE OF HIGH BRIGHTNESS
ELECTRON GUNS IN LITHOGRAPHY

BY

JOHN C. WOLFE

ABSTRACT

The development of reliable, high brightness, temperature-field (TF) emission electron guns promises greater flexibility in electron beam lithography. Detailed pattern analysis of two IC mask sets was performed for the purpose of identifying those areas of electron beam lithography where high brightness guns could be applied to advantage. Significant throughput advantages can be realized in both VSS Vector Scanning Systems and in ultra-high speed Raster Scanning Systems.

ACKNOWLEDGEMENTS

Sponsorship of this work by the Air Force Systems Command, Air Force Office of Scientific Research and the Air Force Avionics Laboratory is gratefully acknowledged.

It is a pleasure to thank John Blasingame, Bryan Hill, Jim Skalski and Bob Werner of AFAL, Wright-Patterson AFB for their assistance and interest in this work. Thanks are also due the members of AFAL/DH and AFAL/DHE for their kind hospitality during the author's stay during the summer of 1979. Many useful discussions with J. Edmond Wolfe are gratefully acknowledged.

I. INTRODUCTION

The ultimate goal of the tri-service very high speed integrated circuit (VHSIC) program is the fabrication of VLSI circuits with $1/2\mu\text{m}$ minimum feature size. The attainment of this goal will certainly require development of a scanning electron beam lithography machine with this capability. Throughput is a major concern for such fine-line VLSI circuits.

Reliable, high brightness electron guns have been developed in recent years at Burroughs Corporation (1) and at the Oregon Graduate Center (2) since the original patent of Wolfe et al. (3) typical beam current densities of $1000\text{--}2000\text{ A/cm}^2$ have been reported (1,2). This should be compared with typical densities of 150 A/cm^2 and 50 A/cm^2 in systems with LaB_6 (4) and W (7) thermionic cathodes, respectively.

II. OBJECTIVES

The objectives of this project was:

To evaluate design problems in electron beam lithography machines which would be developed under the VHSIC program.

III. A. Throughput Considerations in Vector-Scan Lithography:

In the vector-scan approach to electron beam lithography (c.f. ref 5), the mask patterns are first divided into primitive patterns (sometimes called "shapes"). These can be squares, rectangles, trapezoids, parallelograms, etc., depending upon the level of sophistication of the lithography machine. The type, location, size, exposure level or other information about a primitive pattern can be described by a few words of code (usually less than six, sixteen bit words). The codes describing each of the myriad primitive patterns in the mask are stored in the core memory of the system computer. When a particular pattern is to be exposed, the code for its execution is transferred to a "pattern generator" which directs the electron beam to the designated location and exposes, in raster fashion, the primitive pattern.

The design of pattern generators has been evolving for several years toward the goal of higher throughput. The most significant advance has been the variable shaped spot (VSS) idea (c.f. ref. 6,7). In early pattern generators, the finest lines of the pattern were exposed by raster scanning a gaussian beam with a diameter of $1/4$ of the minimum line width for fill-in. In the VSS approach, the smallest lines are filled in by stepping a rectangular beam with exactly the width of the line. Larger rectangles are used for wider lines. Since the exposure time per spot is independent of spot size, the economy is apparent. Other shapes can also be made available (e.g. trapezoids). The more versatile the pattern generator, the more flexible can be the circuit design rules.

Overhead refers to the time required to execute a lithographic pattern which is not actually used in resist exposure. Overhead includes wafer loading, stage slewing and wafer alignment. These functions together contribute (5) about 1 sec/wafer level/cm² if alignment is done once per square

centimeter sized block and 4" wafers are used. There are two types of overhead associated with the pattern generator itself. We call these "pattern overhead" and "line overhead."

A. Pattern Overhead (PO) is the average time interval between the termination of a pattern and the initiation of the next. There are four sources of pattern overhead: 1) Data transfer time from the input buffer of the pattern generator to various control registers; 2) Data computation time; 3) Eddy current decay times; and, 4) DAC settling times. Numerical values for the components of pattern overhead have appeared in the literature (5,8). In reference (5) a total pattern overhead of 3.3 μ sec has been reported. Pattern overhead as low as 1 μ sec may be attainable.

B. Line Overhead (LO) is the average time interval between termination of a line and initiation of the next within the same primitive pattern. In the IBM VSI machine (8) line overhead was the limiting factor. The source of line overhead was the slow data transfer rate to the digital counters and steppers which control line writing. In an analog fill-in pattern generator, line overhead is accounted for by the time required to turn the beam around at the end of a line. If electrostatic deflection is used for fill-in (vectoring would have to be electromagnetic) line overhead may be reduced to .1 μ sec. If a pattern contains only one line there is no line overhead.

III. B. Sample Circuit Characteristics:

Two circuits were analyzed. The first was an RCA 256 X 4 CMOS/SOS RAM (RCA TCS072). The circuit is made up entirely of rectangular patterns oriented on orthogonal axes. The minimum line width is 5 μ m. The circuit has 7 levels. The second circuit is an ECL Multifunction Arithmetic Array designed by AFAL/Hughes and fabricated under AFAL contract by signetics. This circuit is made up of rectangular patterns oriented on orthogonal axes and

parallelograms oriented at 45° to the rectangle axes. The minimum linewidth is $5\text{ }\mu\text{m}$. The circuit has 11 levels. The design rule of both circuits could be implemented by the VSS system described by Pfeiffer (6).

III. C. Mask Pattern Analysis:

The mask patterns were first decomposed (with pencil and ruler) into a minimum number of primitive patterns. These were all rectangles for the RCA circuit but included also slanted parallelograms (as indicated above) for the AFAL/Hughes/signetics circuit. Rectangles were classified as to length and width modulo units of twice the minimum line width. For example, a width was classified as n units wide if it was between $2(n-1)$ and $2n$ times the minimum line width. Slanted parallelograms could be classified as one unit wide and their lengths were classified as for the case of rectangles. An $n \times m$ ($n \leq m$) shape was then said to contain n -line and $n \cdot m$ spots. The total numbers of patterns, lines and spots obtained in this way for each wafer level can be identified with the number of patterns, lines and spots which a VSS system would have to execute to expose the level if the spot were continuously variable in both directions for rectangles and in the long direction for slanted parallelograms from one to two times the minimum line width.

The pattern, line and spot statistics were determined over the active area of all wafer levels with the exception of the bonding pads (see below).

The grand total of patterns, lines and spots for all levels (pads excepted) were calculated for each circuit, divided by the chip active area in cm^2 and multiplied by the area scaling factor (100, in this case) required to reduce the minimum line width to the VHSIC goal of $.5\text{ }\mu\text{m}$. The numbers P of patterns, L of lines and S of spots thus obtained would be the totals required for a VSS system with a $.5\text{-}1\text{ }\mu\text{m}$ variable spot to execute all levels of a chip constructed by scaling down each circuit to have $.5\text{ }\mu\text{m}$ minimum line width and

placing them side-by-side to form a 1 cm x 1 cm VLSI chip. Although these statistics do not refer to a functional circuit it is believed by the author that a fair simulation of fine-line VLSI pattern statistics has been obtained.

Bonding pads should not, of course, be scaled (they were not). In fact they can be neglected in a throughput analysis. One can expose 1000 4 x 4 mil bonding pads in 1 sec for an exposure time of .1 μ sec per spot. This is a negligible amount of the total write time for the chip (see below).

The analysis was repeated for .5-2 μ m and .5-4 μ m variable spot size. The results are summarized in Table 1 for the RCA circuit and in Table 2 for the AFAL/Hughes/signetics circuit. The following definitions are used.

P = number of patterns/cm² (all levels)

L = number of lines/cm² (all levels)

S = number of spots/cm² (all levels)

Throughput Analysis of Composite Chips:

We shall now estimate the throughput for the chips with the pattern statistics obtained above.

We shall take the total time T required to expose all levels of the chip as the measure of throughput. We have,

$$T = [S \{ \frac{P}{S} \cdot PO + \frac{L}{S} \cdot LO + t \}] + \bar{L} \text{ (sec)}$$

where t is the exposure time per spot, \bar{L} is the number of wafer levels and the other symbols are defined as before. Mechanical and alignment overhead has been taken as 1 sec. The term in square brackets is the time required to write the pattern including pattern generator overhead. The last term (\bar{L}) is the mechanical and alignment overhead time. For practical purposes, it can be neglected.

VARIABLE SPOT SIZE	.5-1 μ m	.5-2 μ m	.5-4 μ m
S	2.77X10 ⁸	1.04X10 ⁸	5.66X10 ⁷
L	5.34X10 ⁷	3.86X10 ⁷	3.63X10 ⁷
P	3.60X10 ⁷	3.60X10 ⁷	3.60X10 ⁷

Table 1: Pattern statistics as a function of variable spot size for circuit based on RCA TCS02 (CMOS/SOS).

VARIABLE SPOT SIZE	.5-1 μ M	.5-2 μ M	.5-4 μ M
S	4.04X10 ⁸	1.79X10 ⁸	5.93X10 ⁷
L	5.59X10 ⁷	3.55X10 ⁷	3.10X10 ⁷
P	3.03X10 ⁷	3.03X10 ⁷	3.03X10 ⁷

Table 2: Pattern statistics as a function of variable spot size for
circuit based on AFAL/Hughes/Signetics Universal Arithmetic
Array (ECL).

The dependence of T on the time t is shown for the AFAL/Hughes/signetics circuit in figure 1 for the various possible variable spot sizes. P_0 was taken as 1 μsec and L_0 as .1 μsec as explained above.

It is clear that these curves all reach the overhead limit for spot exposure times less than .05 μsec . This limit is determined by the pattern overhead because the line overhead is much shorter than the pattern overhead and the ratios P/S and L/S are comparable for VSS systems.

The number of patterns in the AFAL/Hughes/signetics circuit and in the RCA circuit are practically identical. The dependence of T upon t is shown in figure 2 for the RCA circuit. For short dwell times ($<.05 \mu\text{sec}$) the throughput of the two circuits are practically the same. It is a characteristic of the lithography machine and not of the particular circuit being executed.

III. D. Throughput of the Raster Scan Lithography Machines:

Advanced Raster Scan Lithography Machines, of which there are none, would step a .5 μm square shaped beam across the wafer in a serpentine raster. The beam would be blanked where exposure is not wanted. Such a system would require a change in the design rules of the two circuits considered above because only integral multiples of the minimum line width are allowed and because slanted lines are not possible. This is not thought to be a serious drawback (it would be for chevron magnetic bubble circuits).

The sources of overhead in such a machine are mechanical and alignment overhead, and line overhead. Line overhead is the time required to turn the beam around at the end of a line. Since large deflections are required, electromagnetic deflection must be used and this results in a relatively long turn around time of 5 μsec (9). The net effect is small however. The time T required to write and \bar{L} level, 1 cm^2 circuit is given by

$$T = (2 \times 10^4 \text{ lines} \cdot 5 \times 10^{-6} \text{ sec/line} \\ + 4 \times 10^8 \text{ spots} \cdot t + 1) \cdot \bar{L}$$

The graph of T versus t for the advanced raster scan system for the two circuits are shown on figures 1 and 2. The overhead limit is approximately $1.1 \bar{L}$ seconds per circuit. This is very small compared to the overhead limit of the VSS vector machine but ultra high speed writing (>100 MHz) is required for the raster scan machine to realize a throughput advantage over the vector machine.

III. E. Discussion

At this point it is useful to establish some spot exposure time limits. The sensitivity of PMMA electron resist is approximately $50 \mu\text{C}/\text{cm}^2$. The maximum current density normally obtained from a tungsten thermionic electron gun is $50 \text{ A}/\text{cm}^2$ (6). Thus, the minimum spot exposure time for PMMA using the tungsten source is $1 \mu\text{sec}$. With the LaB_6 gun (4) the minimum spot exposure time can probably be decreased to $.5 \mu\text{sec}$ but Pfeiffer (6) reports that it is difficult to achieve uniform illumination of the spot forming aperture using the LaB_6 gun. For the T-F gun, with a current density of $2000 \text{ A}/\text{cm}^2$, the minimum spot exposure time is 25 nsec . With these numbers in mind, we can draw the following conclusions.

1. It is clear from figures 1 and 2 that circuit exposure times reach the overhead minimum for spot exposure times shorter than 50 nsec and that this limit is independent of spot size variability. This is because pattern overhead dominates all other types of overhead. For longer spot exposure times, the dependence of throughput on spot size variability is much stronger. At $1 \mu\text{sec}$ spot exposure time, the total exposure time for the ECL circuit decreases from 7.3 min to 1.1 min as the spot size variability increases from $.5\text{-}1 \mu\text{m}$ to $.5\text{-}4 \mu\text{m}$.

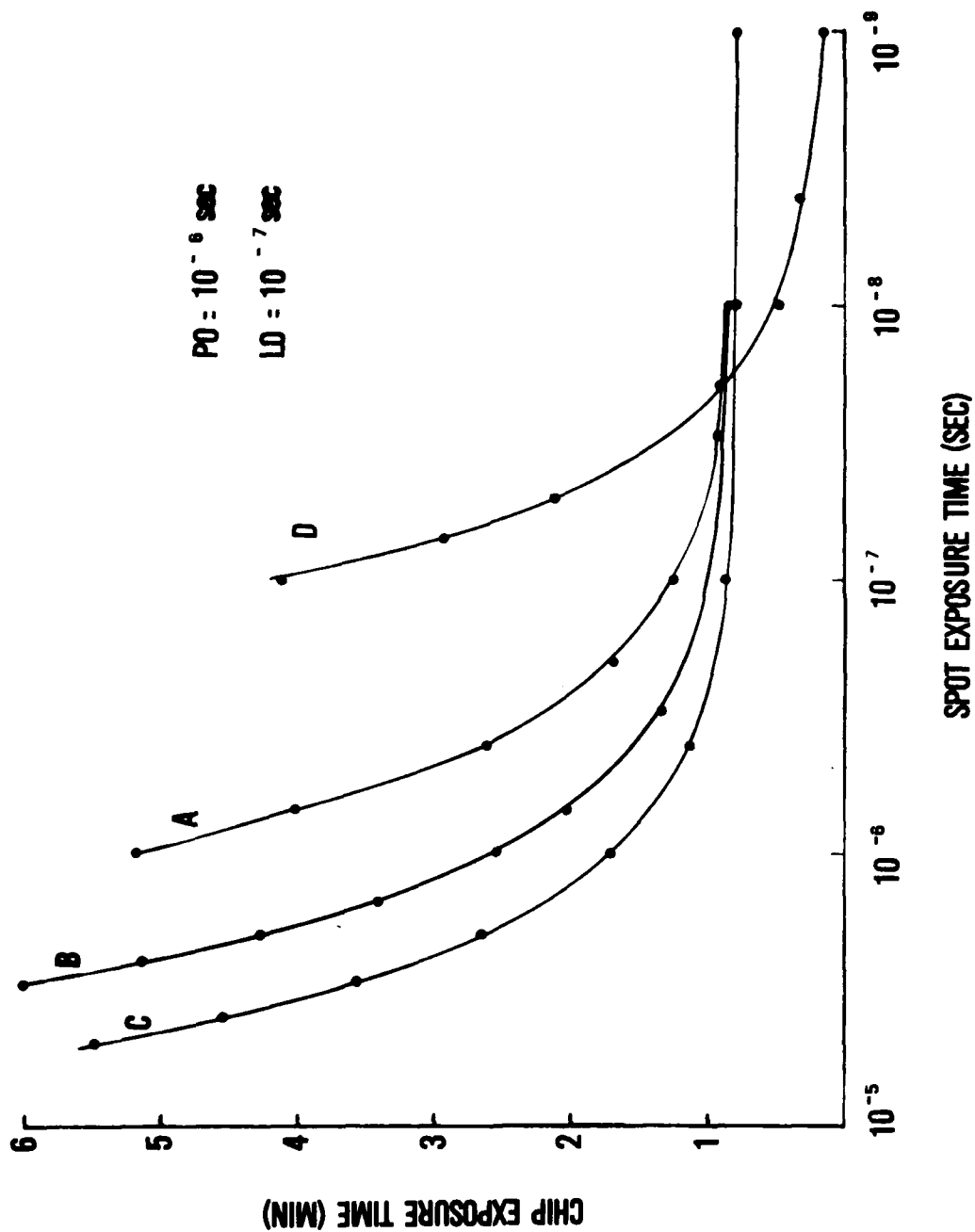
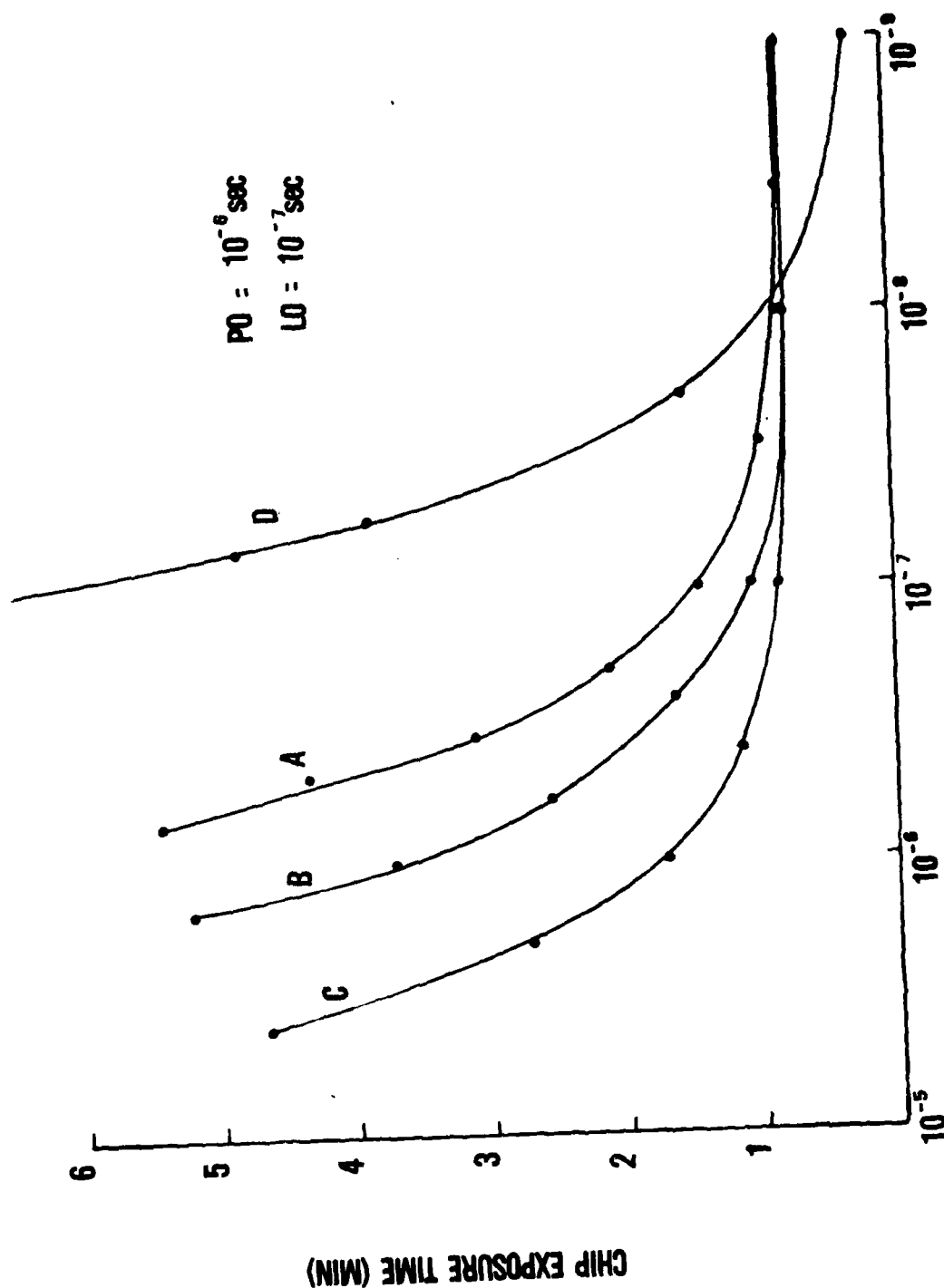


Figure 1: Time to expose all 7 levels of a single 1 cm^2 chip on a 4" wafer (based on RCA circuit statistics) for: A) $.5\text{-}1\mu\text{m}$ VSS Vector; B) $.5\text{-}2\mu\text{m}$ VSS Vector; and, C) $.5\text{-}4\mu\text{m}$ VSS Vector; and D) $.5\mu\text{m}$ square spot raster scanning lithography system.



SPOT EXPOSURE TIME (SEC)

Figure 2: Time to expose all 11 levels of a single chip on a 4" wafer (based on AFAL/Hughes circuit statistics) for: A) .5-1 μ m VSS Vector; B) .5-2 μ m VSS Vector; C) .5-4 μ m VSS Vector; and D) .5 μ m square spot raster scanning lithography system.

It is desirable to operate the vector scan system near the overhead throughput limit at 50 nsec spot exposure time (or 20 MHz exposure rate). Operation in the region placed very modest requirements on spot size variability. Pfeiffer has pointed out (6) that small spot size variations are desirable because of space charge effects.

Operation near the overhead limit requires either sensitive resists or high beam current density. The T-F electron gun can expose PMMA at a rate of 20 MHz with 1000 A/cm². This density is within present capabilities. The tungsten thermionic source would require a resist with a sensitivity of 2.5×10^{-6} C/cm². Development of a high resolution production resist with this sensitivity is far in the future.

We conclude that the T-F electron source would be of significant value in VSS Vector Scan Lithography Machines.

2. It is also clear from figures 1 and 2 that if the advanced raster scan system is to compete with the VSS system operated near the overhead limit, then the spot exposure time will have to be less than 10 nsec. Substantial throughput gains can be realized, however at a 200-300 MHz exposure rate. If, for technical reasons it is not possible to operate the VSS system near the overhead limit or if the overhead times (particularly pattern overhead) cannot be reduced to the somewhat optimistic levels used here, then the exposure rate of the advanced raster system for which its throughput equals that of the VSS system will decrease. For example, if the .5-1 μ m VSS system were operated at 1 MHz exposure rate, (the rate for PMMA and the tungsten electron source), the advanced raster system will have better throughput if its exposure rate is greater than 10 MHz and a throughput advantage of a factor of 10 at 100 MHz for the ECL circuit.

We have previously shown that the maximum exposure rate for PMMA and the T-F gun is 40 MHz. To operate the T-F gun at 200 MHz requires a resist sensitivity of $10 \mu\text{C}/\text{cm}^2$. Such resists may well become available with high resolution.

We conclude that the T-F electron source gives one sufficient current density to consider the advanced raster scan system. The advanced raster scan system has a higher throughput potential than the VSS vector scan system and even at moderate writing rates has a significant throughput advantage over the VSS system with the thermionic tungsten source for PMMA exposure.

IV. RECOMMENDATIONS

High brightness electron guns have been shown to be potentially very valuable in improving throughput and reducing resist sensitivity requirements in VSS Vector Scan and Raster Scan Lithography Machines.

Electron gun research should be continued with particular emphasis on the following problems:

- 1) Develop a sturdy gun mount. Current mounting arrangements are too flimsy for high resolution, production lithography machines.
- 2) Develop a gun capable of high voltage operation.
- 3) Develop a vacuum system capable of supporting the T-F gun in a production environment.

It was shown that a square spot raster scan system is superior to a VSS vector system if the former is operated at ultra-high speed. Research into the problems associated with high speed data transfer and beam blanking should be carried out.

1979 - SCEEE SUMMER FACULTY RESEARCH PROGRAM

Sponsored by the

AIR FORCE OFFICE OF SCIENTIFIC RESEARCH

Conducted by the

SOUTHEASTERN CENTER FOR ELECTRICAL ENGINEERING EDUCATION

FINAL REPORT

IMPURITIES IN COMMUNICATION GRADE GaAs

Prepared by:	Richard G. Yalman
Academic Rank:	Professor
Department and University:	Chemistry, Antioch College
Research Location:	Electronic Research Branch AF Avionics Laboratory, WPAFB OH
USAF Research Colleague:	Dietrich W. Langer
Date:	11 September 1979
Contract No:	F49620-79-C-0038

IMPURITIES IN COMMUNICATIONS GRADE GaAs

by

Richard G. Yalman

ABSTRACT

Molecular beam and chemical vapor phase (Ga/AsCl₃/H₂) epitaxy are used to grow device quality GaAs at the Electronic Research Branch, Electronic Technology Division, Avionics Laboratory, Wright-Patterson Air Force Base, Ohio. Reproducible growth of communications grade GaAs has not been achieved. Practical considerations for the reduction of impurities in these materials are confined to the manipulation of the physical arrangement and chemistry of the "as is" systems. Because the order of desired impurities in GaAs is 1 ppb additional attention must be given to clean rooms, additional traps, modification of flushing and burn-out techniques, elimination of teflon and silicon grease, the in-house preparation of bulk GaAs, and changes in the composition of the carrier gases in the Ga/AsCl₃/H₂ system. A new reactor system has been designed and is being assembled for the determination of growth parameters. A complete determination of the equilibrium state within the reactor tube as a function of furnace profile, composition and pressure of carrier gas and Ga/As, Cl/H and O/H ratios would aid in the statistical design of a new set of experiments with this equipment.

ACKNOWLEDGEMENTS

The author would like to thank the Air Force Systems Command, Air Force Office of Scientific Research, and the American Society of Engineering Education for providing him the opportunity to spend a most worthwhile and interesting summer at the Electronic Research Branch, Avionics Laboratory, WPAFB, Ohio. Special acknowledgement is due to Dr. Dietrich Langer of the Electronic Research Branch for guidance and encouragement. Other members of this organization who have been particularly helpful in setting an unusually stimulating atmosphere include Major Robert J. Almassy, Don Reynolds, Cole Litton, Gary McCoy and Krishan Bajaj.

I would also like to acknowledge my indebtedness to the SCEEE operations office for maintaining an effective program which not only brought me into contact with the local scientists, but also Tom Clarke from North Dakota, Laurence Eaves from Nottingham, and Hans Hartnagel from Darmstadt.

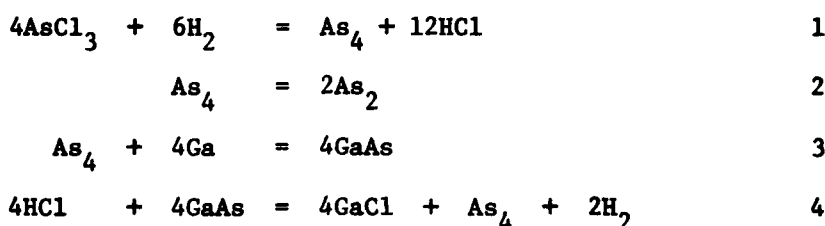
I. INTRODUCTION: Epitaxial GaAs is used in a variety of electronic devices (LEDs, FETs, IMPATTs, etc.). Its relatively wide bandgap and high electron mobility gives GaAs an edge over silicon in microwave applications including solid state transmitters and receivers for radar and communications systems. Unfortunately the preparation of epitaxial GaAs is still largely an art, and its properties have not been adequately correlated with starting materials and/or growth parameters. This lack of a clear understanding of the growth process leads to low yield, high cost, and components of questionable reliability.

One of the missions of the Electronic Research Branch is to develop reproducible techniques for the epitaxial growth of communications grade GaAs. Currently molecular beam and Ga/AsCl₃/H₂ vapor phase epitaxy are being used to provide materials for a variety of in-house physics experiments, but improved techniques are still required to provide materials with consistently low impurities (less than 10^{14} cm^{-3}) and high mobilities (over 120,000 at 77°K). A new design for the Ga/AsCl₃/H₂ system is now being built and the apparatus for organometallic epitaxy is being assembled.

Molecular beam epitaxy¹ consists in the high vacuum transport of Ga and As from sources in Knudsen cells to a GaAs substrate. In the Electronic Research Branch the pumping pressure is in the range of 1×10^{-9} - 5×10^{-11} Torr, with deposition pressures in the range of 10^{-6} to 10^{-7} Torr. Epitaxy growth occurs in an hydrogen atmosphere, the substrate temperature is 540°C, the Ga oven is maintained at 1000°C and the As oven at 350°C. A vacuum lock system has been installed for changing the substrates and the heating elements have cryogenic shields. Carbon has been identified as a major contaminant and carbon and silicon are inherent to the system. To reduce the introduction of carbon and silicon the Pd hydrogen purifier has been modified to eliminate the stainless steel Pd support coil. Nonetheless the system is characterized as having all of the problems inherent in high vacuum technology.²

Organometallic epitaxy³ consists in the pyrolysis of trimethylgallium and arsine in an hydrogen atmosphere in the vicinity of a GaAs substrate mounted on a graphite or boron nitride coated substrate. The susceptor is maintained at 750°C by rf induction heating. Again carbon is an inherent impurity due to reactions of methyl free radicals and the catalytic nature of the GaAs itself.⁴ When a plasma is used to generate Ga and As, silicon from the silica glass reactor will also be an inherent impurity.

The Ga/AsCl₃/H₂⁵ method uses a temperature profile in which Ga and As vapors generated in a high temperature region are transported downstream where they deposit on a GaAs substrate at a lower temperature. In this laboratory purified hydrogen is used to carry AsCl₃ into the high temperature region of a silicon dioxide glass reactor tube. Some of the reactions in this region include



The GaCl and As₄ (and As₂) are transported downstream by hydrogen where the reverse of reaction (4) occurs on the substrate in the low temperature region.

A series of reactions involving hydrogen, hydrogen chloride and Silicon dioxide (from the silica glass reactor tube) give rise to SiO and compounds of the series SiH_xCl_{4-x}. These can react at the surface of the newly formed GaAs to produce elemental Si or to condense as SiO and, by reacting with water, as SiO₂. Thus Si and O are inherent impurities in this system. Zn, presumably from AsCl₃, can be detected at levels as low as 10¹⁴ cm⁻³ by high resolution photoluminescence techniques in high mobility GaAs (greater than 10⁵ at 77°K).⁶

In addition to the major contaminants of concern in this laboratory nearly twenty additional elements have been identified at concentration levels ranging from 2×10^{14} to 10^{17} cm^{-3} by SSMS and SIMS. Because these concentrations are close to the detection limits for most elements⁷ there is some question regarding the true value for any element reported at concentrations below 1 ppm ($4 \times 10^{16} \text{ cm}^{-3}$).

Low levels can also be achieved by photoluminescence techniques.⁹ Unfortunately the exceedingly small differences of energy levels in GaAs for many different donors preclude the use of this technique for differentiating between such impurities. However, the chemical shifts for acceptors range from a few meV to several tenths of an eV and this method can be used for these impurities. Confusion may arise due to the poor quality of the material and to shifts due to high doping. Nonetheless using a high resolution spectroscope with samples maintained at 1.2-2.1K, Zn can be consistently identified in this laboratory at concentrations down to 10^{14} cm^{-3} .

Electrical measurements can detect impurities at 10^{13} cm^{-3} or less i.e. at levels below elemental identification. The goal in this laboratory is to produce such materials. In order to do so the Electronic Research Branch made the decision to reexamine the chemistry of the epitaxial growth processes and to use a chemist in the Summer Faculty Research Program for this examination.

II. OBJECTIVES OF THE RESEARCH EFFORT

1. Initially the stated objective of this research effort was to examine the sources of impurities in the epitaxial growth of GaAs by the pyrolysis of organometallic compounds and arsine in an hydrogen atmosphere in order to reduce the magnitude of these impurities by selecting the highest grade starting materials and modifying the apparatus under construction.

2. The initial goal was subsequently broadened to include:

- a. the TMGa/AsH₃/H₂ system
- b. the Ga/AsCl₃/H₂ system
- c. the molecular beam Ga/As system

3. Given the inherent restrictions of the respective apparatus, the in-house experience with the respective systems and the potential for achieving the desired objective of communications grade GaAs within the near future (1-2 years) the research effort ultimately focussed on the potential sources of impurities in the Ga/AsCl₃/H₂ system.

III. METHODOLOGY

The approaches to the determination of the sources of impurities in epitaxial GaAs include:

1. The identification of trace element impurities in all of the source materials by collating information supplied by the manufacturers through correspondence and by telephone, analytical information available on these materials as a result of elemental analysis in this and other interested laboratories and the Bureau of Standards and a study of the methods of preparation of these materials.
2. A comparison of impurities in GaAs grown by the various techniques in this and various interested laboratories through a study of information available in the literature and to the extent possible, by talking directly with the principal investigators in the various laboratories. The differences in the impurities found in GaAs prepared by different methods identifies, in part, non-identifiable impurities in the source materials and impurities which may be inherent in the growth techniques themselves.
3. A thermochemical study of the possible chemical reactions occurring within the various systems in order to identify the magnitude of potential impurities within different systems and to anticipate modifications which might decrease the magnitude of these impurities.

IV. RESULTS

1. With few exceptions the materials supplied by the manufacturers are used "as-is" in nearly all GaAs growing laboratories, i.e. they are not further purified. These materials are listed as Electronics Grade,

but they vary in purity from 7N for gallium to 5N for the organometallics and arsenic compounds. Although manufacturers will supply lot analysis upon request, specifics, including manufacturing, analytical and sensitivity of analytical techniques, are often considered trade secrets. The analysts themselves report impurities which vary from .02 ppm copper in gallium to 4 ppm germanium in arsenic trichloride. Unfortunately there is no clear correlation between these or other reported impurities and the impurities found in GaAs.

As indicated previously the limits of detection of chemical analysis, whether by atomic absorption, spark emission spectroscopy, secondary ion mass spectroscopy or spark source mass spectroscopy, is less sensitive than photoluminescence. Unfortunately the latter is limited to a few elements at concentrations greater than 10^{14} cm^{-3} . The final criterion is the mobility of the sample, but the desired levels are less than those detected by elemental analysis.

Cr doped GaAs is the common substrate for epitaxial GaAs. In this and other doped substrates the GaAs boule is generally saturated with the desired dopant in order to completely compensate the donors (or acceptors) present. The result is a complete masking of all other impurities which, unless a special analysis is made, are present in unknown quantities.⁸ Thus diffusion across the junction between the substrate and the epi layer is a potential source of impurity. The magnitude of this impurity may be reduced by applying stress to the back of the substrate.¹¹

It is clear that the various processes for the epitaxial growth of GaAs are still in a state-of-the-art stage. This is indicated in the lack of correlation between known impurities in the source materials and the growth materials, in the selection of source materials by the various laboratories from different suppliers and the lack of correlation between growth parameters and incorporated impurities. Few laboratories have the capabilities of further purifying the source materials due to their corrosive and pyrolytic nature. Exceptions are the Naval Research Laboratory which is preparing its own substrate material and the Rockwell Laboratory which is planning to purify trimethylgallium.¹²

A comparison of epitaxial growth methods suggest impurities inherent in the given method. For example, zinc is one of the important contaminants in device grade GaAs grown in the Ga/AsCl₃/H₂ system whereas zinc impurities are less important in liquid phase epitaxy. A second example is the high carbon content of epi layers made by molecular beam and organometallic epitaxy but not the Ga/AsCl₃/H₂ system using Cr doped substrates. Third, systems grown in silica glass reactor tubes contain higher silicon content than those grown in stainless steel or other pure metal systems.

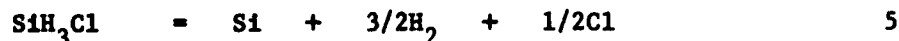
The source of zinc in the Ga/AsCl₃/H₂ system may be AsCl₃ since both the liquid phase and molecular beam epitaxy use metallic arsenic. A suggested source of zinc may also be the vaporization of the brass tips of the torches used in the fabrication of the reactor tubes. The level of zinc in epi layers grown in this system has been reduced to 10¹⁴ cm⁻³. This degree of purity indicates that this system purifies the starting materials. A similar purification in molecular beam epitaxy depends on the so-called "sticking" coefficient of the zinc (and other) impurities on the substrate while purification in liquid phase epitaxy depends upon the distribution coefficients of impurities between the solid and liquid phases. Because of the generally low and unknown concentrations of impurities in the starting materials and the epi layers values of sticking and distribution coefficients are not well known and their elimination depend on empirical experiments.

The sources of carbon, silicon and various metals in molecular beam epitaxy has been described in some detail and are inherent in radiation effects upon the support, insulation and other materials required in ultra high vacuum technology.² Sources of carbon in organometallic vapor phase epitaxy include the presence of small amounts of hydrocarbons in the starting materials, reactions involving the methyl radicals and the catalytic nature of the gallium arsenide itself as there is evidence for the formation of the complex, CGaAs.⁴ The result of the latter factor is that the carbon content is greater than expected from thermodynamic calculations.

Empirical methods in different laboratories to reduce impurities include the use of boron nitride¹³ instead of silica glass boats, the use of a nitrogen atmosphere instead of hydrogen atmosphere,¹⁴ the use of a single rf induction furnace³ in the organometallic system to eliminate the long profile furnace used in the Ga/AsCl₃/H₂ system, the use of constant¹⁵ or lower¹⁶ substrate temperatures, an increase in the partial pressure of AsCl₃¹⁷ and the "gettering" of substrates. In a series of experiments based on a suggestion by Weiner¹⁸ water was deliberately added to the In/PCl₃/H₂ system to suppress the incorporation of silicon in indium phosphide.¹⁸ These variations can reduce the concentration levels of specific elements, particularly silicon, but there are no correlations between the various experimental modifications and the total level of impurities which remain at 10¹⁵ cm⁻³ or greater.

2. In order to estimate the amount of elemental silicon which may be incorporated into epitaxial GaAs a number of authors have made thermochemical studies of the Ga/AsCl₃/H₂- SiO₂ system.^{20,21,22} This system is particularly important as the reactor tube consists of silica glass. Furthermore, because of both custom and convenience silica glass will continue to be the material for the reactor tube even where a boron nitride boat is used.

There are a number of problems connected with these calculations. First, there have been revisions in the thermodynamic data themselves so that species i.g. SiH₃Cl, which were emphasized in earlier calculations now appear to be less prominent. Second, because of the misnomer, i.e., the term "quartz" for silica glass, thermodynamic data for quartz instead of silica glass has been used. Third, because of the complexity of the system under investigation there has been little agreement as to the possible species which may be present or the possible reactions responsible for the formation of elemental silicon in the epitaxial growth. Thus, DiLorenzo and Moore²¹ cite the reaction



as the source of silicon whereas this author prefers the overall reaction



Fourth, a misinterpretation of experimental data which resulted in the statement²¹ that whereas three moles of hydrogen chloride per mole of hydrogen chloride are generated by the reaction



only two of these are used to generate GaCl. This error is due to the fact that over the experimental range of P_{AsCl_3} there is only a small change in the equilibrium ratios of $P_{\text{GaCl}}/P_{\text{As}}$, where P_{GaCl} and P_{As} are the equilibrium partial pressures of volatile gallium and total volatile arsenic compounds, respectively, in the reactor tube (Table I). Unfortunately, this error continues to be repeated.

Table I
Gallium/Arsenic/Ratios as a Function of Initial
 P_{AsCl_3} , $T = 1131\text{K}$

P_{AsCl_3}	Gallium/Arsenic Ratio	
	Observed ^a	Calculated
.001	-	2.58
.00152	1.88	-
.0025	-	2.49
.00291	1.82	-
.0056	-	2.40
.00627	1.93	-
.00745	1.84	-
.010	-	2.32

a. Ref 21.

Free energy values for a number of reactions occurring during the epitaxial growth of GaAs in this laboratory are given in Table II. The higher temperature, 1131 K, corresponds to the temperature of the boat where volatile GaCl is formed while the lower temperature, 1003 K, is the temperature of deposition of GaAs on the substrate. Table IIA contains values for the formation of volatile silicon compounds, Table IIB the values for reactions which lead to the formation of elemental silicon and the values for the "clean-up" reaction for the removal of elemental silicon from the surface of GaAs are given in Table IIC.

Table II

Free Energies, Kcal mole⁻¹

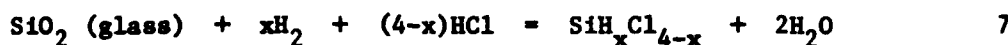
Reaction	Temperature, K	
	1131 ^a	1003 ^b
A		
Volatile Silicon Compounds		
SiO ₂ + 2Ga = Ga ₂ O + SiO	71,404	80,779
SiO ₂ + H ₂ = H ₂ O + SiO	65,701	71,819
SiO ₂ + 3H ₂ + HCl = 2H ₂ O + SiH ₃ Cl	81,238	78,660
SiO ₂ + 2H ₂ + 2HCl = 2H ₂ O + SiH ₂ Cl ₂	65,341	63,200
SiO ₂ + H ₂ + 3HCl = 2H ₂ O + SiHCl ₃	51,462	49,170
SiO ₂ + 4HCl = 2H ₂ O + SiCl ₄	42,064	39,320
SiO + 2HCl = H ₂ O + SiCl ₂	1,824	-2,779
B		
Elemental Silicon Formation on GaAs		
2SiCl ₂ = SiCl ₄ + Si	-26,715	-30,560
SiH ₃ Cl + GaAs = GaCl + 3/2H ₂ + As ₄ + Si	-13,785	-6,790
SiH ₂ Cl ₂ + 2GaAs = 2GaCl + H ₂ + 1/2As ₄ + Si	1,784	12,340
SiHCl ₃ + 3GaAs = 3GaCl + 1/2H ₂ + 3/4As ₄ + Si	16,849	30,040
SiCl ₄ + 4GaAs = 4GaCl + As ₄ + Si	26,676	43,560
C		
Removal of Silicon From GaAs		
Si + 4HCl = 2H ₂ + SiCl ₄	-24,960	-28,880

a. Temperature of the Reactor

b. Temperature of the Substrate

Because of the ratio of P_{As_4}/P_{As_2} has a value of two under the conditions of the experiments in this laboratory ($P_{AsCl_3} = .0056$ atm.) the species As_4 is used in the reactions in Table II. Table II is also based on the thermodynamic data for silica glass and not quartz. More recent thermodynamic data²³ show that the species $SiCl_4$ and $SiHCl_3$ are more stable than had been previously recognized. In spite of these changes the amount of elemental silicon formed on the surface of the epi GaAs is of the same order of magnitude as that reported by DiLorenzo and Moore²¹ and decreases rapidly for P_{HCl} greater than .001 atm.

In the overall reaction of hydrogen chloride with silicon dioxide two moles of water are formed. If this amount of water is introduced



into the reactor tube along with the carrier gas, the amount of volatile silicon compounds will be greatly reduced producing a corresponding reduction of elemental silicon in epitaxial GaAs. The calculations here are in agreement with the suggestion made earlier by Weiner¹⁸ and in view of the fact that his calculations were based on quartz and not silica glass this suggestion becomes more important. The effect of introducing water on the formation of gallium and arsenic oxides during the growth and cooling of GaAs will be negligible as there will be virtually no change in the total amount of water in the reactor tube.

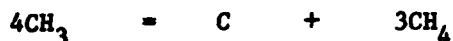
Although zinc is not reported as an impurity in the source materials (gallium, arsenic trichloride and GaAs substrates) but is found in epitaxial GaAs, it was assumed to be present in each of the source materials. Zinc boils at 1180°K, which is higher than the temperature maintained in the hot part of the reactor tube. If present in the elemental gallium, it might be removed by baking out the gallium at 1200°C, the maximum operating temperature of the furnace, in an hydrogen chloride atmosphere. Zinc chloride would then be swept out of the furnace. This procedure is used to purify gallium used in molecular beam epitaxy²⁴.

Since present as an impurity in the manufacturers arsenic trichloride would be in the form of non-volatile ZnCl_2 . The volatility of this and other metal chloride impurities could be further reduced by the formation of anionic chloro complexes by the addition of $(\text{C}_2\text{H}_5)_4\text{NCl}$ or hydrogen chloride. However, whenever an additional substance is added it also acts as an additional source of impurity.

Arsenic trichloride is transferred from a bubbler tube to the reactor tube with the aid of hydrogen gas. The flow rate of the hydrogen gas varies from 50 - 200 ml/min. This is a very rapid flow rate and even though bubbling appears smooth, the presence of a spray cannot be ignored. Thus a potential technique for the reduction of impurities carried from the arsenic trichloride bubbler into the reactor tube is the introduction of large surface traps or baffles.

Where semi-insulating substrates (Cr and O doped GaAs) are used, the concentrations of impurities are of the order of magnitude or larger than those found in the epitaxial GaAs.^{25,26} Although the diffusion rate of zinc in GaAs is low, the rates of diffusion of Group IA and IB elements is quite high.²⁷ Thus substrates may be sources of impurities in the epitaxial material. Rates of diffusion may be reduced by "gettering".¹¹ It may ultimately be necessary to prepare the substrate itself.

Carbon appears to be ubiquitous to GaAs grown by molecular beam and organometallic epitaxy and to other III-V materials. Sources of carbon were discussed in Section 2. A chemical source would be produced by the reaction



where the methyl radical, CH_3 , is produced during the decomposition of trimethyl gallium during organometallic epitaxy. However, thermodynamic calculations show that the amount of carbon formed in this reaction would only correspond to 10^8 cm^{-3} . Other carbon producing reactions involve the cracking of hydrocarbons. Although these reactions normally occur at negligible rates, they occur rapidly on a catalytic surface. GaAs must be considered as such a surface. In order to avoid carbon contamination all freshly prepared GaAs surfaces must be kept in hydrocarbon-

free atmospheres.

Finally, it is not surprising that a listing of elements found in various III-V compounds²⁸ correspond to those occurring most frequently as measured by natural abundancies. This raises the obvious question as to whether dust in the laboratories may be the source of these impurities and that all exposed surfaces of materials and equipment should be done in a dust and hydrocarbon-free clean room.

V. RECOMMENDATIONS:

a. This Work:

The following recommendations have been made to the appropriate personnel in the Electronic Research Branch for the enhancement of the quality of epitaxial GaAs prepared by the Ga/AsCl₃/H₂ system and, where appropriate, molecular beam and organometallic epitaxy.

1. The work should be performed in a "clean room", i.e., an area containing an airlock system with filtered air. There should be no smoking or custodial services in this area nor solvents, oil pumps and other sources of volatile carbon and silicon compounds.
2. Modifications in the reactor tube should be made so that back diffusion of environmental gases cannot occur during the removal and insertion of substrates and epi layers.
3. Traps should be introduced between bubbler systems and reactor tubes.
4. All organic materials including teflon and silicone greases should be eliminated from the reactor system.
5. After the reactor tube is cleaned with the H₂SO₄-HF mixture, the tube should be baked out at 1200°C in an hydrogen chloride atmosphere.
6. All hydrogen chloride used in this system should be generated by the reduction of AsCl₃ with H₂ (this recommendation was already

planned for the new apparatus under construction).

7. Gallium should be baked out at 1200°C in an hydrogen chloride atmosphere.

8. The effect of introducing water via the hydrogen carrier gas at concentrations corresponding to the amount of water currently produced in the hot reactor tube should be investigated.

9. Epitaxial GaAs can be prepared with a lower concentration of impurities than the source materials including the substrate. Because of this fact the preparation of bulk GaAs using the $\text{Ga/AsCl}_3/\text{H}_2$ should be given serious consideration. In this way all of the material used in this process with the single exception of hydrogen gas will have been purified in this laboratory. The new equipment now under construction can be used for preparing the bulk GaAs, for the preparation of pure hydrogen chloride and the transport of gallium and arsenic from the bulk GaAs to the substrate.

b. Recommendations for Future Work:

The equilibrium states of the $\text{Ga/AsCl}_3/\text{H}_2\text{-SiO}_2$ system should be determined along the reactor tube from the hot to the cold region. These calculations should take into consideration the variations in the temperature profile as well as variations in the source materials and substrate, the variations in the partial pressures of volatile constituents as well as the total pressure in the system and variations in the elemental composition within the reactor tube as functions of the Ga/As, Cl/H and O/H ratios. The determination of the equilibrium states is done by minimizing the free energy of the system. The iteration method of Cruise²⁹ will be modified as needed.

The proposed calculations should take into consideration the reaction of the silica glass boat with gallium, the reaction of the silica glass reactor tube with both hydrogen and hydrogen chloride and the reactions of water formed in the latter reactions with Ga, As and GaAs.

An important aspect of these calculations is to determine the turning point between growth and etching and the reactions which may occur between the volatile components within the reactor tube and epitaxial GaAs during periods (heating and cooling) when neither growth nor etching occur.

A program should be prepared which can be used with the Hewlett-Packard 9852A calculator with appropriate accessories now available to the laboratory used for the preparation of epitaxial GaAs. It is anticipated that the program will be used during the course of the experimental program to determine the effect of changing a given variable on the other components of the system. Finally, the program will help in the statistical design of a new series of experiments.

It is clearly recognized that thermodynamics says very little about the kinetics and mechanism of the growth of GaAs. It should also be recognized that the GaAs surfaces have catalytic properties and that previously ignored reactions must be considered.

REFERENCES

1. Cho, A. Y., and J. R. Arthur, "Molecular Beam Epitaxy," Prog in Solid State Chemistry, 10, pp 157-191, 1975.
2. Covington, D. W. and E. L. Meeks, "Unintentional Dopants Incorporated in GaAs Layers Grown by Molecular Beam Epitaxy," J. Vac. Sci. Technol., 16, pp. 847-850, 1979.
3. Manasevit, H. M., and W. I. Simpson, "The Use of Metal-Organics in the Preparation of Semiconductor Materials," J. Electrochem. Soc., 116, PP. 1725 - 1730, 1969.
4. Schlyer, D. J., and M. A. Ring, "An Examination of the Product Catalyzed Reaction of Trimethylgallium with Phosphine and the Mechanism of the Chemical Vapor Deposition of Gallium Phosphide and Gallium Arsenide," J. Electrochem. Soc., 124, pp. 569-573, 1977.
5. Shaw, D. W., "Chemical Vapor Phase Epitaxial GaAs," J. Crystal Growth 31, pp. 142-7, 1975.
6. Reynolds, D. C., Electronic Research Branch, WPAFB OH, private communication.
7. Ahearn, A. J., Trace Analysis by Mass Spectrophotometry, New York, Academic Press, 1972.
8. Look, D. C., "The Electrical Characterization of Semi-Insulating GaAs: A Correlation with Mass-Spectrographic Analysis," J. Appl. Phys., 48, PP. 5141-5148, 1977.
9. Ashen, D. J., P. J. Dean, D. T. J. Hurle, J. B. Mullin, A. W. White and P. D. Greene, "The Incorporation and Characterization of Acceptors in Epitaxial GaAs," J. Phys. Chem. Solids 36, pp. 1040-1053, 1975.

10. Reynolds, D. C., Electronic Research Branch, WPAFB OH.
11. Magee, T. J., J. Peng, J. D. Hong, C. A. Evans, Jr., V. R. Deline and R. M. Malbon, "Back Surface Gettering and Cr Out-Diffusion in VPE GaAs Layers, Appl. Phys. Lett. 31, pp. 277-279, 1979.
12. Dapkus, P. D., Rockwell International, Anaheim CA, private Communication.
13. Swiggard, E. M., S. H. Lee and F. W. Von Batchelder, "GaAs Synthesized in Pyrolytic Boron Nitride (BN)," Proc. Sixth Intl. Symp. on GaAs and Related Compounds, St. Louis 1976, Inst. Phys. Conf. Ser. No. 33b, pp. 23-27, 1977.
14. Ihara, M., K. Dazai, and O. Ryuzan, "Vapor-Phase Epitaxial Growth of GaAs in a Nitrogen Atmosphere," J. Appl. Phys., 45 pp. 528-531, 1974.
15. Seki, H., A. Kookitu, K. Ohta and M. Fujimoto, "New Methods of Vapor Phase Epitaxial Growth of GaAs," Jap. J. of Appl. Phys., 15, pp. 11-17, 1976.
16. Hallais, J., D. Boccon-Gibod, J. P. Chane and L. Hollan, "Diverse Quality GaAs Grown at Low Temperature by the Halide Process," J. Electrochem. Soc., 124, pp. 1290-1294, 1977.
17. DiLorenzo, J. V., G. E. Moore and A. E. Machala, "Effect of Arsenic Trichloride on Silicon Impurities in Epitaxial GaAs," J. Electrochem. Soc. 117, pp. 102-8, 1970.
18. Weiner, M. E., "Si Contamination in Open Flow Quartz Systems for the Growth of GaAs and GaP," J. Electrochem. Soc. 119, pp. 496-504, 1972.
19. Groves, S. H. and Plonko, M. C. Seventh Intl. Symp. on GaAs and Related Materials, St. Louis, Sep 78, Institute of Phys. Conf. Ser. No. 45 pp. 71-77, 1978.

20. Cochran, C. N. and L. H. Foster, "Reactions of Gallium with Quartz and With Water Vapor, With Implications in the Synthesis of Gallium Arsenide," J. Electrochem. Soc., 109, pp. 149-154, 1962.
21. DiLorenzo, J. V. and G. E. Moore, Jr., "Effects of AsCl_3 Mole Fraction on the Incorporation of Germanium, Silicon, Selenium and Sulfur with Vapor Grown Epitaxial Layers of GaAs," J. Electrochem Soc. 118, pp. 1823-1829, 1971.
22. Rai-Choudhury, P., "Thermodynamics of $\text{Ga-AsCl}_3\text{-H}_2$ System and Dopant Incorporation," J. Crystal Growth 11 pp. 113-120, 1971.
23. Hunt, L. P. and E. Sirtl, "A Thorough Thermodynamic Evaluation of the Silicon-Hydrogen-Chlorine System," J. Electrochem. Soc., 119, pp. 1741-1745, 1972.
24. Litton, C., Electronic Research Branch, WPAFB OH, private communication.
25. Kim, H. B., D. L. Barrett, G. G. Sweeney and T. M. S. Heng, Sixth Intl. Conf. on GaAs and Related Materials, St. Louis, 1976, Inst. of Phys. Conf. Ser. No. 33b pp. 136-144, 1977.
26. Brozel, M. R., J. B. Clegg and R. C. Newman, "Carbon-Oxygen and Silicon Impurities in Gallium Arsenide," Appl. Phys 11, pp. 1131-1139, 1978.
27. Kendall, D. L., "Semi-Conductor and Semi-Metals, Vol 4 (Ed. by R. K. Willardson and A. C. Beer) Academic Press, pp. 163-259, 1968.
28. Duchemin, J. P., M. Bonnet, G. Beuchet and F. Koelash, "Organo-Metallic Growth of Diverse-Quality InP by Cracking of $\text{In}(\text{C}_2\text{H}_5)_3$ and Ph_3 at Low Pressure," Seventh Intl. Conf. on GaAs and Related Materials, St. Louis 1978, Inst. of Phys. Conf. Ser. No. 45, pp. 10-18, 1978.
29. Cruise, D. R., "Computer Program for Equilibrium States," J. Phys. Chem. 68, pp. 3794-3808, 1964.